

UNIVERSITY OF MARYLAND AT COLLEGE PARK

DEPARTMENT OF AEROSPACE ENGINEERING



ASIMOV CITY:

DEVELOPING A PERMANENT

EARTH-INDEPENDENT SETTLEMENT ON MARS

ENAE484 SENIOR CAPSTONE, CLASS OF 2015

1. Introduction

1.1. Names

Faculty Advisors: Dr. David Akin, Dr. Mary Bowden, Dr. Andrew Becnel

Graduate Advisor: Jarred Young

Student Team Members:

Wiam Attar	April Claus	Laura Martinez
Rob Bailey	Jacob Cummings	Aly Nada
Marlin Ballard	Patrick Dunleavy	Lauren Powers
Will Bentz	Matt Eastman	Alexander Raul
Joshua Bernstein	Yoseph Feseha	Kevin Reich
Chris Bohlman	Frank Hackenburg	Jaclyn Rupert
Adam Buckingham	Ryan Joyce	Conner Taylor
Jason Burtnick	Scott Kindl	David Valentine
Bernadette Cannon	Jigna Lad	Sam Walters
Lemuel Carpenter	Aaron Lash	Chris Wells-Weitzner
Kevin Chuang	Henry Ludgate	Dustin Zrelak

1.2. Report Overview

1.2.1. Table of Contents

1. Introduction	2
1.1. Names	2
1.2. Report Overview	3
1.2.1. Table of Contents	3
1.2.2. List of Figures.....	10
1.2.3. List of Tables.....	14
1.2.4. Glossary of Acronyms	16
1.3. Program Introduction	18
1.3.1. RASC-AL Program	18
1.3.2. Mission Statement	19
1.3.3. Requirements	19
1.3.4. RASC-AL Requirements.....	20
1.3.5. Program Architecture Overview.....	21
2. Phase I: Exploration	22
2.1. Phase Overview	22
2.2. Lunar Exploration	23
2.3. Mars Exploration	24
2.3.1. Mars 2020.....	24
2.3.2. DSx Missions.....	25
2.3.2.1. Mission Overview	25
2.3.2.2. Primary Mission: Hellas Planitia	26
2.3.2.3. Secondary Mission: McLaughlin Crater	30
2.3.2.4. Concept of Operation	31
2.3.2.5. Vehicle Overview and Science Package.....	32
2.3.2.6. Avionics	34
2.3.2.7. Power Requirements.....	34
2.3.2.8. Aeroshell Design	35
2.3.2.9. Program Cost.....	36
2.3.2.10. DSx Mission Benefits.....	36
2.4. Phobos and Deimos	37
2.4.1. Introduction and Motivation	37
2.4.2. Exploration Program.....	38
3. Phase II: Resource Acquisition and Infrastructure Setup	39
3.1. Introduction	39
3.2. Lunar Resource Acquisition	39
3.2.1. Introduction/Overview.....	40
3.2.2. Concept of Operations	40
3.2.3. Lunar Mining Vehicle.....	41
3.2.3.1. Miner Avionics.....	42
3.2.4. Lunar Processing Plant	44

3.2.5.	Mobile Roving Settlement	44
3.2.6.	Lunar Cargo Delivery	49
3.2.7.	Lunar Lander.....	53
3.2.8.	Crew Support Mission Overview	55
3.2.8.1.	Initial Crew Operations.....	55
3.2.8.2.	Long-Term Crew Support	56
3.2.9.	Spacesuits	57
3.3.	Fuel Transport Vehicle	58
3.3.1.	Overview	58
3.3.2.	Design Constraints.....	58
3.3.3.	Structure.....	60
3.3.4.	FTV Avionics.....	63
3.4.	EML1 Fuel Depot.....	64
3.4.1.	Introduction.....	64
3.4.2.	Design Overview.....	67
3.4.3.	Structural Design	68
	Outer Radius (m)	69
	Thickness (m)	69
	Length (m)	69
	Limit Load (MPa)	69
	Factor of Safety	69
	Margin of Safety	69
3.4.4.	Active and Passive Cooling System.....	69
3.4.5.	Station-Keeping	70
3.4.6.	Reaction Control System	71
3.4.7.	Power Requirements and Avionics.....	77
3.4.8.	Assembly	79
3.4.9.	Concept of Refueling Operations	80
3.5.	LMO Fuel Depots.....	82
3.5.1.	Introduction.....	82
3.5.2.	Design Specifications	84
3.5.3.	Refueling Schedule	86
3.5.4.	Refueling Operations.....	87
3.6.	μNet	88
3.6.1.	Overview	88
3.6.2.	Architecture.....	88
3.6.3.	Launch and Mission Planning	89
3.6.3.1.	Launch	89
3.6.3.2.	Mission Activities and Lifetime.....	89
3.6.3.3.	Flight Plan	89
3.6.3.4.	Destination	90
3.6.4.	Vehicle Layout	91
3.6.4.1.	Structure.....	91
3.6.4.2.	Propulsion System	91
3.6.4.3.	Power System	92
3.6.5.	Electronics	92
3.6.5.1.	Transponder and Antenna.....	92
3.6.5.2.	Link Budget.....	92

3.7.	“Iris” Earth-Mars Relay.....	93
3.7.1.	Overview	93
3.7.1.1.	Required Data Rates: Analysis and Comparison.....	93
3.7.1.2.	Possible Technologies.....	94
3.7.1.3.	Final Design Plan.....	94
3.7.2.	Launch Date & Flight Plan	94
3.7.2.1.	Mission Activities and Lifetime.....	96
3.7.3.	Vehicle Layout	96
3.7.3.1.	Structural Overview.....	96
3.7.3.2.	Propulsion.....	96
3.7.3.3.	Power	97
3.7.4.	Electronics	97
3.7.4.1.	Laser Comm System	97
3.7.4.2.	Ka Band Backup	97
3.7.4.3.	ELECTRA and Transponder	97
3.7.4.4.	Antenna	98
3.7.4.5.	Attitude Control System	98
4.	Phase III: Habitat Transport	98
4.1.	Introduction.....	98
4.2.	Habitat Entry, Descent, and Landing.....	99
4.2.1.	Cargo EDL Architecture	99
4.2.2.	Trajectory Design.....	101
4.2.3.	Inflatable Decelerator.....	103
4.2.4.	Attitude Control	104
4.2.5.	Propulsive Terminal Descent.....	109
4.2.6.	After Landing	109
4.2.7.	Cargo EDL Landing Structure	110
5.	Phase IV: Crew Transport.....	112
5.1.	Crew Selection	112
5.2.	Crew Transport Architecture	113
5.2.1.	Launch	113
5.2.2.	SpaceTrain	113
5.2.2.1.	Concept of Operations	113
5.2.2.2.	Propellant Mass Limits	114
5.3.	Crew Rotations	115
5.4.	Crew Transport Vehicle	116
5.4.1.	Structure and Structural Analysis	116
5.4.2.	Airlocks.....	119
5.4.3.	Power System.....	120
5.4.4.	Thermal Management.....	123
5.4.4.1.	Radiator Sizing.....	123
5.4.4.2.	Thermal Loop.....	124
5.4.4.3.	RCS Thermal	125
5.4.5.	Reaction Control System	127
5.4.5.1.	Moment of Intertia.....	127
5.4.5.2.	Thrust	127
5.4.6.	Interior Layouts	130

5.4.6.1.	Overview	130
5.4.6.2.	Habitability	133
5.4.6.3.	Sleeping Quarters	134
5.4.6.4.	Hygiene Facility.....	135
5.4.6.5.	Lavatory	137
5.4.6.6.	Dinner Table	137
5.4.6.7.	Exercise.....	138
5.4.6.8.	Control Center	138
5.4.7.	Life Support and Environmental Control System	138
5.4.7.1.	Food.....	138
5.4.7.2.	Atmosphere	140
5.4.7.3.	. Radiation Shielding.....	143
5.4.7.4.	Regenerative Human Waste System	148
5.4.8.	Avionics	152
5.4.9.	Crew Transport Vehicle Repair.....	163
5.4.10.	Crew Transport Vehicle Science Missions	168
5.4.10.1.	Martian Surface Virtual Reality Experiment	169
5.4.10.2.	Long-Duration Psychological Evaluations	169
5.4.10.3.	Astro Palate V2	170
5.4.10.4.	Mars Lighting Schedule Experiment	171
5.4.10.5.	E-Learning	172
5.4.10.6.	Product Shelf Life in Microgravity.....	173
5.4.10.7.	Astroseismology Experiment	173
5.4.10.8.	Chromosome-3 Experiment.....	174
5.4.11.	Leisure	174
5.4.12.	Mass and Volume Breakdowns	175
5.4.13.	CTV Payload - Restocking Logistics	176
5.4.14.	Risk Analysis	178
6.	Phase V: Mars Habitation.....	180
6.1.	Crew Entry, Descent, and Landing	180
6.1.1.	EDL/A Introduction.....	180
6.1.2.	EDL/A Vehicle	181
6.1.3.	EDL/A Crew Pod.....	183
6.1.4.	Ascent/Descent Vehicle Landing Structure	186
6.2.	Mobile Roving Settlement.....	189
6.2.1.	Magellan 2.1 Modifications.....	189
6.3.	Martian Resource Use	191
6.3.1.	Mars Miners	191
6.3.2.	Processing Plant	192
6.3.3.	Nitrogen Production.....	193
6.3.4.	Carbon Dioxide Freezers.....	194
6.4.	Habitat.....	198
6.4.1.	Structural Analysis	198
6.4.2.	Airlock Design	203
6.4.3.	Crew Module Layouts.....	214
6.4.4.	Food.....	220
6.4.4.1.	Climate Control.....	220

6.4.4.2.	Nutrition	220
6.4.4.3.	Crops.....	221
6.4.4.4.	Fish	222
6.4.4.5.	Spirulina.....	223
6.4.4.6.	Greenhouses.....	224
6.4.5.	Bioregenerative Systems	228
6.4.5.1.	Atmosphere Management	228
6.4.5.2.	Waste Cycle	229
6.4.5.3.	Anaerobic digestion.....	230
6.4.5.4.	Aerobic Digestion	230
6.4.5.5.	Soil	230
6.4.5.6.	Water Cycle	231
6.4.5.7.	Habitat Lighting	233
6.4.6.	Regolith Tunnels.....	235
6.4.7.	Habitat Power Requirements	241
6.4.8.	Solar Power	242
6.4.9.	Nuclear Power	248
6.4.10.	Habitat Power Management	255
6.4.11.	Habitat Thermal Control.....	259
6.4.12.	Habitat Avionics and Sensors	263
6.4.13.	Habitat Communications.....	264
6.4.14.	Habitat Emergency Preparedness	265
6.4.15.	Risk Analysis	266
6.4.16.	Habitat Mass and Volume Breakdowns.....	269
6.5.	Construction	270
6.5.1.	Overview	270
6.5.2.	Settlement Layout	271
6.5.3.	Construction Timeline	272
6.5.4.	Crane	276
6.5.4.1.	Crane Structure	276
6.5.4.2.	Communications and Avionics	279
6.5.4.3.	Propulsion and Power	280
6.5.4.4.	EDL Vehicle Egress.....	283
6.5.4.5.	Crane Deployment.....	284
6.5.4.6.	Crane Attachments.....	289
6.5.5.	Welding and Repair on Mars	293
7.	Earth Independence.....	295
7.1.	Settlement Expansion	295
7.2.	Science Missions	297
8.	Conclusion	298
8.1.	Budget and Costing Analysis.....	298
9.	Appendix A. Reference Information for Current Design.....	309
9.1.	Introduction.....	309
9.1.1.	Requirements	309
9.1.2.	Full Mission Architecture.....	318
9.2.	Phase I: Exploration	320

9.3.	Phase II: Resource Acquisition and Infrastructure Setup	323
9.3.1.	Miner	323
9.3.2.	Lunar Crew Consumables Mass and Volume Breakdown	325
9.4.	Phase IV: Crew Transport	327
9.4.1.	CTV Mass Breakdown	327
9.4.2.	CTV Resupply Mass and Volume Breakdown	332
9.5.	Phase V: Mars Habitation	335
9.5.1.	Martian Crane Auxilliary Drawings	335
9.5.2.	Nutrition and Diet	338
9.5.3.	Habitat Mass and Volume Breakdowns	344
9.6.	Phase VI: Earth Independence	348
9.6.1.	Costing	348
10.	Appendix B. Akin’s Law #3: The Iterative Design Process	349
10.1.	Phase I Iterations	349
10.1.1.	Mission Architecture Revisions	349
10.2.	Phase II Iterations	351
10.2.1.	Near-Earth Objects	351
10.2.2.	The Omega Relay	353
10.3.	Phase IV Iteration	353
10.3.1.	Crew Transport Concept of Operations	353
10.3.2.	CTV Crew Rotation	354
10.3.3.	CTV Mass Limitations with Falcon Heavy	356
10.3.4.	CTV Experiments	356
10.3.4.1.	Vaccine Development	356
10.3.4.2.	Near Earth Object Mapping	357
10.3.4.3.	Calorimetric Electron Telescope	357
10.4.	Phase 5 Iterations	358
10.4.1.	EDL Fuel Requirements without Refueling	358
10.4.2.	Methane Propulsion Fuel Requirements	358
10.4.3.	Habitat Garage Temperature	358
10.4.4.	The Atlas Martian Crane	359
10.4.5.	Habitat Module Structure	365
10.4.6.	Past Potential Power Sources	366
10.4.6.1.	Solar Thermal	366
10.4.6.2.	Wind Power	367
10.4.6.3.	Geothermal Power	369
10.4.6.4.	Nuclear Power Trade Studies	369
10.5.	Phase 6 Iterations	371
10.5.1.	Evolution of Mission Architecture Costing Strategy	371
10.5.2.	Mars Buggy Revisions	372
10.5.2.1.	Concept of Operations	372
10.5.2.2.	Similarities to Apollo Lunar Roving Vehicle	373
10.5.2.3.	Adjustments to Apollo LRV design	373
11.	Appendix C. MATLAB Code	374
11.1.	Phase I: Exploration	374
11.1.1.	DSx Aeroshell Ballistic Coefficients	374
11.1.2.	Orbital Dynamics Calculations	376

11.2. Phase II: Resource Acquisition and Infrastructure Setup	380
11.2.1. Magellan 2.0 Required Habitable Volume Curves	380
11.2.2. Magellan 2.0 Actual Habitable Volume	381
11.2.3. Solar Power on the Moon	381
11.2.4. Lunar Mining	382
11.2.5. Lunar Regolith Heating	383
11.2.6. Dimensions for Fuel Transport Vehicle Tanks	383
11.2.7. Dimensions for Fuel Transport Vehicle	385
11.2.8. Loads for Cylindrical Lunar Lander Vehicle	386
11.2.9. Dimensions for Moon Gas Station Tanks	388
11.2.10. Loads for Gas Stations	390
11.2.11. Dimensions for Mars Gas Station Tanks	392
11.2.12. Propellant Calculations with Multi-Stage Estimations	393
11.2.13. Payload Mass Calculations	394
11.2.14. EML1 RCS Design	396
11.2.15. Mass Ratio Analysis for EML1 Depot	397
11.2.16. EML1 Power Requirements	399
11.2.17. Propellant Required (CTV back to LEO with SLS Upper Stage)	400
11.2.18. LMO Propellant Required	401
11.3. Phase III: Habitat Transport	402
11.3.1. Parachute Sizing for EDL	402
11.4. Phase IV: Crew Transport	405
11.4.1. Inflatables Optimization – Falcon Heavy	405
11.4.2. CTV Required Habitable Volume Curves	407
11.4.3. Atmospheric Composition Trade Study	408
11.4.4. Mars Surface EVA Allocations as Determined by CTV Water Wall Thickness	409
11.4.5. Reliability Analysis on UPA and WPA Components	411
11.4.6. MLI Thermal Conductivity	411
11.4.7. RCS Actual Propellant	412
11.4.8. Thermal Analysis of Spacecraft to Mars	413
11.4.9. SpaceTrain (On SLS, Launch from LEO-L1 (refuel) - LMO)	414
11.5. Phase V: Mars Habitation	416
11.5.1. EDL/A with Refueling	416
11.5.2. EDL/A without Refueling	419
11.5.3. RCS Thruster Design for EDL/A Vehicle	421
11.5.4. EDL/A Critical Loads and Margin of Safety	422
11.5.5. Freon Pump Radiator and Power Sizing	424
11.5.6. Habitat Thermal	430
11.5.7. Garage Temperature	432
11.5.8. Martian Surface Pressurized Tank Sizing	434
11.5.9. Martian Surface Habitat Structural Optimization	435
11.5.10. Martian Surface Habitat Regolith Loads Analysis	439
11.5.11. Martian Surface Habitat Mass Estimation	441
11.5.12. Crew Food Optimization	442
11.5.13. Solar Power Analysis for Martian Surface Habitat	444
11.6. Auxiliary Trade Studies	447
11.6.1. CTV Inflatables Optimization for Ariane 5	447
11.6.2. CTV Inflatables Optimization for SLS	449

11.6.3.	Zeolite Pressure Swing Absorber for Martian Surface Habitat.....	453
11.6.4.	Solar Power at Alternate Landing Sites	454
11.6.5.	Solar Thermal Power Analysis for Martian Surface Habitat	457
11.6.6.	Feasibility of Wind Power Generation on the Martian Surface.....	458
11.6.7.	Methane-powered EDL/A Crew Vehicle.....	460
12.	Appendix D. Works Cited & References.....	463

1.2.2. List of Figures

Figure 1.	Mars 2020 Rover Instrumentation	25
Figure 2.	DSx Vehicle.....	26
Figure 3.	DSx Exploration Regions at Hellas Planitia. Image Credit: Google Earth ^[151]	27
Figure 4.	DSx vehicle landing locations in the Eastern Lowlands of Hellas Planitia. Image Credit: Google Earth ^[151]	28
Figure 5.	DSx vehicle landing locations in Terby Crater.	29
Figure 6.	DSx vehicle landing locations in the Eastern Highlands of Hellas Planitia	29
Figure 7.	Dsx Vehicle landing locations in McLaughlin Crater. Image Credit: Google Earth. ^[155]	31
Figure 8.	DSx vehicle encased in its aeroshell.....	32
Figure 9.	DSx probe internal layout and primary science package components.	34
Figure 10.	Geometry for a 90° spherical cap section	35
Figure 11.	Aeroshell diameter vs. total vehicle mass for constant ballistic coefficients	36
Figure 12.	Phobos/Deimos - Formation of Mars' Moons ^[4]	38
Figure 13.	Lunar Processing Plane (Tanks represent total volumes and do not reflect actual positioning).....	41
Figure 14.	Lunar Miner	42
Figure 15.	Miner Avionics Block Diagram	43
Figure 16.	Magellan Front View	46
Figure 17.	Magellan Rear View	47
Figure 18.	Magellan Mk2.0 Habitable Volume Curves.....	48
Figure 19.	Magellan Suitport View.....	49
Figure 20.	Initial Miner Delivery System	50
Figure 21.	“LUNOX” Delivery of a Pressurized Rover	51
Figure 22.	Preliminary Magellan Lander	52
Figure 23.	LUNOX Processing Plant Delivery Concept ^[266]	53
Figure 24.	Boeing Reusable Lunar Lander ^[82]	55
Figure 25.	MAX R: Propellant Massing for FTV	59
Figure 26.	MIN R: Propellant Massing for FTV	59
Figure 27.	FTV Inner Structure	61
Figure 28.	FTV Outer Structure.....	62
Figure 29.	FTV Centers of Gravity	63
Figure 30.	FTV Avionics Block Diagram.....	63
Figure 31.	Mass of Prop Left vs Mass PL, LEO-LLO-LMO	64
Figure 32.	Mass of Prop Left vs Mass PL, LEO-L1-LMO	65
Figure 33.	Mass of Prop Left vs Mass PL, LEO-LMO.....	66
Figure 34.	EML1 Fuel Depot Configuration	68
Figure 35.	Starting RCS Prop Mass vs Remaining Prop Mass.....	71
Figure 36.	Diagram of angled thruster nozzle.....	72
Figure 37.	P ratio vs Isp	73
Figure 38.	I _{sp} vs Mass Ratio	74

Figure 39. P ratio vs Exit Mach Number	74
Figure 40. Area ratio vs exit mach number.....	75
Figure 41. Isp vs Mass Flow Rate.....	76
Figure 42. Mdot vs Pump Power	77
Figure 43. Fuel Depot Avionics Block Diagram	77
Figure 44. Image of depot mid-construction, with smaller solar panels on LOX tank expanded.	79
Figure 45. Image of final depot configuration with heat shield and solar panels expanded.....	80
Figure 46. Refueling Con-Ops for typical launch window to Mars.....	81
Figure 47. Mass of fuel in EML1 depot over 5 year period, showing pattern of expected fuel levels for duration of mission.	82
Figure 48. Mass of prop left vs Mass of Start Prop, CTV	83
Figure 49. Starting RCS Propellant Mass vs. Remaining Propellant Mass, LMO	85
Figure 50. Nominal LMO Propellant Depot Fuel Masses 2038-2054	87
Figure 51. μ Net STK Coverage Model	88
Figure 52. μ Net Constellation.....	90
Figure 53. μ Net Vehicle Layout.....	91
Figure 54. STK visualization of phased Mars HEO orbits	95
Figure 55. Earth-Sun-Mars Conjunction and Relay Position	96
Figure 56. CEDL with aerodynamic decelerator deployed.....	100
Figure 57. CEDL Entry Overview	100
Figure 58. CEDL Entry Trajectory	102
Figure 59. Flight Path Parameters for CEDL.....	103
Figure 60. TRN Control Loop.....	105
Figure 61. Lift and Drag on the Cargo Descent Vehicle	106
Figure 62. RCS Thruster Arrangement.....	107
Figure 63. Attitude Control Loop	107
Figure 64. Propulsive Terminal Descent Precision.....	109
Figure 65. CEDL on surface of Mars awaiting cargo extraction	110
Figure 66. Cargo EDL Landing Gear.....	111
Figure 67. Cargo EDL Landing Strut Dimensions	111
Figure 68. Dragon: PL Mass vs Prop Mass	113
Figure 69. CTV Mass Limitations, SpaceTrain	115
Figure 70. CTV Habitable Volume.....	117
Figure 71. Airlock can contain two astronauts.	119
Figure 72. Solar Irradiance vs Distance	121
Figure 73. Specific Energy of Li-Ion Battery	122
Figure 74. Energy Denisty of Li-Ion Battery.....	122
Figure 75. Radiator Area vs Distance	124
Figure 76. Oxygen Boil-Off rate.....	126
Figure 77. Hydrogen Boil-Off	126
Figure 78. Thrust needed vs Maneuver Time (with Dragon)	128
Figure 79. Thrust needed vs Maneuver Time (without Dragon)	129
Figure 80. Upper level accommodations and spatial allocations.....	131
Figure 81. Lower level accommodations and spatial allocations.	132
Figure 82. Attic accommodations and spatial allocations.....	133
Figure 83. Isogrid Floor	134
Figure 84. Sleeping quarter with SPE shield indicated in yellow. Three views are presented: radial inward (left), top down (center), radial outward (right).	135
Figure 85. Hygiene facility with foot and hand restraints.....	136
Figure 86. Dinner table with knee restraints.	137

Figure 87. Seven cubic meters of food storage will be provided by a curved cabinet that is 2.3 m tall, has an outer radius of 2.835 m, inner radius of 2.185 m and spans 108 °.....	139
Figure 88. The experimental work space doubles as a galley.....	140
Figure 89. Prebreathe time with respect to atmospheric oxygen content for various partial pressures.....	141
Figure 90. Aluminum gas storage plate with oxygen (blue), nitrogen (yellow),.....	142
Figure 91. The lowest elevations of Mars may allow for as little as 10-12 REM per year. ^[43]	144
Figure 92. Water Wall Concept.....	145
Figure 93. Allowable weekly EVA hours for both nominal crews and the construction crew. Note that there are only 168 hours in a week. 55 year old men would remain within NCRP-132 limitations even without shielding.....	147
Figure 94. CTV ECLSS Loop.....	148
Figure 95. CO ₂ scrubbing mass over time.....	151
Figure 96. Aerospace Application of Multi-Gas Sensor ^[91]	153
Figure 97. JPL's ENose ^[92]	154
Figure 98. Radiation Assessment Detector (Similar to one aboard Curiosity Rover) ^[93]	155
Figure 99. Passive Dosimeters for Vehicle and Crew Use ^[94]	155
Figure 100. Control loop for GNC/ESP Systems.....	159
Figure 101. System block diagram for CTV avionics. Critical routes are denoted in red. Arrows indicate general data flow direction.....	160
Figure 102. TransHab's MMOD Structure ^[253]	164
Figure 103. Exploded view of the CTV layers (based on this technology of TransHab) ^{[227][250]}	165
Figure 104. Results of HVI test on full-size multi-shock shield for TransHab (Projectile:1.8 cm diameter Al2017T4 sphere, 5.8 km/s, 45 ⁰ impact) ^[250]	166
Figure 105. Caution and Warning System of CTV ^[251]	168
Figure 106. CTV Risk Matrix.....	180
Figure 107. Manned Descent Operation.....	183
Figure 108. Cut-Away View of the EDL/A Crew Vehicle.....	184
Figure 109. Horizontal Cut-Away View of the EDL/A Crew Vehicle.....	185
Figure 110. Exterior View of the EDL/A Crew Vehicle.....	185
Figure 111. Ascent/Descent Vehicle Landing Gear.....	187
Figure 112. Ascent/Descent Landing Strut Dimensions.....	188
Figure 113. PEM Fuel Cell.....	191
Figure 114. PEM electrolyzer.....	193
Figure 115. Nitrogen membrane generator.....	194
Figure 116. Sabatier Reactor, Electrolysis - Methane & Oxygen Production ^[15]	197
Figure 117. Surface Habitat Hall.....	198
Figure 118. Surface Habitat Hall Endcap Stress Analysis.....	199
Figure 119. Surface Habitat Hall Longitudinal Acceleration Stress Analysis.....	200
Figure 120. Surface Habitat Hall Regolith Stress Analysis.....	200
Figure 121. Surface Habitat Hub.....	201
Figure 122. Surface Habitat Hub Endcap Stress Analysis.....	201
Figure 123. Surface Habitat Hub Longitudinal Acceleration Stress Analysis.....	202
Figure 124. Surface Habitat Hub Lateral Acceleration Stress Analysis.....	202
Figure 125. Airlock Exterior View.....	203
Figure 126. Airlock Interior Cutaway View.....	204
Figure 127. Critical buckling as a function of the shell thickness and a half-meter separation between ribs.....	205
Figure 128. Internal Stress SolidWorks Analysis.....	206
Figure 129. Regolith Stress SolidWorks Analysis.....	207

Figure 130. Relative position of the airlock with respect to the hub and hall. This will result in varying depth distribution of regolith among the hub, hall, and airlock	209
Figure 131. Actual Regolith Distribution on the Airlock	210
Figure 132. Conservative Analysis for Regolith Distribution	210
Figure 133. Compressive stress as a function of θ	211
Figure 134. Compressive Stress on Airlock as a Function of θ	212
Figure 135. Compressive Stress on Hall as a Function of θ	213
Figure 136. Crew living quarters.....	214
Figure 137. Hall 1 and Hall 2 top level floor plans.....	215
Figure 138. Crew Hall 1 - Ground Floor	216
Figure 139. Crew Hall 2 - Ground Floor	217
Figure 140. Hub 1 - First Floor.....	218
Figure 141. Hub 1 - Second Floor.....	218
Figure 142. Hub 2 Bisectional Cut.....	219
Figure 143. Bottom Floor (left) and Top Floor (right)	225
Figure 144. Full Greenhouse Hall Assembly.....	226
Figure 145. Greenhouse Hub Layout.....	226
Figure 146. Full Greenhouse Hub Assembly.....	227
Figure 147. Block diagram of closed water cycle.....	231
Figure 148. The United States Energy Administration.....	235
Figure 149. Side-view of Martian habitat and regolith covering.....	236
Figure 150. Various habitat module failures and escape routes	237
Figure 151. Cargo hatch exit, suit port exit, and hallway modules.....	238
Figure 152. Interlocking design of tunnel section.....	239
Figure 153. Geometric properties of column cross section	241
Figure 154. Length of Day representative variables ^[158]	244
Figure 155. Hours of Sunlight on Mars	245
Figure 156. Power over a Summer Day.....	247
Figure 157. Reactor Without Berm.....	249
Figure 158. Labeled diagram of fuel assembly.....	250
Figure 159. Diagram of reactor module, labeled with dimensions.....	250
Figure 160. Reactor Module	254
Figure 161. Reactor With Berm.....	255
Figure 162. Power Path for Asimov City.....	256
Figure 163. LPC Components.....	257
Figure 164. LPC enclosure and radiators.....	258
Figure 165. FSP startup power profile.....	259
Figure 166. Diagram of Pumped Fluid Loop Using Bypass Control.....	261
Figure 167. Radiator Flow Fraction vs. Heat Load Fraction	262
Figure 168. Radiator Outlet Temperature vs. Heat Load Fraction	263
Figure 169. Wireless Network Schematic.....	265
Figure 170. Surface Habitat Risk Matrix	268
Figure 171. Settlement Layout.....	271
Figure 172. Hall extraction: (a) Crane attaching to hall (b) Crane lifting hall out of hub (c) Crane lowering hall to its bed	273
Figure 173. Crane prepared to transport modules from their EDL vehicle to the habitat	273
Figure 174. Stages of construction.....	275
Figure 175. Habitat at the end of Phase 5, fully completed with regolith radiation shielding.....	276
Figure 176. Crane Chassis (1).....	277
Figure 177. Crane's Area of Reach	277
Figure 178. Atlas Continous Track Rocker	278

Figure 179. Retracted Atlas Support Leg.....	278
Figure 180. Methane Boil-Off Rate	280
Figure 181. Atlas Payload Supports.....	282
Figure 182. Atlas Crane Inital Landing Configuration	283
Figure 183. Inital Deoployment of Atlas Crane.....	284
Figure 184. Atlas Support Bed Fully Deployed.....	284
Figure 185. Atlas Crane Fully Deployed	285
Figure 186. Boom Tower Being Raised.....	286
Figure 187. Boom Tower begins to deploy.....	287
Figure 188. Atlas Boom Tower Fully Deployed.....	288
Figure 189. Boom Arm Being Lowered	288
Figure 190. 2nd Half Of Boom Arm Being Lowered and Full Deployment.....	289
Figure 191. Atlas Two Cable System	290
Figure 192. Atlas Gondola	291
Figure 193. Atlas Extracting Crew From Their Decent Vehicle	292
Figure 194. Atlas Regolith Scoop.....	292
Figure 195. Atlas Regolith Counterweight Basket	293
Figure 196. Continous laser keyhole welding process for steel ^[256]	295
Figure 197. Spreading with Varying Cost Fractions.....	301
Figure 198. Mars Descent Vehicle Costing	302
Figure 199. Moon/Mars Miner Costing	302
Figure 200. Development, Productions, and Operations Costs Per Spacecraft	303
Figure 201. Yearly Cost with Various Overhead Factors	304
Figure 202. Cumulative Cost with Various Overhead Factors	305
Figure 203. Cumulative Cost for Different Architecture Strategies	306
Figure 204. Final Yearly Program Budget vs. Cost.....	307
Figure 205. Lunar Miner Truss Loads	323
Figure 206. Lunar Miner Truss Material Properties	324
Figure 207. Martian Crane Top View/Side View	335
Figure 208. Martian Boom Tower and Arm Top View	336
Figure 209. Martian Crane Chasis Top View	336
Figure 210. Martian Crane Truss Segment	337
Figure 211. Mass of Propellant Left vs. Mass of CTV	356
Figure 212. Garage Temperature vs. Time	359
Figure 213. Preliminary Surface Habitat Design	366
Figure 214. Wind Turbine Power Study 1	368
Figure 215. Wind Turbine Power Study 2	368
Figure 216. Previous Strategy Cost Division.....	372
Figure 217. Buggy.....	373

1.2.3. List of Tables

Table 1. Mission Requirements	20
Table 2. RASC-AL Requirements	21
Table 3. Rover Specifications Comparison Part 1	45
Table 4. Rover Specifications Comparison Part 2	45
Table 5. Pressurized Tank Volumes	48
Table 6. Required Mass and Volume Breakdown	56
Table 7. Consumables Resupply Mass and Volume Breakdown	57
Table 8. FTV Tank Dimensions.....	60
Table 9. FTV Tank Loads	60

Table 10. FTV Inner Structure.....	61
Table 11. Specifications of EML1 Fuel Depot.....	67
Table 12: Fuel Depot Dimensions	67
Table 13. Loads on Fuel Depot Tanks	68
Table 14: Intertank Dimensions and Loads	69
Table 15: Docking Truss Dimensions and Loadsg	69
Table 16. Trade study of cryogenic storage systems	70
Table 17. Power requirement breakdown for EML1 depot	78
Table 18. EML1 Fuel Depot Tank Dimensions.....	82
Table 19. LMO Fuel Depot Specifications	84
Table 20. Power Requirement Breakdown for each LMO depot	86
Table 21. μ Net Link Budget.....	93
Table 22. Mars Satellite Elements	95
Table 23. Mass Budget Estimations.....	101
Table 24. Martian Landing Ellipses.....	104
Table 25. Cargo EDL Critical Stress/Margin of Safety	112
Table 26. Crew Rotation Schedule and CTV Assignments	116
Table 27. Inflatable Sizing Optimization Output.....	118
Table 28. CTV Tank Stress Analysis.....	118
Table 29. CTV Power Breakdown.....	120
Table 30. Thruster Specifications	129
Table 31. Habitats will be designed to keep astronauts within the limits of.....	143
Table 32. Redundant parts list for UPA and WPA. “Quantity Old:” is purely a 360 day requirement based upon the life limits and has a reliability of 57%. “Quantity New:” increases low reliability component quantities to bring system reliability up to 90%. Parts list, MTBF, and Life Limit data taken from (Hanford, 2004).	150
Table 33. Mass/Volume/Power/Thermal Dissipation Breakdown	158
Table 34. Avionics Reliability	162
Table 35. Failure Modes and Risk Assessment	163
Table 36. Structural Mass Breakdown.....	175
Table 37. Equipment Mass/Volume Breakdown	176
Table 38. Recurring Mass/Volume Breakdown.....	176
Table 39. Short Expiration Time Mass and Volume Breakdown Summary	177
Table 40. Dragon Payload-to-CTV Logistics	178
Table 41. Ascent/Descent Vehicle Critical Stress Table	189
Table 42. Ascent/Descent Vehicle Margin of Safety.....	189
Table 43. Freezing Points of Martian Atmospheric Constituents ^[11]	196
Table 44. Dietary Requirements	220
Table 45. Rotational Diets	221
Table 46. Extra Dietary Information.....	222
Table 47. Fish Selection Process.....	223
Table 48. Greenhouse Growing Area	227
Table 49. Waste.....	229
Table 50. Anaerobic Digestion Waste	230
Table 51. Water utilized in each of the water cycle processes	233
Table 52. Lighting Power Requirements	235
Table 53. Table of loads on regolith tunnels.....	240
Table 54: 16.7 Hour Power Cycle.....	242
Table 55: 8 Hour Power Cycle.....	242
Table 56. Solar Panel Comparison ^[172-181]	248
Table 57. Table of Dimension Values	251

Table 58. FSP System Component Mass Distribution.....	251
Table 59. Habitat Radiator Design Parameters.....	261
Table 60. Equipment Mass and Volume Breakdown.....	269
Table 61. Consumables Mass and Volume Breakdown.....	270
Table 62. Internal Combustion Engine Specs.....	281
Table 63. The Thermo physical properties of Steel and Aluminum (Aluminum Silicate) ^[254]	294
Table 64. List of Metal Oxides from Martian Surface.....	296
Table 65. Importance of relying on in-situ Martian resources for future habitats construction.....	297
Table 66. SVLCM Model Parameters by Category.....	299
Table 67. Learning Curve Benefits for the Mars Habitat Hall Module.....	300
Table 68. Years with Minimal Cost Margin.....	307
Table 69. System Requirements (Level 2).....	310
Table 70. Sub-System Requirements.....	317
Table 71. Implemented Mission Architecture.....	320
Table 72. DSx Landing Coordinates in the Eastern Lowlands of Hellas Planitia.....	321
Table 73. DSx Landing Coordinates in Terby Crater of Hellas Planitia.....	321
Table 74. DSx Landing Coordinates in the Eastern Highlands of Hellas Planitia.....	322
Table 75. DSx Landing Coordinates in McLaughlin Crater.....	322
Table 76. Lunar Crew Consumables Mass and Volume Breakdown.....	326
Table 77. Lunar Crew Consumables Mass and Volume Breakdown.....	331
Table 78. CTV Resupply Mass and Volume Breakdown.....	334
Table 79. Diet 1.....	339
Table 80. Diet 2.....	340
Table 81. Diet 3.....	341
Table 82. Diet 4.....	342
Table 83. Diet 5.....	343
Table 84. Habitat Mass and Volume Breakdowns.....	347
Table 85. List of All Modeled Vehicles.....	349
Table 86. Mission Architecture Preceding the Final Revision.....	351
Table 87. Crew Rotation Schedule and CTV Assignments.....	355
Table 88. The Atlas Martian Crane Evolution.....	362
Table 89. Boom Arm and Tower Evolution.....	363
Table 90. Crane Attachments Evolution.....	365
Table 91. Nuclear Power Trade Studies.....	370
Table 92. Reactor Trade Study.....	370
Table 93. Small Modular Reactor Trade Study.....	371

1.2.4. Glossary of Acronyms

Acronym	Phrase	Brief Description
ACS	Attitude Control System	Controls pointing and stabilization (attitude) of a vehicle. Could be thrusters, reaction wheels, or control moment gyros.
BRLL	Boeing Reusable Lunar Lander	Vehicle developed by Boeing to carry astronauts to the lunar surface. Designed only
CEDL	Cargo Entry, Descent and Landing	EDL architecture for cargo

CH ₄	Methane	Hydrocarbon found on Mars
EDL/A	Entry, Descent, and Landing / Ascent	The process of entering a planetary atmosphere from space, descending through that atmosphere, and landing on the surface; can include ascent back through the atmosphere from the surface.
EML1	Earth-Moon Lagrange Point 1	A place between the Earth and the Moon where gravitational forces nearly cancel each other out, so spacecraft can 'hover' there with very little fuel expenditure
EVA	Extra-Vehicular Activity	Humans leaving the vehicle to spacewalk or to traverse the surface of a body
FCC	Flight Control Computer	Main computer for a space vehicle
FCTV	Crew Transport Vehicle	Vehicle that carries crew from LEO to LMO and back
FTV	Fuel Transport Vehicle	Vehicle that carries LOX and LH ₂ from the moon to the EML1 fuel depot
GNC	Guidance, Navigation, & Control	System that manages steering, location, and sending actuator commands for a vehicle
HEO	Heliocentric Orbit	An orbit about the sun
HPSC	High Performance Spaceflight Computing	A NASA initiative to develop an FCC
HUD	Heads-Up Display	Display overlaying a viewscreen to provide additional information
IMU	Inertial Measurement Unit	A sensor that uses accelerometers and inertia to determine how much it has moved.
ISRU	In-Situ Resource Utilization	The concept of using local resources in place
LEO	Low Earth Orbit	Orbit around Earth that takes the least energy to get to; usually between 200 and 400 km.
LH ₂	Liquid Hydrogen	Hydrogen (H ₂) in liquid state
LLO	Low Lunar Orbit	Orbit close to the lunar surface
LM	Lunar Module	The vehicle that carried that Apollo astronauts to the lunar surface
LMO	Low Martian Orbit	Orbit close to the Martian surface

LOX	Liquid Oxygen	Oxygen (O ₂) in liquid state
MSL	Mars Science Laboratory	Large science rover that landed on Mars in August 2012
RCS	Reaction Control System	An ACS that uses thrusters
SLS	Space Launch System	NASA's new heavy-lift launch vehicle; still in development
TRL	Technology Readiness Level	NASA standards for how ready a technology is to be used. TRL-1 means purely theoretical; TRL-9 means currently used in flight
TRN	Terrain Relative Navigation	A vehicle locating itself relative to local landmarks based on knowledge of terrain
ZBO	Zero Boil-Off	Technology that insulates a pressure vessel in space sufficiently that no liquid is heated and needs to be vented ("boils off")

1.3. Program Introduction

1.3.1. RASC-AL Program

RASC-AL (Revolutionary Aerospace Systems Concepts – Academic Linkage) is series of student design competitions sponsored by NASA and the National Institute of Aerospace. Every year, RASC-AL releases a series of “themes,” or goals, for students. The University of Maryland ENAE484 class participated in RASC-AL’s Earth Independent Mars Pioneering Architecture theme, which is presented below:

Given a 40 year timespan starting in 2014, and a flat total NASA budget of \$16 Billion a year, derive an architecture that has 24 people continuously living on the surface of Mars. The pioneers on Mars are totally self-sufficient at year 40, with no supplies of any sort except an every other year crew rotation (4 up and 4 down) sent from Earth. The architecture will convey a series of missions (campaign) over the 40 year period that shows the gradual build-up of capabilities, infrastructure and risk reduction. All existing NASA programs will continue with some reduction in annual funding allowed (maintain at least 80% of their current budget) but the total NASA budget will remain flat, adjusting for inflation.

Two exceptions are:

- The International Space Station which will be fully funded to 2024; and
- The Space Launch System and Orion which will be developed and operational through 2035 at their current budgets.

After these points in time, the programs’ budgets can be reduced by any level and applied towards other areas of human exploration.

The lunar surface, asteroids, Mars moons and the Mars surface can be leveraged for In-situ Resource Utilization (ISRU), and all systems must be reusable wherever practical.

All systems required to enable this architecture must be accounted for with respect to the budget. This includes development of new technologies and infrastructure necessary to enable ISRU, and transportation of those ISRU assets. The campaign should be structured so that there is a cadence of significant human activities and missions beyond low Earth Orbit.^[253]

1.3.2. Mission Statement

Our mission statement, developed by Dr. David Akin, is to: “Develop an evolutionary series of technologies and missions within current and projected space exploration budgets that will result in at least 24 people living on Mars independent of Earth by the year 2054.”

1.3.3. Requirements

Mission Requirements (Level 1)

This first level of requirements is derived from the mission statement and those requirements set forth by RASC-AL itself. They include themes and requirements seen throughout the mission and those seen in only one or a few phases. The first three requirements are the most important. The first requirement could be seen as a restatement of the original mission statement, but it helps keeps all lower level requirements focused on the overall goal. The second requirement refers to the overall budget requirement, which is one of the largest limiting factors of the mission. The third refers to the TRL levels of technology, a requirement set forth by RASC-AL. Each of the other requirements covers themes such as resource acquisition, transportation, and communication.

	Mission Requirements (Level 1)	Source
M1	Shall be able to sustainably support 24 people on Martian surface by 2054 with the capability of expansion	Mission Statement
M2	Shall be funded with flat NASA budget as defined by FY 2016 request	
M3	Shall only use technology at TRL 5 or higher, or be capable of raising up TRL 3 and 4 technology through appropriate research time and funding	
M4	Shall be able to transfer crew and cargo between Earth, Mars, and other extraterrestrial locations	
M5	Shall acquire, process, and use resources obtained from extraterrestrial sources	

M6	Shall provide In-Situ Resource Utilization (ISRU) and reusable systems on Martian surface	
M7	Shall be able to support communication with Earth and other extraterrestrial sources	
M8	Shall develop in space refueling capabilities	

Table 1. Mission Requirements

System Requirements (Level 2)

The majority of the level two requirements talk about the development of technologies used throughout the mission. Very few of the vehicles, habitats, or complexes used during the mission have already been developed. All of the technologies needed are represented within the level two requirements. Other requirements at this level include determining a final Martian surface landing site as well as resource availability on Earth’s moon, Mar’s moons, and the Martian surface, and dates of when mining operations should begin to take place. The System requirements can be seen in full in Appendix A.

Sub-System Requirements (Level 3)

Within the third level of requirements, the majority of the requirements are date requirements. Dates of when development needs to end, components must be launched, when construction must be started and completed. A major component of the mission is the time restraint place on it by the mission statement, that the mission must be completed by 2054. Most of the components of the mission are reliant on other previously completed and implemented components. Any failure or pushed back date will not only impact every component that follows from it, but risk failing to complete the mission by 2054. Every date requirement must be planned so that not only will the mission finish on time, but consider certain outside factors such as budget constraints. The Sub-System requirements can be seen in full in Appendix A.

1.3.4. RASC-AL Requirements

	RASC-AL Requirements	Source
RA1	Mission shall be completed by the year 2054 with a crew of at least 24 people living on the surface of Mars independent of support from the earth	NASA RASC-AL Program
RA2	Earth shall only support a rotation of 4 crew members every two years, or once per launch window	
RA3	Mission shall be funded using a budget as defined by NASA’s fiscal year 2016 budget request, and more specifically for the team, the Space Exploration budget	
RA4	Shall pay for the projected amount allocated to Commercial Spaceflight within Space Exploration budget until it is phased out	

	by Fiscal Year 2020
RA5	Shall fund SLS and Orion programs at their full operational budget of \$3 billion per year through Fiscal Year 2035
RA6	International Space Station shall be fully funded until 2024, after which funding may be reallocated by any amount up to its full budget
RA7	Shall have ability to reallocate funds from all other NASA departments as long as those other departments retain at least 80% of their base budget
RA8	All money shall be represented in 2015 dollars and inflation shall be built into the internal budget structure
RA9	Shall receive one SLS rocket and Orion capsule per year from Fiscal Years 2021-2025
RA10	Shall receive two SLS rockets and Orion capsules per year from Fiscal Years 2026-2035
RA11	Shall be able to use resources collected and processed from the Earth's moon, asteroids, the moons of Mars, and the Martian surface
RA12	Any technology used in the mission shall be at least Technology Readiness Level, or TRL, 5. TRL 3 or 4 technologies that can be raised to TRL 5 through appropriate levels of funding and development time shall also be used
RA13	Shall conduct majority of mission operations beyond Low Earth Orbit

Table 2. RASC-AL Requirements

1.3.5. Program Architecture Overview

The name Asimov City was chosen in honor of the science fiction author's story "The Martian Way," in which a settlement on Mars is cut off from Earth but survives due to the astronaut's resilience and ability to support themselves locally. Because the RASC-AL settlement's end goal is independence from Earth, it must support itself from local Martian resources.

Program architecture up until 2054 is divided into five main phases: exploration; resource acquisition and infrastructure setup; habitat transport; crew transport; and Mars habitation. Beyond 2054, the settlement is independent from Earth other than crew rotations at every available launch window. It was assumed that replacement crews from Earth had the resources to launch themselves to low Earth orbit; the Asimov City program does not have to provide Earth launch capability after 2054.

In Phase I, Exploration, missions are sent to the Moon, Mars, and Mars' moons Phobos and Deimos. The goal of this Phase is to determine the type, location, and quantity of available resources and to identify the specific location for the settlement.

In Phase II, Resource Acquisition and Infrastructure Setup, facilities are built to exploit and processes these resources and to enable later mission architecture. Specifically, mining facilities will be built on the

Moon to harvest water, which will be processed into propellants and transferred to fuel depots at the Earth-Moon Lagrange point 1 (EML1) and in lower Martian orbit. In-space refueling allows for heavier payloads to Mars. Spacecraft will be launched for high data rate Earth-Mars communication and fast local Mars communication. By the end of Phase II, the program will have assets on the Moon, at EML1, in heliocentric orbits, and in Martian orbit.

In Phase III, Habitat Transport, habitat components and equipment will be transported to the Martian surface. This includes the structures for the habitat, crew surface vehicles, autonomous construction vehicles, a resource processing plant, and solar panels and nuclear reactors to supply power. This phase requires in-space refueling to move all payloads from Earth to Mars during the time of mandated SLS use.

During Phase IV, Crew Transport, crew will be transported from Earth's surface to the Martian surface. Each crew of four will launch from Earth on a SpaceX Falcon 9 rocket and dock their Dragon spacecraft with an SLS upper stage and with another Falcon 9 carrying an inflatable deep-space vehicle. Transit to Mars will take approximately 180 days. After arriving at Mars, crew will transfer to a reusable powered descent/ascent vehicle, which will take them through the atmosphere to the surface.

Phase V, Mars Habitation, begins when the first crew arrives on the surface. Astronauts will construct the modular surface habitat, set up power systems and resource-gathering infrastructure, and begin growing their own food. This phase continues as more crews arrive on the surface, and ends at 2054 when the settlement becomes independent from Earth.

The full mission architecture can be found in Appendix A.

2. Phase I: Exploration

2.1. Phase Overview

The first phase of the mission will involve the exploration of the lunar south pole, three possible Martian landing sites, as well as the investigation of Phobos and Deimos. JPL's Lunar Flashlight mission will explore the lunar south pole in search of high concentrations of water in the year 2017. Following this mission, Mars 2020 and the DSx missions will explore Hellas Planitia, McLaughlin Crater, and Arsia Mons on the Martian surface to determine an ideal settlement site in the year 2020. Finally, in the year 2029 Phobos and Deimos will be explored by the PADME mission to determine what resources, if any, can be retrieved from the Martian moons.

The lunar exploration mission will be critical for the future plans to refuel using fuel found on the lunar surface. Determining the highest concentrations of water on the lunar surface will allow for more efficient mining and solidify the predicted amount of fuel able to be mined per year. The lunar flashlight mission will also allow for an optimal mining site to be determined by the year 2019 so that mining and eventually refueling can begin as scheduled. This mission will also provide data about the composition of lunar regolith for potential future science missions that could provide a better understanding of the lunar surface.

Mars 2020 and the DSx missions will provide a detailed mapping of the potential landing sites and determine which site is ideal for sustaining human life. Criteria for determining an appropriate settlement site include the availability of water and resources for construction, temperature and other weather, and

radiation levels. The exploratory missions will have science packages to collect data on each of these criteria so that an optimal landing location can be chosen.

Hellas Planitia, the primary candidate for settlement, was selected as a possibility for several reasons. It has minimal radiation exposure as well as between 8 and 12 hours of sunlight per day. The site is relatively flat and is predicted to have subsurface water available. It also contains geological advantages in the construction resources likely to be found within the regolith. The size of the site allows for large scale landing and it was proposed as a MSL landing location. McLaughlin Crater, the secondary landing location and Arsia Mons, the tertiary landing location, were selected as potential candidates for their relatively low radiation levels and potential for subsurface water acquisition.

Phobos and Deimos will be explored by the Phobos And Deimos & Mars Environment (PADME) mission. This mission will determine the feasibility of using the Martian moons for in-situ resource acquisition and will also collect data to enhance the knowledge base on early solar system formation.

The two primary theories for the existence of the Martian moons are the Giant Impact theory and Captured Asteroid theory. The Giant Impact theory poses that a huge collision with the Martian surface launched surface matter from the planet that then coalesced into two moons. This would imply that the moons would be comprised of Mars surface regolith and mining them would not be cost efficient since similar resources could be obtained more easily on the surface of Mars itself. If the Captured Asteroid theory is correct then Phobos and Deimos are captured Carbonaceous C type asteroids picked up by the Martian gravity well.RJB1 If this is the case, then the moons would likely contain Hydrogen and Helium and maybe water. This would imply that mining for fuel could be valuable for EDL refueling.

2.2. Lunar Exploration

The Lunar Flashlight Mission begins in the year 2017 when it is launched aboard the auxiliary flight of the SLS in a Block 1 launch vehicle. The satellite weighs 14 kg and pre sail deployment is 60x10x10cm and 80m² post deployment. The program will cost \$210K which funds a primary mission duration of 2 years.

The satellite reflects 50kw of sunlight off the solar sail to the lunar surface in a 1deg beam. Some of the light diffused is reflected off the lunar surface into a spectrometer aperture which distinguishes volatile ice from the regolith illuminated. The mission will use multiple lunar gravity assists to achieve lunar capture and employ attitude control with the solar sail.RJB2 This mission will be the first attempt at sending a CubeSat to the Moon and will also demonstrate reflecting sunlight using a solar sail for observation.

The Lunar Flashlight avionics package will contain a CubeSat and DSN compatible transponder in order to address the need to have a low mass, low power, and low cost radio that can support Navigation. It will also have the First Iris prototype operating at 8.4/7.2 GHz. The avionics use a PC 104 stack with exciter, receiver, and power supply boards.RJB2 The IRIS provides a downlink rate of 20 kbps at the lunar distance and requires a 10 W DC input.

The data acquired by the this mission will provide a detailed mapping of the availability of water ice on the south pole of the moon. The primary mining location, Shackleton Crater will be examined along with Shoemaker crater, the secondary mining location. The information gathered will solidify the decision to mine in Shackleton crater when it shows what concentration of lunar water is located within the crater. The mission will also provide background information on how volatiles interact with the lunar

surface.RJB3 This will provide further information on the potential for extracting and using the Moon's resources.

2.3. Mars Exploration

2.3.1. Mars 2020

Already scheduled for launch aboard an Atlas 5 in July of 2020, the Mars 2020 rover's initial mission plan had been set before the team acquired this project. The main objectives, as obtained from NASA's Mars 2020 mission pages, are to look for signs of ancient microbial life as well as to fulfill several Strategic Knowledge Gaps prior to human arrival. Chief among these are the demonstration of propellant and Oxygen production from the Martian atmosphere, characterizing atmospheric dust size for its implications in surface instrumentation, and the conduction of surface weather measurements for improving current atmospheric models.

While the specific science packages have already been selected and the Mars 2020 rover designed, NASA has yet to establish a desired landing location. NASA's plan for location selection was to hold Landing Site Workshops later in 2015 for scientists and engineers to pitch their locations.^[113] In the interests of exploring the region where Asimov City will be founded, the team deemed it necessary to select our own landing zone within Hellas Planitia. The main constraint in determining an appropriate landing zone within Hellas Planitia is finding a flat region large enough to contain the mission's projected 18 by 14km landing ellipse.^[114] With a radius of around 100km of flat land surrounding the site at 35°S 95°E, this is the ideal landing location for the first rover to begin the exploration of Hellas Planitia.

Once in the desired landing zone, the Mars 2020 will rely on the use of seven different scientific instruments to conduct the research necessary to fulfill the strategic knowledge gaps identified above. Of these eight instruments, four will focus specifically on determining the mineralogy on the surface of Mars. The Mastcam-Z, a panoramic camera capable of a 3x zoom, will be able to take images in both RGB and visible/near infrared (VNIR). Its images will be used to perform surface mineralogy, specifically for hydrated minerals.^[114] Another instrument, the SuperCam will use Laser-Induced Breakdown Spectroscopy to conduct chemical composition analysis on regolith from up to 20 feet away. The Planetary Instrument for X-ray Lithochemistry (PIXL) will be placed on the rover's arm and rely on X-ray fluorescence spectroscopy to determine more fine scale chemical composition analysis on a specific target spot.^[115]

The last mineralogy instrument selected for the Mars 2020 mission is the Scanning Habitable Environments with Raman & Luminescence for Organics and Chemicals (SHERLOC). This instrument will use UV spectroscopy to detect carbon molecules and organic compounds on a finer scale and create a chemical map of the area around the rover.^[116]

The next instrument, the Mars Oxygen ISRU Experiment, seeks to directly fulfill one of the identified strategic knowledge gaps. This instrument will serve as a reverse fuel cell, using electrical energy to convert the abundant atmospheric CO₂ into O₂ which is critical for establishing a sustainable human settlement on Mars.^[117]

The next instrument, the Mars Environmental Dynamics Analyzer (MEDA), will also be used to fulfill one of the strategic knowledge gaps. By measuring temperature, pressure, relative humidity, and the size

of the dust, MEDA will provide a more complete Martian weather profile, allowing for improvements in current atmospheric model. ^[118]

Another critical instrument, the Radar Imager for Mars Subsurface Exploration (RIMFAX), will use ground-penetrating radar to determine composition profiles upwards of 10 meters below the Martian surface. This instrument will work by tracking Frequency Modulated Continuous Wave patterns to determine composition at different levels beneath the surface. It will specifically be used in the search for the presence of subsurface ice or liquid water. ^[119]

All of these instruments described are shown with their places on the Mars 2020 rover in the graphic below.

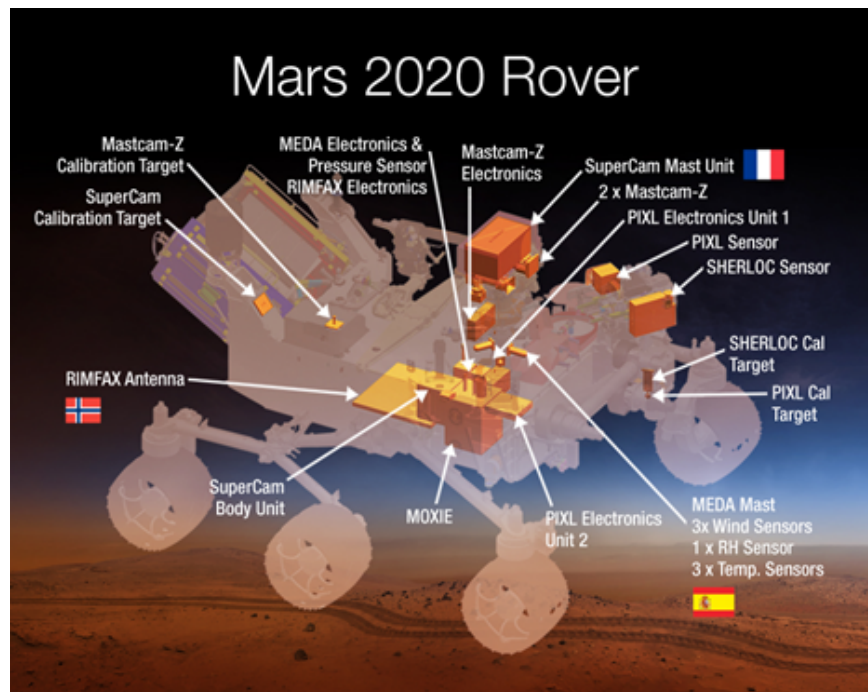


Figure 1. Mars 2020 Rover Instrumentation

2.3.2. DSx Missions

2.3.2.1. Mission Overview

The DSx mission is based on the Deep Space 2 mission launched by JPL in 1999. ^[137] The mission included two miniature space probes, which would penetrate the surface of Mars and collect soil samples. Unfortunately, the mission was deemed unsuccessful due to communication failure shortly after the vehicles descended to the Martian surface. ^[136] The DSx will utilize similar techniques on a larger scale and with some modification in order to explore two potential settlement regions on the Martian surface.



Figure 2. DSx Vehicle

The primary science goal of the DSx mission is to explore the geological area of primary and secondary settlement locations, determine material and water availability in these regions, test communication capabilities at low altitudes on Mars, and select an official settlement site by 2022. Selection criteria for these locations also required:

1. Minimal radiation exposure of 13 rem/year,
2. 8-12 hours of sunlight exposure,
3. Overall flatness of land,
4. Possible subsurface water or ice,
5. Reasonable weather conditions (minimal dust storms)
6. Presence of other geological benefits such as mineral availability,
7. Potential for meaningful science missions, and
8. Large-scale landing capability.

2.3.2.2. Primary Mission: Hellas Planitia

The primary settlement region, Hellas Planitia, is located in Mars' southern hemisphere, centered at 42.43° S and 70.50° E, and has a diameter of about 2300 km, according to the Gazetteer of Planetary Nomenclature. ^[142] Hellas Planitia is one of the solar system's largest impact craters and is the location of Mars' lowest elevations. ^[145] The DSx mission will explore three regions within Hellas Planitia: (1) Eastern Lowlands, (2) Terby Crater, and (3) Eastern Highlands, as shown in Figure 3. The Eastern Lowland region is the primary settlement location with Terby Crater and the Eastern Highlands representing the secondary and tertiary settlement locations, respectively.

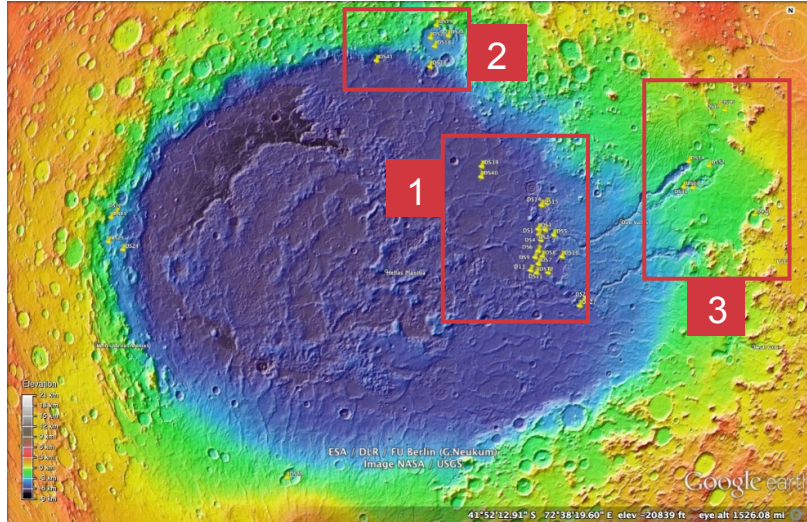


Figure 3. DSx Exploration Regions at Hellas Planitia. Image Credit: Google Earth ^[151]

Eastern Lowlands

The Eastern Lowlands are located on the eastern edge of Hellas Planitia, at the bottom of Dao Vallis and Harmakhis Vallis, and serves as the primary settlement location within Hellas Planitia and for the mission, overall. The Eastern Lowlands consists of large plains with little change in elevation. The region contains some geological features that could act as obstacles; however, these features are widely spread throughout the region and do not propose substantial threats to the settlement given its, relatively, small scale.

The Eastern Lowlands is located at an elevation of approximately -6km ^[151] and experiences temperatures ranging between -96°C to -35°C , or 177K to 238K ^[149] and radiation dosages of between 11 and 12 rem/year. ^[141] Research also suggests that regions of Hellas Planitia once held an abundance of water in the form of giant lakes and even oceans. ^[146]

Nineteen DSx vehicles will be sent to the Eastern Lowlands of Hellas Planitia, primarily in search of water, but also to test the additional science goals previously mentioned. The DSx vehicles will span 630km ; however, twelve vehicles will be concentrated to an 85km span of area, which demonstrates the most promising characteristics for a settlement location. These vehicles are highlighted in red in Figure 4. This region is located at the base of Niger Vallis and Dao Vallis, which is believed to have been formed by large volumes of water or by the collapse of plateau materials. ^[147] In either case, there is great potential for unique and possibly valuable geological features at the base of this region.

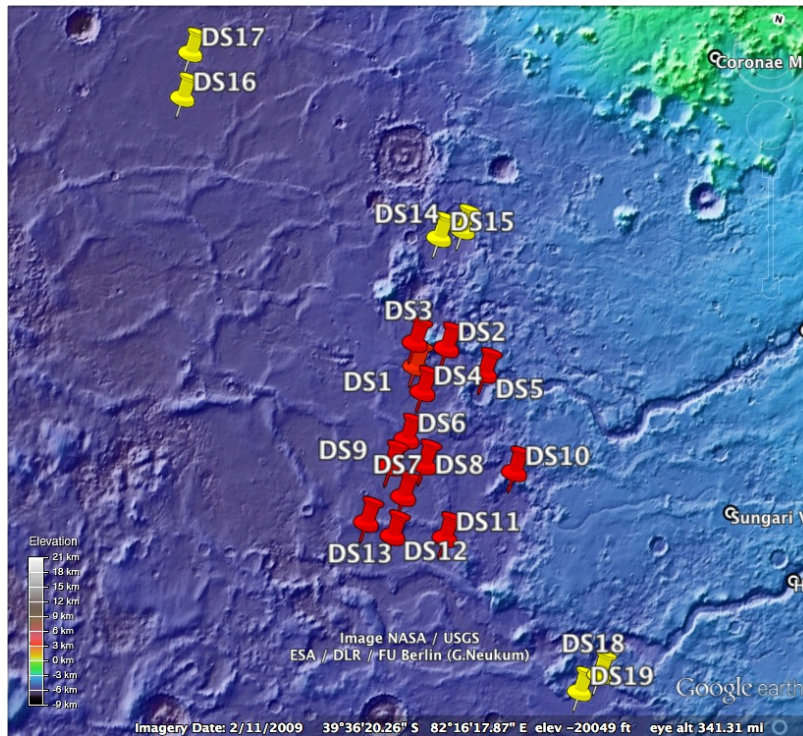


Figure 4. DSx vehicle landing locations in the Eastern Lowlands of Hellas Planitia. Image Credit: Google Earth^[151]

The Eastern Lowlands will host the largest number of DSx vehicles given that it is the primary settlement location prior to receiving data from the exploration missions. A large concentration of DSx vehicles was critical for the success of the mission in the region and, specifically, to ensure that mission scientists and engineers have an accurate and complete understand of the geological conditions of this region before finalizing a settlement location. Furthermore, the dense distribution of vehicles in the Eastern Lowlands ensures that, in the event that one or a few vehicles are unable to perform or relay information, a representative dataset can still be collected from the remaining DSx vehicles in order to gain an accurate representation of the conditions.

Terby Crater

The secondary settlement location, Terby Crater, is a 165km wide impact crater located on the northern edge of the Hellas Planitia impact basin, as shown in Figure 3.^[147] Although Terby Crater is located at a high elevation than the Eastern Lowlands and subsequently experiences high radiation dosages of about 11 rem/year,^[141] it offers a large region of flat planes on which to construct a settlement. Because the crater was also formed from impact of an asteroid, it likely contains additional nonnative minerals that might not be available in other regions of Mars.^[147] According to the European Space Agency, valleys in this crater exhibit channels formed by running liquid.^[138] Terby Crater is of interest for exploration because of its possible history of water and rich geological environment. Due to its increased elevation of about -3km, radiation becomes a heightened concern. For this reason, we will also send two vehicles to explore lower elevations of Hellas Planitia that are still near Terby Crater. A total of six DSx vehicles spanning 280km will be sent to this region, with four vehicles concentrating on a 85km area inside the impact basin as shown in Figure 5.

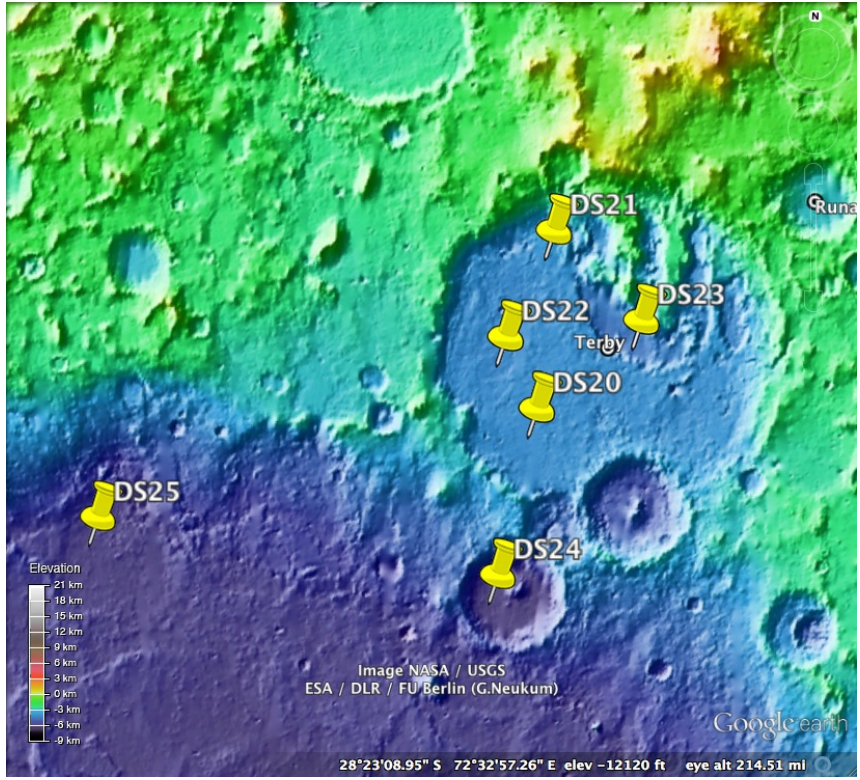


Figure 5. DSx vehicle landing locations in Terby Crater.
Image Credit: Google Earth.^[153]

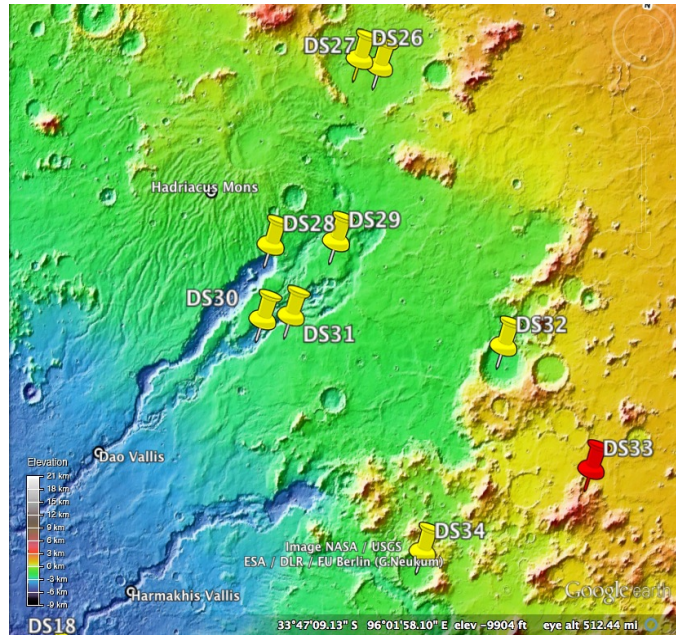


Figure 6. DSx vehicle landing locations in the Eastern Highlands of Hellas Planitia.
Image Credit: Google Images.^[152]

Eastern Highlands

The Eastern Highlands, the tertiary settlement location, is located on the eastern outer edge of the Hellas Planitia impact basin at an elevation of between -2 km and 0 km ^[152]. Because this region is at much higher elevation than the other regions of interest, radiation exposure can be as high as 14 rem/year ^[141]. Although this exceeds settlement location requirements, the Eastern Highlands offers great geological variety, which could be beneficial to resource acquisition and science missions in the event that the primary and secondary settlement locations are deemed uninhabitable.

Nine DSx vehicles will span 690km of this region to study the various geological regions. Of particular interest a region referred to as Three Craters. In 2008, the Mars Reconnaissance Orbiter (MRO) identified concealed glaciers in this region ^[148]. Because water is vital to crew survival and settlement sustainability, Three Craters will become the final settlement location in the event that water is not found at the other two sites. DS33, shown in red on Figure 6, will be sent to this region to more explicitly determine ice concentration. Other regions such as Savich Crater, Niger Vallis, and Sebec Crater will also host DSx missions in order to gain a better understanding of each region and the diverse geography of the Eastern Lowlands.

2.3.2.3. Secondary Mission: McLaughlin Crater

The secondary geographical settlement location, McLaughlin Crater, is centered at 22.13° N and 22.37° W. ^[140] Although this region experiences an elevated radiation dosage of approximately 14 to 15 rem/year, ^[141] NASA studies indicate that the Martian crater may have once held a groundwater-fed lake. ^[139] Rocks on the floor of the crater “show sedimentary rocks that contain spectroscopic evidence for minerals formed through interaction with water.” ^[139] Therefore, the region might still contain areas of surface water. Because of the undesirable radiation levels in this region, McLaughlin Crater will be the secondary settlement region in the event that all three regions at Hellas Planitia are deemed undesirable for settlement.

Three DSx vehicles will be sent to McLaughlin’s crater, primarily in search of water. These vehicles will span a 40 km area to explore the northern, midwestern and southeastern regions of the crater, as shown in Figure 7.

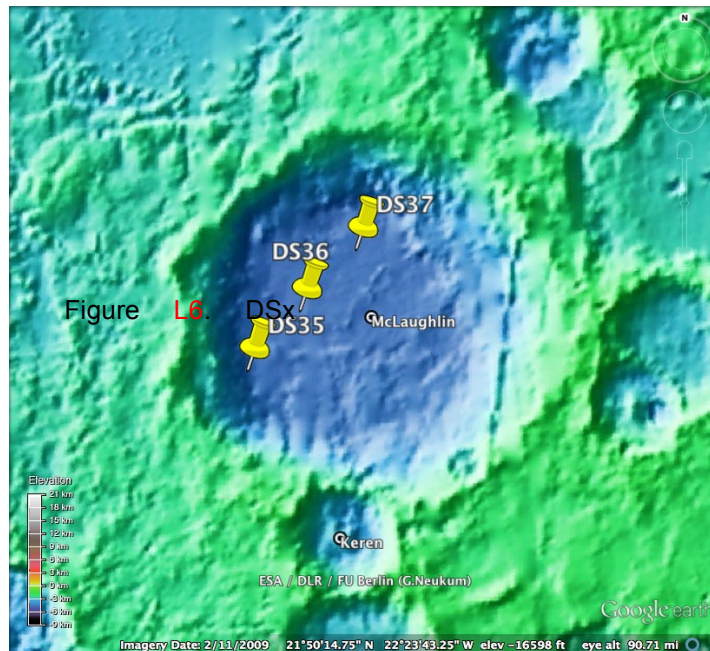


Figure 7. Dsx Vehicle landing locations in McLaughlin Crater. Image Credit: Google Earth. ^[155]

DSx vehicle landing coordinates for all regions can be found in Appendix A1.

2.3.2.4. Concept of Operation

All DSx vehicles will depart for the Martian surface aboard an Atlas V in July 2020 along with the Mars 2020 science rover. The Atlas V will launch from Cape Canaveral, Florida ^[143] and perform a trajectory toward Mars requiring a Δv of 6.6 m/s. The DSx vehicles will arrive at LMO in January 2021, with 1.57 tons of fuel remaining, at which time the Atlas V will jettison its fairing, leaving the DSx holding structure exposed. Each DSx vehicle will be autonomously released from the support structure at different intervals to ensure that the vehicles land within close proximity to their intended landing site. An inclination change at LMO is required to reorient the Centaur, Atlas V second stage, so that the final three DSx vehicles will land in McLaughlin crater in the northern hemisphere. All vehicles will power-up three minutes prior to its release of the first DSx vehicle.

Each DSx vehicle is encased in its own ceramic aeroshell, which will act as the vehicles' Entry, Decent, and Landing (EDL) system. Each aeroshell is an ultralow ballistic coefficient design, which will protect the vehicle from atmospheric heating upon descent and will also break upon impact with the Martian surface, exposing the each DSx to the regolith. Similar to the Deep Space 2 mission, each DSx will host an internal probe that will, upon impact, penetrate the Martian surface up to 1 meter, depending upon soil conditions in its designated region. ^[144] The probe and the main body of the DSx will be connected via flexible cable, similar to the design of the Deep Space 2 ^[136]. The probe will host the primary science package. The central science components are the regolith sample and water sampling experiment. Similar to the Deep Space 2 mission, the sample collector will collect 0.1 g samples of regolith from about 1 meter below the surface using a small drill on the side upper side of the probe. ^[144] Small samples of regolith collected in the drill will drop into a heating cup located below the drill, which closes after the

sample is inserted ^[144]. The water sample experiment will heat the sample, directing any water vapor into a contained chamber where the contents of water vapor is determined by measuring the “difference in light intensity of a laser shining through the vapor.” ^[144] The experiment will continue to heat the regolith sample in increments of 10 K for one hour and will record the water vapor in the contained chamber at each interval. ^[137] Once this process is complete, the sample collector will collect another sample of regolith and repeat the process until the vehicle’s battery dies. This is expected to be approximately two or three Martian days.

All data will be sent back to Earth for analysis. Results for each region will be extrapolated and compared relatively. This data was support the final settlement location decision to which all habitat materials and crew will be sent.

2.3.2.5. Vehicle Overview and Science Package

The DSx vehicles’ design is based on the Deep Space 2 vehicle design, with some modification. This approach allows improvements to be made to the original design while still benefiting from a learning curve in the design and assembly of the vehicles.

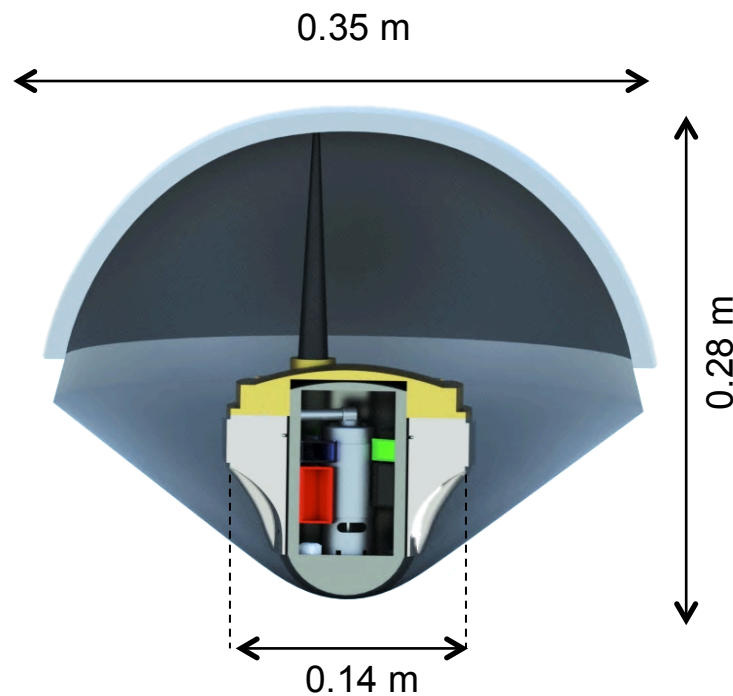


Figure 8. DSx vehicle encased in its aeroshell

The DSx is slightly larger than the Deep Space 2 design, which is due to the use of a slightly longer antenna. The DSx has a height of 250 mm and its largest diameter is 140 mm. The probe located inside of

the DSx, shown in Figure 8, has a diameter of 35 mm and a height of 105 mm. Each vehicle weighs 4.5 kg, including the aeroshell, with a total payload weight of 166.5 kg for all 37 DSx vehicles.

DSx Science Package

The primary science package is hosted inside of the DSx probe. The science package includes:

1. Impact Accelerometer

The accelerometer is primarily used to determine characteristics of the Martian regolith based on impact data. When the DSx vehicle contacts and penetrates the surface, the acceleration data will vary depending on the hardness of the regolith. This information will be collected for all vehicles and extrapolated across the region to gain a better understanding of surface and subsurface regolith conditions. This process is similar to the techniques used in the Deep Space 2 mission ^[144].

2. Internal Temperature Sensors

Temperature sensors are placed inside of the DSx probe to monitor temperature fluctuations and humidity variations ^[144]. An additional temperature sensor is incorporated into the water experiment to monitor the temperatures to which the science equipment is heating the sample of regolith. An initial temperature reading of the regolith sample will also be recorded before the sample is heated incrementally.

3. Drill motor/Sample collector

The drill motor controls the regolith sample collector. After the probe penetrates the Martian surface, the drill motor will drive the sample collector into the soil that surrounds the probe, approximately 1 meter below the Martian surface. The sample collector will gather regolith in its conical grooves as the drive motor extends the collector outward from the vehicle. Rather than rotating the drive shaft in the counterclockwise direction to retrieve the collector and the sample, the drive shaft will continue to rotate in the counterclockwise direction. When the sample collector is at its furthest extended position, the design of the threads allows for the collector to immediately begin moving back into the probe without modifying the clockwise rotation of the drive shaft. This design allows regolith samples to remain within the grooves on the exterior of the sample collector as it makes its way back into the probe. As the head of the sample collector enters the probe, the regolith sample of approximately 0.1 g will fall into the water vapor indication experiment directly below. ^[144]

4. Water sample experiment

After the water sample experiment registers a sample of at least 0.1 g using its internal scale, its upper door will close and an initial temperature of the regolith will be recorded. The sample will then be heated in 10K increments and any water vapor released will be collected in a chamber located behind the sample collection area. ^[144] Similar to the Deep Space 2 mission, a laser will be used to determine vapor concentration in the chamber for each incremental increase in temperature. ^[144] This process will continue for an hour, at which time the sample will be disposed of. The disposal process involves dropping the sample into a used regolith chamber located below the water sample experiment. This area contains all used regolith so that it does not influence future testing. The sample collector will gather another 0.1 grams of regolith and the experimental process will repeat. Results from each trial will be gathered and sent to Earth for analysis and comparison. All science operations will continue until the DSx's primary battery dies, which is approximately 2-3 days. ^[144]

See Figure 9 for DSx probe internal layout and the features of its science package.

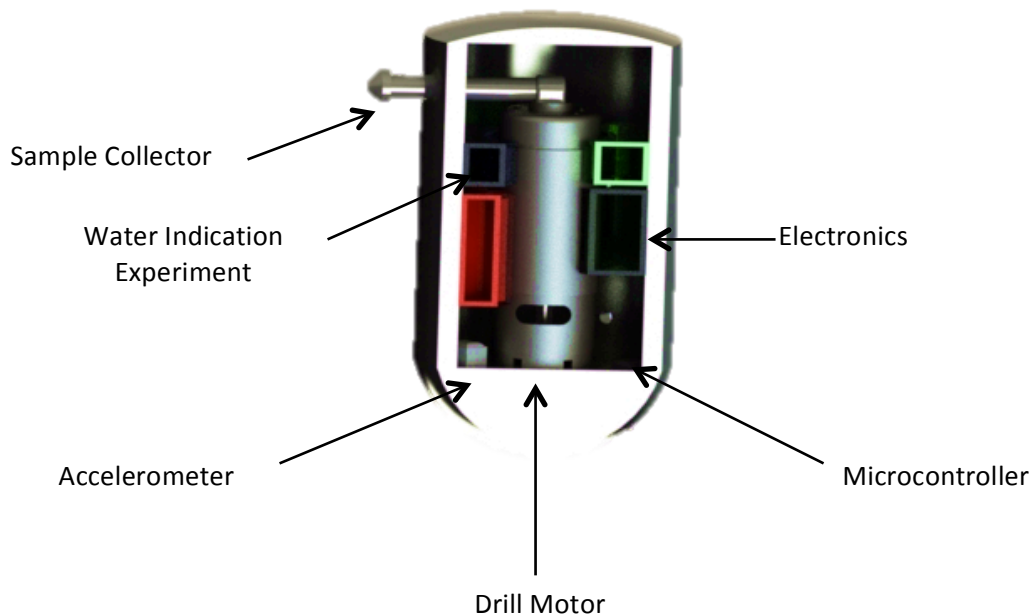


Figure 9. DSx probe internal layout and primary science package components.

2.3.2.6. Avionics

Unlike the Deep Space 2 mission, the DSx mission will not require landers for communication operations. Due to the scale of the DSx mission and budget constraints early in the mission architecture, sending landers to each region of exploration is infeasible. Instead, transmitters will be sent to each region to relay information from each DSx to the Mars Reconnaissance Orbiter (MRO), already in Low Mars Orbit. A small transmitter is required for every 60 km radius in which DSx vehicles are located. This distance is based on the landing requirements for the Deep Space 2 lander.^[137] This transmitter distance will be evaluated during DSx testing prior to launch. In the event that more or fewer transmitters are required to perform all DSx communication procedures, equipment will be added or reduced as necessary. These transmitters will deploy with the DSx vehicles from the Atlas V and will be self-contained in their own aeroshell.

Data recorded from the science package in the probe will be transmitted through the flexible cables connecting the probe and the main body of the vehicle, located about the surface. The main body of the vehicle will transmit this data via the antenna to the local transmitters, then to MRO and ultimately to NASA on Earth where the data will undergo analysis.

2.3.2.7. Power Requirements

Similar to the Deep Space 2 mission, each vehicle will be powered by two non-rechargeable lithium-thionyl chloride batteries, which are stored in the main body of the DSx.^[137] The pair of batteries is

expected to provide 6-14 volts for two to three days, but may last longer depending on Martian conditions. ^[144]

2.3.2.8. Aeroshell Design

The aeroshell is the only EDL feature of the DSx and, therefore, is designed to guide each vehicle to its landing location. The aeroshell is made ceramic material, which will break upon impact with the Martian surface, exposing the DSx vehicle to the regolith below. The blunt surface of the aeroshell is covered with SIRCA-SPLAT (silicon-impregnated, reusable ceramic ablator – secondary polymer layer-impregnated technique), which acts as the heat shield. ^[144] This technique is similar to the technique used in the Deep Space 2 mission. Each DSx vehicle is oriented in its aeroshell such that its center of mass is placed ahead of the aeroshell’s center of pressure. Therefore, the aeroshell will naturally align its blunt heat shield to the oncoming flow (i.e. towards the Martian surface). Consequently, the each vehicle requires neither pointing nor spin-stabilization prior to entering the Martian atmosphere.

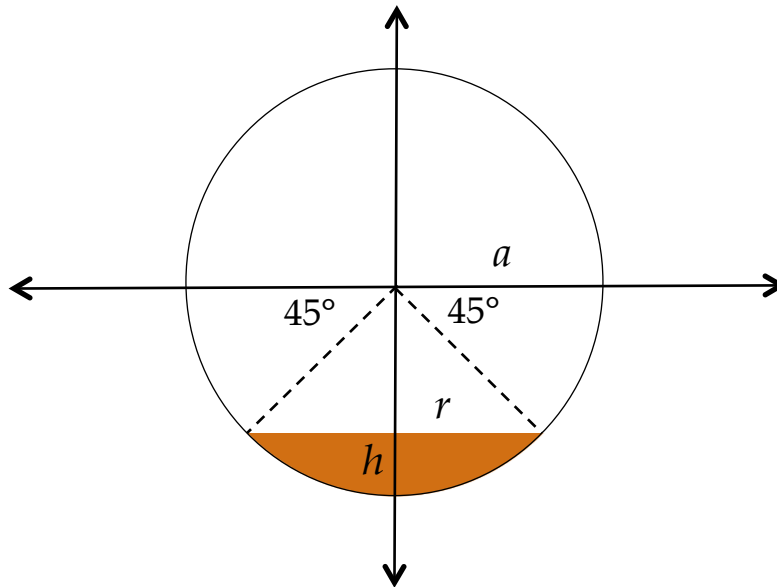


Figure 10. Geometry for a 90° spherical cap section

The aeroshell design is based on a 90° spherical cap section as shown in Figure 10. ^[150] Each DSx and aeroshell unit has a mass of 4.5 kg. In order to achieve a desirable ultra-low ballistic coefficient of between 30 and 40 kg/m², the following equation is used to relate mass, diameter and ballistic coefficient:

$$\beta = \frac{m}{C_D A}$$

Rearranging the equation above yields:

$$m = \beta A C_D$$

Approximating the coefficient of drag, C_D , of a 90° spherical cap as the coefficient of drag of a half cylinder, C_D equals 0.4. Under this assumption, Figure 11 shows the relationship between aeroshell diameter and total vehicle mass for constant ballistic coefficients ranging from 20 kg/m^2 to 150 kg/m^2 . Given DSx sizing constraints and ballistic coefficient requirements, the diameter was designed to be 0.35 m. Consequently, the aeroshell ballistic coefficient is approximately 38 kg/m^2 .

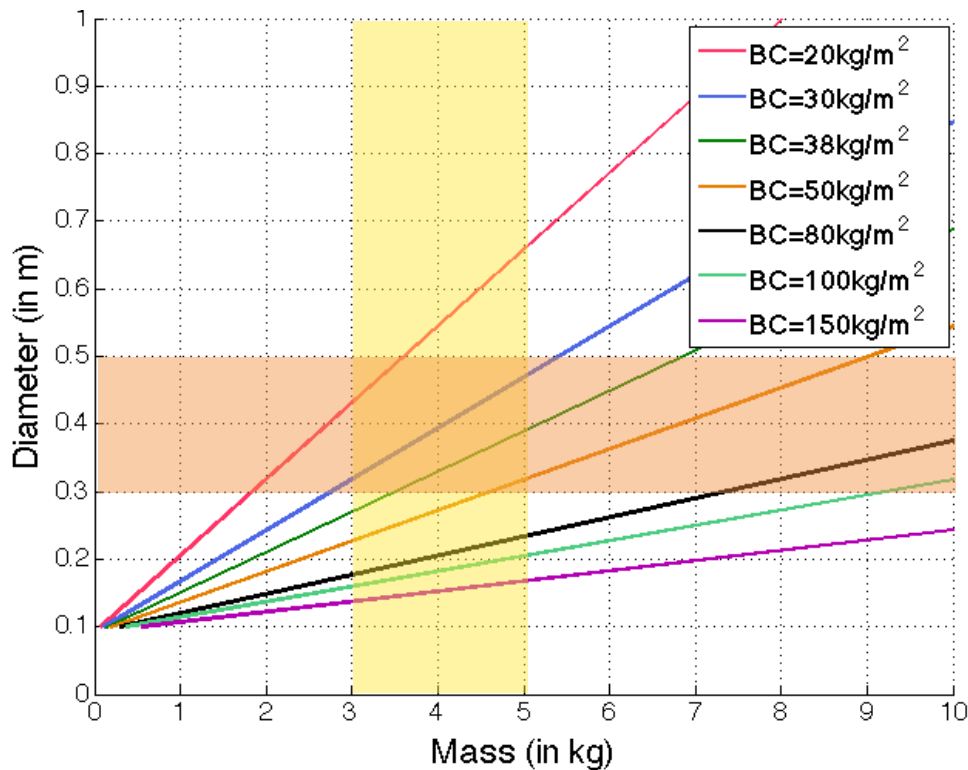


Figure 11. Aeroshell diameter vs. total vehicle mass for constant ballistic coefficients

2.3.2.9. Program Cost

The original development cost of the Deep Space 2 vehicles was \$29.2 million for two probes, or about \$9.73 million each.^[136] Due to similarities between the design of the Deep Space 2 probes and the DSx vehicles, a learning curve of 20% can be introduced into the program cost of the DSx, making the total cost for each vehicle about \$7.79 million and the cost of all 37 vehicles \$288.1 million dollars. An additional \$150 million is added to the program budget to account for costs of the support structure, integration into the Atlas V, launch, and transceivers, bringing the total program cost to \$438.1 million.

2.3.2.10. DSx Mission Benefits

The primary mission of the DSx mission to Mars is to (1) explore the geological area of primary and secondary settlement locations, (2) determine material and water availability in these regions, (3) test

communications capabilities at low elevations on Mars, and (4) select an official settlement location by 2022. The DSx mission plays a critical role in selecting the final settlement location and provides NASA with data to make an informed decision prior to sending humans to Mars. DSx ensures that necessary resources such as water are present in the region and provides indications of the terrain makeup. Without this information, the uncertainties that exist within each location could inhibit the success of the overall mission and increase mission risk for crew and equipment to intolerable levels. DSx is also used to ensure the success of future missions, such as the Mars mining initiative. Because DSx is able to determine water vapor concentration of regolith samples in various regions, it is possible to predict the ability to mine a region and the potential successes or shortcomings associated with these missions. DSx will pave the way for future Mars settlement by giving scientist and engineers the relevant information quickly and effectively.

2.4. Phobos and Deimos

2.4.1. Introduction and Motivation

Phobos and Deimos have been a mystery ever since the 19th century, but in order to determine whether or not a mining mission would be suitable for use by those traveling to and from Asimov City, both planning and exploration are required. To determine whether or not mining operations are worth planning for at this stage, it is vital to understand the likelihood of what kind of orbital body these moons are, and from that, what they contain. In the case of Phobos and Deimos, the best way to determine if a mining operation is worth planning for is to consider both the ideal scenario and the most realistic or probable origins of Phobos and Deimos.

The ideal origin (and thus composition) of Phobos and Deimos would be if they were captured type C asteroids, namely carbonaceous chondrites. In this case, long ago, such an asteroid would have been caught by the Martian gravity well and held there until it acquired a stable orbit. After this, it would have had to transition from its highly eccentric orbit to the much more circular one that it maintains today.^[2]

There are many such asteroids that could have been captured this way, but ideally it is hoped that it would be a type C carbonaceous chondrite because of how much water it would likely contain. A substantial amount of water could be harvested to act as a fuel for spacecraft by making liquid hydrogen and oxygen available. This would be the primary reason to set up a mining mission to Phobos and Deimos - a place in orbit of Mars to facilitate refuelling for travel to and from the rest of the solar system. Based on research of such meteorites that have landed on earth, type C carbonaceous chondrite asteroids have the greatest potential to contain water. Potentially 22% of these asteroids' mass could consist of water. This immense amount of ice, or - thanks to said discovered meteorites being lined with microscopic veins of epsomite - perhaps even liquid water at a range of 20-125°C, could be excellent for a mining mission due to the fact that it would be easily acquirable (given the low gravity of the moons, etc.) and that there would be ample water to make use of for a long time to come. This would make such a mining operation very economical over the long run especially. Given the weight of Phobos and Deimos, this would mean there could potentially be 2.35×10^{15} kg and 3.25×10^{14} kg of water on Phobos and Deimos, respectively, if they were captured type C carbonaceous chondrites.^[1]

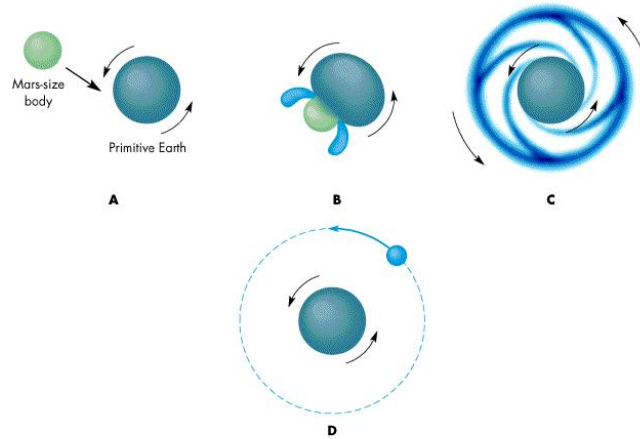


Figure 12. Phobos/Deimos - Formation of Mars' Moons^[4]

Whilst this scenario would be greatly beneficial to humanity's first steps towards another planet, it is unfortunately a not very likely one. Although the captured asteroid theory in general has been a very popular one for a long time in regards to theories for the origins of Phobos and Deimos, it is in fact considerably more likely to have been formed just like Earth's own moon most likely was – by an impact with the planetary body from long ago. This is because of a detected presence of a particular silicate metal – phyllosilicates. These are a very common metal on the Martian surface, and it makes sense that Martian ejecta would still have them after such an impact so long ago. In addition, Phobos and Deimos both have extremely circular orbits, which is very difficult to reconcile within asteroid capture theory. As a result, Phobos and Deimos likely contain only minimal water, not nearly the amount that a captured type C carbonaceous chondrite asteroid would provide. In fact, from what little passing spacecraft have been able to tell, Phobos in particular seems to have the least amount of water on the surface than in almost any other body in the solar system. This in combination with their small masses means that it is not worth it to go to Phobos and Deimos for anything save for exploratory purposes.^{[3][5]}

2.4.2. Exploration Program

Program Metrics

The PADME and LADEE vehicles were built on the Modular Common Spacecraft Bus. This is a modular satellite vehicle that can be reconfigured easily to do different tasks. The total launch mass of LADEE is 383 Kg (248.2 Kg dry). It has a power production of 295 Watts, more than sufficient for the instrument package 157. The total LADEE program cost was \$280 Million, but this included spacecraft development and launch services. The predicted program cost will be closer to ~\$98 million not including launch costs.

Mission Architecture

NASA AMES has already developed the mission architecture in order to use the LADEE vehicle to study the Martian moon. Their mission is called PADME (Phobos And Deimos & Mars Environment). PADME will leave with the Habitat 4 launch, being delivered in Low Mars Orbit, taking care of any increased delta-V concerns. It will arrive in orbit around Mars during 2021, and will initiate a burn putting it in a

highly elliptical polar orbit for ~10 fly-by's of Phobos during a 6-month period before initiating another burn putting it on intersection for ~5 fly-by's of Deimos during another 6-month period before the mission is completed.

PADME Vehicle Instrumentation

The PADME vehicle will have a scientific payload consisting of instruments from LADEE as well as updated instruments. The Mars Orbit Dust Experiment is the same instrument on LADEE that analyzes high altitude ionized dust particles to determine composition. The Mars Moon Camera System is a high resolution camera to produce spatial resolution images. A Neutron Spectrometer will be included to measure the abundance of Hydrogen, hopefully leading to a conclusion regarding the quantitative amount of water in the top layer of regolith. The last instrument of note will be the Radio Science system which measures the Doppler shift during close encounters to map the gravity field of the two moons^[156]

3. Phase II: Resource Acquisition and Infrastructure Setup

3.1. Introduction

The second phase of the Asimov City mission is the “Resource Acquisition and Refueling” phase, which begins in 2025, and lasts until 2054 and beyond as needed by the settlement. The goal of this phase is to utilize in-situ resources, mainly liquid hydrogen and oxygen from the ice found in the permanently shadowed regions of the Moon. The propellant produced on the Moon via automated mining and electrolysis, will increase the Space Launch System’s (SLS) maximum payload to Mars, and will help to save billions of dollars over the course of the mission. Most importantly, it will make crew transport and landing possible.

The first step of the “Resource Acquisition and Refueling” (RA&R) is to establish mining operations on the Moon’s South Pole. This step will include a manned mission, flown on a Falcon 9 rocket in 2027, to assist in the set-up of the two automated miners, the electrolysis facility, the fuel transport vehicles, and the solar panels that will be used to power operations. This human mission is not only essential to the mission itself; it is a chance to test some of the technologies that will eventually be utilized on Mars, such as the Magellan rover. The mining and electrolysis operations on the Moon will be functional by 2029.

Between 2028 and 2030, a propellant depot at the first Earth-Moon Lagrange point (EML1) will be established. The depot will feature zero boil-off (ZBO) technology, including a heat shield, layers of multi-layer insulation and foam insulation, and an active cooling system with a cryocooler. The depot shall be capable of docking with the upper stage of the SLS, as well as the fuel transport vehicles that will be used to carry propellant from the surface of the Moon to EML1. During the early years of the RA&R phase, two smaller propellant depots will be established in Low Mars Orbit (LMO). These depots will eventually be used to fuel crew entry, descent, and landing and to refuel the crew transport vehicle that will carry humans to and from Mars.

The process of setting up this infrastructure on the Moon, at EML1, and in LMO will use a considerable amount of SLS launches and budget during the early to mid years of the mission, but will assure future monetary savings thanks to increased payload, enable humans to actually reach Mars, and move the mission toward its ultimate goal of Earth independence.

3.2. Lunar Resource Acquisition

3.2.1. Introduction/Overview

The Lunar South Pole contains the highest concentrations of water available on the surface of the moon. Because of its low exposure to sunlight, temperatures are much lower on average at the pole and boil off of resources is minimal. For this reason, the most logical place for a mining depot is on the south pole of the Moon. Shackleton Crater, the primary mining site, is found at 89.9 degrees South and 0 degrees East on the lunar surface. The crater is 21km in diameter from rim to rim and 6km in diameter in its interior. RJB4 Shackleton was chosen for its water profile taken by the LCROSS mission which will be confirmed by the Lunar Flashlight mission and the Peaks of Eternal Light found along its rim. The rim of the crater is permanently illuminated by the sun, which is ideal for power generation for the mining process.

Refueling stations throughout the mission path increase payload capacity as increasing fuel requirements reduces payload capabilities. In order to transport high mass cargo such as habitat pieces and construction equipment to Mars, a refueling station utilizing the Moon's resources becomes necessary. With three rockets as the maximum going to Mars in one launch window, and 100 metric tons of fuel required per rocket, a requirement of 300 metric tons every six months becomes the main design criteria. Shackleton Crater at the lunar south pole has been shown through neutron spectrometry to contain high concentrations of hydrogen and up to 55,000 parts per million²²¹ ice throughout the lunar regolith at the base of the crater. This number will be confirmed during the Lunar Flashlight mission when it orbits the moon in 2017.

The power source for the mining equipment and processing plant will come from solar panels laid at the rim on the crater on a Peak of Eternal Light, a region in a permanently shaded region of the moon that receives sunlight throughout the year due to its elevation. Within an earth year, the Peak of Eternal Light at the rim of Shackleton Crater is shaded for two months, with the longest period of darkness lasting seven days and the shortest lasting three days²²². Due to this power restriction, mining within a six month period will be reduced to a five month period. With a twenty percent loss assumed between digging and refueling the fuel transport vehicle, a daily requirement of 45 metric tons of regolith arises. Lunar soil density is 0.75 metric tons per cubic meter²²³ leading to a 60 cubic meter of mined regolith required per day.

3.2.2. Concept of Operations

Lunar mining consists of two major components, miners to collect regolith, and a processing plant to extract the ice, electrolyze the water into LOX and LH₂, and store the fuel until it will be transferred to the fuel transport vehicle. The four miners, tanks, electrolyzer, oven, and other supporting equipment will be shipped together on one decent vehicle. The descent vehicle will land at the outside of the interior crater where it will await crew for initial setup.

Initial setup will be completed by a crew of six over a period of 120 days. Half of this time will be used for laying solar panels to power the mining operation. The LOX and LH₂ tanks will remain on the descent vehicle during the life of the mission, but the electrolyzer, oven with conveyor belts, piping, pumps, refueling boom, miners, and recharging station will be unloaded and placed accordingly. The electrolyzer will be connected with piping directly to the tanks and will be placed near the now permanently stationed descent vehicle. The oven will be connected to the electrolyzer with piping with one conveyor belt placed to bring regolith into the oven and another placed to carry the now ice-free regolith out of the oven. A recharging station consisting of extending plugs placed in the ground will be placed at ten meter intervals away from the descent vehicle. The refueling boom will be attached with piping to the LOX and LH₂

tanks and placed 60 meters away from all other equipment. The solar panels that will have been placed at the Peak of Eternal Light six kilometers away will be connected to the power main on the descent vehicle which provides the necessary power to the electrolyzer, oven, pumps, and recharging station.

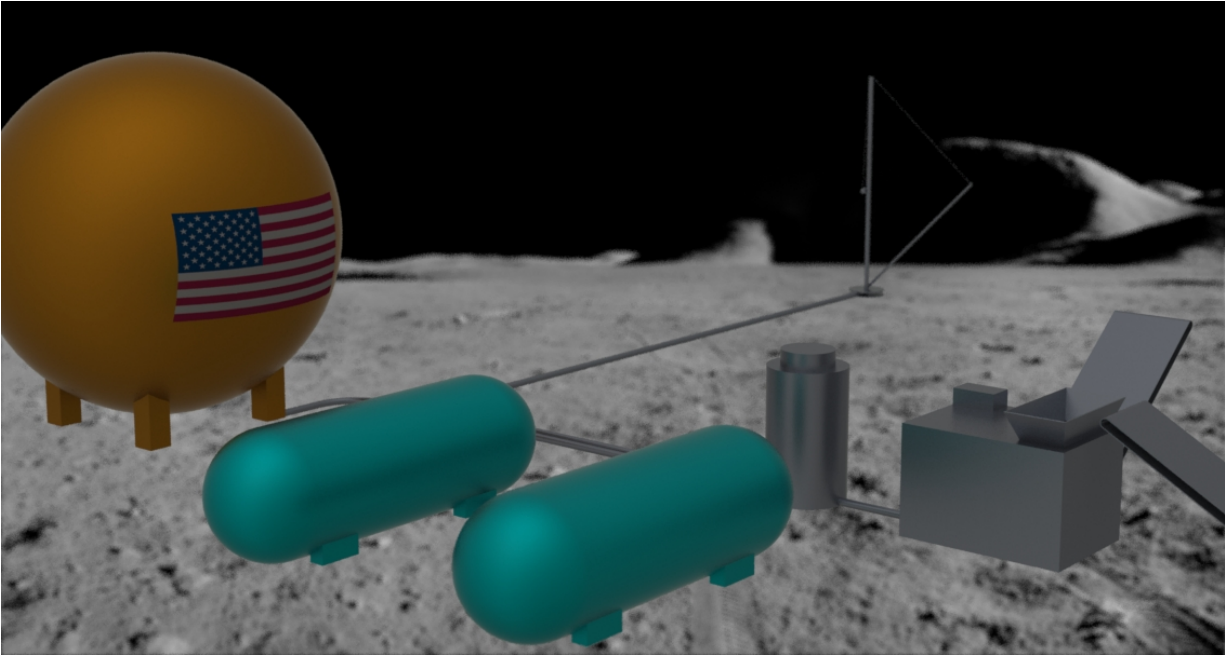


Figure 13. Lunar Processing Plane (Tanks represent total volumes and do not reflect actual positioning)

The total amount of regolith required will be collected by four miners, each working on an eight hour on, eight hour charge, eight hour standby schedule. If one miner becomes no longer operational, remaining miners will begin an eight hour on, eight hour charge cycle with no standby to maintain the 45 metric tons of regolith mined per day requirement. As seen in Figure 14, the miners will have a continuous scoop bucket system on the front which collects regolith as the miner drives in the dump body.

Regolith will be dumped onto the conveyor belt from the miners and brought into the oven where it will be heated to turn the ice into vapor, collected and pumped either into the electrolyzer or directly into the crew rovers when needed. The used regolith will be removed from the oven via a second conveyor belt. Electrodes within the electrolyzer convert the H_2O into H_2 and O_2 which will then be condensed to a liquid and pumped into their respective tanks.

To refuel and recharge the fuel transport vehicle, a refueling boom with a pivoting base will extend to the refueling ports of the FTV where LOX and LH_2 will be pumped from the tanks on the descent vehicle and into their respective tanks on the FTV.

3.2.3. Lunar Mining Vehicle

The mining vehicle will be built around a main truss platform as can be seen around the perimeter of the miner in Figure 14. The truss will be built of 7075 aluminum to withstand a maximum load of 72 kN at

the end of the truss to simulate full load at maximum dump inclination. The dump body has a volume of 17 cubic meters, will be connected to the truss by pivots at the rear and by linear actuators at the front. While in a horizontal, loading position, the dump body sits on stops mounted to the truss. Each of the two linear actuators will be capable of lifting 72 kN, the weight of the entire full dump body for redundancy. The miner's main truss will be mounted to four tracks to support, drive, and steer the miner. Each track system consists of one electric motor to drive the track and another electric motor to rotate the entire track assembly. To reduce ground loading to 20,680 N (3 psi) a track surface area of 4.4 square meters will be required. To ensure the tracks can rotate, the ratio of the length to width must be between 1 and 1.3. Each track will therefore have a surface contact area of 0.95 meters by 1.15 meters.

The front of the mining vehicle will house the continuous scoop bucket powered by two redundant electric motors. The buckets will be 15 centimeters deep and 15 centimeters in height. During mining, the miner moves at 0.5 meters per minute, collecting the top 10 centimeters of regolith for 70 meters to gather the required 15 cubic meters of regolith. The digging process will require 2 hours and 20 minutes each day to complete, but 8 hours of battery life will be available so miners can travel to areas far from the processing plant, and so the miner can pause digging in areas where on board chemical cameras detects areas of low ice concentrations and resume in areas of higher ice concentrations. The maximum speed of the miners will be 5 kilometers per hour such that the round trip to the opposite end of the crater interior will be 2 hours and 40 minutes.

A control panel will be situated on the front left side of each miner will contain the computers required to analyze the data from the chemical cameras, radar imagers, and load cells. This data will be used to determine how much digging will be required and which areas will be most beneficial to mine. Imagers will also be used to position the miners above the charging ports to recharge the batteries. Batteries will be located in the center of the truss between the second and third truss stations. Each battery will have a charge capacity of 25 kW to power the miner for eight hours.

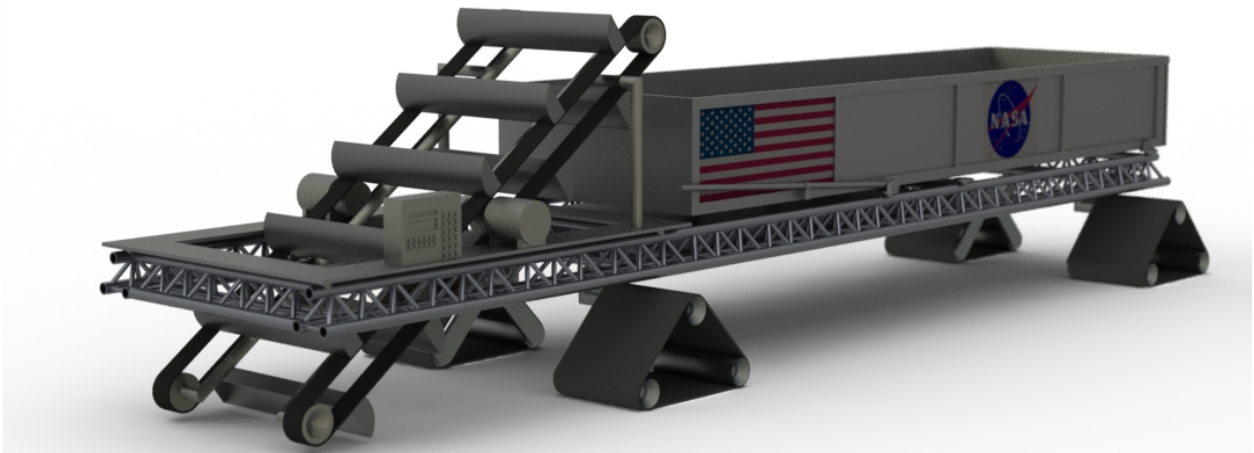


Figure 14. Lunar Miner

3.2.3.1. Miner Avionics

Because both the Moon and Mars miners are going to be designed identical to one another, their avionics packages will also be alike. The primary difference is that the Mars miner will be equipped with an on board GPS receiver that makes use of μ Net. The other requirements for this system include many

actuators to control the vehicle motion, digging mechanisms, dumper mechanisms, and sensors to monitor and control the performance of the system.

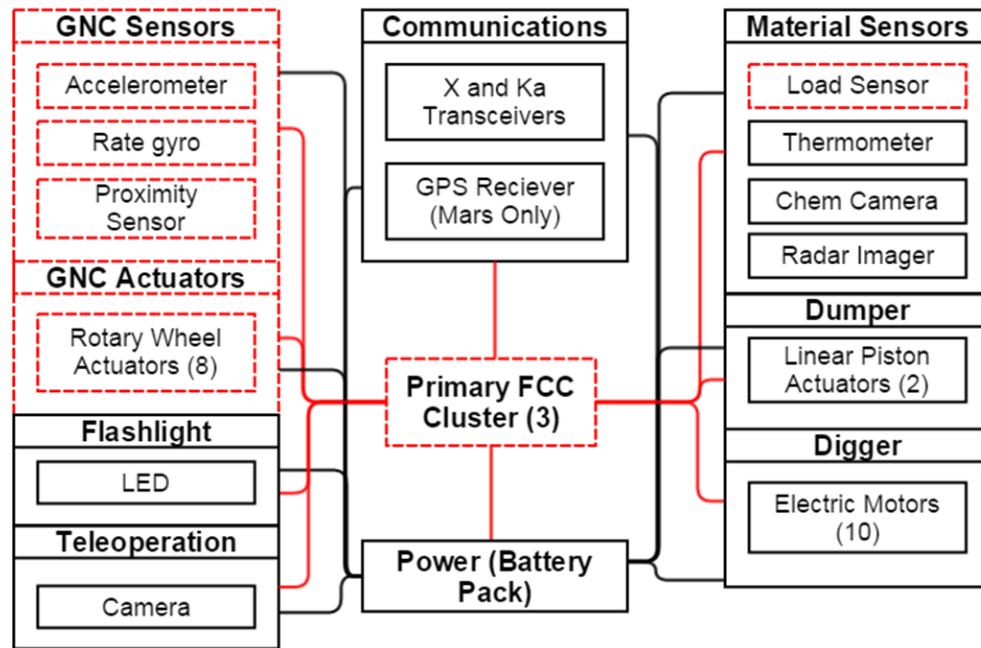


Figure 15. Miner Avionics Block Diagram

Communication

The Moon miner will be more teleoperated from a controller on Earth or on the Moon processing base. To facilitate this long distance control, the miner will use X and Ka band frequency transceiver.

GNC

The miner will use an accelerometer and rate gyro to monitor its' motion on the ground. For digging operations and for dumping loads to the processing facility, the miner will use a proximity camera for precision operations.

Digger/Dumper Electronics

The digger will be actuated by 10 electric motors that work in conjunction with one another similar to vehicle treads. The dumper is operated by two linear piston actuators. These actuators will lift the load at an angle high enough to unload the contents.

Material Sensors

To ensure that the miners are digging in the most prolific regions of regolith, the vehicle will be equipped with a series of science sensors. First there will be a chemical composition camera to evaluate the levels of water/ice particles embedded into the target region. It would not be a wise to waste the energy of the miner and processing plant to collect extra "empty" regolith if it can be avoided. The vehicle will have a radar imager which will give a profile of the underlying regolith to determine if there are any "hard" rocks that could cause damage to the digger. Lastly, there will be a distributed network of load sensors around

the vehicle, specifically atop the wheels to measure the current load of the dump. This way the miner knows when it has reached full capacity and should return to the processing base to dump its contents.

3.2.4. Lunar Processing Plant

The processing plant on the moon will consist of four main components: the oven, the electrolyzer, LOX and LH₂ storage tanks, and a refueling boom. Regolith from the miners will be unloaded onto an electric motor driven conveyor where it will be taken into the oven. In the oven, 150 kW will be used as resistive heating to raise the temperature of the regolith by 400 degrees centigrade to sublimate the ice to water vapor. ^[224] This water vapor will then either bypass the electrolyzer and be directed to the crew rovers when needed or will be pumped into the electrolyzer.

The electrolyzer will use a voltage across two electrodes to separate liquid water into hydrogen and oxygen gas. Water requires 286 kJ/mol to break its bonds and so 367 kW of power will be provided to complete the process. The rate of electrolysis is linearly dependent on the current flow ^[225] such that 250 amperes will allow for 104 kilograms of water processed per hour. Gaseous hydrogen and oxygen will be captured at the top of the electrolysis tank and will be condensed and pumped to their respective storage tanks.

The lunar storage tanks will remain on the descent vehicle to reduce crew work load upon setup. The LOX tanks will have a total volume of 18 cubic meters will be split between four smaller tanks each with a volume of 4.5 cubic meters and a radius of 1 meter. The LH₂ tanks will have a total volume of 1738 cubic meters and will be split between eight smaller tanks each with a volume of 217 cubic meters and a radius of 3.7 meters.

The fuel transport vehicle will take the liquid LOX and LH₂ to the refueling depot every 60 days. To get the fuel from the storage tanks, a refueling boom will be placed 50 meters away from the processing plant. The refueling boom consists of a rotating base, a vertical 20 meter pole, and a boom arm that will be able to extend to 44 meters in length. The arm will be attached to a cable that will go over the top of the pole and down to an electric winch. The ability to adjust the rotation of the base, the angle of the boom, and the length of the boom will allow refueling to the fuel transport vehicle as long as the vehicle lands within a 40 meter radius of the base. After the fuel transport vehicle lands, pumps in the storage tanks will pump fuel, one at a time, into each of the respective tanks on the fuel transport vehicle. While refueling, electrical connections will also be used to recharge the fuel transport vehicle's batteries. When refueling and recharging completes, the boom arm will retract so the refuel vehicle can launch.

3.2.5. Mobile Roving Settlement

The crew will be living in a pressurized rover during the moon mining setup and servicing missions. Due to time constraints and the large scope of this project many different candidate rovers were reviewed and a design was selected that best fit our needs. There are three requirements that must be met. The crew shall be able to live in the rover for up to 120 days. This is the length of the mission to set up the moon mining equipment. The rover shall fit within a Space Launch System (SLS) fairing. The SLS fairing is the largest we can fit a pre-assembled rover. The last requirement is the rover shall be able to autonomously navigate or be teleoperated to meet the crew after landing.

Rover	Travel Rate	Size (LxWxH) (m)	Mass (kg)	Crew	Duration (days)	Contingency
Turtle	25km over 2-3 days	3.45x3.24x2.93	1750	2	6	48 hours
Small Pressurized Rover Concept NASA	240 / 3 rovers	4.5x4x3	3000	2	-	-
SPRITE	100	-	6500		10	-
Magellan	17.6 km/hr	12x5.2	10	3	30	12 days
Arusha	16 km/hr	8.35x3	-	6	28	-

Table 3. Rover Specifications Comparison Part 1

Rover	CO2 Scrubber	Power Source	Fuel
Turtle	LiOH canister	Proton Exchange Membrane	LOX and LH ₂
Small Pressurized Rover Concept NASA	-	-	-
SPRITE	-	-	-
Magellan	2 Bed Molecular Sieve	100 m ² solar array	Electricity
Arusha	-	-	-

Table 4. Rover Specifications Comparison Part 2

The candidate rovers, and their associated features and characteristics, are depicted in table 1 and table 2 for reference. Due to the first requirement, the Turtle and SPRITE rovers were not a viable option as their size limits/restrictions prevent an extended mission. The NASA concept rover and Arusha rovers did not have enough information available to make them viable options. This left the Magellan rover. The Magellan was designed by a previous ENAE484 class for a 42 day mission on the Moon.^[125] This made the Magellan a strong candidate as minimal modifications were needed to meet the increased mission duration and navigation capabilities, and it met the SLS size requirement. Two different modified versions were designed to meet the needs and requirements of each mission. Magellan 2.0 was designed to be used on the Moon and Magellan 2.1 is designed to be used on Mars.

Two Magellan 2.0 pressurized rovers will land on the moon separately from the crew. Because there is no GPS system on the Moon, the rovers will be teleoperated via two radio transceivers operating in the 88-108 MHz range. The crew will walk over the Magellan and enter through the suitports located at the “insert location”. The modifications in the Magellan 2.0 consist of increased habitable volume for extended mission duration as well as extra crew member, increased tank and food storage for oxygen, nitrogen, food, water, added suitports, added refueling compartment for resupplying consumables, and added teleoperation capabilities.

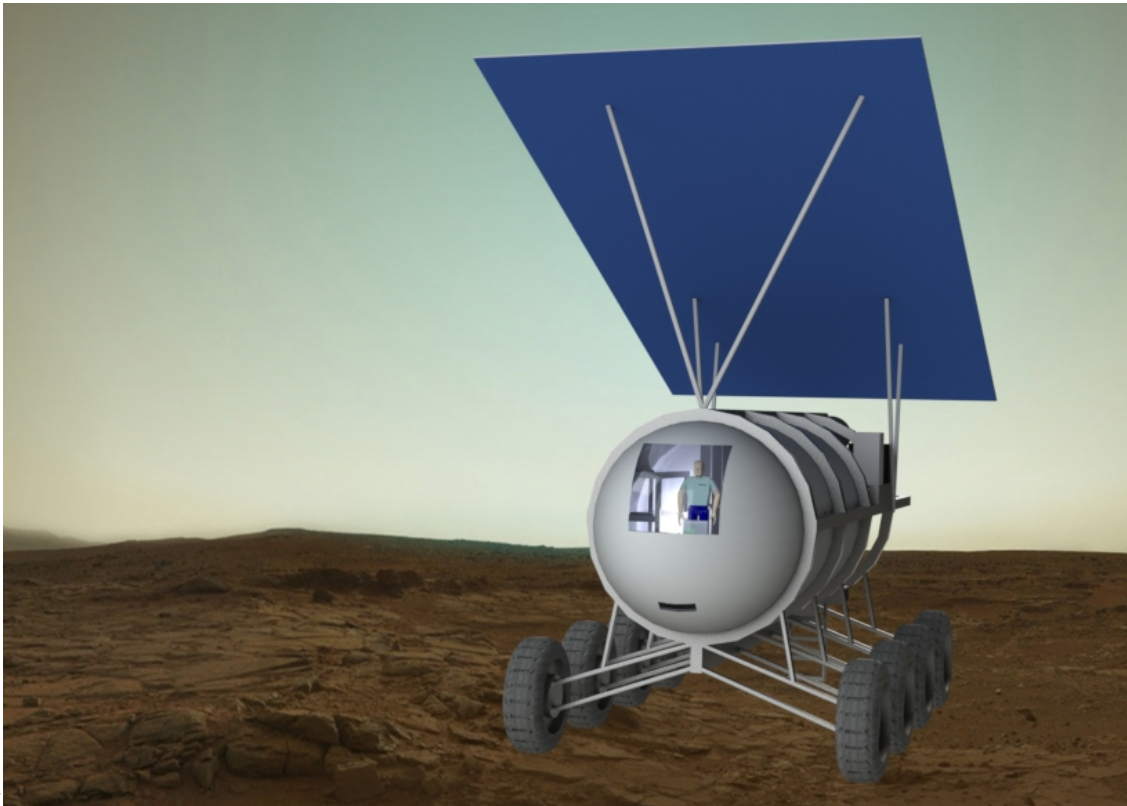


Figure 16. Magellan Front View

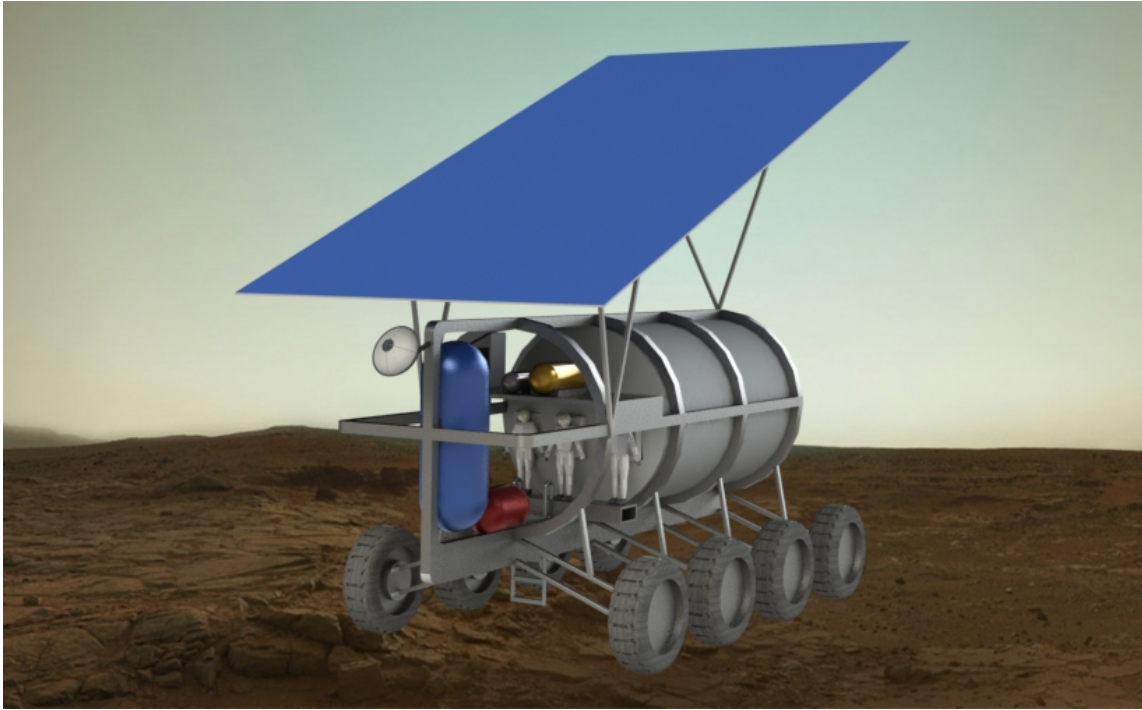


Figure 17. Magellan Rear View

Increased Habitable Volume

The Magellan 2.0 was designed for a nominal mission duration of 90 days with a 30 day contingency; however, the original Magellan was designed for only 42 days. In order to increase the mission duration, the habitable volume was increased according to the NASA 2011 averaged habitable volume curve.^[126] According to this curve, for a total mission duration of 120 days, the volume needed per crew member should be just below 19m^3 for a total of 58.4m^3 (see Figure 18). Thus to meet this requirement, the hull length of the Magellan was increased by one meter such that the each crew member will have 18.9m^3 of habitable space. This habitable volume for each of the crew members was determined through a MATLAB code that considered the total volume of the entire pressurized hull and subtracted the volume of consumables and storage, as well as wall and floor thickness. A third bed was also integrated into the living quarters to accommodate a third crew member.

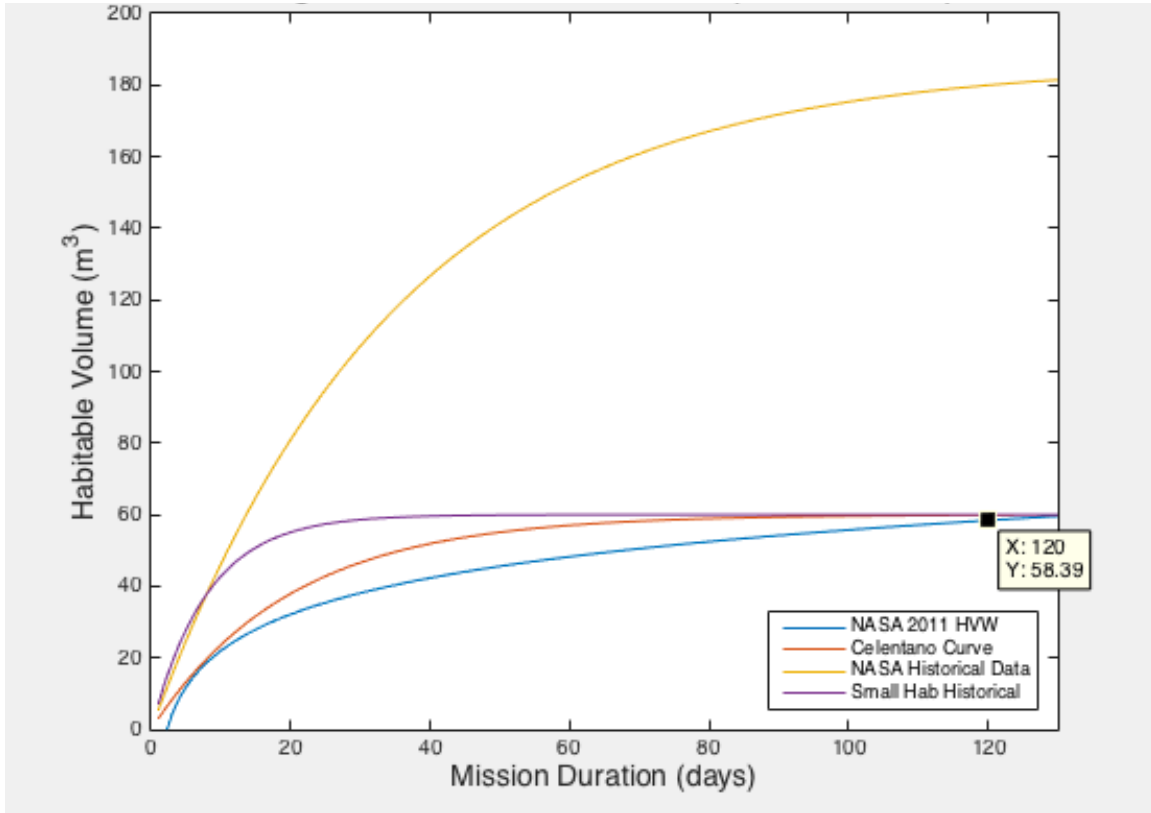


Figure 18. Magellan Mk2.0 Habitable Volume Curves

Gas Storage Tanks

The oxygen and nitrogen tanks have been redesigned to accommodate the extended mission duration. The tanks comprise a cylindrical body with hemispherical endcaps located at either end. The volumes of the tanks were calculated using a MATLAB code. This code accounted for the volume of gas needed to pressurize the habitat as well as the gas that would be lost due to leakage over the 120 day mission duration. The leakage was modeled as an exponential decay. The calculated volumes are listed in Table 5 below:

Tank	Required Volume (m ³)	Radius (m)	Height (m)
O ₂	3.22	0.6	2.05
N ₂	0.60	0.4	0.66

Table 5. Pressurized Tank Volumes

Suitport

The original design for the Magellan used a separate airlock that allowed the crew to change into and out of their suits for extra-vehicular activities (EVAs). A separate airlock does not utilize space efficiently and allows dust particles to enter interior space of the rover. Because of these negative aspects, suitports

were implemented for the Magellan 2.0. The suitport allows for a rear-entry space suit to be attached to and sealed against the exterior of the rover. When the astronaut wants to begin an EVA, s/he will enter the suit feet first from inside the pressurized rover environment. Then they will close and seal the space suit backpack as well as the vehicles hatch. The last step is the astronaut unseals and separates the suit from the rover and steps out for his/her EVA. Once outside the rover, the astronaut can use a ladder on the left side of the rover to descend to the surface. The suitports decrease the amount of time required for the crew to enter their suits and exit the Magellan as well as prevent dust from entering the interior space of the rover. Pictured below are the three suitports and a ladder for their descent.

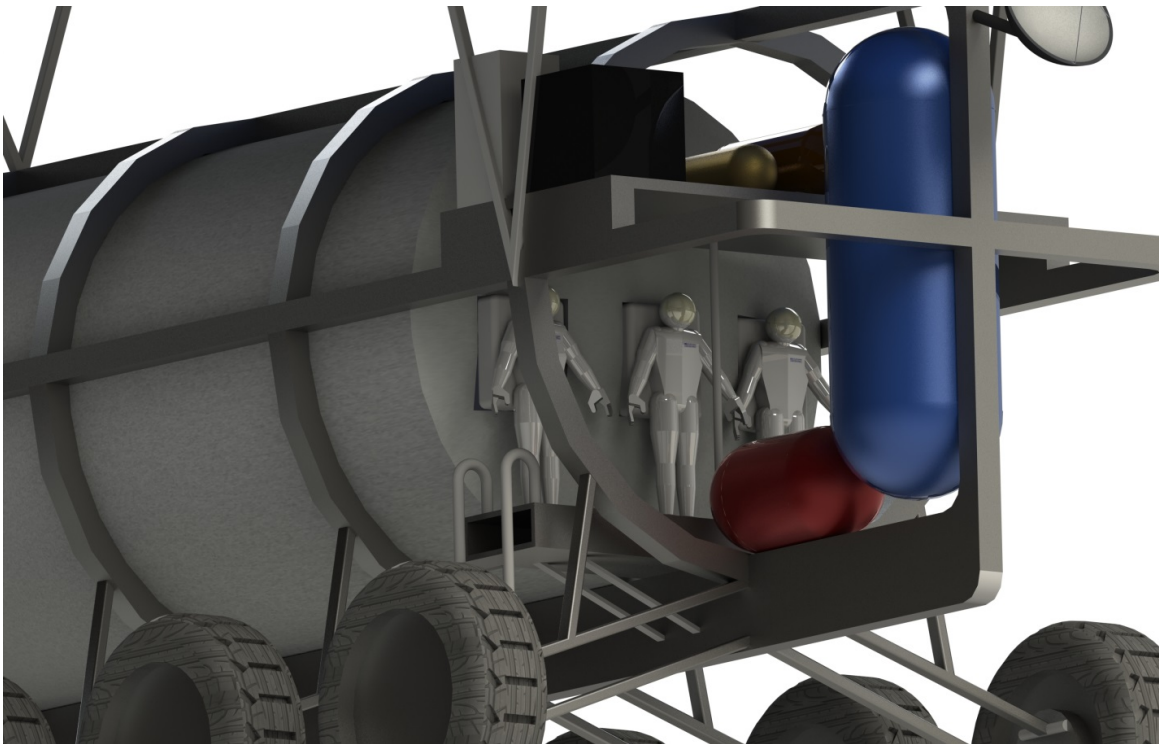


Figure 19. Magellan Suitport View

Refueling Compartment

Once the initial moon setup mission is completed, the Magellan 2.0 will be reused for servicing missions. The servicing missions have nominal mission durations of 30 days. The refueling compartment will allow the crew to refuel the Magellan 2.0 with food, clothing, and other consumables. The refueling compartment has two access hatches. One hatch is on the bottom of the rover and leads to the exterior. The second hatch is from inside the compartment to the inside of the crew habitable portion of the rover.

3.2.6. Lunar Cargo Delivery

Landing on Earth's Moon

The scope of this project covers a large amount of needed infrastructure and covers years' worth of research in order to go into depth about every aspect of the project. As a result, EDL on the Martian

surface was designed from scratch, but landing on Earth's Moon was set as a secondary architecture. However, completely overlooking the needs for lunar landing was not acceptable. As a result, a feasible outline for lunar landing was developed.

Landing the Miners

Due to budgetary restrictions, one SLS Block1B was allotted to transport four mining vehicles to the lunar surface at once. Initial designs for lunar EDL focused on tight packing of equipment and ease of deployment, but overlooked common things such as a shifting center of mass upon fuel usage. Below is an image of one of the early iterations. It contains ramps that are deployed after landing to allow for the miners to drive directly off and be ready for use. It also had three massive tanks that were to be used as the holding tanks for LOX and LH₂, as well as being used as the fuel source for landing. This created the shifting center of mass as mentioned earlier. Four RL-10 engines are used for landing and can be stripped from the vehicle and used on the FTV as a replacement engine to extend the life of the vehicle.

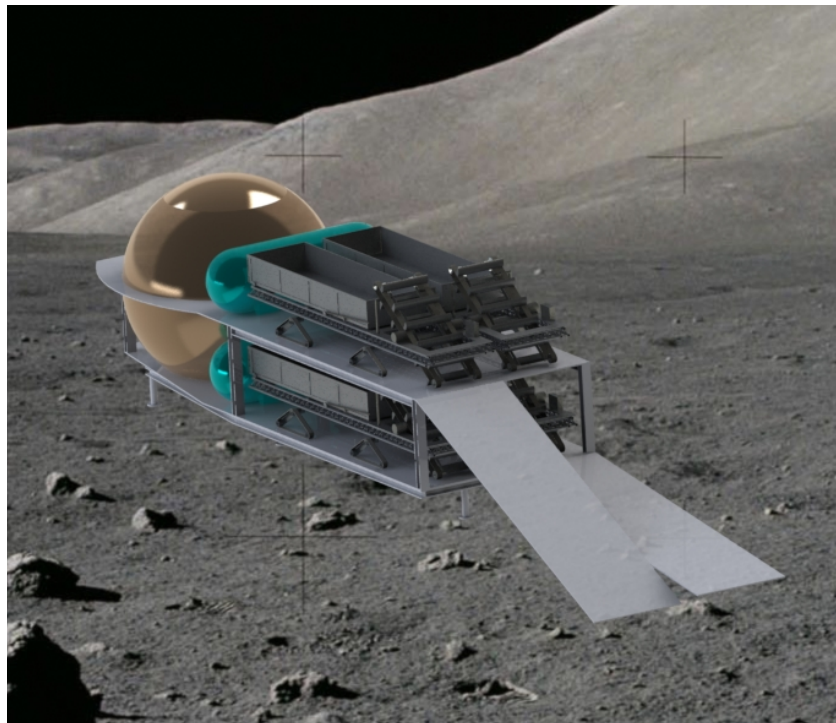


Figure 20. Initial Miner Delivery System

Later iterations focused on coming up with a design that could efficiently be packed in the fairing, and also have a center of gravity that is more centralized and stable throughout the landing procedure. This new design is based off of the NASA/JSC "LUNOX" proposal from 1993. With this design the miners are able to stow in the middle of the landing vehicle and be lowered by wires. Just as the earlier plan, all four will be delivered at once and will be stacked two by two. Also, now with this design, instead of delivery a few small tanks, each of the tanks used for propulsive landing will be the primary holding tanks for processed water. This design also uses four RL-10 engines.

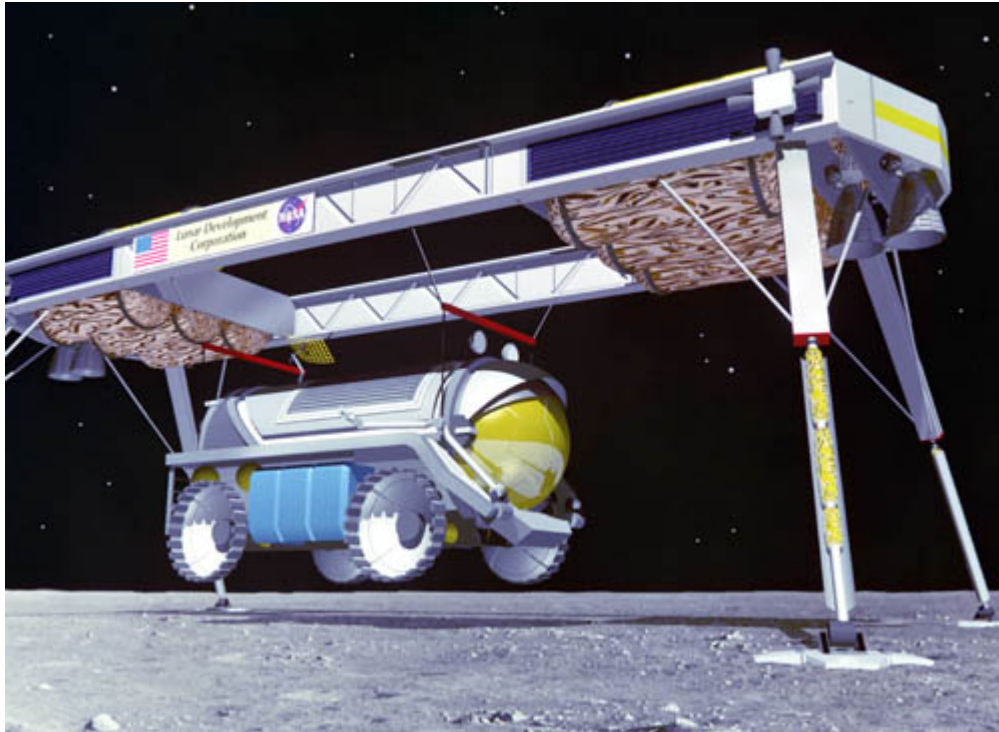


Figure 21 "LUNOX" Delivery of a Pressurized Rover

Landing Magellan

The Magellan is much bigger than a lunar miner but is lucky enough to have one SLS Block 1b allocated for each of the two Magellans. Again, the initial design had a vehicle that was very unbalanced while attempting to land, but still aimed for the simplicity of having a vehicle that requires little to no human interactions to unpack. Below is an Image of the initial attempts at designing this landing structure.

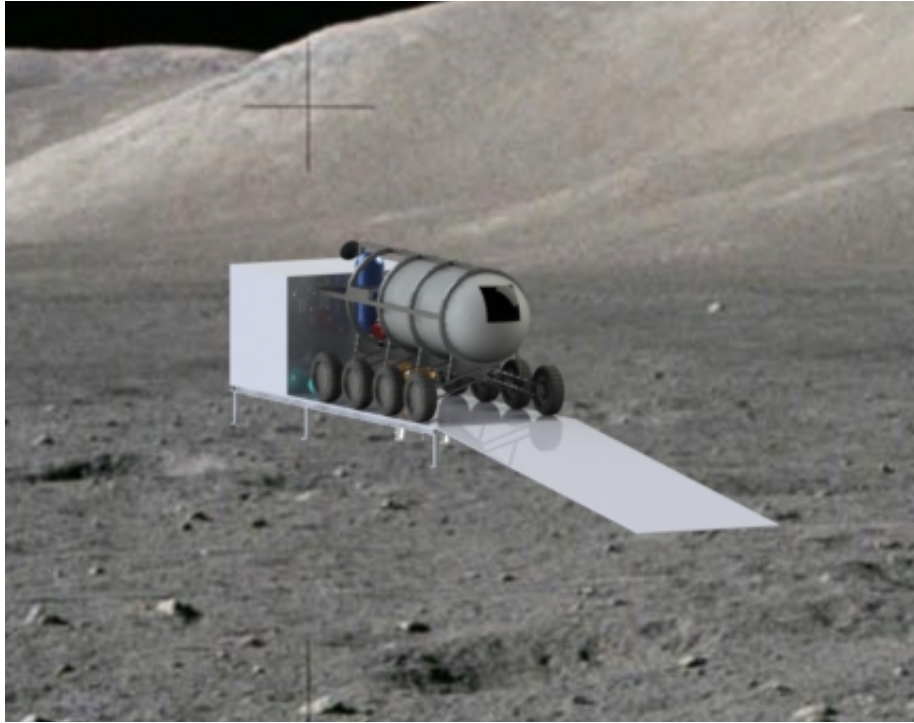


Figure 22. Preliminary Magellan Lander

Just as the other craft, it has a ramp that is autonomously deployed after touchdown. It also has a compartment in the rear that is used to store and deliver parts for the processing plant. This design also needed redesign so the new landing vehicle is also similar to the “LUNOX” lunar lander platform and will lower the Magellan to the ground using cables. It will also have four RL-10 engines and its fuel tanks will also be used to store the processed propellant on the lunar surface. All together this leads to twelve RL-10 engines that will be used to land vehicles on the lunar surface. This means the FTV will have up to twelve replacement engines, if it ever needs a replacement part or entire engine overhaul. Below is concept of what the lander will look like, except it will carry one large Magellan rather than the six small robots it was designed to deliver.

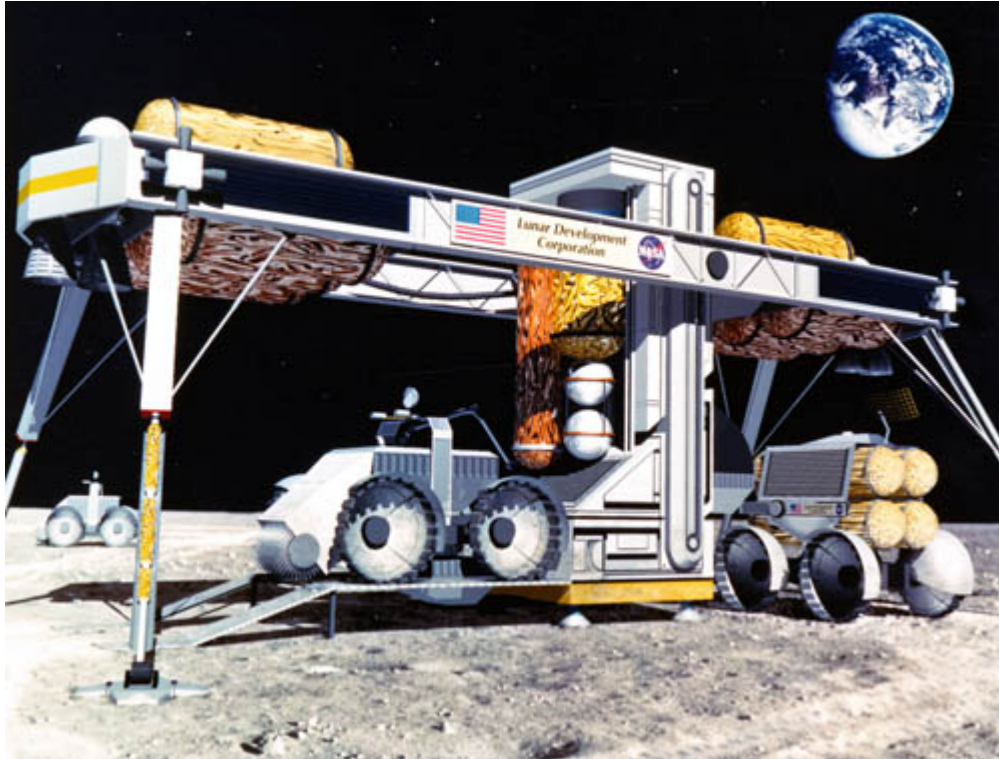


Figure 23. LUNOX Processing Plant Delivery Concept ^[266]

3.2.7. Lunar Lander

As a result of budgetary concerns, the decision was made to modify a previously-designed vehicle to better suit this mission rather than to design something new from the ground up, which would be a more expensive option due to non-recurring development costs.

Requirements

In order to choose a vehicle that would require the fewest modifications, a set of constraints and requirements were created. The two most important of these were reusability (single stage unlike the Apollo Lunar Module (LM) that had ascent and descent stages) and fuel type, both stemming from budgetary concerns. The budget could not accommodate sending new vehicles with every crew or additional fuel, so the vehicle would be required to use Liquid Oxygen (LOX) and Liquid Hydrogen (LH₂) because that is what will be mined and refined on the surface of the moon. In addition, SLS launch vehicle payload fairing sizing constrained the outer diameter to no more than 5m, which is the minimum diameter of the tapered section of the fairing where it will need to be transported in. Finally, in order to support the mission requirement of 6 crew members, it needed to be capable of carrying 6 astronauts to the surface.

Research

After setting the above set of specific design constraints and requirements, research into previously designed lunar landers was conducted. Multiple vehicles were considered, with the top three contenders being the Apollo LM, Altair, and the Boeing Reusable Lunar Lander.

The Apollo LM design, while reliable during every moon landing from 1969 to 1972, would have required intense modifications to meet mission requirements. These would have included increasing its crew capacity from only 2, overhauling both ascent and descent engines to use LOX and LH₂ rather than hypergolic fuel, and upgrading the life support technologies and avionics.^[81] It also would not have been reusable unless the entire structure was changed, so for these reasons the Apollo LM was removed from consideration.

Altair, much larger than the Apollo LM, was a primary component of the now cancelled Constellation Program. It was designed for a crew of 4 and mission durations of 7 to 210 days, but was extremely heavy at over 45 tons, oversized with a height of 9.7m and diameter of 7.5, and was multi-stage. The avionics and life support were advanced and would have required few modifications, but only the descent stage utilized LOX and LH₂, with the ascent stage using hypergolics.^[80] However, even with its upgrades, ultimately the immense size of Altair proved to be too large for the payload fairing, and thus, was also discarded.

The Boeing Reusable Lunar Lander (BRLL) was the first design found to be fully reusable with LOX/CH₄ engines^[83] and sized to fit into the payload fairing at under 5m. It had a gross mass of about 21.5 tons, with 5.5 tons of dry mass and 16 tons of propellant, far less than the Altair, but could only hold 2 crew members.^[82] While its design still did not meet every design constraint or requirement, the fact that it was reusable and fit into the payload fairing was enough to move forward with.

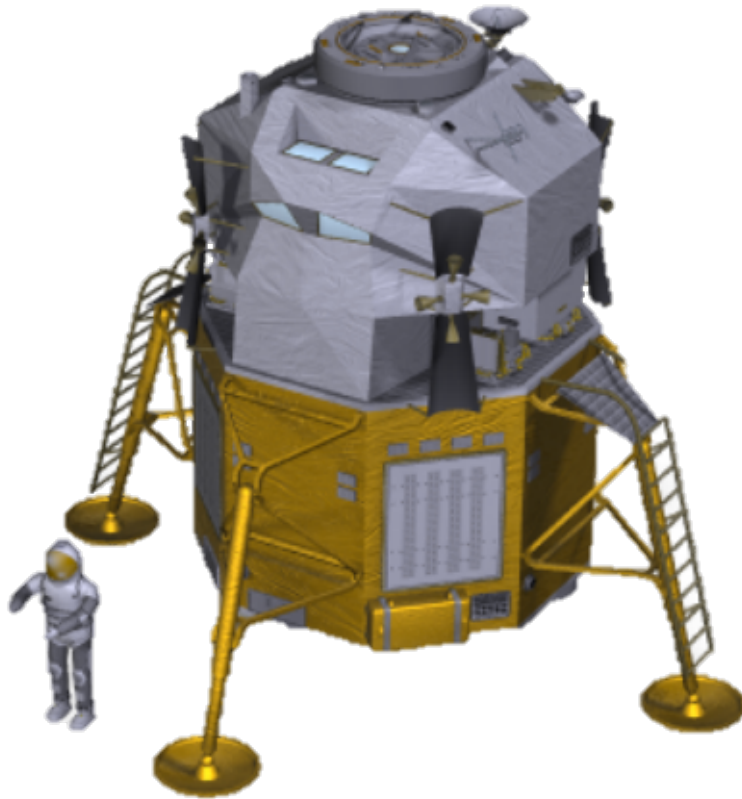


Figure 24. Boeing Reusable Lunar Lander ^[82]

Modifications

Since methane will not be produced in the processing facility on the Moon, the BRL engines needed to be modified to use LH_2 instead. Also, the current crew capacity was only two, but 6 crew members will need to get to the surface. Therefore, the vehicle was slightly modified to add a third crew member, and two BRL vehicles will be used to take the entire crew to the surface. A second vehicle also will provide redundancy in the event that there is a failure in one of the landers.

3.2.8. Crew Support Mission Overview

3.2.8.1. Initial Crew Operations

The main objective of crew operations on the Moon is to set up the $3,650\text{m}^2$ of solar panels required to operate the miners and processing facility. The solar panels will be brought down to the surface in the same shipment as the miners and processing plant and therefore will be located at the base of the crater. They will need to be loaded into a Magellan rover by the crew and transported up a 25° slope to the rim of the crater, where they will rest in eternal sunshine. ^[79]

Each day, 100m² of solar panels will be transported to the rim and installed by one team, with each Magellan rover and its 3 crew members considered a team. Teams alternate every other day; for example, Team 1 will work Monday, Wednesday, Friday and then have the weekend off, and Team 2 will work Tuesday and Thursday and will also have the weekend off. Then, the following week, the teams will alternate schedules. Using this operational schedule, all solar panels will be installed within 8 weeks. The next four weeks are specifically allocated for monitoring miner and processing plant operations in addition to completing any required maintenance. Science experiments, leisure activities and exercise will occur on off-days or weekends.

While the primary mission on the Moon is to set up the required resource acquisition infrastructure to get future crews to Mars, this lunar mission is also a testing grounds for new technologies and vehicles. The Magellan rover, while only the Mk2.0 version and not the Mk2.1 Mars version, as well as the modified Z-2 spacesuit are being tested on the Moon in partial gravity for the first time. This will provide the opportunity to make modifications and improvements before the long-duration Mars mission.

Consumables Mass and Volume Breakdowns

The required consumables for the initial crew will be delivered to the surface of the Moon with the rovers and will not need to be transported in the Dragon with the crew. The detailed breakdown of items in each category can be found in Appendix A.

Item / Category	Mass (kg)	Volume (m ³)
Hygiene	62	1.16
Medical	3	0.01
Clothing	157	0.87
Food	1267	3.46
O ₂	1139	3.22
N ₂	425	0.60
H ₂ O	3051	3.05
Miscellaneous	60	0.75
Total	6164	13.11

Table 6. Required Mass and Volume Breakdown

3.2.8.2. Long-Term Crew Support

In addition to the original crew, there will be 30-day duration maintenance missions once every 5 years in order to upkeep the facility and equipment. These crews will be comprised of 3 astronauts who will live and work in one Magellan rover with the second kept as a backup.

The individual missions of each of these maintenance crews will be determined through telemetry data received from health monitoring systems installed in the miners, solar panels and processing facility. However, the missions will likely consist of repairing solar panels, replacing the linear actuators on the miners, and replacing life-limited parts or parts that have worn down or failed.

These crews will need to bring all of their required consumables with them in their Dragon capsule and then down to the surface in the BRLL due to the long timespan between missions. The extended Dragon

trunk with its 34m³ of unpressurized volume will be utilized to store these consumables before they are transported over to the BRLL for descent to the lunar surface. Consumables will include food, clothing, medical products, hygiene products, oxygen, nitrogen and any specific science experiments that NASA wishes to conduct. The pressurized gas masses and volumes were calculated by a MATLAB code (see Appendix C). The detailed breakdown of items in each category can be found in Appendix A.

Item / Category	Mass (kg)	Volume (m ³)
Hygiene	10	0.20
Medical	3	0.01
Clothing	24	0.16
Food	158	0.43
O ₂	94	2.48
N ₂	168	1.22
Miscellaneous	30	0.40
Total	487	4.91

Table 7. Consumables Resupply Mass and Volume Breakdown

3.2.9. Spacesuits

In order for astronauts to be successful in their mission, they will require a versatile spacesuit that meets the following requirements:

- Maneuverable in both micro and partial gravity
- Zero prebreathe capability
- Comfortable for long-duration EVA
- Suitport capabilities
- Safety harness
- Sustainable LSS system
- HUD system
- Durable and maintainable suit system

After extensive research into TRL5 or higher suits including the I-Suit (3rd generation), H-suit (Mk3 hybrid), and the ILC Dover Z-2, the Z-2 was chosen as the option with the most features and the fewest number of required modifications in order to meet all requirements. The Z-2 is a hard/soft shell hybrid suit and at only 63 kg is fairly light and maneuverable, which is conducive for partial or micro gravity environments.^[219] Astronauts can be 3-D scanned and modeled in order to help build a Z-2 that fits them more precisely than any other spacesuit in the past, which increases comfort.^[217] In addition, the upper torso section is resizable, which for a 13-year duration mission is important in the event that astronauts grow or shrink or need to use a suit that is not theirs for emergency egress. The hard, impact-resistant composite upper torso increases the durability of the suit, and is also where the built-in suitport is located.^[215] This is an extremely important feature in order for astronauts to travel in-and-out of the Magellan rovers and the Mars habitat modules once they arrive on the surface. The life support system is sustainable through the use of a regenerative Rapid Cycle Amine Swingbed CO₂ scrubber, which should reduce maintenance time between EVA missions. Also, equally as important is the operating pressure range, from 0 to 8.4 psi, which allows this suit the capability to be used without any prebreathe time. In

the event of an emergency, having a zero prebreathe suit is far safer for crews, and also increases productivity during regular operations because astronauts only need about 20 minutes to get into the suit rather than the hours of prebreathe prior suits required. In addition, with the ability to vary the pressure, astronauts can begin an EVA at a higher pressure for zero prebreathe, then once they have begun the EVA, gradually decrease the pressure in order to decrease the differential between the suit pressure and outside environment to increase mobility.^[216]

In addition to all the features currently included in the design will be several that are specific to this mission. A safety harness will be built into the structure of the suit so an astronaut can clip a carabiner, located on the hard upper torso, and the harness will distribute the load throughout the suit. These clips will be utilized by crew members mainly during construction activities and descent from landers on the the surfaces of the Moon and Mars.

Another special feature, the BAE QWarrior HUD system, will be added to the suit in order to increase productivity during EVA and allow for better monitoring of suit systems. The BAE QWarrior was developed for soldiers on the battlefield and can provide enhanced situational awareness. This HUD is a light-weight, high resolution,^[214] fully-color, translucent display, which allows symbols, text and video to be seamlessly overlaid on the user's actual field of vision. It has the capability to display waypoints in addition to paths on how to navigate to those locations. It can track other personnel and vehicles, which during an EVA is an extremely attractive features because it ensures that if an astronaut is injured, other crew members can easily track their location and the navigational aids would help ensure that they reach them as quickly as possible.^[213]

3.3. Fuel Transport Vehicle

3.3.1. Overview

The Fuel Transfer Vehicle (FTV) will have a payload consisting of propellant tanks, filled with liquid hydrogen and liquid oxygen processed on the Moon's surface. This propellant will be meant for the refueling of multiple SLS upper stage vehicles. The FTV's purpose is to transfer this propellant from the surface of the Moon to the fuel depot located at the L1 Lagrange Point.

3.3.2. Design Constraints

The Fuel Transfer Vehicle (FTV) had to be able to transfer approximately 110t of propellant to the EML1 Fuel Depot per SLS upper stage in need of refueling. The maximum number of vehicles that the EML1 Fuel Depot will need to refuel without an FTV refueling in between is three (SLS upper stage) vehicles. An SLS upper stage vehicle uses approximately 110t of propellant to reach EML1 from Low Earth Orbit. If 110t is required for each upper stage, then three upper stages in a row would require 330t total. The 110t value is conservative; in reality, the value is closer to 107t. The amount that the FTV could carry as a payload for a single trip was the main determining factor in the frequency of these refueling trips. The desired payload mass for a single trip was 40t. Taking into account the structural mass of the FTV (estimated 15t), payload mass (estimated 40t), I_{sp} of the RL10 engine (460 seconds), and the total delta-V cost from the surface of the moon to L1, an optimal starting propellant mass was determined. The two plots below (Figures 25 and 26, respectively) display the results of this calculation. There are two plots in

order to account for the slight change in distance between the Moon and the EML1 Lagrange point; Figure 25 uses the maximum L1 radius, while Figure 26 uses the minimum L1 radius. The total range of distance was determined to be approximately $5.81(10^4)$ km to $6.49(10^4)$ km, which provided a range of delta-V costs.

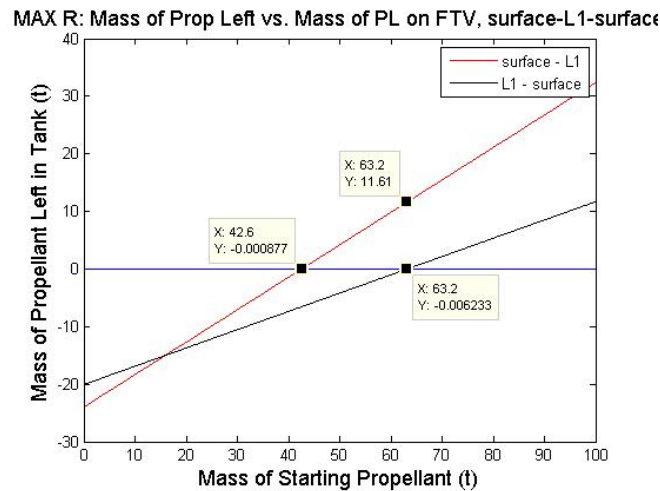


Figure 25. MAX R: Propellant Massing for FTV

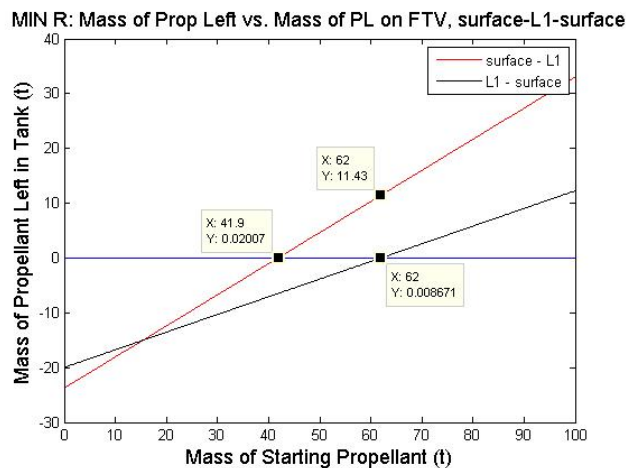


Figure 26. MIN R: Propellant Massing for FTV

According to these plots, the difference in propellant usage to reach L1 at its two most extreme distances is very slight. The plots show that the FTV requires approximately 43t of propellant to reach L1 with a 40t payload. Specifically, the plots are showing that the FTV will arrive at L1 with zero propellant remaining in its tank if it were to start off with only 43t of propellant. Therefore, this amount was too small to be the starting propellant mass. The FTV is not refueling at the L1 depot, so it would require enough initial propellant to reach L1 and make it back to the surface. The plots show that if the starting propellant mass is about 63t, the FTV can launch from the surface of the Moon, reach L1, and fly back to

the surface with zero propellant to spare. There is a 4% margin built into each of the delta-Vs used in these calculations. Therefore, 63t is a conservative estimate for the starting propellant mass of the FTV. This was the design choice for FTV propellant mass in order to successfully carry out the mission of transporting 40t to the L1 depot.

3.3.3. Structure

Tank Design

The possible tank designs included spherical tanks or cylindrical tanks with rounded endcaps. Both designs were initially considered, but spherical tanks were eventually chosen to reduce the structural mass of the vehicle. In addition, spherical tanks reduced the height of the vehicle which allows it to fit easier into an SLS payload fairing while also lowering the center of gravity for easier landing.

The fuel transport vehicle has two fuel tanks, one with LH₂ and one with LOX. The tanks were sized to hold 103 metric tons of total fuel, with 40 metric tons for fuel as a payload and 63 metric tons of fuel for flight. The RL-10B engine was chosen so that the FTV would use the same engine as the upper stage of SLS. The fuel was split into a ratio of 5.85:1 LOX to LH₂ due to the RL-10B engine choice. The FTV is able to deliver 6.84 metric tons of LH₂ and 33.2 metric tons of LOX to the fuel depot at the L1 LaGrange point between the Earth and Moon. The diameter of each tank was calculated to fit the volume of each liquid. The dimensions of the two tanks are listed below in relation to each other.

Tank	Diameter (m)	Thickness (m)
LOX Tank	4.44	0.05
LH ₂ Tank	6.62	0.07

Table 8. FTV Tank Dimensions

Since the FTV is in a permanently shadowed region of the moon, it does not have any active cooling system inside the tanks. The FTV only briefly travels between Shackleton Crater and the L1 fuel depot, so the boil-off during transit is assumed to be within the fuel margin. The FTV tanks are simply hollow shells of Aluminum-6061 which reduces structural mass. The tanks are only expected to experience pressure loads due to the required pressure needed to maintain liquid oxygen and liquid hydrogen inside the tanks. The pressure needed to maintain the fuel at a liquid state is 1 MPa for hydrogen and 4.7 MPa for oxygen. The expected stresses are listed below, with a safety factor of 2 used to comply with NASA technical standard.^[197]

Structure	Limit Load (MPa)	Factor of Safety	Margin of Safety
LOX Tank	22.2	2	0.24
LH ₂ Tank	23.6	2	0.17

Table 9. FTV Tank Loads

Inner Structure

The FTV was designed to withstand several extreme loads. The highest design load on the FTV would come from a crash load on one landing strut at 5g. This load might occur if the avionics or propulsion fails during the landing on the moon. The next highest loads would come from the force of that crash load when it is distributed across the intertank truss (the truss connecting the LH₂ tank to the LOX tank) and the docking truss (the truss connecting the LOX tank to the docking mechanism). Other possible loads that the inner trusses are expected to experience include loads due to thrust and docking, but the crash load is the design load since it is the highest. The inner trusses are made of Aluminum-6061 with varying radii and thicknesses. All of the trusses and struts are designed with a safety factor of 3, since failure in any of the trusses would lead to loss of the vehicle. The dimensions for the trusses and the expected loads are shown below.

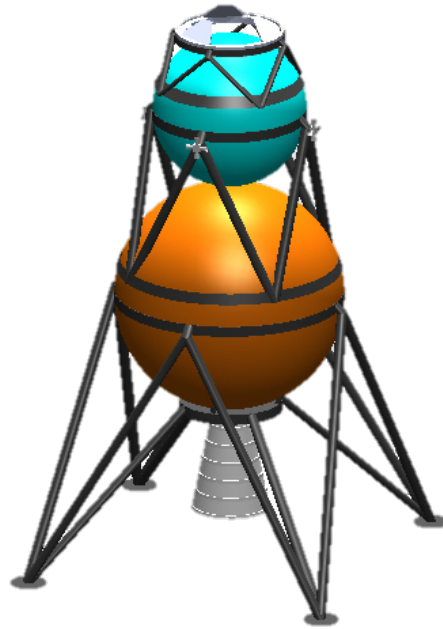


Figure 27: FTV Inner Structure

Structure	Outer Radius (m)	Length/s (m)	Thickness (m)	Limit Load (MPa)	Factor of Safety	Margin of Safety
Landing Struts	0.15	8.80, 8.98	0.02	16.6	3	0.11
Intertank Truss	0.05	5.64	Solid rod	14.0	3	0.32
Docking Truss	0.05	2.69	0.02	10.9	3	0.69

Table 10. FTV Inner Structure

Outer Structure

The fuel transport vehicle has a micrometeorite shield to protect it during transit between the Moon and the EML1 fuel depot. The micrometeorite shielding is made of a 1 centimeter thick aluminum plating that will wrap around the outermost radius of each section of the inner trusses as well as the upper part of the engine block. The landing struts will be wrapped in Kevlar to provide additional protection, since a failure of the landing struts would lead to mission failure. The structural mass of the fuel transport vehicle with shielding is 15.4 metric tons, and the mass when fully fueled is 117.9 metric tons. The center of gravity for the fully loaded FTV is at 8.9 m from the ground while the emptied FTV's center of gravity is at 5.8 m from the ground. The outer structure of the FTV, and the centers of gravity for different configurations are shown below.

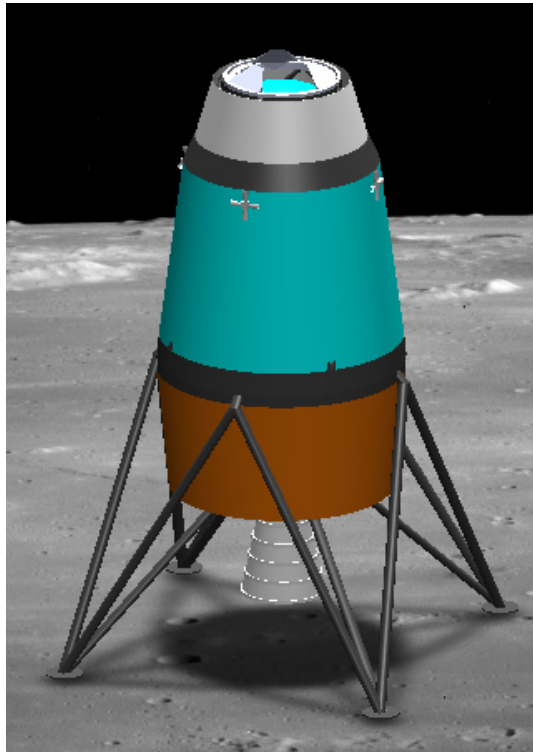


Figure 28: FTV Outer Structure

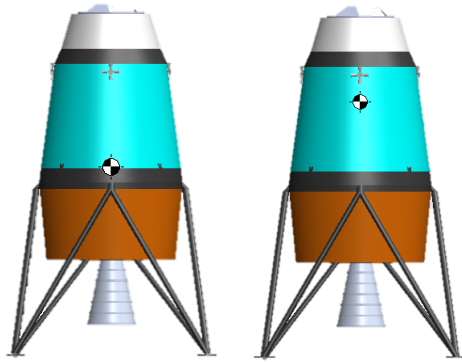


Figure 29: FTV Centers of Gravity

3.3.4. FTV Avionics

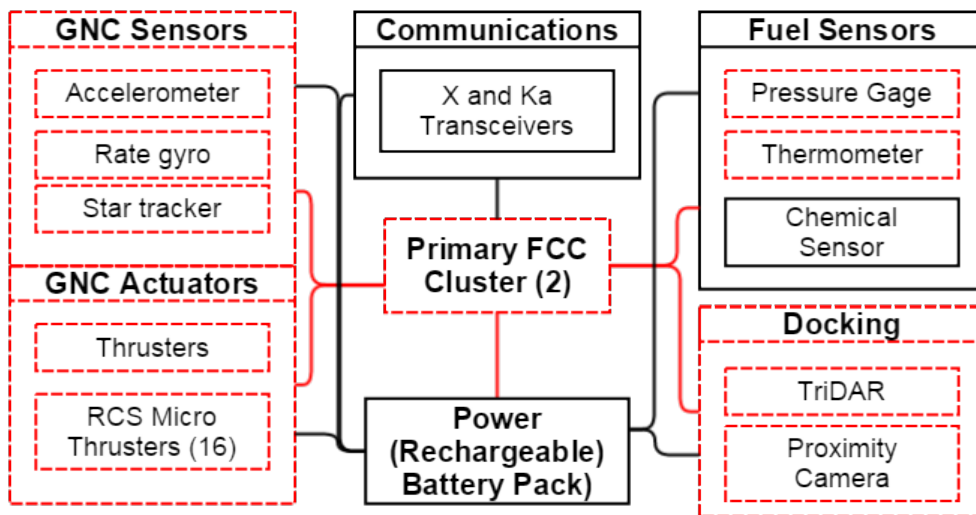


Figure 30. FTV Avionics Block Diagram

GNC

The FTV uses stander GNC sensors for its ascent and descent maneuvers to the fuel depot. This includes the accelerometer, rate gyro and star tracker. The vehicle is actuated by its specially designed RCS Micro-Thrusters that give the vehicle maximized stability and direction control. To assist with docking to the Lunar Fuel Depot, the FTV uses TriDAR.

Docking Mechanisms

To assist with docking to the Lunar Fuel Depot, the FTV uses TriDAR in conjunction with the proximity camera.

Housekeeping

To monitor the health of the storage tanks, the FTV tanks are equipped with pressure gages, thermometer, and chemical sensors. The data collected by these instruments will be available to be uplinked to other spacecraft using the X or Ka band transceiver.

3.4.EML1 Fuel Depot

3.4.1. Introduction

The EML1 Fuel Depot, as its name suggests, is located at the Earth-Moon L1 Lagrange Point located between the Earth and the Moon. The L1 Lagrange Point is an unstable Lagrange point, meaning that objects stationed there without any stabilizing thruster system will gradually drift away from its initial desired location. As a result, station-keeping is required. The propellant for the RCS thrusters providing station-keeping for the depot will be drawn directly from the LOX and LH₂ tanks. The fact that the propellant would be decreasing slightly over the course of year due to this was taken into account.

The initial refueling concept still consisted of the placement of an in-space fuel depot, but the depot was to be placed in lower Lunar orbit (LLO) at about 100km above the Moon's surface.

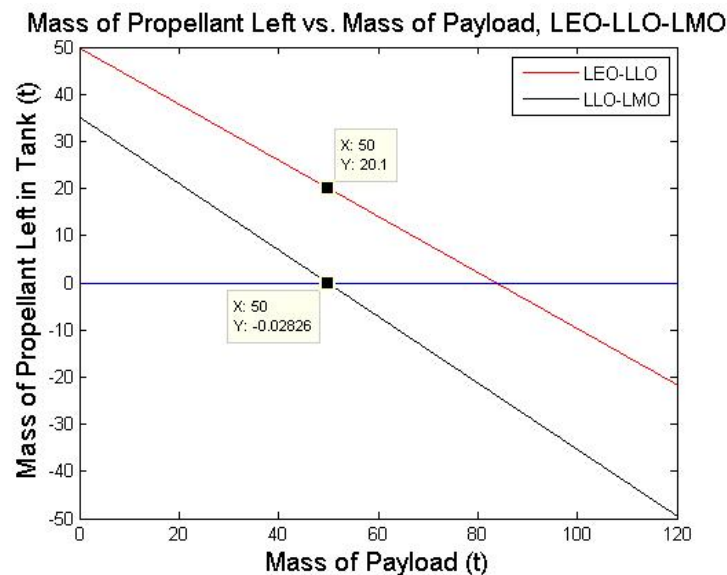


Figure 31. Mass of Prop Left vs Mass PL, LEO-LLO-LMO

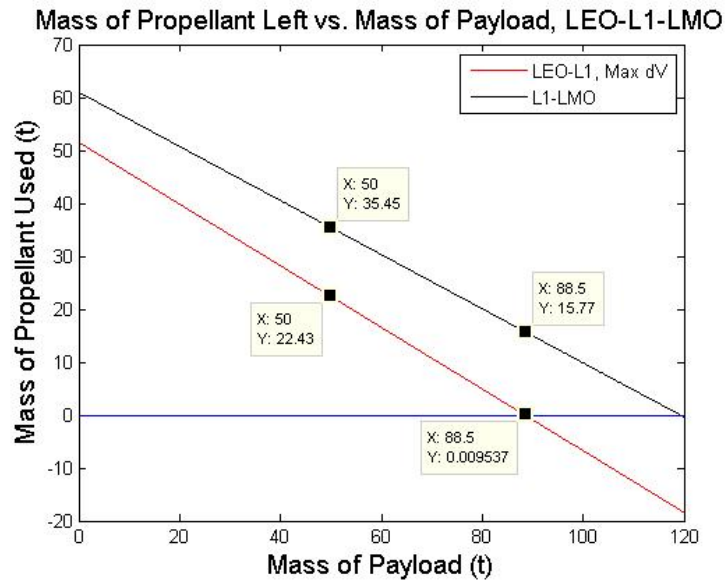


Figure 32. Mass of Prop Left vs Mass PL, LEO-L1-LMO

If the fuel depot had been placed in LLO, the SLS upper stage would require more fuel to enter a parking orbit. This would mean that more propellant would be required to fully refuel the SLS upper stage tanks, which would in turn increase the amount of propellant that the fuel depot would have to contain. An increase in the propellant requirements would then cause an increase in every aspect of the fuel depot, particularly mass and power requirements. By placing the fuel depot in the EML1 position, approximately 3t of propellant is saved during the trip there. This reduces the overall mass and power requirements of the fuel depot. The main advantage that the EML1 position has over a placement in LLO is the difference in propellant requirements to move from the fuel depot to Low Mars Orbit (LMO). Figure 31 indicates that the SLS, with a payload of 50t, would leave from LLO and arrive at LMO with zero propellant remaining in its tanks. A 4% delta-V margin was accounted for in these calculations, so technically this would be fine. However, excess propellant from the SLS tanks will be needed to supply the LMO Fuel Depot (to be discussed in the LMO Fuel Depot section). Therefore, excess propellant is required. Figure 32 shows that an SLS that leaves EML1 with a 50t payload would arrive in LMO with about 35t of propellant to spare. This propellant could then be deposited in the LMO fuel depot and kept in good condition for future use.

Figure 32 (above) shows that the limiting factor in the case of the EML1 depot (as opposed to the LLO depot option) is the payload mass that can be carried from LEO to L1. The maximum payload mass that can be carried by the SLS upper stage from LEO to L1 is about 88.5t. With a payload of 88.5t, the SLS upper stage would arrive at the EML1 Fuel Depot with nearly zero propellant remaining in its tanks. This would then require 129t of propellant from the depot to fully refuel the propellant tanks. A complete refuel at the depot would allow the SLS to arrive at LMO with nearly 16t of propellant to spare.

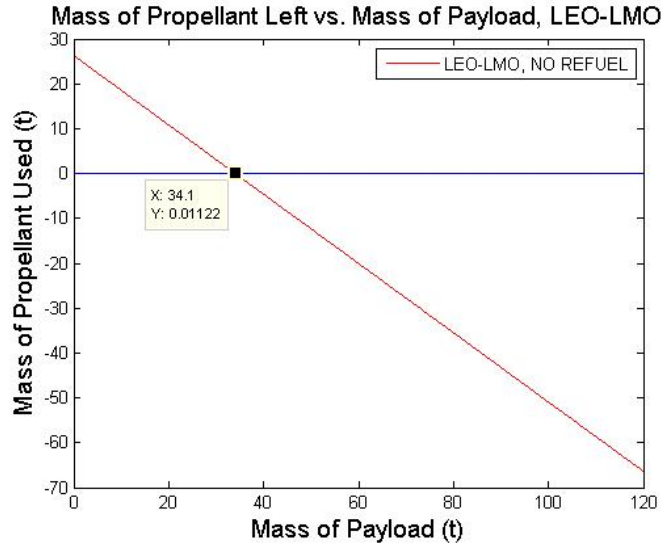


Figure 33. Mass of Prop Left vs Mass PL, LEO-LMO

Figure 33 (above) shows that the maximum payload mass that the SLS upper stage can carry from LEO to LMO with no refuel along the way is about 34t. The addition of the fuel depot at EML1 allowed the maximum payload to be increased by 54.5t, or about 260%, creating an 88.5t payload. Once payloads began being assigned to rockets, it became clear that almost 90t payloads would often not fit into the SLS payload fairing due to volume constraints, and that an after cargo payload containing habitat pieces, landing vehicles, and secondary payloads would be approximately 50t. When volume was discovered to be the limiting factor for payload size, it was decided to set the “average” payload mass to 50t, and design the depot around the constraint that it must support three refuels of the SLS upper stage that were large enough to get a 50t payload to LMO. Another way that the SLS volume constraint set the size of the propellant depot was that it actually limited the size that they hydrogen and oxygen tanks could be. Each hydrogen tank is almost the maximum size that can fit in the SLS payload fairing, so a larger depot would require extra launches in order to complete the depot. For these reasons, the average 50t payload was chosen, and the 330t capacity propellant depot was designed.

Dry Mass	10 t
Gross Mass	340 t
Dimensions	LOX tank height: 9.4m LOX tank diameter: 7.2m LH ₂ tank height: 12.7m LH ₂ tank diameter: 7.7m Width: 26 m
Launch Date	Sept 2025, Jan 2026, May 2026

Launch Vehicle	SLS Block IB
Destination	Earth-Moon L1
Power	339 W
Payload	330 t of fuel

Table 11. Specifications of EML1 Fuel Depot

3.4.2. Design Overview

Tank Design

The EML1 fuel depot is designed to hold 330t of fuel for the upper stage of the SLS. Since the upper stage of the SLS uses an RL-10B engine, the fuel on the depot is split into a 5.85:1 ratio, which is the fuel ratio for that engine type. The fuel ratio means that the fuel depot would need to hold 273.6t of LOX and 56.4t of LH₂. In order to maximize storage volume, the tanks were designed to be cylindrical with spherical endcaps. The tanks themselves are limited radially by the payload fairing of the SLS, which means that the tanks would have to be fairly tall to accommodate all of the fuel. The storage volumes for LH₂ and LOX were calculated based on their respective densities, and then the lengths of the cylindrical portions of the tanks were calculated to fit the storage volume into a cylindrical tank with spherical endcaps. The high density of LOX made it easy to store in a relatively short tank, but the low density of LH₂ lead to very long tanks. A single LH₂ tank would not be able to fit in the payload fairing of an SLS due to its length, so the LH₂ tank was split into two tanks of equal lengths. In order to balance mass for the whole structure, the two LH₂ tanks are connected on either side along the cylindrical portion of the LOX tank. A more detailed explanation of the analysis behind the design of the EML1 depot is included in Appendix C. The dimensions for the tanks and their arrangements are listed below, as well as the full configuration of the fuel depot.

Structure	Diameter (m)	Total Length (m)	Length of Cylindrical Portion (m)
LOX Tank	7.2	9.40	2.90
LH ₂ Tank	7.7	12.7	5.66

Table 12: Fuel Depot Dimensions

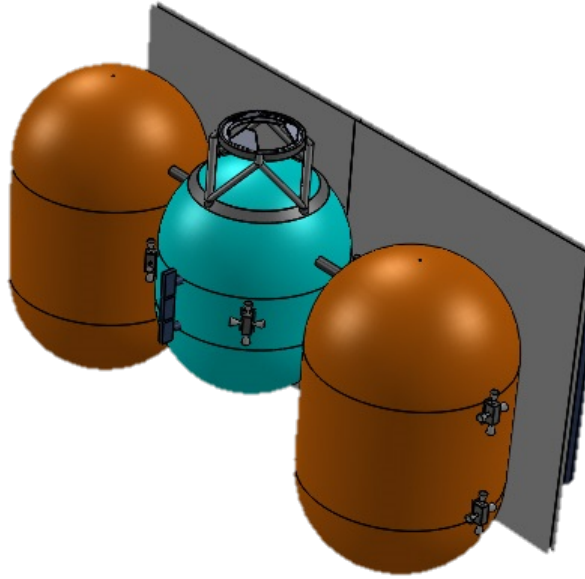


Figure 34. EML1 Fuel Depot Configuration

3.4.3. Structural Design

Loads in Tanks

The highest expected load for the tanks will come from the pressure inside the tanks. In order for the hydrogen and oxygen to remain at a liquid state, the LH₂ and LOX tanks will need be pressurized to 1 MPa and 4.7 MPa respectively. All three tanks will be made of Aluminum-6061, so each of their thickness were estimated to minimize structural mass while also satisfying a safety of 2 as per NASA technical standard.^[197] The calculated stresses in the tanks are shown in the table below.

Structure	Limit Load (MPa)	Factor of Safety	Margin of Safety
LOX Tank	28	2	0.53
LH ₂ Tank	29.3	2	0.43

Table 13. Loads on Fuel Depot Tanks

Intertank Connectors

The LH₂ tanks and LOX tank are connected via the intertank connectors. The intertank connectors are simply hollow rods made of Aluminum-6061. The highest expected load for the intertank connectors should come from the moment created by the RCS thrusters firing. The RCS system only briefly fires twice per year to correct the orbit of the EML1 depot around the LaGrange point, but in an emergency the RCS system might have to fire for a longer period all at once. The intertank connectors are designed to withstand an emergency RCS thrust load, with a safety factor of 3 since a failure at the connectors would

destroy the depot and lead to loss of mission. The dimensions and loads analysis of the intertank connectors are shown in the table below.

Structure	Outer Radius (m)	Thickness (m)	Length (m)	Limit Load (MPa)	Factor of Safety	Margin of Safety
Intertank Connector	0.075	0.02	1	14.7	3	0.88

Table 14: Intertank Dimensions and Loads

Docking

The docking mechanism on the fuel depot is the International Low Impact Docking Standard. This docking standard is easily adaptable between all vehicles that will either refuel or remove fuel from the fuel depot, and so it will be used on the fuel transport vehicle as well. The highest expected load from docking would be limited to 9000 N, since the docking mechanism will not latch at a higher impact load. However, the highest expected load would actually come from launch at roughly 5g. The docking truss is made of hollow rods, with the same dimensions and loads analysis as for the FTV shown below.

Structure	Outer Radius (m)	Length/s (m)	Thickness (m)	Limit Load (MPa)	Factor of Safety	Margin of Safety
Docking Truss	0.05	2.69	0.02	10.9	3	0.69

Table 15: Docking Truss Dimensions and Loads

3.4.4. Active and Passive Cooling System

In order to create efficient and manageable refueling operations, the propellant depots required a zero boil-off (ZBO) system. ZBO propellant storage is still in the experimental phase of development, but most of the components of the system: the multi-layer insulation (MLI), insulating foam, heat shields, and cryocoolers, have been demonstrated in lab and space settings, and are above TRL 5. Some issues with the current systems include that most combinations of these components are not quite at ZBO and most of these systems currently designed function at much smaller scales than the 330t EML1 propellant depot.

Zero boil-off cryocooler technology is a topic of great interest in the aerospace community currently because of its many possible applications, including the development of In-Situ Resource Utilization (ISRU) and to enable longer space missions^[118]. This project will aim to use the technology for ISRU, and has identified ZBO as a critical technology for making the propellant depots possible.

A trade study of five different ZBO propellant storage designs was conducted, and the results are shown in Table 16. Unfortunately, many of the numbers for comparison were not listed in the papers consulted, and these papers were part of a small group that could be found. It seems that there is not yet much published on this research, but the promise of ZBO propellant storage systems in the near future is made in each. For the purpose of this project, an average power requirement per volume of propellant was found and then scaled by the propellant volume of the fuel depot. When finding the power requirement, case #3 was not considered because it was much higher than the other two cases with power requirements listed, and seemed to be an outlier. The total power requirement for the active cooling system was found to be 19.6kW. It was also noted that the cooling systems had between 30 and feature 35 layers of MLI, along with a layer of insulating foam. Most designs considered in the trade study mentioned this foam layer, but did not give much detail on how thick it might be, but case 1 did include its mass in the total cooling mass for the design, and that was accounted for when calculating this project's propellant depot masses.

Case	Tank volume (m ³)	Propellant type	MLI Layers	MLI and Foam Mass (kg)	Power Req (W)	Power Requirement/ Volume of Propellant
1 ^[108]	14.1	LOX	30	25.1	290	20.6
2 ^[109]	11.5	LN ₂	34	26	150	13.1
3 ^[110]	18.1	-	-	-	11500	635
4 ^[111]	87.1	LH ₂	45	-	-	-
5 ^[112]	44.6	LOX	30	-	-	-

Table 16. Trade study of cryogenic storage systems

3.4.5. Station-Keeping

Based on the estimates made by Folta and Vaughn^[203], it was determined that the yearly delta-V cost for a vehicle stationed at EML1 would require approximately 10 m/s to 150 m/s. Assuming that Reaction Control System (RCS) thrusters designed for this vehicle will have an I_{sp} of at least 350 seconds, it was determined that the range of propellant costs on a yearly basis were between 1.0t and 14.5t. These values were determined based on the assumption that the fuel tanks were at its maximum mass of 330t. At this mass, the fuel tanks are completely full; the payload mass of this depot would never exceed this amount.

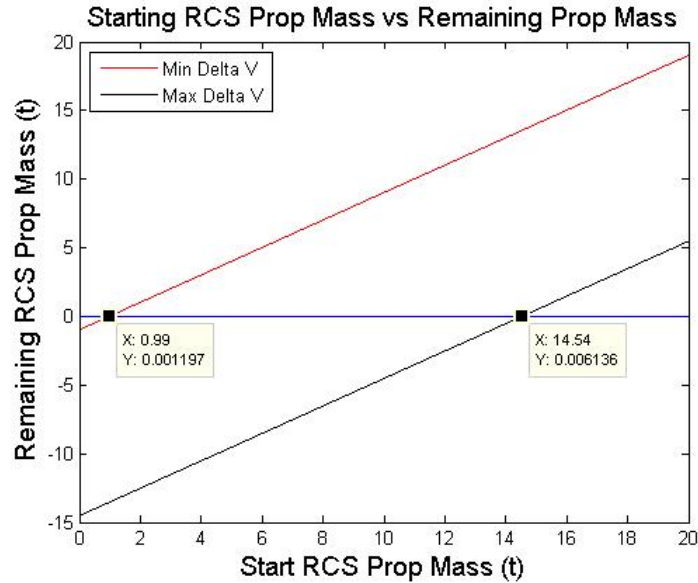


Figure 35. Starting RCS Prop Mass vs Remaining Prop Mass

3.4.6. Reaction Control System

Propellant Limitations

To maintain the goal of ultimate independence and sustainability, the RCS thrusters had to be limited to using liquid oxygen (LOX) and liquid hydrogen (LH₂) as propellant. No other propellant would be available, due to the fact that only LOX and LH₂ were being processed on the Moon and sent up to the fuel depot. RCS thrusters that could use this as propellant would be extremely useful; they would be able to draw their propellant directly from the fuel inside of the EML1 Depot tanks. The amount that they would require was discussed in the previous section, and the physical amount of propellant they would draw from the tanks has been accounted for in the propellant requirement calculations.

Decision of desired I_{sp}: multiple step process to determine what I_{sp} we should aim for with the thrusters.

The initial step in the design of these thrusters was deciding upon a desired I_{sp}. The best possible I_{sp} for the RCS thrusters would be about 450 seconds. However, to remain conservative, a range of 300 to 400 seconds was initially used and tested. Using a maximum delta-V cost of 150 m/s per year and a maximum fuel depot mass of 340t (including the 10t tank mass), an instantaneous acceleration could be calculated. Before doing so, it was decided that the system would be designed for a 6% duty cycle; in other words, these thrusters would fire twice per month to maintain the depot's position (summing up to 24 days of a total 365 days of use). With this in mind, an instantaneous acceleration was calculated.

$$dV_{max} = 150 \text{ m/s}$$

$$g_0 = 9.81 \text{ m/s}^2$$

$$m_{depot} = 340 \text{ t}$$

$$a_{instant} = \frac{dV_{max}}{\text{seconds in 1 year} * (\frac{24}{365})} = \frac{150}{(1 * 365 * 24 * 3600) * (\frac{24}{365})} = 7.23(10^{-5}) \text{ m/s}^2$$

$$F_{thrust} = m_{depot} * a_{instant} = 24.6 \text{ N}$$

From the instantaneous acceleration, the required thrust force for each thruster was determined to be about 24.6N. However, the nozzle of the thruster would need to be positioned at an angle in order to reduce the problem of plume impingement. The exhaust leaving the nozzle could potentially damage the exterior material of the propellant tanks. Therefore, it would be desirable to angle the nozzles away from the tanks. It was decided that the nozzles would be positioned at a 15° half-angle. This 15° angle would cause the thrust vector to have both a vertical and horizontal component, rather than just a horizontal component. Figure 36 below displays this situation.

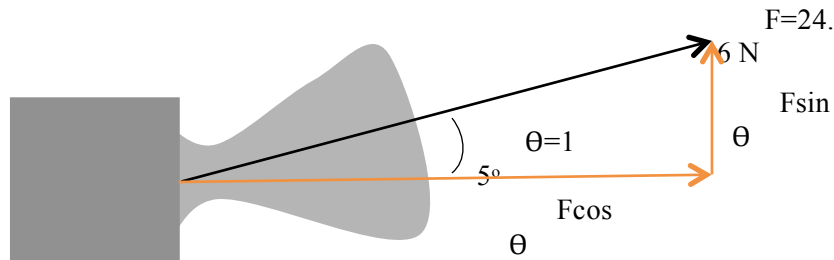


Figure 36. Diagram of angled thruster nozzle

The overall thrust would be less than 24.6N due to the fact that only the horizontal component ($F \cos \theta$) of the thrust force is contributing to the horizontal movement of the vehicle, instead of the full 24.6N of thrust. To maintain a horizontal thrust force of 24.6N, as was originally intended, the total thrust would need to be increased so that the horizontal component by itself is equal to 24.6N. The following relationship was used to determine this desired total thrust.

$$T_{des} \cos \theta = 24.6 \text{ N}$$

Provided that $\theta = 15^\circ$, T_{des} was determined to be 25.5N. Therefore, a thrust force of $F_{thrust} = 25.5\text{N}$ would be required to maintain a horizontal thrust of 24.6N.

The next step in the design process was to determine the mass flow rate required for this system in order to achieve the required thrust. The following equation was used to determine this value.

$$\dot{m} = \frac{F_{thrust}}{I_{sp} * g_0}$$

However, there was still the matter of determining the optimal I_{sp} for the thrusters. In order to choose a desired I_{sp} , the impact that changing the I_{sp} slightly had on the propellant usage was studied. Tsiolkovsky's rocket equation was used to observe this effect.

$$\Delta v = I_{sp} * g_0 * \ln \left(\frac{m_{initial}}{m_{final}} \right)$$

The delta-V (Δv) used in this analysis was the maximum possible yearly delta-V cost, 150 m/s. By observing the change in the mass ratio over a range of I_{sp} values, the impact of the I_{sp} could be observed. The final mass would be slightly less than the initial mass, due to the fact that a certain amount of propellant mass is lost while carrying out the delta-V burn required. As the mass ratio increases, it indicates that the final mass is becoming lower and lower relative to the initial mass. In other words, less fuel is being used up during the burn. In this way, a high specific impulse is desirable. It would allow the exhaust velocity to increase while using minimal propellant. However, a high specific impulse would also require a much larger combustion chamber temperature, as well as a much lower P_e/P_0 ratio (exit pressure/ chamber pressure). A decreasing pressure ratio indicates that the chamber pressure is becoming increasingly larger in comparison to the exit pressure. A higher chamber pressure would require a higher mass chamber to withstand the force. This would create further challenges with the materials being used for the thrusters, the minimizing of thruster mass, and the maintaining of the operational state of the thrusters.

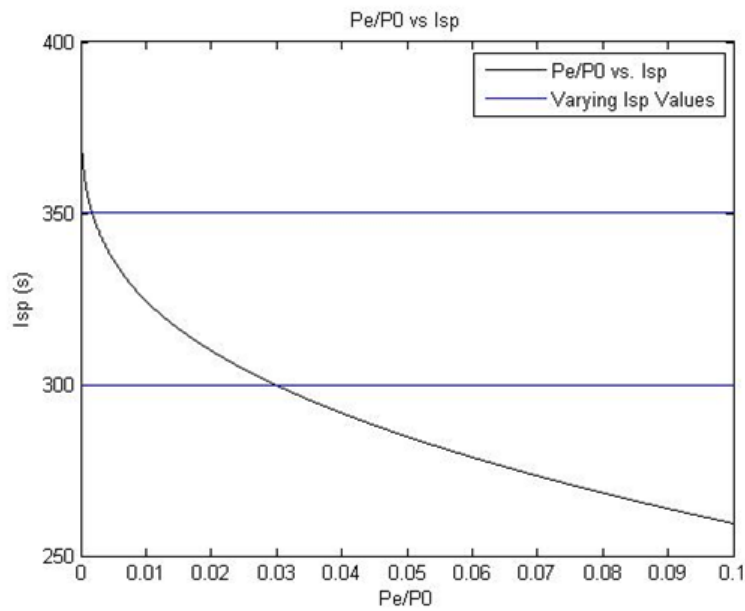


Figure 37. P ratio vs Isp

The figure above shows an exponential increase in the pressure ratio as the I_{sp} decreases. An I_{sp} of 400 seconds requires a significantly lower pressure ratio than I_{sp} of 350 seconds, and the same can be said for an I_{sp} of 350 seconds in comparison to 300 seconds. The figure below displays the change in the mass ratio (initial mass/ final mass) that occurs as a result of increasing or decreasing I_{sp} .

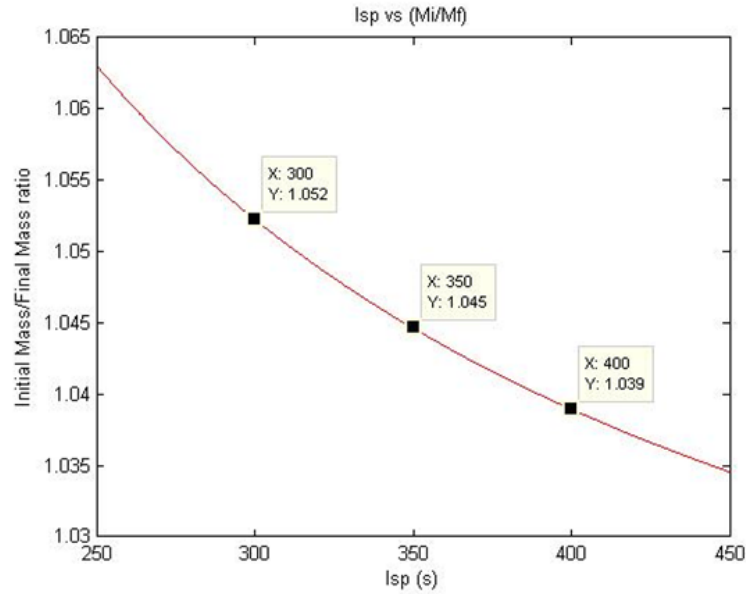


Figure 38. I_{sp} vs Mass Ratio

According to this plot, increasing the I_{sp} from 350 seconds to 400 seconds decreases the mass ratio by about 0.6 %. This means that the propellant mass required by a thruster with an I_{sp} of 350 seconds is approximately 1.006 times that of a thruster with an I_{sp} of 400 seconds. Such an increase is negligible, therefore making it impractical to keep the specific impulse at 400 seconds. By designing the thruster to have a specific impulse of 350 seconds, the pressure ratio is much more reasonable (about 10^{-3}) and the increase in propellant mass is extremely slight. With a desired I_{sp} and pressure ratio, the system's exhaust velocity, exit temperature, and exit Mach number could be determined.

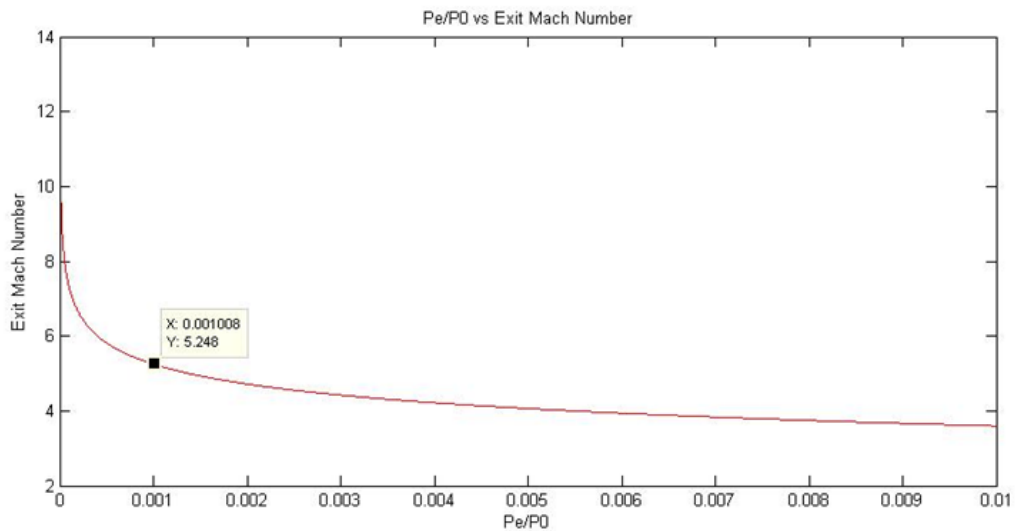


Figure 39. P ratio vs Exit Mach Number

Nozzle Sizing Methods

According to the previous two figures, a pressure ratio of 10^{-3} corresponds to an exit Mach number of about 5.3. Figure 40 shows that a Mach number of 5.3 corresponds to an area ratio (exit area/throat area) of 45. By choosing an exit diameter of 5.0cm, the throat diameter was calculated to be 7.5mm. This is how the sizing of the nozzle was determined.

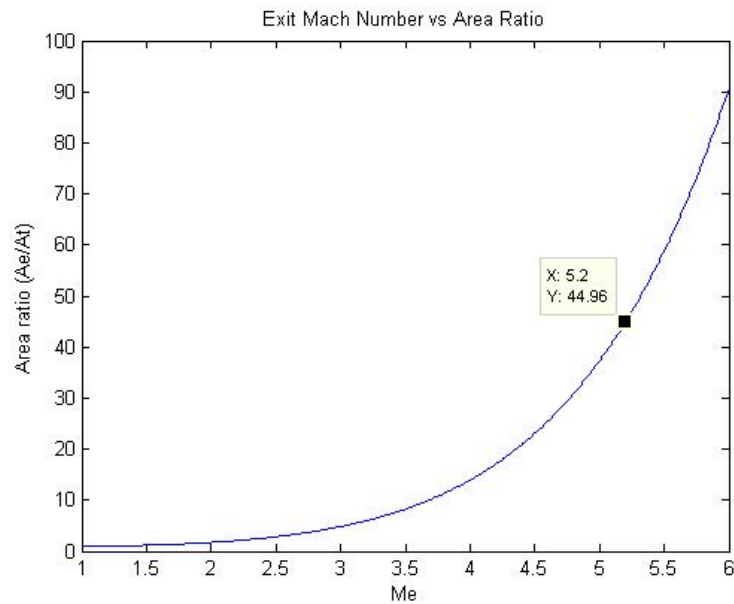


Figure 40. Area ratio vs exit mach number

RCS Power Calculations

The following equations were used to determine the pump power requirements for the EML1 Depot RCS thrusters. The pressures within the fuel and oxygen tanks were chosen to maintain the liquid state of the propellant. The figure below shows the graphical representation of power requirement calculations.

$$p_{1,ox} = 4.7 \text{ MPa}$$

$$p_{1,fuel} = 1 \text{ MPa}$$

$$p_2 = 15 \text{ MPa}$$

$$\eta_{pump,fuel} = \eta_{pump,ox} = \eta_{pump} = 0.8$$

$$\rho_{ox} = 71 \text{ kg/m}^3$$

$$\rho_{fuel} = 1141 \text{ kg/m}^3$$

$$P_{pump,fuel} = \frac{\left(\dot{m} * \frac{1}{6.85}\right) (p_2 - p_{1,fuel})}{\rho_{fuel} * \eta_{pump}} = 267 W$$

$$P_{pump,ox} = \frac{\left(\dot{m} * \frac{5.85}{6.85}\right) (p_2 - p_{1,ox})}{\rho_{ox} * \eta_{pump}} = 71.6 W$$

$$P_{total} = P_{pump,ox} + P_{pump,fuel} = 339 W$$

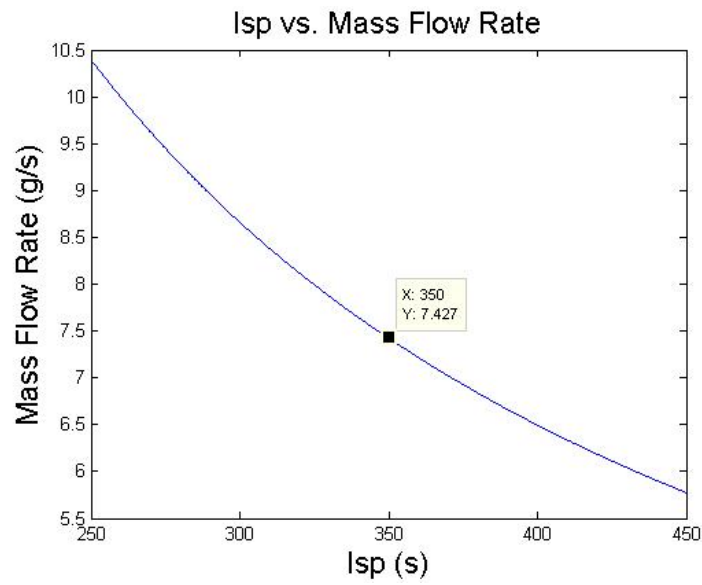


Figure 41. Isp vs Mass Flow Rate

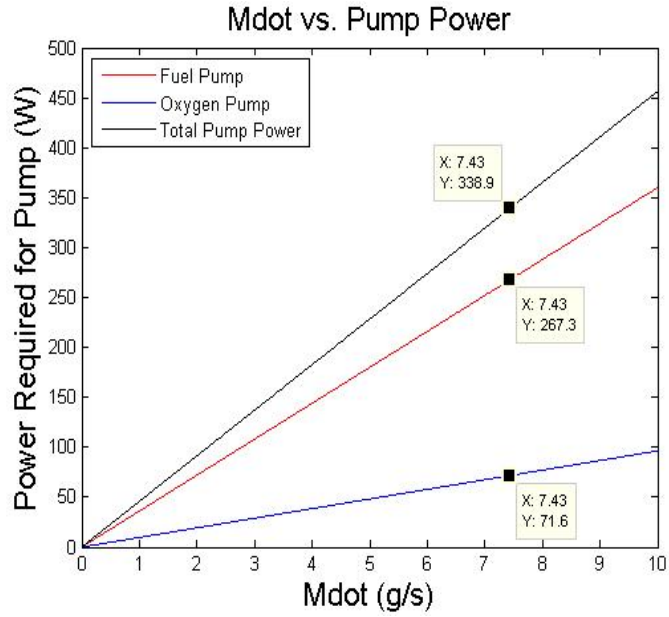


Figure 42. Mdot vs Pump Power

3.4.7. Power Requirements and Avionics

The two fuel depots, located in Mars orbit and at the L1 Lagrange point will have identical avionics packages as seen in the image below.

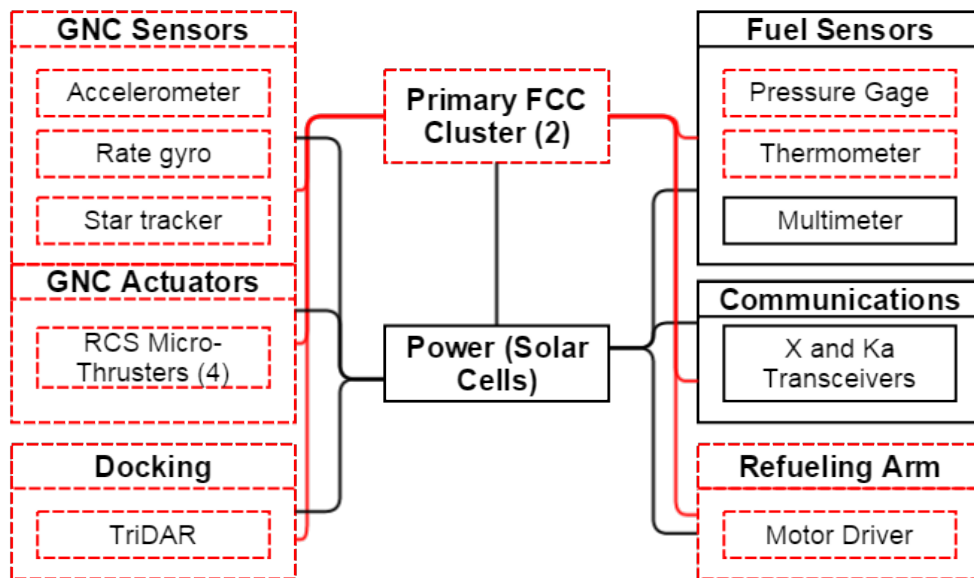


Figure 43. Fuel Depot Avionics Block Diagram

Communications

This mission will require minimal communication capabilities as there are no humans involved in this system. The only requirement is that the system shall be able to downlink housekeeping data to inform the stations of its performance as well as current fuel quantities. This will require an antenna and transceiver that supports X, UHF, Ka, and K frequency band communication at a data rate of 2-11 Mbps.

Control and Docking Avionics

The fuel depots will be configured with attitude control system thrusters. Each of these thrusters will act in order to maintain the orbital positioning of the spacecraft and to help will reaction control when docking with the FTV. These actuators will be controlled by the main computer which will use GNC sensors including an IMU, rate gyro, accelerometer and star tracker to monitor its attitude and movement. The computer will collect this flight data to compute reaction control maneuvers to be executed by the micro-thrusters.

The fuel depot will be equipped with a TriDAR system within the docking port to enable the fuel transport vehicle to berth with this system.

Housekeeping

To monitor the health and current fuel availability on board the depot, there will be a series of sensors on board the vehicle. This will include a pressure gage, thermometer and multimeter for monitoring the chemical composition of the fuel. This data will then be downlinked through the vehicles communication system.

Power Requirements

The power requirements used for sizing the solar panels were calculated by considering the requirements for avionics, radiation losses, the RCS thruster system, and the active cooling system (a considerable portion of the power budget). A 15% margin was added in to ensure that all power requirements were met. The active cooling system power budget calculation is explained in the “Active and Passive Cooling System” section. An estimate for avionics and radiation losses was acquired from the Avionics team, based off of industry standards. Overall, the EML1 fuel depot requires 25kW of power, provided by the solar panels on the sun-facing side of the depot.

EML1 Fuel Depot Power Requirements (kW)	
Active Cooling	19.6
Avionics	1.2
Radiation Losses	0.72
RCS System	0.34
Total	22
With 15% Margin	25

Table 17. Power requirement breakdown for EML1 depot

3.4.8. Assembly

To keep the fuel depot development costs as low as possible, it was decided that autonomously docking tanks would be preferable to a manned mission to EML1 to put the depot together. To accomplish this, each tank was to be outfitted with RCS thrusters (explained in more detail in the “RCS” section), and while the main computer and avionics system would be located on the oxygen tank in the center of the depot, each hydrogen tank features its own, smaller, avionics package outfitted with the minimum possible electronics needed for locating these tanks and lining them up with the oxygen tank, which will do most of the “work” during the docking process.

The components of the EML1 fuel depot are launched on 3 SLS rockets. The first launch will contain the central liquid oxygen tank, which has its own small solar panels used to power its avionics and RCS systems initially. Each hydrogen tank will then be launched in its own SLS, also outfitted with avionics and RCS systems, and the heat shield and larger solar panels that will be used over the course of the mission to protect and power the depot. The heat shield and solar panels will be in a stowed configuration during launch. The launch configurations of each tank, and well as the oxygen tank configuration before docking are shown in Figure 44 below.

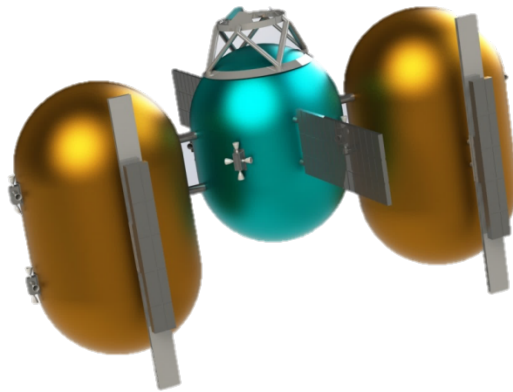


Figure 44. Image of depot mid-construction, with smaller solar panels on LOX tank expanded.

When a hydrogen tank gets to EML1, the oxygen tank will locate the hydrogen tank, and will dock with it. At that point, the smaller oxygen tank solar panels will retract, and the half of the heat shield and solar panels on that hydrogen tank will expand. The process will repeat on the other side of the oxygen tank once the second hydrogen tank arrives at EML1. An image of the final docked configuration is shown below.

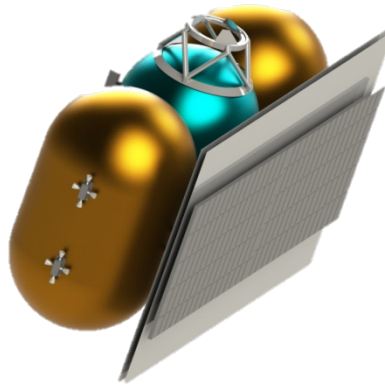


Figure 45. Image of final depot configuration with heat shield and solar panels expanded.

3.4.9. Concept of Refueling Operations

The EML1 fuel depot was designed to accommodate three 110t refuels of the SLS upper stage within a two week launch window, and have time to fully refill before the next launch window (approximately 26 months) A visual representation of the EML1 refueling concept of operations for a typical launch window is shown in Figure 46. This procedure assures that three SLS upper stages can be refueled within each launch window. Because of the limited mass of fuel that can fit into the depot (330t) due to size constraints of the SLS payload fairing, if an SLS upper stage refuel were to fail, it would take some time to replenish fuel before that spacecraft could refuel. This could result in the payload missing its launch window, but it would be possible to shift future launches to accommodate for this, creating a fairly redundant and reliable system. Since launches are more spread out later in the prime mission, a refueling failure would not affect the mission's 2054 deadline of having 24 people on Mars independent of Earth.

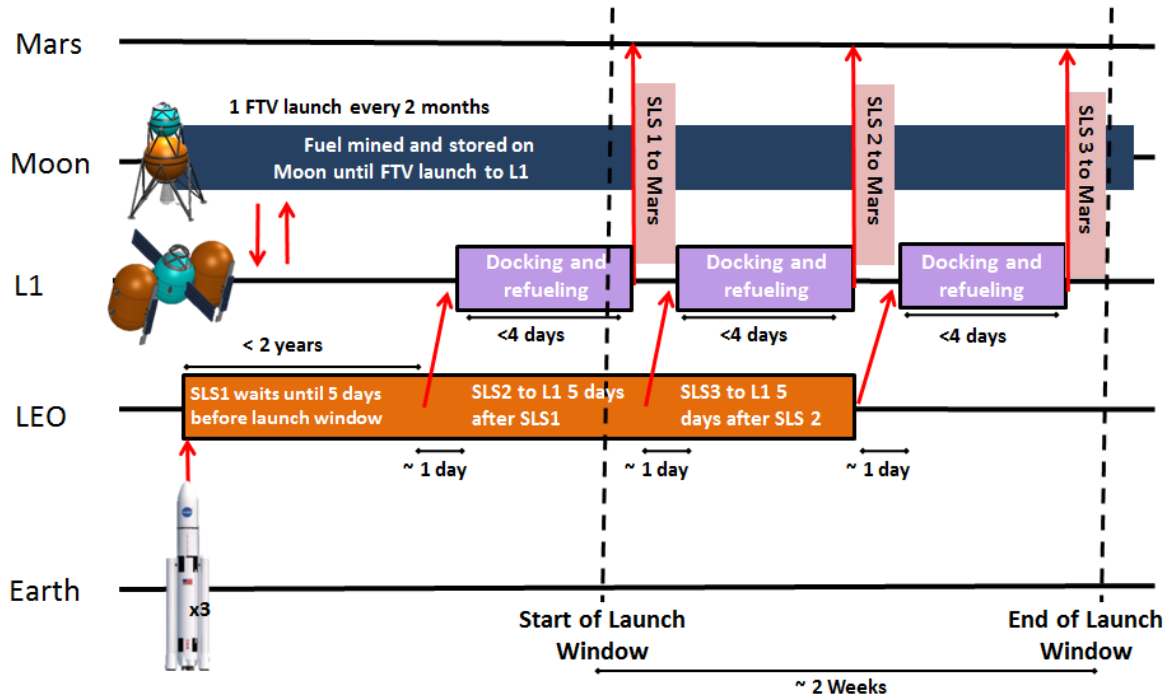


Figure 46. Refueling Con-Ops for typical launch window to Mars.

A graphical representation of the mass of fuel in the EML1 fuel depot over 5 years is shown in Figure 47. The depot takes less than 26 months to fully refuel, and actually does so in about 17 months, meaning that if an FTV fuel transfer were to fail, the depot would have 9 months to reach full capacity with extra trips of the FTVs before a refuel would need to take place. Some launch windows only have one or two SLS upper stage refuels, especially once crew transport begins, so for some years the minimum amount of fuel in the depot would be more than the graph shows, so within the current mission architecture, the depot will always have enough fuel to support the necessary refuels barring any catastrophic failures such as a loss of both FTVs, fuel leaks, or multiple SLS upper stage refueling failures.

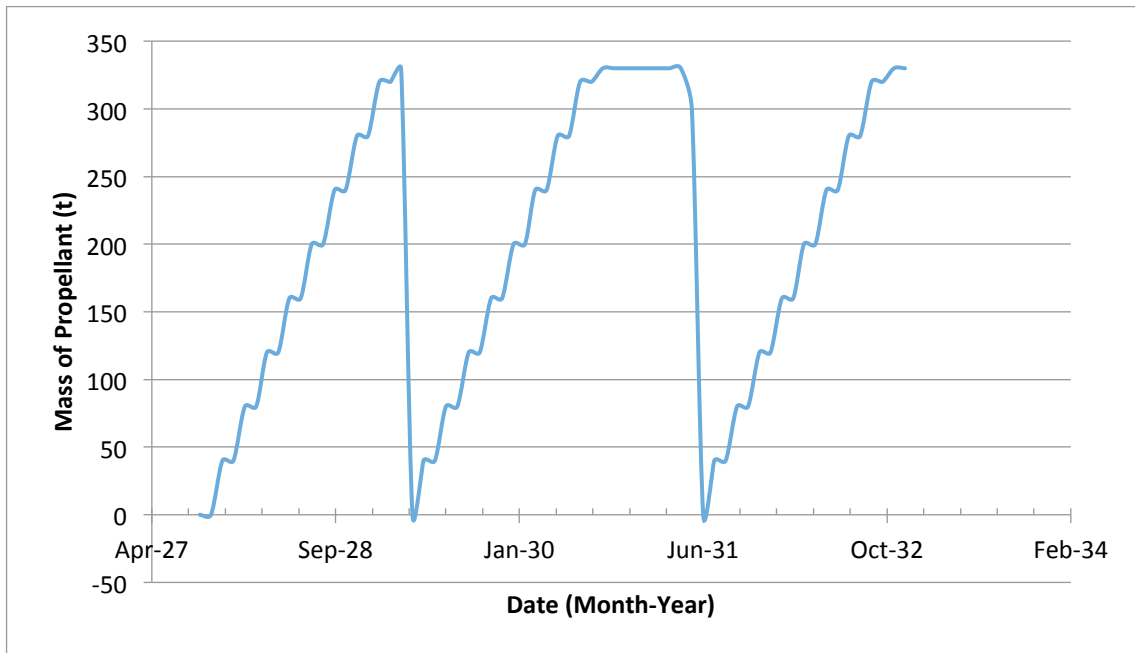


Figure 47. Mass of fuel in EML1 depot over 5 year period, showing pattern of expected fuel levels for duration of mission.

3.5. LMO Fuel Depots

3.5.1. Introduction

Two LMO Fuel Depots will be located in Low Mars Orbit, and will each have the capability to hold 120t of liquid oxygen and liquid hydrogen propellant. Several vehicles, particularly the CTV and the Ascent/Descent vehicle, required additional propellant in order for them to successfully accomplish their individual tasks. The LMO Fuel Depots will provide that propellant, thus aiding mission success.

Tank Design

The LMO fuel depots are similar in design to the EML1 fuel depot. They hold LH₂ and LOX in the same 5.85:1 fuel ratio, and they have all of the same features of the EML1 fuel depot, but they are designed to hold only 120t of propellant each. The LMO fuel depots are basically scaled down versions of the EML1 fuel depot. The dimensions for the LMO fuel depot are included below.

Structure	Diameter (m)	Total Length (m)	Length of Cylindrical Portion (m)
LOX Tank	7.2	9.40	2.90
LH ₂ Tank	7.7	12.7	5.66

Table 18. EML1 Fuel Depot Tank Dimensions

Limiting Design Factors

The LMO fuel depots were limited by volume in the same way that the EML1 fuel depots were, but they face another limitation. The EML1 fuel depot has 3 SLS launches available to send parts and construct it at the Lagrange point, but the LMO fuel depot would only have 2 SLS launches for sending parts and construction. A single LMO fuel depot that would hold enough fuel for several Martian landers and Crew Transport Vehicle launches would be too large to fit in just 2 SLSs. The team calculated the largest amount of storable fuel on a fuel depot that would be able to fit the LOX tank and two LH2 tanks into a single SLS. That amount was found to be 120t of fuel, with a more detailed explanation behind that analysis included in MATLAB code in Appendix C. Unfortunately, 120t would not be enough for all vehicles that needed refueling at Mars, which lead to the need for a second LMO fuel depot. Both LMO fuel depots are simply copies of each other.

CTV Requirement

The CTV will be brought from LMO to the L1 Lagrange point by the SLS upper stage. The maximum mass of the CTV is 29t. To bring a CTV of 29t from LMO to L1, the SLS would require a minimum initial propellant mass of 36t. According to the figure below, a starting propellant mass of 36t will allow the SLS and CTV to arrive at L1 with zero propellant remaining in the SLS's fuel tanks. When in LMO, the SLS tanks will be empty; they lack the active cooling system that is required to maintain the propellant. Therefore, it would need to draw a minimum of 36t of propellant from the LMO fuel tank in order to successfully carry the CTV to the L1 depot.

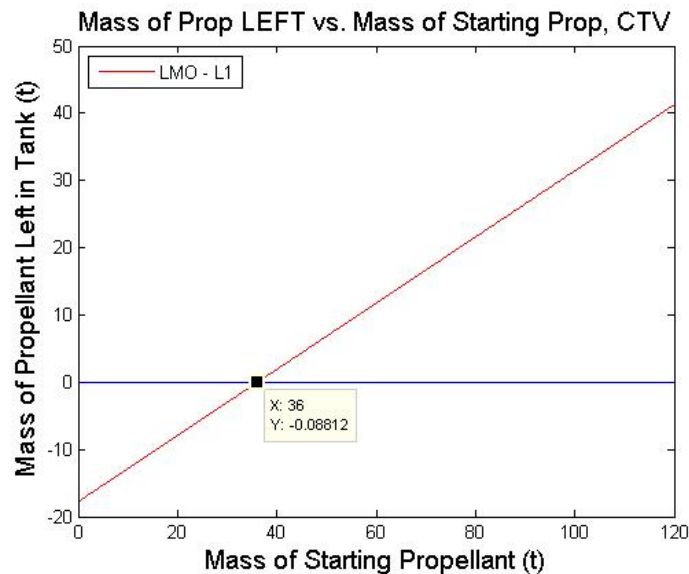


Figure 48. Mass of prop left vs Mass of Start Prop, CTV

Ascent/Descent Vehicle Requirement

The Ascent/Descent vehicle will require 13t of propellant to reach the Martian surface from a position at Lower Mars Orbit (LMO). This has been accounted for in the propellant mass of the LMO fuel depot.

Dry Mass	6.3t
Gross Mass	126t
Dimensions	LOX tank height: 4.8m LOX tank diameter: 7.2m LH ₂ tank height: 6.1m LH ₂ tank diameter: 7.7m Width: 23 m
Launch Date	2028 and 2032
Launch Vehicle	SLS Block IB
Destination	Low Mars Orbit
Power	126W
Payload	120t of fuel

Table 19. LMO Fuel Depot Specifications

3.5.2. Design Specifications

The same minimum and maximum yearly delta-V requirements as the EML1 fuel depot were used to estimate the yearly propellant required for LMO station-keeping. The only difference was that the LMO depot has a significantly smaller mass (about 126t total). The figure below shows that the range of propellant required for an RCS system would be between 0.37t and 5.4t on a yearly basis.

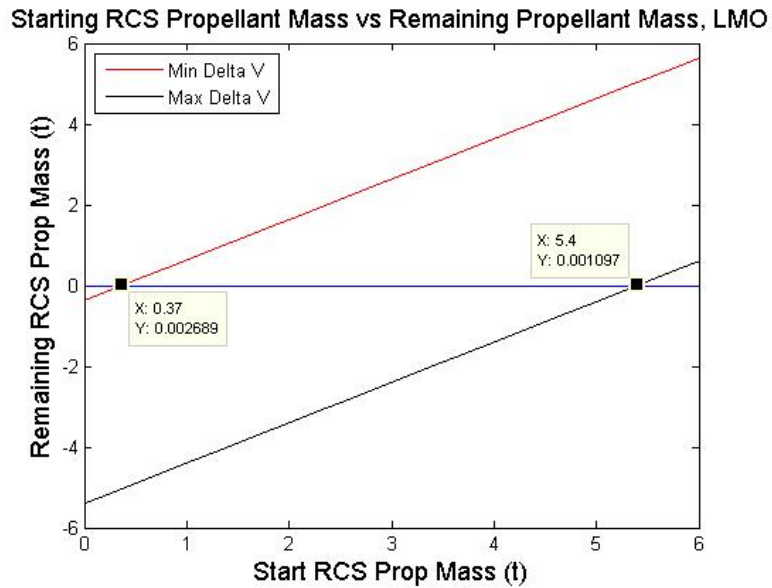


Figure 49. Starting RCS Propellant Mass vs. Remaining Propellant Mass, LMO

Thrust

A duty cycle of 6% was assumed for the LMO Depot RCS thrusters. In other words, the thrusters would fire two times per month. Using the same equations that were used in another section to find the thrust requirements, it was determined that the thrust would need to be 9.46N. This is including the adjustment for the thrust decrease due to the 15° angled nozzle.

RCS Thruster Power Requirements

By using the same methods that were used to determine these variables in [section XX \(same reference as previous section\)](#), it was determined that the \dot{m} required to produce this thrust (assuming an I_{sp} of 350s) would need to be 0.0028 kg/s. This mass flow rate would then result in a fuel pump power requirement of 99.1W and an oxidizer pump power of 26.5W. Thus, the total power required for the LMO depot RCS thrusters would be about 126W.

RCS Thruster Sizing

The RCS thrusters for the LMO depot have the same size dimensions as those of the EML1 depot.

LMO Fuel Depot Power Requirements

The power requirements of the LMO propellant depot were calculated in the same way as that of the EML1 propellant depot requirements were, but using this smaller structure, they turned out to be smaller. The estimate of power needed due to avionics and radiation loss remains the same, since the LMO depot will have the same avionics system as the larger depot. The RCS thrusters also required less power due to the lower mass of the LMO depot. A lower mass corresponded to a lower required thrust, which in turn reduced their mass flow rate. The lower mass flow rate required to produce the needed thrust allowed the

power requirements for the RCS thrusters to be significantly lower than those of the EML1 depot. A breakdown of the power requirement per LMO depot is shown below.

LMO Fuel Depot Power Requirements (kW)	
Active Cooling	6.3
Avionics	1.2
Radiation Losses	0.72
RCS System	0.13
Total	8.4
With 15% Margin	9.6

Table 20. Power Requirement Breakdown for each LMO depot

3.5.3. Refueling Schedule

The docking and refueling operations at the LMO fuel depots will be very similar to that of the EML1 depot. Figure 50 shows the mass of fuel in each depot from the year 2038 until the end of prime mission in 2054. Starting with the Habitat #7 and 8 launches in 2037, the depots will begin to be filled with excess fuel from the SLS upper stage. Each SLS upper stage with an approximately 50 t payload (including EDL vehicle) will arrive at LMO with 35 t of fuel. The small dips in the fuel levels starting in 2045 represent the 13 t of fuel used by the crew EDL vehicle after refuel. These dips are immediately replenished thanks to the extra fuel contained in the SLS upper stage carrying the CTV and Dragon capsule. The larger drops in fuel levels are representative of the SLS upper stage refuel needed to return the CTV to EML1 to pick up another set of crew members. For the CTV to get back to EML1, it requires a 36 t refuel. After 2054, each propellant depot will be full, and there will be enough propellant left within the depots to support six trips of the CTV back to EML1. This means that in the case of an emergency, all 24 crew members could be brought home over the course of 2 launch windows without the need for replenishing the depots. The 2 launch window limitation is due to the capacity and number of the CTVs, not the refueling capabilities. In an emergency situation, having two propellant depots would also be useful, because 2 SLS upper stages could be refueled simultaneously, allowing for all three CTVs to make it back to EML1 within the two week launch window.

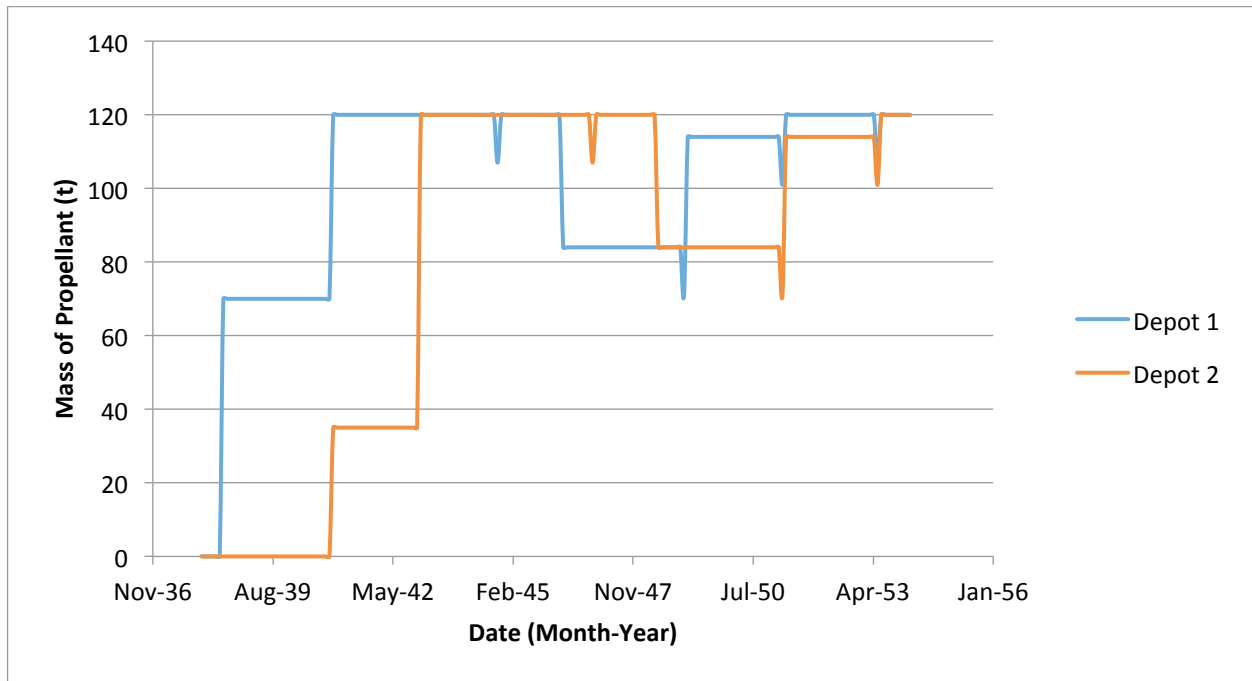


Figure 50. Nominal LMO Propellant Depot Fuel Masses 2038-2054

3.5.4. Refueling Operations

The refueling infrastructure constructed in in the Resource Acquisition and Refueling phase offers many benefits to the Asimov City mission. By investing time and money into the mining operations on the Moon, the FTVs, the EML1 propellant depot, and the LMO propellant depots, the program was able to increase average payload to 50t and max payload to almost 90t, up about 260% from the 37t without refuel. Each SLS costs the program approximately \$500M, making the cost of launching payload to Mars on an SLS about \$13,500/kg. With at least 13t added to each payload and up to 53t, this could mean savings between \$3B and \$12B over the Habitat Transport Phase. This also means that the mission will need less rockets to reach completion.

The cost savings due to refueling are large, but the main benefit of refueling is that fact that the propellants produced on the moon allow both crew transport and crew entry, descent, and landing to be possible. The crew EDL vehicle refuels at the LMO propellant depots before landing, and the CTV transport configuration utilizes refuels of the SLS upper stage at EML1 and LMO to allow the crew transport vehicle to move from LEO to LMO and back.

Once all depots are established, the Asimov City mission will be Earth-independent in regards to propellant other than the propellant needed to get rockets from the Earth’s surface to the EML1 propellant depot. All other propellant will come from either the Moon or Mars, and this propellant will be essential to the success of the overall mission to create an Earth-Independent Mars settlement by the year 2054.

3.6. μ Net

3.6.1. Overview

As the mission begins to inhabit the surface of Mars and establish independence from Earth, it will be essential to have global communication capability to ensure that any Martian explorer is connected to the rest of the crew no matter where they are on the planet. That is why the program has developed the architecture for a Mars Universal Communications Network or μ Net for short. This system shall have the ability to serve the missions' pre-habitation phase in assisting for high precision entry descent and landing maneuvers and then it will serve the habitats of Mars as a communication relay network, satellite internet provider and a global positioning system (GPS).

3.6.2. Architecture

The architecture of the μ Net constellation will require fifteen microsattellites. This number was determined through modeling different combinations of walker constellation satellites using the System Tool Kit (STK) software. Variations on the constellations not only included the number of satellites, but also the orbital elements (altitude, eccentricity, right ascension of the ascending node, true anomaly, inclination, and argument of perigee), and visibilities of the on board antenna dish. The goal of the constellation configuration is to get maximum global coverage, such that the entire planet has 100% communication coverage at all times. This goal was optimally achieved with 15 satellites spread across five different orbital planes with each plane holding 3 satellites. Each of these satellites will require an antenna visibility of at least 35 degrees. This means that the conic angle of the antenna disc must be at a minimum of 35 degrees from horizontal. This configuration not only maximizes ground coverage, but it also minimizes the effects of station keeping required that resulted from gravitational perturbations. In other words, the satellites are kept at a high altitude. Below is a screen shot of the STK model showing the final configuration of the satellite constellation with coverage visibilities of each satellite.

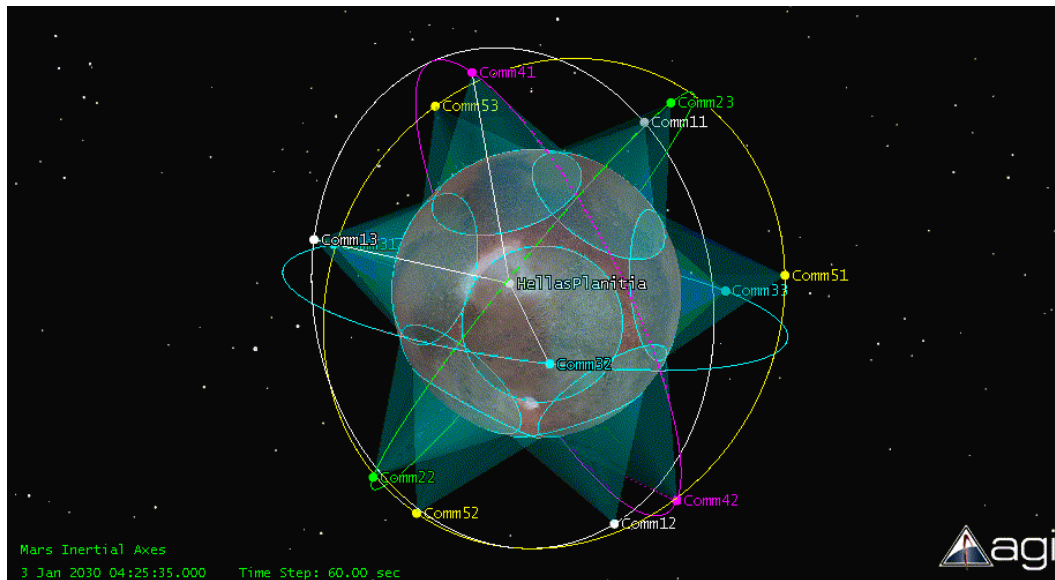


Figure 51. μ Net STK Coverage Model

3.6.3. Launch and Mission Planning

3.6.3.1. Launch

The system shall be launched on the first SLS payload before most Mars payloads are launched. This will be in 2031. The satellite fleet will be bundled into a NanoRack structure. NanoRack will be an internal fairing to the SLS that will house all of the μ Net satellites and will serve as the primary delivery vehicle for deploying the satellites into their destination orbits.

3.6.3.2. Mission Activities and Lifetime

After being launched to Mars in 2027, the μ Net satellites will be deployed into their parking orbits. At this point, other mission critical payloads will be in transit to Mars. Upon their arrival, μ Net will be up and running to aid in our entry, descent and landing activities. By using μ Net's GPS system, the radius of our landing zones will be greatly reduced. This is especially important as later down in our mission timeline, those landed payloads will need to be hauled from their landing site to their designated location on the main base. If this distance can be minimized, the amount of resources and power especially that will be exhausted for payload movements will be reduced.

As astronauts arrive to the settlement, the μ Net satellites will be deployed and used as a communication relay system. The satellite will use its receivers to collect signals from ground transceivers and it will also transmit data that may have been relayed from outside of the Mars space, or from a sister satellite to receivers on the surface of Mars. Overall, the system is very analogous to the Tracking and Data Relay System that is used by NASA on Earth.

The habitat crane, miner, rovers, and astronauts will make use of μ Net for GPS when traveling away from the main base. Each of these assets will be able to acquire a GPS message from at least 3 satellites at any given time, and then the local computer will generate a navigation and guidance solution based on the data. Additionally, μ Net will be able to serve the habitat as an internet provider. This is primarily for people or vehicles that are out of range of the wireless network set up at Asimov City.

The lifetime of the constellation is expected to be at a minimum of 20 years. Due to the relatively cheap costing of this system, it will be possible to replace defective or non-operational elements of the system before resources from Earth get cut off. Before 2053, some or all of the μ Net satellites will be upgraded and replaced to reflect the current technologies of that year.

3.6.3.3. Flight Plan

When the SLS fairing carrying the μ Net payload arrives in LMO, each satellite will be strategically dropped off into their designated orbits from the NanoRack fairing. This will require an orbital extraction maneuver. Each satellite must be released from the NanoRack one by one while the payload block is in LMO. Because the constellations' orbits are spread across 5 planes, the fairing will need to be able to perform plane changes for each group. This will require 3.03 km/s of delta V per plane change which is a maneuver that changes the angle of the right ascension of the ascending node by 72 degrees. While in plane, the fairing will release one satellite as they are separated evenly by true anomaly. From there, each satellite will use its thrusters to perform orbit correction maneuvers to precisely position itself into its

parking orbit. The total delta V required from the NanoRack is 12.12 km/s which does not include any maneuvers into the initial orbit or out of the last orbit to a graveyard orbit. The dimensions of the NanoRack fairing is 3m x 3m x 10m and this delivery vehicle will be equipped with ion thrusters to support the relatively high delta V required.

Below is an image that shows the configuration of all 15 satellites when in their final orbit around Mars.

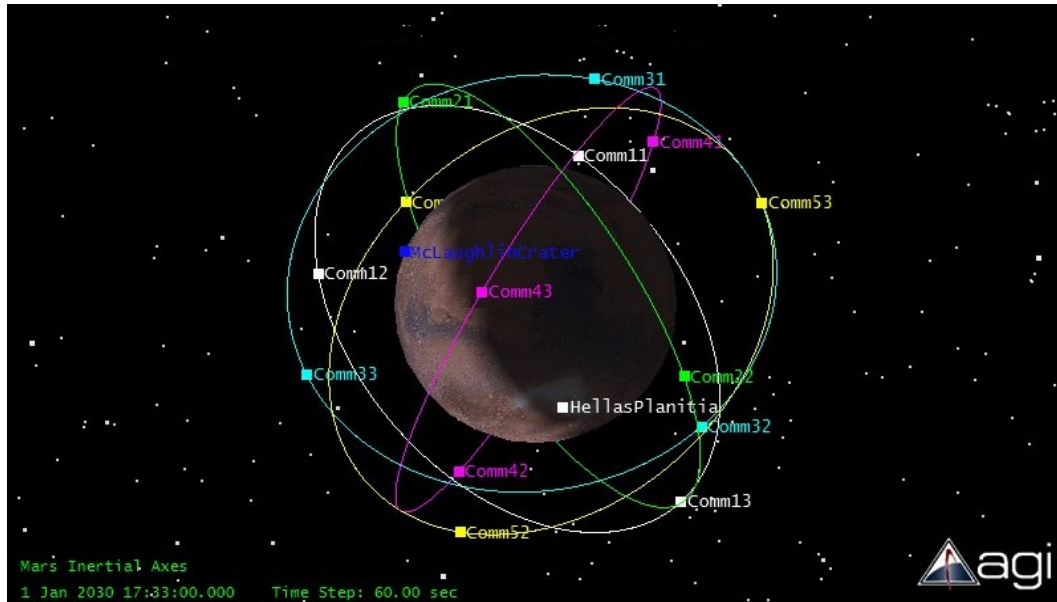


Figure 52. μ Net Constellation

3.6.3.4. Destination

The satellites will be placed in orbit around Mars separated evenly by right ascension of the ascending node and by true anomaly. There will be five orbital planes which each inclined at 60 degrees, but vary by 72 degrees of right ascension of the ascending node. In each plane, there are three evenly separated satellites 120 degrees of true anomaly apart from each other. These satellites will remain in areosynchronous orbit throughout their lifetime.

3.6.4. Vehicle Layout

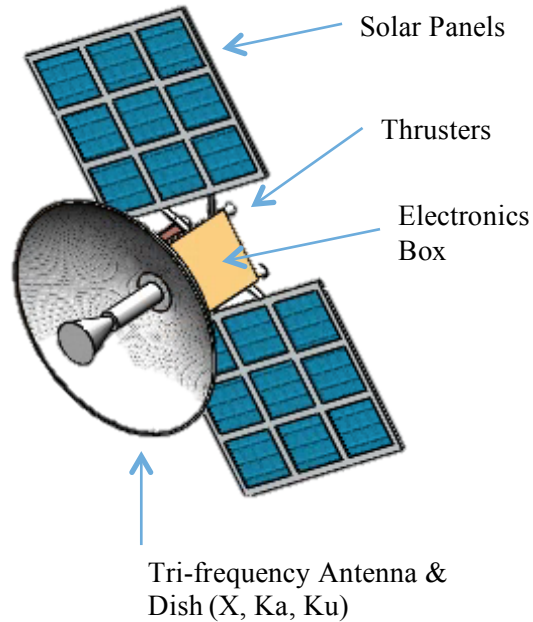


Figure 53. μ Net Vehicle Layout

3.6.4.1. Structure

Each satellite will be structured identically. The satellite design will be a microsatellite weighing 42 kg in total. Within the heart of the satellite is the main electronics box. This houses the central computer, ports, channels and power supply. The box has dimensions of 0.45m x 0.45m x 0.45m and a total mass of 37 kg. The mass includes the weight of the instruments and structure. The antenna has a diameter of 1.5 m which is sized to accommodate an antenna gain of 35.15 dB and antenna dish angle of 35 degrees.

3.6.4.2. Propulsion System

The μ Net satellites will have on board four electric thrusters. Electric propulsion is ideal for the

microsatellite size of the vehicle and the power requirements needed for maintaining their orbits. The thrusters will be a micro pulsed plasma thruster developed by Busek Space Propulsion and Systems that have an impulse of 600 N-s. The only need for thrusters is for orbit correction that will need to be done as a result of perturbations from gravitational effects.

3.6.4.3. Power System

Each satellite in the constellation will have its own solar array made of Ultra-lightweight photovoltaic Si 17%. The efficiency of the solar panel ranges from 15-20%. Based on the power requirement of the satellite, the solar array shall have an area of 1.57 m² and a mass of 3.1 kg which will give a power output of 350 watts. The solar panel dimensions are 1.43m by 1.1m. During nominal operations, the power requirement for this vehicle is 256 watts. This gives us a 26% margin to account for the photovoltaic array inefficiency. The power required for the electronics is 62 watts. All excess power will be directed to powering the electric propulsion system for station keeping and for antenna data transmission.

3.6.5. Electronics

3.6.5.1. Transponder and Antenna

The μ Net satellites will use a modified version of the Small Deep Space Transponder developed by General Dynamics. This transponder only supports X and Ka frequency signal transmission, however, it will be upgraded to include channels for Ku frequency as well. Additionally, the transponder shall also facilitate UHF communication for short-range communication. The transponder is a full duplex system that reaches a maximum data transfer rate of 300 Kbps with a power requirement of 17 watts. The antenna dish is a 1.5 m diameter dish with a conic angle of 35 degrees. This sizing was based on the optimum antenna gain value and the optimum antenna visibility of the Mars surface.

3.6.5.2. Link Budget

μ Net will use X band communication most often. Below is a table showing the link budget for each of the satellites. The calculations took into account losses in signal power due to polarization, space path and antenna pointing. The bit error rate was determined by the transponder hardware specifications. The resultant link margin amounts to 3.83 dB which allows for the system to be able to handle a realistic amount of anomalous signal attenuations.

Fn	7.2 GHz
Antenna Gain	35.15 dB
Σ Losses	
Polarization	0.67 dB
Space (path) loss	177.5 dB
Antenna pointing	0.5 dB
Total Loss	178.67 dB
BER	1.2×10^{-5}
EIRP	12.3 dBW
Eb/No required	4.86 dB
Eb/No received	1.03 dB
Link Margin	3.83 dB

Table 21. μ Net Link Budget

3.7. “Iris” Earth-Mars Relay

3.7.1. Overview

The main Earth-Mars communications link is a piece of architecture vital to the success of the mission. This communications link will support the activities of all astronauts on the surface, as well as all data collection, in addition to supporting the MuNet system and teleoperation controls structures for mars based vehicles and landers. To do this, the team has decided to use a laser communications system, the first ever used for Martian communication. A laser link of this scale has never been planned before, but in order to satiate the requirements of 24 astronauts on mars, as well as the teleoperation of all tools, the data speeds it provides will be required. Radio communication, even in the fastest currently used radio band, is simply not fast enough (though a Ka-band radio link will be used as a backup).

3.7.1.1. Required Data Rates: Analysis and Comparison

Ka band (the new NASA standard deep space radio band) provides up to 4 mb/s data rate under ideal conditions. This alone is not enough to support our mission and all its Martian components. This is fine to send scientific data, but to support all the activities of a colony it is lacking. Orbiters like the MAVEN orbiter used X-band radio communication with the Deep Space Network, operating with downlink budgets of 550 kb/s. To support the mars habitat wifi and MuNet, data speeds far in excess of current radio technologies are needed. A link of the planned scale could easily support video streaming and a faux internet for the colony, but more importantly will provide the necessary bandwidth to sustain communication with the mission’s extensive assets.

3.7.1.2. Possible Technologies

Optical (Laser) With the LLCD (Lunar Laser Communications Demonstration), previously unproven laser communications technology was tested. The LLCD used an optical link to send data at a rate of 622 Mb/sec, far in excess of anything achieved in space up to that point. A scaled up version of this technology will be used in the main earth-mars communications link. The proposed (and terminated in 2006) Mars Telecommunications orbiter (MTO) would have used a 1.06 micron laser and supported data rates of 30 Mb/s. This link is a scaled up version of that. The proposed MARS2022 will also contain a laser communications system. This project will use MARS2022's development resources as its own.

3.7.1.3. Final Design Plan

Mars Satellites

At Mars, a dual HEO orbit has been chosen because it allows for greater coverage versus mars-synchronous. This also allows for communication with polar MuNet satellites, and polar orbit-ground communications (to support polar exploration possible in future of mars settlement). 2 phased orbits are chosen to provide maximum coverage of settlement and all assets. 2 HEO satellites also provide the possibility of multi-link transmittance, which can double the data rate given 2 available earth receivers.

Heliocentric relay

This heliocentric satellite would eliminate the communications outage caused by a major earth-sun-mars conjunction, which can last up to 45 days every 780 days. Once there are enough humans on mars, this outage becomes unacceptable should an emergency occur. This relay has the added benefit of reducing the necessary apertures of the antennas and transmitters because the maximum distance travelled by the laser is considerably less. It also reduces the necessary pointing and tracking accuracy.

Ground Station

The team originally planned to have geosynchronous earth relays to ground receivers because of atmospheric disturbance, but not enough launches are available. Large ground based receivers will be made use of, though at least one new facility should be constructed much closer to 2054. Ideal ground stations are high altitude, with large mirrors (up to 10m ideal). For example, the W.M. Keck Observatory in Hawaii sits at an altitude of 4,145 meters and contains a 10m optical receiver. This ground station is ideal, and will be the main earth receiver.

3.7.2. Launch Date & Flight Plan

The Iris Relay satellites will be launched in 2031, along with other Martian assets. The 2 Mars satellites and the heliocentric satellite will be launched separately. One launch will take the 2 mars satellites, along with other payloads to mars orbit, where the satellites will use their onboard electric propulsion to get into orbit. The heliocentric satellite will do the same, except from GEO.

The Elliptical Mars Satellites have the following orbits, so as to maximize viewing time. They are phased at 90 degrees true anomaly from each other.

Here are the elements for the two Mars Satellites and a visualization in STK:

Satellite #	1	2
Semimajor Axis	16390 km	16390 km
Eccentricity	0.732	0.731
Inclination	92 deg	45 deg
Arg. Of Perigee	250 deg	280 deg
True Anomaly at start of orbit	0 deg	90 deg

Table 22. Mars Satellite Elements



Figure 54. STK visualization of phased Mars HEO orbits

Heliocentric Orbit

The orbit of the heliocentric satellite will be a stabilized heliocentric orbit (so as to avoid earth trailing or earth leading movements over time). During the satellite's 20 year lifetime, it will need to perform several maneuvers to stay in orbit. A heliocentric orbit moves around the solar system's barycenter, which is located not at the center but at the surface of the sun. Therefore one side of the orbit will be closer to mars depending on its location.

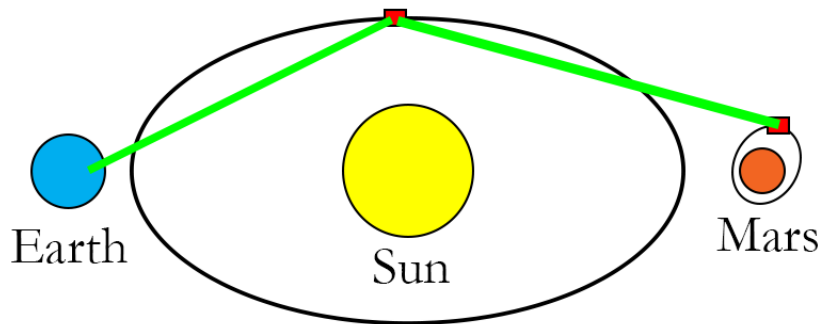


Figure 55. Earth-Sun-Mars Conjunction and Relay Position

3.7.2.1. Mission Activities and Lifetime

Mission lifetime on each of the satellites is 15 years. The main day-to-day activities for the satellites will be station keeping and maintaining correct link orientation, which will be discussed further in a few sections. After the propellant on the satellites has run out, the satellites can maintain link effectiveness using gyroscopes, but as orbits degrade, further effective lifetime will be limited.

3.7.3. Vehicle Layout

3.7.3.1. Structural Overview

Both the Mars satellites and the heliocentric satellites will have very similar designs. The main body of the satellite will be 3m x 4m x 3m without the solar panel (the actual electronics box and main truss structure is smaller), which includes the large mirror antenna and laser substructure. The solar panels fold out for a total craft size of 4m x 8m x 4m. Solar panel sizing is discussed in the power section. Additionally, a 4-pronged UHF antenna will be deployed for communicating with surface assets. The total dry weight of each Mars satellite is 1100 kilograms.

3.7.3.2. Propulsion

All 3 satellites will make use of a high-isp solar electric ion thruster for station keeping purposes. This thruster will not activate unless the communications subsystem is inactive as the solar panels are sized for use of one or the other. The thruster will be a xenon based ion thruster similar to the NSTAR thruster used on Deep Space 1. These thrusters have been chosen for their reliability on missions with many thruster starts and long operation hours.

3.7.3.3. Power

The general power requirements of the Martian satellites are 1.4 kW. In this range of power requirement, a nuclear power source is bordering on unfeasible. Photovoltaic energy generation is the best choice for a long term mission. The solar panels were sized based on the aforementioned 1.4 kW power requirement, and a 300 W/m² Flux Density at mars. The type of solar cell chosen was a 3-Junction GaAs/Ge/GaInP2 cell, with a power rating of 350 W/m² and a mass of 1.76 Kg/m², as well as a reliability rating (calculated for 5kw array) of .9999. This resulted in a calculated solar array size of 17.67 m² for the martian satellites, and a weight of 31 kg. Backup power will be provided by 2 nickel-hydrogen batteries providing 1.6 kW at max capacity.

3.7.4. Electronics

3.7.4.1. Laser Comm System

The satellite will use a laser with an output of 100W (input power 1 kW), at a wavelength of 1.07 microns. The laser will be a MOPA (master oscillator power amplifier) design. This design uses a “Master” laser, which is amplified to the required output power, along with a distributed feedback fiber laser system. The communications pulses are created by a modulator which reads the incoming data stream and then translates it into pulses, which are read by an optical receiver at the antenna on the opposite side of the link and translated back into data.

3.7.4.2. Ka Band Backup

A Ka- band backup radio will be used in case of failure of the laser communications system. A transmitter operating at 30W will be used (only when the laser system is offline) to transmit at around 4 mb/s when necessary. A Ka- band antenna will be mounted directly on the UHF antenna base.

3.7.4.3. ELECTRA and Transponder

Two ELECTRA transceivers will be used to receive and transmit UHF signals from ground based sources and from MuNet. The ELECTRA receiver was used on MAVEN and due to its small power requirements and size will be used once again on our Martian relay. Two Ka band transponders will be included on the craft (Small Deep Space transponders include hardware for both Ka band and X band, and the craft does not include X band functionality).

Data rates from UHF assets will max out at 1 Gbps, with an average of 100Mbps. With our maximum Earth-Mars data rate at 10Gbps. Using this peak data rate, 108 Terabytes of storage would be required to store a full 24 hours worth of data at maximum rate. The power requirements of the laser subsystem limit the amount of SDRAM that can be used. Therefore the data storage will be limited to less than an hour of maximum data rate storage. Data storage systems in the habitat will be used to offset this limitation.

3.7.4.4. Antenna

A large 2.5m mirrored receiver is required with the heliocentric relay reducing the distance traveled (without the relay, up to a 5m mirror would be needed). Using a one piece mirror like Hubble is not possible. Hubble weighs 11,000 lbs, and much of that is the weight of the single piece mirror (also 2.5m). Alternatives are multi segment mirrors and membrane type mirrors. Membrane mirror technology would be ideal but is not TRL5. Therefore a multi segment receiver will be used..

Link Pointing and tracking. Required tracking accuracy is on the order of 6×10^{-7} rad. (3db laser beam at maximum 1.7AU distance, need one tenth of the beam for information transfer). The team chose a combination of two tracking options for this laser link, star Tracking and IR Tracking. Star Tracking uses the positions of distant stars to correctly find the position of and orient the satellite towards the opposite receiver, though this requires an accurate clock and ephemeris data. IR Tracking works as the satellite finds an object with 270K temperature on the 4K background of deep space. These two systems will work in combination to provide the required level of tracking accuracy.

3.7.4.5. Attitude Control System

The satellites will use 3-axis stabilization provided by reaction wheels, as well as gyroscopes for inertial sensing. The required pointing accuracy will be provided by the Fine Guidance Sensor system, the one currently in use on the hubble space telescope, which provides 0.01 arcsec pointing accuracy.

Link Noise and Disturbance

The noise bandwidth (narrowest filter) is 10GHz wide. Industry peak quantum efficiency for optics (reception) is estimated at 90%, and at 50% for transmission at an average distance of 329,120,000 km, this results in a path loss $[(4\pi R/\lambda)^2]$ of 371.8 dB. On the receiving end, a 280THz laser output has an effective system temperature given by

$$T = \frac{hf}{\alpha k}$$

where α is the receiving efficiency. This gives a 26,904 K effective temperature, which leads to a noise power on the receiving end of -84 dBW for 10GHz noise bandwidth. The Effective Isotropic Radiated Power is calculated as 166.4 dBW which with a noise power of -84 dBW gives a Carrier to Noise ratio of 9.2 dB, sufficient to use the maximum 10 Gb/sec speed at distances at or less than the average (50% of the time).

4. Phase III: Habitat Transport

4.1. Introduction

The third mission phase is the Habitat Transport phase, which begins in 2031 and ends in 2042. The purpose of this phase is to prepare the landing site for human arrival by sending all necessary construction materials and resources to the surface of Mars and to Mars orbit. These components include first the

communication satellites as a secondary payload to the first habitat mission. These satellites will assist with the landing of future payloads and will reside in Mars orbit. A crew ascent/descent vehicle will also be placed in Mars orbit until it needs to be used to land the first Martian crew. On the surface, habitat pieces, cranes for construction, pressurized and unpressurized rovers, solar panels, nuclear reactors, and Mars mining equipment for water and propellant production will be landed, along with supplies that the astronauts will need to live such as freeze-dried foods and other objects that will not expire.

Initially it was the intention of this program to complete the Habitat Transport phase between 2021 and 2035, because during that time period, the SLS program needed to be funded, and thanks to this funding, the project would receive “mandated” SLS to use. From 2021 to 2025, the program has one SLS per year, and from 2026 to 2035, the funding provided to fund SLS provides the program with 2 rockets per year. This made it seem that it would be most fiscally responsible to complete the habitat transport phase during this time period and then cut funding for the SLS program, opting for Falcon 9 and Falcon Heavy to be used for crew transport to save money.

Once overhead was added into the monetary needs of the program, it was concluded that the budget in the middle years of the project could not support so many components launch in such a short period of time, so the mission architecture was shifted to expand the Habitat Transport phase to 2042, and to keep the SLS program alive. Though this would seem to be more expensive, by spacing out the development costs of the different components, and saving many launches until later in the mission when the budget experiences an increase of \$3B/year, this change actually made the program fit into the budget better. Thanks to this change, it was not necessary to cut any components from the mission plan due to the addition of overhead costs.

By the end of the Habitat Transport phase, everything will be in place on Mars for when the first crew arrives in 2045, and construction will be ready to begin.

4.2. Habitat Entry, Descent, and Landing

4.2.1. Cargo EDL Architecture

This Mars settlement program will require landing very large payloads on the surface of Mars. To accomplish this, a two-stage expendable descent vehicle has been designed to handle large packages, such as habitat modules, construction vehicles, and reactors. The Cargo Entry, Descent, and Landing (CEDL) vehicle will be decelerated primarily by an inflatable hypersonic aerodynamic decelerator, followed by a final propulsive descent to the Martian surface. The vehicle has been designed to fit inside of the 10m SLS payload fairing and support a cylindrical EDL payload envelope of 8.9m diameter by 16m height. The CEDL weighs 15t fully fueled, and is capable of landing up to 35t on the surface of Mars.

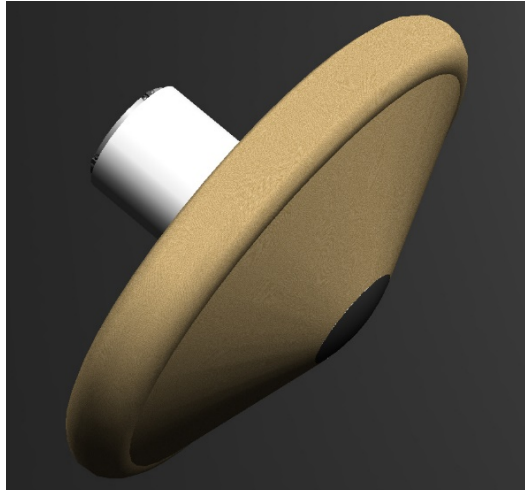


Figure 56. CEDL with aerodynamic decelerator deployed

This two-stage design was chosen in order to obtain a high payload mass fraction for descent. The equipment and modules that need to be landed on Mars to support a self-sustaining human settlement will be at least an order of magnitude more massive than the heaviest payload we have taken to the Martian surface to date. In order to minimize the amount of construction taking place on the surface of Mars, it is helpful to keep the equipment and habitat modules as intact as possible, without breaking them up into smaller payloads for EDL. The payload limit for the vehicle was set to 35t to support landing all surface vehicles and habitat modules with minimal assembly on the surface.

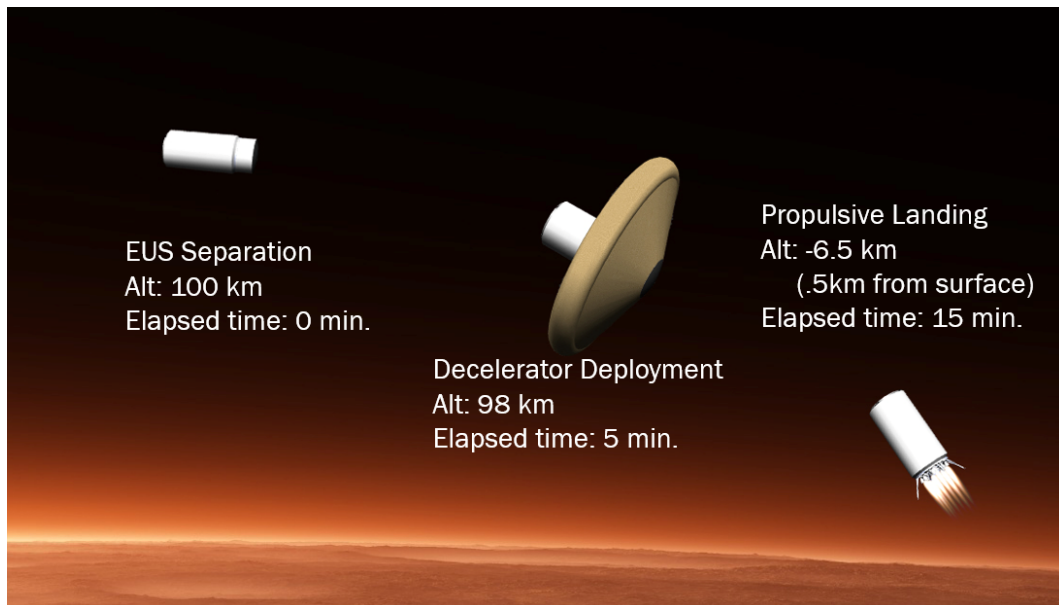


Figure 57. CEDL Entry Overview

The vehicle mass budget estimations^[220] are as follows:

Component	Mass (tons)
Payload	35
Fairings	8.5
Aerodynamic Decelerator	3
Fuel	2.5
Tanks, Propellant Management, Avionics, and Thrust Structures	1
Total	50

Table 23. Mass Budget Estimations

4.2.2. Trajectory Design

Settlement cargo will be transported to Mars via SLS Block 1B's. The SLS upper stage will arrive at Mars and park in LMO at 100km altitude before sending the descent vehicle to the surface. The initial burn to begin the descent will be done by the SLS. The vehicle will need to decelerate through the atmosphere aerodynamically to the surface of Hellas Planitia, which is 7km below Martian altitude 0. Landing in Hellas Planitia is beneficial to our EDL design, as the atmosphere get thicker in the basin, providing more aerodynamic deceleration. However, due to the thin Martian atmosphere, that can be two orders of magnitude less dense than that of Earth, it would take an extremely large decelerator to slow the descent vehicle to a safe landing speed.

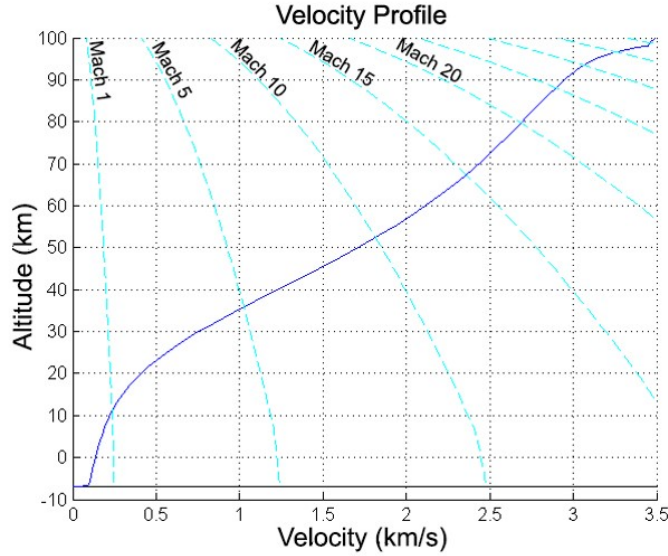


Figure 58. CEDL Entry Trajectory

In order to achieve a safe landing after terminal velocity has been reached, the vehicle has been designed to decelerate to 95 m/s at an altitude of 500m above the surface and begin a propulsive burn for the last half kilometer. For a 50t descent vehicle (including maximum payload), this terminal velocity can be achieved with a ballistic coefficient of 28 kg/m².

The descent vehicle was modeled as a point mass on a ballistic trajectory. For the purpose of establishing a nominal entry trajectory, any lifting effects from small angles of attack were neglecting to model the vehicle as a pure ballistic entry vehicle. Small lift/drag coefficients (on the order of 0.3) can be achieved by inducing an angle of attack using RCS thrusters located on the aft section of the vehicle, but these will be primarily used for course correcting maneuvers during descent to keep the vehicle on the nominal trajectory. The following equations of motion were used to model the descent of the vehicle:

$$\frac{dV}{dh} = \frac{g[\frac{Q}{\beta} - \sin(\gamma)]}{V \sin(\gamma)} \quad \frac{dt}{dh} = \frac{-1}{V \sin(\gamma)}$$

$$\frac{d\gamma}{dh} = \frac{\cos(\gamma)[-g + \frac{V^2}{R+h}]}{V^2 \sin(\gamma)} \quad \frac{dr}{dh} = R \frac{d\theta}{dh} = \frac{-R \cos(\gamma)}{(R+h)\sin(\gamma)}$$

Altitude h (meters) is used as the integration variable here, solving for velocity V (m/s), time t (seconds), flight path angle γ (radians, defined as positive below horizontal), and range r (meters). Q is dynamic pressure (N/m²); β is the ballistic coefficient (kg/m²); g is the gravity (m/s²) at altitude h ; R is the radius of Mars (meters).

The numerical MATLAB solver ode45 was used to calculate the state variables V , t , γ , and r as functions of h . An additional variable a (acceleration) was calculated from velocity and time. The MATLAB function EDL.m and script cargoEDL.m handle these calculations and produced the above velocity profile as well as the following results:

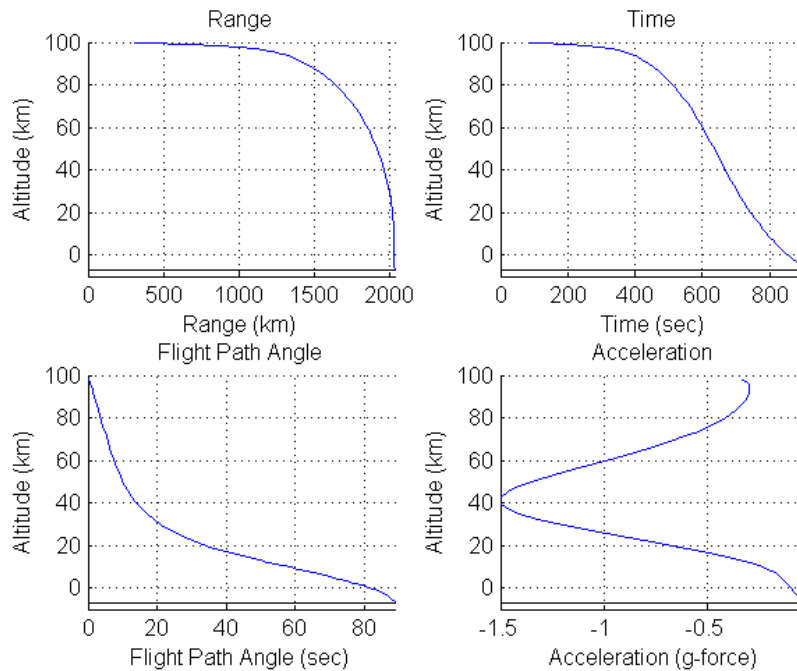


Figure 59. Flight Path Parameters for CEDL

Following this nominal trajectory, the vehicle will cover 2000km over the Martian surface from the time it begins its descent until its final landing on the surface of Hellas Planitia. The vehicle is expected to experiences up to 1.5 G's during the aerodynamic descent.

4.2.3. Inflatable Decelerator

To achieve this nominal descent trajectory, the CEDL must have a ballistic coefficient of 28 kg/m^2 with the decelerator fully inflated. The design presented here can satisfy this requirement using a decelerator with a 40m diameter, 70° half-angle clamped torus, with a 1.4 drag coefficient. The inflated toroidal tube has a diameter of 5m. A two-stage solid gas generator will provide the initial inflation and maintain pressure in the toroidal tube for the aerodynamic descent, similar to the gas generator used to inflate the airbags on the Mars Exploration Rover landers.

With the toroidal tube fully inflated, the incoming hypersonic flow will pull the fabric attaching the torus to the vehicle taut, causing the decelerator to behave as a rigid body. The vehicle will maintain its rigidity from the gas generators and incoming hypersonic flow for the 10 minute duration of the aerodynamic descent. At the end of this stage, the fabric will separate from the vehicle, detaching from the propulsive fairing and tearing radially along the conical section, so that the descent vehicle will fall through the fabric and free of the torus. This decelerator does not need to be recovered, since the vehicle is designed is purposed for a one-way trip. The heat shield on the nose of the vehicle will then separate along with the thruster fairing, and the propulsive descent will begin.

4.2.4. Attitude Control

In order to establish a successful and sustainable settlement on the surface of Mars, all of the equipment and cargo need to be highly localized. While the team has established means for transporting different portions of the habitat during setup, it is important that all components land in a very close proximity. Therefore pinpoint landing, landing within a 100m radius, was set as a high-level mission requirement. As is evidence in the table below, which shows the landing accuracy as well as the entry control means for all seven of NASA’s successful Mars landers, no previous mission has approached the accuracy needed required for this settlement. This data was found online via NASA’s mission pages for several of the landers. The most recent lander, Curiosity, was able to achieve an order of magnitude reduction in landing error over the initial landers by relying on guided entry. This significant improvement in landing accuracy was due in large part by allowing the descent vehicle to adjust its course during descent rather than rely on traditional ballistic entry. However, this mission’s overall success relies on a further decrease in the landing margin by another two orders of magnitude.

Mission	Landing Year	Entry Method	Ellipse Size (km)
Viking I, II	1976	Ballistic	280 x 100
Sojourner	1997	Ballistic	200 x 70
MERs	2004	Ballistic	150 x 20
Phoenix	2008	Ballistic	70 x 30
Curiosity	2012	Guided	20 x 7

Table 24. Martian Landing Ellipses

These large landing ellipses are the product of many factors which are impossible to precisely predict prior to Mars atmospheric entry. Chief among these factors are delivery error at atmospheric entry, the state uncertainty throughout EDL, environmental uncertainty, and the vehicle’s performance. A product of inaccuracies in the trajectory correction maneuvers en route to Mars, the delivery error is the difference between the actual and predicted states at entry. The state uncertainty is a byproduct of propagation of navigation update inaccuracies, as well as the time in between those updates. The environmental uncertainty is due to varying density and wind profiles during the descent phase. Lastly, error margins due to the vehicle’s performance is a function of inaccuracies in the physical model of the descent vehicle, i.e. aerodynamic forces, mass properties, and the performance of the GNC system.^[242]

Among these four factors, the one most feasible for correction during the descent phase is the state error. Having examined studied several options for improving the accuracy of state estimate, the team has decided to rely on the μ Net GPS system as the primary system. With full Mars coverage by four or more constellation satellites at any given time, it will be possible to rely on trilateration and least squares to produce state estimates on the order of 10m. This is a significant improvement over the state estimation precision which is on the order of 5000m.^[243]

While the GPS system provides the most precise state estimate of all the methods studied, it is important to have a contingency plan should some of the satellites fail at any time. For the backup method, the team has settled on using Terrain Relative Navigation, or TRN, which relies on landmark tracking during descent. The system works by utilizing computer vision algorithms conducted on images taken during descent in comparison to surface maps. By tracking these landmarks during descent, the system is able to

determine its location relative to center of the landing ellipse. The basic control loop is shown below. TRN also has the advantage of making it easier to identify, and ultimately to avoid, hazardous landing zones in the final stages of descent. While not particularly useful for Earth landings, TRN was heavily studied for better state estimates prior to the existence of GPS. More recently however, this technique has been researched for underwater navigation systems where GPS signals cannot be received.^[244]

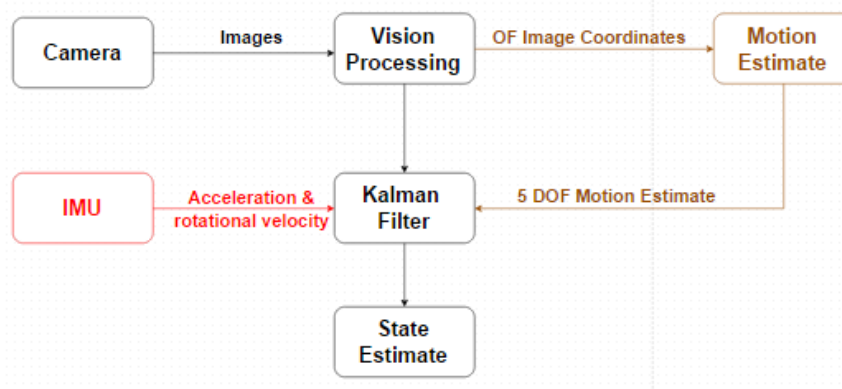


Figure 60. TRN Control Loop

Additionally in recent years, scientists and engineers have done extensive research into employing TRN for precision Mars landings. Simulations of Mars landing conducted by JPL using images taken by the Mars Exploration Rovers during the descent phase has shown that TRN software can run in real time and produce position estimates accurate to around 40m.^[246] While this 40m accuracy is not as good as utilizing GPS systems, it is still a drastic improvement over the 5000m of previous missions.

The only caveat that comes along with TRN is that it relies on the existence of a high-resolution map of the entire landing zone. The same JPL study suggested that the ideal map for TRN would have a resolution of around 5m/pixel. Fortunately this is already in place for all of Hellas Planitia thanks to images taken by the Mars Reconnaissance Orbiter's HiRISE camera, which generates images with a resolution of less than one meter.

With more accurate state information, the team set about improving upon the attitude control guidance of the MSL mission, the only other lander to employ guidance during Mars descent. For the cargo landing missions, the descent vehicle will be brought into the Mars atmosphere at a stable angle of attack. During hypersonic entry, altering this angle of attack for guidance would require far too much energy and result in destabilization. Therefore other means for attitude control, including the one employed by the Curiosity lander, were considered.

The main reason for bringing the descent vehicle in at a non-zero angle of attack is that this allows for the generation of lift for the axisymmetric cargo descent vehicle, shown below with the forces acting on it. It is significant that lift is generated during descent, as controlling the direction of the lift can be used to correct the course of the vehicle. This angle of attack is achieved through a center of gravity offset prior to atmospheric entry, accomplished by ejecting ballast. This method for generating the angle of attack was chosen over the alternative employment of hypersonic trim tabs. Although hypersonic trim tabs would save mass over ballast ejections, and was thoroughly considered for use on MSL,^[245] they could not be employed for the cargo descent missions due to the presence of the large deployable heat shield.

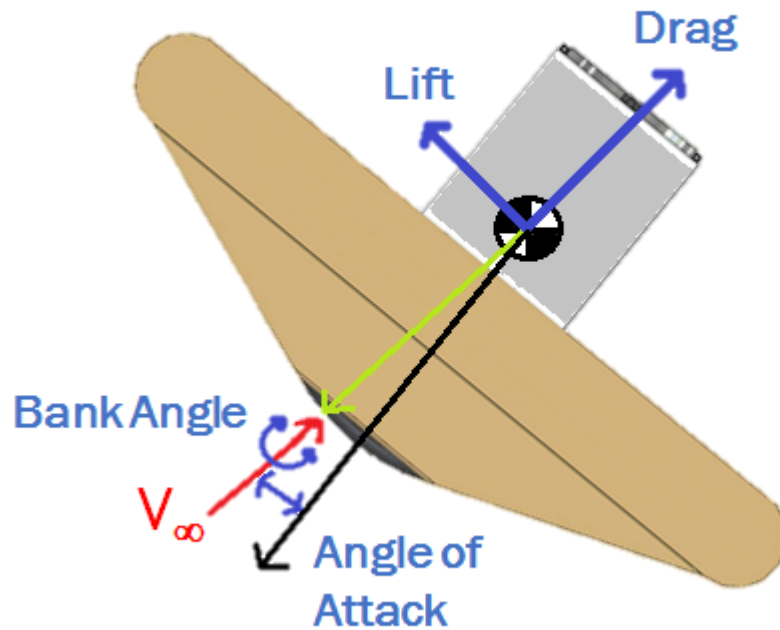


Figure 61. Lift and Drag on the Cargo Descent Vehicle

In order to control the direction of the lift vector, the descent vehicle will rely on reaction control system (RCS) thrusters which will allow for roll rotation through a bank angle. These roll rotations serve to rotate the lift vector around the velocity vector, allowing the control of both roll and yaw. The thruster arrangement, as shown below, consists of two thrusters pointing in opposite directions at four locations 90 degrees around the craft. Each able to achieve a maximum thrust of 500N would allow for a full 360° bank angle maneuver in about 60 seconds.

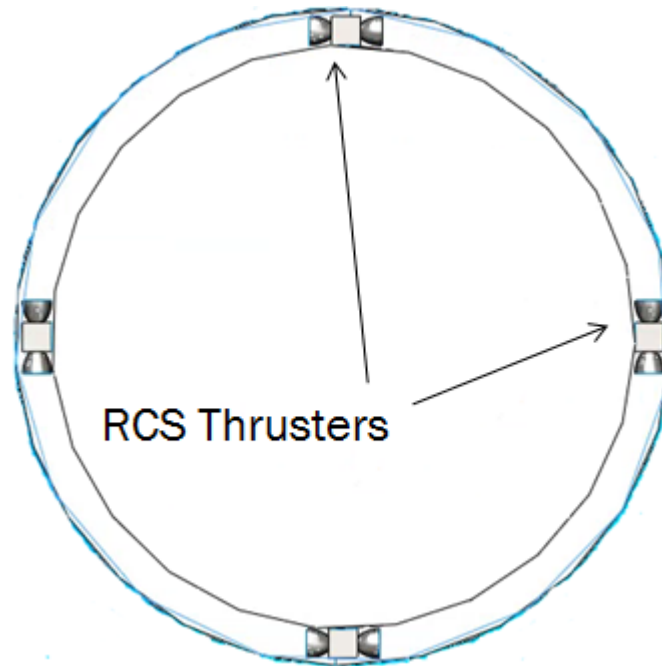


Figure 62. RCS Thruster Arrangement

The performance of the guidance system in directing the vehicle towards its destination relies heavily on the performance of the controller shown below. As shown in the block diagram below,^[247] the state estimate is fed into the Attitude Profiler, which will determine the desired attitude the descent vehicle would be needed to point the lift vector appropriately to guide the craft towards the desired landing point. This desired attitude will then be fed into the Attitude controller, which is a PD controller that controls the RCS thruster burn times to stabilize the descent vehicle around the desired bank angle.

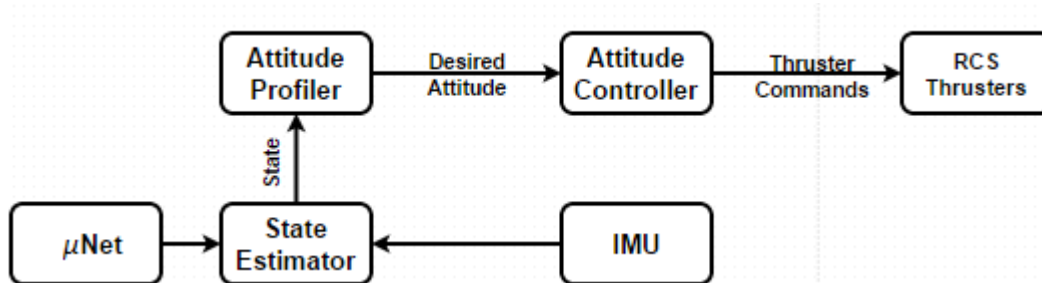


Figure 63. Attitude Control Loop

This serves as the method for guidance until the deployable heat shield is attached from the rest of the descent vehicle at an altitude of 500m. At that point the final stage, powered terminal descent, begins. From there until soft landing, the main engines are gimballed to control the thrust vector in slowing down the craft. For this final stage, the team conducted a trade study of several different pre-existing algorithms targeting controlling the thrust vector direction. The ultimate design considerations were finding a system that could fuel optimally perform the largest position correction from only 500m up.

All of the different methods examined worked on the idea that the acceleration relative to the desired landing zone was represented by the equation below, where g is Martian gravity, T_c is the thrust vector, and m is the mass which is a function of the thrust and the fuel consumption rate. The chief difference among these is how the acceleration relative to the target is modelled as a function of time.

$$a = g + T_c/m$$

The simplest of the thrust vector control algorithms studied was the Apollo guidance algorithm modified for Mars landing. This algorithm models the acceleration profile as a quadratic function of time given as:

$$a(t) = C_0 + C_1t + C_2t^2$$

where C_i are coefficients solved for from the initial and the desired end state, as well as the time of flight, denoted t_f , to determine the acceleration^[248]. A major problem with this approach, however, is that it fixes t_f and provides no allowance for fuel cost optimization or constraints on maximum thrust. Therefore this approach would consume the most fuel of the algorithms studied, with a propellant mass fraction of above 0.3.^[242]

Several modified versions of the Apollo guidance algorithm have been shown to result in better performance. One version improves upon the Apollo model by having t_f be a free parameter, and choosing a time of flight, and therefore the acceleration profile, off of the one that minimizes fuel consumption. To do this, a fuel cost function has been defined as:

$$J_F = \int_0^{t_f} \sqrt{a^T(\tau)a(\tau)} d\tau$$

where $a(t)$ is the same quadratic function of time given in the unmodified Apollo algorithm.^[248]

Further modifications to the Apollo guidance algorithm focused on modelling the acceleration profile as a higher order polynomial function of time.

$$a(t) = C_0 + C_1t + \dots C_Nt^N$$

Linear algebra is then used to solve for the coefficients from the desired end state for each t_f . Just as before, the time of flight which minimizes the fuel cost is then chosen for guidance. This approach has been shown to reduce the necessary propellant mass fraction down to around 0.25.^[242]

A final approach for pinpoint landing using thrust vector control, studied at the University of California, Irvine, focused on reducing the optimum fuel guidance system to a finite-dimensional convex programming problem.^[249] The semi-definite programming approach, while significantly more complicated and involving many more iterations, than the previous methods has shown to be the most fuel optimal, with a propellant mass fraction hovering below 0.2.^[242] However, a major problem with this approach is that to date it has not been demonstrated to run in real-time,^[249] which is necessary for EDL. The thrust vector control algorithms discussed have been plotted below,^[248] showing how large a position correction can be achieved given the altitude and downrange distance from the target when propulsive terminal descent begins. Based off of this information, as well as the feasibility of use of each algorithm, the team has selected the 3rd order modified Apollo guidance algorithm with fuel optimization. As shown in the dark black line, using this thrust control algorithm, the cargo descent vehicle will be able achieve pinpoint landing from up to 750m downrange at only 500m altitude.

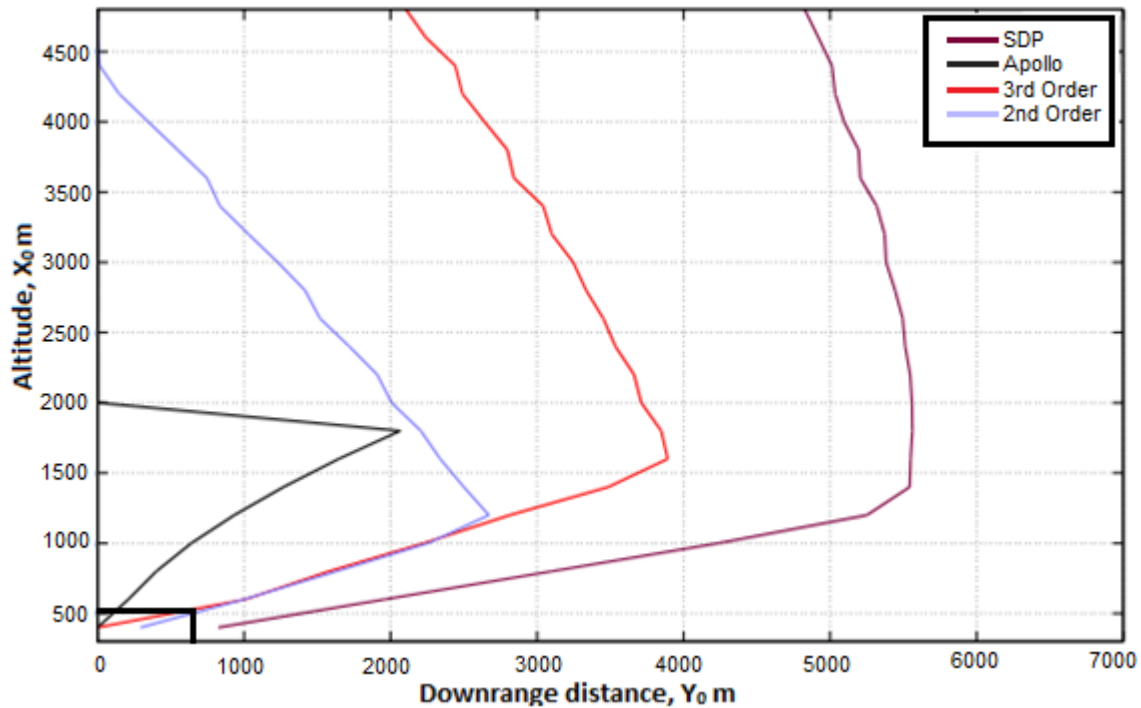


Figure 64. Propulsive Terminal Descent Precision

4.2.5. Propulsive Terminal Descent

The final propulsive descent will be accomplished using eight retrothrusters. Multiple thrusters were chosen as opposed to a single retro thruster to allow for additional attitude control during the final descent, in addition to redundancy in case of engine failure. The CEDL will require a payload mass fraction of 0.05 for the last 500m of descent to landing, or 2.5t. The propulsive descent will use monopropellant hydrazine. Hydrazine was chosen since it can be stored for long periods of time during its travel to Mars with no boil off. Since this vehicle is designed for a one-way trip, fuel does not need to be readily available in orbit or at Mars, such as LH2 and LOX, but can be manufactured on Earth and sent with the descent vehicle. For these reasons, hydrazine was an excellent candidate for final descent propellant.

4.2.6. After Landing

After landing on the surface of Hellas Planitia, cargo will be extracted using cranes. The CEDL will land oriented with the payload on top, so that the crane will be able to easily remove the payload fairing. The CEDL vehicles will remain on the surface of Mars for extended periods of time after landing, until the cranes arrive to extract the cargo and begin construction. They will remain inside their respective payload fairings to protect from harsh weather conditions. The Habitat halls and hubs will be stacked inside of

each other, and will need to be lifted vertically for removal. Cranes will be able to deploy autonomously from the CEDL, without the assistance of other vehicles. This process will be addressed in later sections.



Figure 65. CEDL on surface of Mars awaiting cargo extraction

4.2.7. Cargo EDL Landing Structure

NOTE: The landing structure for the Cargo EDL vehicle is very similar to the landing structure on the manned ascent/descent vehicle, and as such a more in depth analysis of the design process can be found in that section.

The landing structure for the Cargo EDL vehicle will have to be robust to survive potential rough landings on the Martian surface. In addition to withstanding a number of different loads associated with landing, the structure must also provide an adequate base to prevent tipping during the ground handling and extraction of cargo from inside the vehicle, while attempting to limit the vertical distance the vehicle is located from the ground to help ease cargo extraction. The landing structure must also be retractable within a fairing that covers the thrust section of the vehicle in order to properly integrate with the vehicles re-entry envelope.

In the stowed configuration the four, 4m long legs fold underneath the vehicles thrusters, safely stored in a protective fairing. Actuators deploy the legs out to their final configuration, at an angle of 45° the total width of the landing structure is approximately 13.7 meters, allowing for the safe ground handling of cargo.



Figure 66. Cargo EDL Landing Gear

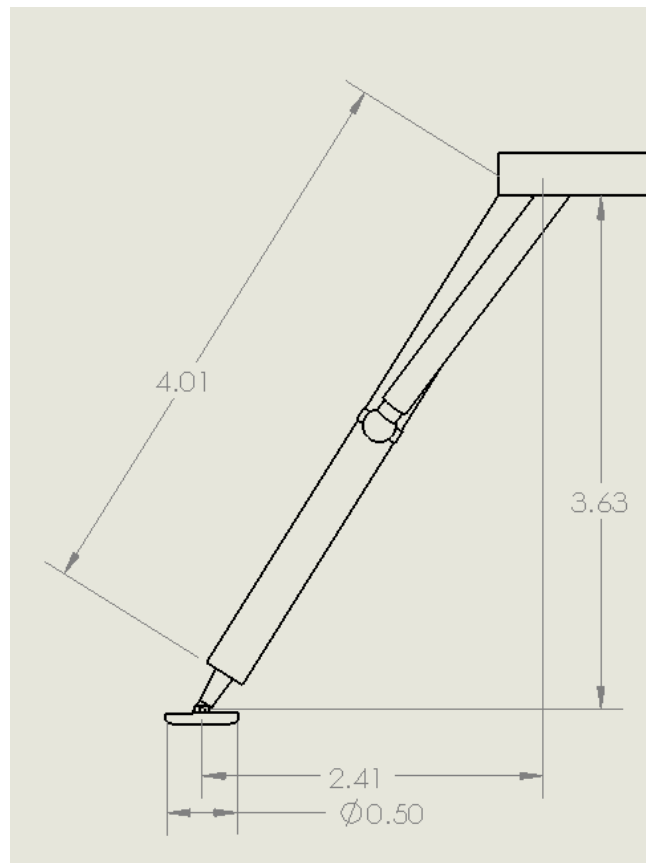


Figure 67. Cargo EDL Landing Strut Dimensions

Loads generated using MATLAB script, *CargoEDLCriticalLoads.m*, that can be located in Appendix C. Note: All factors of safety used are NASA standard.

Al 6061-T6 Alloy σ_u	316 MPa
Critical Buckling Stress	46.82 Mpa
Total Design Stress	22.19 MPa
MOS (σ_u)	10.9
MOS (Buckling)	0.78

Table 25. Cargo EDL Critical Stress/Margin of Safety

5. Phase IV: Crew Transport

5.1. Crew Selection

The various crews sent to Mars will be required to perform many different tasks calling upon many varied skills. The major areas of skills lie in operational, greenhouse, medical, and engineering and technical fields. In operations, the crew will need to know how to pilot their various space crafts and vehicles, from the CTV to the crew landers to the Magellan 2.0 and 2.1. In the greenhouse, the crew will need to have an understanding of biology, and botany to help ensure plant health. All crew will need to be trained in gardening and plant cultivation skills as well as harvesting and post processing. In the medical field, the crew must have the skills of a general practitioner, a psychologist, an optometrist, and a surgeon. All crew members will be trained in human nutrition to monitor their own diets and trained as emergency medical technicians for emergency situations. As for the various engineering disciplines, the crew will need to have an understanding of computer, nuclear, aerospace, mechanical, sustainability, environmental control, construction, and systems engineering. It would also be useful to have a crew member trained as a geologist for various Mars based experiments. These skills will need to be split between each of the 4 initial crew members, thus each crew will need to know on average between 5 -6 of the skills discussed. As the crew size increases, the skills load will be lessened and altered. For example, after initial construction phase is finished, construction engineering skills will not be a priority.

5.2. Crew Transport Architecture

5.2.1. Launch

Crew transport to the Martian surface will begin in April 2044. The first CTV (CTV 1) will launch from Cape Canaveral, Florida to LEO aboard an SLS Block 1B in mid April 2044 and remain in LEO for 3 weeks, before departing for the first Lagrange point (L1). The transit from Earth's surface to LEO will require a Δv of 9.1 km/s. The first crew of four will launch from Cape Canaveral, Florida three weeks later aboard a Falcon 9 with a Dragon capsule. The Falcon 9 will travel directly to L1 from Earth's surface, requiring a Δv of approximately 13 km/s.

The current design of the Dragon spacecraft has an initial propellant mass of 1.290. However, according to the figure below, a starting propellant mass of 1.290 would not be enough for the Dragon to escape the L1 Lagrange point with a payload of any size. The maximum payload that the Dragon would need to carry out of L1 and back to Earth would be 1t. In order for the Dragon to be able to do this, it would need to have a starting propellant mass of 1.85t. This is an increase of 0.56 t of propellant in the Dragon's tanks. With this increase in propellant, the Dragon would be able to escape L1 with a payload of 1t and return to Earth. The figure below displays this capability.

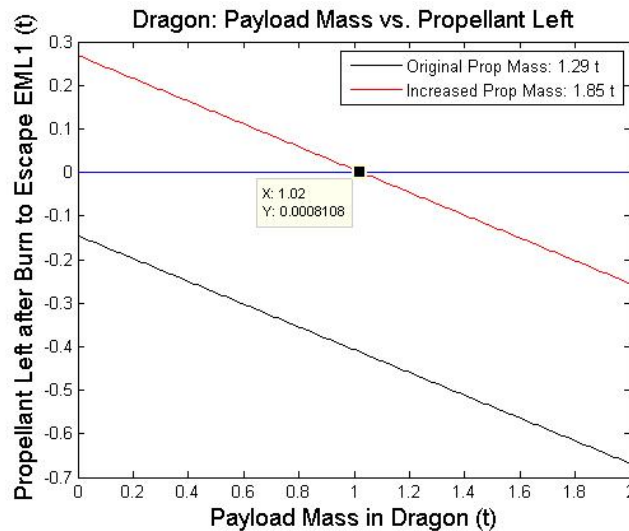


Figure 68. Dragon: PL Mass vs Prop Mass

5.2.2. SpaceTrain

5.2.2.1. Concept of Operations

When the SLS stage two carrying the CTV arrives at L1, the vehicle will jettison its fairing. Shortly after, the crewed Falcon 9 will also arrive at L1. The Dragon capsule and trunk will detach from Falcon 9 stage

2 and, RCS thrusters on the exterior of the Dragon will be used to orient the crew capsule in a position in which it is ready to accept the incoming CTV.

The Dragon will dock to a compatible docking mechanism on the forward end of the CTV. Once docking procedures are complete, the inflatable CTV will pressurize. At the completion of pressurization operations, all systems will be tested and confirmed normal by NASA Mission Control before crew transfer begins. Crew will transfer from the Dragon to the CTV and transport supplies stored in the Dragon capsule. After successfully transporting these items, two crewmembers will prepare for an EVA in order to retrieve the extra supplies from the unpressurized Dragon Trunk. The crew will unload these items, and store them in the now unpressurized airlock. When the airlock is full, the crew will close the airlock and allow it to pressurize. The two crewmembers inside the CTV will quickly unload the airlock, and close the airlock again, allowing the two crewmembers performing an EVA to continue loading the airlock. This process will continue until all items are loaded onto the CTV or until the two crewmembers outside of the vehicle meet their maximum EVA time. In this situation, the crew inside would take over the EVA responsibilities.

Once all items have been successfully loaded into the CTV, all crewmembers will board the CTV and will trigger the detachment of the Dragon capsule on which they arrived. The crew will then initiate the refueling docking process from within the CTV by activating the RCS thrusters and allowing the Space Train to align with the refueling depot. The depot will refuel the SLS stage two. See section XX for refueling details. Once refueling operations are complete, the CTV will undock from the refueling depot using its RCS thrusters and orient itself toward its Mars-bound trajectory. The SLS stage two will then perform a burn, requiring a Δv of 0.699 km/s, sending the Space Train on a trajectory to LMO.

All crew transport missions to LMO from L1 will require 180 days of transit time. Upon arrival at LMO, the SLS stage two will complete a burn, requiring a Δv of 2.72 km/s, to enter into LMO. The CTV will orbit in LMO until it meets with the crew EDL descent pod, which was previously sent to LMO. RCS thrusters are used to align the CTV with the descent pod. The descent pod will dock with the available airlock on the CTV. Crew will put on their spacesuits, enter the airlock and, ultimately, board the descent pod after pressurization operations are complete. The descent pod will undock from the CTV and the crew will begin their descent to the Martian Surface. The Space Train will continue to orbit, performing a long stay at LMO, until the next available launch window, 545 days later. At this time, the Space Train will return to L1 for refueling, unless it has already transported two crews to Mars. In this case, the CTV will remain in LMO and a new CTV will transport the remaining crews (see section 5.3 for crew rotations).

5.2.2.2. Propellant Mass Limits

The Space Train configuration consists primarily of a Crew Transport Vehicle (CTV) and a Dragon. The CTV and Dragon will be carried to the L1 Lagrange point on an SLS Block 1B upper stage. This trip would not create any concerning mass limitations for the CTV as long as the SLS refueled at the EML1 Depot. If it was not refueled, the total mass of the CTV would be limited to about 28t; this can be seen in Figure 69 below. With the refuel at L1, the mass could potentially be over 50t and still arrive at LMO with propellant to spare. The maximum mass of the CTV, when taking all required CTV payload components into account, will be 29t. An SLS carrying a 29t CTV, as well as a 6.1t Dragon spacecraft, would arrive at L1 with 31t of propellant in its tanks. It would then require a refuel of 98t at the L1 fuel depot in order to fill the tanks to their maximum propellant mass of 129t. Once refueled, the SpaceTrain configuration would leave for LMO and reach its destination with 43t of propellant leftover.

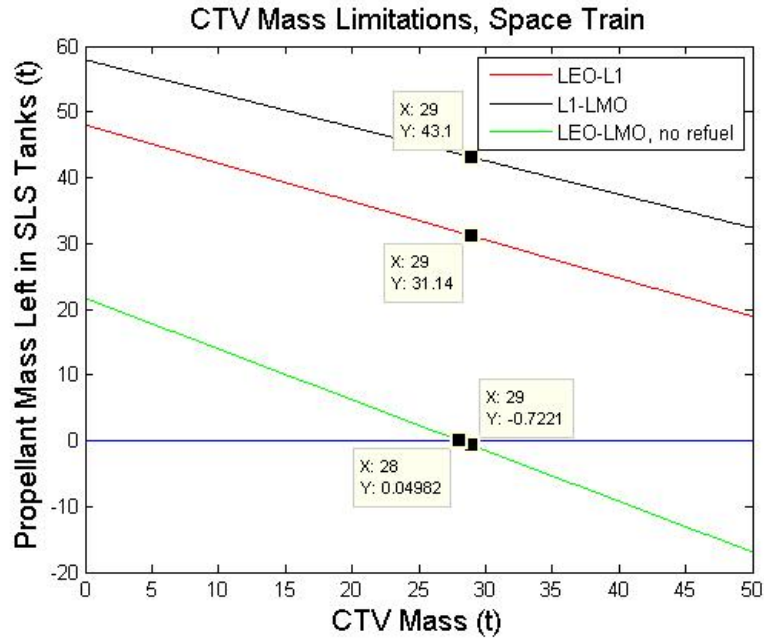


Figure 69. CTV Mass Limitations, SpaceTrain

5.3. Crew Rotations

Primary crew transport to Mars will begin in May 2044 and will end in June 2053. 24 crewmembers will be transported to Mars in crews of four (six crews total). The first crew will depart Earth in May 2044 aboard CTV 1. The first crew will arrive at LMO 180 days later, in October 2044. The crew will immediately depart for the Martian surface and the SpaceTrain will perform a long stay at LMO, orbiting for 545 days. CTV 1 will refuel at and depart LMO in April 2046 and begin its 180-day transit to L1, arriving in October 2046. Here, CTV 1 will be stored until crew 3 is launched in September 2048. Crew 3 will board CTV 1 at L1 and continue to LMO, arriving in February 2049. CTV will again refuel and depart LMO 545 days later, in August 2050 and arrive at L1 180 days later in February 2051 and await Crew 6 transport in June 2053.

Before Crew 3 launches in September 2048, crew 2 will launch in July 2046 and meet CTV 2 at L1. Crew 2 will depart for LMO after all L1 operations are complete and arrive in December 2046, after a 180-day transit. After the crew evacuates the vehicle, the SpaceTrain will continue to orbit in LMO for 545, performing a long stay. The SpaceTrain with CTV 2 will depart LMO in June 2048 and arrive at L1 in December 2048. CTV 2 will remain at L1 for approximately 680 days awaiting the arrival of Crew 4.

Crew 4 will launch from Earth in November 2050 and meet with CTV 2 at L1. Following all L1 preparation and refueling operations, Crew 4 will depart for its 180-day transit to LMO and arrive in April 2051. Upon arrival at LMO, the crew will descend to the Martian surface and the SpaceTrain with CTV 2 will remain in LMO for future missions and emergency use.

Crew 5 will launch in mid-December 2052 and meet with CTV 1 at L1. Three weeks later, CTV 3 and Crew 6 will launch at meet in L1. After all L1 preparations are complete, Crew 5 and 6 will depart for LMO in January 2053, arriving in June 2053, after a 180 day transit time. Crew 5 and 6 will depart for

the Martian surface upon arrival at LMO and the two. At this time CTV 1 and CTV 3 will have completed all initial crew transport missions and it will remain in LMO.

By June 2053, all 24 crew will be on the Martian surface with three SpaceTrain vehicles orbiting in LMO for future crew rotation missions, exploration missions, and possible emergency egress operations. Beginning in 2054, the crew will rotate every 13 years via the three SpaceTrain vehicles in LMO.

Manned Mission No.	Launch Date	Assigned CTV No.	Short Stay/Long Stay at LMO	Arrival Date at LMO	Departure Date from LMO	Return Arrival at L1
1	May-2044	1	Long	Oct-2044	Apr-2046	Apr-20
2	Jul-2046	2	Long	Dec-2046	Jun-2048	Dec-2048
3	Sep-2048	1	Long	Feb-2049	Aug-2050	Feb-2051
4	Nov-2050	2	Long	Apr-2051	-	-
5	Jan-2053	3	Long	Jun-2053	-	-
6	Jan-2053	1	Long	Jun-2053	-	-

Table 26. Crew Rotation Schedule and CTV Assignments

5.4. Crew Transport Vehicle

5.4.1. Structure and Structural Analysis

Inflatable Structure

The structure of the Crew Transport Vehicle (CTV) was originally designed to be a metal cylinder, much like the modules of the International Space Station (detailed design of this iteration can be found in Appendix B). However, due to updated budgetary constraints, the SLS program was not continued in the mission architecture post-2035. The original iteration was sized to fit snugly in an 8.4m SLS payload fairing, but would not be able to fit into a Falcon Heavy fairing with only 4.6m of usable diameter, or an Ariane with only 4.57m of usable diameter. Therefore, a redesign was necessary in order to fit the CTV in one of these alternative launch vehicles while still being able to provide the required habitable volume for the crew.

While the idea of another hard-structure was entertained, research was conducted on the possibility of using an inflatable structure. Inflatables provide a higher ratio of habitable volume to mass, both of which are very significant in this situation seeing that both Falcon and Ariane have far less payload capability both in terms of mass and volume than SLS. Ariane and Falcon were both considered as an alternative launch vehicle to SLS, but Ariane did not have a large enough payload capacity-to-orbit, so Falcon was chosen.

NASA's Transhab and Bigelow Aerospace inflatable modules were researched in order to identify sizing parameters of structures that have already been designed. After research and speaking with an engineer from ILC Dover, the following design constraints were identified:

- Expansion ratio (Inflated - to - deflated ratio): between 1.2 and 2 based upon current designs of inflatable modules

- Deflated (or packed) diameter: less than 4.6m, which is the maximum diameter of the Falcon fairing.
- Length: between 2m and 6.6m because the length of the section of the payload fairing with a 4.6m diameter is 6.6m and the average ceiling height is 2m.
- Inflatable shell thickness: equal to 0.5m, which includes the shell material and waterwall thickness
- Habitable diameter: greater than 2.5m
- Habitable volume: between 110 and 120 m³ based upon the fact that the crew requires around 100m³ of habitable volume and some of the volume will be taken by equipment and storage.

The habitable volume of 100m³ was determined through the use of multiple habitable volume curves (as shown below in Figure 70). The four curves shown below are from the NASA 2011 Habitable Volume Workshop,^[127] the Celentano, the historical NASA data and small habitat historical.^[128] As a result of the NASA 2011 Habitable Volume Workshop curve (99m³) lying between the historical NASA data (248m³) and Celentano (80m³) curves, it was determined to be the best fit for the CTV since it provided enough space for plenty of movement, yet not enough that there was extra, wasteful space.

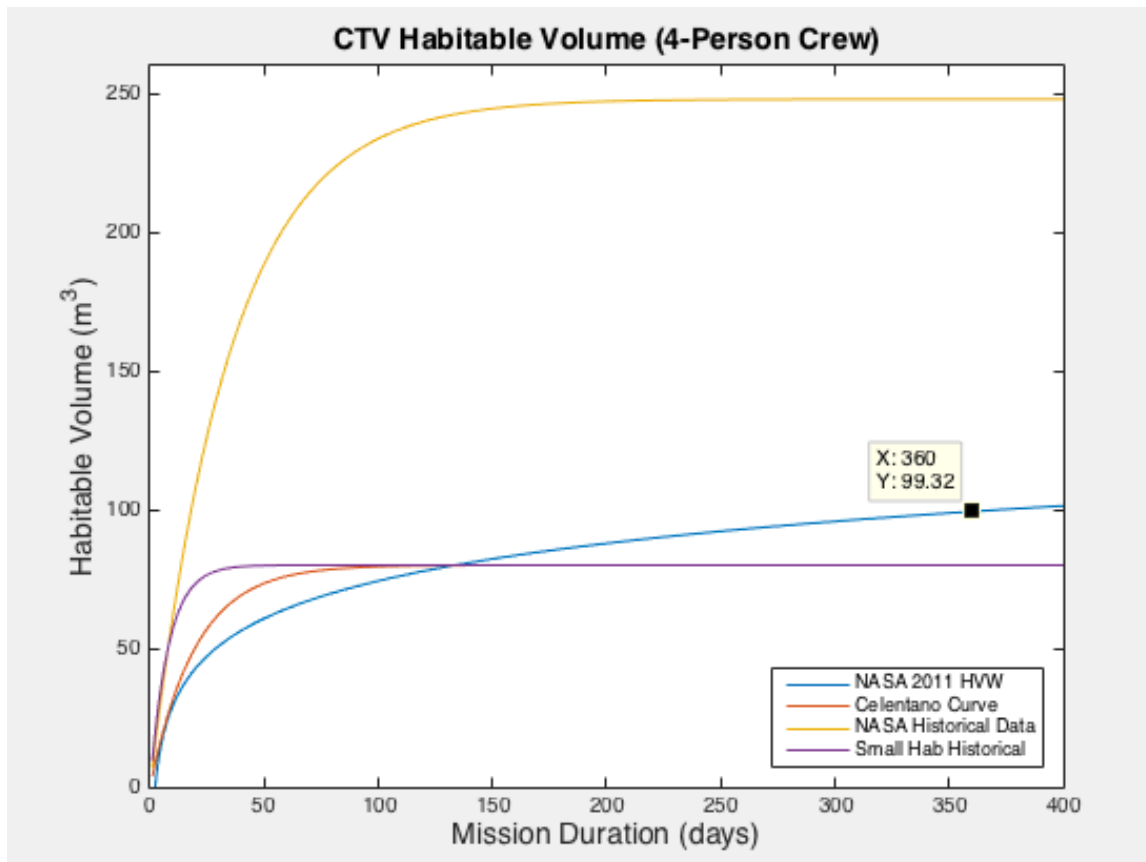


Figure 70. CTV Habitable Volume

In order to optimize the volume and dimensions of the inflatable in order to remain within all design constraints, a MATLAB script was developed (see Appendix C) and a set of five solutions were

produced, which can be found in the table below. The third output was chosen because of the five options it had the largest habitable volume as well as one of the largest expansion ratios.

#	Length	Expansion Ratio	Habitable Diam.	Packed Diam.	Packed Diam. (with cylinder)	Habitable Vol.	Habitable Vol. (with cylinder)
1	5.3	1.50	5.90	4.37	4.54	117.6	112.3
2	5.6	1.45	5.67	4.22	4.40	116.1	110.5
3	5.7	1.45	5.67	4.21	4.39	118.7	112.9
4	6.0	1.40	5.44	4.07	4.26	116.2	110.0
5	6.1	1.40	5.44	4.06	4.25	118.5	112.2

Table 27. Inflatable Sizing Optimization Output

CTV Tanks

For the tanks of the CTV, both for the Attitude Control System and the pressurization of the inflatable, a safety factor of 1.4 was used. For spherical tanks, the limit load was calculated using hoop stress. For the toroidal ACS liquid hydrogen tank, longitudinal stress was used.

$$\sigma_{Hoop} = \frac{p * R}{t} \quad \sigma_{Long} = \frac{p * R}{2 * t}$$

With a tank thickness of 2mm for the toroidal ACS liquid hydrogen tank, a relatively high margin of safety was obtained. This was accepted due to the tank being located on the front of the CTV and having a higher risk of contact with micrometeorites.

Tank	Material	Volume (m ³)	Tank Pressure (MPa)	Tank Thickness	Limit Load (MPa)	MOS
ACS LOX	Al 2090-T86	1.12	4.7	1cm	303	0.22
ACS LH ₂	Al 2090-T86	3.10	1	2mm	70	4.28
Habitat O ₂	Ti-6Al-4V	0.42	20	7mm	434	0.44
Habitat N ₂	Ti-6Al-4V	0.65	31	1cm	472	0.32

Table 28. CTV Tank Stress Analysis

5.4.2. Airlocks

Egress from any particular section of the spacecraft will always occur through a portal or tunnel located in the center of that section. This tunnel is surrounded by three support structures designed to withstand the axial loads associated with launch. This open portal in the center is 1.225 meters in diameter and is concentric with 1.225 meter diameter tunnels at both ends of the CTV. The access tunnel above the upper level has a small door along the inside wall allowing access to the attic as evident in Figure 82. The end of this access tunnel is a docking port designated for the crew descent vehicle. Docking with this vehicle will occur in LMO. There is a second access tunnel located below the lower level that accesses the airlock. The access tunnel is 1.4 meters long with a diameter of 1.225 meters and expands into a 2 meter long airlock with a diameter of 2 meters (large enough to hold two astronauts). A pressurized hatch has been placed at the point of the tunnel's connection with the lower level. The end of the airlock terminates with a second docking port designated for the Dragon spacecraft. The airlock is presented in Figure 71.

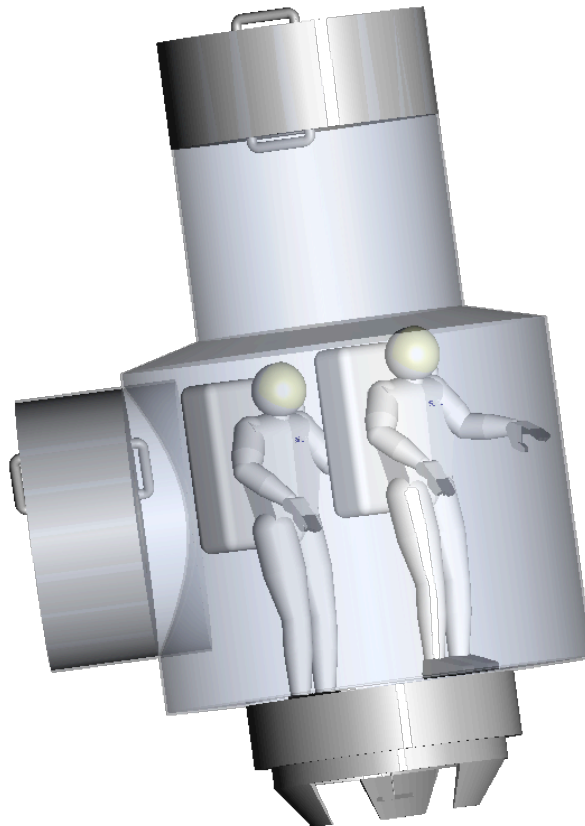


Figure 71. Airlock can contain two astronauts.

5.4.3. Power System

Here is a table showing the power breakdown that is going to be needed on the CTV vehicle while in operation with the crew:

System	Power Requirement
Avionics	5 kW
RCS pumps	1 kW
Thermal Control	0.02 kW
Crew Systems	2 kW
Science Experiment Equipment	3 kW
Total	11.02 kW

Table 29. CTV Power Breakdown

The CTV is going to be powered solely on solar electricity, and these solar panels are going to need to provide around 11kW consistently. The sizing calculation for these solar panels was based on the worst case scenario for these solar panels distance wise. The solar panels were sized with the idea that they would be traveling during the summer season of Mars where Mars is around 1.65AU away from the sun. This significantly decreases the amount of solar irradiance hitting the solar panels. The graph below shows how the solar irradiance quickly decreases as the distance from the sun increases.

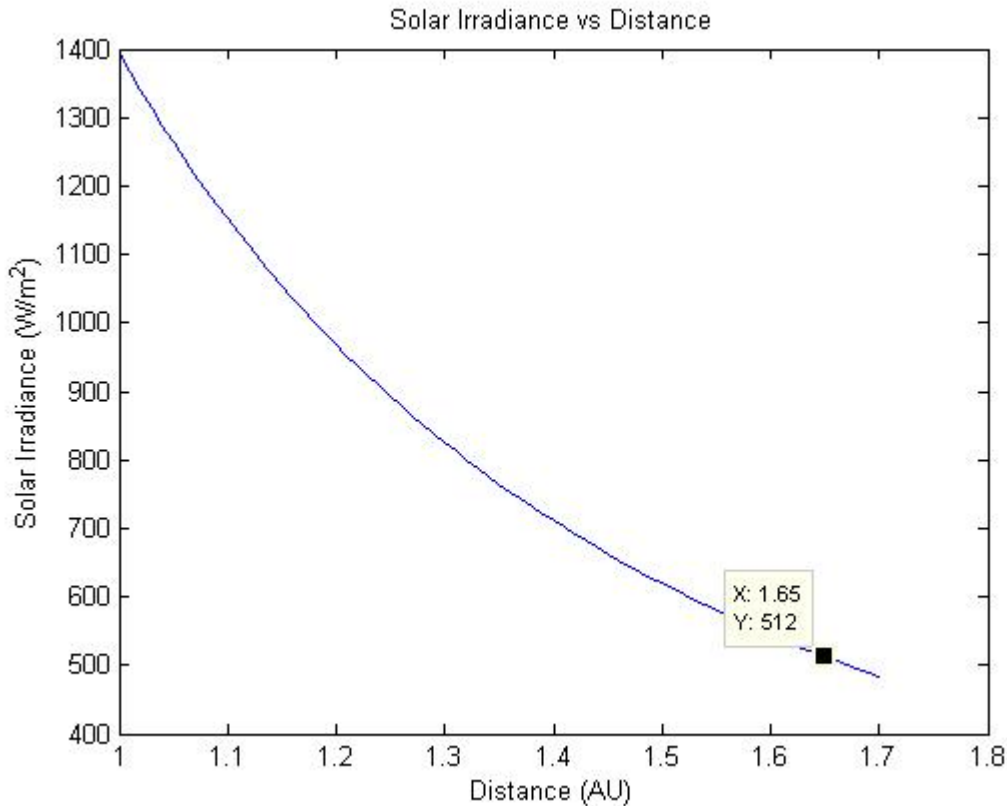


Figure 72. Solar Irradiance vs Distance

The solar panels on the CTV will be able to track the sun allowing for a constant energy production. With the solar panels tracking the sun this will neglect the effect of the zenith angle on the power production of the solar panels. So based on the power required, efficiency of the solar panels, and the solar irradiance it is possible now to size the solar panels needed to provide the required energy to the CTV.

$$A_{solar} = \frac{P_{req}}{\eta_{solar} I_{summer}} = \frac{11020}{.29 * 512} = 74 m^2$$

The CTV will require the minimum of 74m² worth of solar panels, however it was chosen that the CTV will have 78m² based on symmetry proposes when placed on the airlock section of the CTV. The airlock module has a hatch which eliminates the ability to have 4 symmetrically sized and placed solar arrays. Since there are going to be only 3 sets of arrays that means each array is going to require 26m² worth of solar panels.

In addition to the power production, the CTV is going to need a way to store the excess energy that is not being used to power the CTV. The decision was made to use a lithium ion battery over another energy storage system such as hydrogen fuel cells. This decision was made for multiple reasons, one being the overall charge/discharge efficiency of a lithium-ion battery (90%) is greater than the charge/discharge efficiency of the fuel cells (50%). In addition, fuel cells are a lesser known technology than a battery, and it was decided that for the vehicle in space it should have the technology that is known to be reliable. However, hydrogen fuel cells should be under consideration later on in this mission's life cycle to replace the battery energy storage system when fuel cells become a more efficient technology.

The battery was sized to produce 11kW for a 24 hour period, which corresponds to 264 kW-hr. It was decided that a 24 hour period would be enough time to fix any problem that arise with the solar panels. This was based off the duration of time it took the astronauts on the ISS to fix a solar array on the station, about 7 hours, with an additional factor of safety of about 3.5. Using a linear progression of battery technology over the course of a 10 year period it is possible to estimate the mass and size of the lithium ion battery^[161]. Here are the graphs showing the progression:

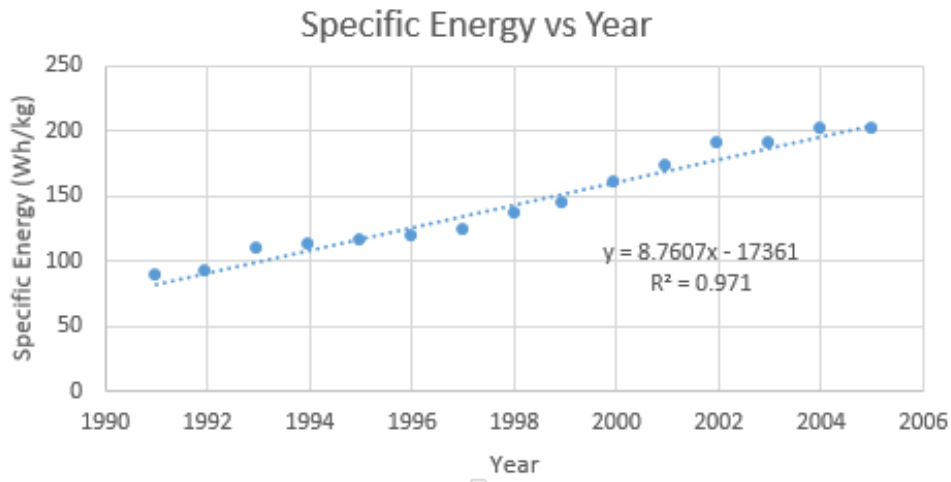


Figure 73. Specific Energy of Li-Ion Battery

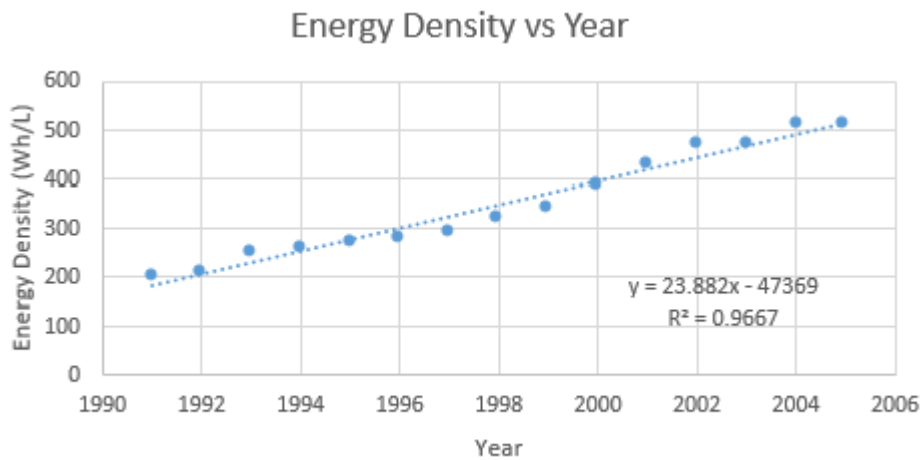


Figure 74. Energy Denisty of Li-Ion Battery

Based on these graphs and the linear progression of the data, the energy density and specific energy of the lithium ion battery can be estimated for the year 2035 which is when the first CTV launch takes place. By the year 2035 lithium ion batteries will have a specific energy value of 467 W-hr/kg, and an energy density value of 1230 kW-hr/m³. From knowing that 264 kW-hr is required of this battery the mass and

the size of the battery can be calculated. It turns out that the battery will weigh 570 kg and will have a volume of 0.21m³.

5.4.4. Thermal Management

5.4.4.1. Radiator Sizing

The CTV's inflatable structure is going to be based off the NASA proposed design of the Transhab attachment to the ISS, which is an inflatable structure that would have been originally used as crew quarters but had the possibility of being used for future planet transit missions.^[163] The Transhab concept uses the idea of multiple layers for the inflatable material. For this section, the most important material is going to be the multi-layer insulation that is located in the layers of inflatable material.^[164] It can be calculated just how much heat will be transferred out of the habitat based on the change from room temperature on the inside of the CTV (293 K) to the temperature facing deep space (4K).

$$\dot{Q}_{out} = k_m * A_{surface} * \left(\frac{T_{hot} - T_{cold}}{t} \right) = \left(3.24 * 10^{-5} \left[\frac{W}{m^2K} \right] \right) (207[m^2]) \left(\frac{293 - 4 [K]}{.01[m]} \right) = 200W$$

The thermal conductivity of the MLI was based on the Spacecraft Thermal Control Handbook where it determines the thermal conductivity based on the hot and cold temperatures (See Appendix C "MLI_Thermal_Conductivity"). The surface area radiating out was based on the assumption that half of the roughly cylindrical vehicle would be radiating to deep space, and the actual number value can be calculated by using the surface area equation of a cylinder and the dimensions of the CTV previously given. In addition the thickness was assumed to be around 1cm thick, which was chosen to allow most if not all of the input heat from solar radiation to be lost on the deep space side of the CTV. This will allow the thermal system to just focus on radiating the waste heat from the electronics inside the habitat.

Now knowing how much heat is radiating out it is time to calculate how much input heat is going to be generated from the solar radiation. That is based on the absorptivity of the MLI insulation along with the surface area illuminated and the solar irradiance.

$$A_{illum} = l * d + \pi \left(\frac{d}{2} \right)^2 = 72 m^2$$

With "l" and "d" representing the length of the CTV and the diameter respectively.

$$\dot{Q}_{solar} = I_{solar} * A_{illum} * \alpha = \left(1394 \frac{W}{m^2} \right) (72 m^2) (0.0037) = 375 W$$

This heat input will change over the duration of the mission as the crew transport vehicle gets farther away from the sun due to the change in solar irradiance, which will essentially change the size needed for the radiators. However, just like the solar panels in the CTV power section, these radiators will be sized for the worst case scenario and that would be during the time the CTV is starting its journey to the L1 LaGrange point in LEO. Here is a graph showing the necessary sizing of a Kapton film, aluminum backed radiator that has an average emissivity of around 0.85, and radiating temperature of 323K:

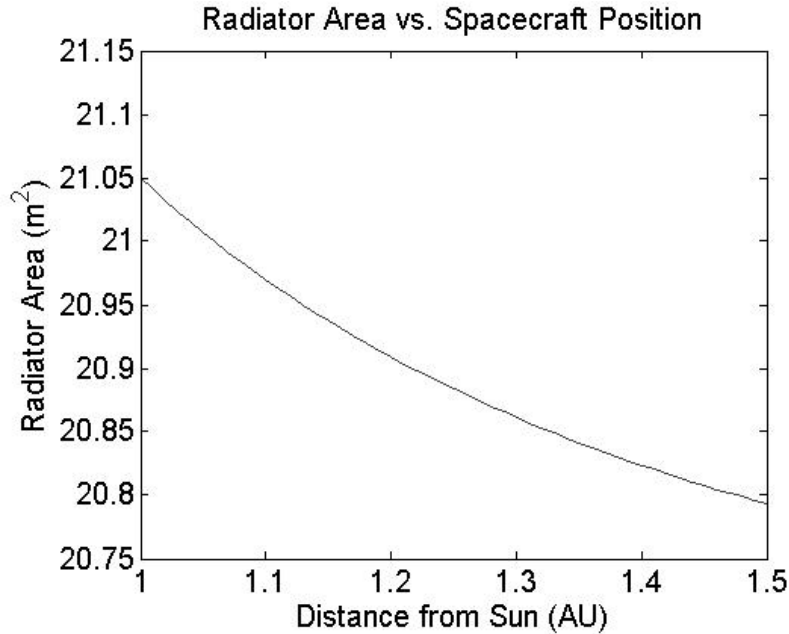


Figure 75. Radiator Area vs Distance

To determine the area of the radiators required, this graph just iterates on the power equilibrium equation to find the area need for the radiators:

$$A_{rad} = \frac{Q_{solar} + Q_{int} - Q_{out}}{\epsilon\sigma T_{rad}^4}$$

Based on the fact that only 200 watts of power will be leaving the CTV, the thermal system is going to have to be able to radiate out the waste heat of 11 kW from the power consumption inside the CTV, which this graph takes into account of. This graph shows that the CTV is going to require 21m² worth of radiators (See Appendix C “SC_thermal” for full calculation). With there being a 4 arrays of radiators this results in each array being 5.25 m² worth of radiators.

5.4.4.2. Thermal Loop

The thermal system for the CTV is going to be an active two fluid pumped loop with the internal loop being the water from the water shell and the external loop being ammonia. The water and the ammonia are going to pass through a heat exchanger that will allow the heat that was absorbed by the water inside the CTV to be transferred over to the ammonia to be taken to the radiators. This system is considered an active system due to the fact that there is going to be a temperature sensor, a bypass valve and a regenerative heat exchanger. The temperature sensor is going to measure the temperature of the ammonia exiting the radiator and if that temperature starts to get within 30 K of the freezing point of ammonia (196K) a bypass valve will open. Once the bypass valve is open, that will divert some of the ammonia to a regenerative heat exchanger that inlet ammonia is flowing through and this will allow the exit ammonia to pick up extra heat allowing the temperature of the fluid to rise. This system is being used to prevent ammonia freezing in the pipes outside of the CTV.

5.4.4.3. RCS Thermal

As mentioned in the previous RCS propulsion section, this vehicle is going to be carrying 1500 kg worth of propellant and an issue that arises from cryogenic propellant storage in space is boil-off. Boil-off results in the cryogenic liquid vaporizing inside the tank and then the tank has to release some of that new vapor to lower the pressure inside of the tank so it does not explode. That released vapor is a loss in propellant and ways to combat this problem are by insulating the storage tanks. However insulation can only lower the boil-off rate to a certain point and not reach zero boil-off. Based on the thickness and specific properties of the tanks and the insulation themselves the boil-off rate can be computed from the equation:^[167]

$$r_{boil} = \frac{\Delta T(k_m + k_s\alpha)\beta}{\rho\Delta hH_{vap}}$$

Where “ ΔT ” is the temperature difference between the ambient temperature and the cryogenic liquid, “ k_m ” and “ k_s ” are the thermal conductivities of the multi-layer insulation and the material of the storage tank, Aluminum 2090-T86, respectively. The “ α ” term is the ratio between the support junction area and the total surface area of the inner shell. The support junction is what would be supporting the outer layer allowing room for insulation, and 0.003% was the chosen average value for this term. “ β ” corresponds to area density of the storage tank, which is just the surface area of the tank over the volume of the tank. The “ ρ ” represents the density of the propellant being store, and the “ Δh ” is the thickness of the insulation. Finally, the “ H_{vap} ” term is the energy of vaporization of the cryogenic liquid, which was determined using an analytical function corresponding to liquid oxygen and hydrogen^[169].

Now from using this equation the thickness of the insulation can be iterated on to determine how the boil-off rate is affected by the thickness of the insulation. Here are the graphs showing the boil-off rates of each cryogenic liquid related to the thickness of the insulation:

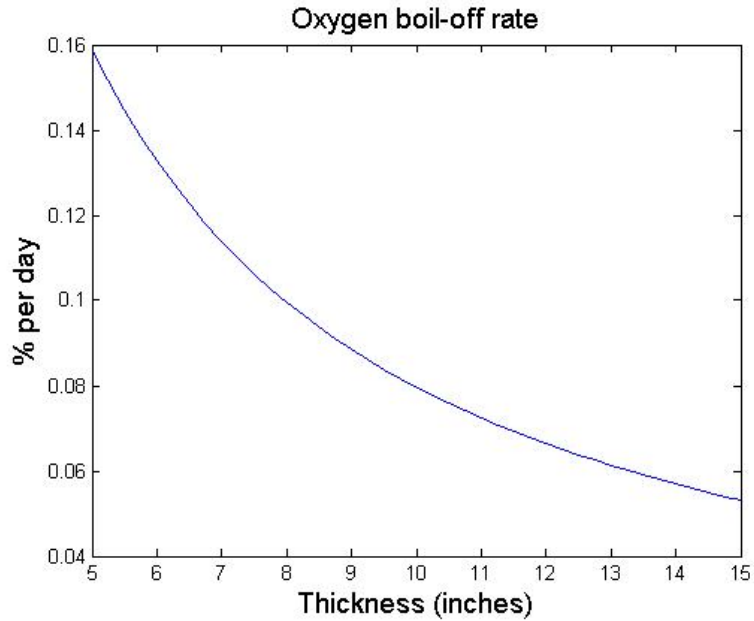


Figure 76. Oxygen Boil-Off rate

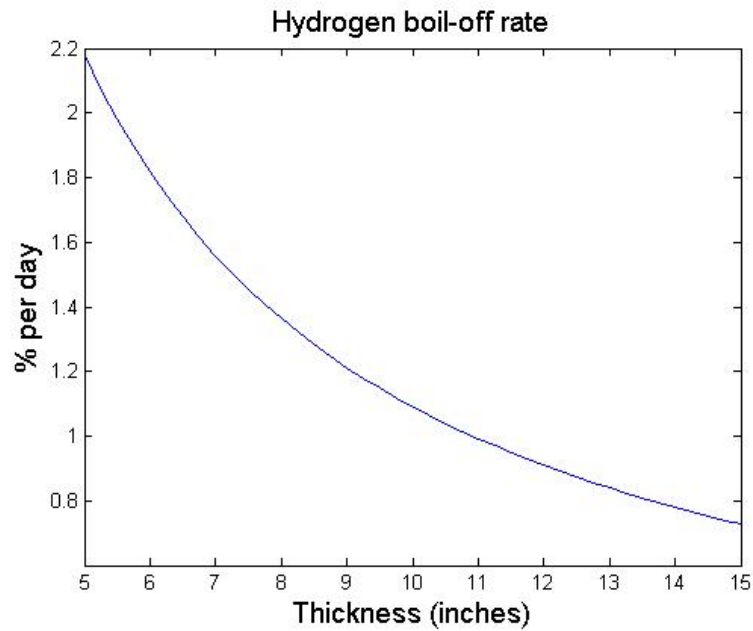


Figure 77. Hydrogen Boil-Off

Liquid oxygen based on the higher boiling point and higher density results in a much lower boil off rate than liquid hydrogen. The LH₂ storage tank has enough space to hold 15 inches worth of insulation and but only 10 inches for the LOX tanks due to spacing constraints on the airlock module. This corresponds to a 0.7% a day for the Hydrogen boil-off rate, while the Oxygen boil-off rate is around 0.08%. Due to

boil off over the course of a roughly 260 day trip to Mars only 20% of the LOX supply will be lost, which corresponds to 1040 kg worth of LOX. However, even with the 15 inches of insulation for the hydrogen storage tank it will still result in total boil-off by half way through the mission. To counteract the total boil-off of hydrogen over the course of the mission the CTV would have to use adopt a cooling system like the one used on the fuel depots that allows there to be theoretically zero boil-off.

5.4.5. Reaction Control System

5.4.5.1. Moment of Intertia

The Space Train is going to have a 6 axis thruster system that will help this large vehicle dock with the EDL vehicle in low Mars orbit. To determine the type of thrust needed for these RCS thrusters the required torque to move this vehicle is needed, which relates to the moment of inertia. To determine the moment of inertia of the vehicle assumptions were made about the general shape of each attachment of the space train. The SLS upper stage was assumed to be two spherical bodies, which represent the LOX and LH₂ storage tanks. If we use the moment of inertia equations for a spherical structure we can find the moment of inertia of the SLS upper stage by using the mass and the radius of each given tank:

$$I_{zz} = I_{yy} = \frac{2}{3}(m_{LOX})(r_{LOX})^2 + \frac{2}{3}(m_{LH_2})(r_{LH_2})^2 = 1152000 \text{ kg m}^2$$

Next, the SpaceX dragon capsule was assumed to be a cone, and the moment of inertia for a cone can be related to the radius of the Dragon's base, mass of the Dragon, and the length of the Dragon:

$$I_{zz} = \frac{3}{10}(m_{dragon})(r_{dragon})^2 = 5830 \text{ kg m}^2$$

$$I_{yy} = \frac{3}{5}(m_{dragon})\left(\frac{r_{dragon}^2}{4} + l_{dragon}^2\right) = 33100 \text{ kg m}^2$$

Finally, there is the CTV which was assumed to be a hollow cylinder:

$$I_{zz} = \frac{1}{2}(m_{CTV})(r_{out}^2 + r_{in}^2) = 230000 \text{ kg m}^2$$

$$I_{yy} = \frac{1}{12}(m_{CTV})(3(r_{out}^2 + r_{in}^2) + l_{CTV}) = 180000 \text{ kg m}^2$$

The total moment of inertia values come out to be: $I_z = 1388000 \text{ kg m}^2$ and $I_y = 1365000 \text{ kg m}^2$

5.4.5.2. Thrust

Now having the moment of inertia for the total space train the total amount of torque required to move the vehicle can be calculated. However, this is based on the total time it takes for the space train maneuver and the moment of inertia, which we can see in this equation:

$$\tau_z = \frac{2(\theta - \theta_o)(I_{zz})}{t^2} - \tau_{dragon}$$

Torque depends on the moment of inertia so to find the max amount of torque the moment of inertia in the z direction will be used because that is the greater moment of inertia value. In addition, the torque should be based off the max rotational angle change which corresponds to the theta terms in the equation. This max rotational angle change will be assumed as 180 degrees, however based on the acceleration and deceleration of the vehicle the theta term in the equation will only correspond to 90 degrees. The reason being is that once you rotate the initial 90 degrees the vehicle is still going to keep rotating however the Space Train will only need to wait to thrust again once the vehicle reaches 180 degrees. This is will double the total amount of maneuver time, however do to the reduction in the angle change from 180 degrees and the maneuver time corresponding to 90 degrees the torque value will decrease causing the thrust required from the RCS thruster to be significantly lower. The Dragon capsule's RCS thrusters are also going to help with reducing the total amount of thrust required by the CTV's RCS thrusters.

To figure out the required thrust needed of the RCS thrusters this equation will be used:

$$F_{RCS} = \frac{\tau_z}{2 * d_{arm}}$$

This equation is just the moment equation where torque is equal to force multiplied by the distance, where the distance is just the total length of the truss structure holding the RCS block, which is 3.2725 meters long. Additionally, the distance was multiplied by two for the reason that there is going to be two truss arms extending opposite of each other and applying a force to move the space train in a specific direction. The total maneuver time can be iterated on to find the total amount of thrust required for the RCS.

Here is a graph of the thrust required of the RCS thrusters vs the total maneuver time it would take to rotate 180 degrees with the dragon providing additional thrust (See Appendix C "RCS_Actual" for code of computation):

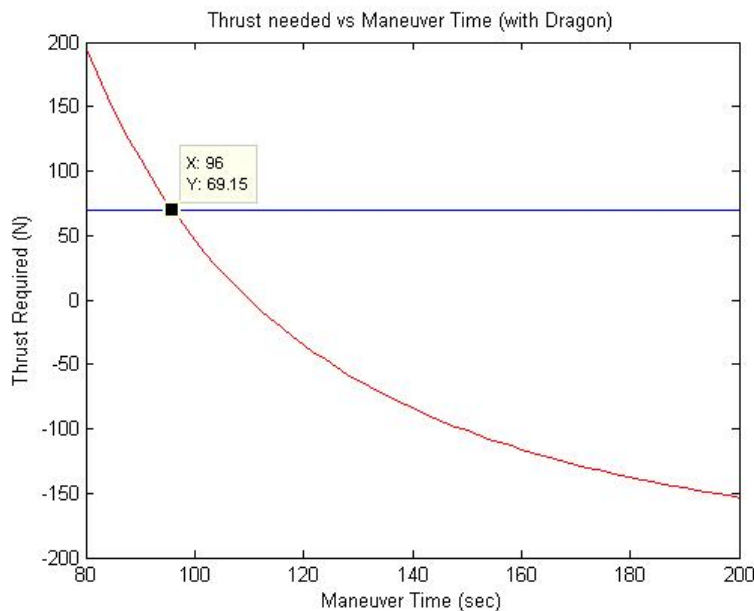


Figure 78. Thrust needed vs Maneuver Time (with Dragon)

As you can see on the graph that a total amount of thrust of 70 N was chosen for multiple reasons. It would allow the CTV to do a complete axis rotation in about a minute and a half, and additionally it will allow the space train to also do a rotation without the dragon in about 3 minutes. Here is a graph showing the maneuver time without the Dragon’s RCS thrusters helping with the rotation:

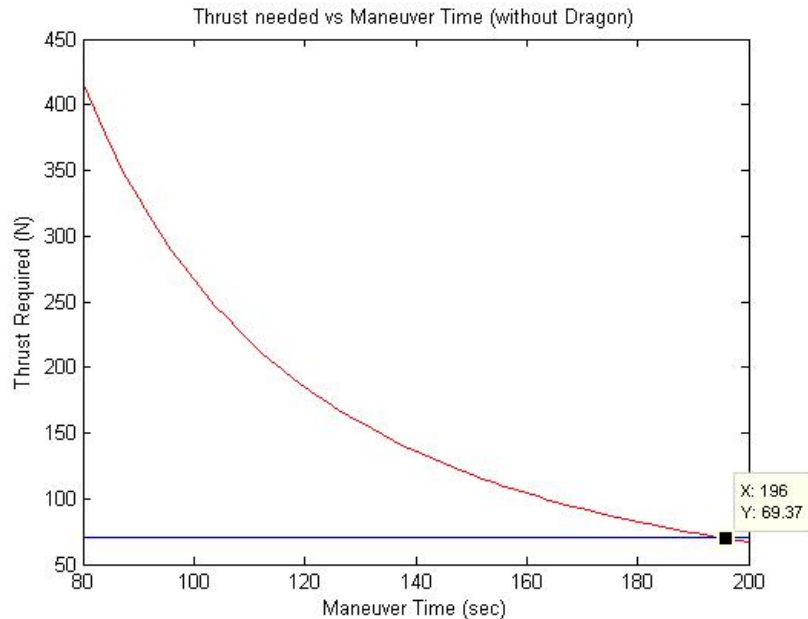


Figure 79. Thrust needed vs Maneuver Time (without Dragon)

This is important to know because if the Mars settlement is going to be Earth independent in the future, the space train cannot rely on the Dragon’s RCS thrusters forever due to the fact that these thrusters are propelled by Hydrazine and Nitrogen Tetroxide ^[166]. These are two propellants that the settlement are not going to be able to create.

This RCS system on the CTV has the same design that was created for the earth-moon fuel depot, and this was decided based on the simplicity of designing one thruster used on multiple systems verses multiple thruster designs for multiple systems. As previously mentioned in the fuel depot RCS section, these thrusters are combustion engine thrusters using LOX and LH₂. Here is a small table showing the specifications of the thruster:

Thrust	70 N
Nozzle Material	Niobium
Mixture Ratio	5.85:1
\dot{m}	20 g/s
Pe/P0	10 ⁻³
Ae/At	37.5

Table 30. Thruster Specifications

There is a total of 1500 kg worth of propellant stored for the CTV's RCS system, and with a mixture ratio of 5.85:1 that results in 1280 kg of LOX and 220 kg of LH₂. Based on the total amount of propellant and the mass flow rate the total amount of time the system can run can be determined as:

$$t = \frac{m_{prop}}{\dot{m}} = \frac{1500}{.02} = 75000 \text{ sec} = 20.8 \text{ hours}$$

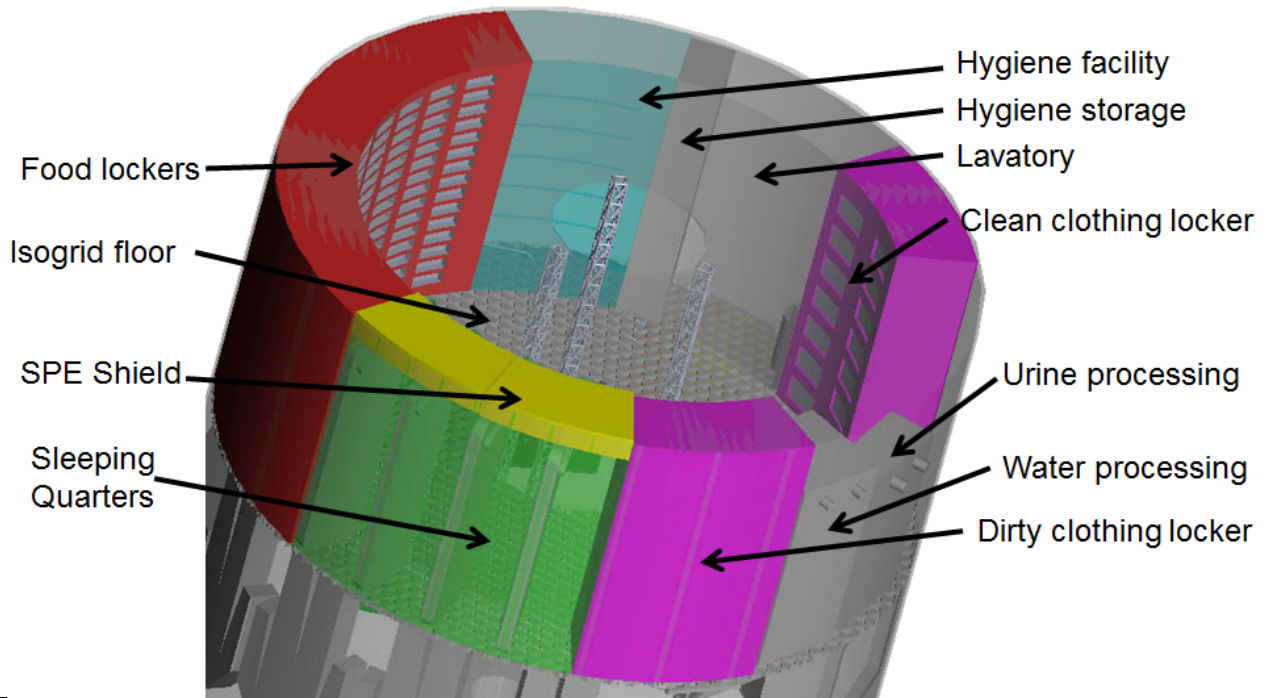
The total amount of pulses that this system can provide is based on the total amount of usage time, which was previously calculated above and the pulse time an RCS thruster would normally have. In this case the pulse time of the RCS thrusters on the space shuttle were used, which corresponds to about 80 milliseconds.^[168]

$$Pulses = \frac{75000}{.080} = 940000 \text{ pulses}$$

5.4.6. Interior Layouts

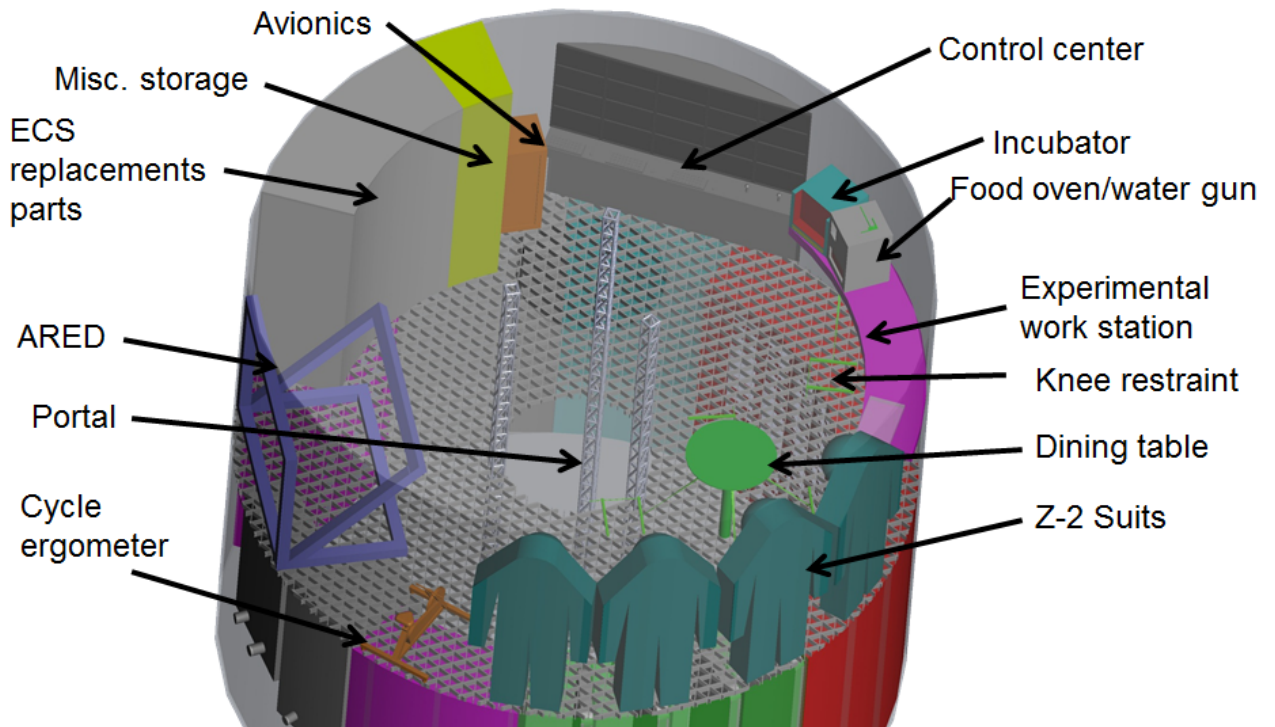
5.4.6.1. Overview

The interior of the CTV contains two primary habitable floors. The upper level is primarily dedicated to sleeping, hygiene and storage while the lower level will be used for a galley, experimental space, control center, exercise facility and general crew meeting area. There will be a small crawl space known as the "attic" with about a ½ meter tall ceiling which astronauts may access on their stomachs. However, the attic is located outside of the radiation shielding water wall and should only be accessed if work is required on the Sabatier reactor or septic system. Additional space allocations in the attic are possible for systems such as cooling pumps, dehumidifiers, etc. These three sections are presented in Figures 80, 81 and 82. Note that the upper and lower levels utilize the same isogrid floor. Therefore, there is a 180° change of orientation between the levels.



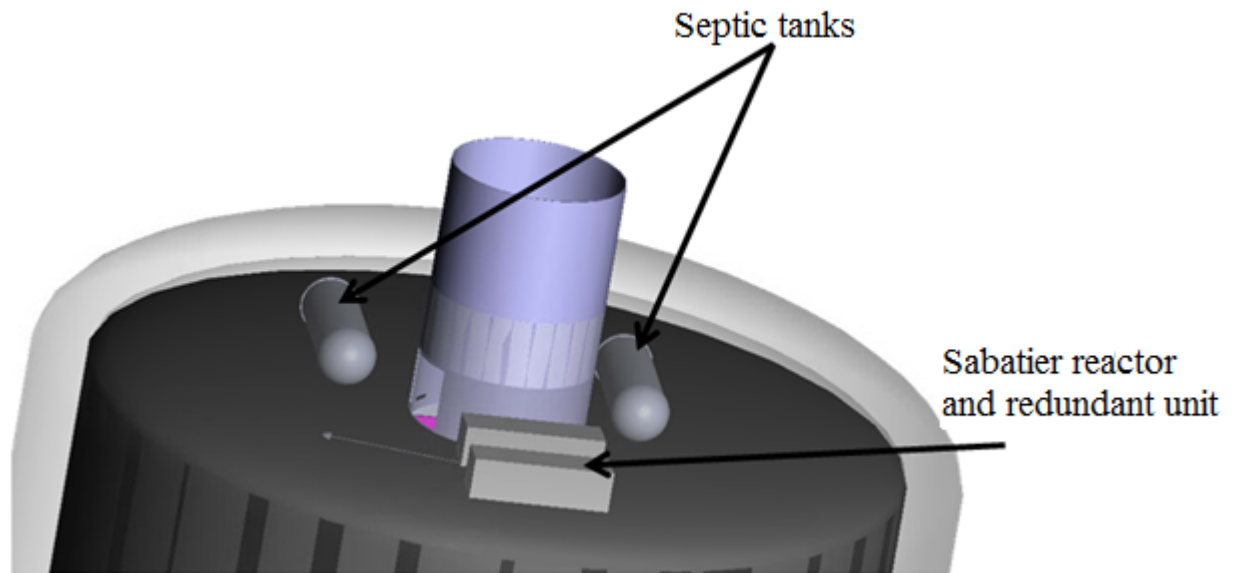
Item	Floor Area (m ²)	Volume Allocation (m ³)
Food lockers	3.07	7.07
SPE Shield	0.37	0.07
Sleeping quarters	0.37	0.86
Hygiene Facility	0.88	2.0
Hygiene storage	0.22	0.51
Lavatory	1.14	2.62
Clean clothing locker	0.88	2.02
Dirty clothing locker	0.88	2.02
Urine processor assembly	0.35	0.52
Water processor assembly	0.64	1.10

Figure 80. Upper level accommodations and spatial allocations.



Item	Floor Area (m ²)	Volume Allocation (m ³)
Avionics containment	0.20	0.20
Misc. storage	0.43	0.99
ECS replacement parts	1.46	
ARED	1.98	2.77
Portal	1.18	N/A
Cycle ergometer	0.51	0.26
Dining table	0.45	0.45
Experimental work station	1.36	1.36
Control center	0.76	1.44

Figure 81. Lower level accommodations and spatial allocations.



Item	Volume (m ³)
Septic tanks	0.3
Sabatier reactor	0.09
Redundant Sabatier reactor	0.09

Figure 82. Attic accommodations and spatial allocations.
The attic is located above the upper level.

5.4.6.2. Habitability

In both the surface habitat and in previous design iterations of the CTV, the ceiling heights were set at 2.5 meters as this is a habitability standard for both weightless and partial gravity environments.^[128] However, in the final CTV design this was reduced to 2.3 meters. This was primarily due to length restraints on the vehicle as it was originally sized to fit within the Falcon Heavy payload fairing. With 2.3 meter ceilings, there is still approximately 0.4 meters of ceiling clearance for a 95th percentile male. Additionally, this slightly lowered ceiling height may be beneficial in microgravity as it increases the number of grasp points for shorter astronauts. With a 2.3 meter high ceiling, a greater proportion of the astronauts will be capable of placing a foot on the floor and stabilizing with a hand on the ceiling.

The floor of the spacecraft will use an isogrid pattern originally adopted by Skylab. This will consist of a matrix of triangular holes in the floor. This is presented in Figure 83. The astronauts will be provided with shoes whose soles have been mounted with triangular cleats that fit into the floor slots. This form of restraint was praised by Skylab astronauts as one of their favorites in mission debriefs. The astronauts found the floors to be very useful even when they were not wearing their shoes as the grid provided toe and finger grasp points all over the spacecraft. The primary complaint of Skylab astronauts was that the grid was not more widespread. Skylab astronauts had a tendency to drag their feet across the grid while wearing the shoes thus ablating the toes. This will be remedied by installing plastic caps on the end of the shoes during manufacture.^[31] Due to the inflatable nature of the CTV, the floor will have to be stored between the support beams during launch. The floor will be assembled in space from smaller panels which will be snapped together after the spacecraft is inflated.

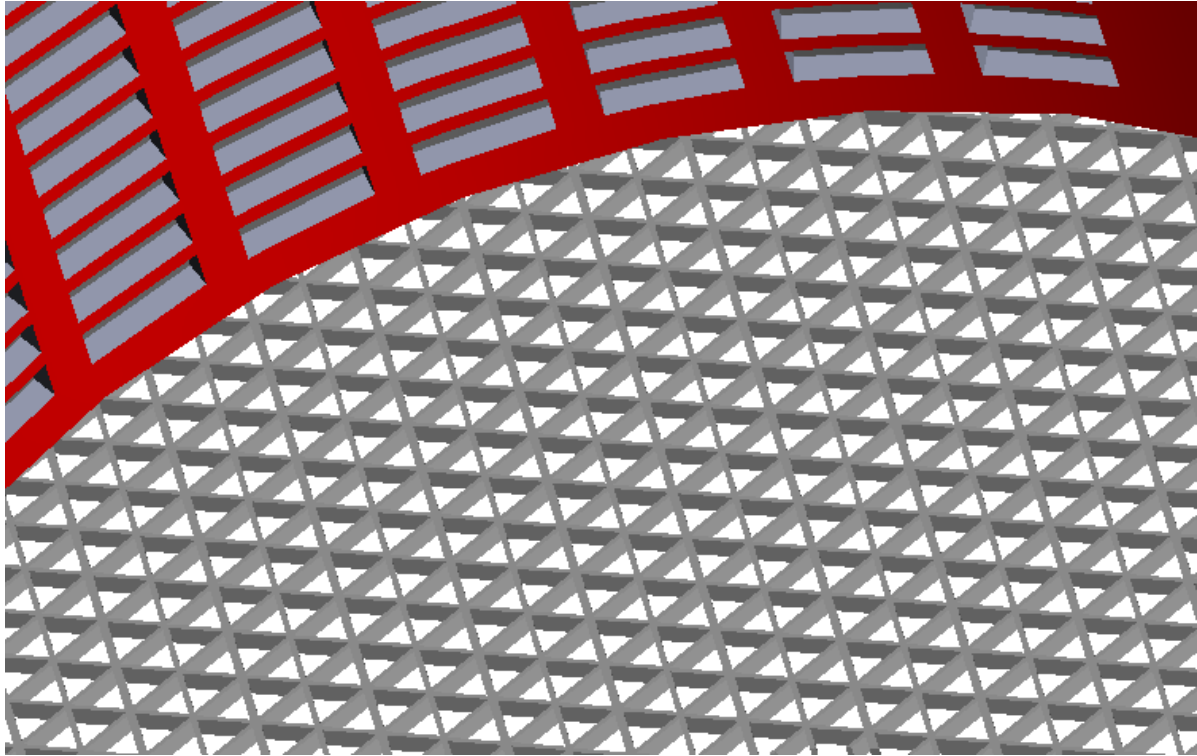


Figure 83. Isogrid Floor

As one will note in reviewing the CTV's floor layout, most storage and crew quarter areas have been placed around the perimeter of the interior. This was done to maximize the open volume of the spacecraft to mitigate isolation or feelings of crampedness. This configuration allows for the open space to be more or less a solid cylinder on both floors. Placing volume allocations for sleeping quarters, food storage, etc. in the center of the spacecraft would have resulted in open spaces being restricted to cylindrical shells surrounding equipment. Astronauts confined to cylindrical shell passageways would have been forced to climb over one another in passing thus contributing to feelings of crowdedness. The final layout of the CTV allows for all crew members to be in view of one another at all times unless confined to a private space such as the hygiene facility, lavatory, or sleeping quarter.

5.4.6.3. Sleeping Quarters

The sleeping quarters will be adapted from those used on the ISS. Each astronaut will have a personal space that is essentially a vertically oriented locker. A sleeping bag will be attached to the wall with a small storage area on the opposite wall for personal items such as a laptop or photographs. Astronauts will be able to take personal calls in this space as long as time delays in transmission permit. They have been sized around a 95th percentile male with a shoulder grip length of 0.715m, shoulder width of 0.505m, and height of 1.865m.^[32] To comply with the shoulder grip length constraint, the two radial walls will have a separation distance of ~0.8m. To comply with the shoulder width constraint, each wall will be 0.65 meters wide. A 20cm polyethylene SPE shield is installed above the astronaut's head, thus the ceiling height is 2.1m in this sleeping quarter. This sleeping quarter is presented in Figure 84.

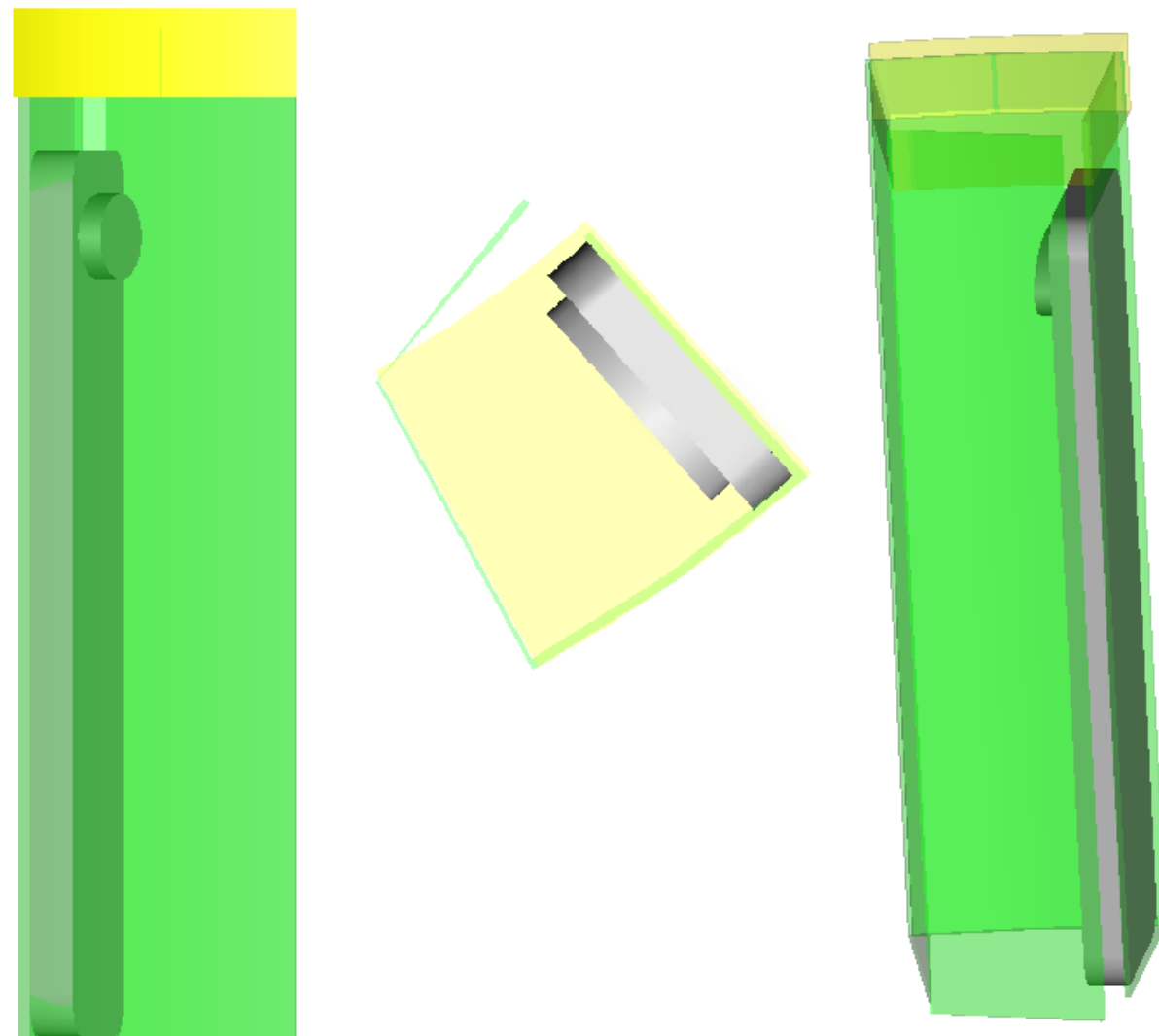


Figure 84. Sleeping quarter with SPE shield indicated in yellow. Three views are presented: radial inward (left), top down (center), radial outward (right).

5.4.6.4. Hygiene Facility

A Skylab shower had initially been considered for the hygiene facility; however, reviewing crew evaluations of the system performance indicated that considerable effort was spent cleaning the shower after every use. Rather than force crew members to become sweaty immediately after hygiene activities, the crew members will use prepackaged wet towels to take sponge baths in a dedicated hygiene facility. The facility has been equipped with a foot restraint as well as several hand restraints at increasing heights to accommodate crew members of various sizes. Like the sleeping quarters, the hygiene facility's inner and outer walls are curved to fit tangent to the inner wall of the pressurized CTV. The separation between the radial walls is around 1.2-1.3 meters depending upon the measurement point. This will allow a 95th

percentile male with a bust depth of 28cm and a thumb tip reach of 88.2cm to stand at the foot restraint and comfortable extend their arms in all directions.

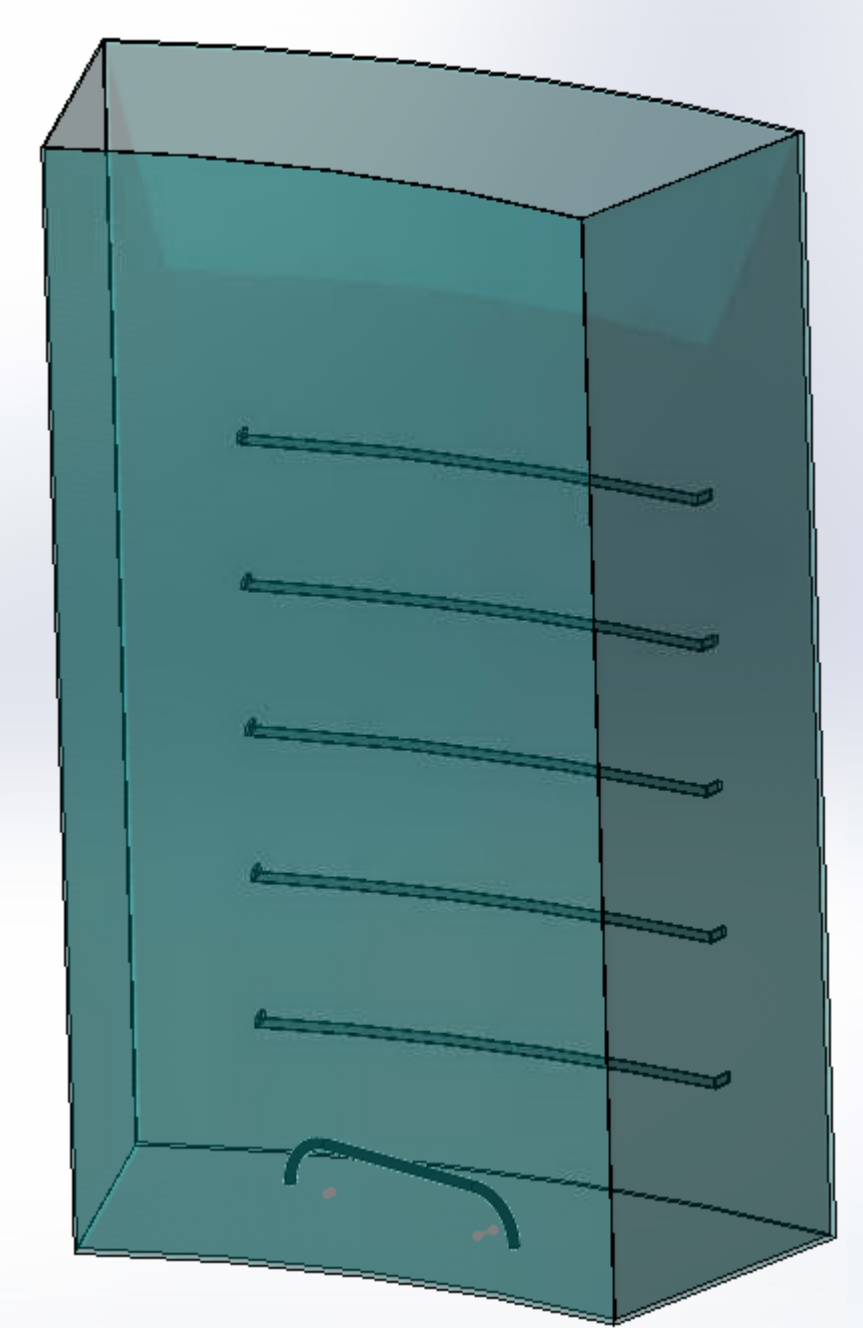


Figure 85. Hygiene facility with foot and hand restraints

5.4.6.5. Lavatory

The lavatory will be adapted from the ISS Tranquility node's unit. Urine will be collected with a vacuum hose. The hose will have an individualized adapter for each crew member. Fecal matter will be compressed and routed to the septic tank. The Lavatory will also have a 5m³ cabinet for hygiene and grooming products as well as wet wipes and toilet paper for clean ups.^[33]

5.4.6.6. Dinner Table

The crew will be using a modified Skylab dinner table. The light duty foot restraints have been removed due to dissatisfaction among Skylab astronauts due to an incompatibility with the cleated shoes. However optional knee restraints extend from the lower surface of the table and have been sized for 95th percentile adult men in the neutral body position. They may be extended or lowered to accommodate astronauts of different sizes. Under the 95th percentile assumption, the knee restraints sit at 61cm above the floor. The upper and lower arms of the restraint nominally sit 19.1cm apart to accommodate 95th percentile thigh clearance; however, they are also adjustable. The surface of the dinner table will be outfitted with slots to accommodate space shuttle meal trays and the surface will have Velcro to attach small instruments and miscellaneous objects. The dinner table has a close proximity to the command center and will serve as a central meeting location for the crew. The dinner table is presented in Figure 86.

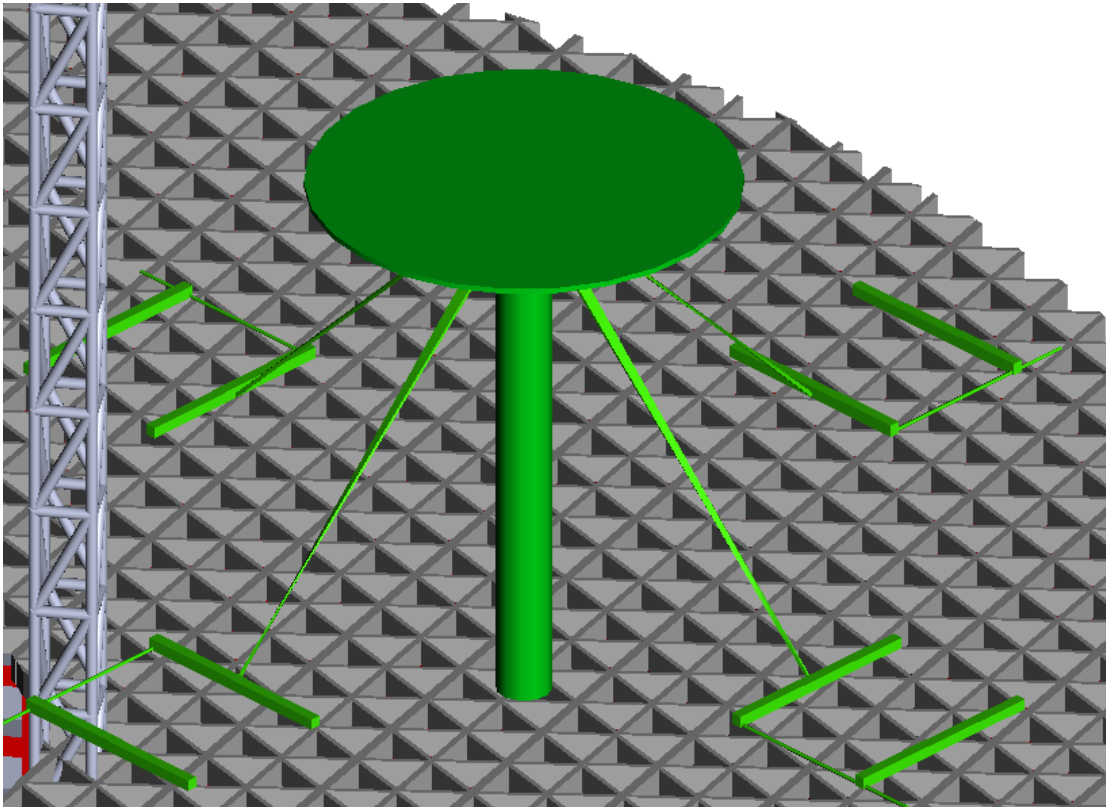


Figure 86. Dinner table with knee restraints.

5.4.6.7. Exercise

Long duration exposure to microgravity can contribute to significant bone and muscular mass losses. The astronauts will mitigate these effects using two pieces of equipment on board the CTV. They will use an Advanced Resistance Exercise Device (ARED) and a cycle ergometer. The ARED has been demonstrated on the ISS and proper use can provide high impact joint compressions, which are essential to musculoskeletal health. The ARED will be used for core and upper body exercise. The cycle ergometer will provide a vigorous cardiovascular exercise to help maintain heart health and endurance. Astronauts will exercise two hours per day on an individualized plan developed by a personal trainer.

5.4.6.8. Control Center

The CTV's control center consists of all the crew I/O to interface with all of the vehicle's critical and auxiliary functions. Information output is handled by 20 18.5" high-definition touchscreens arranged in a 4x5 grid. Crew input is done through the touchscreens, one of 20 peripheral sets (keyboard, touchpad, magnetically-adhering mice + surface), or via analog physical controls (joysticks, buttons, switches, speakers, microphones, etc.). Touch input capabilities allow great flexibility of crew input as well as manipulation of data. Peripheral sets act as a backup to touch capabilities but may also be used as the primary input method if preferred. The physical controls act as absolute backups to the primary inputs but only exist for all critical functions. Every touchscreen is capable of displaying and interfacing every possible function of the CTV, providing 20 paths of redundancy amongst all the touchscreens. This setup also allows for crew flexibility with the ability to customize the control center's purpose for various tasks and operations.

5.4.7. Life Support and Environmental Control System

5.4.7.1. Food

The deep space diet will be composed entirely of prepackaged retorted and freeze dried food. This decision was made in response to the research conducted by the surface habitat greenhouse team. Their optimization efforts indicated that 53.4m² of crop space would be required for each crew member. In order to meet all caloric and nutritional needs, additional space would have to be devoted to fish farming. Although the bioregenerative nature of this system is essential for Earth independence of the surface habitat, it would not provide any volume or mass savings in the context of a six month flight to Mars. This is especially apparent in considering the possibility of a crop failure which could reduce food production for months. This contingency is accounted for in the surface habitat with months of prepackaged food reserves. Rather than implement a bioregenerative system with prepackaged reserves onboard the CTV, freeze dried and retorted foods will be the primary source of sustenance for the crew.

The Space Shuttle program demonstrated that shelf-stable freeze dried and retorted foods can provide astronauts with diverse and palatable meals without the need for refrigeration. Astronauts could

personalize their food options based upon a menu of over 350 items. Their selections would then be sent for approval to a dietician who could recommend substitutions to ensure that all nutritional needs were being met. The astronauts rarely issued complaints and many shuttle derived menu items were brought into the ISS program.^[36] Currently, foods of these types have shelf-lives of around 18 months^[34] However, NASA's Advanced Food Technology Project is actively working to extend this figure significantly. They have completed a series of 36-month accelerated shelf-life tests which demonstrate the potential for room temperature storage of meat up to 8 years, fruit up to 5 years, dairy up to 3.25 years, and vegetables up to 4 years.^[35] Such products will be of vital importance to our crews.

The CTV mass and volume allocations for food storage have been designed around a 2,800 daily calorie intake. Food storage for this diet will amount to 1.76 kg and 0.0048m³ per crew member-day. This figure includes food as well as packaging and a storage container.^[37] Four astronauts on a 360 day round trip flight to Mars will thus require approximately 7m³ of food storage. This has been provided via a 7m³ food locker located on the upper level of the CTV (see Figure 87).

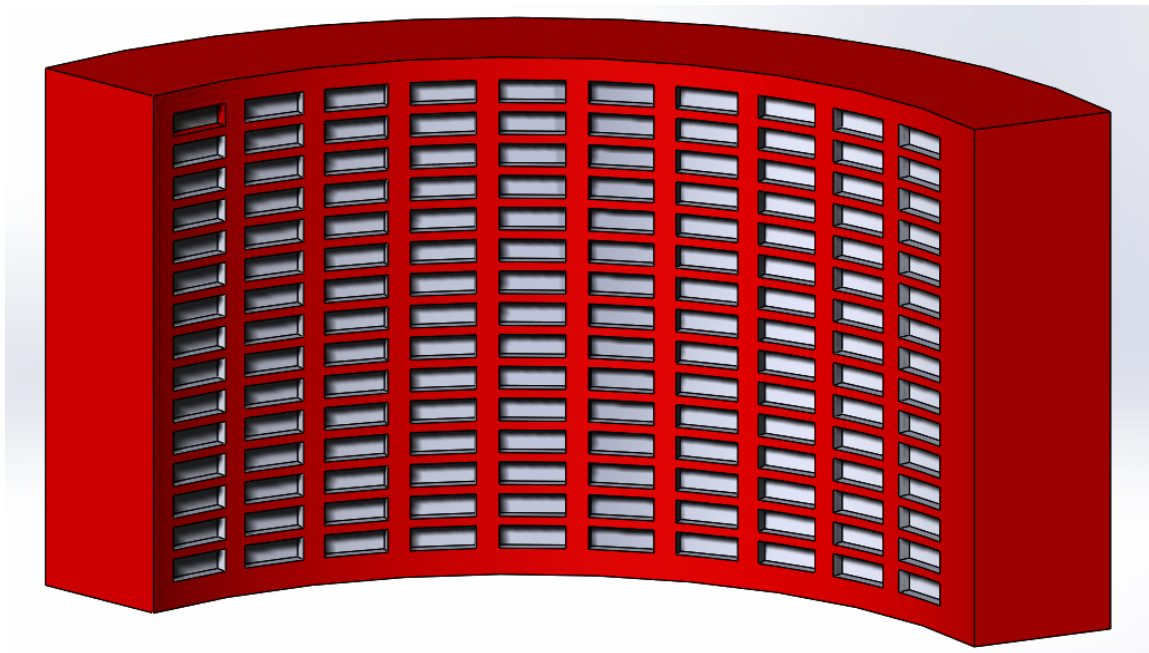


Figure 87. Seven cubic meters of food storage will be provided by a curved cabinet that is 2.3 m tall, has an outer radius of 2.835 m, inner radius of 2.185 m and spans 108 °.

Food preparation and consumption will occur on the lower level of the CTV. The experimental work station doubles as a food preparation area and will be outfitted with a space shuttle derived conduction oven and rehydration apparatus. This system has a mass of 36.3kg and a volume of 0.094m³. When in use, it will draw a maximum of 0.960kW.^[37] This system will allow for a meal for four to be prepared in about a half hour with only five minutes of prep on the part of the crew members.^[38]

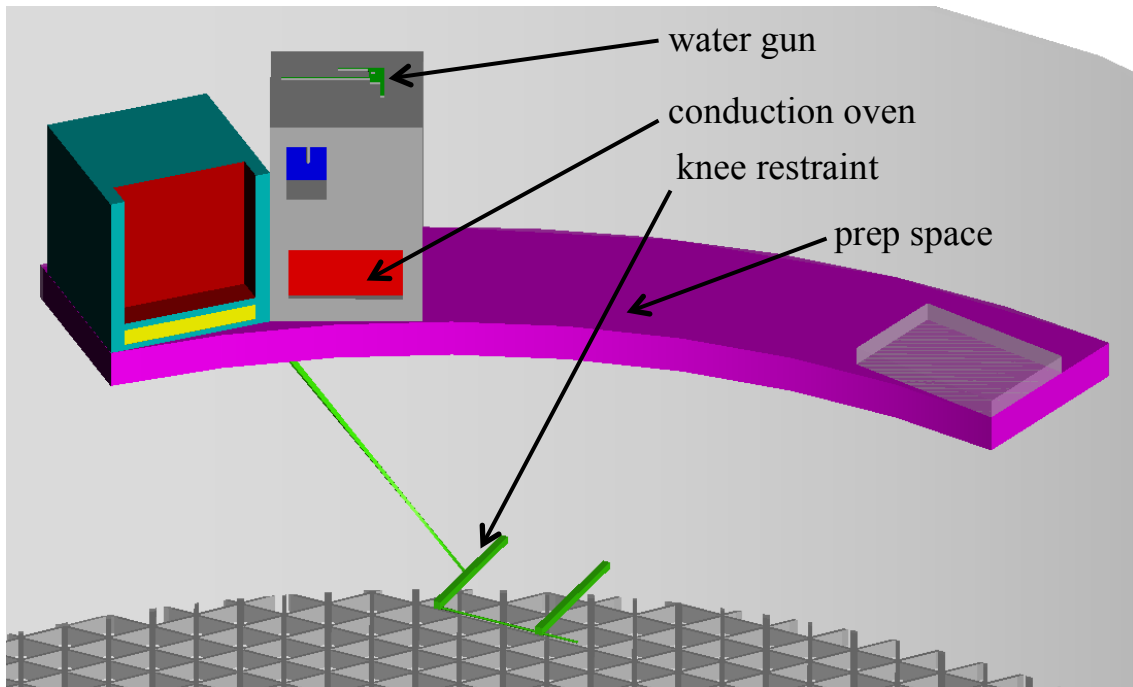


Figure 88. The experimental work space doubles as a galley.

5.4.7.2. Atmosphere

In selecting a gas composition for the cabin atmosphere, a number of factors had to be considered. The ISS uses an atmosphere of 21% oxygen at a total pressure of 101.3 kPa. This composition is very close to that of the Earth and allows for far fewer question marks in using non-metallic, off-the-shelf materials in the cabin. However, the pre-breathe procedure coupled to this composition is rather arduous. Supplemental exercise while breathing pure oxygen can only decrease the pre-breathe time from four hours to two.^[39] Thus, a mission architecture which emphasizes exploration through extra vehicular activity would certainly require a higher percent oxygen composition. However, this desire must be weighed against concerns of material flammability.

Any materials used within the cabin of the CTV will have to comply with NASA-STD-6001 which sets forth flammability tests to evaluate the potential for self-extinguishment of a material. NASA tests materials in various gas compositions up to 30% oxygen which is the assumed flammability limit for general use materials.^[39] A trade study was commissioned to determine the prebreathe times necessary of various atmospheres less than 30% oxygen. An R value of 1.6 was chosen as this is considered to be generally safe.^[250] Using this R value and an assumed ISS spacesuit pressure of 29.6 kPa, the desired tissue pressure of N₂ post pre-breathe was calculated as such

$$p_{N_2-Tissue} = R * P_{suit}$$

This tissue pressure was subbed into the left hand side below to solve for the time required for pre-breathe. The half time was chosen conservatively as 240 minutes.

$$p_{N2-Tissue}(t) = p_{N2-Tissue}(0) \exp \left[-(\ln 2) \frac{t}{t_{1/2}} \right]$$

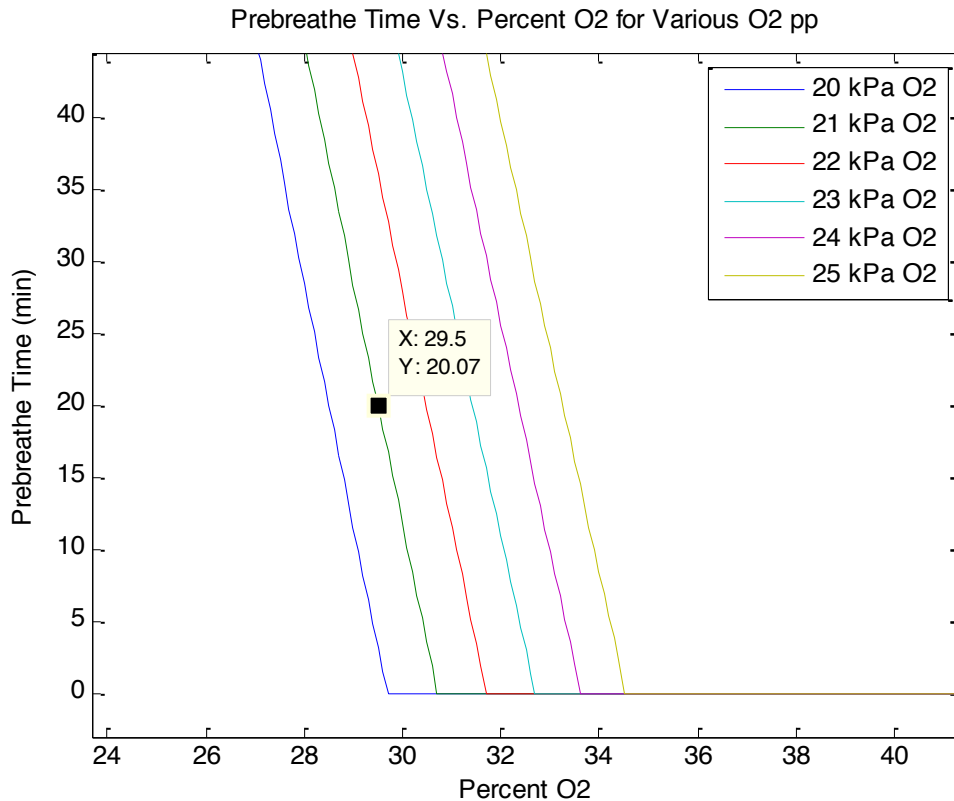


Figure 89. Prebreathe time with respect to atmospheric oxygen content for various partial pressures.

Numerous cabin atmospheres were evaluated and are presented in Figure 89. The code used to generate this figure is presented in Appendix C as ‘Atmospheric Composition Trade Study’. Lower partial pressures of oxygen (as low as 16 kPa) were initially considered; however, it was decided that a sea level partial pressure of oxygen (21 kPa) was essential for crew health and would prevent the need for high altitude ground training. Using a sea level partial pressure also gives the crew more time to respond in the event of a hull breach. A decision was made to use 29.5% oxygen and 70.5% nitrogen at a total pressure of 71.2 kPa. This atmosphere will be used for all human habitats in this architecture. The decision was motivated by the atmosphere only necessitating a 20 minute pre-breathe. From historical systems, twenty minutes seems to be about the amount of time that is necessary to prep a spacesuit and complete its start-up checklists. Therefore, thus twenty minutes can be considered “free” when evaluating systems against their pre-breathe times.

The CTV's atmosphere will be provided by spherical pressure vessels stored in a ring concentric with the CTV's docking mechanism for the crew EDL vehicle. There will be ten tanks in total, four for oxygen and six for nitrogen. They will be mounted upon an aluminum plate which radiates from the docking mechanism. Space is allocated underneath the plate for the radiator panels to extend from. As an inflatable spacecraft, the CTV has very few rigid sections. The egress tunnels at either end of the spacecraft are the only rigid structures upon which to mount equipment such as tanks, panels, and trusses. The circular plate devoted to tank storage had to house all of the compressed gas tanks as well as the toroidal ACS propellant tank in a section no longer than 0.5m to avoid contact with the EDL vehicle. Thus spatial restrictions dictated that either a ring of spherical tanks or toroidal tanks be used. Spherical tanks were chosen for their strength to weight ratio, and inherent redundancy as a loss of pressure in any one tank would not seriously impact the mission. This arrangement can be viewed in Figure 90.

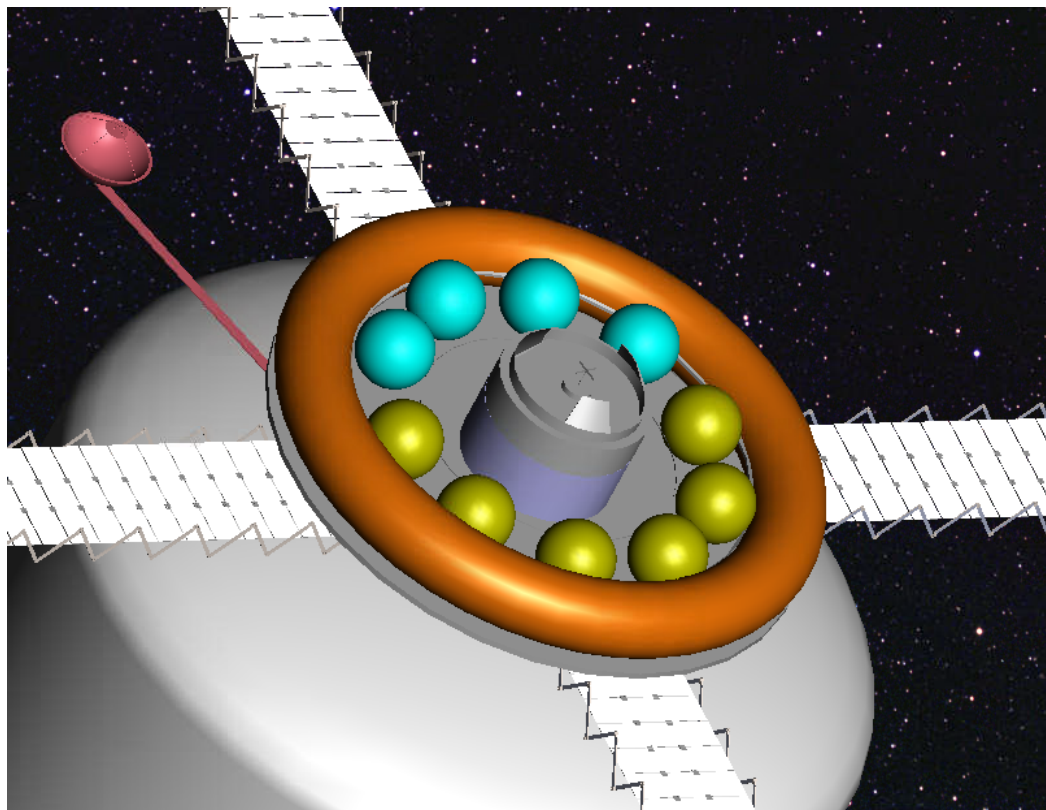


Figure 90. Aluminum gas storage plate with oxygen (blue), nitrogen (yellow), and ACS propellant (orange).

The CTV gas tanks were sized such that they would allow for the CTV to be fully pressurized three times. A quantity such as this will fully mitigate the effects of cabin leaks (0.14% per day)^[37] and allow for continued mission success in the event of a rapid depressurization event. Such an event would require the astronauts to move into the dragon spacecraft to use as a lifeboat while performing EVA's to repair damage to the CTV's hull.

Using the ideal gas law and an internal volume of $\sim 100 \text{ m}^3$ at $\sim 300 \text{ K}$, the pressurant requirements were 2530 mols O_2 and 6040 mols N_2 . Tank pressures were selected to be 4500 psi for nitrogen and 2900 psi

for oxygen. The nitrogen pressure was selected as it is a standard gaseous N₂ storage pressure for spacecraft.^[252] The oxygen pressure was selected somewhat arbitrarily due to its prevalence as an operating pressure for most small industrial pressure vessels. The tank volumes were determined using the ideal gas law with the chosen pressures and an assumed worst-case scenario tank temperature of 400 K after prolonged exposure to direct sunlight. This resulted in a tank size requirement of 0.42m³ for oxygen and 0.65m³ for nitrogen. This volume requirement was satisfied with the ten tanks assuming an inner radius of 0.3m. Titanium was chosen as the material due to its high strength to weight ratio. The outer radius was determined by assuming a safety factor of two (later reduced to 1.4 to produce a positive margin of safety) and yield strength of 880 MPa (Ti-6Al-4V (Grade 5)). From the thin walled equation for hoop stress, the thickness was found to be 7 mm for the oxygen tanks and 1 cm for the nitrogen tanks. A titanium density of 4430 kg/m³ would produce tank masses of 35.9kg per O₂ tank and 51.8kg per N₂ tank.

$$\frac{\sigma_y}{SF} = \frac{pr}{2t}$$

5.4.7.3. Radiation Shielding

The absence of a magnetic field surrounding Mars significantly complicates the goal of achieving Earth independence. Radiation in the form of galactic cosmic rays (GCR) and solar particle events (SPE) will plague astronauts both in the journey to Mars as well as on the surface. GCR's originate outside of the solar system and are typically composed of protons and small nuclei. They bombard astronauts omnidirectionally at a relatively constant rate thus slowly contributing to cell damage over time. Conversely, an SPE shower results from a coronal mass ejection of the sun and can blast astronauts with a massive dose of radiation over the course of a few hours.

NASA has traditionally attempted to restrict astronaut flight hours based upon a 3% limit for the increased risk of exposure induced death (REID) when applied to an average U.S. population. Although this is still the official flight policy of NASA as presented in NCRP-132, recent research efforts are demonstrating that the problem is substantially more difficult and varies between people of the same age and demographic. In particular, the risks associated with never-smokers may be substantially lower than previously thought. Also, there has been a recent push to replace the entire concept of the REM with a more probabilistic risk assessment based upon quality factors.^[40] However, these efforts have not yet been unified into an overarching risk mitigation plan. As a starting point for this architecture, systems will be designed to keep astronauts within the NCRP-132 limitations over the course of a 14 year round trip stay on Mars.

Age at Initial Exposure (Yr)	Female Limit (REM)	Male Limit (REM)
25	40	70
35	60	100
45	90	150
55	170	300

Table 31. Habitats will be designed to keep astronauts within the limits of NCRP 132 over their 14 year mission.^[40]

Measurements taken in deep space by Mars Science Laboratory predict that astronauts may receive a BFO dosage of approximately 66.2 REM during the 360 day round trip flight to Mars.^[42] While living on the surface, dosages will range from 10-20 REM per year depending upon elevation. This is deduced from Figure 91. At these levels, it is clear that a long stay on Mars would be impossible without adequate shielding. A 35 year old woman would surpass all career limits during the transport portion alone.

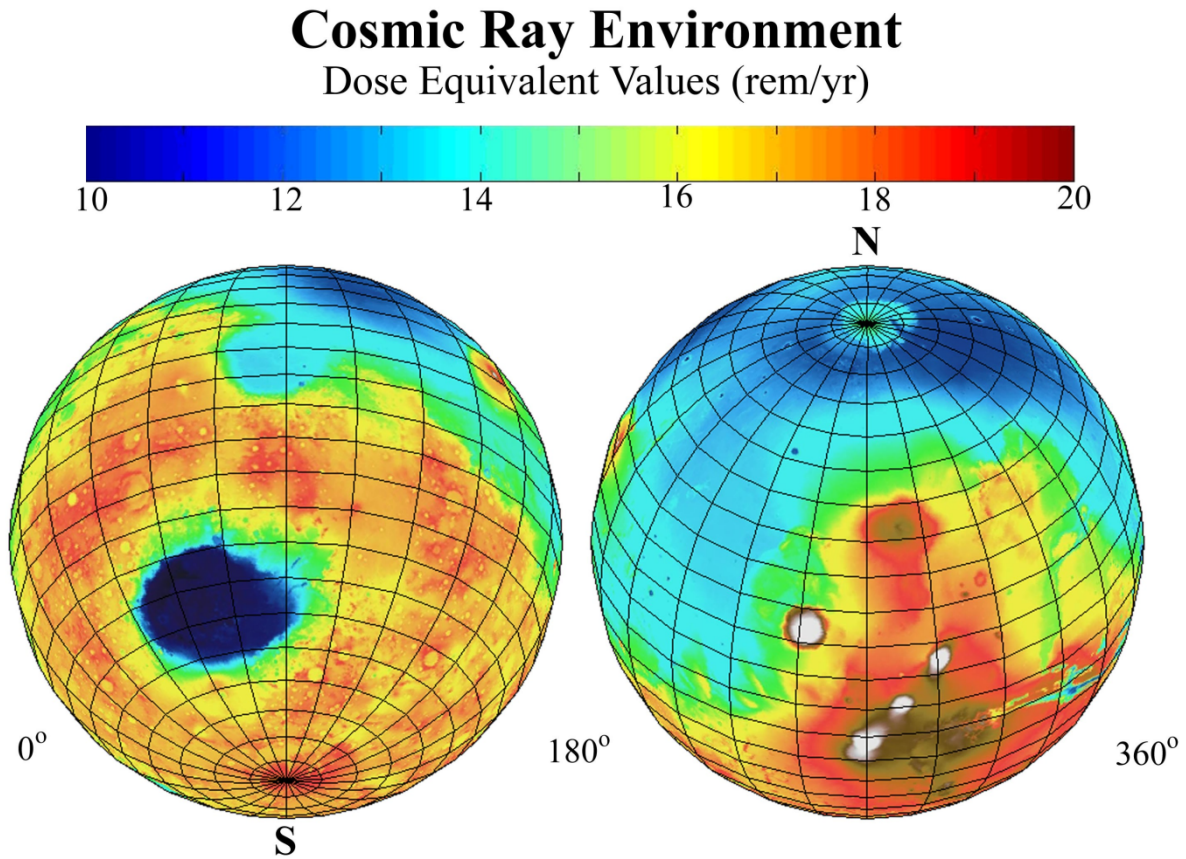


Figure 91. The lowest elevations of Mars may allow for as little as 10-12 REM per year.^[43]

A logical first approach to radiation exposure reduction was to select a landing site with a low elevation. Initial recommendations included the Korolev Crater, Hellas Planitia, Valles Marineris, and Arsia Mons. All of these sites have low elevations with the exception of Arsia Mons. The MPA team reviewed my suggestions and discounted Korolev due to concern for ground instability from the seasonal sublimation of CO₂ sheets. Valles Marineris was discounted due to the anticipated EDL difficulties associated with precision landing among cliffs. Arsia Mons is a large volcano located at a high elevation. A habitat at this location would have to be built deep within the volcanic shafts thus offering natural shielding for the astronauts. However, a massive infrastructure would be required to move equipment up and down the slopes. Additionally, radiation exposure on the outside of the slopes would have been incredibly high. Ultimately Hellas Planitia was chosen for its predictable terrain, low elevation, and the potential for thousands of cubic kilometers of subsurface ice as identified by MRO.^[44]

The selection of Hellas Planitia allows for radiation exposure to be reduced during typical EVA's; however, any architecture which hopes to achieve Earth independence with the potential for lifelong stays on Mars will require complete radiation protection in the habitat. This is especially important in considering the possibility that children may eventually be born in the habitat. For our purposes, complete protection may be interpreted as less than 2% of the ambient exposure. An analysis of GCR reduction with depth using the GEANT4 Monte Carlo simulation tool kit suggested that this requirement may be met with a 5 meter layer of regolith piled above the habitat.^[45] This method will be adopted for Asimov City.

With the habitat shielding in place, astronaut surface EVA hour limitations are correlated directly with the amount of shielding that will be employed in the CTV. Water and polyethylene are the two most effective shields per unit mass.^[251] As large amounts of water will already be required for the life support systems, the most intuitive form of passive shielding for the CTV was to simply build the potable water tank into a shell surrounding the habitable portion of the spacecraft.

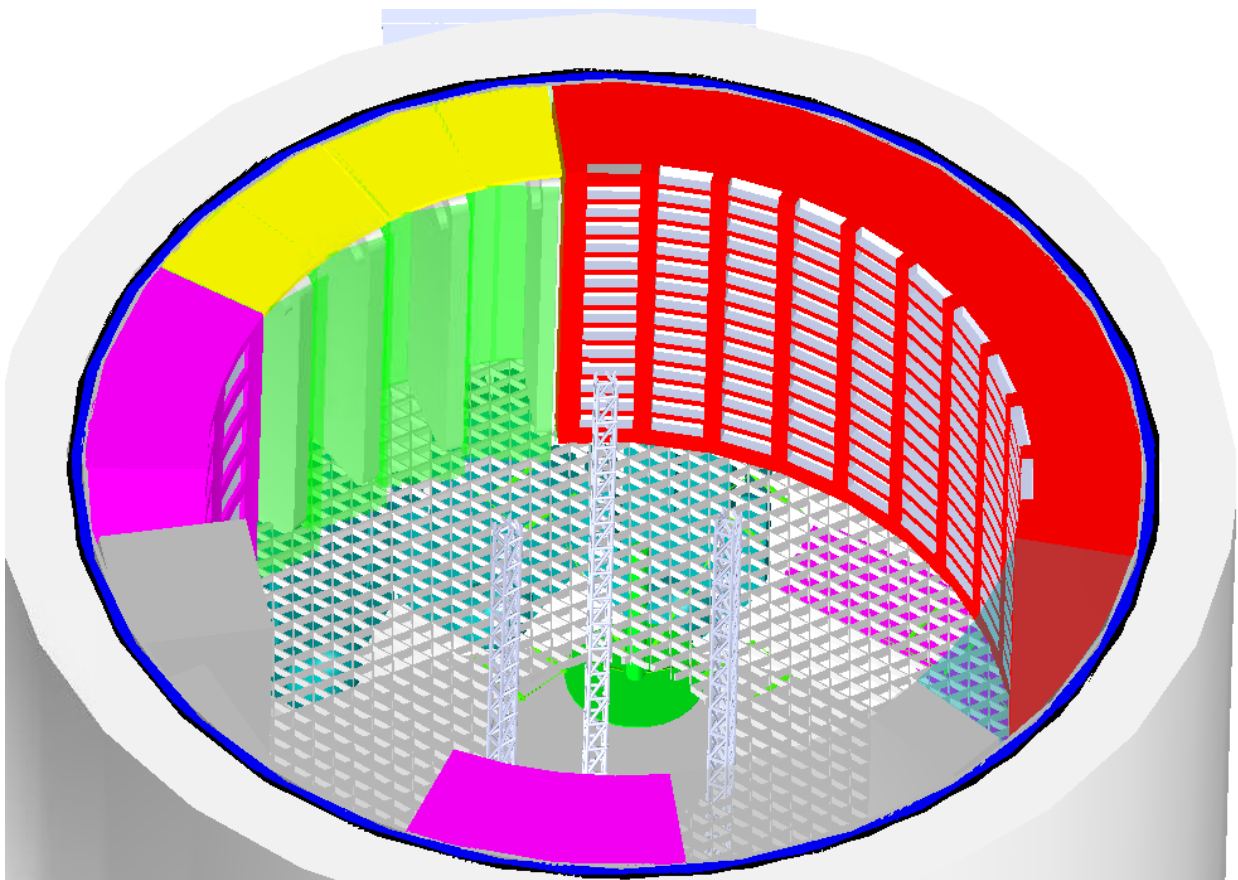


Figure 92. Water Wall Concept

To quantify the dose reduction effects of water with respect to thickness, “Effective Dose Based on Shielding” was taken as a reference.^[251] Points from the “GCR polyethylene” trend (polyethylene is

assumed as nearly equivalent to water) were visually estimated and placed into a MATLAB file and fitted to a decaying exponential curve. This exponential relationship is thus estimated as:

$$\text{Yearly Deep Space REM} = 17e^{\text{water thickness (m)} \cdot (-39.12)} + 53$$

The thickness of the wall was governed by two primary constraints. First, it should be thick enough to allow 35 year old women to perform EVA's on the surface. Second, it should be thick enough to keep the astronauts alive for 360 days in the event that the water processing and urine processing equipment fail. In such a scenario, hygiene activities would be restricted and mission control would have to make one of two calls: abort the mission if younger crew members will be rendered ineligible for surface EVA due to deep space radiation exposure, or continue the mission on a reduced EVA schedule. Regardless, there will always be enough water to support the Sabatier reactor and human metabolic needs long enough to return the astronauts to Earth alive. This requirement was found to be 5.28 tons and is based upon an estimated need of 1.25 kg/CM*day for food prep, 1.6 kg/CM*day for drinking water, and a 360 day Sabatier need of 1.179 tons (this figure will be discussed in the ECS section).

To evaluate the first constraint, a MATLAB trade study was conducted which analyzed the water wall thickness with respect surface EVA hours per week for various crew member types. The trade considered an ambient deep space exposure rate of 70 REM/yr, and a surface rate of 13 REM per year for the region surrounding Hellas Planitia. The time frame was assumed to be 13 years on the surface and one year in deep space. A fraction of the weekly surface time was to be spent inside the habitat where shielding is 98% and the rest of the time outside where the exposure is assumed total. The trade thus calculated the amount of time the astronauts could spend outside and still stay under their NCRP 132 limits during the mission. A similar trade was conducted for the construction crew assuming a four year construction period with no shielding followed by a nine year period with shielding. The results are presented in Figure 93. The code is presented in Appendix C under the title "Mars Surface EVA Allocations as Determined by CTV Water Wall Thickness". The design point was chosen to be 5 cm as this will allow 35 year old women to perform 1 hour per week of EVA and it results in a 5.3 ton water wall which is essentially equivalent to that of the open loop water contingency discussed previously. Contained along the inside edge of the pressurized region of the CTV, the water wall will be a cylindrical shell with endcaps (minus a 1.255 m diameter cut at each end to allow space for the docking tunnels). The inner radius of the wall will be 2.36 meters and the outer radius will be 2.41 meters.

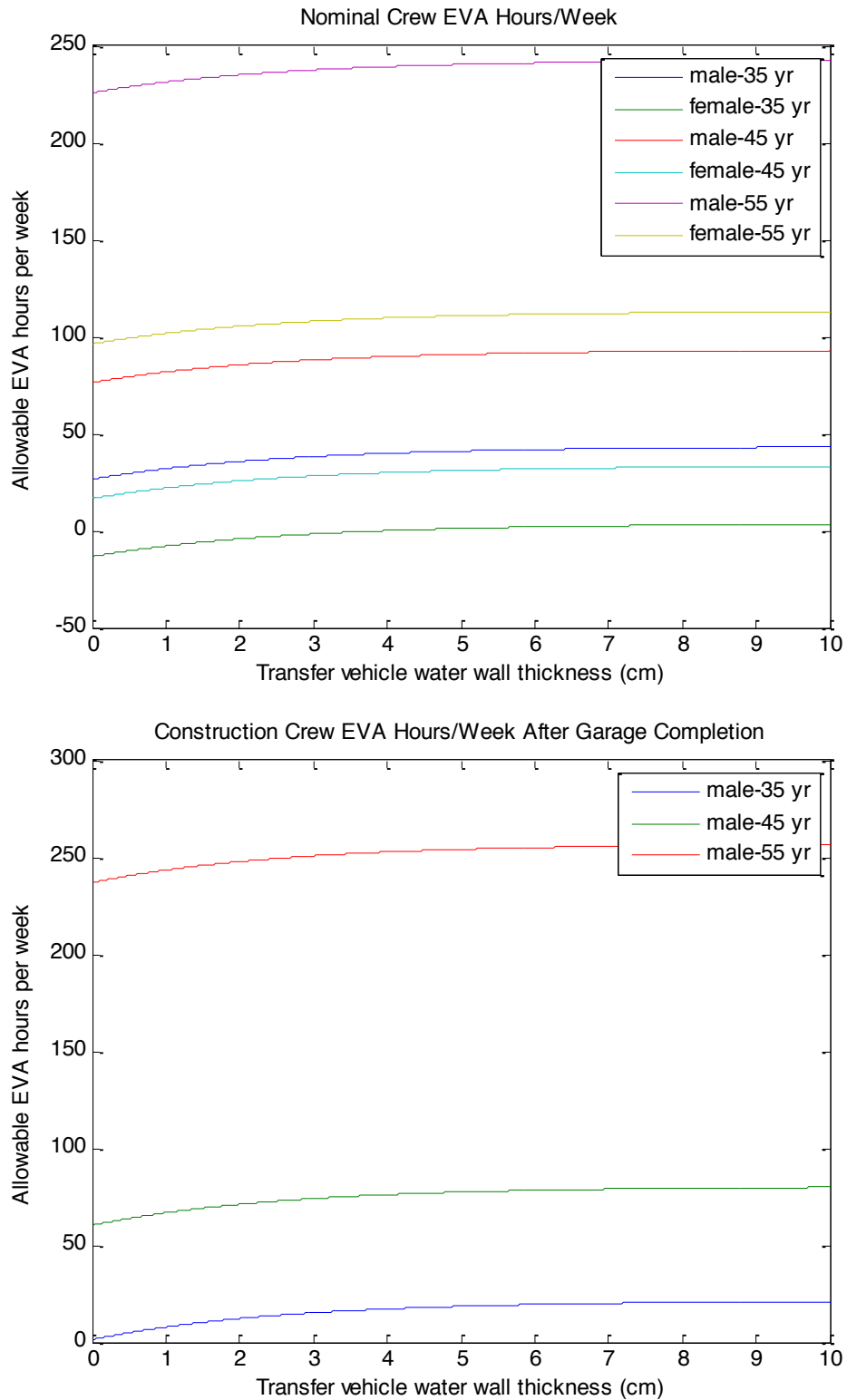


Figure 93. Allowable weekly EVA hours for both nominal crews and the construction crew. Note that there are only 168 hours in a week. 55 year old men would remain within NCRP-132 limitations even without shielding.

The true dangers of SPE's are realized in reviewing a case study of the August 1972 SPE. Although no astronauts were in space during the event, it occurred in the middle of the intervening months between Apollo 16 and Apollo 17. Had astronauts been on the moon during this event, they would have received a 25 hour skin radiation dosage of ~15 Gy and a bone marrow dosage of 0.8 Gy which both exceed the UNSCEAR low-dose-rate criterion. Such a dosage would have resulted in acute effects such as erythema, nausea, vomiting, and blood count changes.^[41] The incredibly high levels of radiation possible in an SPE dictate that a specialized storm shelter be built on the CTV to deal with this scenario. Capitalizing on the fact that SPE's originate from the sun and are thus unidirectional in nature, it has been decided that blocks of polyethylene will be placed above the astronauts sleeping quarters. In the event of an SPE, the spacecraft RCS will rotate the spacecraft to face the polyethylene blocks toward the sun. The astronauts will then retreat into their sleeping quarters until the storm has passed. The blocks will be 20 cm thick. With 20 cm of SPE shielding, annual exposure will be reduced to less than 1% of unshielded levels.^[46]

5.4.7.4. Regenerative Human Waste System

Over the past 17 years, the ISS program has served as a test bed for demonstrating the regenerative technologies that will make long duration spaceflights possible. Our mission architecture will make use of their research by adapting ISS systems for the CTV's environmental control and life support system (ECLSS). Elements which will remain essentially unchanged include the urine processor assembly (UPA) and the water processor assembly (WPA). The CAMRAS system for scrubbing CO₂ will be replaced with a Sabatier reactor.

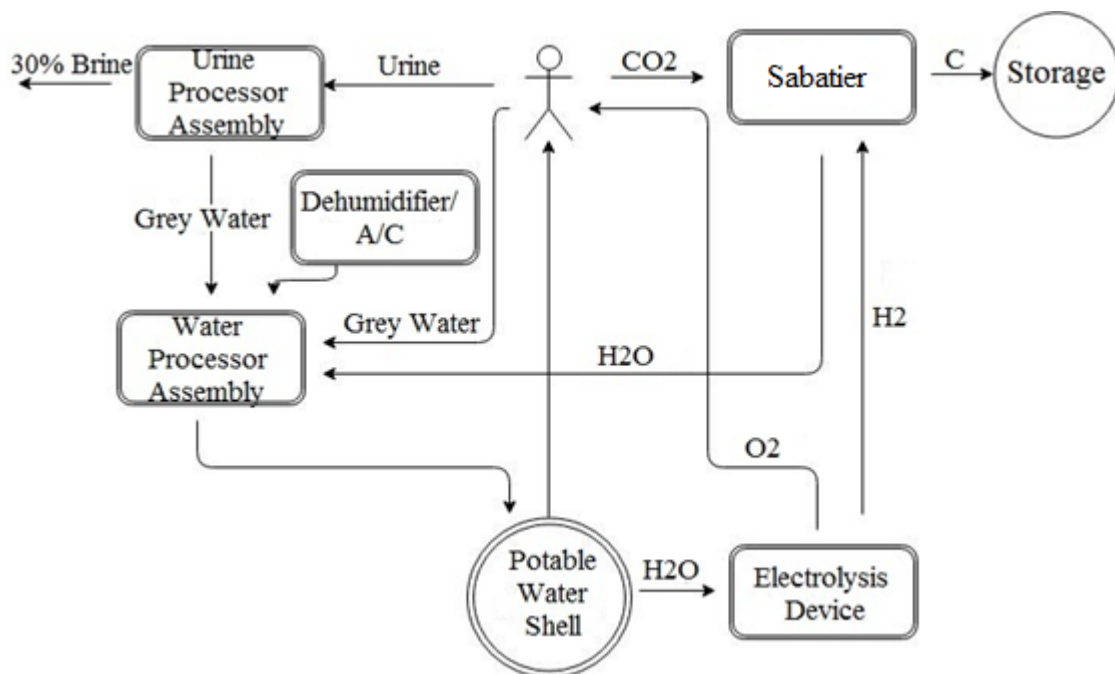


Figure 94. CTV ECLSS Loop.

The UPA uses a vacuum distillation process to recover water from urine. The remaining salty brine solution will be vented from the CTV. In its initial ISS design, the UPA was designed to operate with 85% efficiency in the recovery of water. However this figure has dropped to about 70% during use on the ISS. This is most likely due to excess levels of calcium in the urine of astronauts. Calcium deposits in urine may result from bone loss due to microgravity.^[47] The CTV's UPA will be assumed to have an efficiency of 70% for all water conservation calculations. The WPA uses a series of multifiltration beds and a catalytic reactor to purify water sourced from both the UPA's output as well as the dehumidifiers and any grey water used for hygiene.^[48]

Proper functioning of the UPA and WPA are essential to mission success and thus a thorough reliability analysis is in order. The initial method for determining necessary quantities of replacement parts was based upon the life limits of individual components—sufficient replacement parts would be brought such that each component in the UPA and WPA could be replaced at the end of its individual life limit. However, this resulted in only 57% reliability for the two combined systems. To remedy this, additional redundancies were allocated for a few of the least reliable components thus bringing the system reliability up to 90%. The necessary redundancies are presented in Table 32 and the code used to generate this analysis is presented in Appendix C under the title “Reliability Analysis on Urine Processor and Water Processor Assembly Components”. As stated in the Radiation section, even an irreparable failure of this system would not be a loss of life situation. The water wall would still contain enough reserves to either continue the mission with a reduced EVA schedule for the surface or in a worst case scenario to return the crew safely to the Earth.

Component:	MTBF (h)	360-Day Reliability (%)	Life Limit (yr)	Quantity Old	Quantity New
Distillation Assembly	142525.2	94.118	2	2	2
Firmware Controller Assembly	27331.2	72.89703	2.4	2	3
Fluids Control and Pump Assembly	90140.4	90.85999	4	2	2
Pressure Control and Pump Assembly	181507.2	95.35138	2	2	2
Recycle Filter Tank Assembly	199640.4	95.76453	0.08	14	14
Separator Plumbing Assembly	384651.6	97.77885	1	2	2
Wastewater Storage Tank Assembly	184222.8	95.41831	10	1	2
Catalytic Reactor	25579.2	71.33562	2.25	2	3
Gas Separator	84008.4	90.22651	1	2	2
Ion Exchange Bed	296701.2	97.12997	0.16	8	8
Microbial Check Valve	143488.8	94.15632	1	2	2
Multifiltration Bed #1	296701.2	97.12997	0.36	4	4
Multifiltration Bed #2	296701.2	97.12997	0.36	4	4
Particulate Filter	717356.4	98.8028	0.22	6	6
pH Adjuster	137181.6	93.89602	1	2	2
Process Controller	87950.4	90.64339	7.72	1	2
Pump Separator	42398.4	81.56408	2	2	3
Reactor Health Sensor	56677.2	85.86085	1	2	3
Sensor	143664	94.16324	10	1	2
Separator Filter	359072.4	97.62252	0.84	3	3
Start-up Filter	226884	96.26348	19.92	1	2

Wastewater	53611.2	85.11556	4.71	2	3
Water Delivery	64561.2	87.47418	5	2	3
Water Storage	44676	82.41585	3.92	2	3

Table 32. Redundant parts list for UPA and WPA. “Quantity Old:” is purely a 360 day requirement based upon the life limits and has a reliability of 57%. “Quantity New:” increases low reliability component quantities to bring system reliability up to 90%. Parts list, MTBF, and Life Limit data taken from (Hanford, 2004).

The CTV’s water loop is not entirely closed. The most significant losses are in urine brine, fecal matter, and Sabatier exhaust; however, some water is also lost in the form of humidity due to cabin air leakage. Assuming that astronauts produce 1.562 kg of urine per day^[37] and quoting our 70% UPA efficiency, the crew of four will vent approximately 675 kg of water in the form of brine over 360 days. Feces are approximately 75% water and the CTV will not reclaim fecal water. On average, humans produce about 0.123 kg of feces per day which will correspond to a loss of 133 kg of water over 360 days. The Sabatier reactor will dump carbon waste overboard in the form of CH₄. This corresponds to a 2 to 1 molar loss of H₂O with respect to CO₂. Humans produce 1 kg of CO₂ per day so a basic stoichiometric calculation puts the 360 day water loss for four crew members at 1179 kg. Humidity losses due to cabin leaks were found to be extremely small. 100% humidity (very conservative estimate) in a 68 degree Fahrenheit cabin results in a water partial pressure of 2.3 kPa. Substituting this value into the ideal gas law with a ~100 m³ cabin results in approximately 90 moles of water in the cabin air at any given time. A leak rate of 0.14%^[37] would produce a 360 day water loss of less than 1 kg due to cabin air leaks. Thus the expected 360 day water loss in the CTV ECLSS will be around ~1988 kg. This will only result in a decrease in water wall thickness of approximately 2 cm over the course of 360 days. This loss could be compensated for by restocking the CTV with water at MRO.

Feces will be stored within septic tanks located in the attic. The tanks have a cumulative volume of 0.3 m³ and will have to be emptied at least once every 180 days. The fecal matter should be dumped from the vehicle immediately before either the trans-Earth or trans-Mars injection burns. This 0.3 m³ sizing is based upon the NASA requirement that any fecal collection system be capable of storing 300 ml per crew member per day^[37]

Three carbon dioxide removal technologies were initially considered: Sabatier, Bosch, and ACRS. A trade study was commissioned to determine which would have the least mass on a 360 day mission. This was rather simple as the ACRS and Bosch systems are both closed water loop. For the three system masses the following assumptions were made: 91 kg/crew member for Sabatier with an additional 60 kg/crew member for ACRS, and 700 kg/crew member for Bosch^[252]. For the Sabatier reactor, an additional consideration was made for the mass of water stoichiometrically associated with the methane dumped into space over the course of the 360 day flight. The results are presented in Figure 95. The trade initially prompted the selection of the ACRS system for PDR. However this was changed out for a Sabatier reactor in the final design. Despite the mass savings of ACRS, the technology brings several complications to the CTV—namely, the need for additional machinery for solid carbon processing and a high temperature pyrolysis oven. Very few practical examples of ACRS systems have been found in this body of research and thus the more flight ready Sabatier reactor will be used.

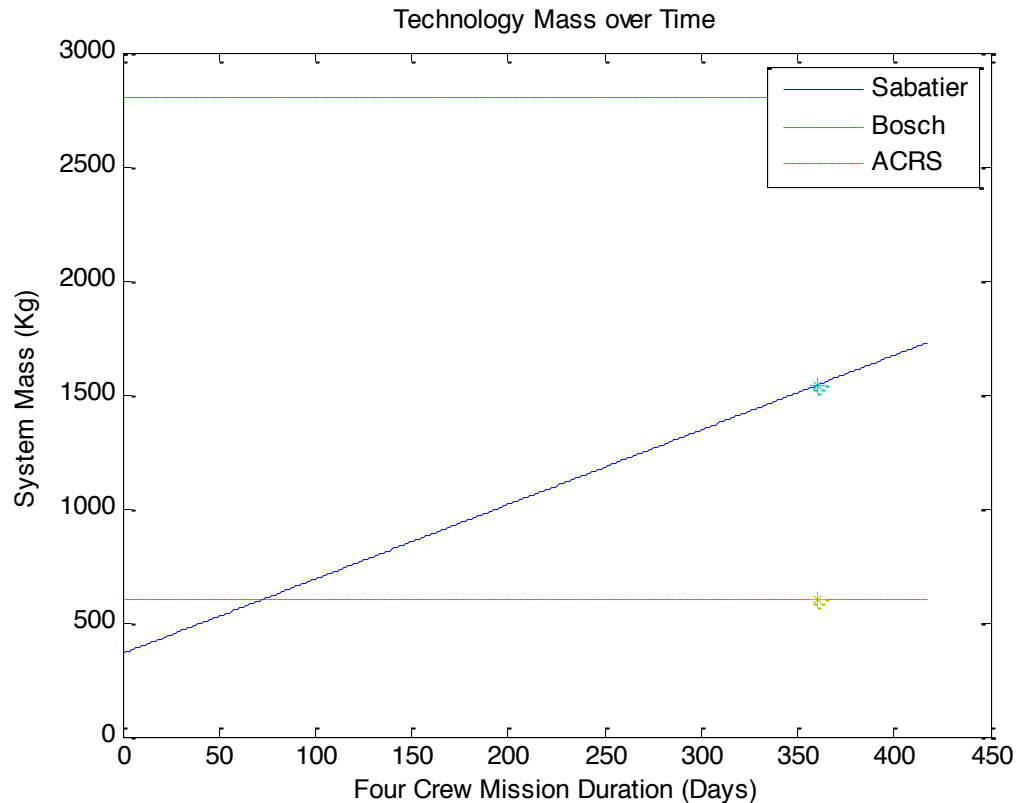
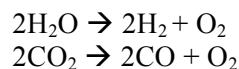
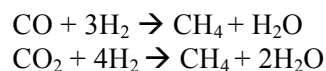


Figure 95. CO₂ scrubbing mass over time.

Carbon dioxide will be removed from the cabin with a three stack solid oxide electrolysis (SOE) and embedded Sabatier reactor system. This system was developed by Christine S. Iacomini, Director of R&D for Paragon Space Development Corporation, and is presented in detail in the associated reference.^[49] A scaled version has been demonstrated in a laboratory setting for the NASA Small Business Innovation Research contract. The system contains a series of plates arranged on top of one another into three stacks. Each stack is a nonporous ceramic oxide electrolyte contained between two electrodes. The first and third stacks electrolyze water and carbon dioxide in the following manner:



The center stack functions as the Sabatier reactor:



This three-step process allows for the products necessary for a Sabatier reaction to be generated directly from electrolyzing exhaled water vapor. The system can support the metabolic needs of four astronauts under the assumption that 28.7% of exhaled water vapor is available for the intake of the system. The system will consume approximately 1 kW, have a mass of 41.3 kg and a volume of 87.2 L. The stacks will be stored in the attic of the CTV along with a second redundant system.^[49]

5.4.8. Avionics

Avionics Components

Flight Control Computers - The FCCs that are used for all avionics applications will be NASA's High Performance Spaceflight Computing (HPSC) initiative.^[90] General specifications that are expected out of the HPSC units are 100-1000x the performance of the RAD750 with similar power requirements of around 7 W. It shall have a built-in MMU, system clock, and wide variety of I/O ports. It has a TRL of 6 and an expected initial deployment date of FY 2018, well in time for the first CTV launch in 2037. Given that the RAD750 has nominal clock rates of up to 200 MHz, these computing units should have performance that is at least on par with current (FY 2015) consumer-grade computers (4-5 GHz multi-core (up to 10) processors, up to 32 GB of volatile memory, and 1 TB solid state drives). All data that does not need to be immediately stored aboard the CTV can be offloaded and stored elsewhere in order to conserve the 10 TB total capacity, which should be sufficient for the CTV's purpose. All FCCs are minimally radiation hardened for CTV applications due to being housed in a special avionics containment unit. FCCs being deployed in other vehicles, particularly FTVs, fuel depots, and construction equipment, will be more heavily radiation hardened to comply with expected reliability values. With 10 FCCs aboard each CTV, there is much more than enough performance available for all critical functions, with plenty to spare for ad hoc computing needs. Data throughput analyses follow later to justify the existence of excess available computing resources.

Guidance, Navigation, and Control

1. IMUs - IMUs, or Inertial Measurement Units, are inertial navigation instruments that often consist of accelerometers, rate gyros, and magnetometers combined in one unit. These are often used as a component for INS (Inertial Navigation Systems), traditionally known as "dead reckoning" for terrestrial applications. While the CTV's navigation solution does involve implementing an INS, the reliability parameters for several IMUs that have been scouted are simply too low for a long 17 year mission. Instead, magnetometers are discarded interplanetary travel does not involve exposure to significant magnetic fields. Accelerometers and rate gyros will be sourced and operated separately as each individual unit has a much higher MTBF compared to that of IMUs.
2. Accelerometers - Accelerometers collect real-time linear acceleration data from all 3 linear degrees of freedom (DOFs) at polling rates of several times a second. There will be several accelerometers placed in different locations inside the CTV to provide differential data. This data is primarily used for interplanetary orbit correction.
3. Rate gyros - Rate gyros collect real-time angular rate data from all 3 angular degrees of freedom (DOFs) at polling rates of several times a second, similar to the accelerometers. There will also be several rate gyros to provide differential data, similar to the accelerometers. This data is used for not only interplanetary orbit correction, but also to augment docking operations.
4. Star trackers - Star trackers contain a database of many celestial objects that for the purposes of space navigation, are essentially stationary. Using the known positions of celestial objects, the star tracker determines range data between the CTV and celestial body of focus. Star trackers will provide supplemental navigational data to the accelerometer/rate gyro INS and can to some extent still provide a navigational fix should some component of the INS fail. The star trackers will also act as an effective sun sensor by considering the sun as a celestial body. This is useful for positioning the CTV relative to the sun to allow for optimal shielding against solar particle events.

5. TriDAR - TriDAR, otherwise known as Triangulation and LIDAR Automated Rendezvous and Docking, is used for all docking operations by the CTV. TriDAR is also deployed on other spacecraft that will perform active docking duties. Using a combination of LIDAR and thermal sensors, TriDAR units are able to construct a 3-D representation of the docking target and consequently provide heading and bearing data to allow for autonomous docking to occur. As such, TriDAR is a passive system that does not require any active interaction with the docking target. This setup is augmented by the usage of the the International Docking Adaptor (IDA) on all docking ports to allow for androgynous docking operations. The reason docking operations are chosen over berthing is due to the speed required in emergency egress events. Berthing would simply be too slow for such contingent events.

Environmental Sensor Package (ESP)

1. Thermometer - Electronic thermometers will constantly monitor various compartments of the habitable volume of the CTV. They will provide real-time data to the FCCs and will dictate the modulation of the habitat in order to maintain a livable and comfortable environment.
2. Barometer - Electronic barometers will constantly monitor the cabin pressure in various compartments of the CTV primarily in order to detect leaks and slow depressurization. They will provide real-time data to the FCCs and will dictate troubleshooting behavior to eliminate loss of pressure. Analog barometers will also be deployed as a backup to the electronic counterparts due to the importance of knowing the cabin pressure at all times.
3. Multi-Gas Sensor - The multi-gas sensor that will be deployed in the CTV will be capable of sensing and monitoring levels of critical gases such as oxygen, carbon dioxide, ammonia, and water vapor. Real-time data from the multi-gas sensor will modulate actuators such as the carbon dioxide scrubbing process as well as the humidifier to maintain optimal conditions for both humans and electronics. Electronics require fairly low humidity levels in order to maximize lifespan.



Figure 96. Aerospace Application of Multi-Gas Sensor^[91]

4. JPL's ENose - JPL's ENose is a device that will be capable of measuring and monitoring air quality in order to ensure that concentrations of harmful particulates and other pollutants are within safety

thresholds. Pollutant sources are often from spills or leaks. Elevated levels of such pollutants will prompt additional precautionary measures to decontaminate the habitat environment. This may be accomplished by ensuring that all air filtration units are operating nominally as well as employing additional contamination cleanup methods.

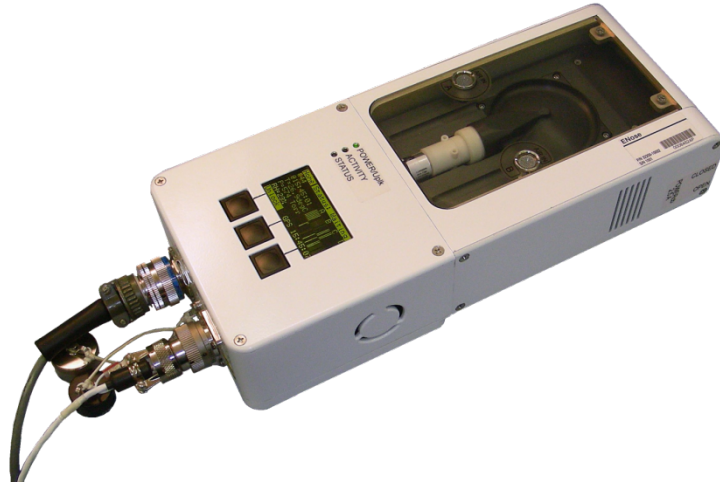


Figure 97. JPL's ENose^[92]

5. Smoke Detector - Smoke detectors in the CTV environment will operate around the clock to detect abnormally elevated levels of smoke particulates that may indicate a fire event. These sensors will be highly sensitive at the cost of false alarms as fire events in the CTV are of much higher criticality compared to fire events in typical terrestrial applications. These smoke detectors will not only produce audible notification of elevated levels of smoke, but will also notify the central computing clusters of such an event. Human intervention is necessary.
6. Water Quality Sensor - Water quality sensors will monitor the dissolved concentration of various pollutants and contaminants in the primary water source. Any elevated levels of any pollutants will trigger warnings via the central computing system, alerting and prompting the crew to take action to purify the water source. Water quality sensors will monitor water from different sources in the CTV and will also ensure that the closed water loop is functioning properly.
7. Radiation Assessment Detector - The Radiation Assessment Detector, or RAD, is an active radiation measuring device that will primarily be measuring radiation exposure due to cosmic rays and other cosmic sources of radiation. The RAD will also provide immediate detection of solar particle events in the event of a communications blackout which would prevent Earth stations from notifying the CTV of SPEs. Cumulative radiation exposure measured by the RAD will be logged in order to monitor cumulative crew exposure. Real-time monitoring of the RAD will also expose potential compromises in the radiation shielding measures put in place.



Figure 98. Radiation Assessment Detector (Similar to one aboard Curiosity Rover)^[93]

8. Dosimeter - The dosimeters that will be deployed for use in the CTV are passive by nature and simply change color upon exceeding a certain preset radiation dosage. They will be placed all around the CTV to monitor cumulative radiation exposures to different areas of the CTV, particularly the sleeping quarters. Dosimeters will also be used on crew wearables to indicate any excessive doses of radiation that a crew member may sustain.



Figure 99. Passive Dosimeters for Vehicle and Crew Use^[94]

9. Multimeter - Multiple multimeters will be deployed in the CTV to monitor every major avionics component with enough for redundant monitoring of voltage and current levels as well as power usage. Multimeters act as the first step of troubleshooting faulty avionics equipment.

Miscellaneous

10. Vacuum depressurization valve - Two vacuum valves will be present in the CTV to allow for full depressurization of the vehicle in the case of a fire. The mechanism is extremely simple: linear actuators open the vacuum valve which empties the CTV gases into space. The CTV is designed to

withstand up to 3 full depressurization events. The CTV crew will first be evacuated to the Dragon capsule in such events.

11. Crew wearables - Crew wearables will be a vest that is worn over standard crew clothing. This vest is outfitted with various sensors for measuring and monitoring human vitals such as heart rate, heart murmur, blood pressure, body temperature, and radiation exposure (dosimeters). The data will be captured cumulatively by the computers and will be analyzed to determine abnormal trends.
12. X/Ka Band Transceivers - High power transceivers will operate on the X and Ka bands to communicate with both Earth and Martian stations. Communications will primarily be used for transferring non-critical information and whatever data the crew may need. The CTV is capable of functioning completely autonomously so any loss of communications will only reduce the quality of living in the vehicle but pose no short term threats.
13. Replacement parts - Sufficient replacement parts will be brought for all avionics components, especially for those with lower reliability values.

Mass/Volume/Power/Thermal Dissipation Breakdown

Component	#	Mass (kg)	Volume (m ³)	Power (W)	Notes
FCC	10	16	0.256	1,000	Volume included in main avionics containment
Main avionics containment	1	100	2.0	N/A	Vertical "rack/cabinet". 1x1x2 m. or convenient
Accelerometer	8	1	0.001	16	Placed around diameter of CTV
Gyros	16	64.8	0.001	3.6	Placed around diameter of CTV
Star trackers	4	22	0.002	36	Placed around diameter of CTV
TriDAR	2	150	0.4	1,000	Only one will be in operation, meaning 500 W consumption. Only on during docking.
Smoke detectors	16	1	0.003	24	Spread out in interior.
Thermometer	4	2	0.001	0.1	Spread out in interior.
Barometer	12	6	0.001	18.9	Spread out in interior.
Multi-gas sensors	4	2	0.001	100	Spread out in interior.
Water quality sensors	4	0.2	0.001	4	In water supply.
RAD	1	10	0.01	5	Can be placed anywhere.

JPL's ENose	4	12	0.0136	40	Spread out in interior.
Multimeters	42	11.34	0.001	N/A	Around 21 components requiring multimeter monitoring. 2x redundancy. Negligible power consumption by design.
Fire suppression vacuum	1	N/A	N/A	N/A	Probably just a valve that releases cabin pressure into space.
Dehumidifiers	2	32	0.1	960	Spread out in interior. In practice, only one should be running which means 480 W consumption.
Pressure/Fluids Control and Pump Assembly	2	100	0.14	100	Power consumption depends on actual use time and mass flow rate of fluids being moved.
Wearables (vest and wristband)	8	4	N/A	8	1 set per crew.
X and Ka band transceivers	6	10.8	0.03	60	Placed around CTV near exterior.
Touchscreen, peripheral set, solid state storage	20	200	0.3	1,000	Spread out in interior.
Wiring	N/A	~1,000	0.112	1,000	More accurate wiring massing when M0 of launch vehicles are obtained. Power column contains heat losses (TDP) only since wiring doesn't consume power.
TOTAL		1,750 kg	3.4 m³	4,400 W	Summed upper bound values (all above estimates have already been rounded up with positive safety factors).
DESIGN		2,000 kg (2 MT)	3.5 m³	5,000 W (5 kW)	Round up with safety margins for design parameters. For CAD, should only draw in a 2 m ³ containment for the FCC cluster with cooling tubes built in. Most of the other volume is spread out in the interior and around the CTV. Maybe want to allocate 1 more kW extra for science missions?

TDP*		N/A	N/A	1,600 + 500 = 2,000 W	Includes 15-50 W waste heat per crew (100 W * 4 = 400 W) added to TDP. Please revise if not accurate.
DESIGN*		N/A	N/A	3,000 W (3 kW)	For radiator sizing.

Table 33. Mass/Volume/Power/Thermal Dissipation Breakdown

*TDP - thermal dissipation power (max bound waste heat)

Calculated power column is power consumption, not TDP except for the shaded rows:

100% TDP

50% TDP

25% TDP

Control Modes

Autonomous - The primary control mode of the CTV will be autonomous via control loops that run in the background on the critical FCC cluster. These autonomous control loops will modulate both the CTV's navigation fix as well as docking operations and habitat environment moderation. As such, crew intervention is not necessary for orbit correction, docking operations, or environmental moderation. If any monitored values exceed certain thresholds that cannot be reversed by the CTV's standard actuators, the crew will be notified and will take appropriate action.

Teleoperation - Teleoperation of the CTV is only critical for roughly half the total expected operation time of the CTV when it is not manned and operates on the same X and Ka bands as the onboard transceivers. This control mode will primarily be used for ad hoc mission changes (i.e requiring a CTV in a parked orbit earlier than anticipated) when the CTV is not manned and only reachable via telemetric means. Due to the long signal travel time, all teleoperation commands cannot be time-sensitive.

Manual - The manual control mode allows the crew to access and control any function of the CTV. Manual commands always take precedence over the other two control modes, especially when manual overrides are utilized to amend situations that the autonomous control mode is unable to handle. Manual redundancies and backups exist for all autonomous features, including docking should the autonomous docking operation prove to be too erroneous. The crew interfaces with the CTV's manual controls via the standard command center (explained in-depth later) as well as the redundant physical controls should the need for them arise.

Control Loop Algorithm

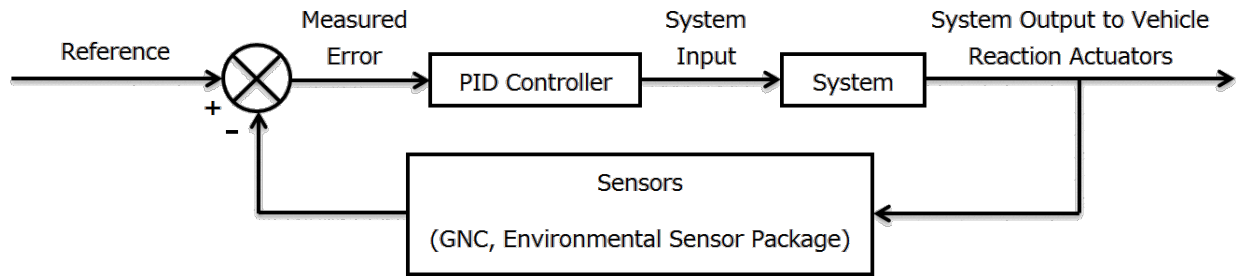


Figure 100. Control loop for GNC/ESP Systems

All control loops will use a fairly simple closed-loop system implementing a PID controller to modulate parameters of interest within operating and desired thresholds. Example parameters include orbit trajectory, relative vehicle heading and bearing for autonomous docking, environmental moderation, etc. Apply “rule of thumb” to choose controller sample rate⁹⁵. If a system settling time of 1 second is desired (this is very short for the purposes of orbit correction), the sample interval should just be 1/10th to 1/100th of the settling time. Let $T_s = 0.0333$ sec. and the sample rate = 30 Hz. If a lower sample rate can be used such as 10 Hz without resulting in a divergent control loop, it will be used. This would entail a practical sample rate of around 30 Hz for all sensors to be consistent with the star tracker.

UD Factorization Extended Kalman Filter (UD-EKF) will be used for the star tracker. Loop rate at 30 Hz to match star tracker inbound data stream sample rate. Performs U-D factorization every iteration, slightly decreasing computation requirements. Performance is mostly similar to most other Kalman filters i.e a handful of linear calculations on ~2640 kbit data payloads per cycle.

Data Throughput Analysis

GNC Example Inbound Data (sample rates are common instrument maxima):

- 3-axis vehicle-mounted accelerometers - 640 samples per second * 8 units * 3 DOF * 32 bit floating point double (4 bytes) = 491.52 kbps
- 3-axis active rate gyro - 400 samples per second * 16 units * 3 DOF (change in roll, pitch, yaw) * 32 bit floating point double (4 bytes) = 614.4 kbps
- Star tracker - 30 * (330 kB or 2640 kbit) (1280x720) HD pictures per second = 79.2 kbps
- Star tracker uses a UD factorization Extended Kalman Filter (UD-EKF) to smooth inbound star ranging data.
- Star trackers tend to have fairly high power usage, similar to the magnitude of an IUVS, for example.
- 57 celestial objects are normally used for autonomous celestial navigation. A comprehensive celestial database may be needed for deeper space travel.
- Even with much higher sample rates than the control loops will actually use, it is noted that having 5 FCCs in the main critical cluster with the expected capabilities outlined in the HPSC initiative will provide much more than enough computational power to handle the full load of every single control loop.

Networking Strategy

All avionics will be connected with double full-duplex SpaceWire connections in order to provide the necessary bandwidth as well as full redundancy for data routing. Multiple paths exist between all

electronic endpoints in order to maximize failover route options. This networking strategy ensures that individual component failures will never compromise the integrity of any of the other avionics. Universal bus interfaces will be implemented in order to simplify installation, upkeep, and maintenance of the overall avionics systems.

Shown below is the system block diagram illustrating the connections and data flow between the major avionics systems onboard the CTV. Red paths indicate critical paths between critical sensors and actuators. Path arrows indicate data flow schemes, with data flow generally leaving sensors and being received by the FCC clusters and processed commands leaving the FCC clusters and being received by the respective actuators. The primary FCC cluster is illustrated to be the center of all critical functions but is capable of drawing upon the standby FCC cluster for additional computing resources in the event of overload or failure. Multiple failover routes and combinations can be implicated by the diagram as well.

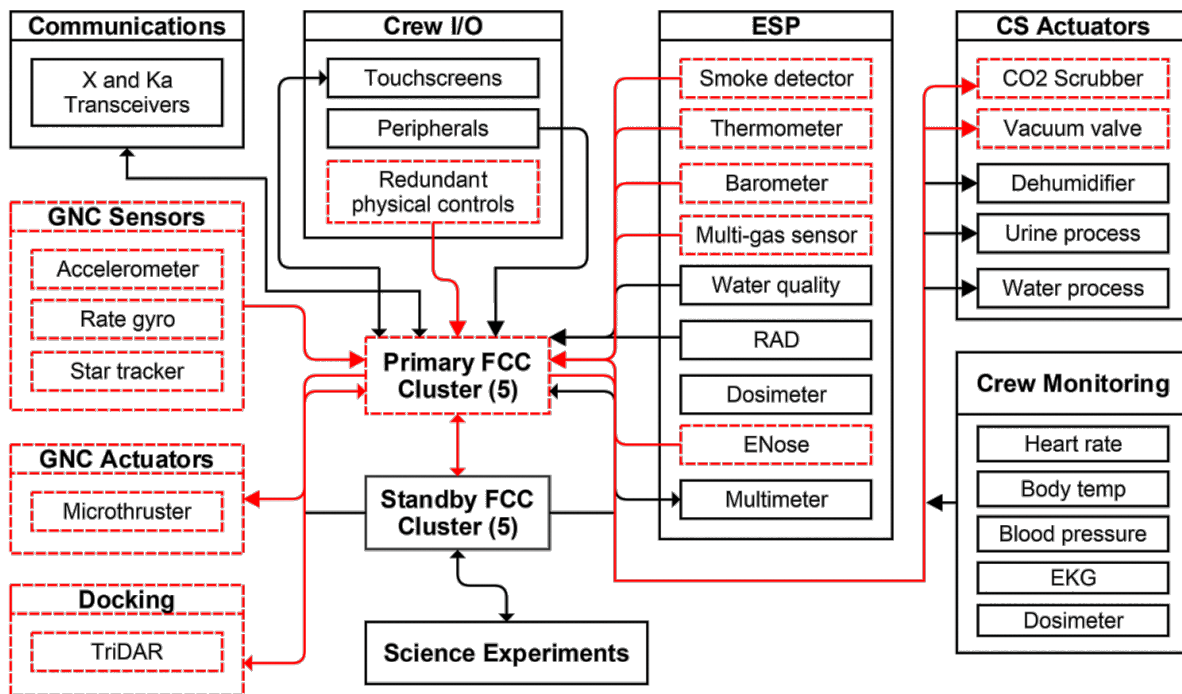


Figure 101. System block diagram for CTV avionics. Critical routes are denoted in red. Arrows indicate general data flow direction.

Avionics Reliability

Total reliability values are calculated as follows:

Individual Reliability $P = e^{-N/MTBF}$. Individual reliability in this context is defined as the reliability of a single unit for the maximum CTV operational lifespan of 17 years (first CTV launch in 2037 to Earth independence in 2054).

Total Reliability = $1 - (1 - P)^{\# \text{ components}}$. Total reliability in this context is defined as the reliability of the entire set of the unit for the maximum CTV operational lifespan as defined above with some notable

exceptions (i.e TriDAR). This is calculated by subtracting the probability of every single unit failing by 100%. Very high total reliabilities were a design goal especially with regards to critical components.

Component	#	MTBF (yr)	Minimum Mission Time (yr)	Individual Reliability (%)	Total Reliability (%)	Notes
FCC	10	30	17	56.74	99.98	-
Accelerometer	8	25	17	50.66	99.65	Effective component of IMU
Gyros	16	11.4	17	22.51	98.30	Effective component of IMU
Star trackers	4	114.08	17	86.16	99.96	Main backup to “dead reckoning” navigation by accelerometer/gyro
TriDAR	2	2.85	0.0137	99.52	99.998	Reliability limited by LIDAR (thermal imager has MTBF ~ 8 yr). Cannot afford docking failure, hence 2 units.
Smoke detectors	16	11.4	17	22.51	98.30	-
Thermometer	4	60	17	75.33	99.63	-
Barometer	12	18.2527	17	39.4	99.75	-
Multi-gas sensors	4	35	17	61.53	97.81	-
Water quality sensors	4	68.4477	17	78.01	99.77	-
JPL’s ENose	4	35	17	61.53	97.81	-
Multimeters	42	11.4	17	22.51	99.998	-
CO2 Scrubber	16	9.13	17	15.54	93.29	16 units means 15 sets of replacement parts (mainly the radial fan). Backup is passive CO2 scrubbing canisters.

Fire suppression vacuum	4	113.167	17	86.05	99.96	Simple electric actuator controlling valve.
Dehumidifiers	8	22.82	17	47.48	99.42	2 units, but 6 sets of replacement parts
Pressure/Fluids Control and Pump Assembly	16	11.4	17	22.51	98.30	-
Wearables (vest and wristband)	8	10	17	18.29	80.09	Not critical
X and Ka band transceivers	6	11.4	8.5	47.44	97.89	If failure, possible end of mission if unmanned as teleoperation will no longer be available. MMT is half of 17 because that is the approximate time that CTV is unmanned and comm. failure is critical.
Touchscreen, peripheral set, solid state storage	20	28.52	17	55.10	~100	Using (industrial) touch screen monitors as limiting factor. SSDs have higher MTBF.

Table 34. Avionics Reliability

Failure Modes and Risk Assessment

Below are some of the most significant avionics components along with failure effects, associated criticality values, and fallback/mitigation factors. Criticality values range from 1 to 5, with 5 being the most critical and 1 being the least critical. Of notable importance are the accelerometers and rate gyros which constitute the Inertial Navigational System and the star tracker that acts as an auxiliary backup to the INS. TriDAR has such a large reliability due to the importance of docking success.

Component	2054 Reliability	Failure Effects	Criticality (1-5)	Fallback/Mitigation
FCC	99.98%	GNC/ESP Failure	5	Half on standby, modular design

Accelerometer	99.65%	Loss of 3 DOF	3	Star tracker
Rate gyro	98.30%	Loss of 3 DOF	4	Replacement parts
Star tracker	99.96%	Lost in space	5	Multiple units
TriDAR	99.998%	No docking ops	5	2 units (1 standby)
Smoke detector	98.30%	No fire detection	5	Replacement parts
Thermometer	99.63%	No automation	3	Manual control
Barometer	99.75%	Pressure leaks	4	Analog equivalent
Multi-gas	97.81%	No monitoring	3	Filters still run
Transceivers	97.89%	No comms/teleops, unaware of SPE	3	Replacement parts

Table 35. Failure Modes and Risk Assessment

5.4.9. Crew Transport Vehicle Repair

CTV Repair

The CTV, being the transport vehicle for the crew to Mars, is one of the critical parts of the mission. NASA has been researching on inflatable habitats for decades. In the 90s, NASA spent millions of dollars to produce a possible potential crew quarters for the International Space Station and for future travel to Mars. In Johnson Space Center in Houston, Texas, scientists experimented and tested the inflatable flight module that they hoped to be the living quarters of the ISS. By improving the habitat after In addition they also start to add more capabilities and standards into this module. Moreover, the habitat will be used not only for ISS but also a habitat for future Mars-bound journeys. Unfortunately, because of the budget crisis and continuous cost over runs, the inflatable program was cancelled and NASA stopped all the research associated with the inflatable Habitat. ^{[227][226]}

In 2000, Bigelow Aerospace bought the license and patent of the inflatable habitat from NASA to conduct further research Bigelow Aerospace after taking over the research on inflatable habitats, it has been conducting continuous research to improve the capability and reliability of inflatable space habitats. Starting 1999, the company has achieved big milestones. In 2006, the company launched Genesis I, the first inflatable habitat to space. Genesis I proved that an expandable habitat can withstand launch environment. In addition, in 2007 the company launched Genesis II, the advanced version of the Genesis I, which contain more sensors, cameras and other technologies. Genesis I and Genesis II have been a tremendous success in the application and usage of inflatable materials. Today both spacecraft are in space being experimented on and transfer a huge data for the company, which will help for future improvements. Currently the more advanced and stronger versions of inflatable habitats, BEAM and

B330 are being developed. The CTV was designed based on the current technologies of Bigelow Aerospace. ^{[227][251]}

CTV Building Materials

In order to survive in the non-forgiving environment of space, the CTV is made from strong materials that can withstand extreme temperature changes, radiation, space debris and other potential problems. The structure of CTV is built from a unique combination of strong materials with the capability of a load-bearing hard structure. These materials provide temperature insulation, protection from space debris, and optimized restraint layer, and a redundant bladder with a protective layer. With more than twenty layers, the structure's inflatable shell is strong and unique. The outer layers are layered to break up particles of space debris and micrometeorites that may hit the shell at high speeds. ^{[227][230]}

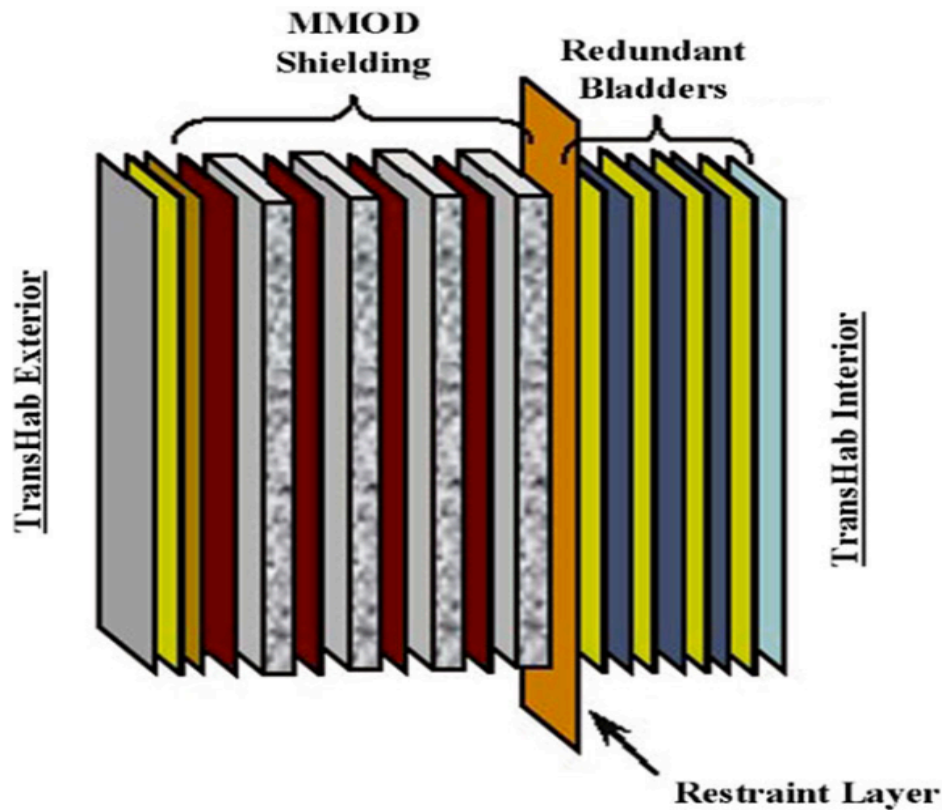


Figure 102. TransHab's MMOD Structure ^[253]

The primary structure of the CTV, which evolved from TransHab of NASA, is structural restraint, constructed from strong materials called Kevlar and Vectran. The shield assembly comprising several bumper layers, spacing layers, and adhesive. Each of these layers protects astronauts from meteorite and

orbital impact. The inflatable shell, which is a primary structure, is composed of four functional layers: the internal scuff barrier and pressure bladder, the structural restraint layer, the micrometeoroid/orbital-debris shield, and the external thermal protection blanket. Its function is to provide the crew with living space, and provide debris protection and thermal insulation. ^[227]

The key to the rugged protection is a successive layer of Nextel spaced between several-centimeter-thick layers of open cell foam. Particles hitting at hypersonic speeds expend energy and disintegrate on successive Nextel layers, spaced by the open cell foam. For extra protection, the shell includes a thin layer of Kevlar. The layering has been tested extensively and repeatedly, including having projectiles fired at the fabric sandwich at speeds of seven kilometers per second.

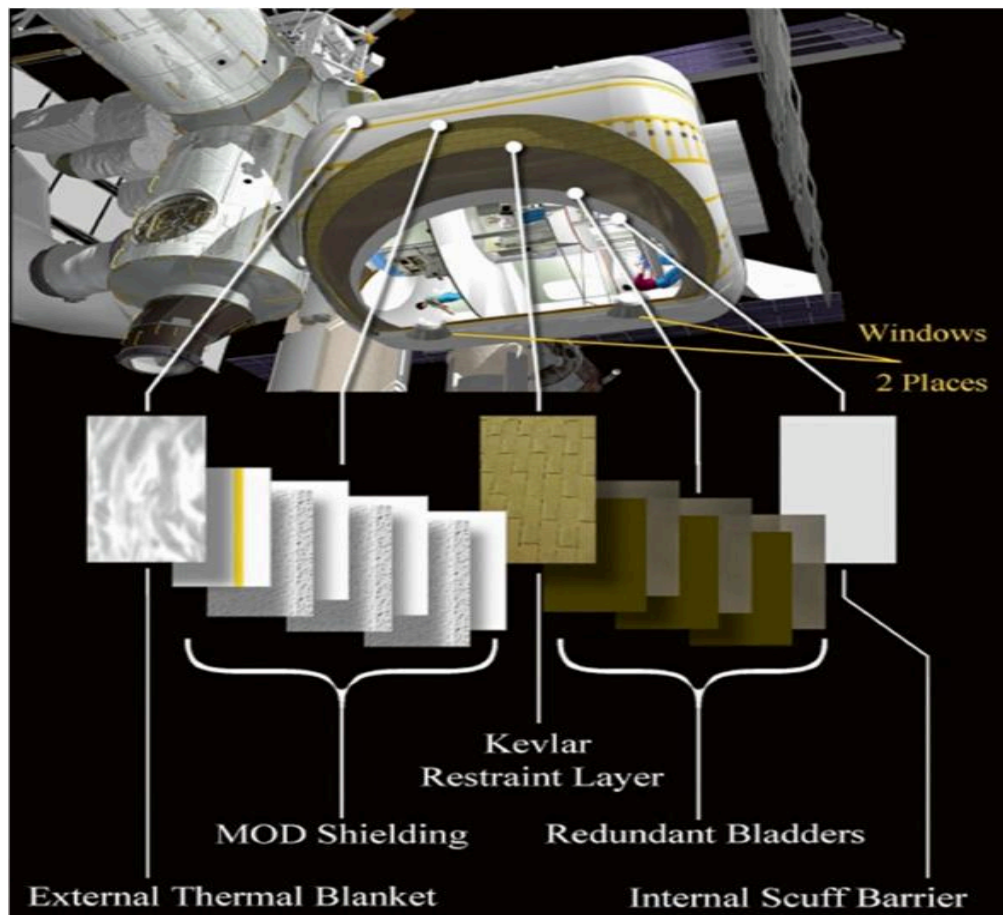


Figure 103. Exploded view of the CTV layers (based on this technology of TransHab) ^{[227][250]}

Space Debris and Micrometeorites

In this mission to Mars, one of the challenges that transportation to Mars will face will be space debris. Since space debris moves at high speed in space, even small dust particles can bring a significant damage to the CTV and the crew. Although space debris has been studied in detail for the last few decades there is a lot unknown factors for experts. Especially orbital debris around earth orbit has been tracked and a lot

of research has been done. NASA and other international space agencies have been studying space debris using both ground based instruments and satellites. ^{[228][250]}

From the beginning of the space age, it become important for the US military and the Russians to detect and track the movement of any space objects. They operate space surveillance systems that not only permanently monitor functional space systems but also the whole space debris population. Therefore, a lot has been known about space debris. A lot of methods that will protect space vehicles have been suggested and implemented.

The key to the debris protection is a successive layer of Nextel, a very strong webbing of ceramic fiber, on the skin of CTV. The Nextel and foam layers cause a particle to shatter as it hits, losing more and more of its energy as it penetrates deeper. Many layers into the shell is a layer of super strong woven Kevlar that holds the module's shape. The innermost layer, forming the inside wall of the module, is Nomex cloth, a fireproof material that also protects the bladder from scuffs and scratches. The structural integrity of CTV has been tested repeatedly since TransHab days. ^[228]

In order to know how strong and safe is inflatable structure different rigorous testing and passed all with more than satisfactory result. In order to accomplish the mission the CTV requires a continuous check up and repair. In the figure below it is shown one of the pictures of the test that was taken a hyper-velocity object, representing micrometeorites, hitting the inflatable structure. After repeated tests the structure have proven that it has Micrometeoroid and Orbital Debris Protection (MMOD) capability. Moreover, it has shown the inflatable technology in which the CTV is built is the best type of shielding against MMODs. ^{[228][250]} The following picture shows the strength of the CTV structure hit by a simulated MMODs.



Figure 104. Results of HVI test on full-size multi-shock shield for TransHab (Projectile: 1.8 cm diameter Al2017T4 sphere, 5.8 km/s, 45° impact) ^[250]

Aside from resisting impact of space debris, the structure is sealed against leakage. The wall material is impermeable to air to limit potential leak paths. An inflatable structure is not vulnerable to puncture than

aluminum habitat. The internal framework of the CTV supports the floors, walls, and equipment inside the habitat will also support the relatively lightweight pressure envelope. The other factor that needs to be detected in CTV is the amount of radiation. The journey to Mars is exposed to higher levels of radiation from space. Space radiation is comprised of atoms in which electrons have been stripped away. Ionizing radiation has so much energy it can literally knock the electrons out of any atom it strikes ionizing the atom. This can damage the atoms in human cells, leading to future health problems such as cataracts, cancer and damage to the central nervous system. Many of the materials considered for use in inflatable space structures will provide good protection from radiation exposure. Due to lack of the metal skin, the CTV will provide reliable protection from radiation.^{[229][253]}

Caution and Warning System

The CTV will have a series of sensors and warning systems that will warn the crew on the condition that may endanger the crew and the spacecraft. This system is called the Caution and Warning System. NASA and its international collaborators have developed an efficient and reliable monitoring and display systems. The ISS and the now retired space shuttle have a reliable and efficient caution and warning systems. These systems, being tested through years have shown their reliability in protecting both the spacecraft and the crew. Since the mission to Mars focus using the current technologies rather than developing new ones, in this mission to Mars, similar display and warning system will be used.

The caution and Warning system will contain sensors, radio frequencies (RF) communications and cameras that detect leakages, punctures, and pressure differences. They continuously measure both from inside and outside, and will feed the data to the monitoring and display system. This system collects signals from the distributed sensors, cameras, and RF communications nodes, and interprets the data through a microprocessor for crew and controller use. The configurations of this system has algorithms for comparing materials property data and making predictions for performance and life, as well as charting and tracking of different potential problems all around the structure. The hardware and software of this system will measure and warn based on this algorithms.

The CTV's sensors continuously scan its surroundings for potential danger including space debris, excessive radiation, temperature difference, fire or any other potential problems. Because these sensors are distributed in the different part of the CTV both inside and outside the detection method is very reliable. If space debris or other danger is detected in advance, the spacecraft can avoid the potential dangers. If the problem detected the alarm will warn the crew to take the necessary step. The following diagram shows the system of the Caution and Warning System.

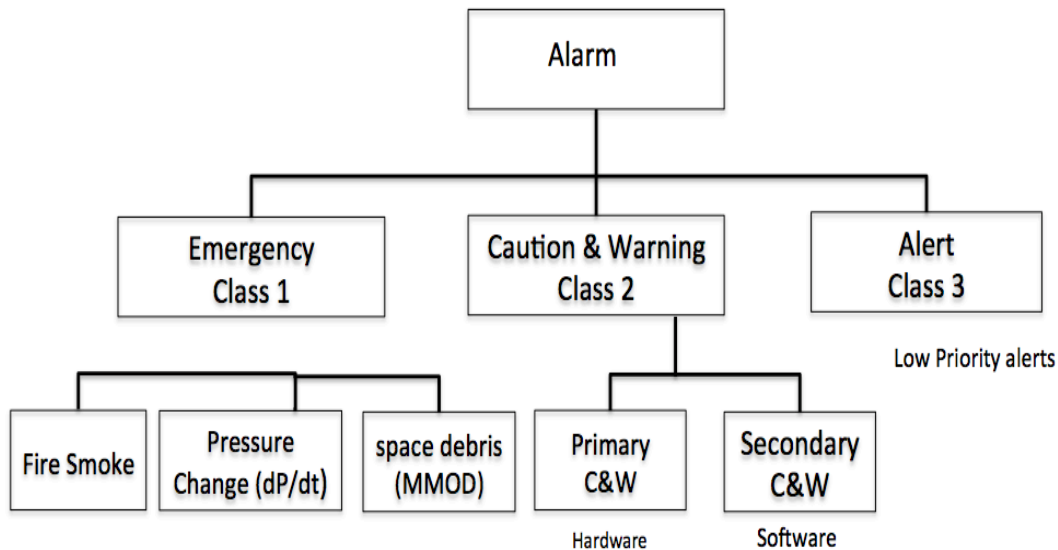


Figure 105. Caution and Warning System of CTV^[251]

The class-1-Emergency system detects and warns potentially dangerous or catastrophic incidents like fire, rapid depressurization, and space debris. This is the highest level of alert system, which can be from simple fix to complete catastrophe. For fire/smoke and pressure detection, the system uses hard-wired sensors, to monitor parameters and to issue alarms. These sensors detect a very small pressure difference or smoke presence. Because of the nature of the class 1 alarms, they always receive the highest priority for resolution. This class also detects the direction of space debris toward the CTV. If dangerous debris system detected in the direction of the CTV, it warn the crew to take the necessary steps. However, because of the speed and the small size of some debris, some of the debris hit the CTV before detection. In this kind of situation the procedure will be in order to fix the puncture that was caused by space debris. If the sensors detect punctures, leaks and other repairs due to space debris or other causes on the outer structure of CTV, which is class 1 emergency alert, EVA will be conducted to fix the problem. NASA has a patch repair system called Rubbn'Repair for servicing structural components in space during puncture and leakage. Rubbn'Repair will stop the leakage once it sticks on the surface of the CTV.

The class-2 system consist the Primary and the secondary Caution and Warning system. The primary system is a hardware system while the secondary one is a software and backup. Because the alert system integrated with different systems of the CTV, this system will alert problems like power loss, machine failures and other issues. The class-3 warning system is a low priority alert that will notify the crew a potential danger that is not priority, but still needs to be fixed.

5.4.10. Crew Transport Vehicle Science Missions

Science mission aboard the CTV are a critical component of overall mission success, future development and crew wellbeing. All crews will spend at 180 days in transit to the Martian surface. This long-duration mission provides ample opportunity to conduct experiments aboard the CTV. The CTV missions to Mars

will be the furthest humans have ever traveled in space. This presents a unique environment in which to conduct experiments that have not otherwise been done.

Because the overall mission is founded on the successful establishment of a Martian settlement, the science experiments conducted onboard the CTVs tend to support crew health, the transition to the Martian environment and independence and sustainability apart from Earth. Many of these experiments are nontraditional in nature; however, each provides valuable data that supports the success of the overall mission and crew wellbeing.

The following missions will be conducted on specified CTV missions:

5.4.10.1. Martian Surface Virtual Reality Experiment

Overview of Experiment

Using commercially available virtual reality equipment developed for use in the space environment, crews shall get themselves familiar with the Martian surface and the habitat and perform preset tasks in that environment. Task selection shall be informed in part through the feedback of the crew already on the Martian surface. Movement will be controlled through a movement treadmill, or a platform where the crew member will be harnessed in and movement tracked through motion trackers in the base of the platform. Using a virtual reality headset to provide audio and visual input to the crew member, the crew member shall be able to interact within the environment using a virtual reality glove apparatus. Heart rate of the crew member performing the experiment shall be taken before and after the experiment.

Equipment Needed

Movement treadmill with harness, specialized treadmill shoes, virtual reality headset, virtual reality glove set, Martian surface environment and task software, heart rate monitor

Assigned Crews

Every crew shall perform this experiment.

Results and Future Benefits

While the crew members shall receive training on earth before departing to Mars, this simulation will allow them to train during their transit and use input from the previous crews to tailor the simulation to be most beneficial. Using the results from the heart rate monitor, it can be determined what tasks the crew will perform to be most and least stressful. These results can be used to not only influence how the tasks are carried out on the Martian surface but also what tasks are included within the training in later missions. The simulation will also give the crew the ability to escape the confines of their transport vehicle and explore a different environment while keeping the focus on the mission.

5.4.10.2. Long-Duration Psychological Evaluations

This study will explore the psychological state and relationships of crewmembers during their transit to Mars. Of primary interest are how these relationships and feelings develop over time and how

crewmembers mitigate possible issues among the crew. This study will also explore how the crew naturally organizes themselves in terms of social structure.

Objective

In particular, the objectives of the study are to:

1. Determine the psychological state of each crew member and how it progresses and develops through the transit to Mars ¹²².
2. Determine crewmembers' opinions of and feelings towards one another ¹²¹.
3. Determine how the crew organizes themselves in terms of leadership and hierarchical standing.

Procedure

All astronauts aboard all CTVs will complete a survey every three days of the missions. The survey will require approximately 20 minutes to complete and will ask crewmembers questions pertaining to their own emotional well being, feelings, and feelings toward other crew members. It will also ask astronauts about possible conflicts and the actions they have taken or will take to resolve the conflict, if any exist. Last, crewmembers will be asked to describe the roles of other crewmembers in the last three days and report any instances that diverge from previously agreed leadership arrangements and roles. While taking the survey, each astronaut will wear a blood pressure monitor and any fluctuations in blood pressure will be correlated to their responses.

This experiment will require survey, which will be sent to each crew member's individual computer tablet and a Space Medicine Blood Pressure Unit to collect blood pressure metrics. The total mass of equipment for this experiment is approximately 2.5 kg and requires a volume of 0.3 m x 0.25 m x 0.2 m ¹²³.

Results and Future Benefit

These results will be collected and analyzed relatively to determine patterns throughout the duration of the mission. Results from each CTV mission will be used to forecast trends in crew relationships on Mars and to monitor each astronaut's overall wellbeing. This information could also be used when making crew selections for latter CTV missions.

5.4.10.3. Astro Palate V2

This study explores to use eating as a way to minimize stressful aspects of long duration space travel and the psychological consequences of allowing astronauts to eat meals together or apart. This study will also transition the astronauts from a traditional astronaut diet to a "Mars diet" in order to prepare them for their arrival at Mars. Studies will be conducted to determine how crew reacts and adjust to this transition.

Objectives

The objectives of this study are to:

1. Determine if eating alone or eating with others directly correlates with psychological benefits or concerns ¹²³.
2. Determine if "rewarding" crew with snacks helps to relieve stress related to tedious or unenjoyable activities ¹²³.
3. Determine how the crew reacts and adjusts to elements of the Martian diet over time.

Procedure

All crewmembers aboard all CTV missions will participate in this research study. After two weeks aboard the CTV, crewmembers will be surveyed and asked to rank their three least favorite tasks for which they are responsible. Objective 2 will be implemented before and/or after these tasks occur¹²³. During the third week of flight, crew members will be instructed to complete their least factor task (task ranking 1) as usual, and will complete a psychological survey after the task is complete. Blood pressure and heart rate measurements will also be taken before and after the task¹²³.

The next time a crewmember completes the tasks, he or she will undergo similar pre-activity evaluations. After completing the task, the crewmember will be instructed to eat a snack of their choosing from the designated selection¹²³. The crew member's heart rate and blood pressure will be recorded before and after eating the snack. This process will continue for two months.

Objective 1 will be tested beginning in week three and will continue for up to three weeks prior to arriving at Low Mars Orbit. Crewmembers will be randomly selected throughout the week to eat with or without the rest of the crew. All crewmembers will be surveyed and undergo heart rate and blood pressure tests to better understand how they react to the presence or lack of presence of (a) team member(s).

Objective 3 will be tested throughout the entire CTV mission. At the beginning of the flight (1.5 months), astronauts will consume a traditional space diet. In the last three months of the missions, flavors and food items of the Mars diet will be gradually introduced into the freeze-dried meals. By the time the crew arrives at Mars, they will have been consuming freeze-dried meals that resemble the Martian diet for two weeks. Surveys, heart rate and blood pressure tests will be used to evaluate objective 3.

This experiment does not require additional medical equipment give that blood pressure and heart rate readings can be collected using the same Space Medicine Blood Pressure Unit mentioned above¹²³. The experiment does, however, require an additional supply of desirable snacks onboard the CTV. All astronauts will be interviewed prior to launch to determine what snacks are appropriate for the crew.

Results and Future Benefit

The results of this experiment will determine whether rewarding crewmembers with snacks and improve morale on long-duration space flights. Furthermore, it will help the crew to adjust physically and psychologically to the Mars diet before their arrival. By doing this, crewmembers are less likely to be surprised by the drastic change in their diet and limited options. Results from crew surveys regarding eating or not eating with other crewmembers will be compared with psychological evaluations from objective 2 of the previous experiments to determine how these two datasets correlate.

5.4.10.4. Mars Lighting Schedule Experiment

The length of an Earth day is 23 hours and 56 minutes compared to the length of a Mars day, which is 24 hours and 37 minutes (NASA, Mars Facts). This 41-minute difference might seem insignificant on a day-to-day basis, but over time, it can drastically affect the crewmembers internal clock.

This study will utilize the lighting system inside of the CTVs to help astronauts adjust to the Mars day throughout the mission. The study will use surveys to determine astronauts' response to the change in schedule over time.

Objective

The objective of this experiment is to:

1. Determine if adjusting the lighting schedule inside the CTV will help crew members adjust to Mars time in preparation for their arrival

Procedures

All crewmembers on all CTV missions will participate in this study. At the beginning of the mission, light dimmers will be used to gradually adjust lights in the CTV to the “on” position, mimicking Earth sunrise. A similar process will be used to mimic Earth sunset at the end of each day. Throughout the mission, the lighting will autonomously adjust such that, by the time the crew arrives at Mars, the light schedule will mimic Mars day and Mars night. Crewmembers will complete weekly surveys regarding fatigue, alertness and their internal clock to determine the psychological effects of the study. Post-testing on Mars will also be utilized to determine if the experiment was effective in preparing the crew for Mars living conditions.

Results and Future Benefit

If the results of this experiment appear too successful for crews 1, 2 and 3, the technique will be implemented, without the experimental component on all remaining crew missions. Furthermore, if the results show that technique was successful in preparing crews for the Mars day, the lighting method will also be used during return trips to Earth, in the opposite sense, to help crews adjust from the Mars day back to the Earth day. In the event that the study is deemed unsuccessful, alternative methods will be researched and developed for future crews.

5.4.10.5. E-Learning

This study will allow crew members to utilize E-learning technology to promote continuous learning as a mean of reducing stress related to space travel ¹²⁹.

Objective

1. To determine if E-learning can reduce stress levels of crew members while promoting continual learning

Procedures

All crewmembers aboard all CTV missions will use E-learning technology for one hour every other day through the entire duration of the mission. Particular learning programs such as virtual art and language courses will be used to determine if E-learning can reduce crew stress. Before and after participating in this study, each astronaut will record his or her heart rate and blood pressure using the Space Medicine Blood Pressure Unit ¹²⁹. These results will be compared relatively between astronauts and over time to identify a correlation between stress levels and E-learning.

This experiment will utilize the already required crew’s tables and computers.

5.4.10.6. Product Shelf Life in Microgravity

This experiment will investigate the physics of colloid phase changes in microgravity¹²⁴. The study might allow the use of non-freeze-dried food and hygiene products on extended research missions from Mars to have longer shelf life.

Objective

The objective of this experiment is to:

1. Determine if new formulations can be used to extend product shelf life on long-duration space flights¹²⁴.
2. Measure phase separation rates in microgravity to develop a model for predicting product shelf life in space¹²⁴.

Procedure

Crews 2 and 4, which will fly aboard CTV 2, will conduct this experiment. Astronauts will homogenize 12 samples of solutions to perform initial experiment setup¹²⁴. The samples will be held in a clear container, which includes three non-homogenized control samples. The astronauts will take control photographs of all samples during experiment setup. A Nikon digital camera will be autonomously programmed to take pictures of the sample every hour for 4 weeks. A crewmember is required to perform one daily status check and record the results. This check requires that the astronaut identify a crystal formation in the samples¹²⁴. After four weeks, the crew will end the experiment and reconstruct the testing environment for a new trial. Results from each test throughout the missions will be compared relative to the leg of the transport mission and the surrounding environment. Analysts on Earth will also look for patterns between all testing phases.

Results and Future Benefit

This experimental research will help to if and how product shelf life varies in different regions of the solar system. The study also might allow additional food, hygiene and clothing products to accompany long duration missions from Mars during exploration and crew transit missions. In effort to support future crew independence from Earth, scientists and researchers must identify alternative methods for supporting crew food and product needs. Eventually, freeze-dried food supplies will diminish and alternative methods will need to be implemented. This experiment sets the foundation for alternative food and product supply methods for crew missions after 2054. In the event that this experiment is deemed unsuccessful, NASA will research, develop and test alternative methods on later crew missions. Crewmembers already on the Martian can also aid in this research, assuming time allows.

5.4.10.7. Astroseismology Experiment

Objectives

The primary objectives of this experiment is to:

1. Observe the stars with great accuracy,
2. Discover a host of short-period extrasolar planets,
3. Detect fluctuations from accretion onto our central black hole
4. And research microlensing from a variety of stars^{130 132}.

Procedure

Crews 2 and 4 will conduct this experiment aboard CTV 2. Because the Sun is in the direction of the galactic center during December and January and would disrupt the experiment, this experiment will be conducted during summer, spring and fall months¹³⁰. Therefore, crew 2, which launches in July 2046 will perform this experiment in the first four months of their transit. Crew 4, on the other hand, will conduct the experiment in the last two months of their transit given that they depart from Earth in November 2050. The experiment will require a small telescope mounted to a rigid science platform on the CTV. The telescope will monitor local stars and results will be sent to both the astronauts onboard the CTV and NASA officials on Earth. Both parties will analyze results.

5.4.10.8. Chromosome-3 Experiment

Overview of Experiment

Using hair follicles collected from crew members, shall extract DNA samples to see the effect of deep space radiation. Once hair follicles are extracted, they are broken down using organic solvents. The solution is then placed within a centrifuge with the solids extracted after the centrifuge process is completed. This process is repeated until only useful organic material remains. The remaining solid material is then incubated for at least two days before the results are studied.

Equipment Needed

Hair follicles, organic solvents, test tubes, petri dishes, microscope slides, centrifuge, incubator, microscope

Assigned Crew

Crews 1, 3, 5, and 6 shall perform this experiment.

Results and Future Benefits

Not much is known about the effects deep space, and more specifically deep space radiation, has on the human body. While there have been similar experiments performed on the International Space Station, none of those covered this particular human feature and were performed within Low Earth Orbit. This could help not only help our understanding of the human body grow, but help create similar experiments to be carried out in other missions. In the short term, it may help inform how vehicles need to be designed in order to mitigate any unwanted effects seen.

5.4.11. Leisure

Aside from continuous maintenance of the CTV and science mission, crew members will require ways to relax during their 6 month voyage to Mars. Each crew member will be allotted 10 kg of personal mass on the CTV, in addition to other items that will be shipped directly to Mars. Currently on the ISS, crew members are allowed 0.682kg in their Personal Preference Kits^[208] in addition to crew care packages that arrive once or twice throughout the duration of a mission and are a maximum of 5kg each.^[207] Since the

average stay on the ISS is about 6-months, the same duration as the CTV voyage to Mars, there are no known negative psychological effects stemming from not allowing crew to take more personal items with them.

Items could include the following: modified musical instruments, cards, cameras, games, personal posters or photographs, specialty clothing items. All crew members will be bringing a tablet computer with them. Movies, TV shows, books, audiobooks, computer games and music can be uploaded to these devices before the mission and will cut down on mass from bringing such items in non-digital form.

5.4.12. Mass and Volume Breakdowns

The structural mass of the CTV can be summarized in the following table and is responsible for about a third of the gross mass of the vehicle.

Element	Mass (kg)
Inflatable Shell	5700
Internal Beams	45
Airlock 1	101
Airlock 2	406
Docking Mechanisms (2)	600
Hatches (2)	600
Solar Panels/ Trusses	200
Radiators/ Trusses	200
Attitude Control System	203
Total	8055

Table 36. Structural Mass Breakdown

The equipment breakdown details all permanent CTV items that are non-recurring items that will not be replenished with each new crew.

Category	Mass (kg)	Volume (m³)
Urine Processing Assembly	744	2.27
Water Processing Assembly	2696	3.54
Sabatier Reactor/ Electrolysis System	84	0.17
Rehydration Apparatus/ Conduction Oven	36	0.09
Pressurized Gas Tanks	455	1.13
Battery	570	0.21
SPE Storm Shelter – Polyethylene Blocks	885	0.45
Crew Quarters	27	4.5
Medical Equipment	38	0.17
Exercise	350	5.8
Science Missions	180	4

Miscellaneous	23	0.44
Total	6088	22.77

Table 37. Equipment Mass/Volume Breakdown

The recurring mass and volume breakdown details all consumables and items that will need to be restocked either with each new crew or on an as-needed basis. Consumables are sized for the 180 day journey to Mars in addition to a 180 day contingency reserve in the event that the crew is required to turn around and come back to Earth. This breakdown includes three separate totals: the overall sum of all items (11.8 tons), consumables that will be exhausted and need to be replenished with each crew (3.3 tons), and consumables that only require resupply on an as-needed basis (8.5 tons).

With the 180 day contingency included, crews will arrive to Mars with 180 days worth of hygiene products, clothes, food, medicine and vitamins that they have not used. These items will be brought to the surface with them to increase the stores for the Mars settlement and therefore will need to be fully restocked by the next crew.

Water, O₂, N₂ and the ACS propellant are only resupplied on an as-needed basis because they should not be completely depleted with each mission since there is reserve built in to the tanks. O₂ and N₂ will require resupply if there is a depressurization of the CTV or through leakages associated with airlock operations. Additionally, as a result of the water loop not being 100% closed, 1 ton of water is depleted with each crew's 180 day mission.

Category	Mass (kg)	Volume (m ³)
Hygiene	167	3.26
Clothes	308	1.65
Spacesuit	252	11.6
Food	2534	6.91
Medical/Vitamins	6	0.01
Crew Personal Items	40	0.50
Water*	6750	6.75
Oxygen*	80	0.32
Nitrogen*	169	0.75
Propellant*	1500	4.22
Total	11806	35.97
Total (resupply each mission)	3307	23.93
Total (resupply on an as-needed basis)*	8499	12.04

Table 38. Recurring Mass/Volume Breakdown

5.4.13. CTV Payload - Restocking Logistics

There are three types of items that will require restocking with each CTV mission:

1. Recurring consumables
2. Occasionally recurring consumables (water, O₂, N₂ and propellant)
3. Short expiration time item transport for use by crews on Mars

Recurring Consumables

As mentioned previously, the CTV will require a full resupply of 3.3 tons of recurring consumables with each new crew of hygiene products, clothes, food, medicine and vitamins. These items will be transported to the CTV in the same Dragon and Dragon extended trunk that the crew launches in.

Occasionally Recurring Consumables

Every 180 days the water supply will be depleted by 1 ton, so in the event of an emergency, the CTV could lose up to 2 tons of water traveling from L1 to LMO and then back to L1. Therefore, 2 tons of water must be able to be resupplied at a time. Each depressurization of the CTV causes a loss of 26.7 kg of O₂ and 56.3 kg of N₂, which before the Mars mining and processing plant are operational is resupplied via the Dragon and Dragon extended ndable trunk that the crew launches in, and afterwards is resupplied via the EDL/A vehicle in LMO. Propellant loss from L1 to LMO is about 36 tons and is replenished at the LMO refueling station.

Short Expiration Time Items for Mars

Time sensitive items such as medicine, vitamins and some hygiene and cleaning products cannot be sent in advance to Mars with other cargo because they will expire before any crews arrive. Therefore, these items will need to be continually sent to Mars with each CTV crew. Each CTV crew will bring enough of these consumables to sustain all crews that landed on Mars before then until the arrival of the next crew. For example, Crew 3 must bring enough for themselves as well as Crews 1 and 2, until the arrival of Crew 4. Table 39 summarizes this mass and volume breakdown, with a more detailed breakdown in Appendix A.

Crew	Mass (kg)	Volume (m ³)
1	183	0.44
2	425	1.03
3	918	2.22
4	1292	3.13
5/6	737	1.78

Table 39. Short Expiration Time Mass and Volume Breakdown Summary

Logistics

The Dragon capsule contains 10m³ of pressurized volume with the extended trunk adding another 34 m³ of unpressurized volume. The maximum Falcon payload to L1 (including the crew) is 7,500 kg. Table 40 details the exact breakdown of how much payload each crew Dragon (payload is defined here as including crew members in their spacesuits) will be carrying during launch. Crews 3 and 4, due to the larger amounts of short expiration time items, will not be able to bring the full 2 tons of water that would be required to restock the CTV water wall in the event a crew needs to return to Earth without landing on Mars. However, this is not expected to present any problems considering only 1 ton of water is lost during the regular mission duration and both crews 3 and 4 can carry at least 1 ton.

After the Dragon with its crew and cargo launches and flies to L1, it will dock with its respective CTV at L1. After docking, astronauts can perform an EVA to the Dragon trunk in order to manually remove the cargo and transport it into the airlock. Once all cargo has been successfully transported inside the CTV, the CTV will undock from the Dragon and Dragon trunk before it begins its refueling docking maneuvers. After docking to the L1 Refueling Depot and refueling, the CTV will undock and continue on its voyage to Mars.

Crew	CTV	Dragon Payload Mass (kg)	Dragon Payload ³ Volume (m ³)	Notes
1	1	4420	24.37	Fully supplied via CTV launch
2	2	4662	24.96	Fully supplied via CTV launch
3	1	7390	28.03	1.5 tons of H ₂ O resupply
4	2	7264	28.44	1 ton of H ₂ O resupply
5	3	4974	25.71	Fully supplied via CTV launch
6	1	6971	26.31	2 tons of H ₂ O resupply

Table 40. Dragon Payload-to-CTV Logistics

5.4.14. Risk Analysis

As a result of the complexity and length of this mission, there is some inherent risk involved. However, major risk items were analyzed and remediation developed in order to decrease the impact severity and likelihood of the event actually occurring. Each risk event includes below list the impact if the event were to occur as well as the remediation steps that have been taken during design or will be taken by the crew. Figure 106 details a risk matrix of likelihood and impact. For reference, an impact level of insignificant is an event that the crew would barely notice, where severe would involve loss of crew.

Analyzed Risk Events

1. Power loss/failure

Impact: Essential equipment failure.

Remediation: The CTV will have batteries for power storage as well as power-saving modes to keep the most essential functions operational until repairs can be completed.

2. Communications blackout

Impact: Crew is unaware of an SPE event and therefore is exposed to harmful levels of radiation.

Remediation: Radiation Assessment Detector can provide immediate detection of SPE radiation.

3. ECS/LSS failure

Impact: Ability to scrub CO₂ and sanitize water is impaired.

Remediation: Replacement parts are available for all systems with life limiting components or that have the potential to fail. The vehicle will have excess oxygen, nitrogen and water in reserves and the crew could use the Dragon LSS/ECS system while the CTV system is being repaired.

4. Depressurization

Impact: CTV structure could begin to shrink, loss of oxygen.

Remediation: Dragon can be sealed off and used as a lifeboat in a rapid-depressurization scenario or crew can don their spacesuits if the leak rate is less severe.

5. Dangerous gasses (CO₂, CO, CH₄)

Impact: Impaired judgement and/or motor skills, unconsciousness, death.

Remediation: Gas masks will be available and if the problem is severe enough the Dragon capsule can be sealed off and used as a lifeboat or crew can don their spacesuits. Sensors are included to detect these gasses and alert the crew.

6. Fire

Impact: Loss of oxygen, smoke inhalation, and equipment and structural failures.

Remediation: The atmosphere contains a low partial pressure of oxygen so combustion is unlikely to occur. In the event of a fire, Dragon can be sealed off and used as a lifeboat while the CTV is fully depressurized in order to deplete the oxygen content and put out the fire.

7. Medical Emergency

Impact: Crew injury or health issue

Remediation: All crew members must complete EMT training and basic medical supplies and equipment will be available.

8. EVA Medical Emergency

Impact: Crew injuries and/or a difficult extraction from spacesuit in the event of a severe injury.

Remediation: Only two crew members will be allowed to EVA simultaneously so the other two are available in the event they need to EVA to rescue or assist their crew mate(s).

9. Solar particle event

Impact: Crew members could be exposed to harmful levels of radiation.

Remediation: Polyethylene blocks will be installed above the sleeping quarters for shielding and the CTV will orient the SpaceTrain to ensure the blocks are between the sun and the crew members.

10. Docking mechanism malfunction

Impact: Inability to dock to Dragon capsule or EDL/A vehicle.

Remediation: Astronauts can perform an EVA via the airlock hatch to repair the docking mechanism. If the mechanism suffers a catastrophic failure, the crew can EVA between spacecraft utilizing tethers and handholds as an alternative to docking.

		Impact				
		Insignificant	Minor	Moderate	Major	Severe
Likelihood	Almost Certain					
	Likely		9			
	Possible		2	5, 7		
	Unlikely			3, 4, 10	1, 6, 8	
	Rare					

Figure 106. CTV Risk Matrix

6. Phase V: Mars Habitation

6.1. Crew Entry, Descent, and Landing

6.1.1. EDL/A Introduction

Martian EDL/A is a crucial part to any mission that will be responsible for delivering humans to the Martian surface and back. It is also something that has never been attempted and a true test on the Martian surface is decades away. Due to its importance to mission success, particular attention was paid to make sure that a feasible and efficient vehicle was designed.

A guiding factor when designing this system was to create a vehicle with a maximum reusability rate. In an ideal world, every part would be reusable. As a result a single stage to orbit rocket is needed. Single

stage to orbit allows for the entire rocket body to remain as one piece and is much more reusable than a two or more stage rocket body that would need parts replaced after each stage separation.

The only part on the EDL/A vehicle that isn't 100% reusable is the entry shielding due to the fact that anything that enters the atmosphere will be at such a high temperature that it is impossible to avoid damages due to heating and friction.

6.1.2. EDL/A Vehicle

Fuel Mass Requirements

Two different fuels were examined for use in the main engines of the EDL/A vehicle. The two fuels considered were hydrogen and methane. Both fuels are available resources on the surface of Mars that could be replenished after each launch. Ultimately, liquid hydrogen was chosen as a fuel because of its increased availability and decreased constraints on mission operations. Liquid oxygen will be mixed in a 6-to-1 ratio with the hydrogen to produce the propellant for the rocket.

Liquid hydrogen fuel and liquid oxygen oxidizer are available at the refueling station in LMO allowing the EDL/A vehicle to refuel after ascent. The required propellant mass for the vehicle was calculated using the rocket equation.

$$\Delta V = -I_{sp}g_0 \ln \left(\frac{m_f}{m_o} \right)$$

Several iterations of the rocket equation were used to obtain a good estimate of the propellant mass. Initially, a value of 450s was assumed for the I_{sp} based on typical values for a LOX/LH₂ engine [70]. The I_{sp} of the engine was later increased to 465s. This is the value of the SLS upper stage engine that operates in the upper Earth atmosphere with similar pressure conditions as the Martian surface [73]. Then, a value of the inert mass of the rocket was estimated. The payload mass was defined by the crew systems team based on the number of astronauts to be transported, the mass of the cargo, and the weight of the capsule.

The propellant mass was calculated for two ΔV s, ascent and descent. Both cases assumed very conservative values to ensure that enough propellant was available. The ΔV for ascent was 4.82 km/s, which assumed an escape velocity from the Martian surface. The ΔV for descent was 3.41 km/s, which assumed a decrease in velocity from 300km LMO to 0 km/s. Tank sizing calculations and inert mass estimates were based on the larger delta-v necessary for the ascent case. This is the limiting case of the rocket and would require the most propellant.

The first iteration was completed with an initial guess of the inert mass. Given the propellant mass obtained from the first iteration, more accurate inert mass numbers were obtained mass estimating relations [220]. These new mass numbers were compared to the initial inert mass estimate allowing for another more accurate estimate to be used in a second iteration. The iterations continued until the estimates agreed. The final inert mass estimate was used when calculating the fuel required during descent from LMO to the surface of Mars.

The results from this analysis reported that the EDL/A vehicle would require 39t of fuel for ascent from Mars, and 13t of fuel during descent from LMO to the surface.

Propulsion

Main Engines

The propulsion system of the EDL/A vehicle will consist of 4 custom engines, each capable of producing 80 kN of thrust at an I_{sp} of 465s. This results in a thrust-to-weight ratio of 1.47 when fully fueled on the surface of Mars. The thrust requirement set for the engines was that if one engine were to fail, then the rocket would still have a minimum thrust-to-weight ratio of 1.1.

The fuel for the engines will be stored at 8 MPa. Each engine nozzle will have an exit diameter of 2.25m and an expansion ratio of 57. These nozzle dimensions were designed to produce perfect expansion at the surface of Mars.

Attitude Control

Just as with the cargo EDL vehicle, the EDL/A crew vehicle will achieve attitude control by using RCS thrusters to control the direction of the lift vector during entry. The RCS thrusters will be laid out similarly to the cargo vehicle, with four sets of two opposing thrusters 90°s around the craft. With each thruster able to produce 311N of thrust, a complete 360° bank angle maneuver in under 60 seconds.

To achieve the desired attitude control of the rocket, the rocket will hold 5.9t of fuel. The CO₂ fuel will be stored in a mixed state of liquid and gas at a quality of 0.28 to fit the sizing constraints of the rocket. The chamber temperature and pressure will be stored at 289K and 5.14 MPa^[74].

The thrusters will have an I_{sp} of 67s, an expansion ratio of 190, and an exit diameter of 15cm.

Atmospheric Entry

During descent, the EDL/A vehicle will experience significant heating from the thin Martian atmosphere. To mitigate the heating, a deployable heat shield will be used in addition to a traditional ablative heat shield. The purpose of the deployable heat shield is to increase the leading radius of the vehicle and separate flow to reduce heating from skin friction along the sides of the EDL/A vehicle. This deployable heat shield will work similarly to the HIADs used for cargo descent. Nitrogen will be used to inflate toroidal rings from the sides of the vehicle. The leading surface of the inflatable will be covered in Nextel 440 fabric, which can withstand heats up to 1600K^{[66][67]}. After the vehicle has slowed to a velocity where heating becomes less serious, valves will open to deflate the heat shield, and the shield can then be reeled in to allow the legs to deploy for landing.

In addition to the inflatable heat shield, an ablative heat shield will surround the engine block at the base of the vehicle. The material must be resistant to the temperatures from the engine exhaust and the incoming flow. An ablative material was chosen because it can be fitted to the shape of the engines to allow the nozzles to be open at all times, and can handle higher temperatures than the fabric material used on the inflatable. One option for the ablative heat shield is PICA-X: a material developed by SpaceX, in conjunction with NASA. This ablator can withstand temperatures up to 2100K while ablating minimal amounts of material with each use^{[71][75]}. This material would increase the operating lifetime of the heat shield before a resupply and restoration of the heat shield becomes necessary.

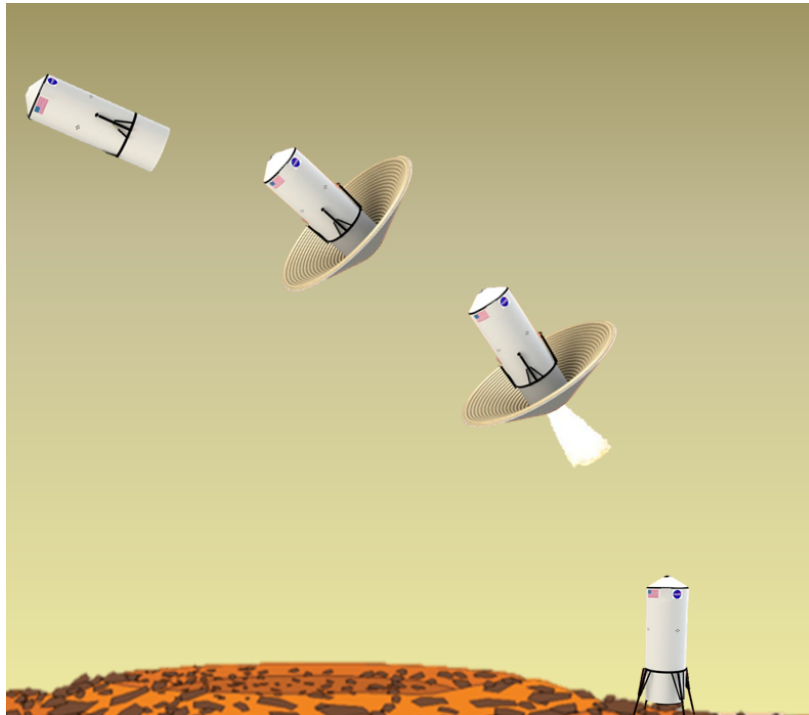


Figure 107. Manned Descent Operation

6.1.3. EDL/A Crew Pod

The primary mission of the EDL/A crew pod is to safely and reliably transport 4 crew members between LMO and the surface, with its secondary mission being the transportation of consumables to the surface from the CTV as well as pressurized gasses and water from refinery to the CTV.

Specific requirements for the EDL/A crew pod included the ability to:

- Transport 4 crew members in their modified Z-2 spacesuits
- Transport a maximum of 3.65 tons and 5 m³ of cargo
- Not exceed a maximum gross mass of 7.6 tons
- Utilize an outer diameter dimension of 6m

- Pressurize to a maximum of 8.4psi
- Dock to the CTV via a universal docking mechanism
- Move crew and cargo from vehicle to the surface of Mars

The EDL/A pod was designed to be a 6m diameter cylinder with a height of 2m. An additional 1.75m in height was added through the blunt-nosed cone shape at the top, where the docking mechanism and hatch are located. While the total exterior height was designed to be 3.75m, the docking mechanism and hatch protrude into the interior of the spacecraft volume (see Figure 108). This was a design choice in order to reduce the height of the vehicle, while still allowing for a pivoting cover to protect the docking mechanism during ascent and descent in addition to making the vehicle more aerodynamic by reducing drag during ascent.

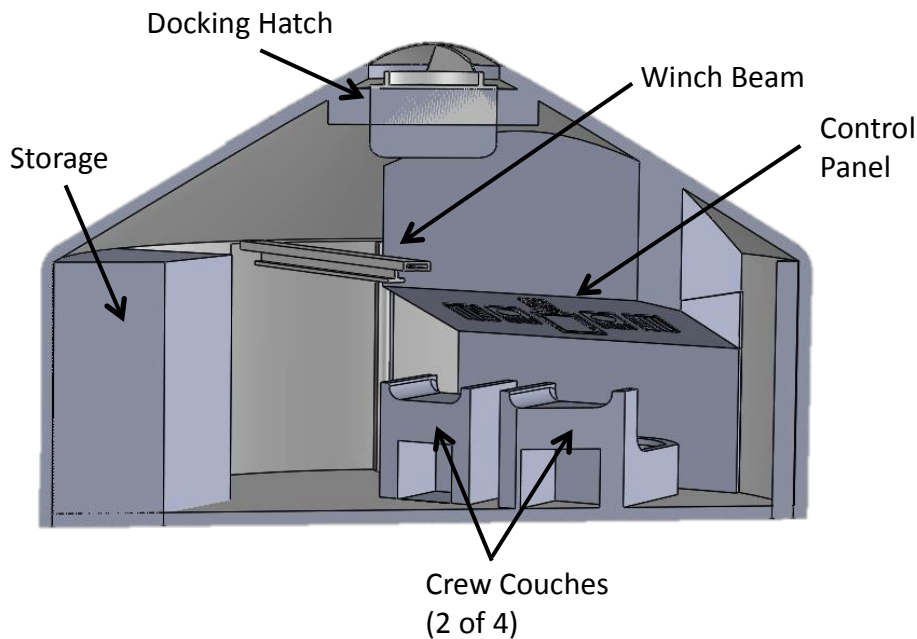


Figure 108. Cut-Away View of the EDL/A Crew Vehicle

All unused floor space was converted into storage (see Figure 109). The combined volume for dry and pressurized gas storage will be 13.7 m^3 , which accounts for the gas required for pressurizing the spacecraft, O_2 and N_2 that will be taken to the CTV during ascent for restocking operations, as well as dry volume for cargo to be brought down to the surface from the CTV during descent. The mass of the vehicle was designed to be 3.95 tons, which allows for 3.65 tons of crew and cargo; a gross mass of 7.6 tons.

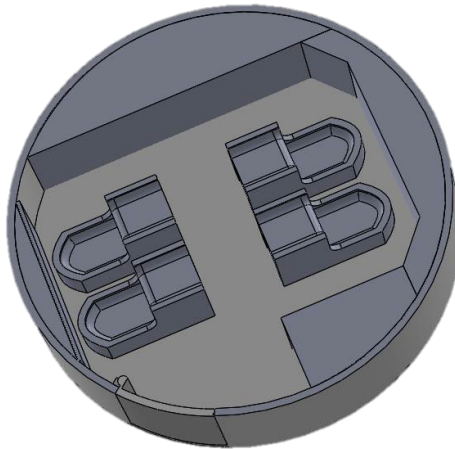


Figure 109. Horizontal Cut-Away View of the EDL/A Crew Vehicle

There will be a total of four crew seats, with two having access to the control panel. In a descent vehicle, couches are not always required, which decreases mass and volume, but in this case, the vehicle will be used for both ascent and descent. The G-forces the crew will experience exceed what would be safe for them sitting in a vertical position, especially considering their deteriorated physical condition after 6 months of zero gravity, which is why couches were required. ^[112]



Figure 110. Exterior View of the EDL/A Crew Vehicle

When the vehicle lands on the surface of Mars, the crew will be unloaded via a special attachment to the end of the construction crane. However, as a backup, the vehicle contains a winch system to lower crew and cargo. The winch is attached to a beam that is stored inside and can be extended about a meter outside

the vehicle after landing. A basket is then attached to the winch and a motor lowers the basket to the surface.

6.1.4. Ascent/Descent Vehicle Landing Structure

The manned landing structure will be required to withstand both the landing loads of the empty Ascent/Descent vehicle, as well as the fully loaded static loads and dynamic loads associated with the ascent of this vehicle. As it is a critical substructure in terms of the vehicle's mission success, the landing structure was also designed to be able to not fail and maintain the stability of the orientation of the vehicle in a number of different contingency situations, such as excess vertical or horizontal speed, crash landing, small obstacles, and angled landing surfaces. In addition, in order to be able to fulfill the mission of the vehicle, this structure is designed to be retractable in order to maintain an acceptable aerodynamic profile.

The landing structure consists of four retractable primary landing struts, along with secondary struts for additional support and motion control. In the stowed configuration these struts align vertically with the outer body of the vehicle to reduce the aerodynamic profile of the landing structure as much as possible while stowed during descent and ascent. These primary struts deploy to an overall length of 8 meters, at an angle from the vehicles longitudinal axis that can vary depending on mission (design angle was 30°).

In terms of design the main loads examined were the fully fueled static loads of the ascent portion of the mission, and the crash-landing loads of the descent portion. In order to withstand these loads a design radius of .13m is chosen for each of the four landing struts.

NOTE: In order to accommodate a number of other design requirements such as angled landing, retractability, and crew factors the legs are to be made using shock damping materials such as a fluid shock absorber. Previous vehicles have used technologies such as crushable aluminum honeycomb cores to accomplish this damping effect, however this technology does not fit the scope of this mission, as it is not reusable. In order to safely accommodate this difference in stress analysis, a much higher factor of safety (~5) was used.



Figure 111. Ascent/Descent Vehicle Landing Gear

Another concern that needs to be addressed is the tipping of the vehicle due to a number of different loads, such as Martian winds or excess lateral velocity at landing. In order to ensure the stability of the orientation of the vehicle the total width of the landing structure had to be wide enough to ensure that the vehicle would not surpass a critical tipping angle. When statically positioned, the Martian winds would have much less of an effect on the angular orientation of the vehicle when compared to lateral velocity at landing. A requirement of at least 2.5 m/s of lateral velocity at landing was set, and using a center of gravity located 8m vertically off the ground it was found that the vehicle would be able to survive a landing with this excess lateral velocity (using NASA safety factor of 1.4).

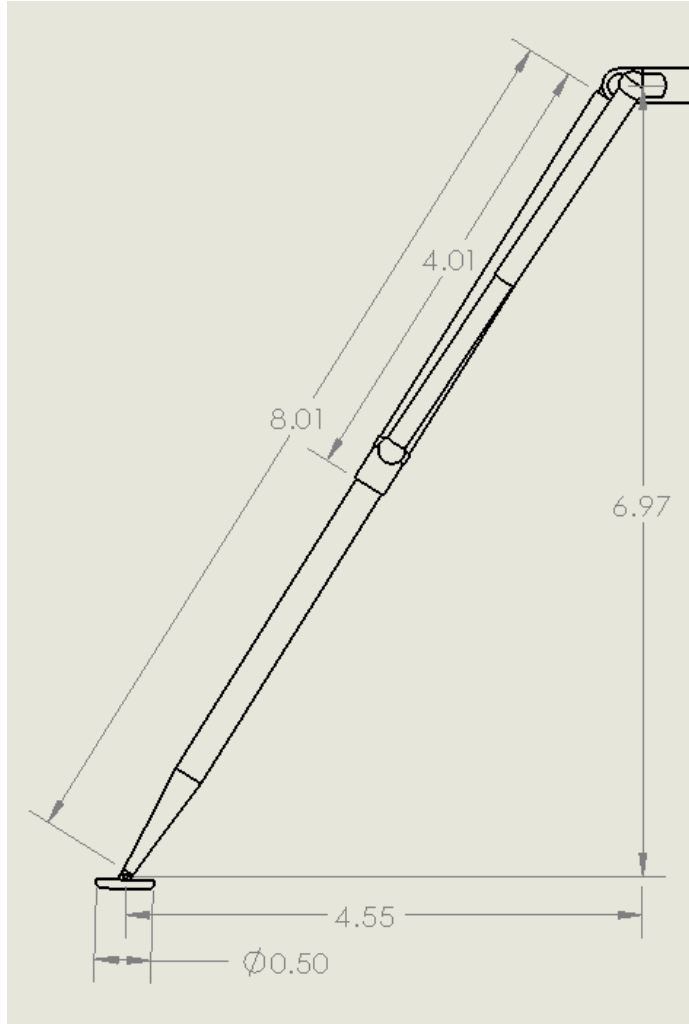


Figure 112. Ascent/Descent Landing Strut Dimensions

In addition to excess landing velocity, another concern that must be considered is an uneven landing surface. Despite precise landing technologies there is still a chance that the targeted landing surface is not perfectly flat. In order to overcome this the use of telescoping landing struts such as fluid shock absorbers are used so that each of the landing feet has a range of travel that can be used to overcome slopes in the landing surface. The feet of the landing structure are also rather large comparatively and have the ability to pivot, allowing them to help alleviate issues involved with landing surface obstructions such as small rocks or inconsistencies.

Loads generated using MATLAB script, *MannedEDLCriticalLoads.m*, that can be located in Appendix C. Note: All factors of safety used are NASA standard.

Load Source	Limit Stresses (MPa)	FOS	Design Stress (MPa)
-------------	----------------------	-----	---------------------

Hoop Stress	48	1.4	67.2
Axial Stress	24	1.4	33.6
Acceleration	8.6	1.4	12
		Total	112.8

Table 41. Ascent/Descent Vehicle Critical Stress Table

The material for these critical components is Aluminum 6061-T6. Originally these parts were designed using a much higher Lithium component alloy of Aluminum: Al 2195. Al 2195 has a history of space and aviation usage, such as on the external tanks of the Space Shuttle. However, upon reconsideration the strength and weight benefits of using Al 2195 were not worth the added cost, thus designing for the more standard Al 6061-T6.

Shown below is the Ascent/Descent vehicle Margin of Safety Table. As with many launch vehicles the critical stress factor is thin walled cylindrical buckling.

Al 6061-T6 Alloy σ_u	316 MPa
Critical Buckling Stress	176 MPa
MOS (σ_u)	2.42
MOS (Buckling)	0.56

Table 42. Ascent/Descent Vehicle Margin of Safety

6.2. Mobile Roving Settlement

6.2.1. Magellan 2.1 Modifications

During the initial construction phase of the Mars habitat, the crew will live in the pressurized Magellan 2.1. They are expected to live in the 2.1 for only a month before being able to move into one of the Halls.

Three Magellan 2.1 pressurized rovers will land on Mars separately from the crew. Upon crew landing, the rovers will autonomously navigate to the crew location. The crew then walk over to the Magellan and enter it through the suitports. The modifications in the Magellan 2.1 consist of adding avionics systems to communicate with μ net, MRO, and Odyssey, upgrading the suspension and wheels for Mars gravity, increasing power capabilities.

Communications

The Magellan rover will communicate with μ net, MRO, and Odyssey to autonomously navigate to where the crew capsule lands. The Magellan will communicate with the satellites via an omnidirectional antennae that supports X band.

Suspension and Wheels

The Magellan suspension and wheels are redesigned for Mars gravity.

Power

The Magellan 2.1 has a power system that works with solar arrays in combination with batteries. The original Magellan was driving constantly and always in the sun. The 2.0 and 2.1 will not be driving very far and so is designed for a lower maximum speed to reduce the power requirement. They will also be stuck without solar power through the night. So the 2.0 and 2.1 have higher battery storage capabilities. Batteries are notorious for losing their charge holding capabilities over time. To counter this loss of effectiveness, the 2.1 has an added proton-exchange membrane fuel cells to allow for continued power once water on mars becomes an available resource. Storage tanks for liquid hydrogen and liquid oxygen have been added to the rover.

Mars Time

The clocks will run on a from 0h0'0'' to 24h39'35'' upon which it will reset to 0h0'0''. This will help keep the crew on the same cycle as the Martian Sol which will help with coordinating and performing EVAs as well as help with crew psychology. The benefit of this time method is that the crew will have an extra 39'35'' each day to spend as they see fit.

Mars Exercise

The crew exercise regimen will be set according to a personal trainer on Earth and modified as needed according to the crew doctor to maintain appropriate muscle, cardiovascular, and bone density levels.

Life Support

A 2 Bed Molecular Sieve comprising of a bed of carbon fiber will be used to extract CO₂ from the atmosphere. O₂ and N₂ will be generated from high-pressure vessels located outside of the pressurize volume. The high pressure at which these gases will be contained at will serve as the means of controlling the associated partial pressures of each of these gases. The thermal control system consists of 2 condensing heat exchangers that will absorb excess heat and moisture and 2 radiators to dump the heat out. Two 60-cm diameter fans will be used to circulate the air around the cabin. In total, this system utilizes 1kW.

Propulsion

The Magellan uses a pair of electric motors situated on each of the axles to propel it. Using an approximate value of 0.3 for the rolling resistance of mars and a desired velocity of 4 m/s, it is calculated that the Magellan would require 20kW to be able to move.

Energy Storage

The Magellan is equipped with solar arrays capable of producing an average of 15kW during day time. When the Magellan lands it will have a 1mt advanced rechargeable li-ion battery containing 265 kW-hr, in case there is a failure with the solar arrays and the crew has to survive on the battery till the recharging station is set setup. For future uses, once the settlement is completely built and the processing plant is up and running, the Magellan is also equipped with a Proton exchange membrane fuel cell and LH₂ and LOX tanks. Advanced rechargeable batteries have short cycle lives (~ 600 cycles) and so a more sustainable option was added. You can see a basic schematic of a PEM fuel cell in the figure below.

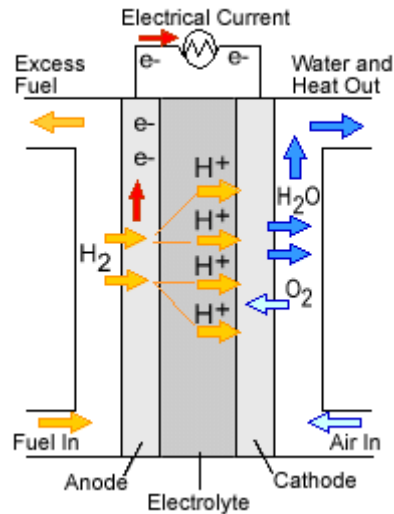


Figure 113. PEM Fuel Cell.

6.3. Martian Resource Use

6.3.1. Mars Miners

Mining on the surface of Mars will be similar to the mining operation on the moon, but with differences. The mining operation on Mars was designed to produce 100 kg of water per day to be provided to the habitat and to produce 30 metric tons of fuel for the ascent vehicle launches every two years. As the requirements for resource acquisition are much lower than that of the moon, only two miners will be sent to Mars, smaller tanks, and no fuel transport vehicle refueling boom.

With the exploration data from the Deep Space X mission, the habitat location will be determined by areas with ice found within the top 10 cm of regolith with up to 5% composition by mass. With 5% water composition, the miners must collect 2 metric tons of regolith each day. This production will increase when fuel is required by the ascent vehicle. As gravity on Mars is roughly double that of the gravity on the moon, the miners will be limited to 22 metric tons of regolith per trip, compared to the 45 metric ton capability on the moon. While this limiting weight is not applicable for daily water production, it limits the rate of soil that the crane will be able to place over the habitat.

Power for the Martian mining operation will come from a 100 kW nuclear reactor. 55 kW will be used to electrolyze 100 kg of water per day when needed, with the remaining power used for the oven, pumps, and conveyor belts.

Compared to the Moon miner, the Mars miner has the advantage that it can use μ Net to communicate with controllers on base. It will also make use of the GPS system within the network for controlled precision navigation.

6.3.2. Processing Plant

The settlement on Mars will have to be able to refuel the CTVs every two years. A processing plant comprising of two miners, a recharging station, an oven and a Polymer electrolyte membrane electrolyzer will process water from the regolith and convert it to H_2 and O_2 . The electrolyzer will run at 55 kW at a rate of 12.5 liter/hour for an 8 hour period every day. A miner would go on an 8 hour mission gathering water, after which the other miner would do the same. The last 8 hours of the day are spent processing the water and recharging the miners. The processing plant contains one of the settlement's power nodes.

Recharging Station

The recharging station would be one of the first things set up. After the first nuclear reactor is up, the recharging station would be put into place. It would be a stand-alone power node that serves one purpose, recharging the vehicles. The Magellan at that point would be containing the first four member crew, thus keeping it powered up will be the main priority. The recharging station will also be powering up the miners during the last 8 hours of the day.

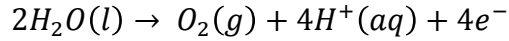
The recharging station is a secondary ELI or "switch panel" located in a zone that would act as parking lot for our vehicles when they are stationary for long periods of time. It would feed directly from the LPC a steady 120 Vdc. It would be able to transmit a maximum of 25 kW when both miners are being recharged. The Magellan would only need to be recharged in case of failure of the batteries or the solar panels, in that case keeping the Magellan up would be the main objective. However, the Magellan only require 1 kW to keep it habitable so it wouldn't be disruptive to the operation. The recharging station needs to also recharge the crane's multiple batteries which would require around 1.5kW.

Electrolysis

Water will be our most valuable resource on mars. It is mission critical that the processing plant be able to produce 100 kg of fuel and oxidizer daily (during the 8 hour processing period) as to meet the requirement of refueling a CTV every 2 years.

An electrolyzer is an electrochemical device to convert electricity and water into hydrogen and oxygen. The PEM electrolyzer utilizes a solid polymer electrolyte (SPE) to conduct protons from the anode to the cathode while insulating the electrodes electrically. Under standard conditions the processing limit of the enthalpy required for the formation of water is 285.9 kJ/mol. A portion of the required energy for a sustained electrolysis reaction is supplied by thermal energy and the remainder is supplied through electrical energy. The following reactions occur at the anode and the cathode:

Anode Reaction



Cathode reaction

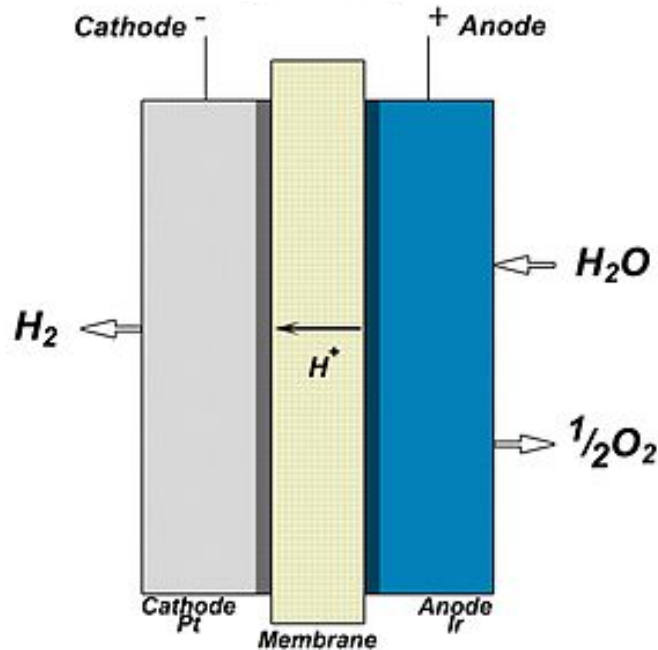
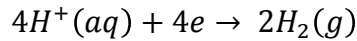


Figure 114. PEM electrolyzer.

The polymer electrolyte membrane is capable of providing high proton conductivity, low gas crossover, compact system design and high pressure operation. The low membrane thickness (~20–300µm thick) is in part the reason for many of the advantages of the solid polymer electrolyte. The low gas crossover rate of the polymer electrolyte membrane (yielding hydrogen with high purity), allows for the PEM electrolyzer to work under a wide range of power input (economical aspect).

Using the following equation and assuming we will have the highest technology available and would be able to operate at the processing limit we find that the electrolyzer would need 55kW to maintain.

$$\frac{286 \text{ kJ}}{\text{mol}} * \frac{\text{mol}}{18 \text{ g}} * \frac{1000 \text{ g}}{1 \text{ kg}} * \frac{100 \text{ kg}}{8 \text{ hrs}} * \frac{1 \text{ hr}}{3600 \text{ s}}$$

6.3.3. Nitrogen Production

Leaks in the habitat will require 50 kg of nitrogen to be replenished each day. The Martian atmosphere contains 2.7% nitrogen so 500 cubic meters of Martian air will be processed each hour. This will be accomplished with eight membrane type nitrogen generators. Martian atmosphere will be pumped into a

heating chamber where its temperature will be raised to 5°C. After heating, the air will be pumped through a polymer membrane where carbon dioxide and other gases will be absorbed by polymer fiber bundles released out of a top pressure release valve. The nitrogen will pass through the membrane where it will be pumped into the habitat. Each nitrogen generator will run continuously, requiring 22 kWh.

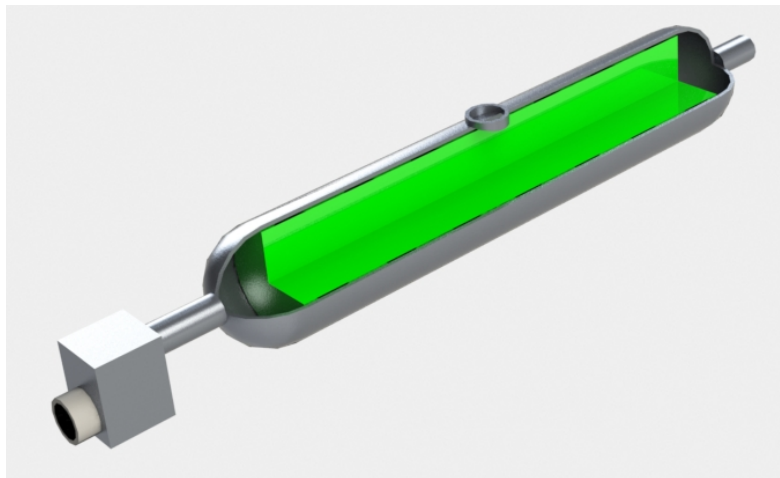


Figure 115. Nitrogen membrane generator

6.3.4. Carbon Dioxide Freezers

When the first settlers arrive on the Martian surface, they will immediately find themselves surrounded by a very valuable resource - the Martian atmosphere. The reason that it is such a valuable resource is because it is made up of 95% carbon dioxide, a very useful feedstock for propellant production. However, in order to make use of it, it needs to be separated from the 5% of other trace constituents present in the atmosphere (N_2 being 2.7% and Argon being 1.6% of that 5%). As such, it is worthwhile to consider various technologies that could be dedicated to the task of capturing and separating this valuable CO_2 in order to ensure the process remains as great an economical benefit as it can be.^[9]

First to consider for this purpose is membrane separation. This method for CO_2 capture and separation has been used in industry for some time, utilizing many different kinds of filters – most of which have been designed to function on Earth. Commercially available membranes are generally polymeric-based. These include poly-acetate, polyamides, polyamides, polysulfone, polyethylene, and polycarbonates. These are materials that continue to be studied for CO_2 gas separation save for zeolite membranes, which separate gases according to the size of the molecule. CO_2 separation, comparatively, is characterized by the solubility of its molecules within the matrix of a given membrane, the dissociation of the molecules from the permeate side of the membrane, and the diffusivity through the matrix of the membrane. The performance of these materials are characterized by their capability to transport CO_2 molecules in gaseous state, selectively. A balance must be struck between permeability and selectivity, as these are competing factors. The majority of these materials permeability is between 100 and 300 barrer ($1 \text{ barrer} = 3.348 \times 10^{-19} \text{ kmol m} / [\text{m}^2 \text{ s Pa}]$). Since carbon dioxide in the atmosphere is in high concentration, lower permeability and a high selectivity is best. The best selection in this case is then the poly(amide-6-b-ethylene oxide) which demonstrated a CO_2 permeability of 122-227 barrer and a CO_2 permeability of 122-227 barrer and a $CO_2:N_2$ selectivity of 71-79 at 25°C. Despite how this compares well against the

other membranes available for Mars, these membranes created for the Martian atmosphere could trade poorly as pressurizing these gasses to the necessary point would likely be cost prohibitive.^[10]

In addition when utilized in the Martian environment, membranes will not separate certain constituents of the atmosphere well - namely Argon and Nitrogen. Unfortunately, these two constituents make up the majority of the trace elements in the atmosphere. In addition, the best of these systems, which utilize membranes, would only recover up to 47% of the carbon dioxide that attempts to pass through it, reducing its efficiency. As such, membranes are not the best choice for ISPP on Mars at this time.

Next are an even newer technology - ionic liquids. These have garnered some increasing interest in the past 15 years, as they can act as replacements for solvents used in many catalytic and organic reactions due to their low volatility and high temperature stability. When used with gasses, they have shown a high affinity for carbon dioxide which makes them ideal for use in green technology geared towards the use of carbon dioxide removal. Carbon dioxide's permeability in membranes which make use of ionic liquids increases from 744 to 1200 barrer in the temperature range from 37-125°C but its selectivity decreases from 8.7 to 3.1 as well; it should be noted that the solubility of carbon dioxide decreases with increasing temperature, however. Whilst these liquid cations and anions have interesting solvent and conductive properties and as such show some promise for the task of carbon dioxide separation, they are rated at a TRL of 1-2. As a result, there is currently a limited understanding of reaction mechanisms and kinetics about the function of the system. On top of that, the current ionic liquids available would only absorb 7% of the carbon dioxide that they encounter. As such, despite their promise, at this time they are not the most viable solution due to their inefficiency and the current limited understanding about these processes.^[10]

The next technologies worthy of consideration are physical absorption/adsorption systems. In these systems, carbon dioxide is allowed to penetrate a solid or liquid under certain conditions, then desorbs under a different set of conditions – a process which is temperature/pressure dependent. This process requires fairly low energy, however the affinity of carbon dioxide for the absorbent is weak, at least compared to chemical solvents. Unlike chemical solvents however, physical absorption has a higher capacity given that it is no longer limited by stoichiometric requirements. These solvents are then regenerated by pressure reduction or heating, commonly Selexol (a bulk carbon dioxide and hydrogen sulfide remover from natural gas streams) or Rectisol. Physical adsorption in particular depends upon the affinity of an analyte for a material's surface without the formation of a chemical bond. Weak interactions (such as van der Waals) allow the separation of the carbon dioxide from a vapor stream – a fascinating phenomenon. Adsorption requires a strong affinity between the absorbent and the carbon dioxide, but unfortunately the stronger the affinity initially is, the more energy intensive it becomes to desorb the carbon dioxide from the adsorbent. Regardless, these are systems that are fairly well understood today, but Asimov City will not include them because these systems tend to utilize very high pressures which result in high energy requirements. This inhibits one of the main points of in-situ resource utilization, and that is to be economical.^[10]

This brings us to carbon dioxide freezers, which is the choice the team – as well as NASA - has gone with. This is because CO₂ freezers obtain relatively pure carbon dioxide, they are highly efficient, and provide an enriched feedstock for buffer gas preparation, a property unique to CO₂ freezers. They have a simple design and to go along with that, a simple concept. Essentially, these will cool carbon dioxide until it can achieve a liquid form. At this point, other portions of the Martian atmosphere will remain in a gaseous form, which means that you will have highly purified Carbon Dioxide as a result. There is a large margin for this freezing point of carbon dioxide as compared to the other trace constituents in the atmosphere, which is why it would be able to be processed in a highly pure form, followed by processing through a Sabatier reactor. This is evidenced by the below table which cites the various constituents in the atmosphere along with their boiling and freezing points.

Martian Atmospheric Constituent	Freezing Point (°C)	Freezing Point (°C)
Carbon Dioxide	-78 (sublimes)	-78
Nitrogen	-196	-210
Argon	-185	-189.15
Oxygen	-183	-219
Carbon Monoxide	-191	-205
Neon	-246	-248
Krypton	-153	-157
Ozone	-112	-192
Methane	-161	-182

Table 43. Freezing Points of Martian Atmospheric Constituents^[11]

Fortunately, the water concentration is low enough that merely 1 gram of water will be captured out of every 700g of CO₂ that is captured from this process. Such low levels are thankfully not of any detrimental effect to the Sabatier process. The captured carbon dioxide will sublimate for sake of providing a pressure of 50 psi, sufficient for the Sabatier reactor. Typically for such systems, two cryocoolers are required to act simultaneously – this is to allow one to facilitate the collection of the carbon dioxide while the other supplies the Sabatier reactor. This will allow for higher efficiency and rate of propellant production, while simultaneously making it less of a detriment to shut the system down if additional power is required in addition to the propellant.

The CO₂ freezer subsystem requires two cryocoolers, for which the geometry, surface area, and thermal mass must be taken into account. The ideal cryocooler head is the ‘Ferris Wheel’ design, designed by NASA’s multi center MARCO POLO. This design has a low thermal mass of 260g, and a larger surface area of 409cm². Despite how the Martian atmosphere has a density of 0.020 kg/m³ compared to Earth’s 1.23 kg/m³ (1.6% of Earth’s density), this will still capture an adequate amount of carbon dioxide at a pressure of 1.066kPa in the Martian atmosphere.^[15]

There are various propellants that are possible to be produced on Mars to varying degrees of difficulty, including methane (CH₄), hydrogen (H₂), hydrazine (H₂NNH₂), and methanol (CH₄O). However, considering the easily acquirable carbon dioxide in the atmosphere, one of the most economical choices available for in-situ propellant production will be methane. There are several reasons why it would be desirable to use this carbon dioxide for the creation of methane in particular. First, it’s more manageable than hydrogen due to its lower boiling and melting point. That is, methane’s boiling point is -161°C and its melting point is -182°C, while for example, hydrogen’s boiling and melting points are -252°C and -259°C, respectively. Methane also requires less storage space due to its high density. It has a density of 0.716 g/L at 0 °C at 1 atm, compared to hydrogen’s density of 0.08988 g·L⁻¹ at the same conditions. Methane only requires passive cooling in order for it to be maintained, and in addition to this, it is actually non-toxic. It also burns cleaner than other fuels such as hydrogen which will be better for the

safety of Martian settlers. Lastly, it causes considerably less wear on engines, which will translate into systems that don't need to be replaced as frequently, which has obvious benefits on Mars.^{[11][12][13]}

There are sources on Mars from which pure methane is released. However, its ultimate presence in the atmosphere is only 10 parts per billion as opposed to the 95% of the atmosphere which consists of carbon dioxide. This is due in part to the photochemistry which leads into the combination of formaldehyde and methanol, which leads to the creation of carbon dioxide. As a result, we cannot rely on these sources as the primary means for methane as we will not know how many there are or where they are for some time to come. Carbon dioxide capture and separation remains the best option for methane propellant production as a result, thanks to its prevalence.^[14]

In order to acquire the methane fuel, an atmospheric processing module would be required. The key components of this module is a vacuum pump which takes in the constituents of the atmosphere, the CO₂ freezer module and its corresponding cryocoolers which together, freeze and separate the carbon dioxide from the other trace elements of the atmosphere. In addition, it makes use of a Sabatier module which utilizes separated CO₂ and hydrogen for processing methane and oxygen. The maximum operational temperature for this module will be no more than 600°C, as beyond this level it would be necessary to shut down the system in order to avoid damage.

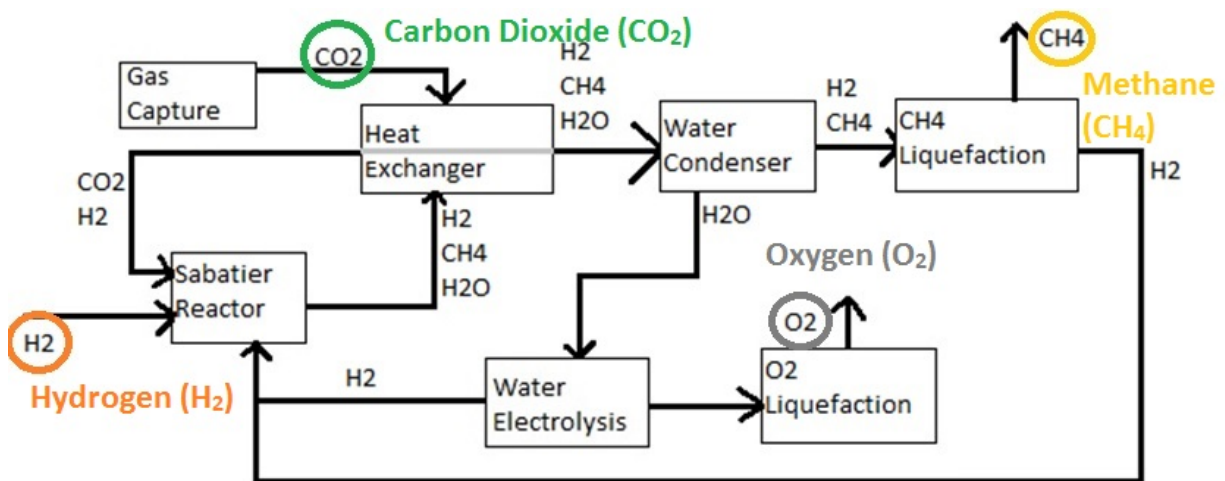


Figure 116. Sabatier Reactor, Electrolysis - Methane & Oxygen Production^[15]

The fundamental process that will be used in order to perform the chemical process that was outlined earlier is pictured above. Here one can see where the carbon dioxide enters the system into the heat exchanger and the hydrogen into the Sabatier reactor. The Sabatier chemical reaction described is as follows: $4\text{H}_2 + \text{CO}_2 \rightarrow \text{CH}_4 + 2\text{H}_2\text{O}$. As it goes through this process including the water condenser, electrolysis, and liquefaction, oxygen (oxidizer) will be produced by the liquefaction module after water electrolysis, and the methane from the methane liquefaction module after the water condenser. Hydrogen can be acquired from electrolysis of water mined on Mars to increase this cycle's efficiency, if a surplus of hydrogen is not brought from Earth with this equation: $2\text{H}_2\text{O} \rightarrow 2\text{H}_2 + \text{O}_2$. This would take further advantage of the virtually unlimited feedstock of carbon dioxide that will be acquired.^[15]

Now that the atmospheric processing module and its integrated CO₂ freezer has been decided upon, this technology will be able to condense, separate, and freeze the carbon dioxide from the atmosphere in order to produce methane with added hydrogen. It is worth emphasizing that in order to bring in this hydrogen into the system, it would be necessary to either bring it from Earth, or utilize some of the hydrogen acquired from water found on Mars. As a result of all of this, the atmospheric processing module will be able to produce 70 kilograms per day of methane and oxygen as fuel, at a 98% purity. This would produce oxygen for the methane propellant's oxidizer as well. In addition, it is a highly efficient system that runs at 15 kW, and its TRL rating is at 4-5, which is a higher TRL rating than the technologies pointed out earlier. Ultimately, this system will allow us to take advantage of one of the, if not the most easily acquirable resource on Mars, and put it to great use.^[15]

6.4. Habitat

6.4.1. Structural Analysis

For the design of the Mars surface habitat structures, certain conditions must be met. First, all structures should be designed to have a margin of safety of zero or greater. For components in which failure would potentially lead to loss of life, a factor of safety of 3 was used. For all other components, a safety factor of 2 was used. The NASA standard for the safety factor for yield of general structure is 1.0. However, a safety factor of 2 was used because a loss of a single habitat hall or hub could lead to a loss of mission. Margin of safety was resolved using the following equation:

$$MOS = \frac{\sigma_{Allowable}}{\sigma_{Applied} * FOS} - 1$$

Second, the habitats should be designed to have a reduced mass since each will be constructed on Earth and sent to Mars. To achieve this, an aluminum-lithium alloy was selected for both habitat hubs and halls. Specifically, Al 2090-T86 was selected for its relatively low density of 2590 kg/m³ and relatively high yield strength of 520MPa^[210].

Halls

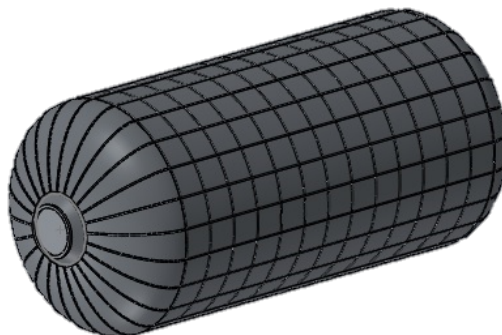


Figure 117. Surface Habitat Hall

Hall Pressure Vessel

The thickness of the hall pressure vessel was first estimated assuming hemispherical end caps and using the equation for hoop stress.

$$\sigma_{Hoop} = \frac{p * R}{t}$$

This led to a thickness just over 1mm. To account for increased stress due to ellipsoidal end caps, the thickness was rounded up to 2mm. With such a thin pressure vessel, the potential of the pressure vessel being punctured by Martian regolith during the construction phase is a concern. To deal with this, the half cylinder EDL fairing will be repurposed and laid over the halls before burying them in regolith.

Stress analysis on the pressure vessel was done using SolidWorks Simulation, which showed a maximum stress of 160MPa. This, along with a safety factor of 3, led to a safety margin of 0.08.

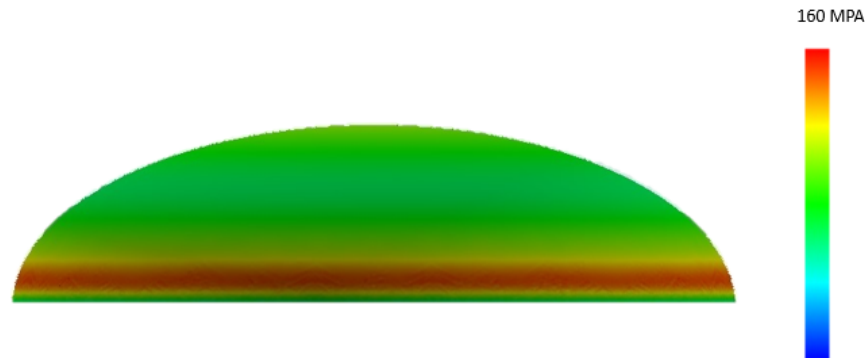


Figure 118. Surface Habitat Hall Endcap Stress Analysis

Hall Longitudinal Struts

For the longitudinal struts, it was determined that the source of their limit load would be longitudinal acceleration during launch. With a maximum acceleration approximated to be 5g's, each hall would experience an axial inertia force of 6g's multiplied by mass. To be conservative, the mass used was the maximum payload mass of the Space Launch System of 70t.

Initial calculations of the required dimensions of the longitudinal struts, which ignored the presence of ribs, proved too conservative and led to masses which exceeded that limitations of the Space Launch System. Through trial and error, cross-section dimensions of 5cm by 2cm with 24 longitudinal struts spaced every 15° radially was determined to be sufficient while keeping overall mass relatively low.

Subjecting an effective cage of longitudinal struts and ribs to the launch load showed a maximum stress of 181MPa. This, along with a safety factor of 2, led to a safety margin of 0.43.

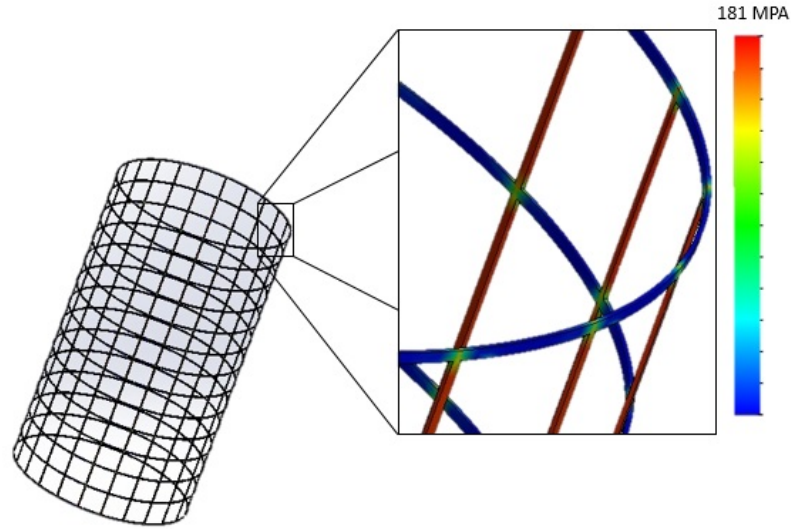


Figure 119. Surface Habitat Hall Longitudinal Acceleration Stress Analysis

Hall Ribs

For ease of manufacturing, the ribs of the hall were designed to have the same cross-sectional dimensions as the longitudinal struts. Each hall will have a rib every meter along the length of its cylindrical portion totaling 14 ribs. The ribs will experience their limit load when the habitats are buried in regolith for radiation purposes on the surface of Mars. With Martian regolith having a density of approximately 1500 kg/m^3 and the halls having a total of 10 m of regolith above them, an equivalent load was applied to the effective cage in SolidWorks. This yielded a maximum stress of 39MPa in the ribs. With a safety factor of 3, this lead to a safety margin of 0.50.

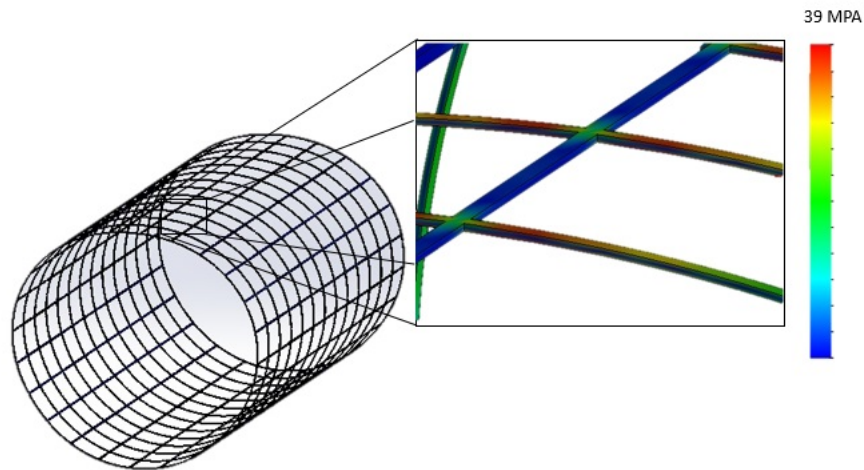


Figure 120. Surface Habitat Hall Regolith Stress Analysis

Hubs



Figure 121. Surface Habitat Hub

Hub Pressure Vessel

The thickness of the hub pressure vessel was, again, initially estimated assuming hemispherical end caps and hoop stress. This led to a thickness of approximately 1.5mm. To account for increased stress due to ellipsoidal end caps and to reduce the risk of regolith puncturing the pressure vessel, the thickness was rounded up to 1cm. Stress analysis with SolidWorks, yielded a maximum stress of 39.3MPa. With a safety factor of 3, this led to a safety margin of 3.41.

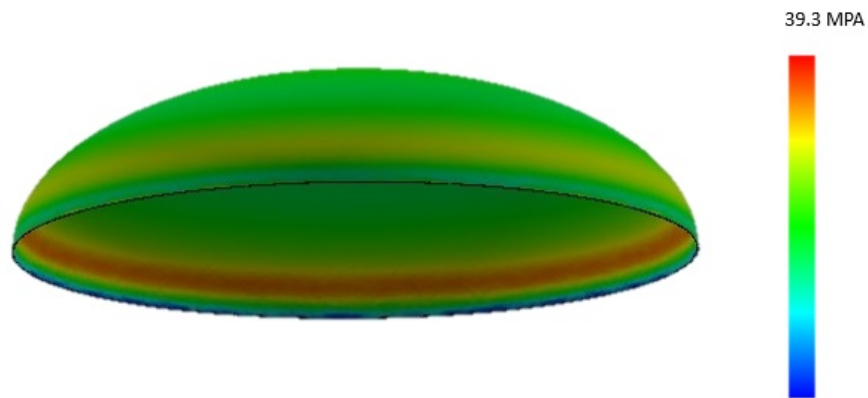


Figure 122. Surface Habitat Hub Endcap Stress Analysis

Hub Longitudinal Struts

Like the hall longitudinal struts, the hub struts will experience their limit load during launch. Cross-sectional dimensions of 5cm by 2cm was again used along with a spacing of 24 struts every 15° radially. The conservative approach of using an inertial load calculated from the maximum payload mass of 70t was also used on the hub. When subjecting the hub's effective cage of longitudinal struts and ribs to this

launch load, the maximum stress was shown to be 238MPa. This, along with a safety factor of 2, lead to a safety margin of 0.09.

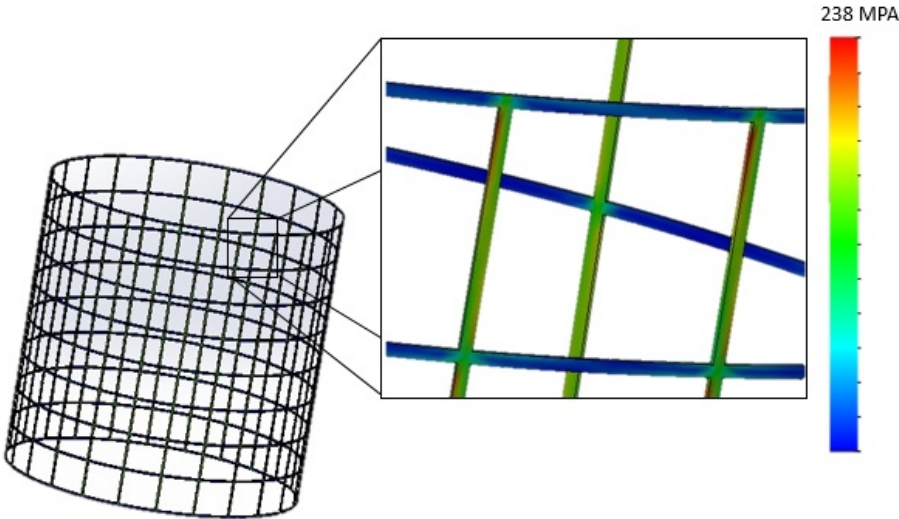


Figure 123. Surface Habitat Hub Longitudinal Acceleration Stress Analysis

Hub Ribs

For the hubs, ribs were also placed every meter along its cylindrical length, which totaled to 9 ribs. Since the hubs will be placed vertically on Mars, their ribs will not be subjected to loads due to regolith. Instead, they will experience their limit load due to lateral acceleration during launch. With an approximated lateral acceleration of 2g’s, a SolidWorks simulation showed the maximum stress to be 62.8MPa. With a safety factor of 2, this lead to a margin of safety of 3.14.

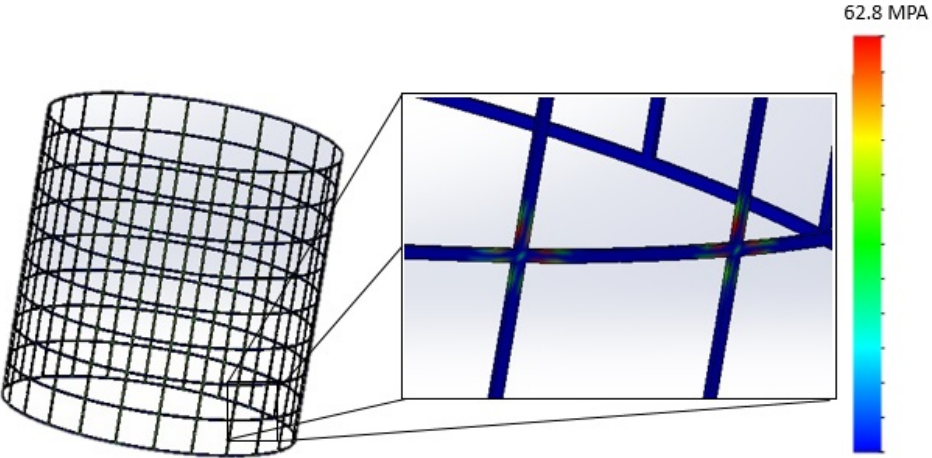


Figure 124. Surface Habitat Hub Lateral Acceleration Stress Analysis

6.4.2. Airlock Design

The first step in designing the airlock was by following these criteria:

- The airlock will have the general geometry of a pressure vessel in order to safely withstand an internal pressure of 72 kPa.
- The material used is Aluminum 2090-T86 (Aluminum Lithium alloy with a high strength-to-mass ratio).
- The airlock design requires having ribs to provide support against internal pressure and regolith pressure.
- The airlock design requires having stringers to provide support against launch loads.
- The airlock diameter needs to be 2.5 m.
- The airlock length needs to be 3.5 m.
- The airlock hatch has a diameter of 1.5 m.
- The airlock needs to have two suit ports.

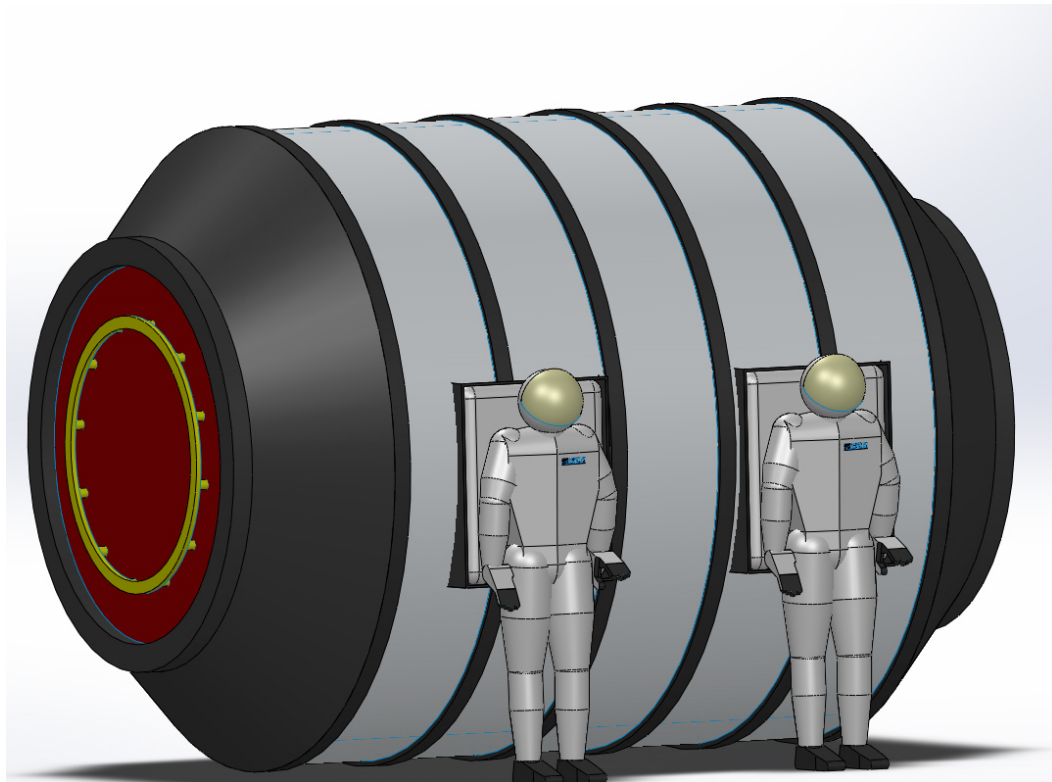


Figure 125. Airlock Exterior View

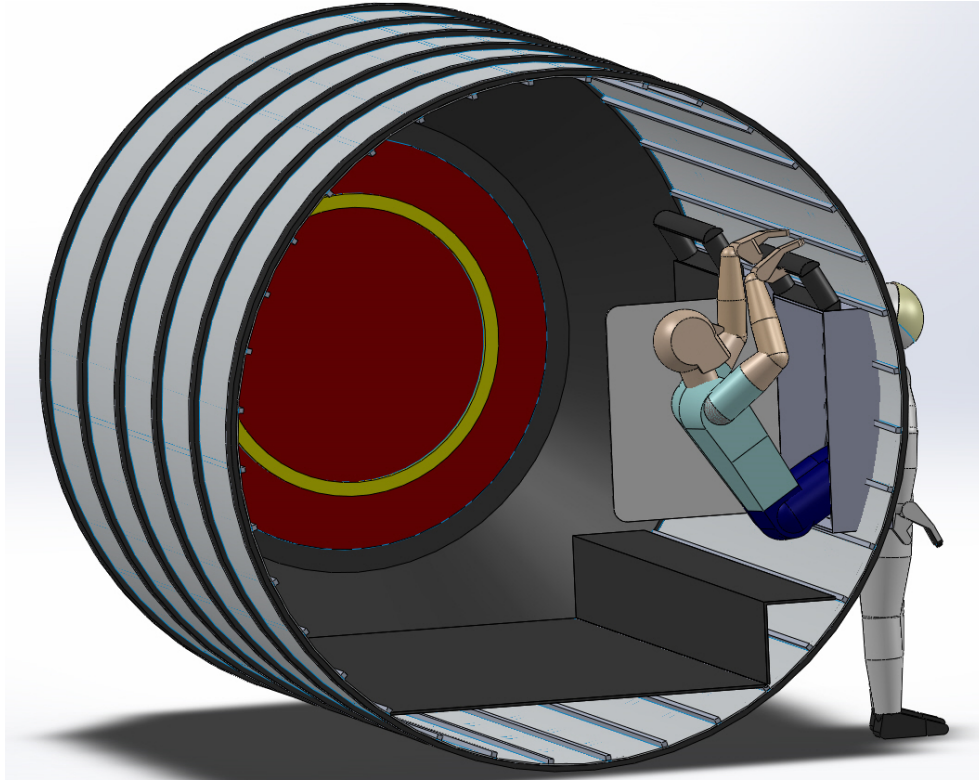


Figure 126. Airlock Interior Cutaway View

Choosing the Shell Thickness

Next, the question that needs to be answered is: What thickness of Aluminum skin is required to keep the airlock from buckling? In order to find a safe shell thickness for the airlock, a series of calculation was made using Roark's Formulas for Stress and Strain.

According to Roark's equation, the critical buckling of a short cylinder with ribs can be found as a function of:

- The separation between the ribs in the cylinder and,
- The thickness of the cylinder's shell.

Furthermore, the Critical bucking expression for the airlock is:

$$\sigma_{\text{buckle}} = 0.807 \left(\mathbf{E} \times \frac{t^2}{Lr} \right) \sqrt[4]{ \left(\frac{1}{1 - \nu^2} \right)^3 \times \frac{t^2}{r^2} }$$

E: Young's Modulus= 76 GPa
 v: Poisson's Ratio= 0.34

t: thickness of Aluminum
 L: separation distance between ribs

Thus, the theoretical analysis to find the critical thickness of the Aluminum shell was calculated based on the separation between the ribs. For the current airlock design, the separation between ribs is 0.5 meters. So, based on this separation distance, the critical buckling thickness of the shell was found by taking into consideration two load sources (each load taken separately):

- Internal pressure, and
- Regolith stress.

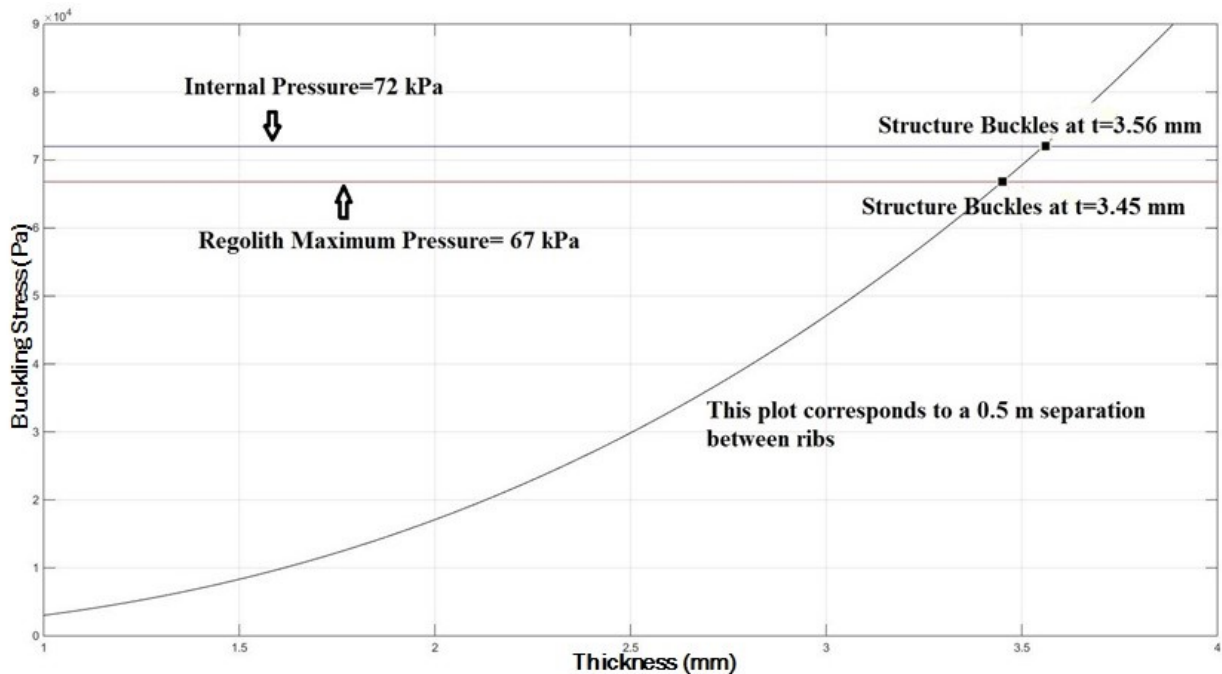


Figure 127. Critical buckling as a function of the shell thickness and a half-meter separation between ribs

The result of the analysis has shown that the major source of buckling would result from the internal pressure. And the buckling thickness of the Aluminum shell was found to be:

$$t_{\text{critical}} = 3.56 \text{ mm}$$

Thus, the shell thickness is required to be larger to t_{critical} to avoid any failure due to buckling. So, the shell thickness was designed to be 6 mm. thick in order to have a large margin of safety.

The internal pressure (72 kPa) will be higher than the regolith stress (67kPa). Thus, the critical buckling thickness due to internal pressure will be higher than the critical buckling thickness due to regolith distribution. Furthermore, the ribs and stringers dimensions were designed based on stress analysis that was studied using SolidWorks:

- Ribs: the airlock has six ribs. Each rib is 7 cm wide and 2 cm thick.
- Stringers: There are twenty five stringers on the inside of the airlock. Each stringer is 2 cm wide and 2 cm thick.

Airlock Stress Analysis

In order to calculate margins of safety of the airlock design with respect to the major load sources, a buckling analysis was studied. The buckling and static simulations/theoretical calculations took into account three major load sources:

- Regolith Stress
- Internal Pressure
- Launch Loads

Moreover, in order to be conservative in doing the analysis, each load source was studied separately. For instance, analyzing the regolith stress and internal pressure together is less conservative since these two loads are opposite in direction. And, it is important to take into consideration the regolith stress before the airlock is pressurized.

Airlock Internal Pressure Analysis

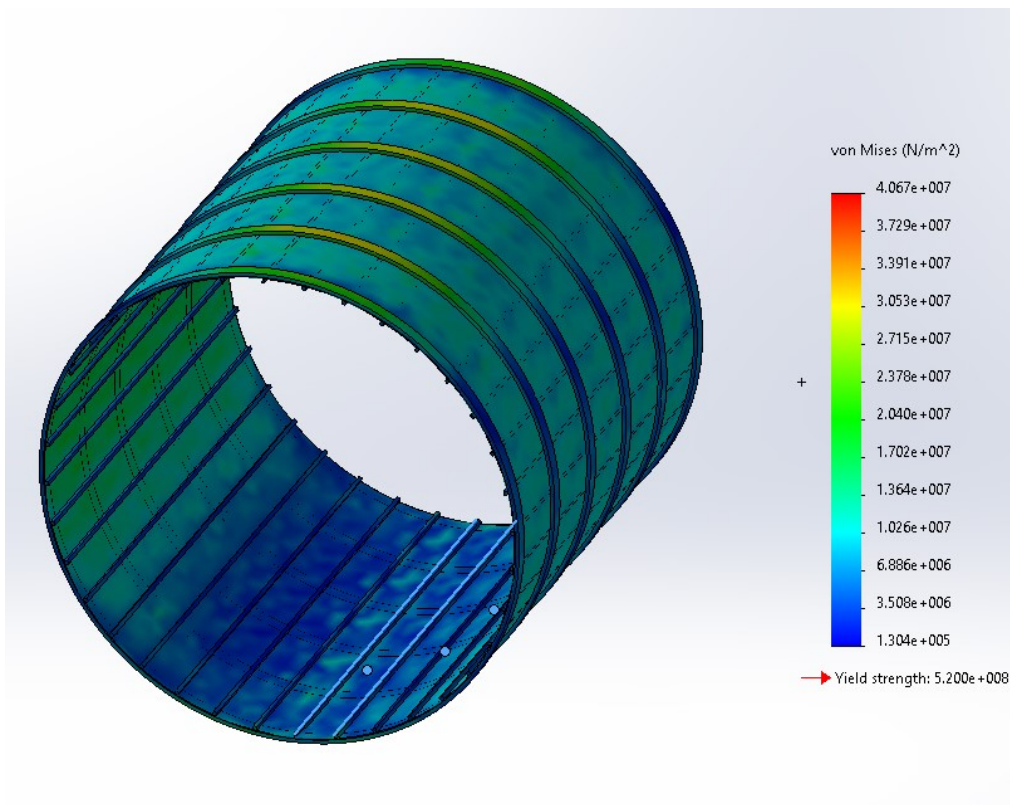


Figure 128. Internal Stress SolidWorks Analysis

As shown in the above figure, the material has yield strength of **5.2 e+08 Pa**. The maximum stress applied is **4.07 e+07 Pa**. By applying a **factor of safety equal to 3**, the **margin of safety is 3.3**.

Airlock Regolith Stress Analysis

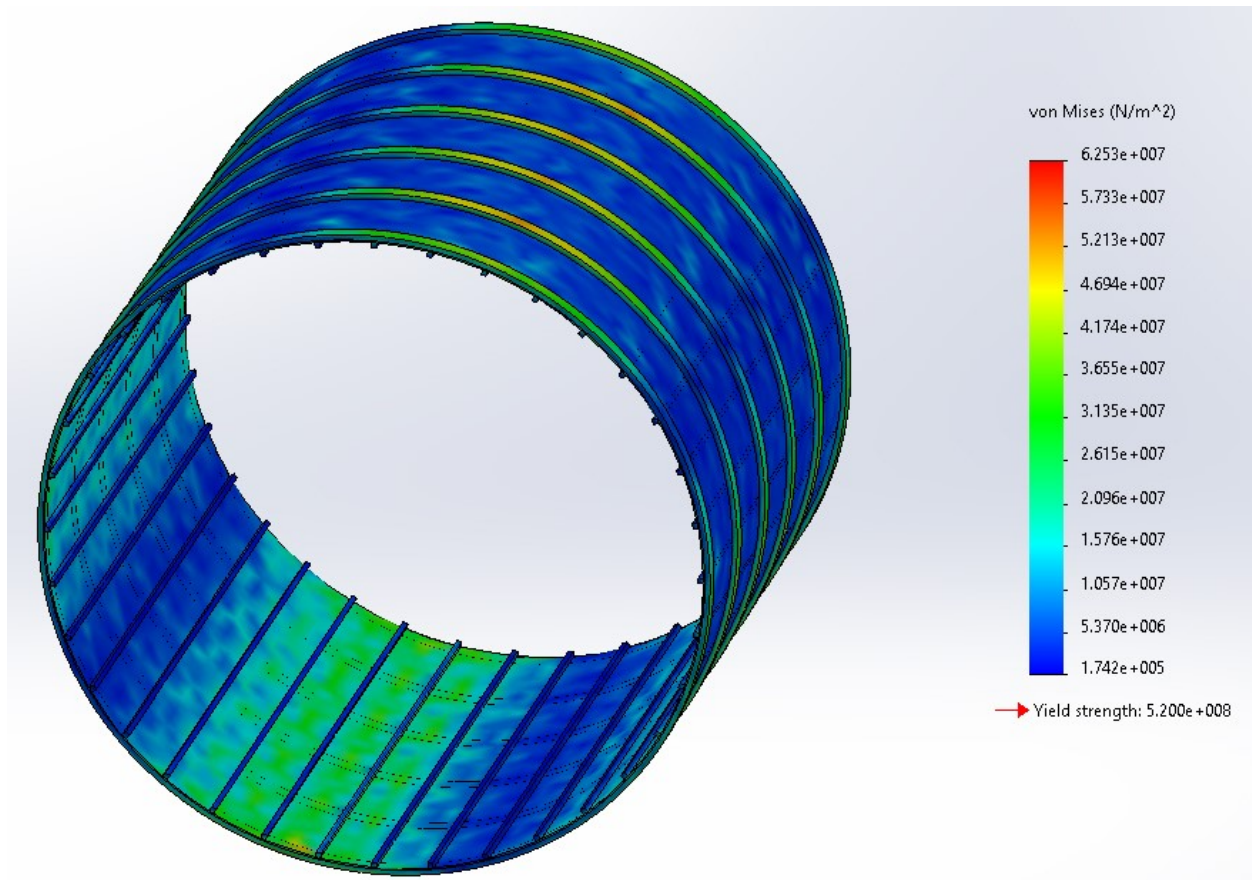


Figure 129. Regolith Stress SolidWorks Analysis

As shown in the above figure, the material has yield strength of **5.2 e+08 Pa**. The maximum stress applied is **6.25 e+07 Pa**. By applying a **factor of safety equal to 3**, the **margin of safety is 1.77**.

Airlock Launch Loads Analysis

In order to do a conservative analysis, the launch loads looked at the stringers and airlock shell only. With these conservative constrains, the maximum stress applied is **6.3 e+07 Pa**. By applying a **factor of safety equal to 2**, the **margin of safety is 3.1**.

Suitport Design

Furthermore, for a planetary surface, like Mars, an airlock could potentially be a major source of contamination from the abrasive Martian dust particles, if astronauts were to enter the airlock with their spacesuits on. Thus, in order to address this issue, the suitport was designed as a two-part system. The

first part of the suitport is attached to the spacesuit, and the other part of the suitport is attached to the airlock. Thus the designed suitport will be on the outside of the airlock, as shown in a previous figure. In order for an astronaut to enter his/her spacesuit, he/she will first open the hatch that is located on the interior of the airlock, then he/she will open the second hatch located on the back of the spacesuit. Then, the astronaut will climb into the spacesuit. Once he/she is inside the spacesuit, astronaut will operate few mechanisms to close and seal both hatches.^[51]

This way, astronauts will be capable to don/doff their spacesuits and do their extravehicular activities without any assistance from other crewmembers. This will be essential for any emergency situation where all astronauts in a certain habitat are required to evacuate at the same time.

Regolith Stress Analysis for Habitats and Airlocks

Mars' surface receives more radiation than the Earth's, and these radiations pose a major risk on Mars' settlers. While the carbon dioxide content of the Martian atmosphere provides an effective shielding against short wavelength ultraviolet radiation, it unfortunately doesn't protect against long wavelength ultraviolet radiation and galactic cosmic radiation (GCR), primarily in the form of ionizing radiation such as alpha particles, beta particles, gamma rays, and x-rays.^[50] Thus, permanent Martian habitats would certainly need an effective radiation protection equivalent to that provided by the Earth's atmosphere.

Furthermore, Mars' habitats (hubs and halls) and airlocks would need to be covered by a Martian regolith to provide a reliable shielding against harmful galactic cosmic rays and ultraviolet rays. An analysis carried out by the Crew Systems team has shown that a 5-meter layer of regolith is required.

However, due to the relative positions of the airlock, hubs and halls:

- The airlock will be subjected to 12 meters of regolith.
- The hall will be subjected to 10 meters of regolith.
- The hub will be subjected to 5 meters of regolith.

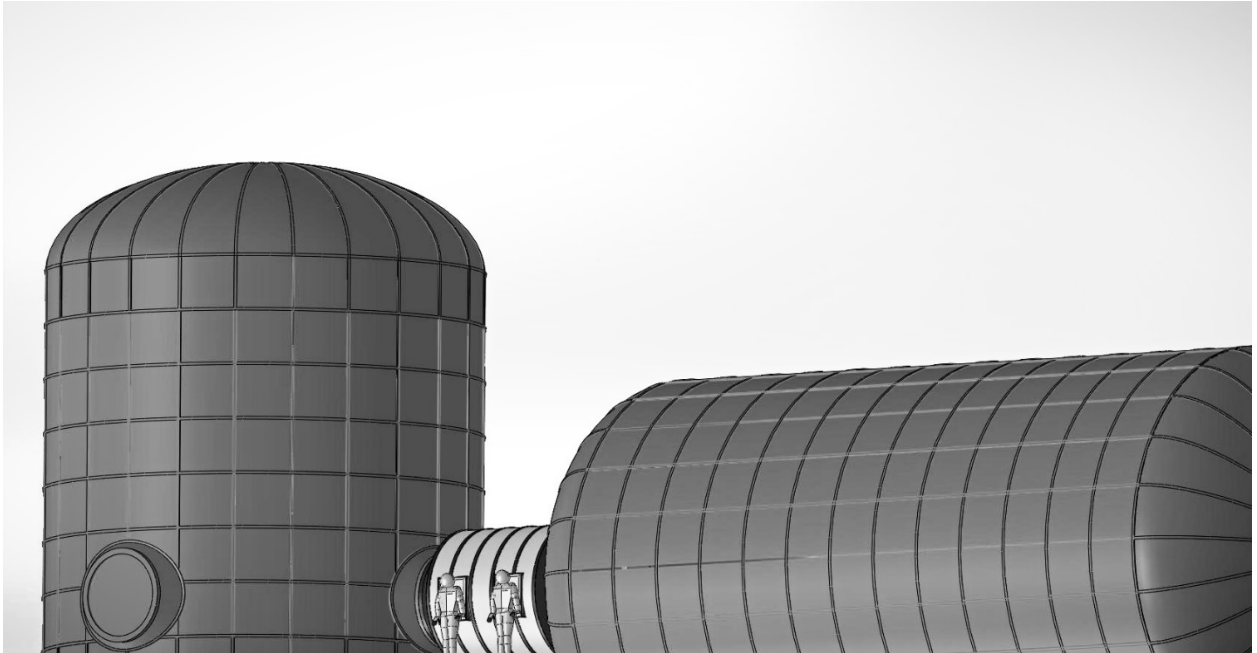


Figure 130. Relative position of the airlock with respect to the hub and hall. This will result in varying depth distribution of regolith among the hub, hall, and airlock

Additionally, the Martian regolith applied to the habitats and airlocks has a density of 1.5 g/cm^3 . The major stress distribution of the regolith will be subjected to the airlock (12 m.) and the hall (10 m.).

Regolith Stress Distribution on Airlock

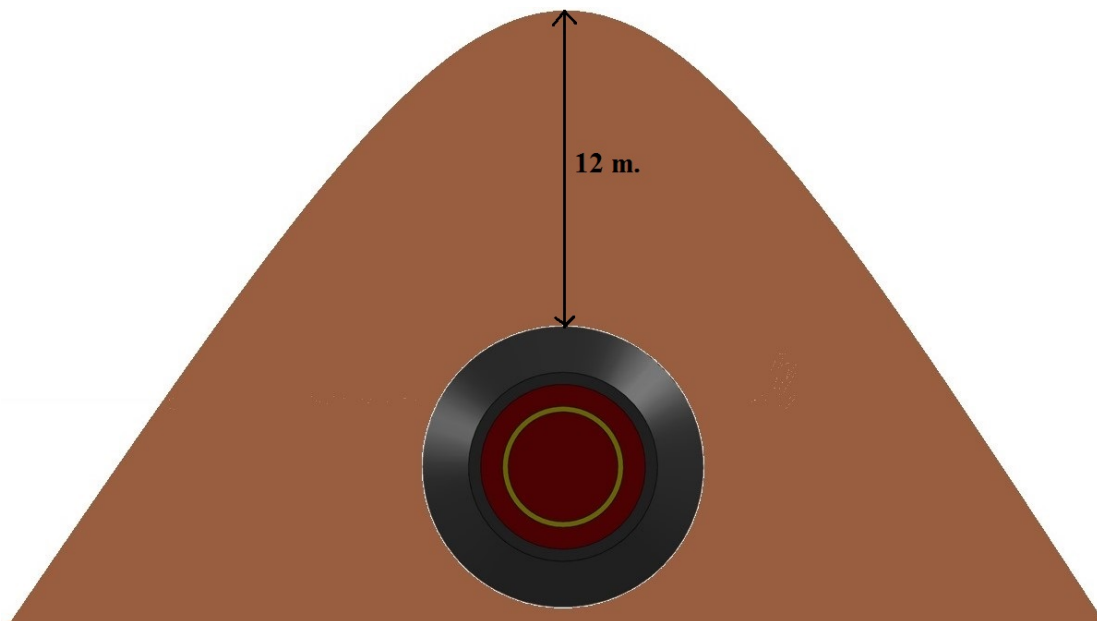


Figure 131. Actual Regolith Distribution on the Airlock

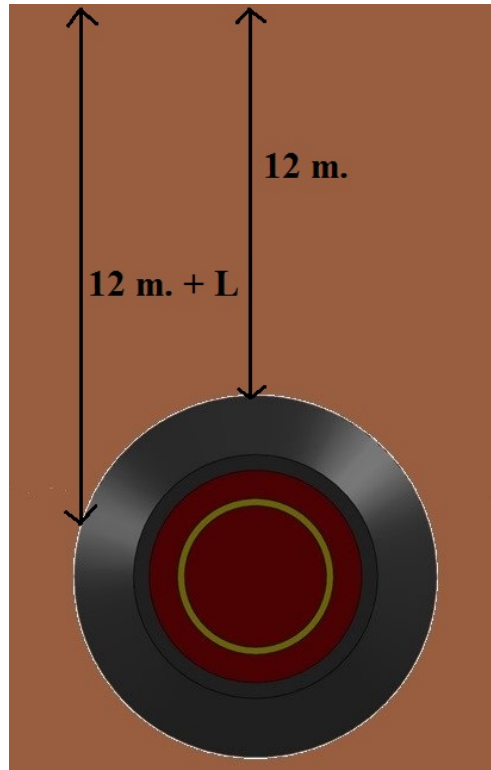


Figure 132. Conservative Analysis for Regolith Distribution

Moreover, the maximum regolith depth on top of the airlock is equal to **12 meters**. Also, the stress distribution of regolith on the airlock will vary from one point to another since the regolith distribution will have a slope as shown. However, in order to be conservative in studying the regolith stress analysis, it has been assumed that the airlock will be under a constant level of regolith distribution. This conservative approach was taken to approximate the regolith stress distribution on the airlock.

Moreover, based on the 12-meter depth of regolith that will be applied to the airlock, a compressive stress analysis was studied in order to find the compressive load on the airlock as a function of the angle θ .

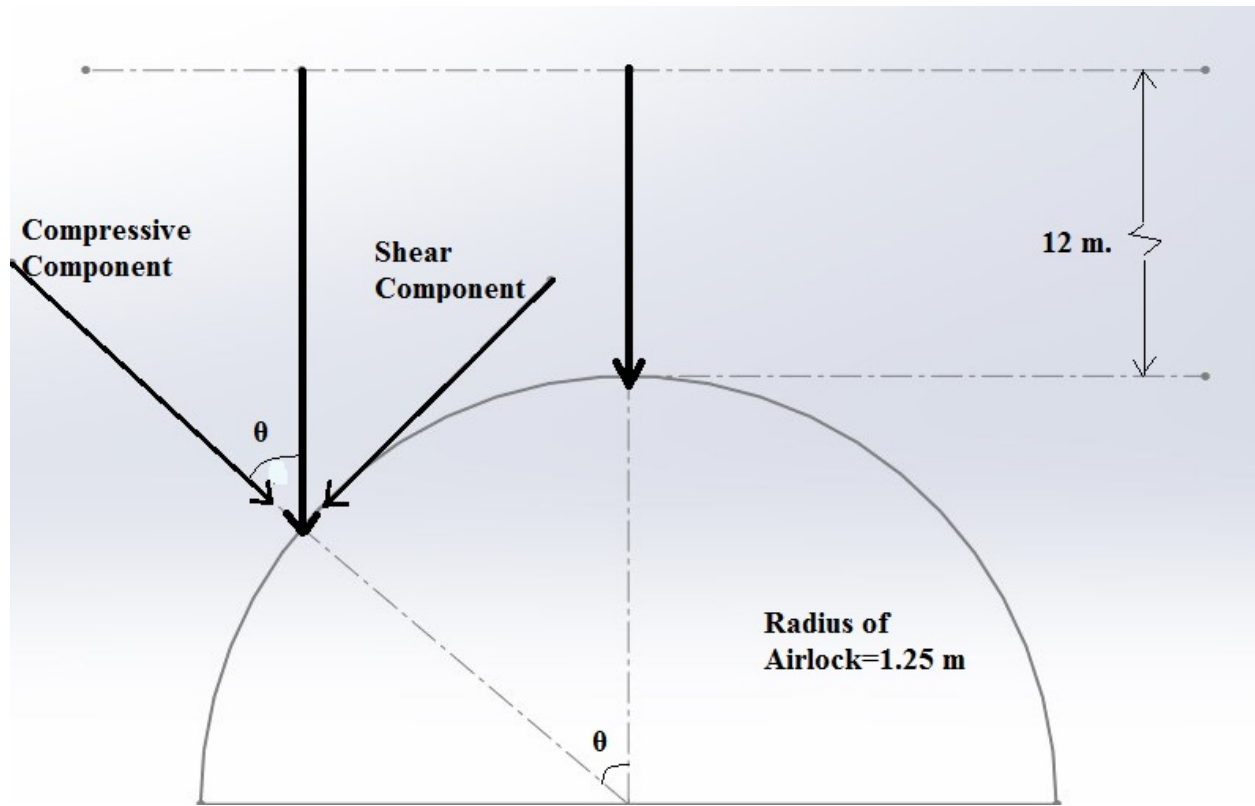


Figure 133. Compressive stress as a function of θ

Also, the compressive stress expression that was derived as a function of the angle θ is:

$$\sigma = \rho * g * [12 + 1.25 - (1.25 * \sin(90 - \theta))] * \cos(\theta)$$

Thus, based on the analysis, the regolith compressive loads plot on the airlock is:

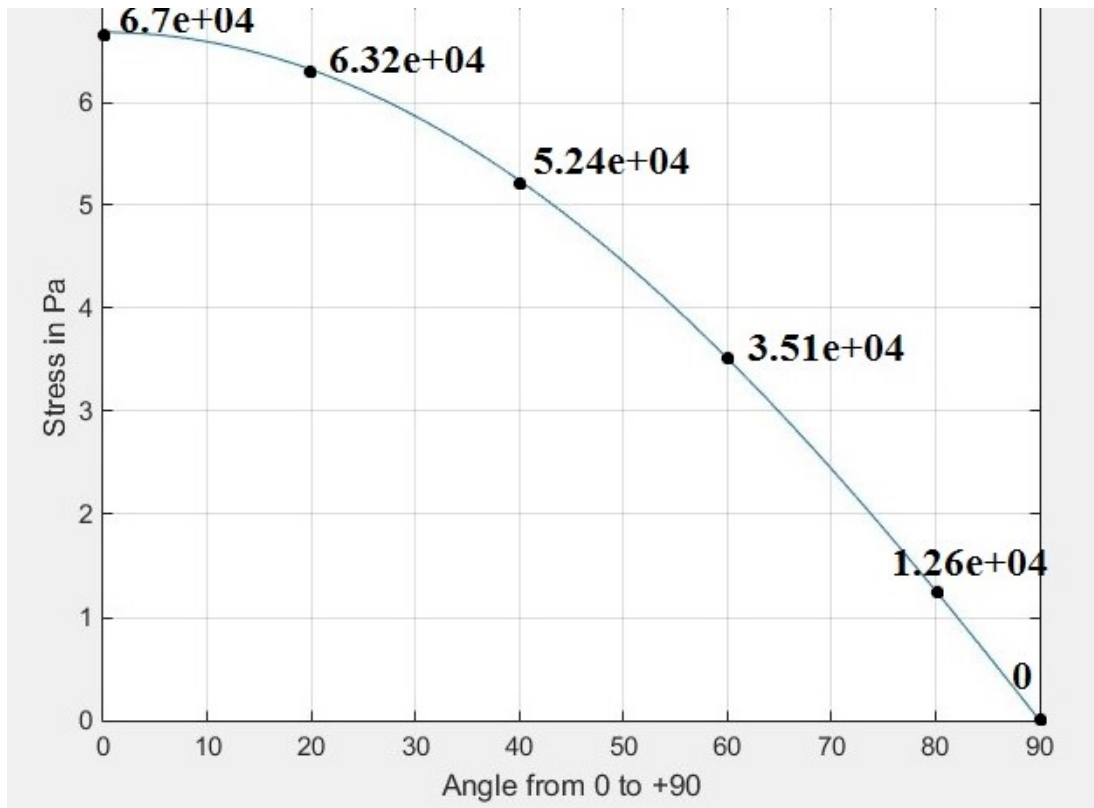


Figure 134. Compressive Stress on Airlock as a Function of θ

Thus, the regolith compressive stress analysis shows that the maximum compressive stress applied to the airlock will be at angle $\theta = 0^\circ$. And, the maximum compressive stress from the regolith is: $\sigma_{\max} = 67 \text{ kPa}$

Regolith Stress Distribution on Hall

A similar approach was taken to study the regolith stress distribution on the hall. However, it is important to note that the stress distribution on the hall will vary because:

- The hall has a different radius ($r=3.5 \text{ m.}$)
- The depth of regolith is also different ($\text{depth}=10 \text{ m.}$)

The following figure shows the regolith compressive stress on the hall:

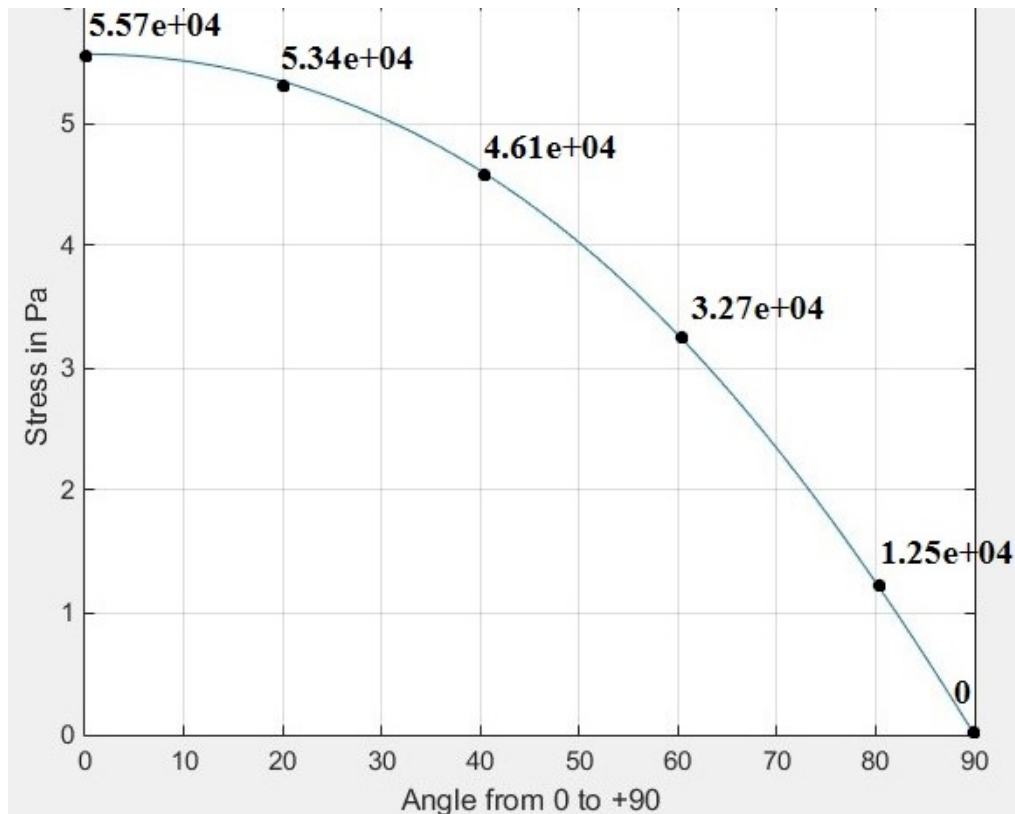


Figure 135. Compressive Stress on Hall as a Function of θ

Thus, the regolith compressive stress analysis shows that the maximum compressive stress applied to the hall will be at angle $\theta = 0^\circ$. And, the maximum compressive stress from the regolith is: $\sigma_{\max} = 56 \text{ kPa}$

An Alternative to Reduce Regolith Pressure on Habitats and Airlocks

As mentioned earlier, airlocks will be subjected to 12 meters of regolith depth, and halls will be subjected to 10 meters of regolith depth. This regolith is essential to eliminate all the radiations for future settlers on Mars.

However, a potential alternative can be taken to reduce the required depth of regolith. This alternative can be achieved by having a shielding material on the inside of the airlock/habitat. This way, this shielding material on the inside, along with less required regolith on the outside, will give the required radiation protection. So, a habitat/airlock design can be a combination of a rigid body on the outside and an inflatable body on the inside. That way, the shielding material can be inflated inside of the rigid habitat/airlock. One relatively new material that could be potentially used is Demron.

Demron is a radiation blocking fabric. It is described as a non-toxic polymer, and it has a radiation protection similar to lead shielding, while being lightweight and flexible. This material can be treated as a normal fabric for cleaning, storage, and disposal. Additionally, this material significantly reduces high energy alpha and beta radiation, as well as low energy gamma radiation. ^[52] The shielding power of Demron becomes greater by laminating several sheets of Demron together.

6.4.3. Crew Module Layouts

In the overall habitat configuration there are four specific modules dedicated specifically to the crew; two halls and two hubs. The halls contain the living quarters, bathrooms, medical wing, exercise room, laundry facilities, maintenance bay and storage. The hubs house the multipurpose room, kitchen, control room, food storage and free space.

The upper level of Hall's 1 and 2 are identical and will be devoted to crew living quarters and lavatory space. There will be six bedrooms on each side of a hall's walkway and two bathrooms at the end of the hall. Each bedroom will accommodate one astronaut and will serve as their personal work and relaxation space. The bedrooms are 2 meters by 3.25 meters and contain a small chair as well as a bed/desk unit, a pole for hanging clothing and a set of cubbies for storage. The bed/desk unit is essentially a folding murphy bed with the desk surface mounted on the bottom which is exposed when the bed is folded against the wall. If cohabitation among astronauts is desired, the wall between any two bedrooms may be removed, dissembled, and stored. As each bedroom is the mirror image of its neighbor, this will allow two beds to fold into one large bed. This is made clear in reviewing Figure 136.

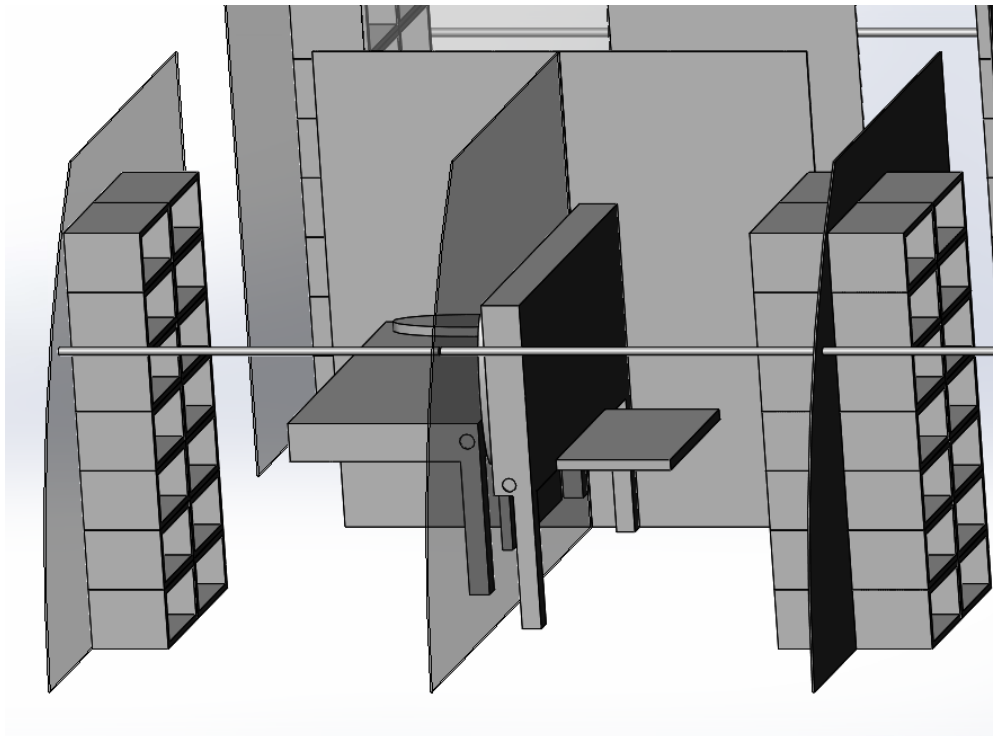


Figure 136. Crew living quarters.

The hall floor plans is presented in Figure 137. The bathrooms at the end of the Hall's each contain one toilet and two sinks. This space will be used primarily for crew hygiene activities in preparation for sleep. The toilet offers the convenience of proximity to bedrooms for late night lavatory trips.

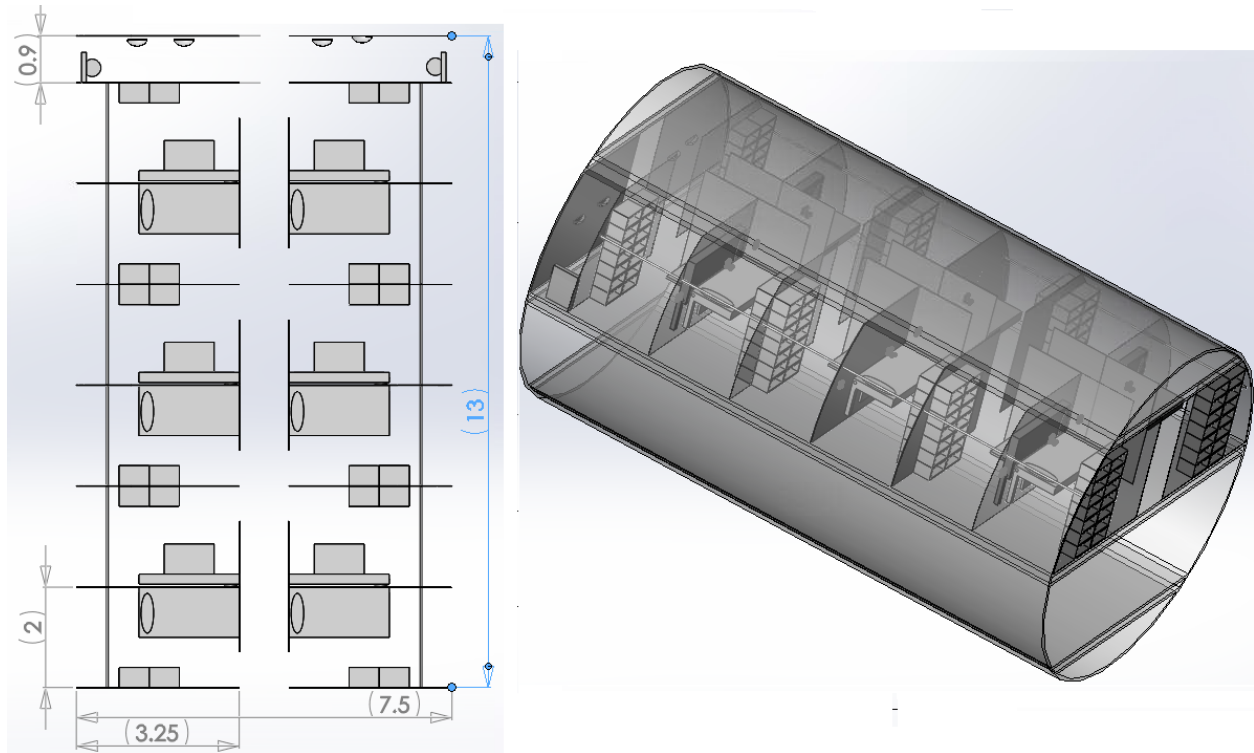


Figure 137. Hall 1 and Hall 2 top level floor plans.

The lower level of Hall 1 was allocated for the medical wing, exercise room, laundry facility and another bathroom.

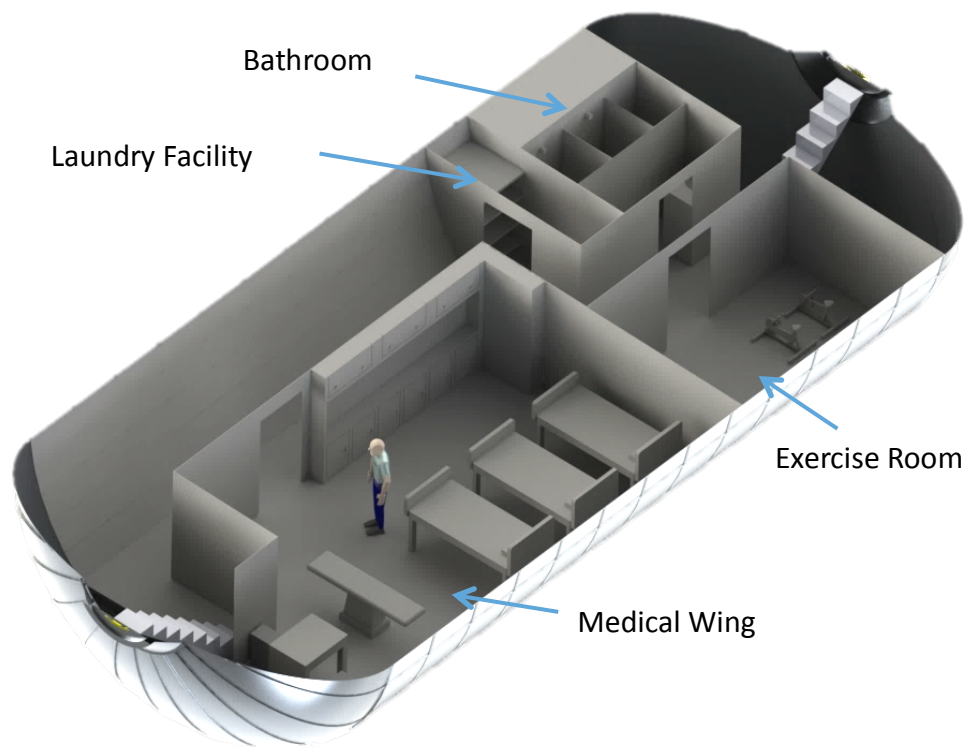


Figure 138. Crew Hall 1 - Ground Floor

The medical wing will contain two full hospital beds, a cot, a desk and set of chairs, surgery table, foldable examination table, and storage for medical equipment. It was designed for versatility in order to make the best use of a limited amount of space. There can be two main configurations; standard and emergency (see Figure 138). The standard configuration will include 2 beds, the surgery table moved against a wall, and the examination table, unfolded. There will be curtains surrounding each bed for privacy as well as around the examination table to create a small room. In the emergency configuration, the examination table can be folded flush against the wall, the beds moved closer together to accommodate a cot in addition to the 2 medical beds, and the surgery table moved away from the wall. Curtains will surround the surgery table as well as one curtain around all 3 beds. There will be rails on the ceiling the curtains attach to, which allow for varying configurations.

The laundry room will contain two washer-dryer combination machines. Each astronaut will be bringing enough clothes with them to last the entire mission duration of 13 years; therefore, being able to wash and reuse them is important in maintaining sustainability.

Exercise is extremely important to maintaining muscle mass and bone density in a $\frac{1}{6}$ Earth-gravity environment. The exercise room will contain two foldable treadmills, two stationary bicycles, a pull-up bar and weight rack. The treadmills can be folded to almost half of their original floor area in order to provide more space for body exercises.

The bathroom will contain two individual shower stalls, one toilet, a vanity and sink, wall storage for hygiene and cleaning items, and a trunk for additional storage and seating.

The lower level of Hall 2 was designed primarily for storage and as a maintenance bay, but will also contain a bathroom that is identical to the one previously described for Hall 1.

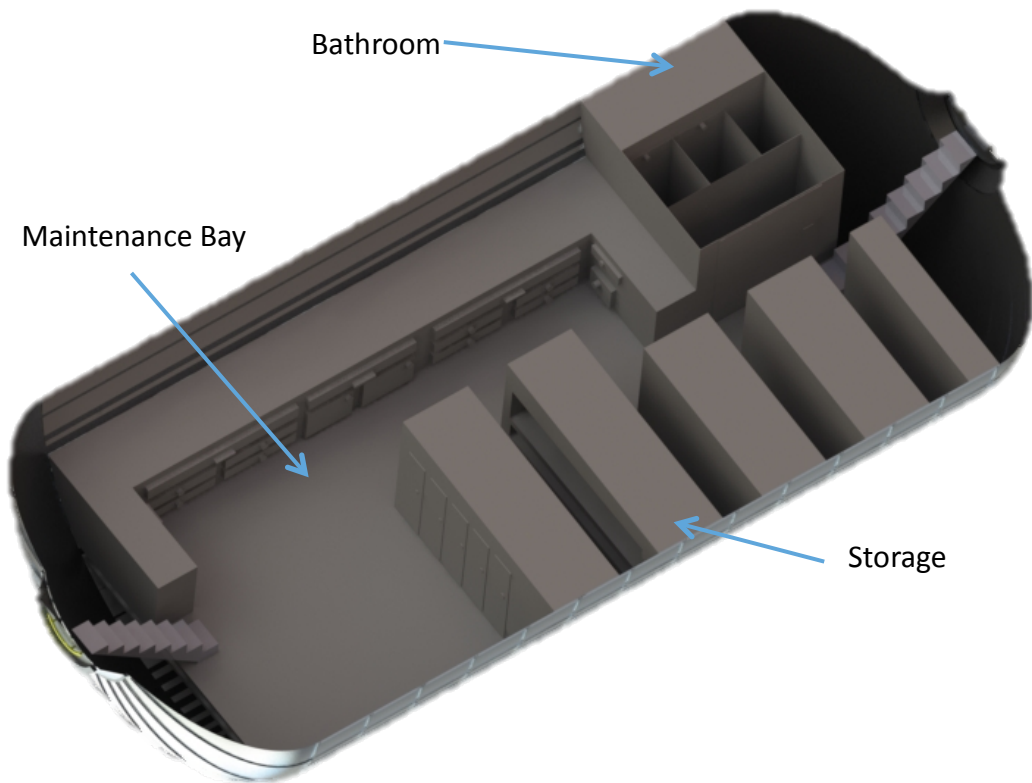


Figure 139. Crew Hall 2 - Ground Floor

The Hub is a three floor vertical structure with four airlocks on the bottom floor. There are two types of Hubs with different purposes for the first and second floors, however, the third floor in each Hub are the same. This third floor is empty and made available to the crew to repurpose as they see fit allowing for increased crew autonomy. Each floor is 7.5m in diameter and 2.9m tall. Each floor is connected by a spiral stair case 1.7m in diameter.

The first floor of Hub 1 is a multipurpose room and kitchen combination. There is a 10 burner stove / dual oven, an industrial sink, and storage cabinets lining the exterior. In the center of the room there are sets of convertible furniture that can be set up as either a couch or table. There is enough seating to allow for all 24 crew members to gather in the multipurpose room at once.

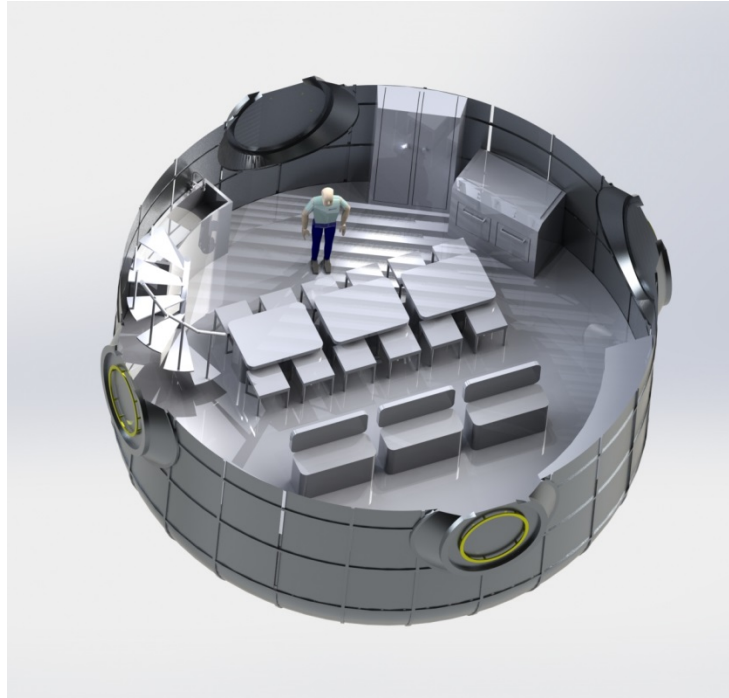


Figure 140. Hub 1 - First Floor

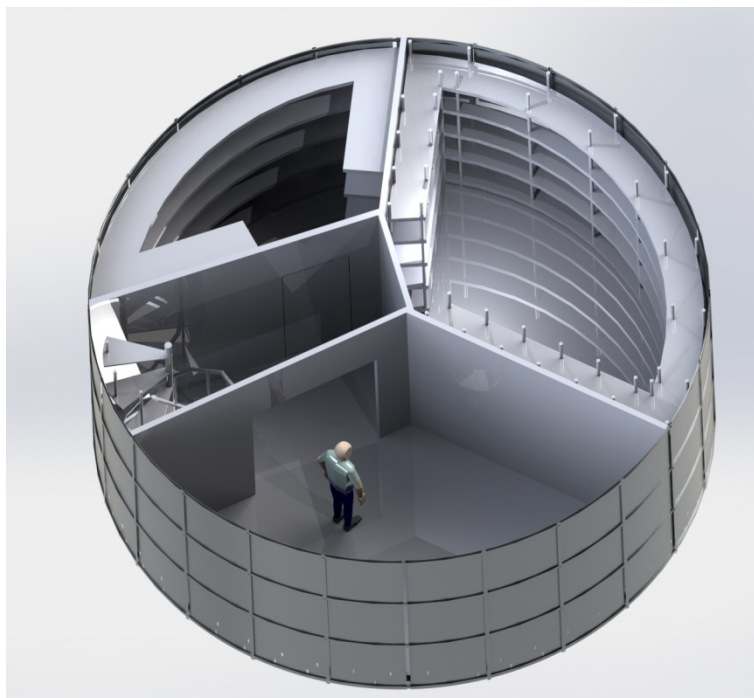


Figure 141. Hub 1 - Second Floor

The first floor of Hub 2 is a control room. This control room is where the crew can view and monitor all processes in the base. The second floor of Hub 2 is a laboratory where the crew can conduct experiments.



Figure 142. Hub 2 Bisectional Cut

Crew Module Lighting

The crew modules of the habitat will be kept at 300 lux, the same light intensity of libraries and classrooms. The reason for this is that 300 lux provides enough light for tasks to be performed efficiently while not providing a detrimental amount of light as higher intensities lead to more difficulty in performing visual tasks as well as more difficulty in judging color⁸⁸. LEDs will be used to provide the lighting for the crew modules just as they provide the lighting for the greenhouses. With current LED technology and the ability to produce 75 lumens / watt, 530 W are required to power a crew hub and 666 W are required to power a crew hall, leading to a total power requirement of 2.39 kW. Using the United States Energy Information Administration's projection of 200 lumens / watt when crew arrives, the power required is 199 W for a crew hub and 250 W for a crew hall, leading to a total power requirement of 898 W.

The composition of the LEDs will be chosen to replicate the visible spectrum of the sun similarly to how LED solar simulators provide a replica of the sun's spectrum in laboratory conditions. The reason for this is that there are psychological benefits to working in sunlight and there is no additional power cost since the same amount of LEDs are required. Exposure to sunlight results in less stress while not being exposed to sunlight can lead to depression and reduced productivity, a fact which has been proven in tests of factory workers who worked in windowless conditions⁸⁹.

6.4.4. Food

6.4.4.1. Climate Control

The Greenhouses will be set between 55 and 80 degrees Fahrenheit in order to accommodate the maximum amount of plants and fish. The humidity will be set between 50-85% in order to accommodate the maximum amount of plants. These levels will also allow us to acquire the correct amount of water needed from the dehumidifiers daily.

6.4.4.2. Nutrition

Requirements

The crew's diet will be based on the USDA's requirements for a 75th percentile active male.^[102] This includes all necessary vitamins and minerals as well as the macronutrients. The nutritional facts for each of the crops and fish were acquired by the USDA food database that listed each nutrient per 100 grams of the given food.^[104] In order to design the most effective diet, an optimization was used that minimized crop and fish tank area while maintaining all the necessary nutrients. This resulted in approximately 34m² of area per crew member of crop space.

Nutrient	kCalories	Protein (g)	Fat (g)	Carbohydrates (g)
Requirement	3200	65	71	360
Nutrient	Magnesium (mg)	Phosphorus (mg)	Potassium (mg)	Sodium (mg)
Requirement	420	700	4700	1500
Nutrient	Selenium (mcg)	Vitamin C (mg)	Thiamin (mg)	Riboflavin (mg)
Requirement	55	90	1.2	1.3
Nutrient	Folate (mcg)	Choline (mg)	Vitamin B12 (mcg)	Vitamin A (mcg)
Requirement	400	550	2.4	900
Nutrient	Fiber (g)	Calcium (mg)	Iron (mg)	Vitamin E (mg)
Requirement	38	1000	8	15
Nutrient	Zinc (mg)	Copper (mg)	Manganese (mg)	Vitamin D (mcg)
Requirement	11	0.9	2.3	15
Nutrient	Niacin (mg)	Pantothenic Acid (mg)	Vitamin B6 (mg)	Vitamin K (mcg)
Requirement	16	5	1.3	120

Table 44. Dietary Requirements

Rotatable Diet

In order to promote a more diverse and amiable food selection plan for the crew, the diet will rotate between 5 various regiments, each lasting between 3 and 4 months (depending on the grow time for the

specific vegetables in each diet). Each diet will still contain all necessary nutrients and they all use the same amount of area within 1m².

Diet 1	Diet 2	Diet 3	Diet 4	Diet 5
Sweet Potato	Sweet Potato	Peanut	Sweet Potato	Peanut
Peanut	Peanut	Wheat	Peanut	Wheat
Wheat	Wheat	Rice	Wheat	Rice
Rice	Rice	Cabbage	Rice	Cabbage
Cabbage	Potato	Carrot	Cabbage	Carrot
Green Onion	Cabbage	Green Onion	Green Onion	Green Onion
Lettuce	Green Onion	Lettuce	Lettuce	Lettuce
Onion	Lettuce	Onion	Onion	Onion
Snap Bean	Onion	Snap Bean	Radish	Snap Bean
Strawberry	Snap Bean	Strawberry	Snap Bean	Strawberry
Kale	Strawberry	Kale	Kale	Tomato
Broccoli	Kale	Broccoli	Broccoli	Kale
Peppers	Broccoli	Peppers	Peppers	Broccoli
Tilapia	Tilapia	Tilapia	Tilapia	Tilapia
Spirulina	Spirulina	Spirulina	Spirulina	Spirulina

Table 45. Rotational Diets

6.4.4.3. Crops

Primary Diet

Approximately 53 m²/CM of crop space is available. The majority of this space (34m²/CM) will be used for the crew's main diet.

Backup Diet

10m² per person will always be dedicated to backup crops. The three most energy dense species will be grown; peanuts, wheat, and rice. They will be stored once harvested, and will be added into the anaerobic digester once they expire.

Personal Plots

5m² per person will be used for personal plots. This allows the crew to grow whatever they like in order to give them more variety in their meals and to give them more autonomy. Gardening is also known to be

associated with reduced stress.^[107] Anything from more wheat to herbs and spices can be grown. Each astronaut can select which seeds they would like to bring in order for them to grow that certain plant.

Medicinal Plants

Due to the short shelf lives of medicine, 4m² per person will be used for medicinal crops. For the astronauts, they will be in a fairly closed loop system with few outside difficulties, meaning that other than the bacteria they bring with them, there should be a very low risk for new ailments. The crew should be vaccinated of most diseases that would be of worry beforehand and extensively screened for any underlying diseases so they do not bring anything that could affect the other crew members. Using several types of plants, certain plant-derived pharmaceutical proteins (PDPs) and therapeutics can be developed.^[103] The proteins chosen to be grown will be based on each astronaut's health factors, so as to combat the diseases that the crew member is most susceptible towards. Bacteria will also be a threat to the crew, so certain fungi will be brought with the crew and reproduced to make things such as penicillin. Plants that offer the active ingredients in anti-inflammatories/pain relievers such as aspirin will be grown in order to synthesize these medicines. Anesthetics can also be synthesized from genetically modified plants in order to help if any crew member must go through any surgery.^[106]

The final row uses the percentage of area that the non-primary diet does not take up and approximates the rest of the numbers from that.

Diet	Area (m ² /CM-day)	Yield Oxygen (g/CM-day)	CO ₂ Uptake (g/CM-day)	Water Uptake (kg/CM-day)	Waste Mass (g/CM-m ²)
1	33.9	1456.1	2002.2	229.7	6485.1
2	34.2	1458.5	2005.8	228.5	6443.2
3	33.5	1423.8	1957.7	228.1	6332.9
4	33.9	1448.2	1991.3	229.7	6442.3
5	33.4	1413.2	1943.1	226.5	6287.9
Non-main diet crop yield	19.0	512.4	704.6	82.1	2280.0

Table 46. Extra Dietary Information

6.4.4.4. Fish

Selection

Using several species known for their aquaponics capabilities, a trade study was performed that reviewed all of the different fish to see which was the best for the mission. For each category, each fish was ranked from 1 to 9, so the lowest total number was the best fish. Access to recommended diet is the easability for the crew to provide the necessary diet to the fish. Ease of breeding signifies how much extra effort must go into making the fish breed. The nutrition and ease of preparation is the nutritious value of the fish and how easy it is to prepare, such as descaling or deskinning time. Durability is how can the fish withstand bad water conditions.

	Access to Recommended Diet	Ease of Breeding	Nutrition/ Ease of Preparation	Durability	Total
--	----------------------------	------------------	--------------------------------	------------	-------

Tilapia	4 ^[240]	3 ^[240]	4 ^[104]	1 ^[240]	12
Largemouth Bass	9 ^[238]	7 ^[238]	3 ^[104]	9 ^[238]	28
Koi	1 ^[239]	1 ^[239]	9 ^[104]	2 ^[239]	13
Goldfish	2 ^[239]	2 ^[239]	8 ^[104]	3 ^[239]	15
Catfish	5 ^[233]	8 ^[233]	7 ^[104]	8 ^[233]	28
Carp	6 ^[232]	6 ^[234]	2 ^[104]	4 ^[232]	18
Jade Perch	3 ^[235]	4 ^[235]	5 ^[104]	7 ^[235]	19
Murray cod	7 ^[237]	5 ^[237]	6 ^[104]	5 ^[237]	23
Trout	8 ^[236]	9 ^[236]	1 ^[104]	6 ^[236]	24

Table 47. Fish Selection Process

The selection of tilapia was chosen for several reasons. The first requirement was that the fish had to be able to do well in aquaponics, which tilapia are well known for. They also needed to be robust, in the sense that they could handle irregular water conditions and able to eat a large variety of plant waste. Their fast growth rates was also a factor. They also have the ability to breed in captivity as opposed to most other fish, and they are appetizing, being a common food dish.

Growth

With high oxygenation, about 56000g of tilapia can be held in every foot cubed of water.^[101] This equates to roughly 0.005m² for every 100g of tilapia if a tank height of 1/3 a meter is used. For optimal growth, the amount of food to provide the fish is 1.8% of their total body mass per day, every day. In order to reach a size of 500g, approximately 220 days will be required for the fish to grow. Since the complete fish will not be consumed the fish will grow for another 6 days in order to reach 550g, leaving 10% or 50g as waste. So with a grow time of 226 days, a max size of 550g and a sizing of 0.005 m²/100g, there will be about 7m² of tank area per crew member, or 2.33m³ per crew member.

Breeding

Two tanks will be set aside for breeding. The first tank will be approximately 1 meter long, 4/3 meters wide, and 1/3meters high. This is the tank in which the male and female will both go. Once the female has laid the eggs, she will place them into her mouth. At this point the female will be moved to a tank with the same dimensions except half a meter long, and the male can be returned to the other tanks. The total volume needed will be 2/3m³. It will take no longer than 1 week for the eggs to hatch and at this point the female can be returned to the other tanks.¹⁰¹ The babies will remain here until they grow to approximately 1 gram and then added into the other tank system.

6.4.4.5. Spirulina

Background

Spirulina is a type of algae that when dried, has high nutritional value. It also grows particularly fast, at 30% its size per day.^[100]

Growth

Spirulina must be dried before it will be consumed. All the mass numbers from here on will be for dried spirulina. The tank sizes can be the same size as the fish tanks at 1/3m. Since the Spirulina grows 30% of its size per day, roughly 1000g will always be present for each crew member, so this way it will take 1 day for the approximate daily dose needed to grow. With constant aeration, the spirulina can handle 10g per every 1 liter. This equates to 0.1m³ for every 1000g.

Drying

Spirulina can be freeze dried in order to be consumed. It can also be taken outside to the Martian surface where the vacuum like conditions will be able to dry the algae.^[100]

6.4.4.6. Greenhouses

Greenhouse Layout

The greenhouse layout for the hub and hall were selected to satisfy a number of different conditions. The first design consideration was to create the maximum area of plant space. The second was to ensure that any plant can be reached by anyone with a grip length of 0.66 m or longer. This was a requirement to ensure that all crew members could contribute to crop harvests without requiring certain crew members to harvest specific areas. In addition, to ensure that there was enough room to walk between aisles with a container, the width of each walkway is designed to be 0.75 m. The final requirement was that the first floor have the ability to exit through all airlocks for potential expansion and crew safety.

A number of different cross sections were looked at to determine which design produced the maximum area while also satisfying all other requirements. The final design that was selected for the hub, provides an area of 29 square meters per shelf. The final hall design was chosen because the minimum area for the paths is achieved by keeping the paths rectangular; this floor plan provides an area of 28 square meters.

Greenhouse Halls

The greenhouse halls are divided into three floors, a bottom floor with dimensions of 5.31 x 13m and a middle floor with dimensions 7.49 x 13m. On the bottom floor there is one 1.33 x 12m space allocated for plants as well as another 1.33 x 12m space allocated for either plants or fish, depending on whether fish are grown in that particular hall. In addition, there is another 0.39 x 12m space allocated for plants which provides one 0.39 x 12m shelf and one 0.61 x 12m shelf. On the top floor, three 1.33 x 12m spaces are allocated for growing plants. This results in 129.3m² of growing space in a hall with fish tanks and 161.3m² of growing space in a hall without fish tanks.

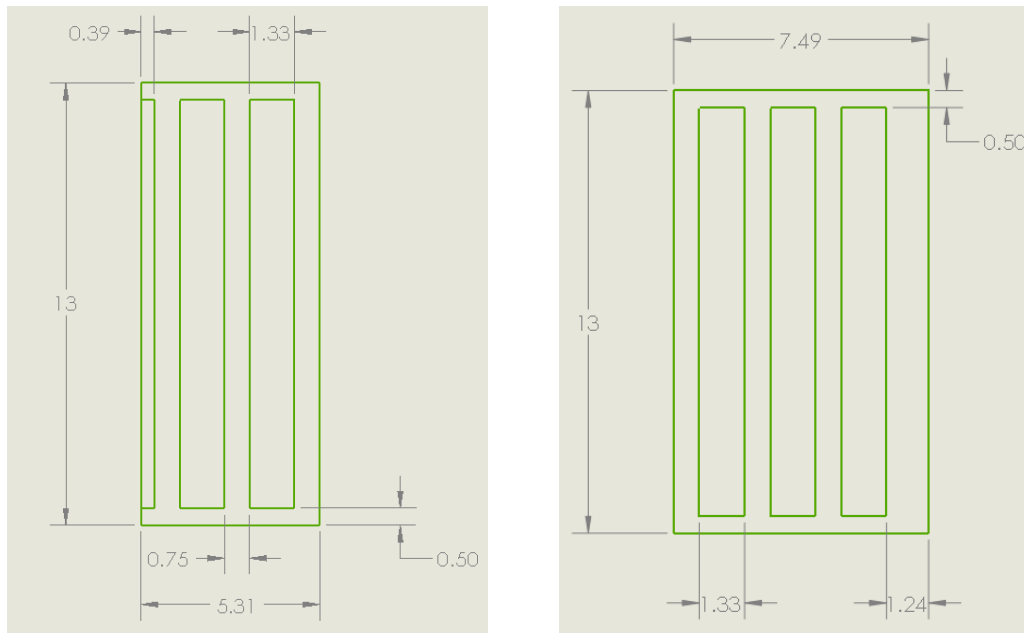


Figure 143. Bottom Floor (left) and Top Floor (right)
Greenhouse Hall Layouts

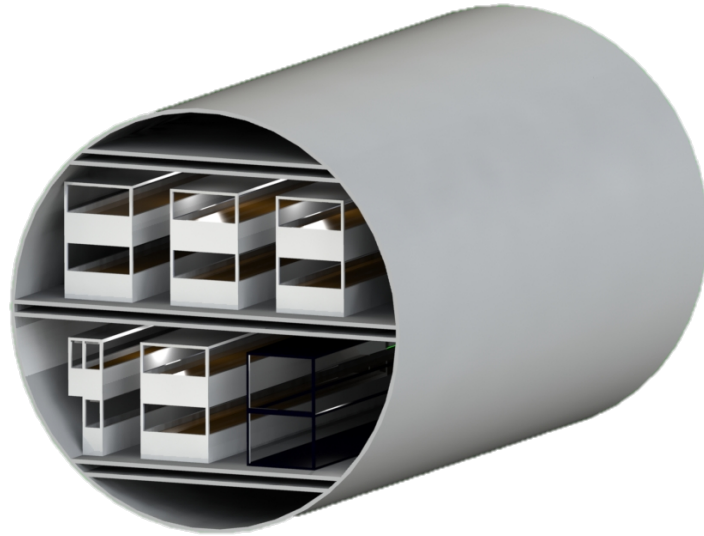


Figure 144. Full Greenhouse Hall Assembly

Greenhouse Hubs

The greenhouse hubs are designed to have 0.75m wide walkways throughout the middle of the hub as well as having all crops within a reachable distance of 0.667m. There is a 1.7m hole in the floor where the spiral staircase to go through floors is located. Shelves which are on the staircase side provide 5.34m² of growing space while shelves on the opposite side provide 5.79m² of growing space. This results in 133.6m² of total growing space per greenhouse hub.

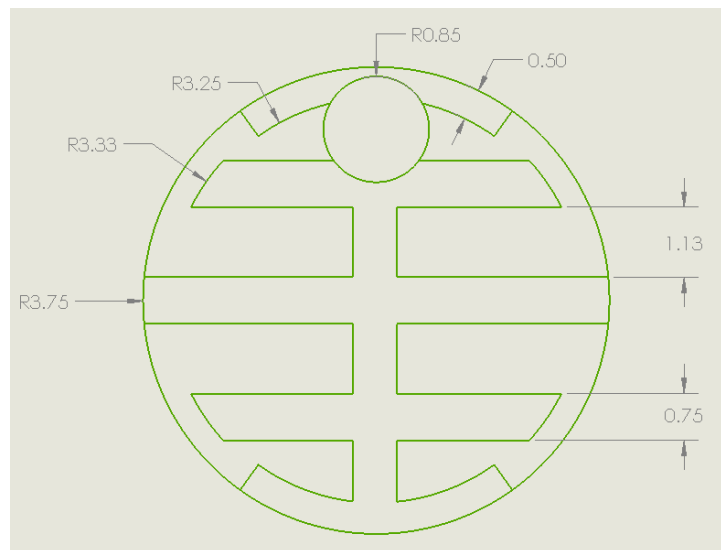


Figure 145. Greenhouse Hub Layout



Figure 146. Full Greenhouse Hub Assembly

Total Greenhouse Growing Area

Module	Growing Space (m ²)	Tank Volume (m ³)	Number of Modules
Hall (with fish tanks)	129.3	80.0	2
Hall (without fish tanks)	161.3	0	3
Hub	133.6	0	4
Total	1276.9	160.0	9
Food Requirements	800.8 – 819.8	109.7 – 116.5	-
Excess Space for Personal Use	457.1 – 476.1	43.5 – 50.3	-

Table 48. Greenhouse Growing Area

Greenhouse Environment

The Greenhouses will be set between 55 and 80 degrees Fahrenheit in order to accommodate the maximum amount of plants and fish. The humidity will be set between 50-85% in order to accommodate the maximum amount of plants. These levels will also allow us to acquire the correct amount of water needed from the dehumidifiers daily.

6.4.5. Bioregenerative Systems

6.4.5.1. Atmosphere Management

Maintaining a consistent and habitable atmosphere for the habitat requires the removal and replenishment of different gases. A large part of the changing habitat atmosphere results from the crops that are grown. Since a large portion of the crew's diet is dependent on grown crops, a large amount of carbon dioxide is required for the photosynthetic process and a large amount of oxygen is released by the plants into the atmosphere.

One issue is that humans do not exhale enough carbon dioxide for the plants to optimally perform photosynthesis and grow as effectively as possible. Humans exhale 1.0kg of carbon dioxide per day, meaning that a crew of 24 will release 24.0kg into the habitat atmosphere. Meanwhile, the plants require 47.4kg of carbon dioxide per a day.

The carbon dioxide discrepancy is solved by the carbon dioxide outputted as a product of the anaerobic digestion system. The amount of carbon dioxide outputted from the anaerobic digesters and the combustion of methane is 24.0kg per day. This leads to a 0.6kg of excess carbon dioxide that needs to be scrubbed via the Sabatier process. The Sabatier process acts as the backup carbon dioxide method in the case of crop failure.

These numbers change if the crew uses all 19m² of their personal space. With the additional crops, all of the plants require 82.3kg of carbon dioxide per a day. Meanwhile, the anaerobic digesters will now produce 41.7kg of carbon dioxide, for a total of 65.8kg of carbon dioxide when combined with the amount that humans exhale. This means that 16.5kg of carbon dioxide will need to be added to the habitat atmosphere per a day from the Martian atmosphere.

Another issue is that the plants output more oxygen than humans inhale, leading to a harmful atmosphere from a human health standpoint as well as increased flammability concerns due to the increase in total partial pressure percentage of oxygen. Humans inhale 0.85kg of oxygen per day, meaning that a crew of 24 requires 20.4kg of oxygen to survive. The plants output 34.5kg of oxygen a day depending on the current diet rotation.

Oxygen from the atmosphere is removed by burning a portion of the methane, which is outputted as a product of the anaerobic digestion system. From the methane produced, up to 17.6kg of oxygen can be combusted, an amount that is more than enough to reach desired habitat oxygen levels. As a backup system, pressure swing absorption (PSA) with zeolite x13 as the absorptive material will be used. PSA isolates the oxygen from the atmosphere by utilizing the different pressures required for the zeolite x13 to absorb different gases. When the pressure is raised, atmospheric nitrogen and carbon dioxide are

absorbed by the zeolite x13, isolating the oxygen. The oxygen is then released or stored and the pressure is lowered, releasing the nitrogen and carbon dioxide back into the habitat atmosphere.^[73]

Similarly to the carbon dioxide numbers, the oxygen numbers will alter if the crew utilizes all 19m² of their personal space. In this case, the plants will output 59.9kg of oxygen. In addition, the methane produced will now be able to combust 30.6kg of oxygen. This means that an extra 8.9kg of oxygen will be present in the atmosphere and that PSA will be required to bring the atmosphere to safe oxygen levels.

6.4.5.2. Waste Cycle

Solid

Solid waste will be coming from the crew, the plants, and the fish. Humans will be creating approximately 150 g/ CM-day of solid waste.^[37] The plants and fish will be creating at most 8750 g/CM-day. 550 g/CM-day will be taken from the plant waste and used as food for the fish. This leaves approximately 8350 g/CM-day of solid mass to feed into the anaerobic digester.

Liquid

Liquid waste includes urine, toilet flush water, and hygienic waste water (dishwater included). This comes to a total of 27 kg/CM-day.^[37] The toilet flush water and urine will be fed into the anaerobic digester while the hygienic waste water is cycled through the subsurface flow.

Other

All trash that cannot be added to the anaerobic digester or is not water will be discarded from the Habitat.

Waste	Mass (g/CM-day)
Feces	130.0
Human Detritus	16.0
Food Waste (fish food excluded)	8215.1
<i>Total Solid</i>	<i>8361.1</i>
Urine	1704.0
Hygienic Waste Water	24450.0
Toilet Flush Water	500.0
<i>Total Water</i>	<i>26654.0</i>
Total	35015.1

Table 49. Waste

6.4.5.3. Anaerobic digestion

The anaerobic digester will be used to create compost from the waste as well as creating methane and carbon dioxide. The digester is split into 5 separate tanks. The first tank is simply the holding tank where the waste collects. It will be able to hold 5 days' worth of waste. The next 3 tanks will be where the digestion occurs and the waste will spend 5 days in each of these tanks. The final tank is used to heat the waste up to approximately 70 degrees Celsius to disinfect the now compost. The system will be duplicated in case of breakdowns. Approximating the volumes of each, the total volume going into the digester is 0.003 m³/CM-day. Each tank will be approximately 0.15m³ in order to hold 10 days' worth of waste for 4 crew members. Using just the solid part of the waste, there will be approximately 872g of solid mass waste/CM-day that will be going into the digester. With current technology, this will equate to 183g of methane/CM-day, 463g of carbon dioxide/CM-day, and 129g of compost/CM-day.^[99]

Waste	Mass (g/CM-day)	Solid Mass (g/CM-day)	Water Mass (g/CM-day)
Feces	130.0	32.5	97.5
Human Detritus	16.0	1.6	14.4
Food Waste (fish food excluded)	8215.1	821.5	7393.6
Urine	1704.0	17.0	1687.0
Toilet Flush Water	500.0	0.0	500.0
Total	10565.1	872.6	9692.4

Table 50. Anaerobic Digestion Waste

6.4.5.4. Aerobic Digestion

The compost that the anaerobic digester creates will work as an aeration system in the greenhouse. Aerobic bacteria will be added to the compost in order to help break it down while consuming oxygen and releasing carbon dioxide as well as nitrate for the soil. Earthworms will also be introduced into the soil (vericomposting) in order to help break down even more of the compost.^[96] The worms have the ability to increase crop yield by breaking down the compost to more fundamental levels that are easier for the plants to access, as well as improve the moisture control of the soil and increasing microbial diversity that allow a more well rounded nutrient abundance.

6.4.5.5. Soil

The soil needed for the plants will be a mixture of the compost created as well as the soil on mars. Martian regolith contains all nutrients needed for plant growth except nitrogen.^[105] The regolith also has a hard time with water carrying capabilities, however the vericompost is known for its moisture control. Nitrogen can be implemented using nitrifying bacteria that live both in the fish tanks as well as the soil. As the fish excrete ammonia, nitrosomonas will oxidize this and produce nitrite. The nitrite then gets

filtered into the soil via subsurface flow where nitrobacter bacteria use the nitrite to produce nitrate. Finally, the nitrate is absorbed by the plants and when the fish eat the plant waste the cycle restarts. pH testing will be heavily used in the beginning of the aquaponic cycle in order to get the correct levels of nitrogen in the soil and water. ^[98]

6.4.5.6. Water Cycle

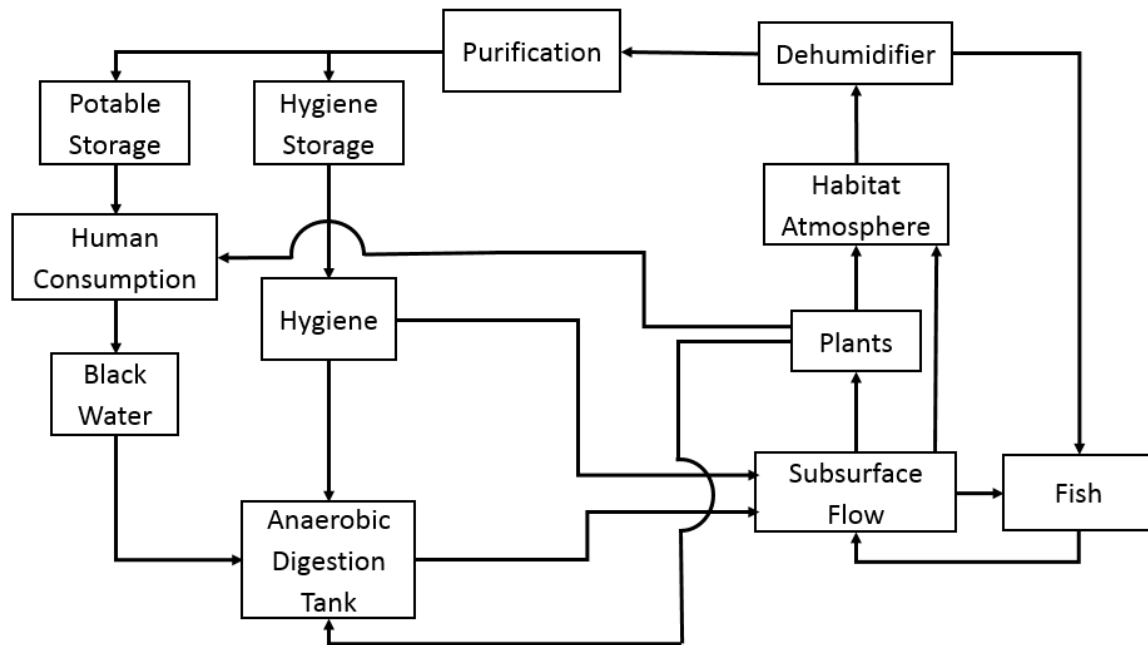


Figure 147. Block diagram of closed water cycle

There will be two kinds of water storage: potable storage for drinking and cooking and hygiene storage for other processes such as hand washing and dish cleaning. The water used for human consumption is converted into urine or feces and turned into black water, where it is directly to the anaerobic digestion tanks. After water from hygiene storage is used, it is directed to either the anaerobic digestion tank or the subsurface flow system depending on how it was used.

After the anaerobic digestion occurs, deoxygenated water is one of the products. The water is directed to the subsurface flow system where the plants can oxygenate and denitrogenate the water.

Once the water enters the subsurface flow system, three different paths can be followed. The water will either be absorbed by the plants, evaporated into the greenhouse atmosphere, or flow to the bottom of the greenhouse shelves where it will be collected and redirected to the fish tanks. The water that is collected by the fish tanks will eventually be redirected back into the subsurface flow system while the water that is evaporated into the atmosphere is collected by the dehumidifiers. The water absorbed by the plants is either transpired into the atmosphere and collected by the dehumidifiers or is inside the plants when they are harvested. The water inside the plants when harvested are either consumed by humans if they are a part of the edible biomass or put into the anaerobic digester if it is a part of the inedible biomass.

Water that is collected by the dehumidifiers is either directed into the fish tanks and eventually reintroduced to the subsurface flow system or is purposed for purification. Three different methods of purification were looked at: chlorination, exposure to ultraviolet (UV) light, and exposure to ozone. The primary method chosen was chlorination with exposure to UV light as a backup method.

While ozone has many positives as a water purification method, it was deemed as the worst of the methods due to the need to create the ozone. One method of creating ozone involves exposing diatomic oxygen to high-energy UV rays, breaking the oxygen's chemical bonds and allowing atomic oxygen to bond to diatomic oxygen molecules and create the ozone. The main issue with this process is that there is no additional benefit over just using the UV lights as the purification method instead of as a part of a more complicated process. Another method of creating ozone is exposing oxygen to an electrical discharge, but this method is much more complicated than chlorination and exposure to UV light.^[85] In the end, ozone exposure was deemed not worth the additional complications and sources of failure such as the need to redirect oxygen to a system that can create the ozone. In addition, ozone does not act as a lasting disinfectant, meaning the use of chlorine may still be required in order to keep the water pure.

For UV light exposure, the water needs to be exposed to the light for several seconds in order to purify it. This is much simpler than ozone treatment with comparable results. The main issue with this is that it also does not act as a lasting disinfectant, meaning that chlorine may still have to be used.^[86]

Chlorine is the primary water purification system with the plan being to bring enough chlorine to last an extended period of time. In order to purify one kilogram of water, 0.0003 grams of chlorine are required. 720kg of water is purified each day for the entire crew, meaning that 0.216 grams of chlorine is required a day to purify all the water that is directed to storage. In addition, while all of the purification methods are not reusable since the chlorine is exhausted and the electronics of UV purification and ozone purification will break down, chlorination has the possibility to become renewable since chlorine has been identified on the Martian surface.^[87]

Process	Water Directed (kg/CM-day)
Potable Storage → Human Consumption	2
Human Consumption → Black Water	2
Black Water → Anaerobic Digester	2
Hygiene Storage → Hygiene	28
Hygiene → Anaerobic Digester	11
Hygiene → Subsurface Flow	17
Anaerobic Digester → Subsurface Flow	13
Subsurface Flow → Fish Tanks	20
Fish Tanks → Subsurface Flow	220
Subsurface Flow → Habitat Atmosphere	<1
Subsurface Flow → Plants	230
Plants → Human Consumption	<1
Plants → Habitat Atmosphere	230
Habitat Atmosphere → Dehumidifiers	230
Dehumidifiers → Fish Tanks	200
Dehumidifiers → Purification	30

Purification → Hygiene Storage	28
Purification → Potable Storage	2

6.4.5.7. Habitat Lighting

Table 51. Water utilized in each of the water cycle processes

General Lighting

The crew modules of the habitat will be kept at 300 lux, the same light intensity of libraries and classrooms. The reason for this is that 300 lux provides enough light for tasks to be performed efficiently while not providing a detrimental amount of light as higher intensities lead to more difficulty in performing visual tasks as well as more difficulty in judging color.^[88]

LEDs will be used to provide the lighting for the crew modules just as they provide the lighting for the greenhouses. With current LED technology and the ability to produce 75 lumens / watt, 530W are required to power a crew hub and 666W are required to power a crew hall, leading to a total power requirement of 2.39kW. Using the United States Energy Information Administration’s projection of 200 lumens / watt when crew arrives, the power required is 199W for a crew hub and 250W for a crew hall, leading to a total power requirement of 898W.

The composition of the LEDs will be chosen to replicate the visible spectrum of the sun similarly to how LED solar simulators provide a replica of the sun’s spectrum in laboratory conditions. The reason for this is that there are psychological benefits to working in sunlight and there is no additional power cost since the same amount of LEDs are required. Exposure to sunlight results in less stress while not being exposed to sunlight can lead to depression and reduced productivity, a fact which has been proven in tests of factory workers who worked in windowless conditions.^[89]

Greenhouse Lighting

The light saturation point, the point where additional light does not increase the amount of growth of the plant, for crops is 32,000 lux. This is where plants grow optimally, with a minimum of 4,000 lux being required for plants to simply survive with no additional growth.^[59] The goal was to provide this optimal amount of lighting because additional space would be required for the crops if they do not produce their maximum amount of edible biomass as well as an inability to accurately predict crop yields when the light saturation point is not met.

The crops are going to be grown indoors with artificial lighting for two main reasons: the nature of the buried habitat is not conducive to utilizing natural light and the natural light received on Mars will be too weak and too variable to be relied upon for the crops. With the habitat being buried, the logistics of circumventing the meters of sun-blocking regolith were deemed not worth the cost. The regolith over the habitat is required to block radiation and there cannot be greenhouse units without it since crew members will spend a large amount of time planting, maintaining, and harvesting crops. A possible method of using natural sunlight in the modules under the regolith was through the use of fiber optic cables to

transfer the sunlight, but this technology was not seen as viable since it is still affected by the weak Martian sun.

When sunlight reaches Earth at a distance of 1 AU, the insolation constant is 1394 W/m². There is no direct conversion of watts to lumens as different wavelengths of light have different conversion rates based on the luminous efficacy of the light, a ratio of luminous flux to the radiant flux of the light source. For the sun's light, the luminous efficacy is 93 lumens/watt,^[60] meaning that the maximum amount of lux at 1 AU is 130,000. Since light is a form of radiation, the inverse-square law can be used in order to determine the amount of lux that reaches Mars. The minimum distance of Mars from the sun is 1.381 AU at aphelion and 1.666 AU at perihelion, leading to a maximum lux that ranges from 46,600 to 68,300.

While this lux range contains values above the 32,000 lux light saturation point, other factors need to be considered. The first is that this is the maximum lux reaching Mars, meaning it will only reach the surface during Mars' solar noon. Any other time will produce lower lux depending on the angle the sun is in the sky. In addition, a percentage of the light will be reflected by the Martian atmosphere. While the Martian atmosphere is much thinner than that of Earth, there is a large amount of dust which causes around 20-25% of light that hits it to be reflected.^[61] Since the habitat is located at the low elevation of Hellas Planitia, there is more atmosphere for the light to be exposed to before reaching the surface.

The large variance of seasons is another reason that natural light is not a viable option. While Mars' 25° tilt is comparable to Earth's 23° tilt, its large orbital eccentricity of 0.0935 is almost six times larger than Earth's 0.0167.^[62] This large eccentricity means that seasons are more extreme and that the winters in Hellas Planitia are longer than the summers due to its latitude, resulting in more days of less sunlight. In addition, during the Martian summers dust storms can form as the Martian surface is warmed, causing the majority of sunlight to be unable to reach the surface in unpredictable intervals.

Once it was determined that artificial lighting was the best course, the type of light bulbs used in the greenhouses was considered. A comparison of incandescent bulbs, compact fluorescent lamp (CFL) bulbs, and light emitting diodes (LEDs) was performed and concluded that LEDs were the best route to take. One main reason for this decision is that LEDs are more efficient at creating light from power than incandescent bulbs and CFLs, meaning that less power would be required to provide the 32,000 lux to the greenhouses. In addition, LEDs have a larger usable life than both incandescent bulbs and CFLs, with a usable life of 50,000 hours compared to 10,000 hours for CFLs and just 1,200 hours for incandescent bulbs. LEDs also produce less heat than both CFLs and incandescent bulbs with none of the heat being emitted from the light source, potentially damaging the plants. Lastly, LEDs are unaffected by humidity, meaning that the humid atmosphere of the greenhouses will not alter the LEDs' light output.^[63]

While LEDs are the best option in terms of the power required, the large amount of greenhouse space made the overall power requirements for greenhouse lighting higher than desired. With current LED technology, LEDs can produce 75 lumens/watt, resulting in 427 W/m² to produce the desired 32,000 lux. This means that for the 815 m² of crops required, a total of 348kW is needed. LED efficiency has been increasing on a yearly basis and since the greenhouses do not need to be operational until the crew arrives in 2037, LED efficiencies around that time can be projected. The United States Energy Information Administration projects that the efficiency of LEDs will level off in 2030 with an efficiency of 200 lumens/watt,^[64] resulting in 160 W/m² to produce the desired 32,000 lux. This leads to a new total power of 130 kW for the greenhouse lighting.

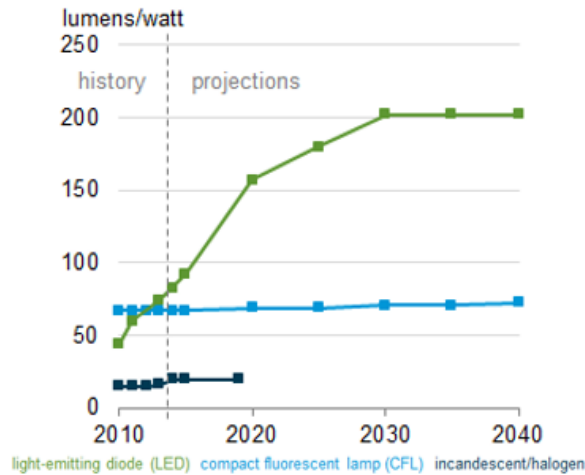


Figure 148. The United States Energy Administration projection for LED efficiency in the future^[64]

A composition of red and blue LEDs will be used in our greenhouses. The reason for this is that plants only require light from the red and blue parts of the visible spectrum in order to grow. Any other colors of light would be wasted as they are either not absorbed by the plants or not utilized in the photosynthetic process.^[65]

Another consideration is that while the 130kW is the minimum amount of power to satisfy that crew’s diet, up to 19m² of space is available to each crew member for their personal gardens as well as the growing of medicinal plants. This means that the maximum of 456m² extra space can be used, resulting in an additional 73.0kW, and a new total power number of 203kW.

Total Lighting Power Requirements

Module	Current LED Technology	2030 LED Projections
Crew Hub	0.530kW	0.199kW
Crew Hall	0.666kW	0.250kW
Greenhouses (Required Diet)	348kW	130kW
Greenhouses (Personal Space)	182.4kW	73.0kW
Total	531.6 kW	233.5 kW

Table 52. Lighting Power Requirements

6.4.6. Regolith Tunnels

The entire Martian habitat was designed to be covered in a thick layer of Martian regolith. At a minimum thickness of 5 m above all habitat modules, the regolith layer is able to shield the habitat from a majority of harmful cosmic radiation. When piled, the soil forms slopes at its angle of repose of about 30°. Any

regolith placed upon the habitat will form a gentle slope to ground level. This means there will be a not inconsiderable horizontal distance between the base of any structure covered in regolith and the Martian surface. Several unpressurized tunnels will traverse this distance from the Martian habitat modules through the surrounding regolith to the Martian surface.

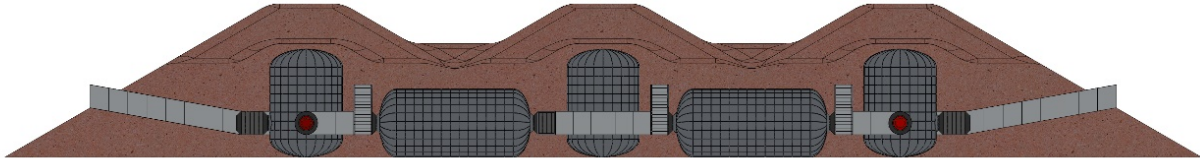


Figure 149. Side-view of Martian habitat and regolith covering

These regolith covered tunnels provide the sole means of egress from the Mars habitat to the Martian surface. As such they are designed around several types of extravehicular activity. The tunnels connect to the airlocks to transition from the unpressurized environment of the tunnels to the pressurized Martian habitat. The tunnels encompass two forms of egress from the airlocks. First, there is a tunnel section attached to the side of the airlocks containing the suit ports. This allows astronauts to don their spacesuit and exit the airlock in the same action. There is also a tunnel section connected to the cargo hatch on the end of the airlock. This allows for astronauts to conduct extravehicular activity with suits not from the airlock suit ports, as well as move larger cargo that could not be moved through the suit ports.

The design requirements for the regolith tunnels were aimed at optimizing their usage to provide surface access for humans and cargo, as well as their accessibility in the event of an emergency. To this end, the dimensions of the tunnels were specified at a 2.5 m height clearance and 2 m width. The tunnel sections connected to the airlocks are larger; they are 2.5 meters wide at the suit port exit and 2.8 meters wide at the cargo hatch exit. This allows for more maneuvering space at the airlocks. The astronauts have adequate space to enter and exit the habitat through the suit ports, as well as to bring large cargo in or out of the airlock cargo hatch. In addition, the ramp sections of the tunnels were designed with a 10° upwards slope to save some distance while keeping the slope angle minimal. The two tunnels connected to the airlock cargo hatches will connect to the surface without an upwards sloping ramp section. These tunnels will be used for the movement of large cargo too difficult to transport up or downhill.

A side-effect of routing all travel to and from the Martian surface through the tunnels is that the regolith-covered tunnels are also the only method of emergency evacuation. Because of this, there is a high degree of redundancy built into the layout of the tunnels. The regolith-covered tunnels allow for emergency evacuation of the habitat in the event of the failure of any two habitat modules. To ensure this, four right-angle sections were placed in the enclosed internal courtyards of the habitat, providing an unpressurized connection between the one inner hall and the four outer halls, by passing the two central hub modules.

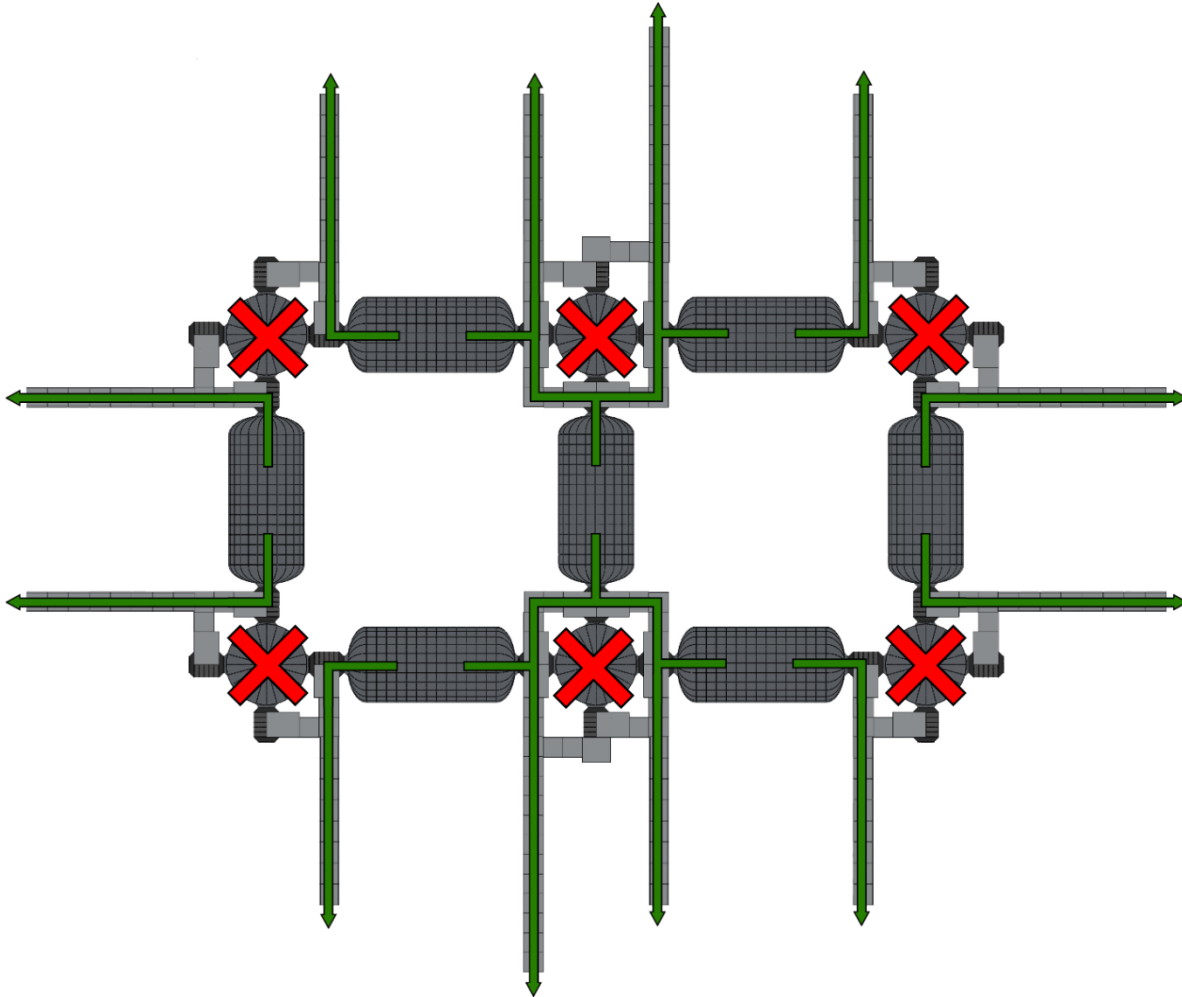


Figure 150. Various habitat module failures and escape routes

The design of the regolith tunnels was based on an inner box frame composed of extruded beams and external panels supporting the regolith. This allows for a highly modular design. The use of repetition greatly simplified design, analysis, and construction of the regolith tunnels. The tunnels modules include flat and ramped 2m wide hallway sections, a 2.5m wide suit port exit, a 2.8m airlock cargo hatch exit. The modules are made from 2 identical roof and floor sections along with two identical or mirrored wall sections.

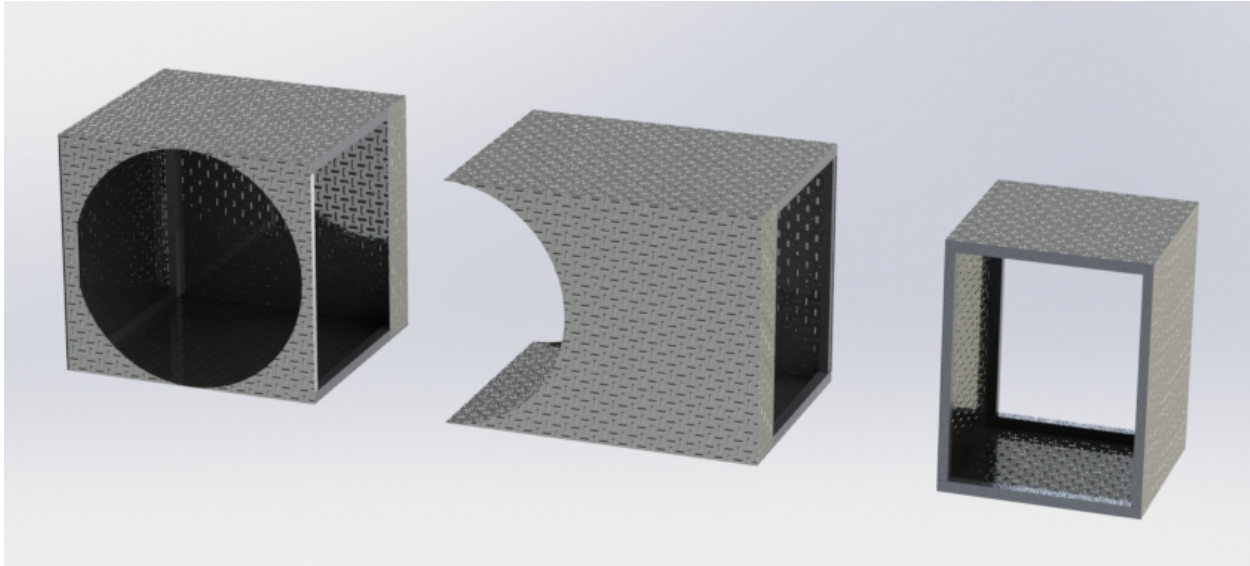


Figure 151. Cargo hatch exit, suit port exit, and hallway modules

The individual tunnel module sections were designed to be partially assembled on Earth. A single wall/roof/floor section consists of two square aluminum extrusion beams welded to a panel. This allows the tunnels to be launched in a compact payload format. On the surface of Mars, they will be assembled by the construction crew during extravehicular activity. The beams of the roof/floors are slightly wider than those of the walls, and have notches cut to insert the beam members from the wall sections. This way the tunnels can be assembled on Mars by extravehicular activity. The tunnel sections are first aligned in place by maneuvering them using the construction crane. An astronaut will manually join the sections with bolts. After the regolith is placed on top of the tunnel, it will secure the orientation of the tunnel sections.

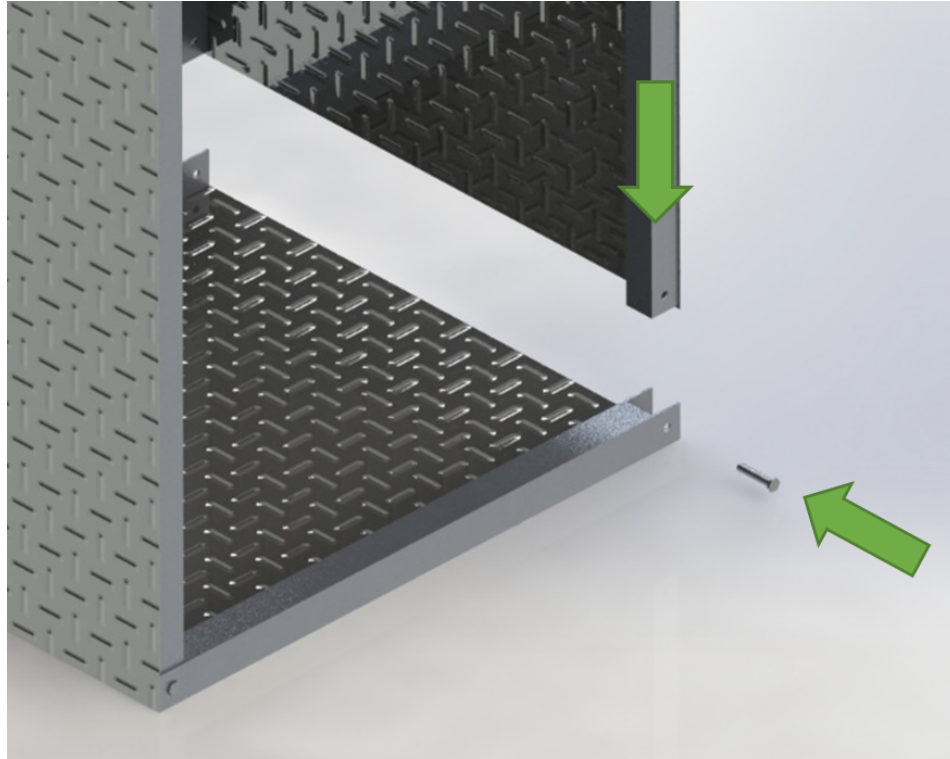


Figure 152. Interlocking design of tunnel section

The major source of loading on the tunnels is the thick covering layer of Martian regolith. While a minimum thickness of 5m is required over all habitat modules for radiation shielding. Because of the tall height of the habitat hubs compared to the halls and airlocks and the low angle of repose of the Martian soil, the regolith will be deeper than necessary in the areas around the hub modules. The regolith layer above the tunnels can measure up to 12m thick above the regolith tunnels. Due to the critical role of the tunnels in providing surface access and emergency evacuation routes, as well as uncertainties in the exact composition and behavior of Martian soil, the tunnels were designed with a high factor of safety of 3.

The loading of the regolith layer was modeled as a pressure load. Calculating for a 12m thick layer of 1.5 g/cm^3 density Martian regolith, in Martian gravity at 3.711 m/s^2 yields an equivalent pressure of 66.8 kN/m^2 . This pressure was applied to the top surface of the tunnel sections. It was assumed that the side and shear loads would be negligible compared to the weight of a regolith layer up to 12m thick. The aluminum alloy Al-2090-T83 was selected for its high yield strength of 520 MPa (Young's Modulus 76 GPa) and its high workability in welding.^[254]

Module	Load Source	Limit Load	Design Load	Safety Factor	Margin of Safety
Cargo Exit	Roof Panel	520 MPa	168.9 MPa	3	0.0260
	Column Buckling	352.9 kN	116.9 kN	3	0.00582
	Column Compression	520 MPa	9.845 MPa	3	16.61
Suit Port Exit	Roof Panel	520 MPa	126.1 MPa	3	0.374
	Column Buckling	352.9 kN	83.85 kN	3	0.403
	Column Compression	520 MPa	7.057 MPa	3	23.6
Hallway	Roof Panel	520 MPa	91.69 MPa	3	0.890
	Column Buckling	352.9 kN	67.08 kN	3	0.754
	Column Compression	520 MPa	5.646 MPa	3	29.7

Table 53. Table of loads on regolith tunnels

In analyzing the regolith loading, the roof panels were treated as thin simply supported plates. Young and Boudynas give an approximate equation for the maximum bending stress in such a case as $\sigma_{max} = \frac{\beta qb^2}{t^2}$ where a is the length of the long side of the plate, b is length of the short side of the plate, β is a constant tabulated as a function of a/b , q is the uniform load, and, t is the plate thickness^[255]. As a , b , and q are constrained by design, a function can be derived for the relationship between plate thickness and maximum stress. Stress will be highest at the panel of largest area. For the cargo airlock, where $a=2.79$, $b=2.5$, this is expressed as $\sigma_{max} = \frac{142000N}{t^2}$. Accounting for a yield stress of 520 MPa and a safety factor of 3, this equation becomes $520MPa = 3 \frac{142000N}{t^2}$. The minimum safe thickness is 28.6 mm. Rounding up to the nearest millimeter gives a margin of Safety of 0.026. This thickness will be used in all panels to simplify manufacture, but sections with less loading will have a higher Margin of Safety. The MATLAB program `alash_1.m` uses these relations to automatically calculate the Margin of Safety for the remaining roof panels given dimensions a , b , and t and a Factor of Safety.

The tunnels were designed primarily around the column buckling load in the vertical aluminum extrusions. The Euler buckling load is calculated as $F_{buckle} = \frac{\pi^2 EI}{(KL)^2}$, where E is Young's Modulus, I is the area moment of inertia, L is the column length, and K is a constant depending on the end conditions. In the worst-case scenario requiring the least loading to buckle, the one end of the columns would be treated as fixed and the other would be allowed to move laterally, for $K=2$. Including a factor of safety of 3, the design load for a single column is $F_{design} = \frac{\pi^2 EI}{12L^2}$. It is assumed that the load will be distributed evenly among the 4 columns. Loading will be highest at the panel of largest area. For the cargo airlock, where $a=2.79$, $b=2.5$, this is expressed as $F_{design} = \frac{1}{4} abg(\rho_{regolith} * 12m + \rho_{Al} * 0.029m) = 117.0$ kN. Accounting for Young's Modulus of 76 GPa and L of 2.5m the buckling load equation can be solved for $I = 2.924 * 10^{-6}m^4$. The area moment inertia for a hollow square cross section is $I = \frac{s_o^4 - s_i^4}{12}$, where s_o is the outer side length and s_i is the inner side length. Thus a relationship $s_o^4 - s_i^4 = 2.254 * 10^{-4}m^4$ can be derived between the outer side length and inner side length. The MATLAB program `alash_2.m` plots this relationship below, along with the cross sectional area. The case of minimum inner side length is a solid cross section with $s_i = 0$ and $s_o = 0.1088$ m, for an area of 0.01184 m². Rounding s_o up to the nearest millimeter gives an area of 0.01188 m² Margin of Safety of 0.00582. At these dimensions, the axial compression stress in a column is $\sigma_p = \frac{F_{design}}{A_{column}} = 9.873$ MPa. With a Safety Factor of 3 over the yield strength of 520 MPa, this represents a Margin of Safety of 16.61, so

compressive failure should not be an issue. These dimensions will be used in all columns, but sections with less loading will have a higher Margin of Safety. The MATLAB program `alash_3.m` calculates the Margin of Safety in buckling and compression for the remaining columns given dimensions a , b , t , L , s_i , s_o , and a Factor of Safety.

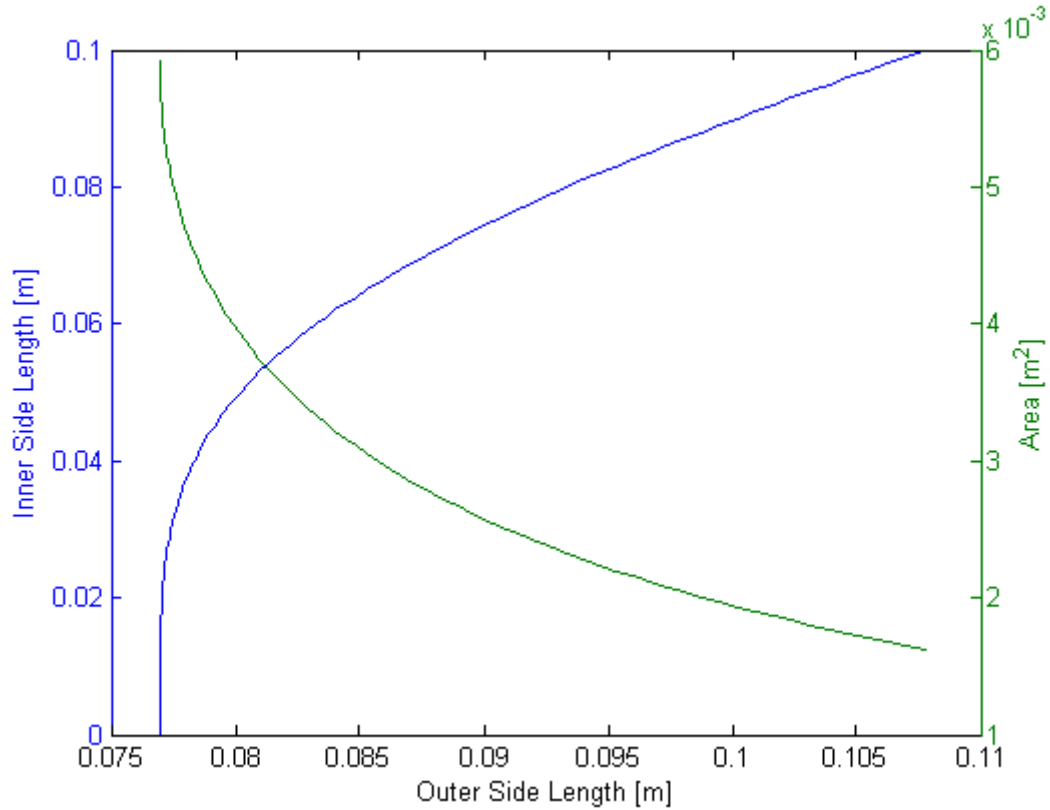


Figure 153. Geometric properties of column cross section

6.4.7. Habitat Power Requirements

The Mars habitat will have 2 power cycles; a 16.7-hour and 8-hour cycle shown in respective order:

Power Load Source	Maintaining Power (kW)
Heating	1
Life Support	18
Food Systems	210
Electronics	2
Miscellaneous	2

Total	233
-------	-----

Table 54: 16.7 Hour Power Cycle

Most of the power consumption for the 16.7-hour cycle comes from the greenhouse habitats where the lighting needs a lot of power to provide the necessary light for the plants to grow. The heating power requirement is only a kilowatt based on the fact that the lighting from the habitat will be keeping the whole habitat warm and the 1 kW will be used to run the pumps of ammonia and water to remove some of the excess heat.

Power Load Source	Power (kW)
Heating	13
Life Support	18
Food Systems	0
Electronics	2
Miscellaneous	2
Processing	75
Vehicles	25
Total	135

Table 55: 8 Hour Power Cycle

Now for the 8 hour cycle is going to be supporting the processing plant that is going to be creating our hydrogen and oxygen along with charging the mining vehicles that need to go out the next day. The heating numbers for the 8-hour cycle rise due to the fact that the lighting inside the habitat has shut off and it will now require some way to keep the habitat warm during the “night” time.

6.4.8. Solar Power

The Mars habitat is going to be run mostly on nuclear power and we came to this conclusion when we realized that nuclear power is a more reliable way to provide a constant amount of power. Solar electricity is based on the amount of solar irradiance making contact with the solar panels themselves, however throughout the course of a Mars day the intensity of solar irradiance hitting the solar panels is going to fluctuate. This is due to the fact that the Sun is going to be changing positions across the Mars sky while the solar panels are lying flat on the Mars surface causing the zenith angle relative to the Sun and the solar panels to be changing. Due to the changing zenith angle, the amount of power will not be constant throughout a Mars day.

Even though solar electricity is not going to be a the main source of power for the habitat, it is still going to be needed to provide the extra amount of power when one of the three nuclear reactors are down for

refueling. The solar panels were sized relative to the amount of extra power needed to take over for the downed nuclear reactor.

Originally it seemed like the best idea would be to have the solar panels attached to some structure that would track the sun across the sky allowing for a relative constant output of power instead of them lying flat. However, the structure when designed would provide an additional 50 metric tons to the mission, which is mass that could not be accommodated for on this mission. So based on this discovery it was decided that the solar panels would be flat on the surface to conserve mass for the mission.

Based on the power breakdown table above you can see that when a nuclear reactor is down for refueling the solar panels are going to need to provide around 30kW of power for the 16.7 hour power cycle. However, due to the fluctuating power output from the solar panels throughout the day it was decided that it would be best that during the day the solar panels would be providing power to the energy storage unit. The reason being that the energy storage unit can take all the energy supplied by the solar panels throughout the time the sun is out and then output a constant power supply to the habitat the next day. In addition, due to the efficiency of power transfer being around the solar panels and the hydrogen fuel cells being roughly 50 percent we now know that the solar panels are going to need to provide 60kW during the sunlit time. Based on the amount of power needed and the amount of time it is needed for we can see that the total amount of energy needed to be provided is going to be 960 kW-hr.

Now that we know the amount of energy needed for the 16.7 hour power cycle, figuring out how much power the solar panels can produce and figuring out how long daylight will last on Mars based on the habitat's location is the next step to size the solar panels.

First it was calculated as to what "season" would be providing the least amount of solar flux to the surface of Mars. Knowing that solar flux is inversely proportional to the distance away from the sun squared it is easy to calculate the corresponding solar irradiance for Mars. All that is needed to know is the solar flux reaching the Earth and the distance Mars would be away from the sun during a specific "season". Knowing that Mars is the greatest distance away from the sun during the "summer" we can find the lowest amount of solar flux that will be provided during a Mars year. ^[182]

$$I_{summer} = I_{summer} \left(\frac{1}{d_{winter}} \right)^2 = 1394 * \left(\frac{1}{1.65} \right)^2 = 512 \frac{W}{m^2}$$

Note that these "seasons" are based on the orbital period of Mars throughout its orbit around the sun. So for the summer season it corresponds to when Mars is 90 degrees in its orbit around the sun.

Now to continue the sizing process of the solar panels we need to find how long daylight normal last in each season on Mars, and which season corresponds to the shortest amount of daylight. If the summer results in the shortest amount of time then we will be able to size the solar panels for worst case scenario.

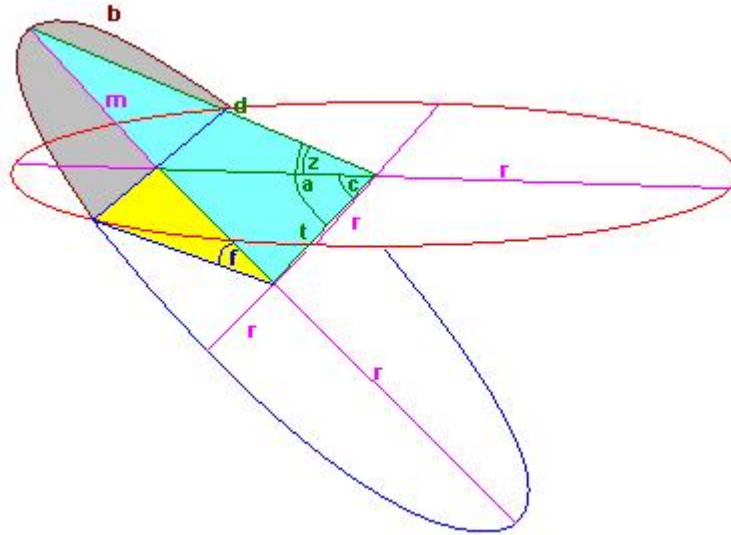


Figure 154. Length of Day representative variables^[158]

This image is a representation of the solar circle relative to the surface of observing plane (Mars surface).

First we need to find the angle between the observing point and the sun's zenith angle:

$$z = 90 - Lat - \cos\left(\pi * \left(\frac{Day}{343.5}\right)\right) * Axis_{tilt}$$

The 348.5 comes from the amount of days it takes for Mars to rotate around the sun (687 days) divided by two. The Axis tilt variable corresponds to obliquity of the ecliptic, which for Mars is 25 degrees.

Next, the angle between the sun's zenith and the solar disc is calculated by:

$$a = z + Lat$$

Distance from zenith angle to observer:

$$d = \frac{1}{\sin(a)}$$

Distance from center of the solar circle to the observer:

$$t = \cos(a) * d$$

Exposed radius part between zenith and solar circle:

$$m = 1 + \tan(c) * t$$

Angle between sunrise or sunset point and the center of the solar circle:

$$f = \cos^{-1}(1 - m)$$

Finally, the exposed fraction of the solar circle can be calculated and if this number is multiplied by 24.7 (length of Mars day) it can show how many hours the sun will shine on the surface of Mars:

$$\text{Hours} = \left(\frac{f}{180}\right) * 24.7$$

Note: all of these calculations were based off figuring out how much sunlight would reach the Earth's surface but adapted to Mars.^[158]

Here is a graph corresponding to a Mars year:

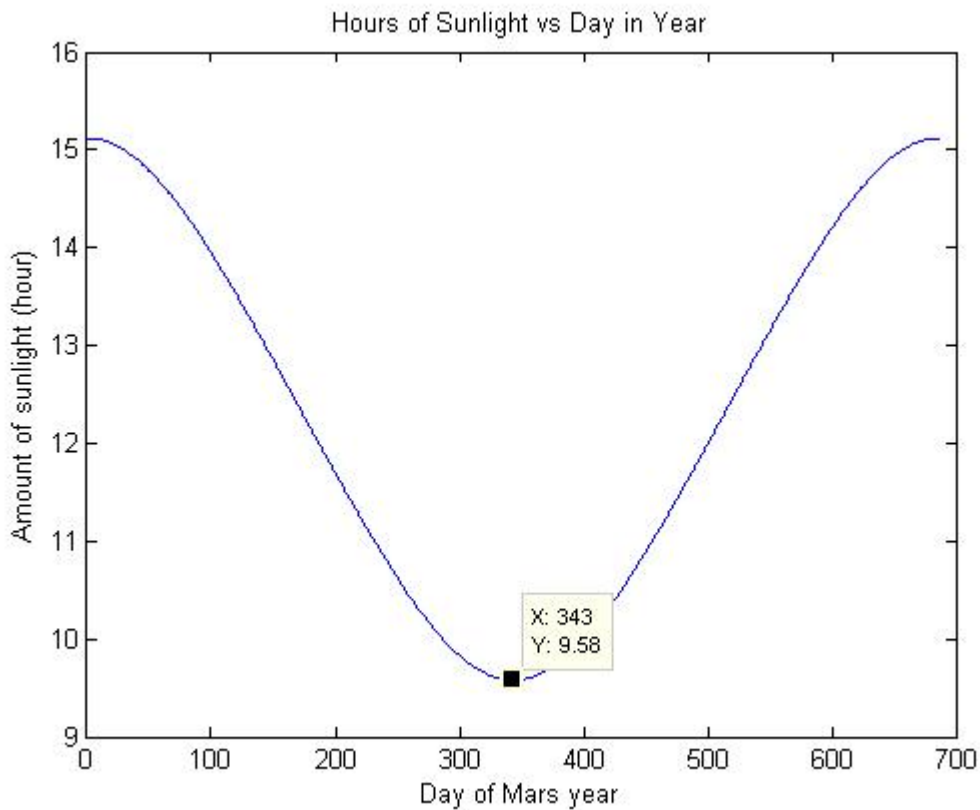


Figure 155. Hours of Sunlight on Mars

Based on this graph you can see that the lowest length of sunlight occurs around day 343 of the Mars year. This day corresponds during the summer season on Mars which occurs during day 199 to 382.^[159] Now it is known that the lowest amount of solar flux and the shortest amount of sunlight occurs during the summer season so we can now size the solar panels based on this information.

To calculate the amount of energy during the sunlight hours we need to iterate every second to find the relative variables at that time such as, hour angle, zenith and solar irradiance. This will then allow us to calculate the total amount of energy over a 9.6 sunlight hour period. The time is iterated from -4.8 hours to 4.8 hours, and this is done so that at time of zero this will correspond to midday where the sun would be at its peak. Here are the basic equation that were used to find the amount of power produced every second throughout the shortest Mars day that was just calculated as 9.6 hours:

$$\text{Hour Angle} = 360 * \left(\frac{t}{24.7} \right)$$

Hour angle is just the angle between an observer's meridian and the hour circle¹⁶⁰ and t represents the time going from -4.8 hours to 4.8 hours.

$$\text{declination} = \sin(\text{Orbital Position}) * \sin(\text{Axis Title})$$

$$\text{Zenith} = \cos^{-1}(\sin(\text{lat}) * \sin(\text{dec}) + \cos(\text{lat}) * \cos(\text{dec}) * \cos(\text{hour angle}))$$

Where the variables "lat" and "dec" correspond to the latitude of the habitat on mars and the declination of the sun, respectively.¹⁶²

Then solar irradiance hitting the solar panels can be computed from the following equation:

$$I_{flat} = I_{summer} * \cos(\text{zenith})$$

Finally the power produced is calculated by using the solar irradiance on the solar panels, area of the solar panels and the efficiency of the solar panels:

$$P_{flat} = I_{flat} * \text{Area}_{solar} * \eta_{solar}$$

Here is a graph corresponding to the Power produced of a solar panel over the course of a summer day with the area of 1m² and the efficiency of 29%.

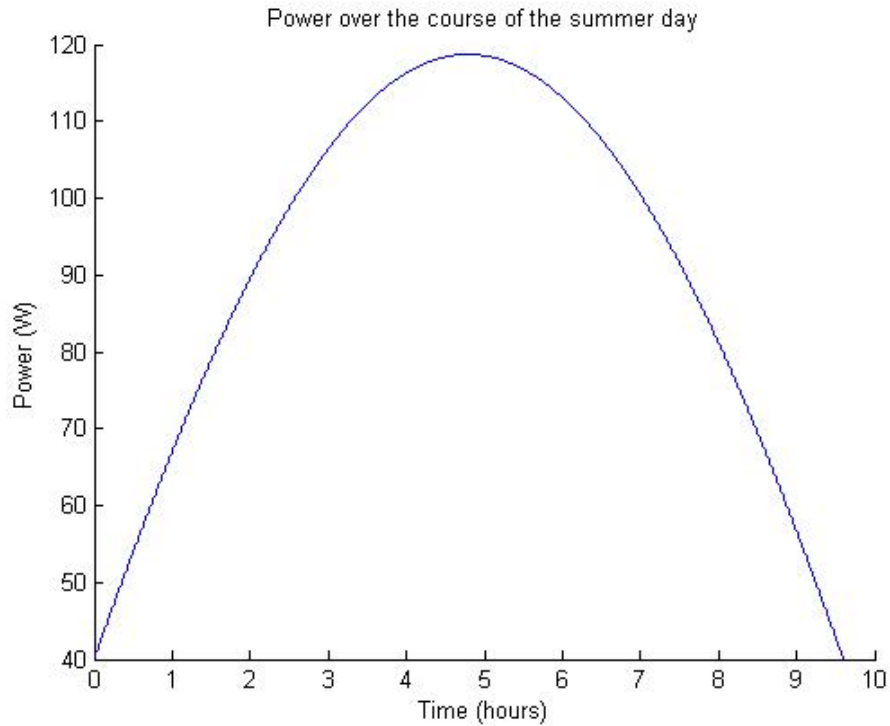


Figure 156. Power over a Summer Day

Now the total energy over a course of a day can be calculated by summing all the power values found through the time iteration process and then dividing it by the 3600 seconds to convert that number to W-hr. This number turns out to be 875 W-hr/m² since we found this number for 1 m² worth of solar panels.

So now we can size the amount of solar panels needed:

$$\frac{960 \text{ kWhr}}{0.875 \left(\frac{\text{kWhr}}{\text{m}^2} \right)} = 1100 \text{ m}^2$$

A comparison table between multiple solar panels was created to decide which solar panels would be the most efficient to use on this mission. In bold shows our decision to use the Emcore multijunction solar panel for the reason that is one of the lightest, most efficient and less expensive compared to the other multijunction solar panel, Spectrolab. This is where we find that the efficiency to use for the solar panels is 29 percent.

Solar Panel	Efficiency	Power decay rate (%/year)	$\frac{W}{m^2}$	$\frac{kg}{m^2}$	$\frac{kW}{m^3}$	Cost $\frac{\$}{m^2}$
Global Solar Powerflex 6	13%	0.87%	34	3.3	11	-----
Solopanel SP3L	10%	0.96%	27	2.4	13	160
Emcore ZTJ PV Cell	29%	0.50%	78	2.9	9.3	10000
SpectroLab XTJ	26%	0.50%	69	2.9	8.1	28000
SunPower E-Series	20%	0.36%	53	11.4	1.2	1200

Table 56. Solar Panel Comparison^[172-181]

6.4.9. Nuclear Power

Description of FSP Reactor

The main power source for the Mars settlement will be three fast-spectrum, liquid-metal cooled fission reactors. Each reactor will be fueled by Uranium-Dioxide and will have a constant power output of 100kWe. These specific reactors were chosen due to their low mass, low required distance from populated areas, and well-tested safety systems. One of the main concerns regarding the use of nuclear technology as a power source is the ability to transport it while maintaining a subcritical state prior to the intended startup time. This would not be a concern when using the Fission Surface Power (FSP) reactors, initially designed by the NASA's Fission Power Surface team led by Donald Palac.^[193]

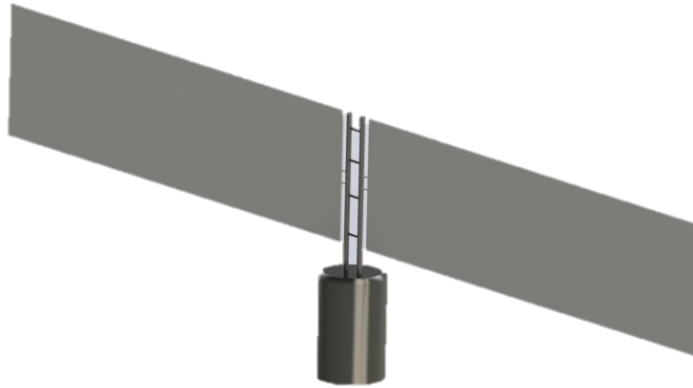


Figure 157. Reactor Without Berm

FSP Scaling and Mass Distribution

The original fission power system discussed in the FSP Team’s Initial Concept Definition Report was said to be readily scalable between 10 kWe and 100kWe.^[193] However, the various sizing calculations in the report revolved around a 40kWe design. The Asimov City settlement would require more power than these reactors could provide, so the design was scaled up to a 100kWe reactor. This changed numerous factors, particularly the volume and mass sizing of the reactor itself.

According to the report, the power density of the 40kWe reactor is about 32 W/cm³, and the thermal power output is 186kWt.¹⁹³ The fuel pin assembly is in the shape of a hexagon. A hexagon has a cross sectional area that can be found through the following formula:

$$A_{hex} = \frac{3\sqrt{3}}{2} a^2$$

where ‘a’ is the length of one of the six sides. The power density given above is in terms of the power (in W) per unit volume of the fuel. Therefore, the volume of the fuel pin assembly can be calculated by dividing the power output by the power density, which results in a fuel pin assembly volume of approximately 5800cm³. This value is an estimate because the packing density of the fuel pins was not taken into account. Using this volume and the above area formula, as well as the known fuel pin height (h) of 69cm, the side length ‘a’ was calculated to be 5.7cm. The radius of the inscribed circle within the cross section of the fuel can be found with the following formula:

$$r = \frac{a}{2} \sqrt{3}$$

By using this formula, the inscribed circle radius (r) was found to be 4.9cm. The fuel pin assembly is now fully dimensioned, as seen in the figure below.

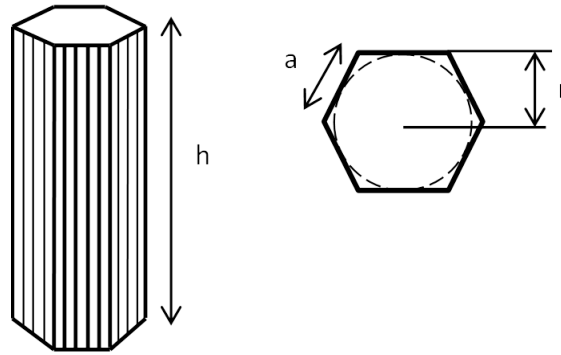


Figure 158. Labeled diagram of fuel assembly

The average density of Uranium-Dioxide is 10.97 g/cm^3 .^[200] Provided this density and the volume (about 5800 cm^3), the initial mass of the fuel within the 40kWe reactor was determined to be approximately 64kg.

The efficiency of a reactor can be found by dividing the electrical power output divided by the initial thermal power output. In the case of the FSP reactor, the thermal power output is 186 kWt and the electric power output is 40 kWe; the efficiency of this reactor would thus be 21.5%. With this efficiency, a thermal power output of 465kWt would be required to produce the desired electrical power output of 100kWe. Assuming the same power density, the fuel volume required to achieve this thermal power output was found to be 14500 cm^3 . To simplify the number of factors being scaled, the height of the fuel pin assembly was kept the same; the volume of the assembly only increased in the radial direction. The new volume was then used to determine the required side length ($a_{\text{req}} = 9.0 \text{ cm}$) and inscribed circle radius ($r_{\text{req}} = 7.80 \text{ cm}$). Using the same value for the density of Uranium-Dioxide as earlier, the required fuel mass to produce an electrical power output of 100kWe was found to be 159kg.

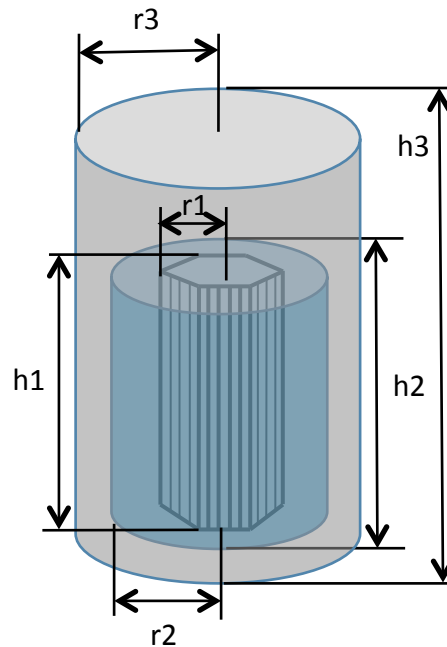


Figure 159. Diagram of reactor module, labeled with dimensions

Component	Dimensions
Fuel Pins	Radius (r1): 7.80 cm Height (h1): 69.0 cm Volume: $1.45 * 10^4 \text{ cm}^3$
Reactor Module	Radius (r2): 38.8 cm Height (h2): 69.0 cm Volume: $3.26 * 10^5 \text{ cm}^3$
Radiation Shielding	Radius (r3): 66.0 cm Height (h3): 230 cm Volume: $8.86 * 10^5 \text{ cm}^3$

Table 57. Table of Dimension Values

The reactor and shield components were each scaled linearly to achieve a reasonable estimate for the sizing of the 100kWe reactor. The component masses were scaled in a similar manner. The mass of the 100kWe reactor was thus estimated to be approximately 14.4t. The mass distribution of the various FSP system components is shown below.

FSP System Component	Mass (t)
Reactor Module	3.60
Power Conversion Module	1.02
Heat Rejection Module	1.90
Power Management and Distribution Module	2.60
Radiation Shield Module	5.20
Integration Structure	1.20
Total Mass of FSP System	14.4

Table 58. FSP System Component Mass Distribution

It should be noted that linear scaling was used to determine a reasonable estimate of the size and mass of the scaled-up reactor. According to FSP team leader Donald Palac, the scaling of a nuclear reactor does not follow an exact linear scale. A more accurate scaling that his team performed resulted in an estimated FSP system mass of $9^{11}t$.^[194] However, this method was more complex and beyond the scope of this course. The linear method was thus used for this project and resulted in an overestimate of the mass for each nuclear reactor.

Fast Spectrum and its Advantages

A fast-spectrum reactor is preferred for this mission due to its ability to operate critically without a moderator. A moderator, often in the form of light water or heavy water, is generally required for induced nuclear fission to occur and be sustained. The nuclear fission of the material produces high speed neutrons; generally, these neutrons are moving at too high of a speed for absorption and fission to take place. This is why a moderator is required. The moderator slows the neutrons down enough that they can be absorbed into the various cross sections of the atoms. However, this type of nuclear reactor has a much higher mass than that of the fast-spectrum reactor. The moderator itself can add a significant amount of mass to the system. The fuel would also have a relatively low enrichment level (ratio of fissile material to non-fissile material), meaning that more fuel mass overall would be required to power the system. Fast-spectrum reactors have highly enriched fuel, increasing the interaction probability of the high speed neutrons.^[199] This counterbalances the initial problem that high speed neutrons move too quickly to be absorbed. A moderator is not needed to slow them down; the enrichment level is high enough such that a steady fission process can be maintained. The FSP reactor has a fuel enrichment of 93%.^[193] In other words, 93% of the initial fuel mass is the fissile U-235 material and the other 7% is the non-fissile U-238 material. This is a very high enrichment, but it significantly reduces the mass of the system while still providing a sufficient power output.

Another potential issue for nuclear reactors is the concept of Xenon poisoning. Xe-135 will begin to appear in the fission products of the nuclear fuel over time, and it can cause serious problems for the reactor.^[198] Xe-135 is a powerful neutron absorber; because of its large cross section, it has a very high interaction probability with thermal (slow) neutrons. As it absorbs neutrons and becomes stable, the Xenon atoms can build up and drastically reduce the reactivity of the nuclear reactor.^[198] This will not be a problem for the FSP reactor, mainly due to the fact that it is a fast spectrum reactor. Instead of dealing with slow thermal neutrons, it deals with fast neutrons.^[199] There is no moderator in the FSP reactor to slow down the fast neutrons. These fast, high speed neutrons are not as easily absorbed by the Xe-135 atoms, therefore significantly reducing the risk of Xenon poisoning.

Fuel Cycle

The fuel cycle was not explicitly stated in the online reports completed by the Fission Surface Power Team at NASA, so it had to be solved for separately. The fission rate (FR) was initially determined using the following equation.^[196]

$$FR = \frac{P_{thermal\ output}}{E_R}$$

$$where\ E_R = 3.2 * 10^{-11} \frac{W * s}{fission}$$

E_R is the conversion factor between fission energy and thermal power.^[196] The desired thermal power output, as mentioned in section b, was determined to be 465kWt.

$$FR = \frac{465 * 10^3 \text{ Wt}}{3.2 * 10^{-11} \frac{\text{Wt} * \text{s}}{\text{fission}}} = 1.453 * 10^{16} \frac{\text{fissions}}{\text{s}}$$

The burn-up rate (BR) was then calculated using the fission rate (FR) from the previous step, the molar mass (M_{fiss}) of the fissile material (U-235), and Avogadro's number (N_{Av}).

$$BR = (FR) * \left(\frac{M_{\text{fiss}}}{N_{\text{Av}}} \right)$$

$$BR = \frac{\left(1.453 * 10^{16} \frac{\text{fissions}}{\text{s}} \right) * \left(235 \frac{\text{g}}{\text{mol}} \right)}{6.02 * 10^{23} \frac{\text{atoms}}{\text{mol}}} = 5.67 * 10^{-6} \frac{\text{g}}{\text{s}} = 0.178 \frac{\text{kg}}{\text{yr}}$$

The burn-up rate describes the rate at which the fuel is used up (on a mass basis) over a certain period of time. This value can thus be used to determine the remaining fuel mass after a certain period of time.

The enrichment of the fuel used in the reactor was said to be 93%.^[193] In other words, 93% of the fuel was fissile Uranium-235, while the remaining 7% was non-fissile Uranium-238. The initial fuel mass was 159 kg. 93% of the initial mass amounts to about 148 kg, meaning that the initial U-235 mass was 148 kg. To determine an approximate final mass of U-235, it was estimated that once the fuel had reached a mass equivalent to that of 5% of the initial mass, the reactor would become subcritical and no longer be able to sustain the nuclear fission process. At this point, the fuel cycle would be over and the reactor would need to be refueled. 5% of the initial mass, 148kg, was found to be 7.95kg. Using the burn-up rate of 0.178 kg/year and the final fissile material mass of 7.95kg, it was determined that the time required for the fuel mass to be reduced to 5% of its initial mass was about 44 years. Thus, the fuel cycle for the 100kWe FSP reactor is 44 years.

Control Systems, Transportation Safety

The reactor module itself consists of six control drums, three start-up control drums and three fine-tune control drums. Each of these control drums are made up of a neutron reflector material and a neutron absorption material. The reflector material, Beryllium (Be), causes an increase in the movement of the neutrons within the nuclear fuel core, which increases the reactivity of the material. The absorption material (Boron-Carbide, B₄C) has the opposite effect, reducing the number of moving neutrons in the core and thus lowering the reactivity. The control drums can be configured in certain arrangements and orientations to achieve a range of reactivity levels. When all six of the control drums are oriented with the B₄C side facing inward toward the fuel core, reactivity will be at its lowest. At this point, it is not possible for the nuclear fuel to reach a critical state. There is not enough reactivity for the fuel to transition from a subcritical state to a critical state, thus it will be safe to transport. The control drums can actually be configured such that the three start-up drums are in their reflector orientations and the three

fine-tune drums are in their absorption orientations, and the reactor will still maintain a subcritical state. The critical state can only be reached the correct number of control drums are oriented in a specific direction and at a certain reactivity level.^[193]

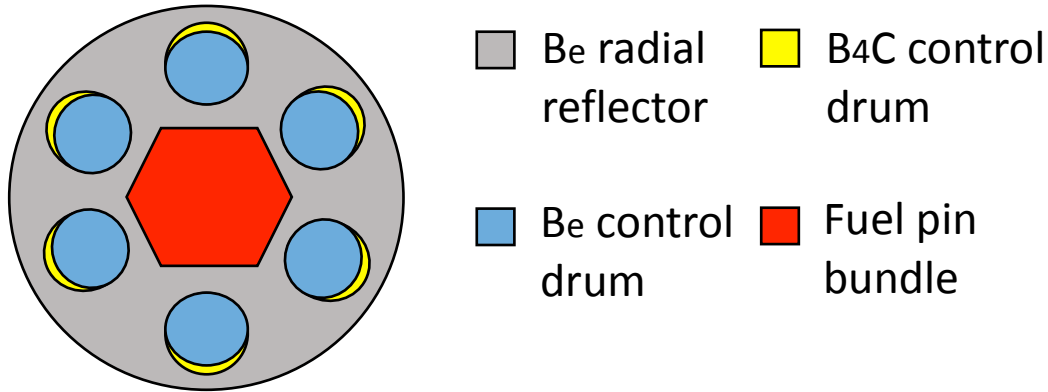


Figure 160. Reactor Module

Safety Features, Assessment

Several safety measures have been used in the reactor system to ensure that a nuclear disaster is not even a possibility. The sixth control drum in the reactor module is there for redundancy in the case that one of the control drums fails. One drum can fail to move to the correct orientation, and the state of the reactor will still be maintained. For instance, if the reactor is in an operational (critical) state and one of the control drums abruptly fails to move to the correct position, the critical state will be maintained. There is no risk of a sudden power change or further system failure. The reactor also has a negative temperature coefficient of reactivity. A change in the temperature of the reactor module has the potential to affect reactivity. This impact on the reactivity is described by the temperature coefficient of reactivity. In the case of this reactor, the temperature coefficient of reactivity is negative; in other words, any increase in temperature in the reactor module will actually result in a decrease in reactivity. This is ideal for nuclear reactors. A sudden temperature spark will not be dangerous to the stability of the reactor. In this way, the reactor essentially has the ability to self-regulate, keeping its own internal reactor temperature relatively constant. In addition, the radiation levels of the reactor are guaranteed to remain below the standard limit of 5 rems/year for unshielded settlement residents, as long as the minimum distance from civilization is regularly maintained.^[193]

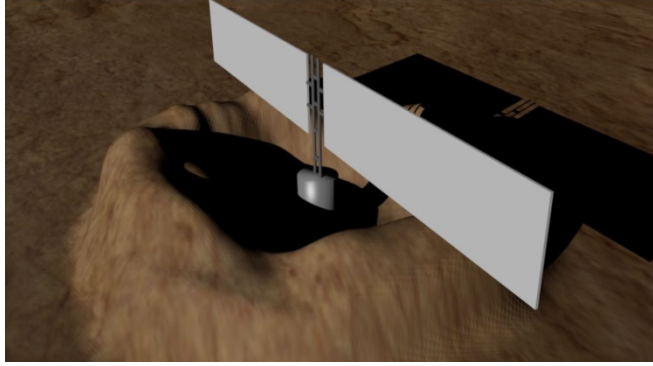


Figure 161. Reactor With Berm

Future Considerations

Future considerations for the nuclear reactor power system would include robotics for refueling, increasing design life of materials, and waste management plan for radioactive materials. A specialized robotics system would need to be developed that is designed to handle the high levels of radiation emitted from the spent nuclear fuel. This robotics system would be used to remove the remaining fuel from the previous fuel cycle and replace it with new fuel. The electronics within this system would require significant protection against the radiation; otherwise, they would not be operational in such a situation.

The FSP team noted that the planned design life was 8 years, though there were few limiting factors.^[195] The design life of the materials that make up the reactor components would most likely be the limiting factor of the FSP system. However, FSP team leader Donald Palac stated that this design life was chosen due to limitations on the available time for life testing, rather than limitations imposed by the actual material lifetime.^[194] He also noted that the design could potentially be extended to 15 years or more if certain steps are taken.^[194] It would be beneficial for further research to be done in order to maximize the extension of the reactor design life.

The fuel cycle of the reactor, as determined in the FSP Fuel Cycle section of this report, will be about 44 years. This would mean that the highly radioactive nuclear fuel remaining in the reactor at the end of 44 years would need to be taken out and stored in a heavily shielded location. A management plan for this nuclear waste would need to be fully planned and tested before the first refueling session takes place. This waste management plan will most likely consist of the use of containers that are heavily shielded against high levels of radiation, in combination with the Martian regolith; the regolith acts as a natural shield against radiation. In addition, sizable radiators could be required to dissipate the large amounts of heat being dissipated by the nuclear waste.

6.4.10. Habitat Power Management

The management of the power output from the FSP will be managed and distributed by the PMAD module, which provides the main electrical control functionality for the FSP system. The module also provides the means by which the users communicate with the FSP. The PMAD includes all the cabling, controls, diagnostics, and power supplies to operate the system including a battery for startup power and can be connected to solar arrays in case of simultaneous failure of the three FSP systems. The PMAD's main purpose is to provide provides a regulated 120 Vdc bus interface that allows users to directly

connect and disconnect loads. The reason a high voltage was used is because most of our power is being consumed by large machinery such as the electrolyzers or charging stations and hence operating at low voltage would not be feasible. The overall design philosophy is based on parasitic load control meaning that the system generates full power continuously and dissipates any excess power not required by the loads via a resistive load bank. This isolates the thermal power system from electrical transients resulting in fewer thermal cycles and longer service life. Most importantly of all, the above characteristics result in the PMAD being autonomous and self-sufficient.

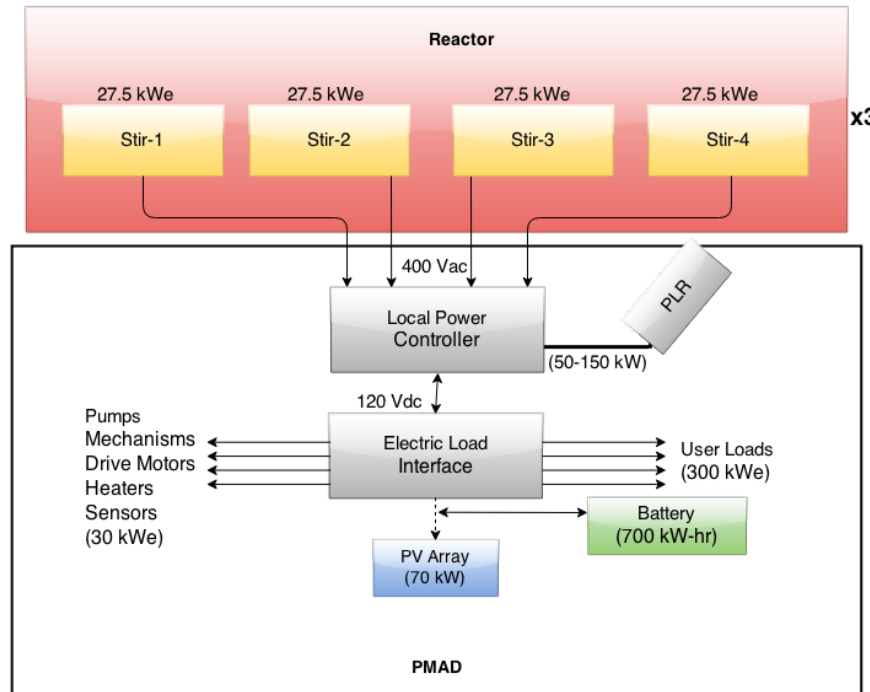


Figure 162. Power Path for Asimov City

Local Power Controller

The Local Power Controller (LPC) contains the reactor and power control computers that receive data signals and issue commands to permit autonomous operation of the FSP system. The reactor control computer interprets instrumentation signals and relays commands to power supplies that move control drums or adjust NaK pump flow. Once at steady operation, conditions would be continuously monitored but reactor module adjustments would be fairly infrequent. The power control computer would monitor the Stirling converters to adjust piston stroke and Parasitic Load Radiator (PLR) set point depending on the desired amount of electric power output. In addition, the power control computer would maintain the heat rejection pumps and water loop auxiliary heating, with constant monitoring but fairly infrequent adjustment. The reference system assumes a master and backup computer for both the reactor and power control computers.

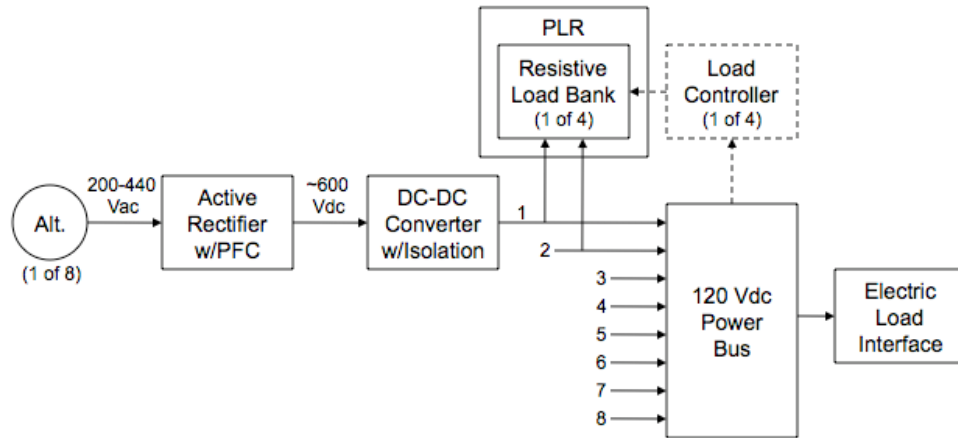


Figure 163. LPC Components

The LPC also includes the electronics to convert the Stirling alternator power from ac to dc and regulate the 120 Vdc output for distribution to the Electric Load Interface as shown schematically in the figure below. Each of the eight Stirling alternators has a dedicated power channel that processes the single phase 60 Hz alternator output. The design-point output voltage is 400 Vac rms at 13.25 kW (reached by scaling up the initial design of 6 kW). Stirling output power can be varied between about 50 and 110 percent, corresponding to alternator voltages between 200 and 440 Vac, while maintaining the regulated 120Vdc bus. The first LPC stage converts the alternator's ac output to 600 Vdc using an active rectifier with power factor control (PFC). This stage delivers a near-constant dc output voltage over a wide range of alternator supply voltages while maintaining optimum power factor. The second stage is a dc-dc converter that converts the 600 to 120 Vdc and provides isolation against electrical faults and grounding issues. Voltage reduction is provided by an inverter and high-frequency transformer-rectifier that can isolate faults. Voltage regulation is performed with a parasitic load controller that senses user load demand and draws any additional current needed to maintain a fixed bus voltage using a resistive load bank. Each pair of Stirling alternators use a separate parasitic load controller. The four parasitic load banks that comprise the PLR are arranged in parallel with the 120 Vdc power bus, separated only by a disconnect switch for each alternator pair. This PMAD architecture permits the system to produce 120 Vdc regardless of alternator voltage, making partial power operation seamless to the power bus. An additional benefit is that the system can provide regulated power during the FSP startup to expedite the switchover from external power sources. The LPC electrical components are housed in a 1 by 1 by 1m aluminum enclosure that includes cold plates and thermal radiators to maintain electronic temperatures below 330 K. The one-sided radiators, providing 2m² surface area, are mounted on the outside of the enclosure and hinged to permit a manual deployment for improved view factor to space. The PLR is sized to dissipate 150kW at 770K. The two-sided PLR, approximately 2m tall by 1m wide, would be delivered separately and attached to the top of LPC at the outpost.

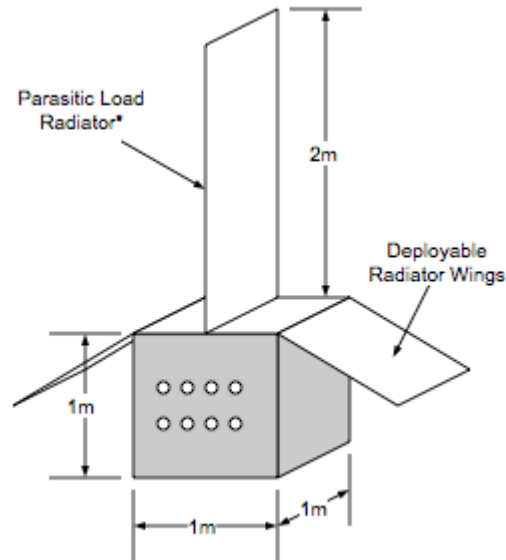


Figure 164. LPC enclosure and radiators.

Electric Load Interface

The Electric Load Interface (ELI) serves as the FSP system's interface to the outpost. It provides the access point for FSP-generated electric power and the communications link for FSP system operations data. There are 4 separate power nodes, habitat & greenhouses user loads, FSP auxiliary loads, processing plant and the recharging station. Each would have its own ELI receiving power from the reactors.

The user load interface is envisioned as an electrical switch panel, similar to a residential breaker box, which would allow users to connect various size loads as required.

The auxiliary power panel, next to the user load interface, would feed individual power supplies located with the ELI that provide the electrical input for FSP pumps, motors, heaters, and sensors. A system interface computer provides supervisory control for the ELI functions. The ELI components are housed in a second 1 by 1 by 1 m aluminum enclosure with external radiators, similar to the LPC.

Transmission Cabling

The transmission cabling for the FSP system includes the main power cable from the Stirling alternators to the LPC, the data cabling from the truss-mounted instrumentation relays to the LPC, and the auxiliary power cable from the ELI back to the reactor installation. All cabling is assumed to be placed on the surface with a 180° view to space. The cabling is based on spaceproven MIL-STD ETFE (ethylene-tetrafluoroethylene) insulated, tin-coated copper conductor rated for up to 600 V and 150 °C. All cables are 600m long which includes 20 percent length margin relative to the 500 m separation distance. The twenty-four 13.25kW, 400Vac alternator power cables carry about 33.1A each and require two 5 AWG conductors. Total resistance is 0.6Ω resulting in about 660W power loss, which is equivalent to 95 percent transmission efficiency. The data cabling is assumed to include four 16 AWG conductors, two primary and two backup. The auxiliary power cabling is assumed to include twenty 10 AWG conductors suitable for up to ten 3kW power loads at 120 Vdc, or 30kW total. The auxiliary power cables would be grouped as necessary to meet the various FSP parasitic loads at the reactor installation.

Solar Array and Battery

A 70kWe photovoltaic (PV) solar array and a 700 kW-hr Li-ion battery are included with the FSP PMAD module and connected to the 120 Vdc ELI at the outpost. The battery is needed to start the reactors, and also if all three reactors fail, it has enough energy to maintain the habitat as habitable for a full day. This provides time for the crew to lay out the solar arrays, which will be used till the reactors are once again operational.

A notional FSP startup power profile for a single reactor is show in the figure below. Startup would be performed over a period of approximately one Earth-day with pauses at incremental steps during the ascent to full power. The first 5 to 6 hours would be the most power intensive and would include radiator panel deployment, water loop charging, NaK and water fluid pumping, and Stirling electrical motoring. Maximum power draw is almost 10kW between hours 4 and 5. At the 8-hr mark, the system is at “breakeven” power. By the 10-hr mark, the system is producing 25 percent power and is no longer dependent on the solar array and battery. By the 18-hr mark, the system is at full power providing 110kW at the PMAD power bus with up to 10kWe available for the auxiliary FSP loads.

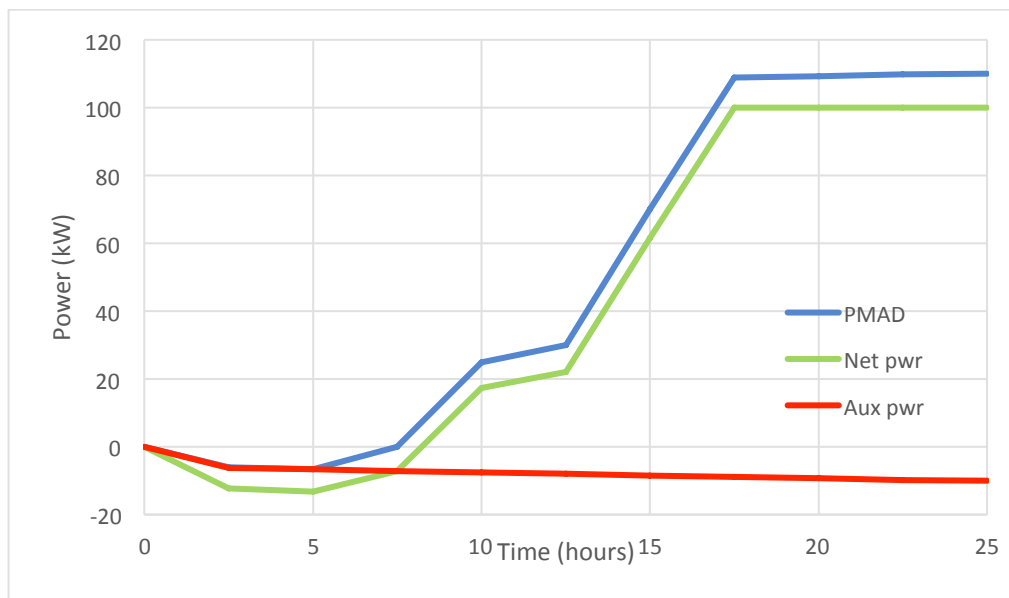


Figure 165. FSP startup power profile

6.4.11. Habitat Thermal Control

Maintaining the temperature inside of the habitat in necessary for the survival of the crew and crops. This prevents a significant challenge because the temperature at Hellas Planitia has been recorded as low as 177K and as high as 297K. Additionally, heat is constantly being generated inside of the habitat. To develop a thermal control solution, a model of the heat transfer in and out of the habitat must first be developed.

One of the major characteristics of this habitat is that it is covered by a 5 meter thick layer of regolith. The regolith barrier not only serves as a radiation shield for the astronauts, but also has the added benefit of acting as thermal insulation for the habitat. A simplified thermal model for the habitat was developed based on conduction of heat through the regolith barrier. The net conductive heat transfer through the regolith based on 1-D heat conduction is:

$$\dot{Q} = 7 \left(x_{reg} k_{reg} L_{hall} (2\pi) \frac{(T_{hab} - T_{env})}{\ln\left(\frac{r_{reg}}{r_{hall}}\right)} + (1 - x_{reg}) k_{reg} L_{hall} (2\pi) \frac{(T_{hab} - T_{ground})}{\ln\left(\frac{r_{ground}}{r_{hall}}\right)} \right) + 6 \left(x_{reg} k_{reg} L_{hub} (2\pi) \frac{(T_{hab} - T_{ground})}{\ln\left(\frac{r_{ground}}{r_{hub}}\right)} + k_{reg} \pi r_{hub}^2 \frac{T_{hab} - T_{env}}{x_{reg}} + k_{reg} \pi r_{hub}^2 \frac{T_{hab} - T_{ground}}{x_{ground}} \right)$$

where n_{reg} is the fraction of the habitat in contact with the regolith radiation barrier. From this equation, we find that the heat loss through the regolith across the entire habitat for an environmental temperature of 177K is 16.5 kW. This is significantly less than the total heat generated inside of the habitat; therefore, additional heat extraction methods are required.

Radiators

In order to maintain a thermal equilibrium within the habitat, all excess heat that is not lost through the regolith barriers must be pulled out of the habitat and dispersed. To do this, radiators will be used. The required size of the radiators corresponds to the design case for the radiators. The design case is a function of the radiator properties, the required heat dissipation, and the environment in which the radiator is operating. Each hub and hall will have its own system of radiators corresponding to the required heat dissipation. The thin Martian atmosphere allows for heat transfer from the radiators through radiation as well as convection. Therefore, the radiator area follows from the equation:

$$A = \frac{\dot{Q}_{diss}}{\sigma \varepsilon (T^4 - T_{env}^4) + h_{env} (T - T_{env})}$$

where A is the radiator area, \dot{Q}_{diss} is the excess heat dissipated, σ is the Stefan-Boltzmann constant, ε is the emissivity of the radiator, T is the temperature of the radiator, T_{env} is the environmental temperature, and h_{env} is the convective heat transfer coefficient of the Martian atmosphere.

Two different design cases were constructed for the radiators, one for the crew modules and one for the greenhouse modules. The design cases are representative of the maximum heat load to the radiators and the maximum heat backload from the environment. The excess heat load in each crew module is 5.5 kW, and the excess heat load for each greenhouse module is 23 kW. The remaining parameters of the design case are as follows:

Variable	Value
----------	-------

σ	$5.67 * 10^{-8} \frac{W}{m^2 K^4}$
ϵ	0.9
h_{env}	$2.929 \frac{W}{m^2 K}$ [78]
T	323K
T_{env}	297K

Table 59. Habitat Radiator Design Parameters

The resulting radiator areas are 24m² for each crew module and 99m² for each greenhouse module.

Much of the excess heat generated by the habitat comes from the LEDs used in the greenhouses. Since the LEDs are operating in a cycle, they will be turned off for a period of time and the amount of excess heat will decrease dramatically. During this period, resistive heaters will be used to recuperate the energy loss through the regolith and maintain a constant temperature inside of the habitat. The resistors will add 13 kW of heat across the entire habitat.

Pumped Fluid Loops

Each module will contain a two loop pumped fluid loop to carry the heat from inside of the habitat to the radiators. The internal loop will use water due to its high heat capacity and non-toxicity. One concern with the external fluid loop is radiator freezing. The lowest recorded temperature at Hellas Planitia is 177K which is below the freezing point of many working fluids used in pumped fluid loops. To rectify this problem, a bypass valve was added to the external loop.

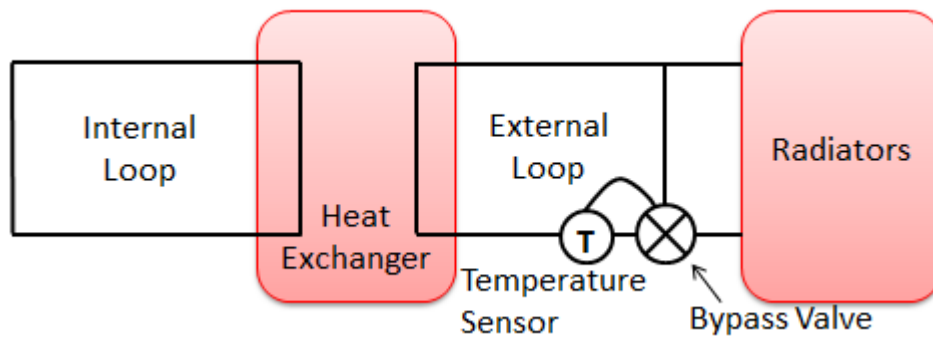


Figure 166. Diagram of Pumped Fluid Loop Using Bypass Control

The bypass valve operates by monitoring the temperature of the flow and comparing it to a set desired value. When the temperature falls too low, the valve can open and allow for more of the warm radiator inlet fluid to mix with the cold outlet fluid. In doing so, the excess heat is used to reheat the outlet flow instead of dissipating to the atmosphere through the radiators. The analysis of this system involves simultaneously solving three equations: [79]

$$\frac{dT}{d\zeta} = \frac{C}{F_{radiator}} (T^4 - T_{env}^4)$$

$$T_{setpoint} = (1 - F_{radiator})T_{radiator,in} + F_{radiator}T_{radiator,out}$$

$$T_{radiator,in} = T_{setpoint} + \Delta T_{design}F_{load}$$

where dT is a differential temperature drop of the radiator fluid, $d\zeta$ is a non-dimensionalized length along the flow path, C is a constant representative of the fluid and radiator, $F_{radiator}$ is the fraction of the flow into the radiator, T is the temperature of the fluid at any given point, T_{env} is the environmental temperature. $T_{radiator,in}$ and $T_{radiator,out}$ are the inlet and outlet temperatures of the radiator fluid, and F_{load} is the fraction of the design heat load that is being dissipated through the radiator. $T_{setpoint}$ is the desired temperature of the flow at the mixing point, and ΔT_{design} is the difference between the radiator inlet temperature and the setpoint temperature.

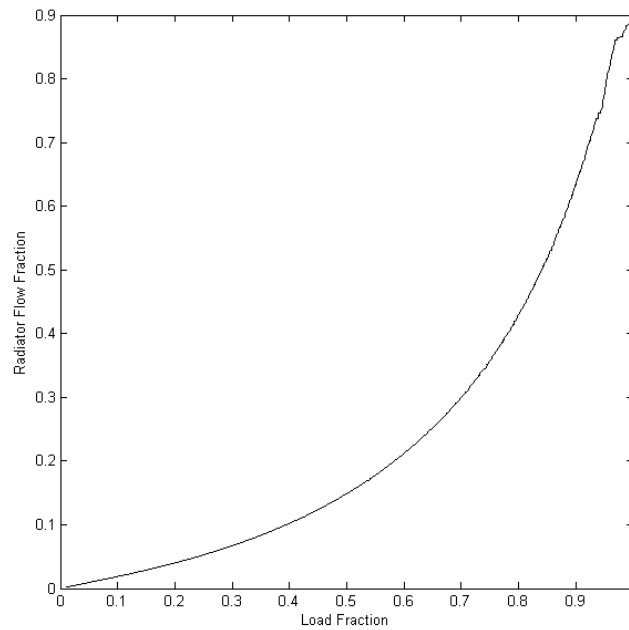


Figure 167. Radiator Flow Fraction vs. Heat Load Fraction

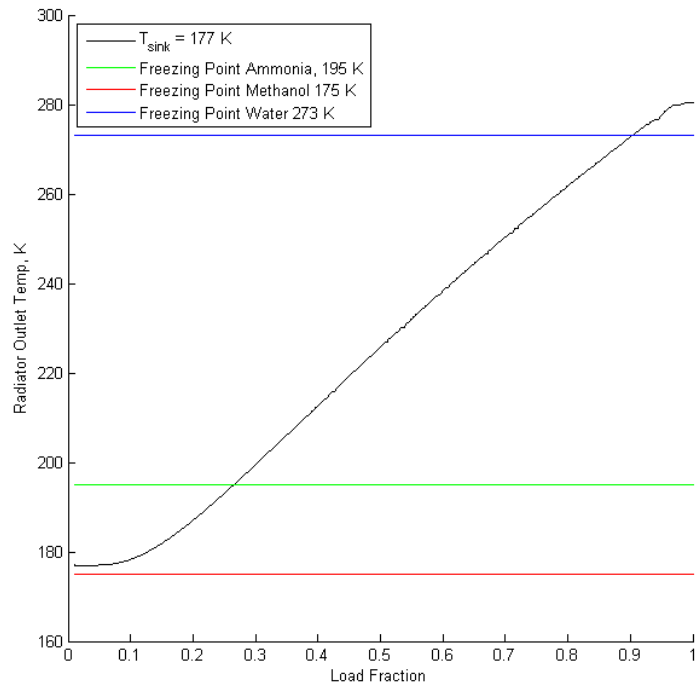


Figure 168. Radiator Outlet Temperature vs. Heat Load Fraction

Figures 167 and 168 show the radiator outlet temperature and the required flow through the radiators for an environmental temperature of 177K. Figure 168 shows that methanol is a good choice as a working fluid for the external loop. The freezing point of Methanol is 175K, which is below the lowest recorded temperature at Hellas Planitia. Methanol will not freeze even with zero excess heat load in the habitat. Additionally, if the temperature at Hellas Planitia does drop below 175K, the bypass valve can be activated to prevent freezing. Finally, if there is a leak in the piping, then Methanol can be created from the natural resources on Mars to replenish the fluid loop.

6.4.12. Habitat Avionics and Sensors

The Habitat utilizes the same Environmental Sensor Package (ESP) as described in the CTV section of Phase 4. This was done in order to create a standard of sensor suites among all of the pressurized vehicles and habitats. This in turn allows for easier repairs and less diversity of unnecessary replacement parts.

The only main difference between the sensors in the habitat, is that they need to be slightly modified in order to be used in the greenhouse portions of the habitat. The sensors in the ESP are normally calibrated for an atmospheric composition designed for human breathing, not a Nitrogen rich environment like that in the greenhouses as previously mentioned.

6.4.13. Habitat Communications

On the surface of Mars, the habitat will require a system which allows for humans to communicate with one other and for electronics, which include sensors and instruments, to be able to uplink data and downlink operational commands. Therefore a combination of a wired and wireless network will be set up as the main communication interface on the settlement.

Internal Command and Data Handling

Each hab and hub, or Module of the Asimov settlement shall have its own internal communication system. This will be an array of space grade Ethernet wire, similar to SpaceWire, which connects each sensor, instrument and electronic equipment to the central computer. The Ethernet will be used for all command and data handling within the unit. This includes uploading of data and downloading of instruction to electronics compiled from the computer. The data flow between instruments will nominally be half duplex as command and downlink will not be necessary simultaneously. Intercom will be facilitated with the use of wall mounted radios. The physical wiring of this network shall be done either along the inner walls of the habitat or through the walls to minimize safety concerns. The Ethernet wire has can reach data rates in the 100's of Gbps range which is incredibly faster than any other C&DH technology and consumes milliwatts of power per byte transferred. The central computer of each module shall handle all outbound communication which will be routed to the Ad Hoc wireless network. The wireless network will connect each node of the habitat with one another.

SpaceWire was the main contending alternative to the Ethernet for primary C&DH as it is already a known and reliable technology. However, after realization that the habitat will be protected from space radiation, it will be an unnecessary to use that reinforcement. Another contender was MIL-STD 1553. Although this technology is reliable and demonstrates great redundancy, the technology is far too behind as the data rate capable is at most 1 Mbps.

Wireless Network

Each habitat module and remote entity such as rovers or traveling astronauts cannot be connected to the habitat via SpaceWire or wired Ethernet. Therefore, it is necessary to implement a wireless network on the settlement. This network will allow for communication between all nodes on the surface which includes habitat modules, rovers and buggies, and roaming astronauts. The radius of reach of the wireless communication will be 6 miles for an optimal link between two nodes. However, the maximum distance that the radio signals reach can span up to a 13 mile radius.

There are two methods of organizing the architecture of this network. One is a centralized infrastructure schematic, whereas the other is a decentralized or Ad Hoc set up. The former method requires that one node in the system be the central routing point. Essentially, all communication will need to be routed through this node before reaching any other as a sort of a clearance point in that this node will need to administer permission for each communication relay before sending it off to the destination node. This structure enforces security and monitors the flow of traffic, but has the constraint that it minimizes the maximum distance from which a node can connect to the network. The Ad Hoc infrastructure allows any node to connect to any other node. This means that there are many different routes that a packet of data can take before getting to its destination node. The Ad Hoc system hence has a very strong built in redundancy. Additionally, this maximizes the distance between two nodes. For instance, as long as a node is in reach of one other in the system, it has the ability to communicate with virtually any other node in the array. Below is a schematic which represents the habitat wireless network. The yellow arrows show possible paths which data can be routed through to get from one node to another.

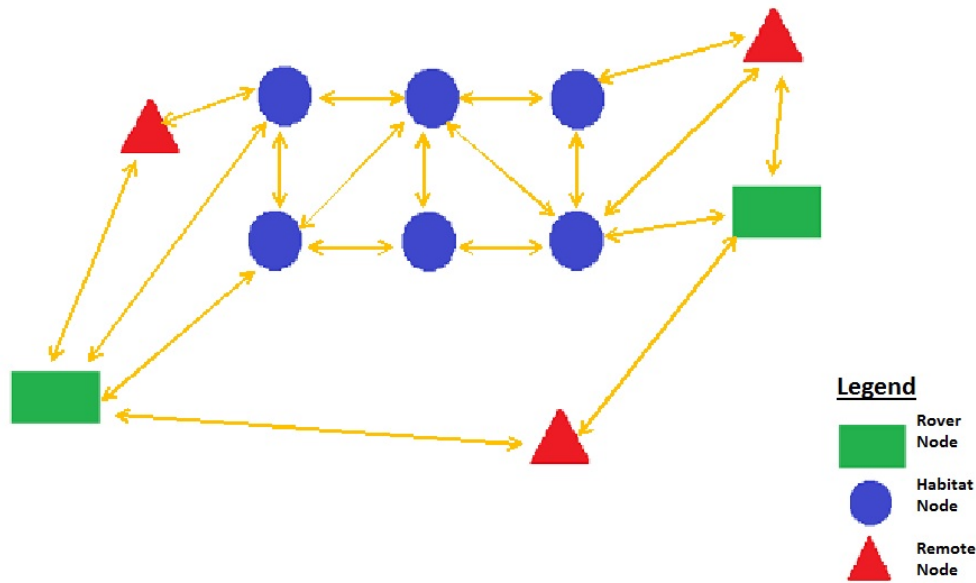


Figure 169. Wireless Network Schematic

Each node that will interface with the network will require a router. This router will support the acquisition and transmission of spread spectrum radio signals. Spread spectrum radio will have a data transfer rate of 2-11 Mbps and will require 40-800 mW per byte of data transmitted.

Interface with μ Net

During the early phases of the mission, communication to earth will be necessary. This will require the use of the communications constellation. To interface with the communication satellites, the wireless network shall connect to the ground station through a ground receiver. This data shall then be encoded and transmitted through the Asimov City Primary ground station antenna which supports communication directly to any μ Net satellite.

6.4.14. Habitat Emergency Preparedness

The habitat and crew will be prepared for a number of different emergency situations that could present themselves on the surface of Mars because of the danger such situations could put the crew in. This is another particularly challenging aspect of sending people to Mars due to the massive delay in communications. As such, the crew must be almost entirely autonomous and capable of handling any such emergency that should present itself because only minimal support can be offered once they arrive at Mars. To combat the potential danger of these situations, the crew will be trained heavily during their pre-mission training, briefed on the potential dangers, potential solutions, and trained to handle unforeseen hazards without help from a support team. When the crews are finally sent to Mars, a physical copy of the emergency procedure books will be sent with them, along with a digital copy, so that when one of these situations arise they have good guidelines for how to act. While it is unlikely that these emergency manuals will be able to handle all of the situations that might arise, and the instructions may not apply

perfectly, the crew will be well versed in these situations and will use the instructions to assist their own judgments in how to solve the problem.

The manuals will contain procedures for handling the following emergencies: power failure, large and small scale communications blackouts, environmental control or life support systems component failure, depressurization, harmful gas levels, fire, biohazard, medical emergency, stranded EVA crew, broken vehicles, and multiple crop failures. With the habitat designed for this mission, the crew will have a number of ways to mitigate the risk and damage associated with one of these emergencies. In the event of a potentially harmful gas level, depressurization, or a bad fire originating from one of the habitat modules, the crew will immediately evacuate the module and trigger the rapid-seal mechanism on the airlocks to effectively isolate the module from all others. The crew will then isolate the source of the problem, determine if the problem can be solved without depressurization of the module, and if possible, get in suits and fix the source of the problem. If the gas levels are too high, or the fire too large, the crew will depressurize the module to atmosphere until it is safe for the astronauts to enter the module in suits and determine the next best course of action to recover. If the fire is small, the astronauts will have one handheld, pressurized fire extinguisher capable of being refilled with in-situ resources. These fire extinguishers will be filled with a compound similar to Inergen, a common household fire extinguisher that is composed of 52% Nitrogen, 40% Argon, and 8% CO₂. This extinguisher was chosen because of the potential ability to refuel it with Martian atmosphere and because it can be used in small areas without posing a major threat to the crew.

In the event of one of these emergencies, a member of the crew will immediately message mission control with the details of the emergency and include any information that the crew has regarding the situation. In addition, a member of the crew will continue to update mission control of the actions taken to avert the crisis. This procedure will allow mission control to stay on top of the situation and as updated as possible. This is imperative so that mission control can assist in solving these situations by ensuring that the astronauts' actions are a good course of action. This also gives mission control the potential ability to assist the crew with future steps or secondary issues that may present themselves as a result of the initial problem, delay in fixing the problem, or faulty steps taken to fix said problem. While it is understood that mission control will be severely limited in their ability to help the crew through these situations due to the communications delay, it is imperative that they still follow the crew's decisions and status in the event that they may be able to offer some critical piece of advice. When handling an emergency that could have significant impact on habitability of the habitat or potentially harm the crew, as much extra help as possible should be provided to the astronauts.

The habitat design also includes a requirement that no two module failures can trap crew members. As a result of this the egress tunnels have a number of redundancies and many airlocks have multiple suit ports. This means that outside of two airlocks around a single hall failing, the astronauts will always have a means to move out of the isolated module. Should a double airlock failure occur, however, determining what caused the airlocks to fail, and how they should be fixed will be the top priority. Fortunately, since the most likely failure for the airlocks would be a leak leading to depressurization, this should be easily manageable to fix. In addition, unless the airlock has a gaping hole, the crew can leave it open while they evacuate the hall module and isolate the airlock to avoid further leaking.

6.4.15. Risk Analysis

As a result of the complexity of the systems and length of this mission, there is some inherent risk involved. However, major risk items were analyzed and remediation developed in order to decrease the impact severity and likelihood of the event actually occurring.

Analyzed Risk Events

1. Power loss/failure

Impact: Essential equipment failure.

Remediation: Redundant systems are built-in so one failure will not negatively impact essential systems.

2. Depressurization

Impact: Loss of atmosphere.

Remediation: Suitports in every airlock and the affected module can be sealed off until the source of the depressurization is detected and repaired.

3. Dangerous gasses (CO₂, CO, CH₄)

Impact: Impaired judgement and/or motor skills, unconsciousness, death.

Remediation: Gas masks will be available. Sensors are included to detect these gasses and alert the crew.

4. Fire

Impact: Loss of oxygen, smoke inhalation, and equipment and structural failures.

Remediation: The atmosphere contains a low partial pressure of oxygen so combustion is unlikely to occur. In the event of a fire, there will be handheld fire extinguishers in each module. In addition, if the fire is extremely severe, the affected module can be sealed off and fully depressurized in order to deplete the oxygen content and put out the fire.

5. Medical emergency

Impact: Crew injury or health issue

Remediation: All crew members must complete EMT training and medical supplies and equipment will be available in the Medical Bay.

6. Stranded EVA crew

Impact: Limited supply of life support in spacesuits and rovers.

Remediation: There will be three pressurized rovers to conduct rescue operations.

7. Crop failure

Impact: Depleted food supply, crew may not have all the nutrients they require for a healthy diet, 3-months until the next crop growth

Remediation: Excess crop area was designed into the habitat as well as food storage space.

8. Fishery failure

Impact: Depleted food supply, crew may not have all the nutrients they require for a healthy diet

Remediation: Excess cryogenically frozen fish-eggs will be brought to repopulate.

9. EVA medical emergency

Impact: Crew injuries and/or a difficult extraction from spacesuit in the event of a severe injury.

Remediation: EMT training, pressurized and unpressurized rovers to transport injured crew member back to the Medical Bay.

10. Nuclear Reactor Malfunction

Impact: Loss of power, radiation exposure.

Remediation: Safety Systems within the FSP Reactor, previously discussed in section 6.5.9, ensure that criticality can only be reached when the control drums of the reactor module are oriented in a very specific direction. Redundancy allows for multiple failures within the control drum system, reducing the

risk of unintended criticality or supercriticality to a negligible level. In addition, there will be three reactors at the Mars habitat. In the case that one of them fails, there will be two reactors remaining in operating condition, along with the secondary solar panel power system. The shielding of the reactor module, as well as the berm of regolith surrounding the module, reduce the level of radiation leaving the reactor enough that the settlers will not be negatively affected.

Impact

		Insignificant	Minor	Moderate	Major	Severe
Likelihood	Almost Certain					
	Likely		2			
	Possible		5, 6	1, 3, 3, 4		
	Unlikely			2, 7, 8, 9	10	
	Rare					

Figure 170. Surface Habitat Risk Matrix

6.4.16.Habitat Mass and Volume Breakdowns

Permanent Equipment

All items in the categories below are sent packed within the habitat modules. A detailed breakdown of items in each category can be found in Appendix A.

Category	Mass (kg)	Volume (m ³)
Hygiene	552	10
Medical Bay	686	6.04
Clothes Washing/ 3-D Printing	194	1.61
Water Pipes	1301	2.60
Backup CO ₂ Scrubbing System	198	0.44
Anaerobic Digestion System	300	3.6
Exercise	305	2
Cleaning	15	0.04
Kitchen/Dining	921	13.56
Crew Quarters	667	9.80
Miscellaneous	49	1.05
Total	5188	50.74

Table 60. Equipment Mass and Volume Breakdown

Consumables and Supplies

These mass and volume quantities provide a 13.5 year supply of each category for all 24 crew members, which are sent with habitat module. All items have long, or no, expirations, unlike the subset of consumables with short expiration times that must be sent on the CTV with each crew. A detailed breakdown of each category can be found in Appendix A.

Category	Mass (kg)	Volume (m ³)
Hygiene	322	7.14
Work Clothes	182	0.5
Packaged Food	15418	42.05

Fertilizer	14000	16.5
LEDs	1508	6.07
Miscellaneous	12	0.18
Total	31442	72.44

Table 61. Consumables Mass and Volume Breakdown

6.5. Construction

6.5.1. Overview

Building such a large-scale settlement on the surface of Mars is an incredibly challenging prospect. A large portion of team effort was focused on finding a way to reasonably complete such a complicated process. The first challenge with completing something of this magnitude is the unpacking and transportation of the large habitat modules. This means, absent a landing system capable of landing inches away from another module, some sort of transportation system is needed to move one of these modules from their landing location and configuration, into position for habitat construction. In addition, when trying to support 24 people on the surface of Mars for an indefinite time period, a massive amount of habitat volume is needed. This further complicates this transportation system by dramatically increasing the scale of the modules that need to be transported. The vehicle designed to handle this particular set of challenges is the Atlas Martian Crane. This vehicle also serves as the unpacking and transportation vehicle for sensitive payloads and general cargo; in addition to being the primary method of crewed egress from the EDL vehicle.

The next challenge that needs to be addressed for a construction process of this size is the need for very accurate landing sites. This was a driving factor on the EDL vehicles designed for cargo and crew transport to the surface because, without the ability to land within a few kilometers of the eventual habitat location, an absurd amount of time would be required to transport habitat modules. This would significantly delay the date which the crew can first move into their habitat, as well as the end date of the construction process. In a massive scale operation like this, every day of delay counts because it is yet another day without radiation shielding and, during the early stages, another day spent living in the pressurized rovers. To combat this problem, the landing locations are two and a half kilometers from the eventual habitat location, and the construction process has been structured such that the top priority is setting up all vital functions so that the crew can move into a habitat module as quickly as possible.

As mentioned before in this paper, a habitat of this size requires a massive amount of power for greenhouse operation, food storage, and other vital functions. As a result, three small nuclear reactors were selected to satisfy the large power requirements. Having nuclear reactors on Mars presents a significant design challenge for the construction process however, due to the potential danger to the crew. In order to handle this specific problem, the Atlas Martian Crane and pressurized rovers will act in tandem to set the reactors in their final location. Through teleoperation of the crane, the crew will be able to remain a safe distance away during setup.

6.5.2. Settlement Layout

There were a number of factors considered when choosing the layout of the habitat and the landing locations. The biggest challenge with creating a habitat layout and the landing locations of the EDL vehicles is balancing a close proximity to the habitat site, while also leaving a sizable gap in the event of issues with the avionics systems during landing. It is extremely important to minimize the risk of a landing vehicle hitting another vehicle, or the habitat itself, but short distances are also required to minimize transportation time for the construction process. Because there are 16 vehicles landing on the surface, a massive amount of time is spent on driving to each landing site, unpacking the vehicle, and then carefully transporting materials back to the habitat.

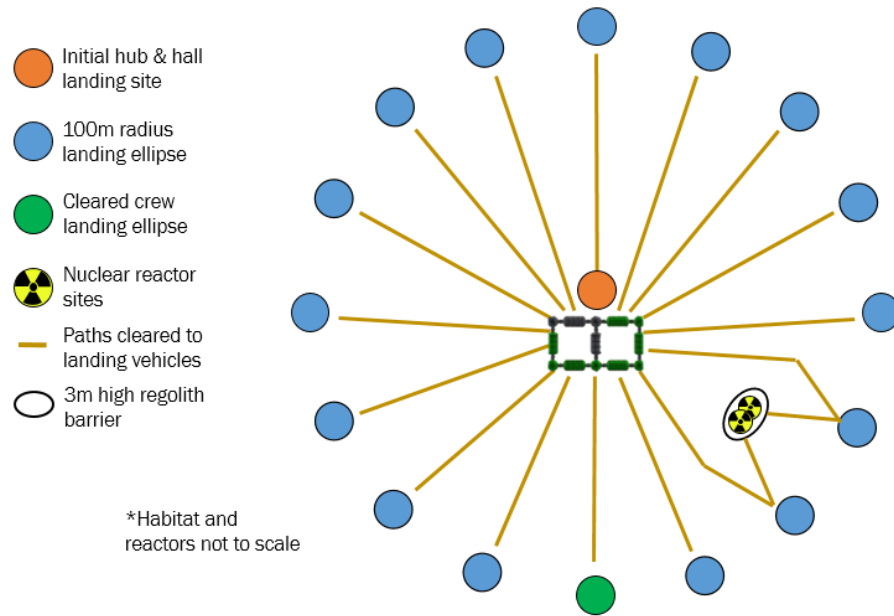


Figure 171. Settlement Layout

The entire habitat layout is centered around the initial hub and hall landing location. This landing vehicle will contain the first modules that will house the crew. Every following vehicle will be landed radially around this landing location to reduce the distance travelling between different landing vehicles. The distance between the center of each landing site and the habitat is 2.5 km. With landing vehicles as accurate as the ones required for a project like this, we determined that a distance of 2.5 km would be a sufficient distance from the habitat to reduce the chances of hitting another landing vehicle dramatically. Specifically, in the event of an avionics error increasing the landing zone to the size that it intersects with another vehicle (approximately 1 km radius), the percentage chance of this error causing the rocket to hit another vehicle is 0.1%, even in the event this faulty rocket tips over. This makes the separation between the external landing locations about 1 km. The southern half of this circle will contain the landing vehicles with the reactors and the vehicle that contains the processing plant and module end caps. These vehicles and their constituents are the immediate priority of the crew upon arrival. This allows quick access of the processing plant and end caps after placing the reactors in position, reducing the time of travel in the early stages of construction.

The reactors are located in the southeast side of the habitat layout, located a minimum of 500 m from the

habitat to reduce radiation exposure to the crew. A regolith wall will also be constructed around these reactors to further reduce radiation. Finally, there will be a designated landing zone for all crews following the first. This zone will be cleared of rocks by the pressurized rovers to remove the risk of the vehicle encountering rocks during landing. In the event that the designated area has rocks too large to be removed from the site, a different landing location will be selected such that a cleared landing site can be made. The remaining descent vehicles will land in other locations around the habitat, and their locations will be determined by GPS and sent to the crew. They will have a detailed map of where each vehicle lands and a list denoting the items contained in each vehicle. For every landing site, a path will be cleared of rocks in advance of the crane such that it never needs to encounter rocks while handling sensitive payloads. In addition, for cargo landings that will happen after the first crew arrives, their landing sites will be cleared of rocks as well. This configuration will enable our crew to complete the initial construction process as quickly as possible, and reduce risk of landing vehicles and cranes being damaged by rocks.

6.5.3. Construction Timeline

Once the crew approaches Low Mars Orbit the cranes and pressurized rovers will be given the signal to deploy themselves from their respective landing vehicles. One of these cranes and pressurized rovers will drive back to the initial hub and hall landing site, which will be used as the eventual habitat location. The crew will then transfer into the entry, descent, and landing vehicle and descend to the surface of Mars. Once the crew lands, the remaining two pressurized rovers and the other crane, with gondola attached, will drive to their landing location to lower the crew to the surface. Now, the crew will live in the pressurized rovers until they complete the first habitat module.

From the pressurized rovers' command station, the crew will teleoperate the crane and drive to the location of the reactor landing vehicle. The reactors will then be carefully removed and placed into the crane bed for transportation. Once the reactors are placed safely in the crane bed, the pressurized rovers will begin driving to the reactor site, clearing the path of rocks on the way via a plow attachment. The crane will follow approximately half a kilometer behind the rovers to avoid unnecessary radiation exposure to the crew. Upon clearing the reactor site of rocks and piling a 3m high regolith barrier between the habitat and the reactors, the crewed rovers will drive a safe distance away and teleoperate the crane as it places each reactor safely behind the barrier. Since this process is understandably delicate, this procedure will not be completed until wind conditions are low enough that the wind force won't create significant oscillations while the reactor is being maneuvered by the crane. Once the reactors are in place, the crewed rovers and crane will lay down the power lines as they drive back to the initial hub and hall landing location to set up the transformer.

During the time the crew is working on setting up the reactors, the uncrewed pressurized rover will be clearing the eventual habitat location of rocks. Additionally, once the habitat site is cleared, one of the mining vehicles will begin digging a trench the full length of the hall so that it will not roll when it is placed down. The other mining vehicle will also have begun stockpiling regolith for the processing plant. After the transformer is operational, the crewed rovers will clear the paths for both cranes and drive to the processing plant vehicle. Once there, they will remove a stack of hub and hall end caps as well as the processing plant. These will be transported back to the habitat location, and the processing plant will be set up a short distance away, near the transformer. Once hooked up to a reactor, the processing plant will begin producing water for habitat use.

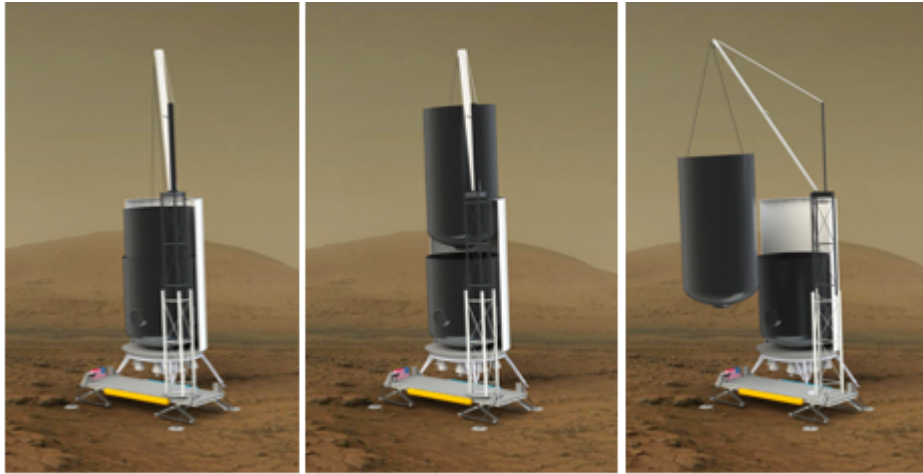


Figure 172. Hall extraction: (a) Crane attaching to hall (b) Crane lifting hall out of hub (c) Crane lowering hall to its bed

At this point, the crew will begin unpacking the first hall from the landing vehicle. Because the halls are being shipped inside the hubs and are also packed into an EDL vehicle, the fairing will first need to be blown out. After the fairing is removed, the crew will use both cranes to remove the airlocks stored above the two modules and lower them safely out of the way. One crane will have the standard hook attachment, and the other will have the gondola attachment with an astronaut in it. This crane will maneuver the astronaut in the gondola next to the attachment points for both the airlocks and the habitat modules. With the airlocks removed, the astronaut in the gondola will ensure both of the crane's winch cables are securely attached to the hall, and the crane will begin lifting it out of the hub. After the hall is lifted out of the EDL vehicle, the crane will place it into its bed and drive a short distance away to the actual habitat location. The support structure for the crane's bed will consist of an adjustable set of wire cables to accommodate transporting both hubs and halls.



Figure 173. Crane prepared to transport modules from their EDL vehicle to the habitat

Once the crane and hall are at the habitat location, the crane will lift the module off of the bed and lay it down in the trench prepared by the mining vehicle. On one end of the trench, there will be a deeper section, although the rest of trench will remain level. This deeper section around the open end of the module will allow the crane to lower the end cap into position. The end cap will then be carefully maneuvered over the flange and gasket of the module and locked in place with bolts. Once all of the bolts are properly tightened, the regolith will be pushed into the trench, filling the deeper section until it is the proper height for the airlock. The airlock will then be lowered into position and dock with the module. Because this process requires precision and cranes are not particularly precise, the attachment points that serve to enable lifting the module will be also be used with guy wires so that the module can be more precisely positioned.

Once the airlocks are mated to the hall and both doors are closed, the hall will be ready for pressurization. The compressed gas canisters that were shipped with these modules will now be opened and pressurize the module. The flange and gasket style connection for the end caps should form an airtight seal once the internal pressure starts pressing the flange towards the outer shell. Once the habitat is pressurized, the crew will officially move in to their new home. This marks the end of Stage 1 of construction.

During Stage 2, additional steps are required to allow the hubs to be operational. The crane will remove a hub from its EDL vehicle and transport it back to the habitat. Then, the hub will be placed into the position by the crane with the assistance of guy wires attached to the pressurized rovers. Through communication with the drivers of these rovers, the hub will be lowered next to the airlock and mate with it. Once the two structures are mated, the regolith will be pushed around the hub to ensure it is securely in place. Then, the crew and crane will begin attaching the hub's airlocks. Once these are attached the crew will place all of the large components, required for the first floor, into the hub with the assistance of the crane. After these components are positioned, the crane will then lower the second floor into the hub. Once the floor is lowered into the proper position, it will be bolted down. At this point, all components required for the second floor will be appropriately positioned. The placement of the third floor and its components will follow. Finally, using the same strategy for attaching the end cap as the halls, the hub will be ready for pressurization and the airlock doors between the hub and the rest of the habitat can be opened, expanding the livable space of the habitat.

Once the modules are put in place for Stage 2, the egress tunnels will be constructed by the astronauts. Though these will not be fully built at this stage, they will be laying the important infrastructure for when Stage 3 begins. This was determined an important step of Stage 2, however, because once the left side of the habitat matrix is completed, it will be challenging to construct these tunnels on the interior. All remaining stages of construction follow the same pattern outlined here for setting up the modules and airlocks and during these stages the crew will make regular trips to finish removing the materials from each payload as necessary

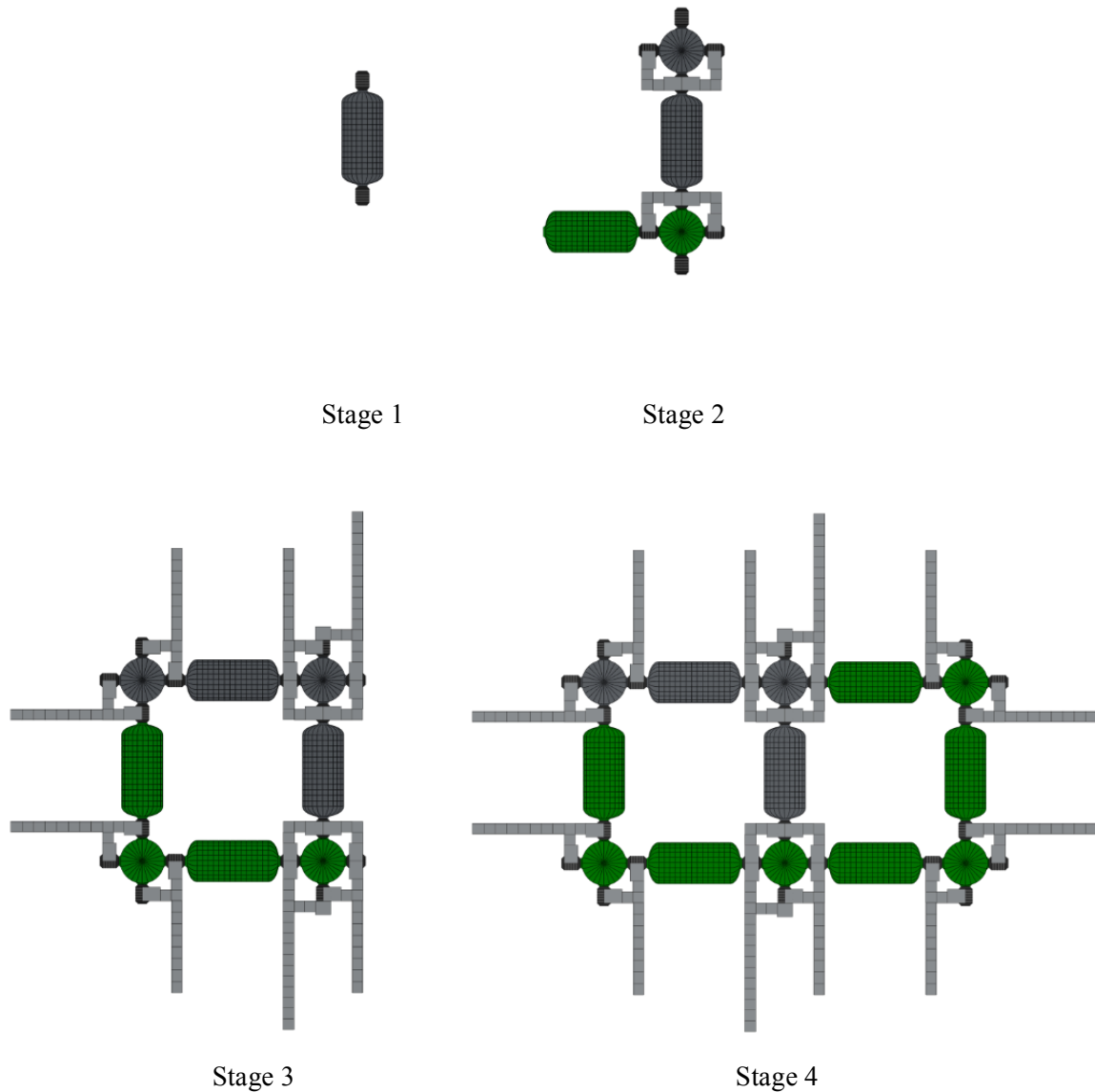


Figure 174. Stages of construction

Stage 1, which consists of the above steps, will take about one month to complete and by the end of that, the crew will move into the first crewed module. This is the minimum completion of the habitat that will allow the crew to move in. In the event this takes longer than expected, the crew is capable of being supported in the pressurized rovers for three full months, yet there is high priority on moving the crew out of the rovers and into the habitat as quickly as possible. This is primarily for the crew's mental health but also helps reduce load on the rovers.

Stage 2, which consists of completing the greenhouses and crewed section such that the crew will soon be entirely capable of supporting themselves, will be completed approximately 9 months after the crew's initial landing. Shortly following the completed greenhouses, crops will begin producing and the crew can slowly shift their diets over to their self-sufficient food source. It is at this point in time, that time will have to start being devoted to maintaining the crops. During this and the remaining stages, until completion of Stage 5, the miners will collect regolith for both regolith deposition and the processing facility. This will speed up Stage 5 of the construction process.

In Stage 3, the crew will be constructing the remaining crewed modules and greenhouses to support the addition of the second crew. At the completion of this stage, the entire left hand side of the habitat matrix will be completed and the habitat will be capable of supporting both crews. This will be completed shortly before June 2040, approximately 2 years after the first crew landed, when the second crew is set to arrive. During this time period, the dried food that the second crew brought with them will be used to supplement their diets until the plants are fully capable of supporting them. This additional food will allow our combined crew to live a full year without any supplement from the crops. Because the greenhouses will also be fully operational before our first crew exhausts their two year supply of dried food, any leftover food will be used in case of an emergency crop failure.

After the second crew's landing, Stage 4 will consist of crews maintaining greenhouses and completing the right hand side of the habitat matrix. Following this stage, the habitat will be fully capable of supporting the entire 24 person crew, and the habitat will be ready for regolith deposition. This will be completed a year late in June 2041, one year in advance of the third crew's landing.

Stage 5 will be the final stage of construction when the habitat is covered with a 5m layer of regolith for radiation shielding. This final stage will be completed by mid 2042 for the arrival of the third crew. From this point on, the habitat will be entirely self-sufficient and the crew will no longer need to worry about exposure to radiation, except during EVA's.

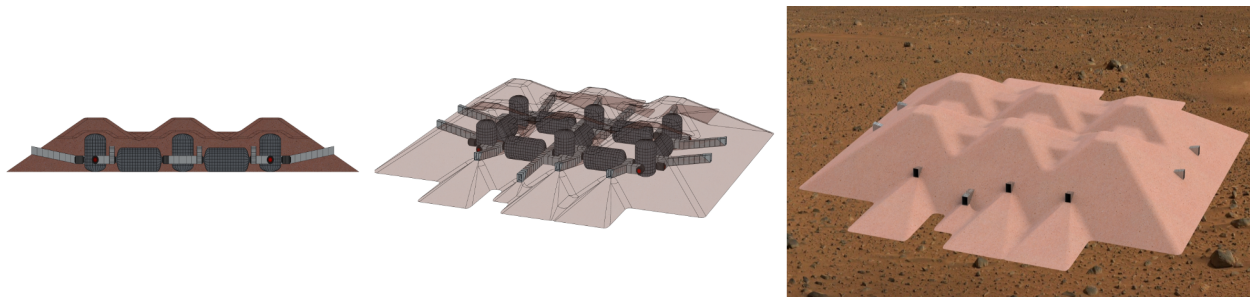


Figure 175. Habitat at the end of Phase 5, fully completed with regolith radiation shielding

6.5.4. Crane

6.5.4.1. Crane Structure

The Atlas Martian Crane has a dry mass of 24 Mt. It has a stowed dimension of 14m long x 5m wide x 4m tall.

As seen in the picture below, the main chassis of the crane utilizes a similar triangular truss structure as the miner. However the crane is slightly wider and longer than the miner in order to provide greater stability when lifting and carrying a payload. The general triangular truss structure however remains the same between the two vehicles. This was done so that if a part were to break on either vehicle, only one set of spare parts is needed.



Figure 176. Crane Chassis (1)

The Crane tower consists of the boom tower, which is made up of 3 parts (two triangular trusses and the top), and the boom arm which is made up of 2 parts. As depicted below, the boom arm has an operating radius of 18m.

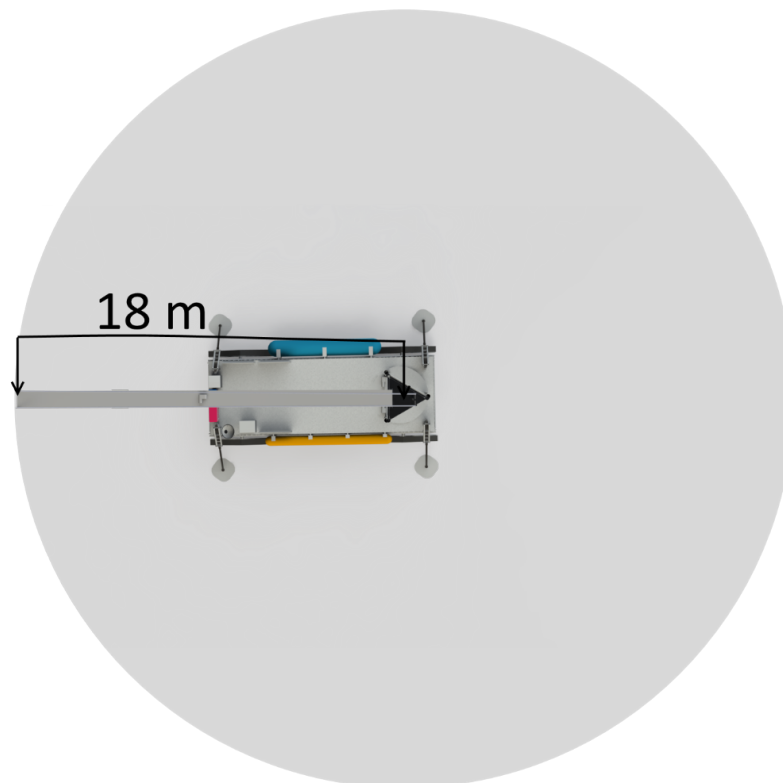


Figure 177. Crane's Area of Reach

Atlas utilizes a continuous track rocker system to gain traction on the loose Martian regolith. Tracks were chosen over wheels for the crane because they provide a larger surface contact area which is needed when driving on regolith.



Figure 178. Atlas Continuous Track Rocker

Atlas uses 4 supports that extend out when the crane needs to lift objects. The collapsed view of these legs can be seen below, these legs extend out from the crane bed, widening the crane's footprint.

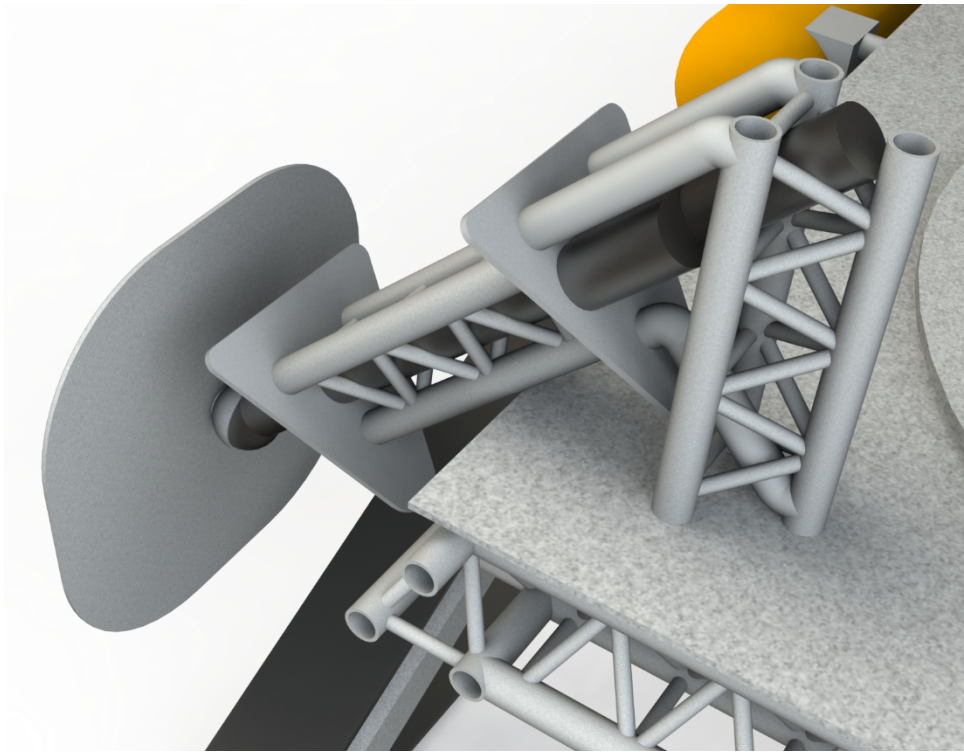


Figure 179. Collapsed View of Legs

Center of Gravity

The center of gravity (COG) for the crane when the tower is deployed without a load is directly in the center of the crane bed (see below.) When the crane lifts one of the hubs or halls, it moves roughly 0.5m away from the base of the tower.

6.5.4.2. Communications and Avionics

The Atlas crane uses a high power satellite dish to communicate with the rest of the base. This dish communicates over the Ka transmission band, as well as the habitat wireless network system that will be developed. Through these communication channels, the crane can be operated through teleoperation. The crane will also have the ability to operate autonomously for specific menial tasks that do not require direct human control. If there is an issue with the dish, an astronaut can take control over the rover manually through a sealed operating panel located on the side of the crane.

The Atlas crane keeps all of its necessary electronics and processing components inside of a radiation hardened box, located near the satellite dish towards the front of the crane.

6.5.4.3. Propulsion and Power

The crane that is going to be used on Mars is going to require a lot of torque, more torque than any electric motor or battery can provide. The amount of torque required to lift a 9 metric ton hall capsule off the ground would be around 3340 N-m, and the only way to provide this amount of torque with current technology would be to use an internal combustion engine run specifically on methane and oxygen. With a factor of safety of 2 the amount of power the engine would need to provide would be about 35kW.

To figure out the power produced by the engine, it was assumed that this engine would be running off a Brayton cycle for simplicity. The oxygen would run along part of the combustion chamber basically as a way to vaporize the oxygen into a gas, which would then flow into the combustion chamber. The methane would then be injected into the oxygen's flow with a fuel injector which would allow for more precise amounts of methane to take part in the combustion process. With this design the engine would be running at 35 cycles per second, which allow for the engine to produce more power at a lower cost to the fuel mass and would allow the engine to produce 36kW worth of power to the crane.

Based on the design of the crane, it will be able to store about 1000kg worth of liquid methane along with 5800kg worth of oxygen. However there is going to be some boil-off from the methane during the trip from LEO to the surface of Mars. The boil-off rate of liquid methane can be represented in this graph as a relationship to the thickness of the insulation around the methane storage tanks:

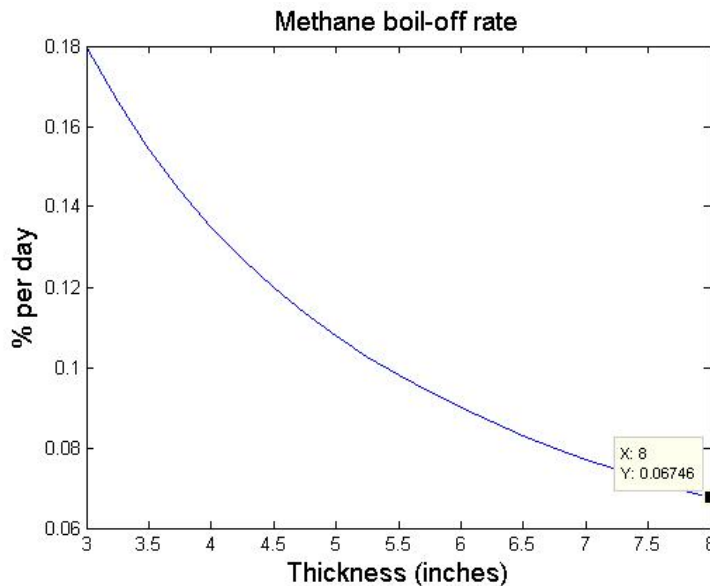


Figure 180. Methane Boil-Off Rate

Now from the graph shown, about 0.07% of the propellant will be lost each day to boil-off on the journey to Mars from LEO with 8 inch thick insulation. However, over the course of the roughly 260 day trip the total amount of propellant lost comes out to be around 20%, which results in 800kg worth of methane left in the storage tank once it reaches Mars.

Here is table showing the specifications of the engine (See Appendix C "Brayton_Cycle"):

Mass of Engine	300 kg
Volume of Engine	0.055 m ³
Mixture Ratio	5.8 : 1
Mass flow of LCH4	1 g/s
Mass flow of LOX	6 g/s
Operation Time	8 day 21 hours
Power Production	36 kW
Combustion Chamber Material	Niobium Alloy
Outer shell Material	Titanium
Coolant	Freon 21
Radiator Sizing	10 m ²

Table 62. Internal Combustion Engine Specs

The operation time was based off the total 800kg of liquid methane being used up in the system. The volume of the engine was based on dimensions of high performance NASCAR engines. The mass was based off the material used and the volume that amount of material took up in the engine.

Niobium Alloy was chosen for the combustion chamber material because it would not melt during the combustion of the methane due to its melting point (2700K) being higher than the combustion temperature (2500K). Based on the Brayton cycle the amount of heat left in the system could be calculated and assuming that the combustion chamber is a black body radiator the temperature left over could be calculated. This value turns out to be 2230K, which then is assumed is going to be radiated to the other material the engine is made out of. The design decision was made to make the outer shell of the engine to be made out of titanium because that would require less heat needed to be removed by the radiators. The reason being is that the melting point of titanium is higher than most common metals, which allows for less power needed to be removed to reach a little bit below that melting point. This would allow for less space required for the radiators, which is important because there is not a lot of available surface area on the Mars crane. To determine the amount of heat needed to be remove assuming a blackbody radiator:

$$P_{rad} = \sigma A_{comb}(T_{left}^4 - T_{melt}^4)$$

Power needed to be radiated away is related to the surface area of the combustion chamber, the temperature left in the system, the melting temperature of the titanium out shell and the Stefan-Boltzmann's constant.

The coolant used to cool down the engine is Freon 21, which was chosen because the temperatures on Mars will never reach the freezing point of Freon 21, -135 degrees Celsius, at the settlement location. The astronauts will not have to worry about Freon 21 freezing up in the pipes during the cold seasons.

Due to the constraint on surface area these radiators are going to need to radiate at higher temperatures because during the hot seasons these radiators are going to have to radiate out to 293K, which with the current radiator technology would take up too much surface area on the crane. The radiator area size is based on the power equilibrium equation:

$$P_{rad} = \sigma A_{rad}(T_{rad}^4 - T_{env}^4)$$

This crane instead of using the current technology for radiators it is going to be using carbon fiber radiators that are able to radiate up to 600K with an emissivity of 0.77. ^[171] These radiators at the moment are TRL 4, however with 6 months of production time and 283 thousand dollars the TRL level could be bumped up to a 5. ^[170] (See Appendix C “Material_For_engine” for more in-depth calculations)

The Atlas also utilizes an onboard CO₂ compressor to pull in CO₂ from the Martian atmosphere to be used for Atlas’ pneumatic actuators.

Hub/Hall Mobility Supports

The crane uses a series of aluminum rods located on the bed of the crane to help hold the hubs/halls steady when driving. The rods are positioned in a circular pattern and can be pinned in such a way that the diameter of the pattern can slightly change to accommodate the different diameters of the halls and hubs as seen below. Steel cables (not shown) run through the rods to provide additional support and can also change length to accommodate the different size loads.

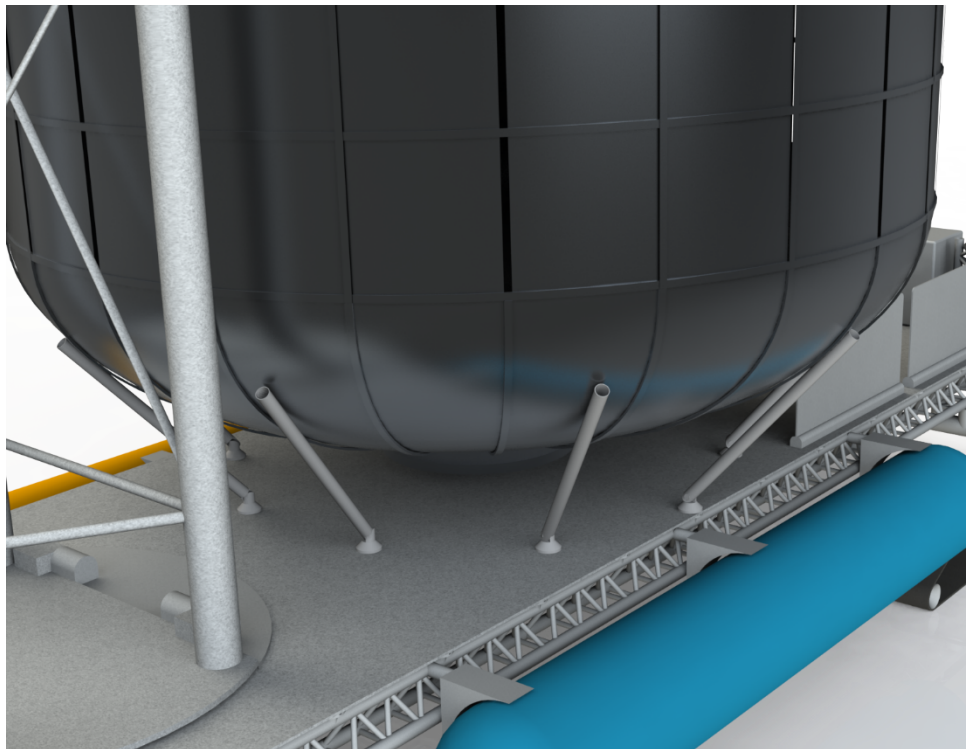


Figure 181. Atlas Payload Supports

LOX and Methane Tanks

With regard to the tanks that will be utilized for oxygen and methane storage, there are certain design requirements that must be adhered to. The materials will be made of aluminum (chosen at a safety factor of two) and a graphite/epoxy composite lined with aluminum. These were chosen for their sturdiness as well as their thermal properties and resistance to changes in temperature. The methane tanks will be

roughly 33% larger in terms of internal volume given the differences in the density for the propellants. In addition, the oxygen tanks will be more susceptible to pressure increases and venting issues during times of heat leaks at different phases (at around 250mW and 167mW, respectively). Lastly, the thickness of the methane tanks will be larger than the oxygen tanks, but only by a margin of roughly 50 percent.^[120]

6.5.4.4. EDL Vehicle Egress

During its final stages of descent, one side of the EDL fairing will be blown off, exposing the underside of the atlas crane along with a lowering bed as seen below:



Figure 182. Atlas Crane Initial Landing Configuration

The continuous track axles are attached to the lowering bed so that the crane does not move during EDL or when being lowered to the ground.

Once Atlas receives the command to begin deployment, a pneumatic actuator pushes the bed from a vertical position to 5 degrees off the vertical where it then releases.



Figure 183. Inital Deoployment of Atlas Crane

The bed is held in place by a steel cable and winch, and is then slowly lowered to the ground. If there is a malfunction, the winch can be operated manually through the use of a hand crank.



Figure 184. Atlas Support Bed Fully Deployed

When the crane is lowered all the way to the ground, the clasps that were connecting the axles on the tank to the bed are blown off, and the crane drives off the bed.

6.5.4.5. Crane Deployment

When the Atlas crane initially exits its fairing, the boom arm and tower still need to be deployed (As seen in image below). This is done autonomously in the following steps:

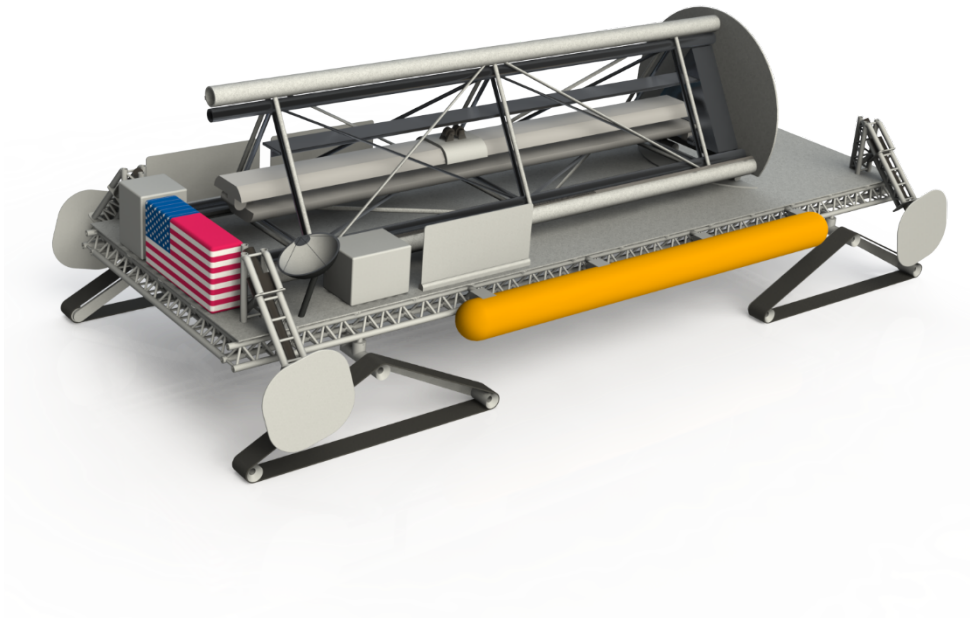


Figure 185. Atlas Crane Fully Deployed

The boom tower is lifted upright to a vertical position by using a pneumatic actuator. Once the tower is upright, it is permanently locked into place using clamps.



Figure 186. Boom Tower Being Raised

If there is an error with the pneumatic actuator, a cable can be attached between the top of the boom tower and the EDL fairing. The crane would then just drive away from the fairing, the tension of the fairing would pivot the boom tower about its hinges bringing it upright.

The boom tower consists of 2 triangular trusses that fit inside one another. Once the tower is upright, the interior truss raises itself through a rack-and-pinion system in between the two trusses.



Figure 187. Boom Tower begins to deploy

Once the interior truss is fully raised a series of solenoids automatically bolt the truss into place. The top platform is then raised using a rack-and-pinion system and bolted into place.



Figure 188. Atlas Boom Tower Fully Deployed

The folded boom arm is then lowered into place by using a winch located on the top platform.



Figure 189. Boom Arm Being Lowered

The second half of the boom arm is unfolded through another pneumatic actuator, and is lowered into place using a winch. When the two halves of the boom arm are parallel, they are permanently bolted together.

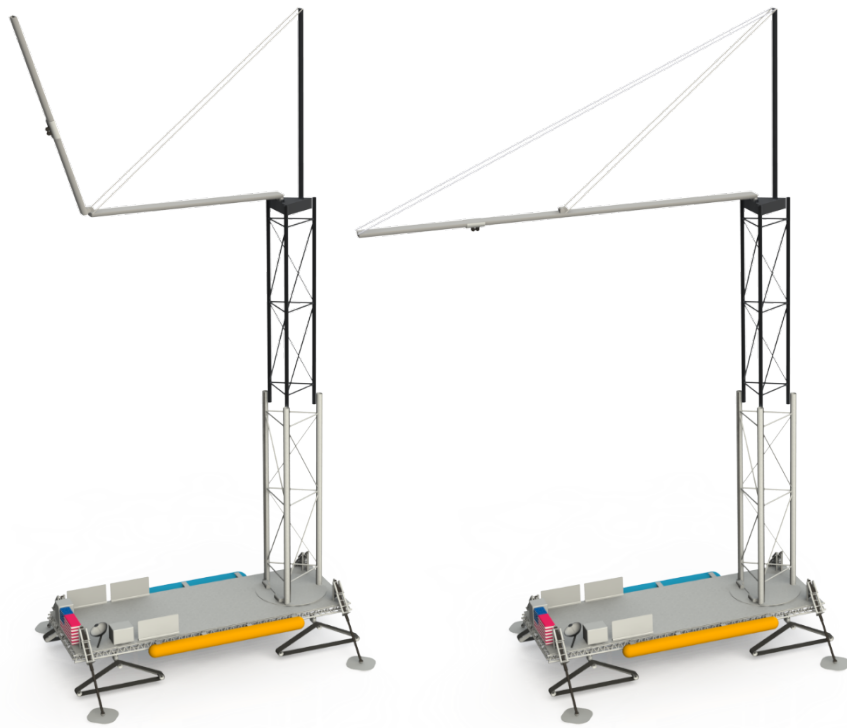


Figure 190. 2nd Half Of Boom Arm Being Lowered and Full Deployment

6.5.4.6. Crane Attachments

Two Cable System

The Atlas uses a two cable system to provide greater stability and maneuverability when lifting and moving the hubs and halls. However since the hooks to be attached manually onto the hubs and halls, the two cables are used in parallel to mimic a single cable that can attach to the various payloads that will not or cannot have astronaut presence. Without manual assistance, the crane uses magnetically assisted hooks to pick up the various payloads.



Figure 191. Atlas Two Cable System

Gondola

The gondola attachment is a basket designed to carry a astronaut in full EVA gear. The gondola's purpose to carry the astronauts out of their EDL vehicle as well as provide them with a vantage point during construction if needed.



Figure 192. Atlas Gondola

In order to get the crew out of their EDL vehicle, the gondola is picked up by the crane and is lifted to the exit door on the crew EDL vehicle where it then magnetically connects to the side of the EDL vehicle. A crew member steps onto the gondola, and then closes the safety gate behind him/her. The magnetic seal is then broken and the gondola is lowered to the ground.

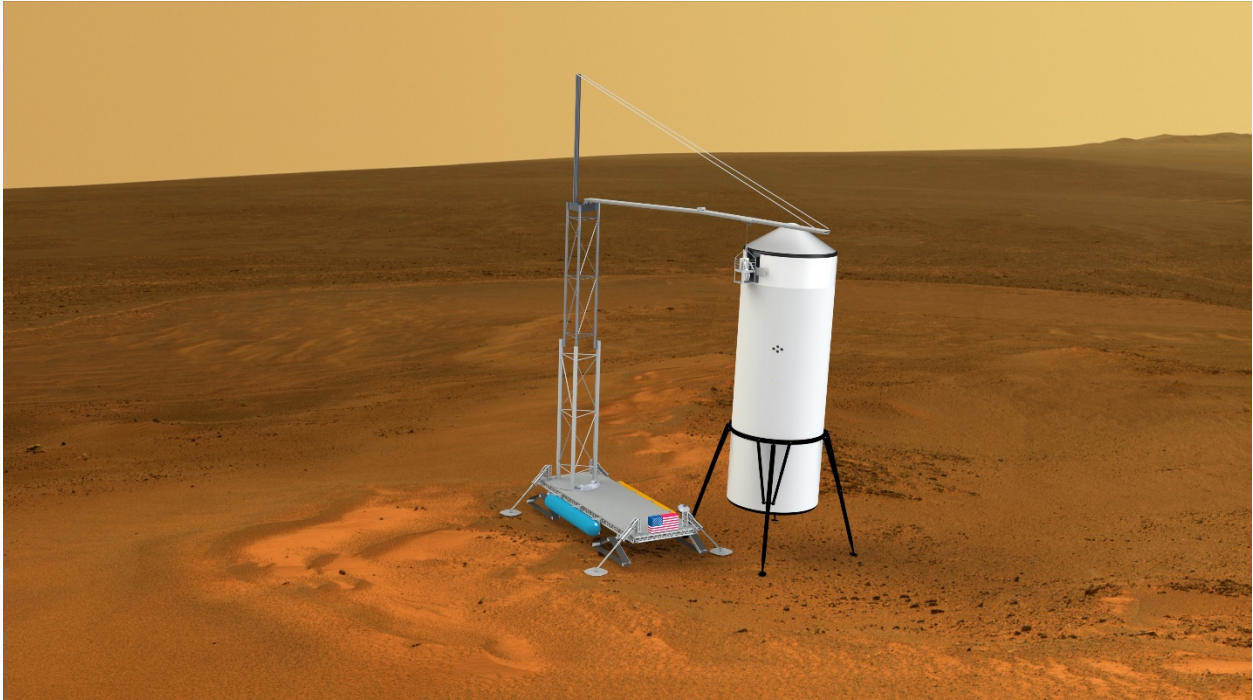


Figure 193. Atlas Extracting Crew From Their Decent Vehicle

Regolith Scoop

The regolith scoop attachment is used during the burial phase of the habitat construction. It attaches to the end of the two cable system and can be moved anywhere under the boom arm's area of coverage. The scoop digs into the regolith, closes its jaws, picks up regolith, and moves it to where it is needed.

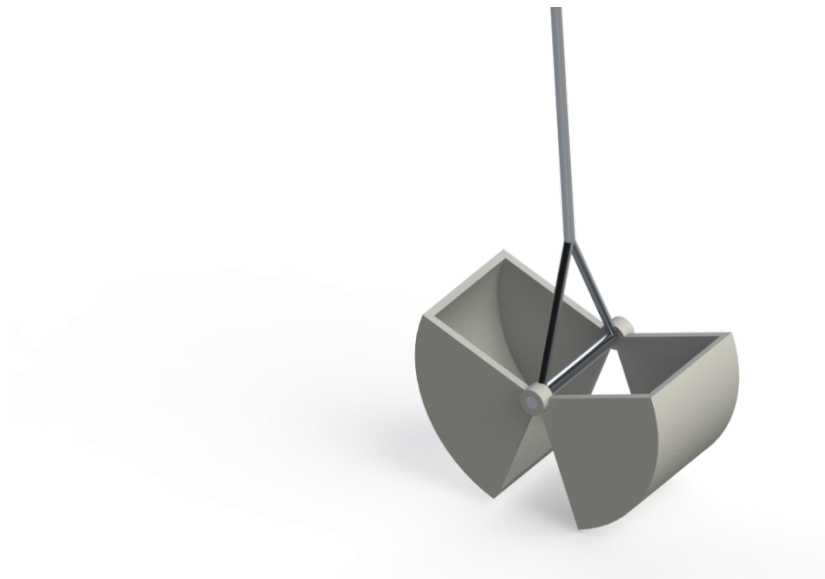


Figure 194. Atlas Regolith Scoop

Regolith Counterweight Basket

The counterweight basket is used to provide additional stability when the Atlas crane transports the heavier payloads. It is shipped empty, and attaches to the back end of the boom tower. Another crane picks up the basket to mount it. Once attached, it is then filled with regolith by using the regolith scoop and holds 8m^3 , which comes to roughly 12t.



Figure 195. Atlas Regolith Counterweight Basket

6.5.5. Welding and Repair on Mars

Once the crew and all the instruments arrive on Mars, things may be broken and might need repair. The habitat, the Magellan and the Crane are among the major equipment that may require welding during breakdown or other fixes. Welding has been done on LEO since 1960s and the technology has evolved a lot from what it was at the beginning. For the mission to Mars, different kinds of welding systems had been analyzed to choose the best and effective methodology for this mission. Welding provides a flexible foundation for assembly, repair and maintenance functions on Space platforms or on other planetary bodies. Flexibility is attained through the ability of the laser beam to interact with practically all materials and through the variety of techniques available to produce and deliver laser power to a work piece.

Construction (assembly), repair, and manufacturing all require joining techniques. Welding has always been the dominant metals joining technique. On earth, there are different kinds of welding techniques. In actuality, only a few techniques will be needed for welding most construction materials encountered in Space structures. Laser welding is obviously the most diverse, being able to work with metals and non-metals alike. Both electron beam (EB) and arc welding processes require that the material being welded be a metal. Electron beam requires a vacuum and arc welding requires an inert gas. Laser beam welding requires neither and can work within either environment. A thorough study of the behavior of molten materials and solidification phenomena was considered in choosing the best method of welding. ^[230,251]

For the last five decades NASA and the Russians have been conducting to know more about space welding. The research is conducted on different materials and in different variables. These research conducted will be used for the implementation of repair and welding on Mars for this mission. The Magellan, the habitat and the crane are made from aluminum and steel. Therefore knowing the properties of the thermo physical properties, and heat distribution of materials is one of the very important requirements to work on the welding of this equipment.

	Steel (carbon)	AISI 316
Thermal Conductivity (W/cm⁰C)	0.24	0.24
Thermal diffusivity (cm²/sec)	0.055	0.045
Absorption coefficient (cm⁻¹)	6.0	6.0
Reflectivity	0.3	0.3
Vaporizing point (°C)	2870	2870
Melting point (°C)	1530	1500

Table 63. The Thermo physical properties of Steel and Aluminum (Aluminum Silicate) ^[254]

Laser welding energy sources utilize either a continuous wave (CW) or pulsed output of photons. With CW systems, the laser beam is always on during the welding process. Pulsed systems are modulated to output a series of pulses with an off time between those pulses. The laser beam is focused on the work piece surface to be welded. These laser beams may be delivered directly to the part via classical hard-optics, or through a highly flexible fiber optic cable capable of delivering the laser energy to distant workstations. ^[255]

The performance of metals, especially Aluminum and steel, when a laser beam is hit the workpiece is an important property that will determine the successful welding and repair task of the crew on Mars. Steel, which is the main building structure of the crane, has been studied in a lot of detail how it perform during laser welding. The steel melts and solidifies when the laser beam hit the surface. The picture below from independent research shows the three-dimensional property of steel during a continuous laser beam penetration welding. This research showed that the predicted/simulated property of steel is very similar to the measured value during laser beam welding. These ‘predictable’ properties of steel help the Mars crew on Mars to analyze and determine the outcome during repairs and welding. ^[255,256] This study was conducted using the 304 stainless steel, with laser power of 2500 W, and radius at focus of 200 μm. In the figure below, it shows that the after 2.0 ms weld pool has reached about close to half of the depth of the workpiece. Therefore, when the crews weld and repair different materials on Mars, the immediate effect of laser beam welding on metals will help them to complete tasks faster.

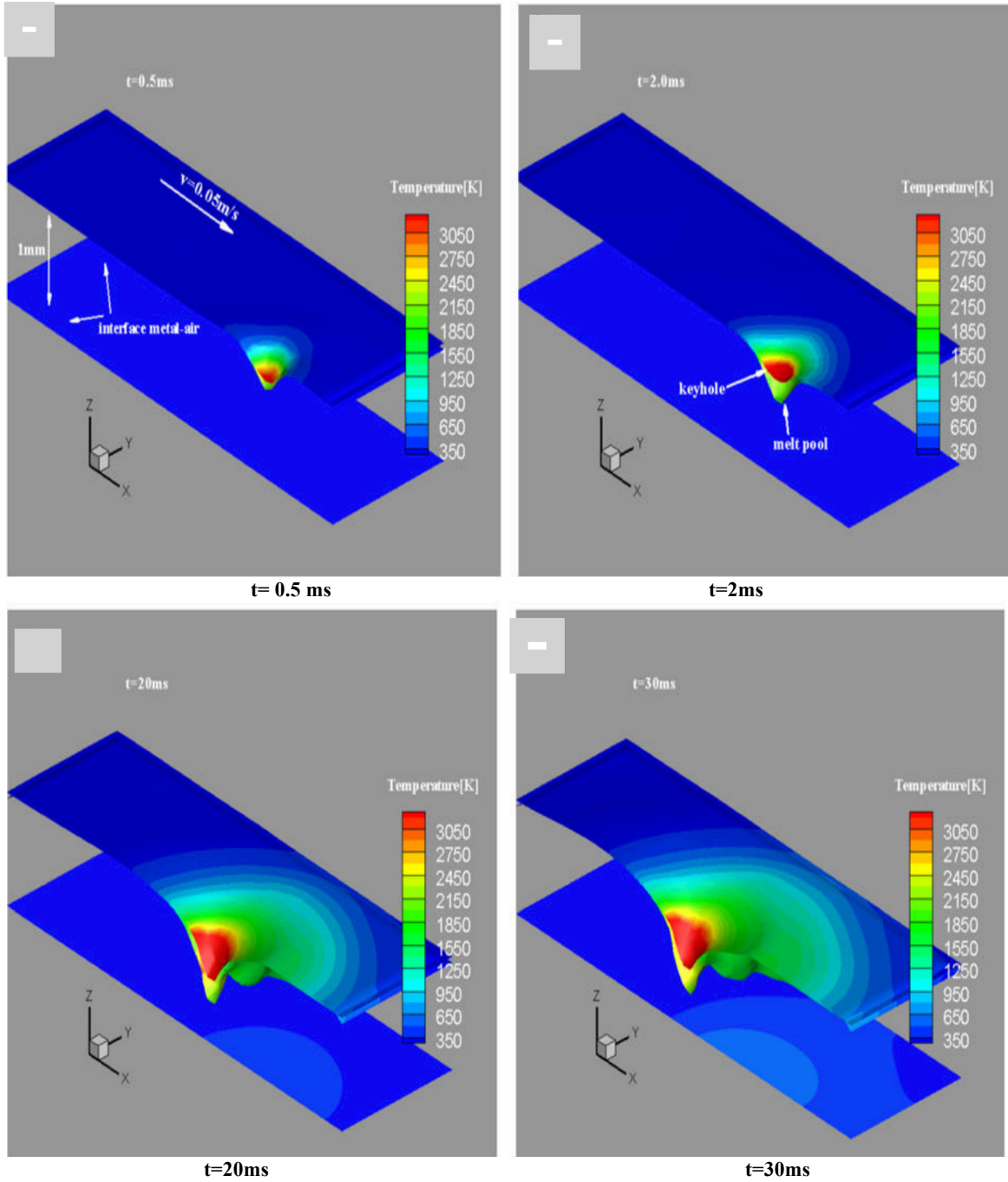


Figure 196. Continuous laser keyhole welding process for steel ^[256]

7. Earth Independence

7.1. Settlement Expansion

Future Expansion: Material for Building Purposes

The Martian atmosphere and soil provide many useful elements that can be utilized in materials production such as metals and glass.

Metal Oxides

The table below lists the main soil (metal oxides) constituents of the Martian Soil.

Constituents	Mars Pathfinder ^[53]	Mars Opportunity ^[54]
SiO ₂	50.2 %	45.5 %
Al ₂ O ₃	8.4 %	8.8 %
FeO	17.1 %	20.1 %
MgO	7.3 %	7.2 %
CaO	6.0 %	7.52 %
TiO ₂	1.3 %	1.09 %
P ₂ O ₅	-	0.82 %
Na ₂ O	1.3 %	1.4 %

Table 64. List of Metal Oxides from Martian Surface

Glass

Additionally, the silicate content of the Martian sand can be used to make glass through thermal fusion. The iron oxide content needs to be removed in order to have a transparent glass, through the reduction with carbon monoxide followed by magnetic separation. Glass fibers can also be used to improve the tensile strength of concrete building blocks that can be potentially produced on Mars. ^[55]

Future Expansion: Building New Habitats from Local Material

For future further expansion, new habitats can be potentially built from locally made bricks. However, due to the poor tensile strength of the bricks, the pressurized new habitats will need to be covered by regolith in order to be able to counteract the internal pressure, and in order to keep the habitat in compression. This will additionally provide the necessary radiation shielding. ^[56] Additionally, it has been estimated that a seven-meter layer of regolith will be sufficient to contain an internal pressure of one atmosphere for this habitat model. Also, glass fibers (previously mentioned) could be added to these local bricks in order to increase their tensile strength.

Additionally, lava tubes and caves can be taken advantage of for further habitation. These structures provide a reliable constant level of thermal protection and radiation shielding. ^[57]

Moreover, the building of future habitat structures can be a combination of more than one building material. This combination can also be from all-local material or from a combination of local and imported materials. ^[58]

- Raw Regolith
- Locally Made Regolith Blocks

- Reinforced Concrete
- Thin Films
- Inflatables
- Deployable Metal Structures
- Glass Products

According to a trade study that was made by ISFR (In-Situ Fabrication and Repair, NASA), a trade study was made to compare various habitat structures integrated technologies. And, an overall ranking/score was given based on NASA Marshall Space Flight Center:

- Current TRL (Technology Readiness Levels)
- Benefit from other technologies/development program
- Radiation shielding capabilities
- Ease of multiple egress

The following table represents the ISFR trade study with its respective overall score and ranking:

Integrated Construction Approach	Overall Score	Overall Ranking
Sandbags/Liner	2.124	1
Reinforced Concrete/Liner	2.108	2
Blocks/Liner	1.989	3
Cave or Lava Tube/Liner	1.920	4
Sandbags/Nested Inflatable	1.878	5
Cave or Lava Tube/Imported Structure	1.840	6
Cave or Lava Tube/Nested Inflatable	1.839	7
Sandbags/Deployable Metal/ Nested Inflatable	1.826	8
Raw Regolith/ Imported Structure	1.770	9
Blocks/Deployable Metal/Nested Inflatable	1.676	10

Table 65. Importance of relying on in-situ Martian resources for future habitats construction.

Thus, the dependence on local Martian Material will be essential for potential expansion and for the building of future habitats and related structures.

7.2. Science Missions

In order to maximize the effectiveness of Asimov City, the crew will perform a series of science missions to better understand Mars' history and the effects of sending humans to another planet for a long duration of time. The main areas of experimentation will focus on the study of geological features, psychological effects of isolating humans on a foreign planet for 13 years, as well as physiological effects of long term Mars habitation.

Geology

Since images of the Martian surface became available scientist have been trying to draw connections between the geologies of Earth and Mars. Specifically, scientist have been looking for microbially induced sedimentary structures (MISS); geological features which could only have been caused by microbes within the rocks. Recently a study has drawn a connection between Mars sedimentary structures with those observed on Earth (Noffke, 2015). Although this study includes an in depth analysis of available images from the Curiosity rover, no definitive conclusion can be reached until first person research can be conducted.

Psychology

A mission of this magnitude will have a psychological effect on any astronaut sent to Asimov City. Long term isolation and closed quarters could lead to depression, anxiety, conflicts between crew members, and even psychosis. In order to combat these unavoidable circumstances alternative activities, other than scientific studies, are needed to protect the mental health of the crew members. Robotic companions, programmed with different personalities, have been tested on the HI-SEAS missions. These pets have already shown promising results, and in 20 years when these psychological outlets are needed they may prove critical to the mental health of the crew.

Physiology

It is known that any time spent in microgravity significantly affects the human body; bone deterioration, muscle loss, decreased heart size, spine elongation. What is not known is how a prolonged stay on the Martian surface, about $\frac{2}{3}$ Earth's gravity, will change an astronaut's body. The time spent on Mars will surely have a profound effect on the crew's body. Regular testing and experimentation will be needed within Asimov City in order to better understand, and potentially stall, the low gravity effects on the human body.

8. Conclusion

8.1. Budget and Costing Analysis

Budget

The Asimov City program budget was prescribed by the RASC-AL competition requirements to be based on the 2016 President's Budget Request.^[190] This would give NASA a yearly budget of \$18,529M, in constant year 2015 dollars. To provide accessible analysis because of this, all analysis was done using constant 2015 dollars. From the entire administration budget, the program could have control of the full Exploration appropriation of \$4,505.9M. Additionally, an allocation of \$3105.6M was made available in 2025 corresponding to a discontinuation of the International Space Station program. The Asimov City program was given partial fiscal control of the rest of the NASA budget. Specifically, the RASC-AL rules allowed for a redistribution of up to 20% of all non-related appropriations to Asimov City. This added a yearly budget of \$2,172.9M.

Though Asimov City was granted control of the Exploration budget, RASC-AL rules required the continued funding of the Commercial Spaceflight program according to the 2016 President's Budget Request. Additionally, the rules require the Exploration Systems Development to be funded at \$3,000M

per year through 2035. This funding is for the development and construction of the Space Launch System launch vehicle and the Orion Multi-Purpose Crew Vehicle.

Cost Estimation

In order to perform a cost estimation of the various spacecraft to be produced throughout the duration program, a number of parametric models were employed. Given that the program design was created without any real-world funding, the Asimov City team did not have access to proprietary cost databases or models. Therefore, free, lower fidelity models were required. Four such models were previously made available by the NASA Johnson Space Center website.^[184] A discussion of how these models were obtained and implemented can be found in Appendix Marlin.1. In their distributed state, the JSC cost models used a variety of real year dollars, so each model's cost estimates were independently scaled into 2015 dollars using the NASA New Start Inflation Indices.^[192]

The recurring cost of spacecraft was derived from the JSC Spacecraft/Vehicle Level cost Model (SVLCM).^[185] The SVLCM uses a database of previous spacecraft missions to statistically generate a power law relation between spacecraft dry mass and program cost, providing the user with a coefficient and exponent to apply to the dry mass. The model maintains separate categories of missions, as tabulated (Table 66). Different parameters are displayed for recurring and non-recurring costs. Each spacecraft and vehicle was matched with the most appropriate category available. Because the SVLCM is a low-fidelity model, the categories do not precisely apply to each vehicle. For example, the Moon/Mars Miner was most closely classified as an "Unmanned Planetary Spacecraft" in the SVLCM.

Vehicle Type	Nonrecurring Cost Coefficient (a m ^b)	Nonrecurring Cost Exponent (a m ^b)	Recurring Cost Coefficient (a m ^b)	Recurring Cost Exponent (a m ^b)
Liquid Rocket Engine	17.551	0.55	0.0884	0.662
Manned Spacecraft	11.016	0.55	0.3173	0.662
Unmanned Planetary Spacecraft	7.412	0.55	0.4921	0.662
Launch Vehicle Stage	4.345	0.55	0.0945	0.662
Unmanned Earth Orbital	2.098	0.55	0.2181	0.662
Scientific Instruments	1.167	0.5	0.141	0.7

Table 66. SVLCM Model Parameters by Category

The model view presented on the 2006 Johnson Space Center website uses spacecraft quantity as an input, and presents the user with a summed recurring cost, applying a learning curve discount over the quantity. As the cost estimation for this program demands scheduling production of spacecraft, a modification was made to incrementally apply the learning curve to each production unit as it is produced. An 80% learning curve was assumed for all spacecraft production. This is applied logarithmically in base two, i.e. every time the number of produced vehicles is doubled, a 20% discount per unit is achieved. This can be seen in the following table of recurring costs for the Asimov City habitat hall module (Table 67). The second unit costs 80% of the first unit, and the fourth costs 80% of the second.

Table 67 also displays that the years where the program incurs the recurring costs are derived from the mission architecture. This is shown for convenience; in the actual model spreadsheet, recurring costs were distributed evenly between the year the spacecraft is launched and the year before.

Hall Module Production Number	Production Year	Production Unit Cost (\$M 2015)	Ratio of Cost to First-Unit Cost
1	2030	178.55	100%
2	2030	142.84	80%
3	2031	125.36	70.21%
4	2033	114.27	64%
5	2033	106.35	59.56%
6	2035	100.29	56.17%
7	2035	95.43	53.45%
8	2036	91.42	51.2%
9	2037	88.02	49.29%

Table 67. Learning Curve Benefits for the Mars Habitat Hall Module

The Spacecraft/Vehicle Level Cost Model was also used as a basis to estimate the nonrecurring costs of the spacecraft using the respective power law parameters. Given that one of the goals of the Exploration and Resource Acquisition phases of the Asimov City program is to begin to develop proof of the viability of the spacecraft design in lunar missions, many of the spacecraft in the Habitat Transport phase are very similar to spacecraft from the Lunar Exploration phase. In order to account for the similarities in design, a block number was added as an input to the nonrecurring cost estimation model. For this, JSC's Advanced Missions Cost Model^[186] (AMCM) was inspected. The AMCM multiplicatively applied the block number raised to a constant exponent of -0.355, which is equivalent to a learning curve of 78.2%. This factor was applied to the nonrecurring costs generated by the SVLCM. The nonrecurring costs and first-unit production costs of the used spacecraft are tabulated in Appendix A.

In order to present the cost over the duration of the program with relation to the budget, the nonrecurring cost for each spacecraft was spread over the duration of its development. JSC's Cost Spreading Calculator^[187] model was used for this. This model internally uses a quintic polynomial relating the fraction of time spent in the program to its cumulative cost. This polynomial approximates a beta distribution function, and its coefficients derive from two inputs to the model: cost fraction and peakedness. The cost fraction represents the fraction of the total (non-recurring) cost that is used by half of the program duration, and is allowed to vary between 3/16 and 13/16. A visualization of a fixed-cost program spread with varying cost fraction is pictured in Figure 197. Taking advice from the RASC-AL Costing Webinar,^[191] each spacecraft has a minimum development time of eight years. Complex spacecraft such as the Crew Transport Vehicle, as well as critical early launches, such as the Lunar Manned Ascent/Descent Vehicle were given a longer development time, up to twelve years.

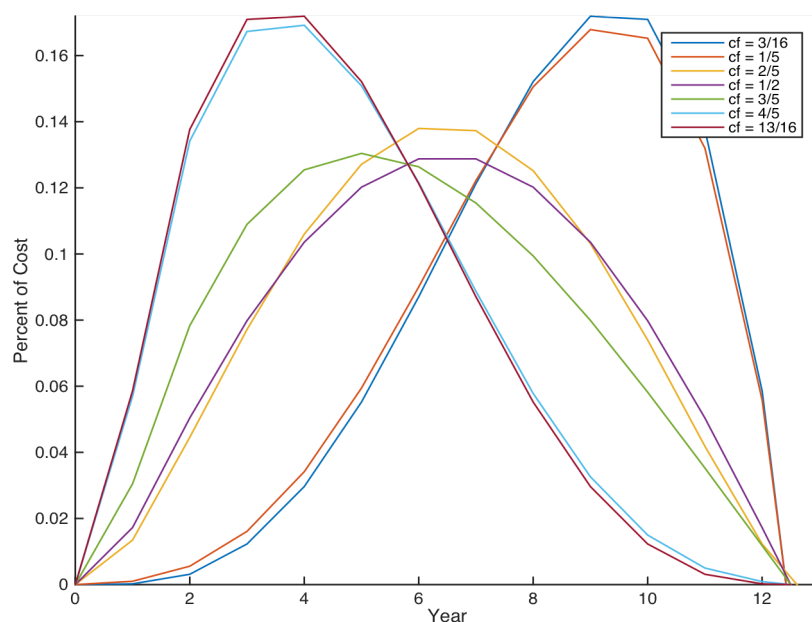


Figure 197. Spreading with Varying Cost Fractions

The spreading of spacecraft nonrecurring cost throughout the program was the main method of manipulating the cost estimation. It allows the total cost curve to move around and fit under the budget curve. For instance, Lunar Exploration spacecraft such as the Lunar Manned Ascent/Descent Vehicle, the Moon/Mars Miner, and the Lunar Ground Transport were set to develop starting in 2015; therefore, they use a maximal 3/16 as the cost fraction. This allows the program to fill as much of the early budget as possible, while still having the launches occur in 2025, 2026, and 2027, respectively. The recurring costs are incurred after the International Space Station is defunded, making that cost manageable, while the nonrecurring costs are incurred before the Martian spacecraft begin to be developed.

Spacecraft operations were modeled using the JSC Mission Operations Cost Model^[188] (MOCM) that estimates the Mission Operations and Data Analysis (MODA) costs for missions after they launch. The MOCM uses a power law similar to the SVLCM, where the total mission cost is used as the base, with coefficient and exponent determined by a separate series of categories than the SVLCM's. This leads to the same issue where the Moon/Mars Miner is most closely labeled as "Physics & Astronomy" in the

MOCM. The MOCM was applied based on the development cost and total production costs and is incurred from the first launch of a spacecraft until its end of life, usually 2054.

In addition to modelling the MODA costs of a single spacecraft, the MOCM was used to model the overall program management and operations cost. This includes features such as crew selection and training, as well as facilities. In order to account for this, a recurring yearly cost was added where the year-to-date total program cost was given as an input into MOCM, and the result became the program MODA.

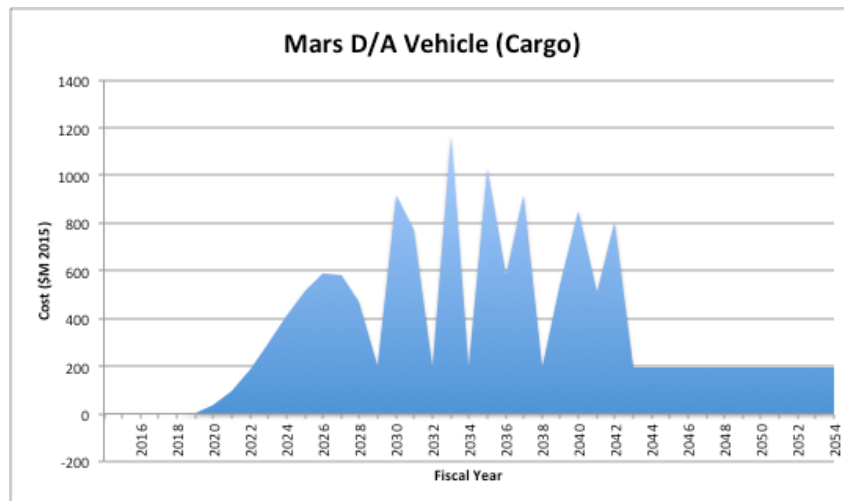


Figure 198. Mars Descent Vehicle Costing

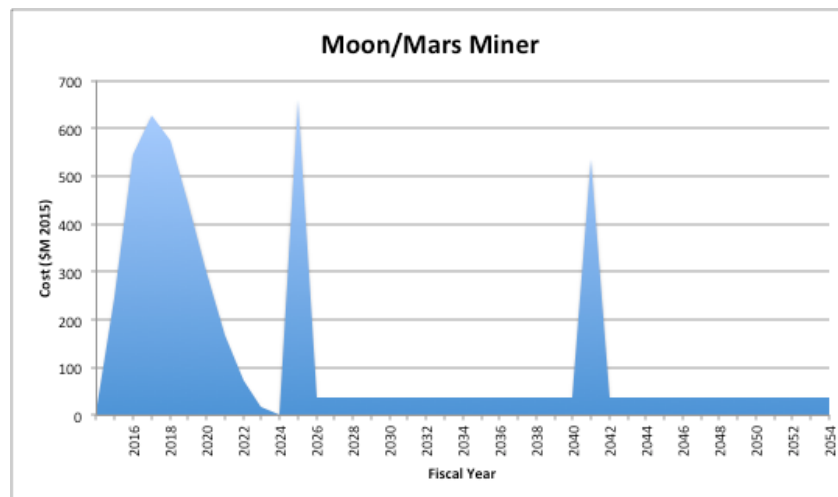


Figure 199. Moon/Mars Miner Costing

Shown in Figures 198 and 199 are examples of two of the spacecraft cost estimations. In both, the preliminary curve is the spread nonrecurring costs, the peaks are single-unit production costs for that year, and the base offset from zero is the mission operations and data analysis. The Cargo Descent Vehicle appears to improperly apply the learning curve, but this is simply because each peak after the first represents two vehicles being produced that year in adherence to the mission architecture. The Mars Descent Vehicle begins its development in 2018 and proceeds through 2030, taking twelve years due to its complexity. This means that for the first seven years of development, the program is running under the minimal budget section of the program, where in the remaining five years, the International Space Station budget has been reclaimed. For this reason, a minimal cost fraction of 3/16 was chosen to ensure the majority of the costs would be incurred when the program has more budget. In contrast, the Moon/Mars Miner is first flown in 2025, so a similar strategy would not be beneficial. In this case, the maximal cost fraction of 13/16 was applied so that the program could make as much use of its 2015 and 2016 as possible. A similar analysis was performed for each spacecraft to determine the appropriate spreading parameters.

The sandplot (Figure 200) below shows the summed cost through the duration of the program of all spacecraft costs. From this view of the cost estimation, the phases of the program become clear. The first peak in 2019 is the development of the Exploration Phase spacecraft. The subsequent peaks are the production of the Lunar Exploration vehicles entwined with the beginning of the development of the Mars spacecraft and vehicles.

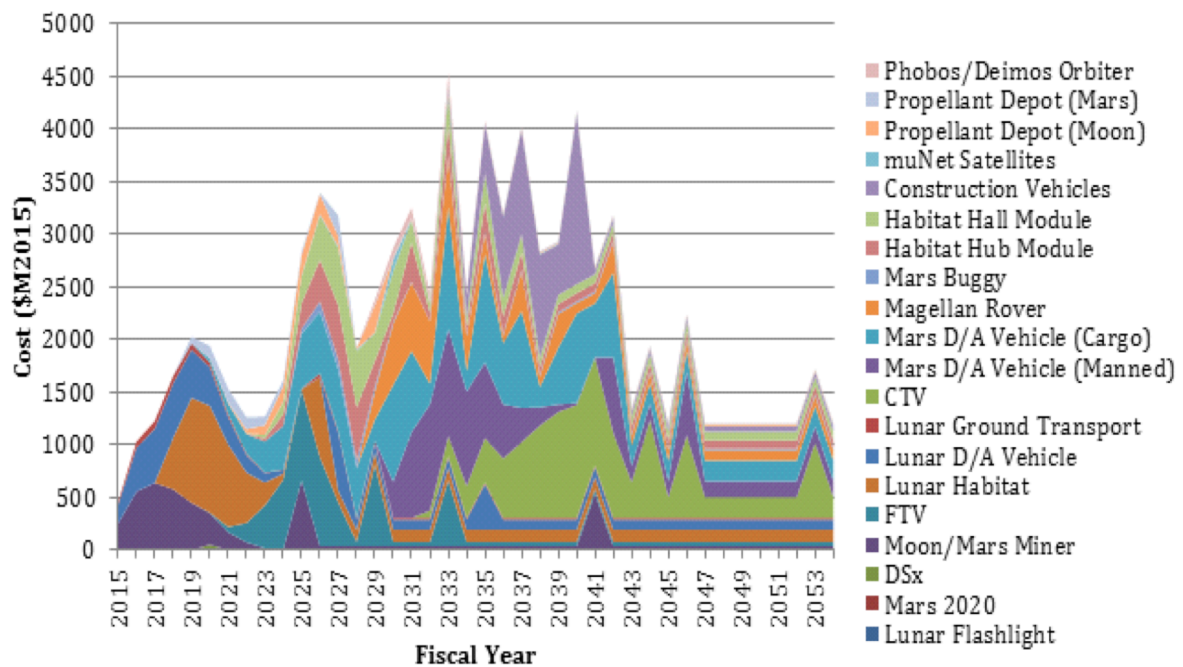


Figure 200. Development, Productions, and Operations Costs Per Spacecraft

The Asimov City program consists of more hardware than the presented spacecraft. Other costs are considered on a case-by-case basis. The nuclear reactors used to power the Mars Habitat were presented

in a NASA paper¹⁹³ to have an expected first-unit cost and a cost for each additional unit. This cost structure is very similar to the structure used in the spacecraft estimating model, so the first-unit cost was broken into a non-recurring cost which was spread over 8 years, and the recurring cost received the benefit of the learning curve. In contrast to this, the program estimated the cost of its SpaceX Falcon Heavy launches using a flat cost of \$90M in accordance to SpaceX’s advertised launch prices^[189]. The Dragon crew capsule was similarly estimated as a flat cost of \$250M, but this cost was from an interview with Dr. Akin. Neither the Falcon nor the Dragon receives learning curve benefit.

All of the models presented represent the direct costs to the program. To properly capture all of the costs associated with a program such as this, an integrated model would include indirect costs as well as the direct costs. One way to do this is to introduce a multiplicative Overhead Factor to each cost. To determine what level of Overhead Factor to use, various values were applied to a previously balanced strategy (see Appendix A) and plotted against the yearly budget (Figure 201). It was assumed that NASA cost estimations had already included indirect costs, so the Overhead Factor was neither applied to the Exploration Systems Development funding nor to SpaceX launch vehicle purchases. Two suggested Overhead Factors were 1.5 and 2. A third factor was obtained by scaling the cost by the ratio of the total budget to the total program cost—to wit, this is the factor that represents what the cost would be if the program spent the entire budget. This ratio was found to be 1.98.

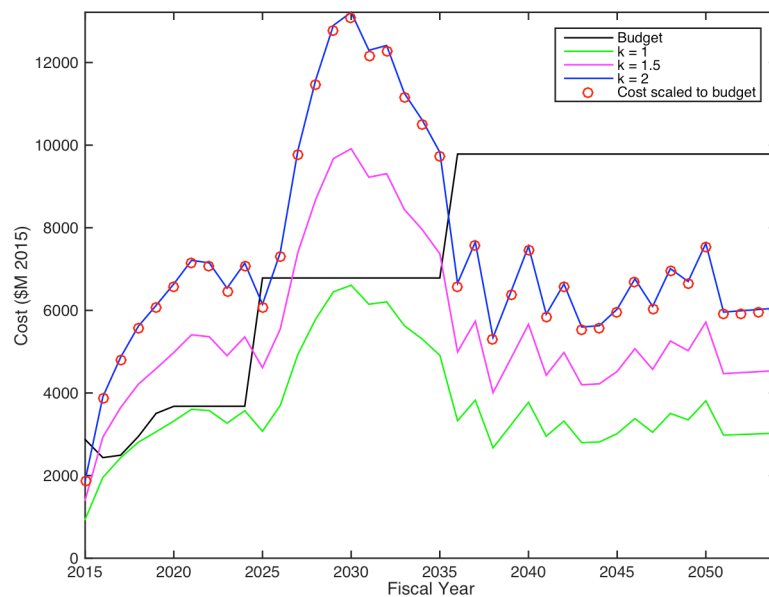


Figure 201. Yearly Cost with Various Overhead Factors

As is clear from the figure, the introduction of the Overhead Factor puts Asimov City, as prescribed by the previous strategy, over-budget in the first half of the program. This is not an issue that can be solved by manipulating model parameters—there simply is not enough available funding in the early phases for this to fit under the budget. This is shown below in a plot of the cumulative costs. (Figure 202). For the Scaling Factor of 1.5, the cumulative cost is not above the cumulative budget curve until 2040, and the Scaling Factor of 2, being larger than the total cost ratio, never returns to positive. The even-budget Scaling Factor is seen to converge to the budget at the end of the program, which occurs by construction.

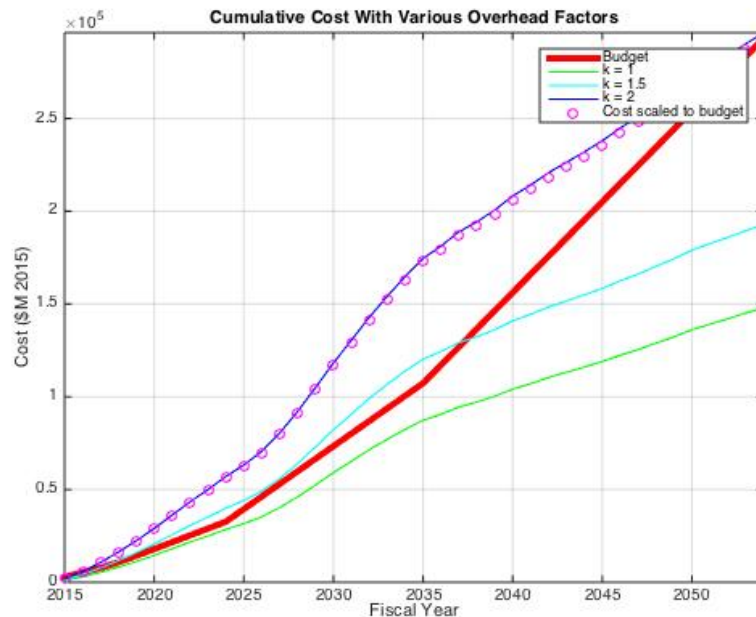


Figure 202. Cumulative Cost with Various Overhead Factors

An observer of the cumulative cost with the Scaling Factor of 1.5 notices that at no point beyond the first year is the cumulative cost below the cumulative budget. This implies that there is no possible spreading that will produce a legal timeline—any spreading would move costs from one over-budget year to another. Clearly, another strategy is needed. The issue with the SLS-lossless strategy is that in order to utilize every SLS, all unmanned objects must be on Mars before 2035, which is when the program recovers the portion of the Exploration budget that was spent on SLS/Orion. Over the 18 years in the program, this equates to \$54B that cannot be spent on development and production of spacecraft. Additionally, because all of the unmanned costs are incurred prior to the first crew launch, the continued funding is also wasted, as there is nothing left to produce. Given this, and the fact that the early years of the program have the minimal funding, a better strategy is to push each mission as far back in the timeline as possible. This allows as much of the cost as possible to be incurred in the later years of the program.

Changes to the architecture started with the crew missions, as they are the last in the program. It was observed that the crews were being transported one per launch window, despite having three Crew Transport Vehicles. Each CTV is in a rotation cycle between Earth Orbit and Mars orbit, so by the pigeonhole principle, at least one launch window exists where two CTVs are around one planet. This implies that there can be two crews sent on a single later launch window. Additionally, the earlier architecture missed Martian launch windows in 2053 and 2044. As a result, it was possible to accommodate all crew launches, in the years 2044-2053.

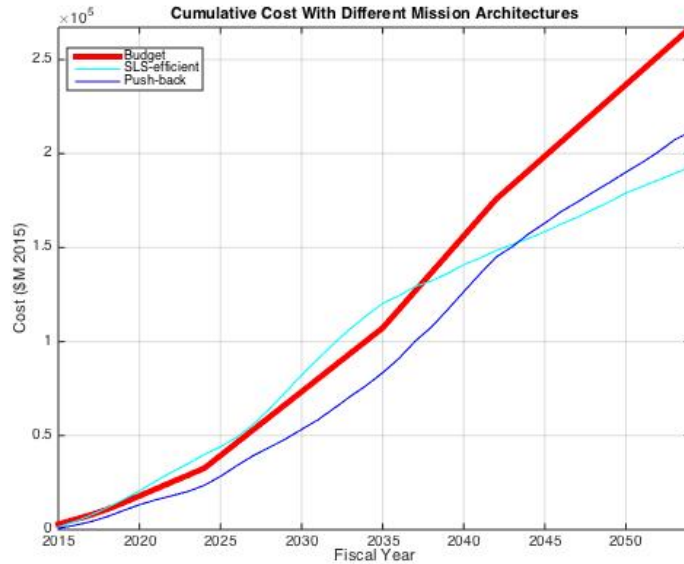


Figure 203. Cumulative Cost for Different Architecture Strategies

Moving the crew missions back allowed supporting equipment to move back as well. Using the L1 Propellant Depot, the program would be able to send 3 SLS payloads in the preceding launch windows. In order to support this, NASA must continue to maintain the SLS program through 2042. RASC-AL rules indicated that while the SLS and Orion are in production, NASA is able to purchase an additional SLS or Orion individually for \$500M. This implies that, when in production, the recurring cost of the two delivered SLS/Orion per year is \$2,000M, with a \$1,000M operations cost. In order to keep the SLS launch team active beyond the 2035 deadline, Asimov City continues to fund the Exploration Systems launch team at \$1,000M per year during the 2036-2053 fiscal years. During that time, thirteen additional SLS vehicles will be produced, never exceeding a production or launch rate of three per year. This means that in addition to the cost increase from the Overhead Factor, the program paid \$25,500M more than the previous strategy in order to maintain its launch capability. Additionally, the mission architecture leaves seven SLS vehicles unused, for an effective opportunity cost of \$17,640M (See Appendix A for effective cost of missing an SLS launch). This is an opportunity cost only to the Asimov City program, though, as other concurring NASA programs will be able to launch on the freed SLS vehicles. Moving the construction and production of later missions moved \$32,120M of spacecraft costs into the post-2035 funding phase, more than doubling the budget utilization in the later years.

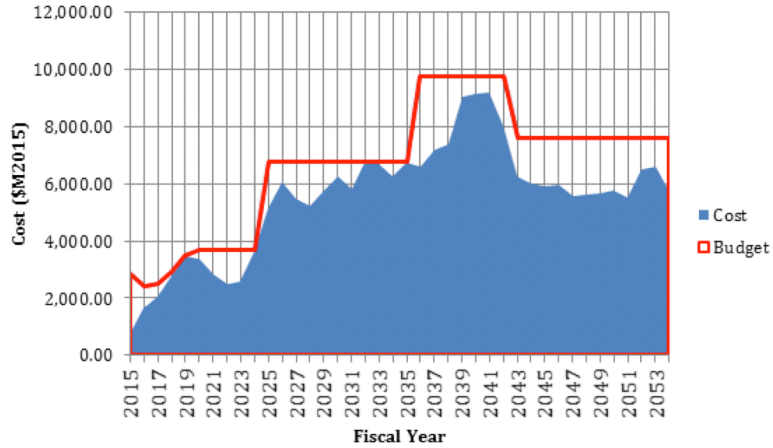


Figure 204. Final Yearly Program Budget vs. Cost

The late-launch scheduling strategy drove each launch, with the exception of Lunar Flashlight, Mars 2020, and DSx back a minimum of 4 years. With each mission moved to the current architecture, the cumulative cost is always less than the cumulative budget, as can be seen in Figure 204. This implied that, by tuning spreading parameters, it would be possible to fit the cost curve under the budget. The result of that analysis is the final cost estimation, shown below in Figure 204. This estimation yields a total program cost of \$211.5B, with an annual average budget margin of 22.46%. It is clear that some years have very low margin, the minimum margin of 1.93% occurring in 2040. The years with margins below 10% are tabulated in Table 68. These are years where the program will not be able to recover from mission failure due to budgetary reasons.

Fiscal Year	Budget (\$M 2015)	Cost (\$M 2015)	Margin
2019	3,510	3,270	6.66%
2032	6,780	6,160	9.27%
2033	6,780	6,290	7.31%
2035	6,780	6,652	1.94%
2037	6,780	6,730	6.03%
2039	9,780	9,270	5.27%
2040	9,780	9,600	1.93%
2041	9,780	9,460	8.07%

Table 68. Years with Minimal Cost Margin

The crew launches at the end of the program was the limiting factor in how far back the development and production costs could be spread. As a result, there was no way to effectively use the full budget as recovered from the Exploration Systems Development program, so in 2043, the Asimov City program returns the 20% budget reallocation to the remainder of the NASA programs as it continues to proceed towards Earth independence.

9. Appendix A. Reference Information for Current Design

9.1. Introduction

9.1.1. Requirements

	System Requirements (Level 2)	Source
S1	Shall determine availability of resources on Moon by 2019	M1,M2,M3,M5
S2	Shall investigate resource availability of each potential landing spot in Hellas Planitia region on Mars	M1,M2,M3,M6
S3	Shall investigate radiation levels of each potential landing spot in Hellas Planitia region on Mars	M1,M2,M3
S4	Shall map surface of each potential landing spot in Hellas Planitia region on Mars	M1,M2,M3
S5	Shall measure atmospheric conditions of each potential landing spot in Hellas Planitia region on Mars	M1,M2,M3
S6	Shall investigate resource availability of each potential landing spot in McLaughlin Crater region on Mars	M1,M2,M3,M6
S7	Shall determine final landing area on Mars by 2022	M1
S8	Shall determine geological composition of Phobos and Deimos	M1,M2,M3,M5
S9	Shall develop pressurized settlement on Lunar surface	M1,M2,M3, M5,M7
S10	Shall select Lunar surface crews from pool of appropriate candidates	M1
S11	Shall use pressurized rovers on lunar surface	M1,M2,M3
S12	Shall use existing suit technology for all missions	M1,M2,M3,M4
S13	Shall develop Lunar Regolith Miner for resource acquisition operations on Moon	M1,M2,M3, M5,M8
S14	Shall develop Lunar Resource Processing Center	M1,M2,M3, M5,M8
S15	Shall begin Lunar mining operations by 2027	M1,M5,M8
S16	Shall develop Fuel Transport Vehicles for use in conjunction with Lunar mining operations	M1,M2,M3, M4,M5,M8
S17	Shall develop Fuel Depot Station at Lagrange Point L1	M1,M2,M3,

		M7,M8
S18	Shall develop Mars Regolith Miner for resource acquisition operations	M1,M2,M3, M6,M8
S19	Shall develop Martian Resource Processing Center	M1,M2,M3, M6,M8
S20	Shall begin Martian surface mining operations by 2045	M1,M6,M8
S21	Shall develop Mars Fuel Depot Station in LMO	M1,M2,M3, M4,M5,M6,M8
S22	Shall select Mars settlement crews from pool of appropriate candidates	M1
S23	Shall develop pressurized settlement on Martian surface	M1,M2,M3, M5,M6,M7
S24	Shall develop structure to shield Martian settlement from radiation	M1,M2,M3
S25	Shall have EVA capabilities on Martian surface	M1,M2,M3,M7
S26	Shall develop Crane Vehicles for use on Martian surface	M1,M2,M3
S27	Shall create flexible daily schedule for crew to follow	M1
S28	Shall develop Crew Transport Vehicle for transit between LEO and extra-orbital locations	M1,M2,M3, M4,M7
S29	Shall use International Docking Standard on all spacecraft	M1
S30	Shall use electronic sensors for all space vehicle GNC and EDL	M1,M2,M3,M7
S31	Shall design and build EDL systems and Ascent/Descent Vehicle for use from LMO to Martian surface	M1,M2,M3,M7
S32	Shall use pressurized rovers on Martian surface	M1,M2,M3
S33	Shall use unpressurized rovers on Martian surface	M1,M2,M3
S34	Shall develop Martian surface based communications system	M1,M2,M3,M7
S35	Shall develop Martian orbit based communication system	M1,M2,M3,M7
S36	Shall develop Martian Global Positioning System	M1,M2,M3,M7
S37	Shall develop space based Earth to Mars communication system	M1,M2,M3,M7
S38	Shall facilitate scientific advancement using technology developed during mission	M1,M2,M3, M4,M5,M6, M7, M8

Table 69. System Requirements (Level 2)

	Sub-System Requirements (Level 3)	Source
B1	Shall utilize Lunar Flashlight mission for Moon resource determination	S1
B2	Shall utilize Mars 2020 mission for investigation of Martian landing sites	S3,S4,S5,S7
B3	Shall develop probes for use in investigation of Martian landing sites	S2,S6,S7
B4	Shall complete development of Phobos and Deimos orbiters by 2033	S23
B5	Shall launch Phobos and Deimos orbiters by 2033	S23
B6	Shall select first Lunar surface crew by 2025	S10
B7	Shall select back up crew of 6 members for each Moon mission	S10
B8	Shall launch crew of 6 members to Moon for Lunar construction by 2027	S9
B9	Shall complete development of Lunar Settlement by 2025	S9
B10	Shall launch Lunar Settlement by 2025	S9
B11	Shall complete construction on Lunar Settlement by 2025	S9
B12	Lunar settlement shall have dedicated living quarters area	S9
B13	Each crew member shall have their own private living quarters in Lunar settlement	S9
B14	Lunar settlement shall have a dedicated medical care area	S9
B15	Lunar settlement shall have dedicated non-work multipurpose area	S9
B16	Lunar settlement shall have electronic controlled Environmental Control System	S9
B17	Lunar Settlement shall have electronic controlled Life Support System	S9
B18	Shall develop emergency response plans for situations within the Lunar Settlement	S9
B19	Shall develop emergency response plans for situations outside the Lunar Settlement	S9
B20	Shall enter and exit Lunar Settlement using suit ports	S9

B21	Lunar settlement shall need a minimum of 100 kW-hr per day	S9
B22	Lunar settlement shall receive power from solar panels	S9
B23	Lunar settlement shall have the capability to store power within on board fuel cells	S9
B24	Lunar pressurized rovers shall receive power from rechargeable fuel cells	S11
B25	Shall complete development of Lunar pressurized rover by 2026	S11
B26	Shall launch Lunar pressurized rover by 2026	S11
B27	Shall finish development of Lunar Regolith Miner by 2025	S13,S15
B28	Shall launch Lunar Regolith Miner by 2025	S13,S15
B29	Lunar Regolith Miner shall mine regolith capable of being converted to 300 metric tons of fuel every 6 months	S13,S15
B30	Shall shut down and service Lunar Regolith Miner at regularly scheduled intervals beginning in 2030	S13,S15
B31	Shall finish development of Lunar Resource Processing Center components by 2025	S14,S15
B32	Shall launch components of Lunar Resource Processing Center by 2025	S14,S15
B33	Shall complete construction of Lunar Resource Processing Center by 2027	S14,S15
B34	Shall finish development of Fuel Transport Vehicles by 2028	S16,S29
B35	Shall launch and have in Lunar orbit Fuel Transport Vehicles by 2032	S16
B36	Shall finish development of L1 Fuel Depot Station components by 2028	S17,S29
B37	Shall launch first components of L1 Fuel Depot Station by 2028	S17
B38	Shall have launched all components of L1 Fuel Depot Station by 2029	S17
B39	Shall utilize autonomous robotics in construction of entire L1 Fuel Depot Station	S17
B40	Shall complete construction of L1 Fuel Depot Station by 2032	S17

B41	Shall finish development of Martian Regolith Miner by 2025	S18,S20,S24
B42	Shall launch components of Martian Regolith Miner by 2041	S18,S20,S24
B43	Shall complete construction of Martian Regolith Miner by 2045	S18,S20,S24
B44	Shall finish development of components of Martian Resource Processing Center by 2041	S19,S20
B45	Shall launch components of Martian Resource Processing Center by 2041	S19,S20
B46	Shall finish construction of Martian Resource Processing Center by 2046	S19,S20
B47	Shall finish development of Martian Fuel Depot Station by 2027	S21,S29
B48	Shall launch first components of Martian Fuel Depot Station by 2027	S21
B49	Shall have launched all components of Martian Fuel Depot Station by 2032	S21
B50	Shall utilize autonomous robotics in construction of entire Martian Fuel Depot Station	S21
B51	Shall complete construction of Martian Fuel Depot Station by 2035	S21
B52	Shall transfer habitat modules from LEO to Martian surface	S23
B53	Shall begin transfer of habitat module payloads by 2031	S23
B54	Shall finish transfer of all habitat module payloads by 2037	S23
B55	Martian settlement shall have dedicated greenhouse modules for plant and animal growth	S23
B56	Martian settlement shall have dedicated experimental workspace modules	S23
B57	Martian settlement shall have dedicated living quarters modules	S23
B58	Each crew member shall have their own private living quarters in Martian settlement	S23
B59	Martian settlement shall have dedicated medical care module areas	S23
B60	Martian settlement shall have dedicated non-work multipurpose module areas	S23
B61	Each crew member shall maintain a diet consisting of at least 3200 calories in Martian settlement	S23

B62	Each crew member shall have regularly scheduled medical evaluations in Martian settlement	S23
B63	Martian settlement shall have electronic controlled Environmental Control System	S23
B64	Martian settlement shall have electronic controlled Life Support System	S23
B65	Shall enter and exit Martian settlement using airlocks	S23,S25
B66	Shall be able to perform EVA's from habitat in Martian settlement	S23,S25
B67	Shall develop emergency response plans for situations within the Martian Settlement	S23
B68	Shall develop emergency response plans for situations outside the Martian Settlement	S23
B69	Martian settlement shall need a minimum of 300 kW-hr of power	S23
B70	Martian settlement shall receive power from nuclear reactors	S23
B71	Martian settlement shall receive power from solar panels	S23
B72	Martian settlement shall have the capabilities to store 50 kW of power	S23
B73	Martian crew shall perform scientific experiments both inside and outside habitat	S23
B74	Shall have installed modules sufficient to support 4 crew members by 2045	S23
B75	Shall have installed modules sufficient to support 8 crew members by 2047	S23
B76	Shall have installed modules sufficient to support 12 crew members by 2049	S23
B77	Shall have installed modules sufficient to support 16 crew members by 2051	S23
B78	Shall have installed modules sufficient to support 20 crew members by 2053	S23
B79	Shall have installed modules sufficient to support 24 crew members by 2054	S23
B80	Shall utilize Crane Vehicles to extract habitat modules from payload fairings	S23,S26
B81	Shall utilize Crane Vehicles to move habitat modules to	S23,S26

	settlement location	
B82	Shall utilize Crane Vehicles to place modules within the correct settlement configuration	S23,S24,S26
B83	Shall finish development of Crane Vehicles by 2040	S23,S24,S26
B84	Shall launch Crane Vehicles by 2040	S23,S24,S26
B85	Shall utilize materials found on Martian surface for habitat construction	S23,S24,S26
B86	Shall utilize Martian Regolith Miner in creation of radiation shielding	S19,S23,S24
B87	Shall incorporate 12 m thick regolith layer along walls for radiation shielding	S24
B88	Shall incorporate 12 m thick regolith layer along roof for radiation shielding	S24
B89	Shall use input from crew already on Mars when selecting new Mars bound crew	S22
B90	Shall select first Mars crew by 2043	S22
B91	Shall launch first Mars crew by 2045	S23
B92	Shall select second Mars crew by 2044	S22
B93	Shall launch second Mars crew by 2046	S23
B94	Shall select third Mars crew by 2046	S22
B95	Shall launch third Mars crew by 2048	S23
B96	Shall select fourth Mars crew by 2048	S22
B97	Shall launch fourth Mars crew by 2050	S23
B98	Shall select fifth Mars crew by 2051	S22
B99	Shall launch fifth Mars crew by 2053	S23
B100	Shall select sixth Mars crew by 2051	S22
B101	Shall launch sixth Mars crew by 2053	S23
B102	Shall select 4 backup crew members for each Mars mission	S22
B103	Shall adjust schedule to reflect Earth-Mars time differences	S27
B104	Shall finish development of 3 Crew Transport Vehicles by 2044	S28,S29,S30

B105	Shall launch first Crew Transport Vehicle by 2044	S28
B106	Shall launch second Crew Transport Vehicle by 2046	S28
B107	Shall launch third Crew Transport Vehicle by 2053	S28
B108	Crew shall conduct scientific experiments while in transit on Crew Transport Vehicle	S28
B109	Crew Transport Vehicle shall have electronic controlled Environmental Control System	S28
B110	Crew Transport Vehicle shall have electronic controlled Life Support System	S28
B111	Shall have emergency plans in place for Crew Transport Vehicle	S28
B112	Shall use propulsive systems for EDL to Martian surface	S30,S31
B113	Shall use inflatable systems for EDL to Martian surface	S30,S31
B114	EDL systems shall utilize Martian satellite network for positioning	S30,S31,S35
B115	Shall finish development of EDL Vehicles by 2031	S30,S31
B116	Shall launch EDL Vehicles by 2031	S30,S31
B117	Martian unpressurized rovers shall receive power from nuclear fuel cells	S33
B118	Shall finish development of Martian unpressurized rovers by 2040	S33
B119	Shall launch Martian unpressurized rovers by 2040	S33
B120	Martian pressurized rovers shall receive power from nuclear fuel cells	S32
B121	Martian crew of four shall be able to live inside of Martian pressurized rovers for a maximum of 30 days	S32
B122	Martian pressurized rovers shall have ability to autonomously find crew landing site	S32
B123	Shall have ability to perform EVA's from Martian pressurized rovers	S32
B124	Shall finish development of Martian pressurized rovers by 2026	S32
B125	Shall launch all Martian pressurized rovers by 2042	S32
B126	Shall finish development of Martian surface communication	S34

	system by 2031	
B127	Shall launch components of Martian surface communication system by 2031	S34
B128	Martian surface communication system shall be fully operational by 2045	S34
B129	Martian orbital satellite network shall provide full coverage of Martian surface	S35,S36
B130	Shall finish development of Martian orbital satellites by 2031	S35,S36
B131	Shall launch Martian orbital satellites by 2031	S31,S35,S36
B132	Martian orbital satellite network shall be EDL functional by 2032	S35,S36
B133	Martian orbital satellite network shall be fully functional by 2045	S35,S36
B134	Shall finish development of Earth-to-Mars communication relay station by 2040	S37
B135	Shall launch Earth-to-Mars communication relay station by 2040	S37
B136	Earth-to-Mars communication relay station shall be placed at Lagrange point L3	S37
B137	Earth-to-Mars communication relay station shall be fully operational by 2045	S37
B138	Earth-to-Mars communication relay station shall relay data at 300 Mbps	S37
B139	Shall utilize technological advances toward space tourism	S38
B140	Shall utilize technological advances toward earth orbit based communications systems	S38
B141	Shall utilize technological advances toward development of space inclusive commuter travel	S38
B142	Shall utilize technological advances toward development of space inclusive cargo transport	S38

Table 70. Sub-System Requirements

9.1.2. Full Mission Architecture

Fiscal Year	Mission/Milestone	Launch Window to Mars	Available SLS Rocket No.		Assigned Rocket Type	Assigned SLS Rocket No.
2015	PHASE 1: EXPLORATION					
2016*		Mar-16	-	-	-	-
2017	Lunar Flashlight Mission	-	-	-	Atlas V	-
2018*		May-18	-	-	-	-
2019		-	-	-	-	-
2020*	Mars 2020	Jul-20	-	-	Atlas V	-
	DSx Mission		-	-		
2021	PHASE 2: RESOURCE ALLOCATION & INFRASTRUCTURE SETUP					
		-	2021-1	-	SLS Block 1B	2021-1
		Sep-22	2022-1	-	SLS Block 1B	2022-1
2022*	DETERMINE SETTLEMENT LOCATION SITE BY 2022 --- BASED ON DSx MISSION AND MARS 2020 ROVER MISSION					
2023		-	2023-1	-	SLS Block 1B	2023-1
2024*		Nov-24	2024-1	-	-	-
	ISS SPLASHDOWN 2024 -- ASSUME ALL BUDGET FROM ISS PROGRAM					
2025	Moon Miner Delivery	-	2025-1		SLS Block 1B	2025-1
2026	Moon Rover Delivery Mission	-	2026-1	2026-2	SLS Block 1B	2026-1
	Moon Mining Magellan Delivery				SLS Block 1B	2026-2
2027	Mars Propellant 1 Depot	Jan-27	2027-1	2027-2	SLS Block 1B	2027-1
	Manned Moon Mining Mission				SLS Block 1B	2027-2
2028	L1 Propellant Depot Launch 1	-	2028-1	2028-2	SLS Block 1B	2028-1
	FTV 1 Delivery				SLS Block 1B	2028-2
2029*	L1 Propellant Depot Launch 2	Mar-29	2029-1	2029-2	SLS Block 1B	2029-1
	L1 Propellant Depot Launch 3				SLS Block 1B	2029-2
2030	Moon Mining Repair and Expansion	-	2030-1	2030-2	Falcon	-
	PHASE 3 BEGINS – HABITAT TRANSPORT					
2031*	Habitat Section 1 + Communication Satellites (No Refuel)	May-31	2031-1	2031-2	SLS Block 1B	2030-2
	Habitat Section 2 Launch				SLS Block 1B	2031-1
2032	Mars Propellant 2 Depot	-	2032-1	2032-2	SLS Block 1B	2032-2
	FTV 2				SLS Block 1B	2032-1
2033*	Habitat Section 3 Launch	Jul-33	2033-1	2033-2	SLS Block 1B	2033-1
	Habitat Section 4 Launch + PADME				SLS Block 1B	2033-2
2034		-	2034-1	2034-2	-	-
					-	-

2035					-	-
	Moon Mining & Gas Station Servicing Mission	Sep-35	2035-1	2035-2	Falcon	-
	Habitat Section 5 Launch				SLS Block 1B	2035-1
	Habitat Section 6 Launch				SLS Block 1B	2035-2
LAST SLS DELIVERY YEAR						
2037*	Mars Magellan 1 Delivery (No Refuel)	-	-	-	SLS Block 1B	Purchase 1
	Habitat Section 7 Launch	-			SLS Block 1B	Purchase 2
	Habitat Section 8 Launch	Nov-37	-	-	SLS Block 1B	Purchase 3
2038		-	-	-		
2039	Mars Magellan 2 Delivery	-	-	-	SLS Block 1B	Purchase 4
2040*	Crane 1 Launch	Jan-40	-	-	SLS Block 1B	Purchase 5
	Crane 2 Launch				SLS Block 1B	Purchase 6
2041	Mars Miner Launch	-	-	-	SLS Block 1B	Purchase 7
2042*	Mars Magellan 3 Delivery	Mar-42	-	-	SLS Block 1B	Purchase 8
	ELD Vehicle Launch				SLS Block 1B	Purchase 9
	Reactors/Solar Panel Delivery				SLS Block 1B	Purchase 10
2043	PHASE 4: CREW TRANSPORT					
2044*	CTV 1 Launch	May-44	-	-	SLS Block 1B	Purchase 11
	Crew 1 Launch				Flacon 9	-
2045	PHASE 5: MARS HABITATION					
2046	CTV 2 Launch	Jul-46	-	-	SLS Block 1B	Purchase 12
	Crew 2 Launch				Flacon 9	-
2047*			-	-	-	-
2048*	Crew Launch 3 (meet with CTV 1)	Sep-48	-	-	Flacon 9	-
					-	-
2049		-	-	-	-	-
2050*	Crew 4 Launch (meet with CTV 2)	Nov-50	-	-	Flacon 9	-
					-	-
2051		-	-	-	-	-

2052		-	-	-	-	-
2053*	CTV 3 Launch	Jan-53	-	-	SLS Block 1B	Purchase 13
	Crew 5 Launch		-	-	Flacon 9	-
	Crew 6 Launch (Meet with CTV 1)		-	-	Flacon 9	-
2054	MISSION INDEPENDENT OF EARTH --- ALL 24 CREW ON MARS					
	REQUIREMENT: Crew Rotates every 13 years					

Table 71. Implemented Mission Architecture

9.2.Phase I: Exploration

DSx No.	Latitude				Longitude			
	Deg.	Min.	Sec.	Dir.	Deg.	Min.	Sec.	Dir.
DS1	39	48	25.34	S	82	18	33.88	E
DS2	39	28	10.92		82	46	6.21	
DS3	39	29	46.25		82	12	24.91	
DS4	40	7	10.74		82	31	54.36	
DS5	39	41	13.14		83	31	9.02	
DS6	40	47	31.53		82	26	41.81	
DS7	41	33	50.93		82	37	17.13	
DS8	41	4	53.08		82	51	23.82	
DS9	41	11	55.07		82	16	28.40	
DS10	40	53	0.87		84	27	1.78	
DS11	41	58	43.95		83	31	57.93	
DS12	42	7	11.74		82	35	41.38	
DS13	42	1	17.14		82	3	59.69	
DS14	37	51	50.48		82	34	30.44	
DS15	38	2	15.10		82	12	39.45	

DS16	36	47	58.28		77	21	12.08	
DS17	36	9	16.07		77	20	18.70	
DS18	43	18	16.40		86	1	48.96	
DS19	43	36	30.35		86	45	38.40	

Table 72. DSx Landing Coordinates in the Eastern Lowlands of Hellas Planitia

DSx No.	Latitude				Longitude			
	Deg.	Min.	Sec.	Dir.	Deg.	Min.	Sec.	Dir.
DS20	28	43	38.42	S	73	26	59.87	E
DS21	27	17	16.80		73	30	37.77	
DS22	28	9	58.89		73	7	35.59	
DS23	27	57	53.37		74	21	31.75	
DS24	30	5	51.64		73	10	58.18	
DS25	29	46	14.97		69	23	2.37	

Table 73. DSx Landing Coordinates in Terby Crater of Hellas Planitia

DSx No.	Latitude				Longitude			
	Deg.	Min.	Sec.	Dir.	Deg.	Min.	Sec.	Dir.
DS26	28	21	45.74	S	95	29	23.14	E
DS27	28	29	3.36		96	3	48.12	
DS28	32	56	49.25		93	34	12.88	
DS29	32	41	14.54		95	26	8.04	
DS30	34	40	25.70		93	32	47.33	
DS31	34	30	40.79		94	22	8.04	
DS32	34	28	13.33		100	42	12.40	
DS33	36	54	60.00		104	9	0.00	
DS34	39	34	56.39		99	19	53.82	

Table 74. DSx Landing Coordinates in the Eastern Highlands of Hellas Planitia

DSx No.	Latitude				Longitude			
	Deg.	Min.	Sec.	Dir.	Deg.	Min.	Sec.	Dir.
DS35	21	39	54.26	N	22	55	13.77	W
DS36	21	54	54.88		22	41	25.57	
DS37	22	10	17.22		22	26	31.98	

Table 75. DSx Landing Coordinates in McLaughlin Crater

9.3. Phase II: Resource Acquisition and Infrastructure Setup

9.3.1. Miner

Model Information

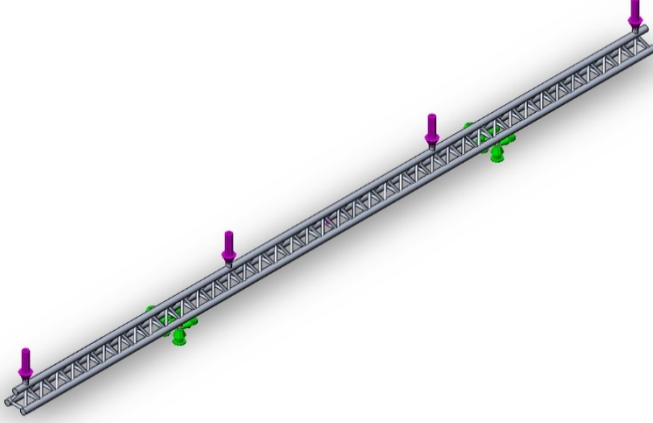
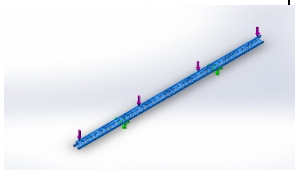
			
Model name: truss1 for sim Current Configuration: Default			
Solid Bodies			
Document Name and Reference	Treated As	Volumetric Properties	Document Path/Date Modified
Boss-Extrude8 	Solid Body	Mass:875.426 kg Volume:0.311539 m ³ Density:2810 kg/m ³ Weight:8579.17 N	G:\truss1 for sim.SLDPRT Apr 27 23:11:42 2015

Figure 205. Lunar Miner Truss Loads

Material Properties

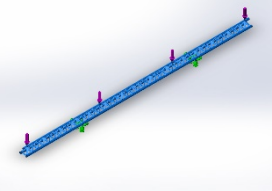
Model Reference	Properties	Components
	Name: 7075-T6 (SN) Model type: Linear Elastic Isotropic Default failure criterion: Unknown Yield strength: 5.05e+008 N/m² Tensile strength: 5.7e+008 N/m² Elastic modulus: 7.2e+010 N/m² Poisson's ratio: 0.33 Mass density: 2810 kg/m³ Shear modulus: 2.69e+010 N/m² Thermal expansion coefficient: 2.4e-005 /Kelvin	SolidBody 1(Boss-Extrude8)(truss1 for sim)

Figure 206. Lunar Miner Truss Material Properties

Study Results

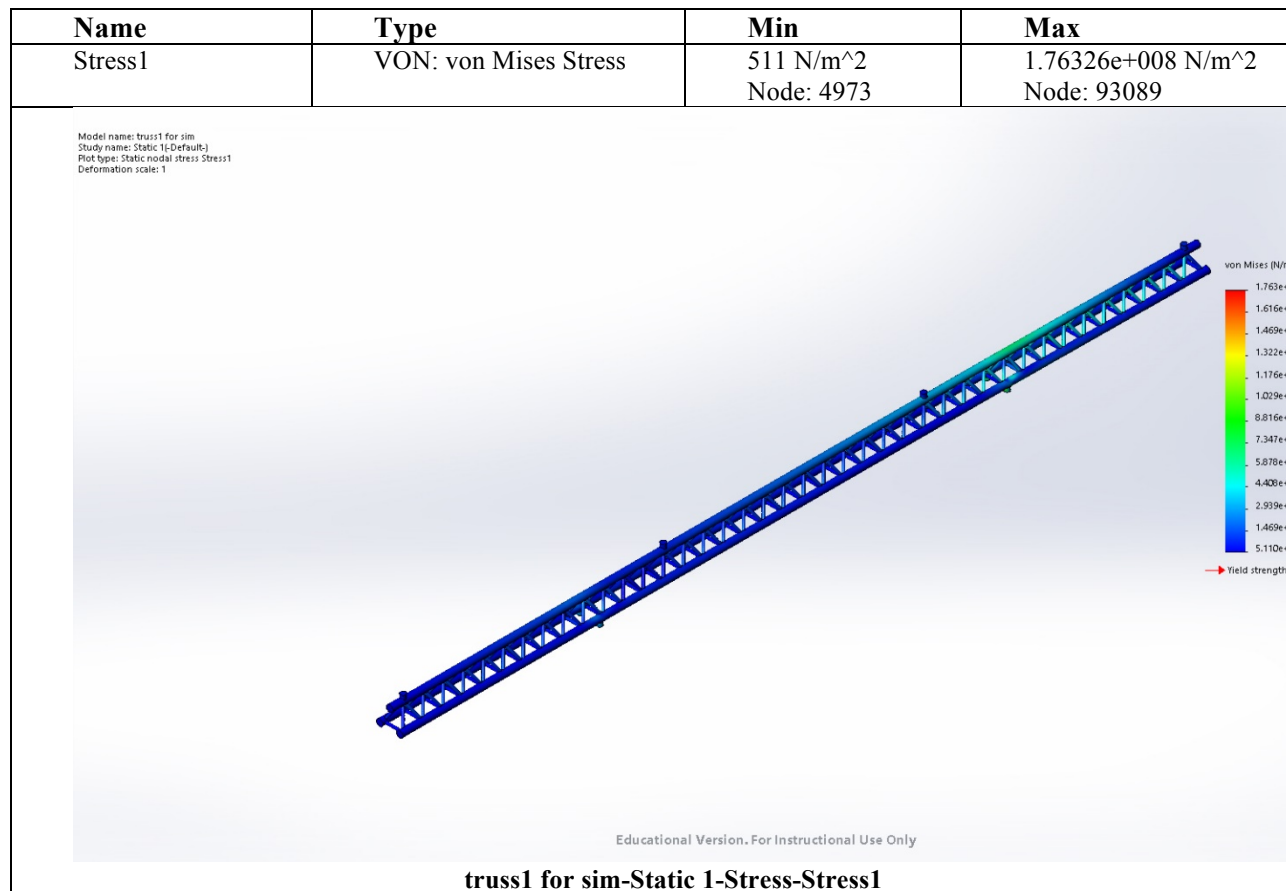


Figure 207. Lunar Miner Truss Stresses

Name	Type	Min	Max
Displacement1	URES: Resultant	0 mm	26.2713 mm

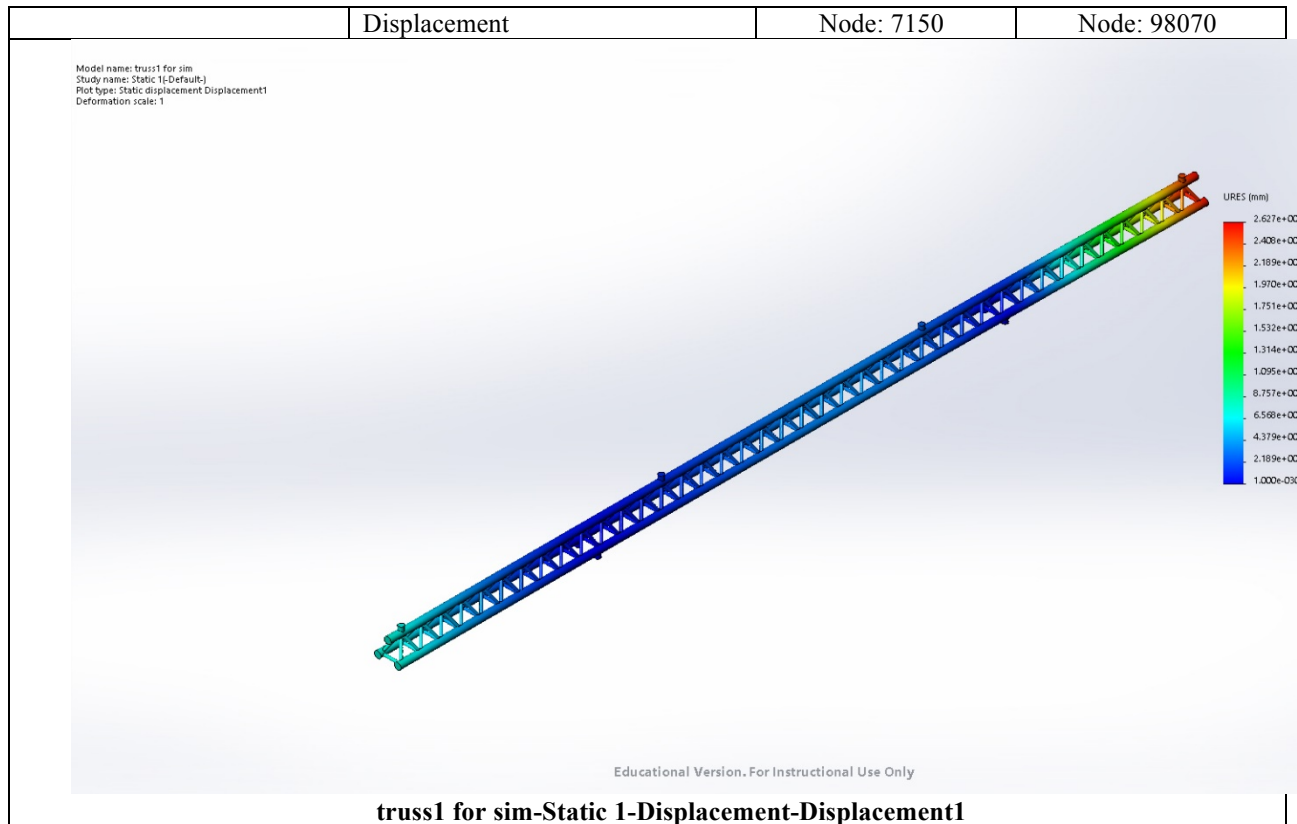


Figure 208. Lunar Miner Truss Displacement

9.3.2. Lunar Crew Consumables Mass and Volume Breakdown

Item	Mass Per Item	Volume Per Item	Quantity	Mass - 6 CM for 120 days (kg)	Volume- 6 CM for 120 days (m ³)	Mass-3 CM for 30 days (kg)	Volume- 3 CM for 30 days (m ³)
Toothbrush	.3 oz	216 in ³	1/ CM/ 3 months	0.05	0.021	0.03	0.011
Toothpaste	5.8 oz	20 in ³	1/ CM/ 4 months	0.99	0.002	0.16	0.000
Floss (100 yd)	.8 oz	59 in ³	1/ CM/ year	0.05	0.002	0.02	0.001
Comb set (2 of each)	.3 oz	5 in ³	1/ CM	0.05	0.000	0.03	0.000
Brush set (2 of each)	3 oz	60 in ³	1/ CM	0.51	0.006	0.26	0.003
No rinse body bath (space soap)	1.12 lb	46.944 in ³	1/CM/2 months	6.10	0.009	1.02	0.002
Disinfectant wipes- pack of 120	4.8 oz	41.664 in ³	3/CM/2 days	1.22	0.006	0.15	0.001
No-wash shampoo	16 oz	53.125 in ³	1/ CM/ 2 months	5.44	0.010	0.91	0.002
Razor handles	3.2 oz	58 in ³	1/ CM + 2 extra	0.73	0.008	0.45	0.005
Razor blades	2.3 oz	4.4 in ³	1/ CM/ 1 month	1.17	0.001	0.20	0.000
Shaving cream	1 lb	31 in ³	1/ CM/ 2 months	5.44	0.006	0.91	0.001
Female hygiene set	.12 lb	45 in ³	1/FM crew	0.33	0.004	0.16	0.002
Deodorant	2.6 oz	14.5 in ³	1/ CM/ month	1.33	0.004	0.22	0.001
Eye drops	.06 lb	0.375 in ³	1/ CM/ year	0.16	0.000	0.08	0.000
Skin lotion	1.1 lb	62 in ³	1/ CM/ 6-months	2.99	0.006	0.50	0.001
Towels	.27 lb	.007 m ²	8/CM/month	17.64	1.008	2.94	0.168
Packaged wet towel (8x8 in)	44 g	9 in ³	1/CM/2 days	15.84	0.053	1.98	0.007
Washcloth (50 pack)	4 oz	41.472 in ³	1 cloth/CM/day	1.63	0.010	0.20	0.001
Hygiene Consumables Totals				61.67	1.16	10.21	0.20
First aid kit (bandages, tape, gauze, pills... etc.)	0.3 kg	96.1 in ³	1	0.30	0.002	0.30	0.002
Vitamin bottle (1 tab per day, 200 tabs per bottle)	.1 kg/bottle	32.5 in ³ /bottle	1 tab/day/CM	0.40	0.004	0.10	0.004
Medications Kit - 90 bottles included (50 pills per bottle)	0.025 kg/bottle	-	1	2.25	0.005	2.25	0.005
Medical Consumables Totals				2.95	0.01	2.65	0.01
T-shirt	6 oz	42.4 in ³	1/CM/3 days & 1/CM/10 days	53.07	0.217	6.63	0.027
Long Sleeve shirts	6 oz	48 in ³	2/CM	2.04	0.009	1.02	0.005
Shoes	6.5 oz	360 in ³	2/CM	2.21	0.071	1.11	0.035
Cargo pants	9 oz	216 in ³	1/CM/10 days	18.37	0.255	2.30	0.032
Shorts	7.1 oz	54 in ³	1/CM/3 days	48.31	0.212	6.04	0.027
Jackets/sweaters	9.9 oz	54 in ³	2/CM	3.37	0.011	1.68	0.005
Undergarments	2 oz	6.3 in ³	1/CM/3 days	13.61	0.025	1.70	0.003
Socks	2 oz	6.3 in ³	1/CM/3 days	13.61	0.025	1.70	0.003
Sweatpants	7.5 oz	216 in ³	2/CM	2.55	0.042	1.28	0.021
Clothing Consumables Totals				157.14	0.87	23.46	0.16
Dried Food	1.76 kg	.0048 m ³	1/CM-d	1267.20	3.456	158.40	0.432
Food Consumables Totals				1267.20	3.46	158.40	0.43
O2 gas	-	-	-	1139.10	3.22	94.00	2.48
N2 gas	-	-	-	424.83	0.6	168.00	1.22
H2O	-	-	-	3051.40	3.05	-	-
LSS Consumables Totals				4615.33	6.87	262.00	3.70
Crew personal items	10 kg	0.5 m ³	1/CM	60.00	0.75	30.00	0.4
Misc. Consumables Totals				60.00	0.75	30.00	0.40
Total Consumables (Recurring) Mass:				6164	13.11	487	4.91

Table 76. Lunar Crew Consumables Mass and Volume Breakdown

9.4. Phase IV: Crew Transport

9.4.1. CTV Mass Breakdown

Item	R/N/S*	Quantity (4 crew; 180 days, Reserve)	Mass Per Item	Mass - 180 days (kg)	Mass- Reserve (kg)	Total Mass including Reserve (kg)	Volume Per Item	Total Volume (in^3) (incl. reserves)	Total Volume (m^3) (incl. Reserves)	Notes
Toothbrush	R/S	8, 8 reserve	.3 oz	0.07	0.07	0.14	216 in^3	3456.0	0.057	
Toothpaste	R/S	8, 8 reserve	5.8 oz	1.32	1.32	1.97	20 in^3	320.0	0.005	
Floss (100 yd)	R/S	4, 4 reserve	.8 oz	0.09	0.09	0.09	59 in^3	472.0	0.008	
Comb set (2 of each)	R/S	4, 4 reserve	.3 oz	0.03	0.03	0.03	5 in^3	40.0	0.001	
Brush set (2 of each)	R/S	4, 4 reserve	3 oz	0.34	0.34	0.34	60 in^3	480.0	0.008	
No rinse body bath (space soap)	R/S	12, 12 reserve	1.12 lb	6.10	6.10	12.19	46.944 in^3	1126.7	0.019	2.4 x 2.4 x 8.15 inches
Disinfectant wipes (3/cm every two days)- pack of 120	R/S	9, 9 reserve	4.8 oz	1.22	1.22	2.45	41.664 in^3	750.0	0.012	4.8 x 2.8 x 3.1 inches
No-wash shampoo	R/S	48, 48 reserve	16 oz	21.77	21.77	43.54	53.125 in^3	5100.0	0.084	8.5 x 2.5 x 2.5 inches
Razor handles	R/S	4, 4 reserve	3.2 oz	0.36	0.36	0.45	58 in^3	464.0	0.008	1.9 x 3.9 x 7.8 inches
Razor blades	R/S	24, 24 reserve	2.3 oz	1.56	1.56	3.13	4.4 in^3	211.2	0.004	1 x 1 x 4.4 inches
Shaving cream	R/S	12, 12 reserve	1 lb	5.44	5.44	10.89	31 in^3	744.0	0.012	2.1 x 7.1 x 2.1 inches
Female hygiene set	R/S	1/ female CM + 1 reserve	.12 lb	0.27	0.27	0.27	45 in^3	180.0	0.003	2.05 x 3.6 x 6.1 inches
Deodorant	R/S	24, 24 reserve	2.6 oz	1.77	1.77	3.54	14.5 in^3	696.0	0.011	
Eye drops	R/S	4, 4 reserve	.06 lb	0.11	0.11	0.11	0.375 in^3	3.0	0.000	1.5 x 1 x 2.5 inches
Skin lotion	R/S	4, 4 reserve	1.1 lb	2.00	2.00	3.99	62 in^3	496.0	0.008	3.3 x 2 x 9.4 inches
Towels (2/wk/cm)	R/S	208, 208 reserve	.27 lb	25.47	25.47	50.95	.007 m^2	-	2.912	1000 x 350 x 2 mm
Packaged wet towel (8x8 in)	R/S	360, 360 reserve	44 g	15.84	15.84	31.68	9 in^3	6480.0	0.106	3 x 3 x .1 inches
Washcloth (50 pack)	R/S	5, 5 reserve	4 oz	0.57	0.57	1.13	41.472 in^3	414.7	0.007	9.6 x 7.2 x 0.6 inches
Hygiene Consumables Totals				84.33	84.33	166.89			3.263	
Urine Processor Assembly (UPA)	N	1, no reserve	291 kg	291	0	291	0.523 m^3	-	0.523	<---Initial System
<i>UPA Replacement Parts Launched with CTV:</i>									1.747	<---Replacement parts through 2054
Distillation Assembly	N	1, no reserve	92.7 kg	92.7	0	92.7	-	-	-	
Firmware Controller Assembly	N	2, no reserve	23.1 kg	46.2	0	46.2	-	-	-	
Fluids Control and Pump Assembly	N	1, no reserve	47.6 kg	47.6	0	47.6	-	-	-	
Pressure Control and Pump Assembly	N	1, no reserve	49.1 kg	49.1	0	49.1	-	-	-	
Recycle Filter Tank Assembly	N	13, no reserve	15.4 kg	200.2	0	200.2	-	-	-	
Separator Plumbing Assembly	N	1, no reserve	16.8 kg	16.8	0	16.8	-	-	-	
Hygiene Equipment Totals				743.6	0	743.6			2.27	
Z-2 space suit	R/S	4, no reserve	63 kg	252	0	252	2.9 m^3	-	11.600	
EVA Consumables Totals				252	0	252			11.600	
Fanny-pack tool bag	N	2, no reserve	10 kg	20	0	20	0.4 m^3	-	0.400	
EVA Equipment Totals				20	0	20			0.400	
Sleeping bag	N	4, no reserve	800 g	3.2	0	3.2	-	-	-	26 x 16 cm / 6l
Sleeping bunk ('phone booth')	N	4, no reserve	6 kg	24	0	24	1.125 m^3	-	4.500	2 x .75 x .75 m
Polvethvlene blocks	N	4, no reserve	105 kg	221.25	0	885	.1125 m^3	-	0.450	.2 x .75 x .75 m

Portable Ultrasound	N	1, no reserve	0.12 kg	0.12	0	0.12	324 in ³	324	0.005	12 x 9 x 3 inches
Portable Defibrillator	N	1, no reserve	2.4 kg	2.4	0	2.4	305.119 in ³	305.119	0.005	
Respirator	N	1, no reserve	30 kg	30	0	30	7200.802 in ³	7200.802	0.118	.38 x .42 x .74 m
EMT kit	N	1, no reserve	3.2 kg	3.2	0	3.2	2160 in ³	2160	0.035	20 x 12 x 9 inches
Surgical Kit	N	1, no reserve	1.4 kg	1.4	0	1.4	~100 in ³	100	0.002	
Superfocus adjustable glasses	N	5, no reserve	~2 oz	0.28	0	0.28	22.5 in ³	112.5	0.002	2.5 x 1.5 x 6 inches
Intravenous fluid system	N	2, no reserve	.02 kg	0.04	0	0.04	~200 in ³	400	0.007	
Medical Equipment Totals				37.44	0	37.44			0.1737	
First aid kit (bandages, tape, gauze, pills... etc.)	R/S	1, no reserve	0.3 kg	0.3	0.3	0.6	96.1 in ³	96.1	0.002	6.2 x 7.75 x 2 inches
Vitamin bottle (1 tab per day, 200 tabs per bottle)	R/S	4, 4 reserve	.1 kg/bottle	0.4	0.4	0.8	32.5 in ³ /bottle	260	0.004	5.2 x 2.5 x 2.5 inches / bottle
Medications Kit - 90 bottles included (50 pills per bottle)	R/S	1, no reserve	0.025 kg/bottle	2.25	2.25	4.5	-	-	0.005	~2 yr shelf life
Medical Consumables Totals				2.95	2.95	5.9			0.0104	
T-shirt (1 per 3 days for exercise, 1 per 10 days)	R/S	312, 312 reserve	6 oz	53.07	53.07	106.14	42.4 in ³	26457.6	0.434	Military roll 6" length, 1.5 inch radius
Long Sleeve shirts (2 per cm)	R/S	8, 8 reserve	6 oz	1.36	1.36	2.72	~48 in ³	768	0.013	Add .1 inch to radius of T-shirt
Shoes (2 per cm)	R/S	8, 8 reserve	6.5 oz	1.47	1.47	2.95	360 in ³	5760	0.094	
Cargo pants (1 per 10 days)	R/S	72, 72 reserve	9 oz	18.37	18.37	36.74	216 in ³	31104	0.510	
Shorts (1 per 3 days for exercise)	R/S	240, 240 reserve	7.1 oz	48.31	48.31	96.62	54 in ³	25920	0.425	
Jackets/sweaters (2 per cm)	R/S	8, 8 reserve	9.9 oz	2.25	2.25	4.49	54 in ³	864	0.014	
Undergarments (1 per 3 days)	R/S	240, 240 reserve	2 oz	13.61	13.61	27.22	6.3 in ³	3024	0.050	
Socks (1 per 3 days)	R/S	240, 240 reserve	2 oz	13.61	13.61	27.22	6.3 in ³	3024	0.050	
Sweatpants (2 per cm)	R/S	8, 8 reserve	7.5 oz	1.7	1.7	3.4	216 in ³	3456	0.057	
Clothing Consumables Totals				153.75	153.8	307.5			1.6451	
Dried Food	R/S	-	1.76 kg/CM-d	1267.2	1267.2	2534.4	.0048 m ³ /CM-d	-	6.912	
Food Consumables Totals				1267.2	1267	2534.4			6.912	
Rehydration Apparatus/Conduction Oven	N	1, no reserve	36.3 kg	36.3	0	36.3	0.094 m ³	-	0.094	
Food Equipment Totals				36.3	0	36.3			0.094	
O2 gas	N	-	80 kg	80	-	80	.32 m ³	-	0.320	
N2 gas	N	-	169 kg	169	-	169	.75 m ³	-	0.750	
H2O	N	-	6750 kg	6750	-	6750	6.75 m ³	-	6.750	
LSS Consumables Totals				6999	0	6999			7.82	
Sabatier Reactor and Electrolysis System	N	1, 1 reserve	42 kg	42	42	84	0.087 m ³	-	0.174	
Water Processor Assembly	N	1, no reserve	781 kg	781	0	781	1.1 m ³	-	1.100	
<i>WPA Replacement Parts Launched with CTV:</i>							2.435 m ³	-	2.435	
Catalytic Reactor	N	2, no reserve	67.042 kg	134.08	0	134.08	-	-	-	
Gas Separator	N	1, no reserve	39.1456 kg	39.15	0	39.15	-	-	-	

Ion exchnage Bed	N	7, no reserve	13.02 kg	91.14	0	91.14	-	-	-	
Microbial Check Valve	N	1, no reserve	5.76 kg	5.76	0	5.76	-	-	-	
Multifiltration Bed #1	N	3, no reserve	149.23 kg	447.69	0	447.69	-	-	-	
Multifiltration Bed #2	N	3, no reserve	149.23 kg	447.69	0	447.69	-	-	-	
Particulate Filter	N	5, no reserve	32.25 kg	161.25	0	161.25	-	-	-	
pH Adjuster	N	1, no reserve	2.54 kg	2.54	0	2.54	-	-	-	
Process Controller	N	1, no reserve	44.9971 kg	45	0	45	-	-	-	
Pump Separator	N	2, no reserve	31.3 kg	62.6	0	62.6	-	-	-	
Reactor Health Sensor	N	2, no reserve	16.8 kg	33.6	0	33.6	-	-	-	
Sensor	N	1, no reserve	4.81 kg	4.81	0	4.81	-	-	-	
Separator Filter	N	2, no reserve	7.66 kg	15.32	0	15.32	-	-	-	
Start-up Filter	N	1, no reserve	9.43 kg	9.43	0	9.43	-	-	-	
Wastewater	N	2, no reserve	103.3 kg	206.6	0	206.6	-	-	-	
Water Delivery	N	2, no reserve	47.5 kg	95	0	95	-	-	-	
Water Storage	N	2, no reserve	56.7 kg	113.4	0	113.4	-	-	-	
ECS Equipment Totals				2738.1	42	2780.06			3.709	
O2 Tanks	N	4, no reserve	35.9 kg	143.6	0	143.6	0.113 m^3	-	0.450	Spherical Tank, R_inner=0.3 m R_Outer=0.307 m. Made of Titanium.
N2 Tanks	N	6, no reserve	51.8 kg	310.8	0	310.8	0.113 m^3	-	0.680	Spherical Tank, R_inner=0.3 m R_Outer=0.31 m. Made of Titanium.
Press. Gas Equipment Totals				454.4	0	454.4			1.13	
Stationary Bike	N	1, no reserve	50 kg	50	0	50	.6 m^3	-	0.600	
Advanced Resistance Exercise Device	N	1, no reserve	300 kg	300	0	300	5.2 m^3	-	5.200	
Exercise Equipment Totals				350	0	350			5.8	
Lighting	N	6, 2 reserves	4 oz	0.68	0.23	0.91	68.796 in^3	550.368	0.009	4.2 x 2.6 x 6.3 inches (1 bulb)
Respirator (gas mask)	N	4, no reserve	0.5 kg	2	0	2	462 in^3	1848	0.030	4 x 10.5 x 11 inches
Battery	N	1, no reserve	570 kg	570	0	570	.21 m^3	-	0.210	
Science missions	N	-	180 kg	180	0	180	4 m^3	-	4.000	
Misc. Equipment Totals				752.68	0.23	752.91			4.2493	
Crew personal items	R/S	4, no reserve	10 kg	36.81	0	36.81	0.5 m^3	-	0.500	
Tablet computer	R/S	4, no reserve	1.76 lbs	3.19	0	3.19	32.8 in ^3	131.2	0.002	11.5 x 7.93 x 0.36 inches
Misc. Consumables Totals				40	0	40			0.502	
Propellant	R	-	1500 kg	1500	0	1500	4.22 m^3	-	4.220	
Propellant. Consumables Totals				1500	0	1500			4.220	
Total Equipment (Nonrecurring) Mass:				5381	42	6087			22.78	
Total Consumables (Recurring) Mass:				8799	1508	11806			35.97	
Total Mass:				14180	1550	17893			58.75	

*N/R/S:

N: Nonrecurring

R: Recurring

S: Reserve will be brought to the surface of Mars with the crew

Table 77. Lunar Crew Consumables Mass and Volume Breakdown

9.4.2. CTV Resupply Mass and Volume Breakdown

Item	General Quantity	Mass Per Item	Volume Per Item	Supporting 1 crew 6 months	Mass (kg)	Volume (m ³)	Crew 1 (supporting 1) 20 months	Mass (kg)	Volume (m ³)	Crew 2 (supporting 1, 2) 20 months	Mass (kg)	Volume (m ³)
Toothpaste	1/ CM/ 4 months	5.8 oz	20 in ³	6	0.99	0.002	20	3.29	0.007	20	3.29	0.007
Soap (shower)- bar	2/ CM/ month	4 oz	13 in ³	48	5.44	0.010	160	18.14	0.034	160	18.14	0.034
Soap (handwashing)- bar	7/ week	4 oz	13 in ³	180	20.41	0.038	620	70.31	0.132	620	70.31	0.132
2-in-1 shampoo/conditioner	1/ CM/ 2 months	25.4 oz	199 in ³	12	8.64	0.039	40	28.80	0.130	40	28.80	0.130
Shaving cream	1/ CM/ 2 months	1 lb	31 in ³	12	5.44	0.006	40	18.14	0.020	40	18.14	0.020
Deodorant	1/ CM/ month	2.6 oz	14.5 in ³	24	1.77	0.006	80	5.90	0.019	80	5.90	0.019
Eye drops	1/ CM/ year	.06 lb	0.375 in ³	2	0.11	0.000	8	0.11	0.000	8	0.11	0.000
Skin Lotion	1/ CM/ 6-months	1.1 lb	62 in ³	4	2.00	0.004	16	7.98	0.016	16	7.98	0.016
First aid kit	1/ crew	0.3 kg	96.1 in ³	1	0.30	0.002	1	0.30	0.002	1	0.30	0.002
Vitamin bottle (1 tab/day)	200 tabs/ bottle	.1kg per bottle	32.5 in ³ per bottle	3.6	0.36	0.002	13	1.30	0.007	13	1.30	0.007
Medications Kit	90 bottles (50pills)	0.025 kg per bottle	0.002 m ³	1	2.25	0.002	1	2.25	0.002	1	2.25	0.002
Clorox/lysol spray	2/month	22 oz	104.94 in ³	12	7.48	0.021	40	24.95	0.069	40	24.95	0.069
All-natural laundry detergent (120 HE washes)	1 /1.25 months for a crew of 24	12.6 oz	60.55 in ³	4.8	2.14	0.005	3	1.07	0.003	6	2.14	0.006
				TOTAL (1 crew)	57.34	0.137	TOTAL (1 crew)	182.54	0.441	TOTAL (1 crew)	183.61	0.444
										TOTAL (2 crews)	367.23	0.888
										+6 months crew 1	57.34	0.137
				TOTAL:	57.34	0.137		182.54	0.441		424.57	1.025

Item	General Quantity	Mass Per Item	Volume Per Item	Crew 3 (supporting 1,2,3) 20 months	Mass (kg)	Volume (m ³)	Crew 4 (supporting 1,2,3,4) 20 months	Mass (kg)	Volume (m ³)	Crews 5&6 (supporting 1,2,3,4) 6 months	Mass (kg)	Volume (m ³)
Toothpaste	1/ CM/ 4 months	5.8 oz	20 in ³	20	3.29	0.007	20	3.29	0.007	-	-	-
Soap (shower)- bar	2/ CM/ month	4 oz	13 in ³	160	18.14	0.034	160	18.14	0.034	-	-	-
Soap (handwashing)- bar	7/ week	4 oz	13 in ³	620	70.31	0.132	620	70.31	0.132	-	-	-
2-in-1 shampoo/conditioner	1/ CM/ 2 months	25.4 oz	199 in ³	40	28.80	0.130	40	28.80	0.130	-	-	-
Shaving cream	1/ CM/ 2 months	1 lb	31 in ³	40	18.14	0.020	40	18.14	0.020	-	-	-
Deodorant	1/ CM/ month	2.6 oz	14.5 in ³	80	5.90	0.019	80	5.90	0.019	-	-	-
Eye drops	1/ CM/ year	.06 lb	0.375 in ³	8	0.11	0.000	8	0.11	0.000	-	-	-
Skin Lotion	1/ CM/ 6-months	1.1 lb	62 in ³	16	7.98	0.016	16	7.98	0.016	-	-	-
First aid kit	1/ crew	0.3 kg	96.1 in ³	1	0.30	0.002	1	0.30	0.002	-	-	-
Vitamin bottle (1 tab/day)	200 tabs/ bottle	.1kg per bottle	32.5 in ³ per bottle	13	1.30	0.007	13	1.30	0.007	-	-	-
Medications Kit	90 bottles (50pills)	0.025 kg per bottle	0.002 m ³	1	2.25	0.002	1	2.25	0.002	-	-	-
Clorox/lysol spray	2/month	22 oz	104.94 in ³	40	24.95	0.069	40	24.95	0.069	-	-	-
All-natural laundry detergent (120 HE washes)	1 /1.25 months for a crew of 24	12.6 oz	60.55 in ³	8	2.86	0.008	11	3.93	0.011	-	-	-
				TOTAL (1 crew)	184.33	0.446	TOTAL (1 crew)	185.40	0.449	-	-	-

Table 78. CTV Resupply Mass and Volume Breakdown

9.5. Phase V: Mars Habitation

9.5.1. Martian Crane Auxilliary Drawings

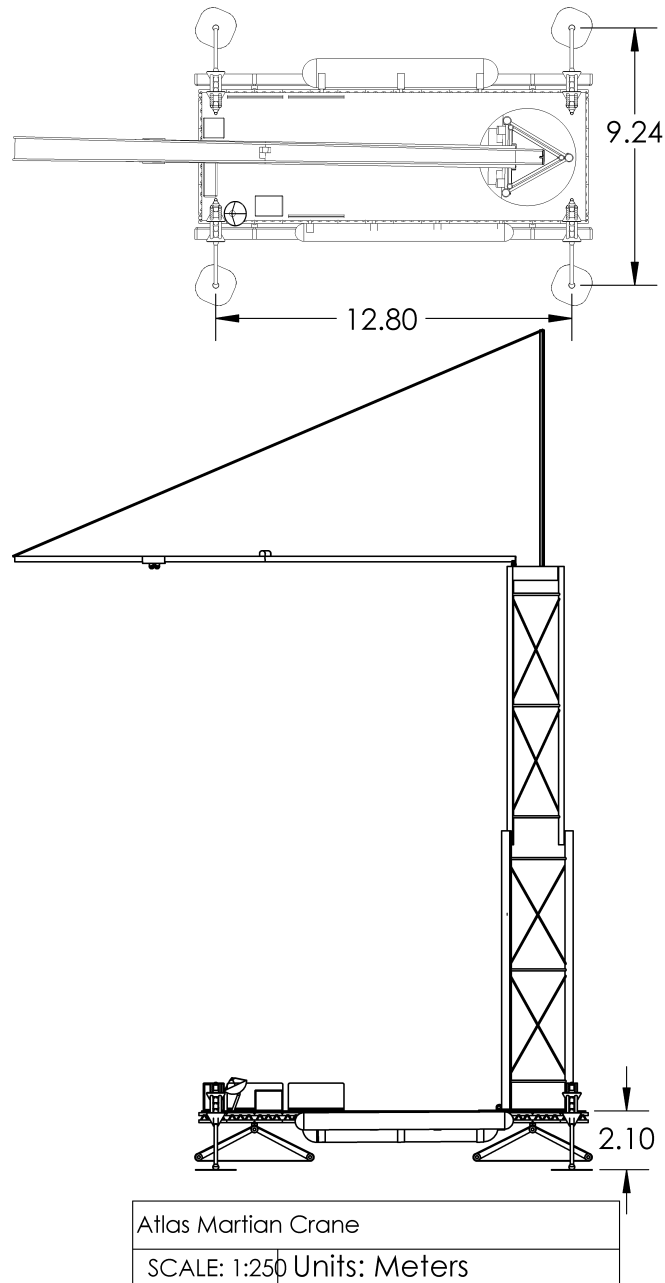


Figure 207. Martian Crane Top View/Side View

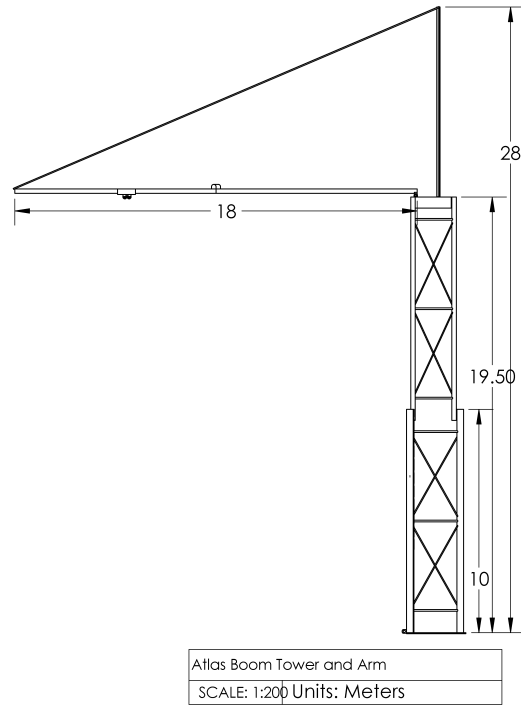


Figure 208. Martian Boom Tower and Arm Top View

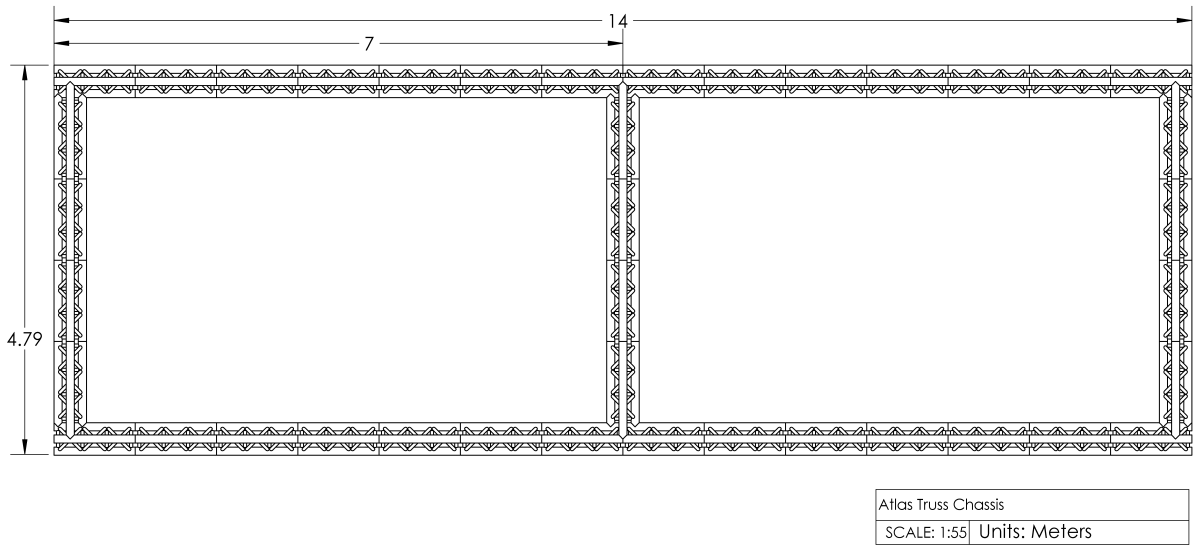


Figure 209. Martian Crane Chassis Top View

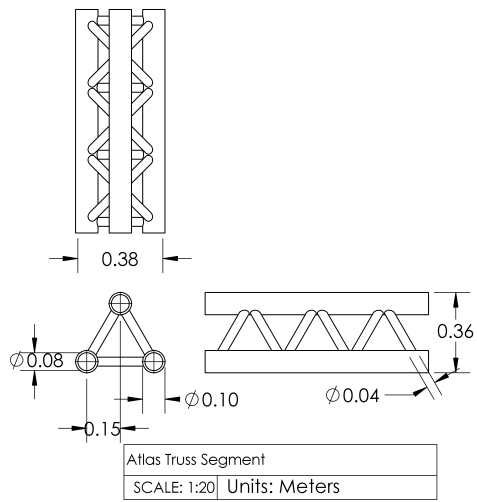


Figure 210. Martian Crane Truss Segment

9.5.2. Nutrition and Diet

Diet 1

Food	Sweet Potato	Peanut	Wheat	Rice	Cabbage	Green Onion	Lettuce	Onion	Snap Bean	Strawberry	Kale	Broccoli	Peppers	Tilapia	Spirulina	Total	Needed	Difference
Grams/100g	0.4	0.6	3.4	0.4	0.4	0.4	0.4	0.4	0.4	0.4	0.5	6.4	0.4	4.8	2.5	21.9	-	-
Grams total	40	64.7	342.1	40	40	40	40	40	40	40	48	644.1	40	483.9	245.2	2187.9	-	-
Calories	34.4	366.7	####	143.2	10	12.8	6	16	12.4	12.8	23.5	219	8	464.5	711.1	3200	3200	0
Protein g	0.6	16.7	46.8	2.6	0.5	0.7	0.5	0.4	0.7	0.3	2.1	18.2	0.3	97.2	140.9	328.6	65	263.6
Fat g	0	31.8	8.4	0.2	0	0.1	0.1	0	0.1	0.1	0.4	2.4	0.1	8.2	18.9	71	71	0
Carbs g	8	10.4	243.3	31.7	2.3	2.9	1.1	3.7	2.8	3.1	4.2	42.8	1.9	0	58.6	416.9	360	56.9
Fiber g	1.2	5.5	0	1.1	1	1	0.5	0.7	1.1	0.8	1.7	16.7	0.7	0	8.8	40.9	38	2.9
Calcium mg	12	59.5	116.3	1.2	16	28.8	14.4	9.2	14.8	6.4	72	302.7	4	48.4	294.3	1000	1000	0
Iron mg	0.2	3	12	1.7	0.2	0.6	0.3	0.1	0.4	0.2	0.7	4.7	0.1	2.7	69.9	96.9	8	88.9
Magnesium mg	10	108.6	492.6	9.2	4.8	8	5.2	4	10	5.2	22.6	135.3	4	130.6	478.2	1428.2	420	1008.2
Phosphorus mg	18.8	243.2	####	38	10.4	14.8	11.6	11.6	15.2	9.6	44.2	425.1	8	822.6	289.3	3700	700	3000
Potassium mg	134.8	455.9	####	30.4	68	110.4	77.6	58.4	84.4	61.2	235.8	####	70	1461.3	3342.2	9699.9	4700	4999.9
Sodium mg	22	11.6	6.8	0.4	7.2	6.4	11.2	1.6	2.4	0.4	18.3	212.5	1.2	251.6	2569.8	3123.5	1500	1623.5
Zinc mg	0.1	2.1	14.2	0.4	0.1	0.2	0.1	0.1	0.1	0.1	0.3	2.6	0.1	1.6	4.9	26.9	11	15.9
Copper mg	0.1	0.7	1.9	0.1	0	0	0	0	0	0	0.7	0.3	0	0.4	15	19.3	0.9	18.4
Manganese mg	0.1	1.3	10.3	0.4	0.1	0.1	0.1	0.1	0.1	0.2	0.3	1.4	0	0.2	4.7	19.1	2.3	16.8
Selenium mcg	0.2	4.7	305.8	6	0.1	0.2	0.2	0.2	0.2	0.2	0.4	16.1	0	202.3	17.7	554.4	55	499.4
Vitamin C mg	1	0	0	0	14.6	7.5	3.7	3	4.9	23.5	57.6	574.5	32.2	0	24.8	747.2	90	657.2
Thiamin mg	0	0.4	1.4	0.2	0	0	0	0	0	0	0.1	0.5	0	0.2	5.8	8.8	1.2	7.6
Riboflavin mg	0	0.1	0.4	0	0	0	0	0	0	0	0.1	0.8	0	0.3	9	10.8	1.3	9.5
Niacin mg	0.2	7.8	23	1.6	0.1	0.2	0.2	0	0.3	0.2	0.5	4.1	0.2	18.9	31.4	88.8	16	72.8
Pantothenic Acid mg	0.3	1.1	3.2	0.5	0.1	0	0.1	0	0.1	0.1	0	3.7	0	2.4	8.5	20.2	5	15.2
Vitamin B6 mg	0.1	0.2	1.4	0.1	0	0	0	0	0.1	0	0.1	1.1	0.1	0.8	0.9	5.1	1.3	3.8
Folate mcg	4.4	155.2	147.1	92.4	17.2	25.6	15.2	7.6	13.2	9.6	67.7	405.8	4	116.1	230.5	1311.6	400	911.6
Choline mg	4.9	34	0	0	4.3	2.3	5.4	2.4	6.1	2.3	0.4	120.4	2.2	205.6	161.8	552.2	550	2.2
Vitamin B12 mcg	0	0	0	0	0	0	0	0	0	0	0	0	0	7.6	0	7.6	2.4	5.2
Vitamin A mcg	283.6	0	0	0	2	20	148	0	14	0.4	240.2	199.7	7.2	0	71.1	986.1	900	86.1
Vitamin E mg	0.1	5.4	0	0	0.1	0.2	0.1	0	0.2	0.1	0.7	5	0.1	1.9	12.3	26.3	15	11.3
Vitamin D mcg	0	0	0	0	0	0	0	0	0	0	0	0	0	15	0	15	15	0
Vitamin K mcg	0.7	0	0	0	30.4	82.8	50.5	0.2	5.8	0.9	338.5	651.2	3	6.8	62.5	1233.2	120	1113.2

Table 79. Diet 1

Diet 2

Food	Sweet Potato	Peanut	Wheat	Rice	Potato	Cabbage	Green Onion	Lettuce	Onion	Snap Bean	Strawberry	Kale	Broccoli	Tilapia	Spirulina	Total	Needed	Difference
Grams/100g	0.4	0.7	3.4	0.4	0.4	0.4	0.4	0.4	0.4	0.4	0.4	0.6	6.2	4.9	2.4	21.7	-	-
Grams total	40	65.7	337.8	40	40	40	40	40	40	40	40	61	618.8	493.4	237.9	2174.6	-	-
Calories	34.4	372.6	1145	143.2	30.8	10	12.8	6	16	12.4	12.8	29.9	210.4	473.7	689.9	3200	3200	0
Protein g	0.6	17	46.2	2.6	0.8	0.5	0.7	0.5	0.4	0.7	0.3	2.6	17.5	99.1	136.7	326.3	65	261.3
Fat g	0	32.4	8.3	0.2	0	0	0.1	0.1	0	0.1	0.1	0.6	2.3	8.4	18.4	71	71	0
Carbs g	8	10.6	240.3	31.7	7	2.3	2.9	1.1	3.7	2.8	3.1	5.3	41.1	0	56.9	416.9	360	56.9
Fiber g	1.2	5.6	0	1.1	0.9	1	1	0.5	0.7	1.1	0.8	2.2	16.1	0	8.6	40.8	38	2.8
Calcium mg	12	60.5	114.9	1.2	4.8	16	28.8	14.4	9.2	14.8	6.4	91.5	290.8	49.3	285.5	1000	1000	0
Iron mg	0.2	3	11.9	1.7	0.3	0.2	0.6	0.3	0.1	0.4	0.2	0.9	4.5	2.8	67.8	94.9	8	86.9
Magnesium mg	10	110.4	486.5	9.2	9.2	4.8	8	5.2	4	10	5.2	28.7	129.9	133.2	463.9	1418.2	420	998.2
Phosphorus mg	18.8	247.1	1716	38	22.8	10.4	14.8	11.6	11.6	15.2	9.6	56.1	408.4	838.8	280.7	3700	700	3000
Potassium mg	134.8	463.3	1456	30.4	168.4	68	110.4	77.6	58.4	84.4	61.2	299.4	1955.4	1490.1	3242.3	9700.1	4700	5000.1
Sodium mg	22	11.8	6.8	0.4	2.4	7.2	6.4	11.2	1.6	2.4	0.4	23.2	204.2	256.6	2493	3049.5	1500	1549.5
Zinc mg	0.1	2.1	14.1	0.4	0.1	0.1	0.2	0.1	0.1	0.1	0.1	0.3	2.5	1.6	4.8	26.7	11	15.7
Copper mg	0.1	0.8	1.9	0.1	0	0	0	0	0	0	0	0.9	0.3	0.4	14.5	19	0.9	18.1
Manganese mg	0.1	1.3	10.2	0.4	0.1	0.1	0.1	0.1	0.1	0.1	0.2	0.4	1.3	0.2	4.5	18.9	2.3	16.6
Selenium mcg	0.2	4.7	302	6	0.1	0.1	0.2	0.2	0.2	0.2	0.2	0.5	15.5	206.2	17.1	553.7	55	498.7
Vitamin C mg	1	0	0	0	7.9	14.6	7.5	3.7	3	4.9	23.5	73.2	552	0	24	715.2	90	625.2
Thiamin mg	0	0.4	1.4	0.2	0	0	0	0	0	0	0	0.1	0.4	0.2	5.7	8.6	1.2	7.4
Riboflavin mg	0	0.1	0.4	0	0	0	0	0	0	0	0	0.1	0.7	0.3	8.7	10.5	1.3	9.2
Niacin mg	0.2	7.9	22.8	1.6	0.4	0.1	0.2	0.2	0	0.3	0.2	0.6	4	19.3	30.5	88.2	16	72.2
Pantothenic Acid mg	0.3	1.2	3.2	0.5	0.1	0.1	0	0.1	0	0.1	0.1	0.1	3.5	2.4	8.3	19.9	5	14.9
Vitamin B6 mg	0.1	0.2	1.4	0.1	0.1	0	0	0	0	0.1	0	0.2	1.1	0.8	0.9	5.1	1.3	3.8
Folate mcg	4.4	157.7	145.3	92.4	6.4	17.2	25.6	15.2	7.6	13.2	9.6	86	389.8	118.4	223.6	1312.4	400	912.4
Choline mg	4.9	34.5	0	0	4.8	4.3	2.3	5.4	2.4	6.1	2.3	0.5	115.7	209.7	157	550	550	0
Vitamin B12 mcg	0	0	0	0	0	0	0	0	0	0	0	0	0	7.8	0	7.8	2.4	5.4
Vitamin A mcg	283.6	0	0	0	0	2	20	148	0	14	0.4	304.9	191.8	0	69	1033.7	900	133.7
Vitamin E mg	0.1	5.5	0	0	0	0.1	0.2	0.1	0	0.2	0.1	0.9	4.8	2	11.9	25.9	15	10.9
Vitamin D mcg	0	0	0	0	0	0	0	0	0	0	0	0	0	15.3	0	15.3	15	0.3
Vitamin K mcg	0.7	0	0	0	0.8	30.4	82.8	50.5	0.2	5.8	0.9	429.7	625.6	6.9	60.7	1294.9	120	1174.9

Table 80. Diet 2

Diet 3

Food	Peanut	Wheat	Rice	Cabbage	Carrot	Green Onion	Lettuce	Onion	Snap Bean	Strawberry	Kale	Broccoli	Peppers	Tilapia	Spirulina	Total	Needed	Difference
Grams/100g	0.6	3.4	0.4	0.4	0.4	0.4	0.4	0.4	0.4	0.4	0.6	5.7	0.4	5	2.5	21.5	-	-
Grams total	62.7	342.8	40	40	40	40	40	40	40	40	63.9	567.2	40	504	254.2	2155	-	-
Calories	355.3	1162	143	10	16.4	12.8	6	16	12.4	12.8	31.3	192.8	8	483.9	737.1	3200	3200	0
Protein g	16.2	46.9	2.6	0.5	0.4	0.7	0.5	0.4	0.7	0.3	2.7	16	0.3	101.2	146.1	335.6	65	270.6
Fat g	30.9	8.5	0.2	0	0.1	0.1	0.1	0	0.1	0.1	0.6	2.1	0.1	8.6	19.6	71	71	0
Carbs g	10.1	243.8	31.7	2.3	3.8	2.9	1.1	3.7	2.8	3.1	5.6	37.7	1.9	0	60.7	411.3	360	51.3
Fiber g	5.3	0	1.1	1	1.1	1	0.5	0.7	1.1	0.8	2.3	14.7	0.7	0	9.2	39.6	38	1.6
Calcium mg	57.6	116.5	1.2	16	13.2	28.8	14.4	9.2	14.8	6.4	95.8	266.6	4	50.4	305	1000	1000	0
Iron mg	2.9	12.1	1.7	0.2	0.1	0.6	0.3	0.1	0.4	0.2	0.9	4.1	0.1	2.8	72.4	99	8	91
Magnesium mg	105.3	493.6	9.2	4.8	4.8	8	5.2	4	10	5.2	30	119.1	4	136.1	495.6	1435	420	1014.9
Phosphorus mg	235.6	1741	38	10.4	14	14.8	11.6	11.6	15.2	9.6	58.8	374.4	8	856.9	299.9	3700	700	3000
Potassium mg	441.8	1477	30.4	68	128	110.4	77.6	58.4	84.4	61.2	314	1792	70	1522	3464.3	9700	4700	5000
Sodium mg	11.3	6.9	0.4	7.2	27.6	6.4	11.2	1.6	2.4	0.4	24.3	187.2	1.2	262.1	2663.7	3214	1500	1713.8
Zinc mg	2	14.3	0.4	0.1	0.1	0.2	0.1	0.1	0.1	0.1	0.4	2.3	0.1	1.7	5.1	26.8	11	15.8
Copper mg	0.7	1.9	0.1	0	0	0	0	0	0	0	1	0.3	0	0.4	15.5	20	0.9	19.1
Manganese mg	1.2	10.3	0.4	0.1	0.1	0.1	0.1	0.1	0.1	0.2	0.4	1.2	0	0.2	4.8	19.2	2.3	16.9
Selenium mcg	4.5	306.4	6	0.1	0	0.2	0.2	0.2	0.2	0.2	0.6	14.2	0	210.7	18.3	562	55	507
Vitamin C mg	0	0	0	14.6	2.4	7.5	3.7	3	4.9	23.5	76.7	505.9	32.2	0	25.7	700	90	610
Thiamin mg	0.4	1.4	0.2	0	0	0	0	0	0	0	0.1	0.4	0	0.2	6	9	1.2	7.8
Riboflavin mg	0.1	0.4	0	0	0	0	0	0	0	0	0.1	0.7	0	0.3	9.3	11.1	1.3	9.8
Niacin mg	7.6	23.1	1.6	0.1	0.4	0.2	0.2	0	0.3	0.2	0.6	3.6	0.2	19.7	32.6	90.4	16	74.4
Pantothenic Acid mg	1.1	3.2	0.5	0.1	0.1	0	0.1	0	0.1	0.1	0.1	3.3	0	2.5	8.8	20	5	15
Vitamin B6 mg	0.2	1.4	0.1	0	0.1	0	0	0	0.1	0	0.2	1	0.1	0.8	0.9	5	1.3	3.7
Folate mcg	150.4	147.4	92.4	17.2	7.6	25.6	15.2	7.6	13.2	9.6	90.1	357.3	4	121	238.9	1298	400	897.5
Choline mg	32.9	0	0	4.3	3.5	2.3	5.4	2.4	6.1	2.3	0.5	106.1	2.2	214.2	167.8	550	550	0
Vitamin B12 mcg	0	0	0	0	0	0	0	0	0	0	0	0	0	8	0	8	2.4	5.6
Vitamin A mcg	0	0	0	2	334	20	148	0	14	0.4	319	175.8	7.2	0	73.7	1095	900	194.5
Vitamin E mg	5.2	0	0	0.1	0.3	0.2	0.1	0	0.2	0.1	1	4.4	0.1	2	12.7	26.4	15	11.4
Vitamin D mcg	0	0	0	0	0	0	0	0	0	0	0	0	0	15.6	0	15.6	15	0.6
Vitamin K mcg	0	0	0	30.4	5.3	82.8	50.5	0.2	5.8	0.9	450	573.4	3	7.1	64.8	1274	120	1154.3

Table 81. Diet 3

Diet 4

Food	Sweet Potato	Peanut	Wheat	Rice	Cabbage	Green Onion	Lettuce	Onion	Radish	Snap Bean	Kale	Broccoli	Peppers	Tilapia	Spirulina	Total	Needed	Difference
Grams/100g	0.4	0.6	3.4	0.4	0.4	0.4	0.4	0.4	0.4	0.4	0.6	6	0.4	4.9	2.5	21.7	-	-
Grams total	40	64.2	342.9	40	40	40	40	40	40	40	57.1	599.5	40	494.1	247.7	2165.4	-	-
Calories	34.4	364.1	1162.3	143.2	10	12.8	6	16	6.4	12.4	28	203.8	8	474.3	718.2	3200	3200	0
Protein g	0.6	16.6	46.9	2.6	0.5	0.7	0.5	0.4	0.3	0.7	2.4	16.9	0.3	99.2	142.3	331.2	65	266.2
Fat g	0	31.6	8.5	0.2	0	0.1	0.1	0	0	0.1	0.5	2.2	0.1	8.4	19.1	71	71	0
Carbs g	8	10.4	243.9	31.7	2.3	2.9	1.1	3.7	1.4	2.8	5	39.8	1.9	0	59.2	414.1	360	54.1
Fiber g	1.2	5.5	0	1.1	1	1	0.5	0.7	0.6	1.1	2.1	15.6	0.7	0	8.9	40	38	2
Calcium mg	12	59.1	116.6	1.2	16	28.8	14.4	9.2	10	14.8	85.6	281.8	4	49.4	297.2	1000	1000	0
Iron mg	0.2	2.9	12.1	1.7	0.2	0.6	0.3	0.1	0.1	0.4	0.8	4.4	0.1	2.8	70.6	97.4	8	89.4
Magnesium mg	10	107.9	493.7	9.2	4.8	8	5.2	4	4	10	26.8	125.9	4	133.4	482.9	1429.9	420	1009.9
Phosphorus mg	18.8	241.5	1741.8	38	10.4	14.8	11.6	11.6	8	15.2	52.5	395.7	8	840	292.2	3700	700	3000
Potassium mg	134.8	452.8	1477.8	30.4	68	110.4	77.6	58.4	93.2	84.4	280.2	1894.3	70	1492.2	3375.6	9700	4700	5000
Sodium mg	22	11.6	6.9	0.4	7.2	6.4	11.2	1.6	15.6	2.4	21.7	197.8	1.2	256.9	2595.5	3158.3	1500	1658.3
Zinc mg	0.1	2.1	14.3	0.4	0.1	0.2	0.1	0.1	0.1	0.1	0.3	2.5	0.1	1.6	5	26.9	11	15.9
Copper mg	0.1	0.7	1.9	0.1	0	0	0	0	0	0	0.9	0.3	0	0.4	15.1	19.5	0.9	18.6
Manganese mg	0.1	1.2	10.3	0.4	0.1	0.1	0.1	0.1	0	0.1	0.4	1.3	0	0.2	4.7	19.1	2.3	16.8
Selenium mcg	0.2	4.6	306.5	6	0.1	0.2	0.2	0.2	0.2	0.2	0.5	15	0	206.5	17.8	558.6	55	503.6
Vitamin C mg	1	0	0	0	14.6	7.5	3.7	3	5.9	4.9	68.5	534.7	32.2	0	25	700.9	90	610.9
Thiamin mg	0	0.4	1.4	0.2	0	0	0	0	0	0	0.1	0.4	0	0.2	5.9	8.8	1.2	7.6
Riboflavin mg	0	0.1	0.4	0	0	0	0	0	0	0	0.1	0.7	0	0.3	9.1	10.9	1.3	9.6
Niacin mg	0.2	7.7	23.1	1.6	0.1	0.2	0.2	0	0.1	0.3	0.6	3.8	0.2	19.3	31.8	89.2	16	73.2
Pantothenic Acid mg	0.3	1.1	3.2	0.5	0.1	0	0.1	0	0.1	0.1	0.1	3.4	0	2.4	8.6	20.1	5	15.1
Vitamin B6 mg	0.1	0.2	1.4	0.1	0	0	0	0	0	0.1	0.2	1	0.1	0.8	0.9	5.1	1.3	3.8
Folate mcg	4.4	154.1	147.4	92.4	17.2	25.6	15.2	7.6	10	13.2	80.5	377.7	4	118.6	232.8	1300.7	400	900.7
Choline mg	4.9	33.7	0	0	4.3	2.3	5.4	2.4	2.6	6.1	0.5	112.1	2.2	210	163.5	550	550	0
Vitamin B12 mcg	0	0	0	0	0	0	0	0	0	0	0	0	0	7.8	0	7.8	2.4	5.4
Vitamin A mcg	283.6	0	0	0	2	20	148	0	0	14	285.3	185.8	7.2	0	71.8	1017.8	900	117.8
Vitamin E mg	0.1	5.3	0	0	0.1	0.2	0.1	0	0	0.2	0.9	4.7	0.1	2	12.4	26.1	15	11.1
Vitamin D mcg	0	0	0	0	0	0	0	0	0	0	0	0	0	15.3	0	15.3	15	0.3
Vitamin K mcg	0.7	0	0	0	30.4	82.8	50.5	0.2	0.5	5.8	402.2	606.1	3	6.9	63.2	1252.1	120	1132.1

Table 82. Diet 4

Diet 5

Food	Peanut	Wheat	Rice	Cabbage	Carrot	Green Onion	Lettuce	Onion	Snap Bean	Straw-berry	Tomato	Kale	Broccoli	Tilapia	Spirulina	Total	Needed	Difference
Grams/100g	0.6	3.4	0.4	0.4	0.4	0.4	0.4	0.4	0.4	0.4	0.4	0.8	5.1	5.2	2.6	21.3	-	-
Grams total	61.9	340.2	40	40	40	40	40	40	40	40	40	78.7	514	523.9	256.2	2134.8	-	-
Calories	350.9	1153.1	143.2	10	16.4	12.8	6	16	12.4	12.8	7.2	38.6	174.8	502.9	742.9	3200	3200	0
Protein g	16	46.5	2.6	0.5	0.4	0.7	0.5	0.4	0.7	0.3	0.4	3.4	14.5	105.2	147.2	339.3	65	274.3
Fat g	30.5	8.4	0.2	0	0.1	0.1	0.1	0	0.1	0.1	0.1	0.7	1.9	8.9	19.8	71	71	0
Carbs g	10	242	31.7	2.3	3.8	2.9	1.1	3.7	2.8	3.1	1.6	6.9	34.1	0	61.2	407.2	360	47.2
Fiber g	5.3	0	1.1	1	1.1	1	0.5	0.7	1.1	0.8	0.5	2.8	13.4	0	9.2	38.5	38	0.5
Calcium mg	56.9	115.7	1.2	16	13.2	28.8	14.4	9.2	14.8	6.4	4	118	241.6	52.4	307.4	1000	1000	0
Iron mg	2.8	12	1.7	0.2	0.1	0.6	0.3	0.1	0.4	0.2	0.1	1.2	3.8	2.9	73	99.4	8	91.4
Magnesium mg	104	489.8	9.2	4.8	4.8	8	5.2	4	10	5.2	4.4	37	107.9	141.4	499.6	1435.3	420	1015.3
Phosphorus mg	232.7	1728	38	10.4	14	14.8	11.6	11.6	15.2	9.6	9.6	72.4	339.2	890.6	302.3	3700	700	3000
Potassium mg	436.3	1466.1	30.4	68	128	110.4	77.6	58.4	84.4	61.2	94.8	386.3	1624.2	1582.1	3491.7	9699.9	4700	4999.9
Sodium mg	11.1	6.8	0.4	7.2	27.6	6.4	11.2	1.6	2.4	0.4	2	29.9	169.6	272.4	2684.8	3233.8	1500	1733.8
Zinc mg	2	14.2	0.4	0.1	0.1	0.2	0.1	0.1	0.1	0.1	0.1	0.4	2.1	1.7	5.1	26.7	11	15.7
Copper mg	0.7	1.9	0.1	0	0	0	0	0	0	0	0	1.2	0.3	0.4	15.6	20.3	0.9	19.4
Manganese mg	1.2	10.2	0.4	0.1	0.1	0.1	0.1	0.1	0.1	0.2	0	0.5	1.1	0.2	4.9	19.1	2.3	16.8
Selenium mcg	4.5	304.1	6	0.1	0	0.2	0.2	0.2	0.2	0.2	0	0.7	12.8	219	18.4	566.8	55	511.8
Vitamin C mg	0	0	0	14.6	2.4	7.5	3.7	3	4.9	23.5	5.5	94.4	458.5	0	25.9	643.8	90	553.8
Thiamin mg	0.4	1.4	0.2	0	0	0	0	0	0	0	0	0.1	0.4	0.2	6.1	9	1.2	7.8
Riboflavin mg	0.1	0.4	0	0	0	0	0	0	0	0	0	0.1	0.6	0.3	9.4	11.1	1.3	9.8
Niacin mg	7.5	22.9	1.6	0.1	0.4	0.2	0.2	0	0.3	0.2	0.2	0.8	3.3	20.4	32.8	91	16	75
Pantothenic Acid mg	1.1	3.2	0.5	0.1	0.1	0	0.1	0	0.1	0.1	0	0.1	2.9	2.6	8.9	19.8	5	14.8
Vitamin B6 mg	0.2	1.4	0.1	0	0.1	0	0	0	0.1	0	0	0.2	0.9	0.8	0.9	4.9	1.3	3.6
Folate mcg	148.5	146.3	92.4	17.2	7.6	25.6	15.2	7.6	13.2	9.6	6	110.9	323.8	125.7	240.8	1290.5	400	890.5
Choline mg	32.5	0	0	4.3	3.5	2.3	5.4	2.4	6.1	2.3	2.7	0.6	96.1	222.6	169.1	550	550	0
Vitamin B12 mcg	0	0	0	0	0	0	0	0	0	0	0	0	0	8.3	0	8.3	2.4	5.9
Vitamin A mcg	0	0	0	2	334	20	148	0	14	0.4	16.8	393.4	159.3	0	74.3	1162.2	900	262.2
Vitamin E mg	5.2	0	0	0.1	0.3	0.2	0.1	0	0.2	0.1	0.2	1.2	4	2.1	12.8	26.4	15	11.4
Vitamin D mcg	0	0	0	0	0	0	0	0	0	0	0	0	0	16.2	0	16.2	15	1.2
Vitamin K mcg	0	0	0	30.4	5.3	82.8	50.5	0.2	5.8	0.9	3.2	554.5	519.6	7.3	65.3	1325.8	120	1205.8

Table 83. Diet 5

9.5.3. Habitat Mass and Volume Breakdowns

Item	General Quantity (Total)	Mass Per Item	Quantity	Equipment		Consumables (1 crew, 13.5 years)	
				Mass (kg)	Vol (m ³)	Mass (kg)	Vol (m ³)
Toothbrush	1/ CM/ 3 months	.3 oz	216	-	-	1.84	0.765
Floss (100 yd)	1/ CM/ year	.8 oz	54	-	-	1.22	0.052
Comb set (2 of each)	1/ CM	.3 oz	4	-	-	0.03	0.000
Brush set (2 of each)	1/ CM	3 oz	4	-	-	0.34	0.004
Towel set (2 big, 2 small, 2 washcloth)	4/ CM total	1 pound	16	-	-	7.26	0.313
Razor handles	1/ CM +2 extras	3.2 oz	6	-	-	0.54	0.006
Razor blades	1/ CM/ 1 month	2.3 oz	648	-	-	42.25	0.047
Female Hygiene set	1/FM crew + 2 extras	.12 lbs	3	-	-	0.16	0.002
Hygiene Consumables						53.65	1.19
Shower	4 total	17 kg	4	68.00	-	-	-
Toilet	6 total	39 kg	6	234.00	-	-	-
Sink+vanity	10 total	25 kg	10	250.00	-	-	-
Hygiene Equipment				552.00	10.000		
Portable Ultrasound	(1 total + 1 extra)	0.12 kg each	2	0.24	0.011	-	-
Portable Defibrillator (parts will need to be replaced starting at 2 yrs)	(1 total + 1 extra)	2.4 kg each	2	4.80	0.010	-	-
Respirator	1, no reserve	30 kg	1	30.00	0.118	-	-
EMT kit	1, no reserve	3.2 kg	1	3.20	0.035	-	-
Small X-ray machine	1 total + 1 extra	47 kg each	2	94	2.200	-	-
EMT kit	(1 total + 1 extra)	3.2 kg	2	6.4	0.071	-	-
2 stretchers	2 total	1.8 kg each	2	3.6	0.030	-	-
1 permanent medical bed	1 total	75 kg	1	75	1.156	-	-
Surgery table	1 total	386 kg	1	386	0.619	-	-
2 foldable cots	2 total	6.4 kg each	2	12.8	0.085	-	-
Exam table	1 total	35 kg	1	35.00	0.432	-	-

Surgical Kit	(1 total + 1 extra)	1.4 kg	2	2.80	0.003	-	-
Intravenous fluid system	5 IV bags and tube sets	.02 kg	5	0.10	0.016	-	-
Desk	1	15	1	15.00	0.300	-	-
Chairs	6	2.8	6	16.80	0.951	-	-
Medical Equipment				685.74	6.04		
Work coveralls	2/ CM	1 pound per CM	8	-	-	18.14368	0.07210324
Gloves for gardening	2 pairs/ CM/ year	~4oz	108	-	-	12.246984	0.011149783
3-D clothes printer	1 total and 1 backup	24 kg	1	24	1.000	-	-
Washer/dryer	2 total	85kg	2	170.00	0.606	-	-
Clothes Consumables				194.00	1.61	30.39	0.08
Dried Food	-	1.76 kg/CM-d	365 days	-	-	2569.6	7.008
Fertilizer	-	-	-	-	-	2333.33	2.75
LEDs	-	-	-	-	-	251.33	1.012
Food Consumables						5154.2600	10.7700
Pipes (water)	-		-	1301.00	2.600	-	-
CO2 Scrubbing backup system	1 total	198 kg	1	198.00	0.438	-	-
Anerobic Digestion System	1 total	300 kg	1	300.00	3.600		
ECS Equipment				1799.00	6.64		
Treadmill	2 total	89.8113 kg	2	179.62	1.400	-	-
Barbell	1 total	20kg	1	20	-	-	-
Exercise bike	2 total	45kg	2	90	0.600	-	-
Pullup Bar	1 total	15kg	1	15	-	-	-
Exercise Equipment				304.62	2.00		
Respirator (gas mask)	1/CM	0.5 kg each	4	-	-	2.00	0.030
Projector	1 total	0.77 kg	1	0.77	0.050	-	-
3D printers	2	24 kg	2	48.00	1.000	-	-
Misc Equipment				48.77	1.05	2.00	0.03

Mops (swiffer wetjet)	1/ module	2 lbs	13 total modules	11.793392	0.026	-	-
Reusable wet/dry swiffer pads (set of 2)	1/ swiffer +2 extra	2.4 oz	15 total	1.020582	0.003	-	-
Rags/towels (4 pack)	4/ module total +2 extra	1.5 oz	54	2.2963095	0.010	-	-
Cleaning Consumables				15.11	0.04		
Stove (Double Oven, 10 burner)	1 total	286 kg	1	286	1.583	-	-
Dining Tables	6 tables total + 1 extra	approx 15 kg each	7	105	3.500	-	-
Kitchen Counter/Work Station	1 total	211 kg	1	211	1.439	-	-
Microwave	1 total	11.5 kg	1	11.5	0.066	-	-
Sink (with drainboards)	1 total	55 kg	1	55	1.566	-	-
Dishes (large plate, small plate, bowl) (shatter proof Melamine)	1 set/ CM +4 extra	0.45 kg per set x 28 sets	28	12.6	0.354	-	-
Silverware (2 forks, 2 spoons, knife)	1 set/ CM +4 extra	0.25 kg per set X 28 set	28	7	-	-	-
Vacuum Sealer	1 set +1 extra	4 kg each	2	8	0.059	-	-
storage cabinets	2 total	57 kg each	2	114	1.091	-	-
Tupperware (50 piece set)	2 total	2.5 kg per set	2	2.5	0.061	-	-
Grain Mill (cast iron) (manual)	1 total	4 kg	1	4	0.021	-	-
Dining Chairs (folding) (plastic seat)	24 total	2.8 kg each	24	67.2	3.803	-	-
Water bottle	1 set/ CM +2 extra	0.1 kg each	28	2.8	-	-	-
Mug and cup	1 set/ CM +2 extra	~0.4 kg per (mug+glass)	28	11.2	-	-	-
Bowls (pyrex - can be used for hot and cold)	Two 14 piece sets	3.5 kg per set	2	7	0.007	-	-

Pots/Pans/Utensils	Two 15 Piece sets	6.8 kg per set	2	13.6	-	-	-
Kitchen Knives	1 Set with Block	2.3 kg	1	2.3	0.011	-	-
Dining/Kitchen Equipment				920.70	13.56		
Desk/Bed	1/ CM total	~25 kg	24	600	6.000	-	-
Chair	1/ CM total	2.8 kg	24	67.2	3.804	-	-
Bedroom Equipment				667.20	9.80		
Totals (1 crew)						5240	12.07
Totals (6 crews)				5187	50.74	31442	72.44
Total Mass (kg)						36629	
Total Volume (m ³)						123.17	

Table 84. Habitat Mass and Volume Breakdowns

9.6. Phase VI: Earth Independence

9.6.1. Costing

Procedure for Obtaining Johnson Space Center Cost Models

Johnson Space Center hosted a Cost Estimating Web Site where the Spacecraft/Vehicle Level Model, Advanced Missions Cost Model, Mission Operations Cost Model, and Cost Spreading Calc tools were made available. However, this website and its associated JavaScript tools are no longer available, as is noted on the RASC-AL website. In order to access the models, Internet Archive Wayback Machine was used. This is a tool that enables users to browse crawled versions of websites. The Wayback Machine has archived versions of the Cost Estimating Web Site, with details tabulated below. From the Wayback Machine's view of the website, Mozilla Firefox debugging tools were used to view the source of the model webpages. Luckily for Asimov City, JSC performed all calculations in client-side JavaScript, so the model parameters were all visible. The equation constants were then translated and integrated into an Excel worksheet, where they could be generated, modified, and linked appropriately. The Excel tool was then populated with the relevant spacecraft architecture information. The original JSC JavaScript tools were used as a check of the Excel tool's correctness, but were not directly used in the cost analysis.

Modeled Costs of All Program Spacecraft with Associated Nonrecurring and First-Unit Recurring Costs

Name	SVLCM Nonrecurring Cost (\$M 2015)	SVLCM First-Unit Recurring Cost (\$M 2015)
Lunar Flashlight	20.73	3.16
Mars 2020	1642.31	301.62
DSx	30.66	2.63
Moon/Mars Miner	3005.19	624.19
FTV	3434.81	733.11
Lunar Habitat	4040.27	356.71
Lunar D/A Vehicle	3014.13	250.70
Lunar Ground Transport	387.06	22.29
CTV	7393.11	738.20
Mars D/A Vehicle (Manned)	5915.30	564.42
Mars D/A Vehicle (Cargo)	3397.60	723.56
Magellan Rover	3158.26	278.84
Mars Buggy	387.06	22.29
Habitat Hub Module	2035.70	164.35
Habitat Hall Module	2180.78	178.55
Construction Vehicles	3980.05	875.35

muNet Satellites	61.12	11.63
Propellant Depot (Moon)	777.90	248.43
Propellant Depot (Mars)	601.49	191.66
Phobos/Deimos Orbiter	361.82	51.35
Heliocentric Communications Satellite	228.54	56.87

Table 85. List of All Modeled Vehicles.

10. Appendix B. Akin’s Law #3: The Iterative Design Process

10.1. Phase I Iterations

10.1.1. Mission Architecture Revisions

The mission architecture underwent 16 major revisions throughout the design process in order to account for a variety of shifting changings. Perhaps the most significant changes to occur in the mission architecture were in the final two revisions. This change was due to the additional of overhead cost in the budget, sending expenses early in the mission over the budget construction. Therefore, the mission architecture was adjusted to distribute cost, and therefore missions, to years in which budget caps were not met. The mission archiecture preceding the final revision is shown below.

Fiscal Year	Mission/Milestone	Launch Window to Mars	Available SLS Rocket No.		Assigned Rocket Type	Assigned SLS Rocket No.
2015	PHASE 1: EXPLORATION					
2016*		Mar-16	-	-		-
2017	Lunar Flashlight Mission	-	-	-	Atlas V	-
2018*		May-18	-	-		-
2019		-	-	-		-
2020*	Mars 2020	Jul-20	-	-	Atlas V	-
	DSx Mission		-	-		
2021	PHASE 2: RESOURCE ALLOCATION					
	Mining Equipment Delivery	-	2021-1	-	SLS Block 1B	2021-1
2022*	Moon Mining Habitat Delivery	Sep-22	2022-1	-	SLS Block 1B	2022-1
	DETERMINE SETTLEMENT LOCATION SITE BY 2022 --- BASED ON DSx MISSION AND MARS 2020 ROVER MISSION					

2023	Moon Rover Delivery Mission	-	2023-1	-	SLS Block 1B	2023-1
2024*	Crew Moon Mining Mission	Nov-24	2024-1	-	Falcon 9	-
	Mars Propellant Depot Delivery 1 (No Refuel)				SLS Block 1B	2024-1
	ISS SPLASHDOWN 2024 -- ASSUME ALL BUDGET FROM ISS PROGRAM					
2025	Mining Equipment Delivery (FTV)	-	2025-1	-	SLS Block 1B	2025-1
2026	Propellant Depot to L1 (Mission 1)	-	2026-1	2026-2	SLS Block 1B	2026-1
	Propellant Depot to L1 (Mission 2)				SLS Block 1B	2026-2
2027	Habitat Section 1 Launch (NO REFUEL) + Comm. Satellites	Jan-27	2027-1	2027-2	SLS Block 1B	2027-1
	Propellant Depot to L1 (Mission 3)				SLS Block 1B	2027-2
2028	Fuel Transport Vehicle No. 2	-	2028-1	2028-2	SLS Block 1B	2028-1
	Habitat Section 2 Launch				SLS Block 1B	2028-2
2029*	Habitat Section 3 Launch	Mar-29	2029-1	2029-2	SLS Block 1B	2029-1
	Habitat Section 4 Launch + PADME				SLS Block 1B	2029-2
2030	Habitat Section 5 Launch	-	2030-1	2030-2	SLS Block 1B	2030-1
	Moon Mining Repair and Expansion Mission				Falcon 9	-
	Habitat Section 6 Launch				SLS Block 1B	2030-2
2031*	Habitat Section 7 Launch	May-31	2031-1	2031-2	SLS Block 1B	2031-1
	EDL A/D Vehicles (NO REFUEL)				SLS Block 1B	2031-1
2032	Habitat Section 8 Launch	-	2032-1	2032-2	SLS Block 1B	2032-1
	Mars Propellant Depot Delivery 2				SLS Block 1B	2032-2
2033*	Rover Delivery Mission	Jul-33	2033-1	2033-2	SLS Block 1B	2033-1
	Rover Delivery Mission (NO REFUEL)				SLS Block 1B	2033-2
2034	Construction Mission 1 (Crane)	-	2034-1	2034-2	SLS Block 1B	2034-1
	Mars Miner Delivery				SLS Block 1B	2034-2
2035	Construction Mission 2 (Crane)	Sep-35	2035-1	2035-2	SLS Block 1B	2035-1

	Moon Mining & Gas Station Servicing Mission				Falcon 9	-
	Solar Panel Delivery Mission (NO REFUEL)				SLS Block 1B	2035-2
LAST SLS DELIVERY YEAR						
2036	PHASE 3: SETTLEMENT					
2037*	CTV Launch 1		-	-	Falcon Heavy	-
	Crew 1 Launch	Nov-37	-	-	Falcon Heavy	-
2038		-	-	-	-	-
2039		-	-	-	-	-
2040*	CTV Launch 2	Jan-40	-	-	Falcon 9	-
	Crew 2 Launch				Falcon 9	-
2041		-	-	-	-	-
2042*	Crew 3 Launch	Mar-42	-	-	Falcon 9	-
					-	-
2043		-	-	-	-	-
2044*		May-44	-	-	-	-
2045		-	-	-	-	-
2046	Crew 4 Launch	Jul-46	-	-	Falcon 9	-
2047*			-	-	-	-
2048*	CTV Launch	Sep-48	-	-	Falcon Heavy	-
	Crew 5 Launch				Falcon Heavy	-
2049		-	-	-	-	-
2050*	Crew 6 Launch	Nov-50	-	-	Falcon 9	-
					-	-
2051		-	-	-		
2052		-	-	-		
2053*		Jan-53	-	-		
2054	PHASE 4: MISSION INDEPENDENT OF EARTH --- ALL 24 CREW ON MARS					
	REQUIREMENT: Crew Rotates every 13 years					

Table 86. Mission Architecture Preceding the Final Revision

10.2. Phase II Iterations

10.2.1. Near-Earth Objects

Introduction

Near Earth Objects offer a variety of benefits but each benefit also has a downside. NEO's offer a variety of materials that are useful to developing a Mars transit architecture. Everything from platinum that can be mined and sold to raise money, to water that can be broken down into LOX and LH₂ which can be used as rocket fuel. Platinum is very abundant in Type S and Type M asteroids, and water is most likely found in Type C asteroids.

Limiting Factors

Despite the abundance of platinum, the time limitations put onto the architecture require refueling to be put ahead of fundraising. Therefore, NEO's will be looked at in terms of determining their viability as uses of refueling. Therefore all of the following calculations are done using Type C asteroids as the targets.

Benefits of NEO's

The nice thing about NEO's is that their gravities are almost negligible. As a result the fuel cost to land and take off from their surface would be minimal, compared to someplace such as the moon. Another good thing is that Type C asteroids are very abundant in our solar system. Type C asteroids make up 75% of the known asteroids.^[260] There is a downside, the majority of these asteroids are on the outer regions of the main asteroid belt. It is estimated that some of these Type C asteroids may contain up to 22% water due to never reaching above 50°C.^[261] This severely limits the amount of Type C asteroids that are feasible to be used as refueling stations.

Possible Architectures

Two main circumstances need to be considered when looking at NEO's. One option is to redirect the NEO into a stable, predictable orbit around a body such as Earth, the Moon, Mars, Phobos, or Deimos. The other option is to keep the NEO in its current orbit and base missions off of the orbital elements of the NEO and its close approach windows. This can be a viable answer that minimizes cost, but it is fairly hard to find a NEO with the right elements. Optimally the NEO would be a pit stop on the path to Mars that would be able to refuel the rocket without the delta v's that are needed to get on and off of Earth's Moon.

Reality of the Circumstance

Despite these limitations, some practical candidates were found. Using the "Near-Earth Object Human Space Flight Accessible Targets Study (NHATS)" catalog, by JPL, potential targets were identified. Four of these targets were as follows: 162173 (1999 JU3); 65679 (1989 UQ); 101955 Bennu (1999 RQ36); 341843 (2008 EV5). The main limiting factors on identifying a useful type C asteroid was to ensure that it was large enough to sustain an extended mining operation. However, the asteroid also needed to be able to have frequent near earth passes so that it could be used as a refueling station for Mars missions. The last and most critical limitation is that it needs to require less fuel to get to the NEO than it would to go to a refueling station somewhere else. This is important because the less fuel needed before arriving at the station means that more mass can be transported longer distances.

Another big issue with NEO mining is the technology readiness level of most of its critical components. There have been many proposed design for removing water from asteroids, but few have been built, tested, or even thoroughly designed. The most likely option requires covering the entire asteroid surface or a large section of it to vaporize the water, but these have yet to be tested and require a burn to place the

asteroid in an optimum orbit. Also, mechanical miners for near zero g are at a TRL level even lower. The only part of the mission that would have a large TRL would be the means of travel to get to the asteroid. Even then, many of the identified type C asteroids have a fairly high uncertainty level on their orbital elements.^[262] The final, and maybe most problematic part of developing a NEO resource system is timing. Every candidate that was located required extended stay times on the asteroid to wait for proper alignment with Mars. This extended time and exposure to radiation would be far from desirable to the crew and is a large reason why NEO mining was not chosen as our main fuel acquisition method.

10.2.2. The Omega Relay

The first iteration of the main earth-mars communications link featured a relay in a non-keplerian artificial “hover” orbit above the solar plane. This would mean that constant earth-mars communication during solar conjunctions could be maintained with the use of only one satellite to form the relay. However, the station keeping requirements of such an orbit were too great for the design to maintain for anywhere near the mission lifetime. Additionally, in-orbit perturbations would greatly decrease the fidelity of the radio link.

10.3. Phase IV Iteration

10.3.1. Crew Transport Concept of Operations

Due to budget adjustments, the mission architecture was redesigned which, subsequently, required redesign crew transport operation. The original crew transport operations before post-Critical Design Review costing adjustments are described below:

Crew transport to the Martian surface will begin in November 2037. The first CTV will launch from Cape Canaveral, Florida to LEO aboard a Falcon Heavy in late October 2037 and remain in LEO for 3 weeks. This will allow SpaceX and NASA time to turn over the launch pad. The transit from Earth’s surface to LEO will require a delta v of 9.1 km/s. The first crew of four will launch from Cape Canaveral, Florida in early November 2037 aboard a Falcon 9 with a Dragon capsule. The Falcon 9 will travel directly to L1 from Earth’s surface, requiring a delta v of approximately 13 km/s. Three days prior to the crew’s departure, the Falcon Heavy with the first CTV will perform a burn in order to get to L1 to meet the first crew.

When the Falcon Heavy with the CTV arrives at L1, the vehicle will jettison the Falcon Stage 2 and the CTV will autonomously dock to one of the three available SLS stage two rockets that were used to transport the Fuel Depot to the first Lagrange point. These SLS stage two rockets have been stored properly to ensure that all rockets are suitable for reuse and multiple trips to Low Mars Orbit (LMO) and back to L1. Just prior to the CTV performing the docking operations, the SLS stage two, which is docked to one of the three fuel tanks of the Fuel Depot, will undock from the Depot by blowing the explosive bolts of the docking mechanism. The procedure will be indicated and controlled by NASA flight control on Earth. RCS thrusters on the exterior of the SLS stage two will be used to orient the rocket in a position in which it is ready to accept the incoming CTV.

In the event that one of the SLS stage two rockets at L1 is deemed to be unacceptable for its expected crew transport mission, whether due to maintenance or other limiting factors, NASA flight operations will first determine the issue and evaluate the severity and complexity of the issue. If the issue is considered to be low in severity and easily repairable, the crew might be asked to perform an additional or extended EVA at L1 to make the necessary repairs. In the event that the SLS stage two is determined to have significant damage, undetermined causes of malfunction or cannot be easily and safely repaired during an EVA, one of the two remaining SLS stage two rockets will be used and standard procedures will continue. Because all three SLS stage two rockets are required for crew transportation missions, any defective or unusable rockets will be replaced with one of the available SLS stage two rockets in Lunar Orbit before the next crew arrives at L1.

After the CTV has successfully docked to the CTV, the crew Dragon capsule will dock to the CTV using RCS thrusters. The Dragon will dock to a compatible docking mechanism on the forward end of the CTV. Once docking procedures are complete, the CTV will pressurize. And crew will transfer from the Dragon to the CTV and transport supplies stored in the Dragon capsule. After successfully transporting these items, two crewmembers will prepare for an EVA in order to retrieve the extra supplies from the unpressurized Dragon Trunk. The crew will unload these items, and store them in the now unpressurized airlock. When the airlock is full, the crew will close the airlock and allow it to pressurize. The two crewmembers inside the CTV will quickly unload the airlock, and close the airlock again, allowing the two crewmembers performing an EVA to continue loading the airlock. This process will continue until all items are loaded onto the CTV or until the two crewmembers outside of the vehicle meet their maximum EVA time. In this situation, the crew inside would take over the EVA responsibilities.

Once all items have been successfully loaded into the CTV, the crew will initiate the docking process from within the CTV by activating the CRS trusting and allowing the Space Train to align with the refueling depot. The depot will refuel the SLS stage two. Once refueling operations are complete, the CTV will undock from the refueling depot using its RCS thrusters and orient itself toward Mars. The SLS stage two will then perform a burn to send the Space Train on a trajectory to Low Mars Orbit.

Most crew transport missions to Low Mars Orbit from L1 will require 180 days of transit time, with the exception of Crew 5 transport, which will perform a short stay at Mars and, subsequently, require 313 days of transit time. Upon arrival at Low Mars Orbit, the SLS stage two will complete a burn to enter into Low Mars Orbit. The CTV will orbit until it meets with the descent pod, which was previously sent to Low Mars Orbit. RCS thrusters are used to align the CTV with the descent pod.

The descent pod will dock with the available port on the CTV. Crew will put on their spacesuits, enter the airlock and, ultimately, board the descent pod after pressurization operations are complete. The descent pod will undock from the CTV and the crew will begin their descent to the Martian Surface. The Space Train will continue to orbit, performing a long stay at Low Mars Orbit, until the next available launch window, 545 days later. At this time, the Space Train will return to L1 for refueling, unless it has already transported two crews to Mars. In this case, the CTV will remain in Low Mars Orbit and a new CTV will transport the remaining crews. For the Crew 5 transport mission, which performs a short stay at Low Mars Orbit, the CTV will remain in orbit for 40 days before beginning its transit back to L1.

10.3.2.CTV Crew Rotation

Primary crew transport to Mars will begin in November 2037 and will end in April 2051. 24 crewmembers will be transported to Mars in crews of four (six crews total). The first crew will depart Earth in November 2037 aboard CTV 1. The first crew will arrive at Low Mars Orbit 180 days later, in April 2038. The crew will immediately depart for the Martian surface and the SpaceTrain will perform a

long stay at Low Mars Orbit, orbiting for 545 days. CTV 1 will depart Low Mars Orbit in October 2039 and begin its 180-day transit to L1, arriving in April 2040. Here, CTV 1 will be stored until crew 3 is launched in March 2042. Crew 3 will board CTV 1 at L1 and continue to Low Mars Orbit, arriving in August 2042. At this time, CTV 1 will have completed all of its initial crew transport missions and it will remain in Low Mars Orbit for emergency evacuation and future crew rotations and exploration missions after 2054.

Before Crew 3 launches in March 2042, crew 2 will launch in January 2040 and meet CTV 2 at L1. Crew 3 will depart for Low Mars orbit after all L1 operations are complete and arrive in June 2040, after a 180-day transit. After the crew leaves the vehicle, the SpaceTrain will continue to orbit in Low Mars Orbit for 545, performing a long stay. The SpaceTrain with CTV 2 will depart Low Mars Orbit in December 2041 and arrive at L1 in June 2042. CTV 2 will experience the longest storage duration at L1 as it awaits Crew 4 transport in July 2046.

Crew 4 will launch from Earth in July 2046 and meet with CTV 2 at L1. Following all L1 preparation and refueling operations, Crew 4 will depart for its 180-day transit to Low Mars Orbit and arrive in December 2046. Upon arrival at Low Mars Orbit, the crew will descend to the Martian surface and the SpaceTrain with CTV 2 will remain in Low Mars Orbit for future and emergency use.

CTV 3 and Crew 5 will launch in September 2048 and meet at L1. After all L1 preparations are made, Crew 5 will depart for Low Mars Orbit, arriving in July 2049, after a 313 day transit time. Crew 5 will depart for the Martian surface upon arrival into orbit and the SpaceTrain with CTV 3 will orbit for 40 days before departing in August 2049. The first rotation of the CTV 3 is the only crew transport mission that will perform a short stay at Mars in order to return to L1 for Crew 6 transport. The CTV 3 will return to L1 in June 2050 and meet with Crew 6, who launches in November 2050. Crew 6 will perform all preparation and refueling operations at L1 and depart for Low Mars Orbit, arriving in April 2051, 180 days later. Crew 6, the final crew to go to Mars before 2054, will depart for the Martian surface immediately after arrival at Low Mars Orbit, and the SpaceTrain with CTV 3 will remain in Low Mars Orbit for future use and emergency egress.

By May 2051, all 24 crew will be on the Martian surface and three SpaceTrain vehicles will be in Low Mars Orbit for future crew rotation missions, exploration missions, and possible emergency egress operations. Beginning in 2054, the crew will rotate every 13 years via the three SpaceTrain vehicles in Low Mars Orbit.

Manned Mission No.	Launch Date	Assigned CTV No.	Short Stay/Long Stay at LMO	Arrival Date at LMO	Departure Date from LMO	Return Arrival at L1
1	Nov-2037	1	Long	Apr-2038	Oct-2039	Apr-2040
2	Jan-2040	2	Long	Jun-2040	Dec-2041	Jun-2042
3	Mar-2042	1	Long	Aug-2042	-	-
4	Jul-2046	2	Long	Dec-2046	-	-
5	Sep-2048	3	Short	Jul-2049	Aug-2049	Jun-2050
6	Nov-2050	3	Long	Apr-2051	-	-

Table 87. Crew Rotation Schedule and CTV Assignments

10.3.3.CTV Mass Limitations with Falcon Heavy

At one point in the design process, it had been thought that there would not be SLS vehicles available to carry the CTV and Dragon to the L1 Lagrange point. It was suggested that Falcon Heavy vehicles should be used. The use of a Falcon Heavy set a limit on the mass of the CTV. The mass of the Dragon was already determined, but the CTV mass could be varied. According to the figure below, the maximum mass that the CTV could be was between 29.2t and 29.7t, depending on the minimum and maximum radius of the L1 point. This was approximated to be a limit of 29t. If the CTV had a mass greater than 29t, there would not be enough propellant in the Falcon Heavy upper stage's tanks to bring the CTV (and Dragon) to L1. This was the reason for the initial 29t limit on the CTV mass. It was later determined that an SLS would be available for each of the crew launches, which allowed significantly more mass to be carried to L1. However, the 29t mass for the CTV was kept to reduce the number of changes that would need to be made.

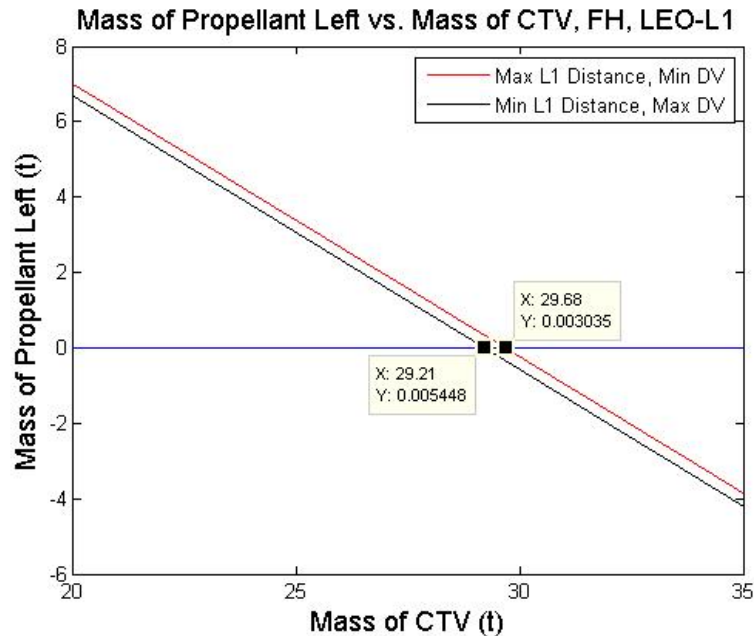


Figure 211. Mass of Propellant Left vs. Mass of CTV

10.3.4. CTV Experiments

10.3.4.1. Vaccine Development

Reasons for Unfeasibility

Within our mission structure, the success of each crew making it safely to the Martian surface is vital to the overall success of the mission. The creation of vaccines primarily rooted in the use of the source virus. While there have been advances in safe and secure ways to transfer and use the viruses, the potential of an outbreak not only puts the crew aboard each transport vehicle at risk, but each crew

already on the surface of Mars when the vehicle itself lands. Previous similar experiments have taken place aboard the International Space Station, however, with their proximity to the earth, the crew aboard could be rescued and returned to earth within a few days, whereas the crew in transport to the Martian surface is stuck in their conditions for the duration of their journey.

Potential for Future Implementation

Any implementation would have to come during phase 6, or the long-term independence phase of the mission. The potential for vaccine creation in space could be very important, be it that the vaccine could only be created in space or the creation is time sensitive and the ingredients can only be obtained on Earth. At that point in history, post 2054; medical technology should have reached the point where an experiment of this content can be done with little risk to crew safety.

10.3.4.2. Near Earth Object Mapping

Reasons for Unfeasibility

It has been determined that the equipment needed is much too large, the mass and power requirements would be too demanding, and the techniques needed are too complex. All space based radar devices are native to their own satellites, which would impose base limits on the volume, mass, and power that the crew transport vehicle cannot successfully sustain. The single satellite systems use SAR, Synthetic Aperture Radar, technology that requires a minimum amount of time to observe its target in order to correctly create an accurate image. The idea of this experiment would have been to attempt to map out Near Earth Objects yet to be seen, but with the speeds of both the crew transport vehicle and the potential Near Earth Objects, the time of observation would be only a few seconds, if not less than that. The SAR also needs to be focused on an object for it to work at its optimum efficiency, and the unknown nature of the experiment would work to the technology's disadvantage.

Potential for Future Implementation

Any future implementation is contingent on future advances in space satellite imaging technology. As stated above, using today's technology, this experiment is unfeasible. As one cannot see into the future, the potential shall remain low for the time being.

10.3.4.3. Calorimetric Electron Telescope

Reasons for Unfeasibility

This experiment is not feasible as there is no real experiment to be done. In the International Space Station version, the only function of the International Space Station is to gather the data and send it back to earth where it will be processed and analyzed. Adding the CALET sensor to the CTV would not be very intrusive, as it takes up negligible mass, volume, and power, but as an experiment for the crew, it is not ideal.

Potential for Future Implementation

There is no potential for future implementation. The computational power needed to process the data is beyond what can be placed on the crew transport vehicle.

10.4. Phase 5 Iterations

10.4.1. EDL Fuel Requirements without Refueling

A previous iteration of the EDL/A vehicle design involved performing the ascent launch and descent without refueling in orbit. This required a tremendous amount of fuel. The fuel requirements for the ascent and descent scheme without refueling were calculated similarly to the procedure explained in the **EDL Fuel** section of the main text. A Matlab script was created to simultaneously solve two rocket equations as follows:

$$\Delta V_a = -I_{sp}g_0 \ln\left(\frac{m_{int}}{m_o}\right) \quad \Delta V_d = -I_{sp}g_0 \ln\left(\frac{m_f}{m_{int}}\right)$$

The script solved for the fraction of propellant mass used after the initial ascent and the total propellant mass. Upon completing the analysis, it was found that the EDL/A vehicle would need 83 metric tons of fuel. An in-orbit refueling strategy was chosen in favor over a single fueling because of the size requirements of vehicle capable of holding 83 metric tons of fuel.

10.4.2. Methane Propulsion Fuel Requirements

A methane fueled rocket was also considered for the EDL/A vehicle, because methane is much easier to store and can be created from the Martian atmosphere. One of the limiting factors of a methane propelled rocket is the fact that it would only be available on the surface of Mars; therefore, the rocket would need to complete the ascent and descent maneuvers without refueling. Additionally, methane rockets are typically limited to an I_{sp} of 380 seconds^{[68][69]}. By completing a rocket equation analysis of a single fueled, methane powered rocket, it was found the EDL/A vehicle would require 150 metric tons of fuel. Not only would this require a massive launch vehicle, but that amount of propellant exceeds the projected capabilities of methane production on Mars. Ultimately, it was decided that a liquid hydrogen rocket would be more feasible.

10.4.3. Habitat Garage Temperature

A previous iteration of the Martian settlement involved placing the habitat underneath a garage structure that would hold the regolith barrier on top of it. One of the design considerations with such a structure was where to place the radiators. If the radiators were placed inside of the garage, would it get too hot? A thermal analysis was completed assuming a constant heat output of the radiators inside of the habitat. This model was simplified and ignored the fact that the radiators would need to increase in temperature as the temperature in the garage structure increased. Instead, the model assumed a constant heat load inside of

the garage structure. The garage temperature increased significantly as evidenced in the figure below. The temperature in the garage still follows a similar trend to the diurnal temperature cycle but is raised by 200 K. Additionally, the design heat load used for this calculation was much less than the final design heat load, so the actual temperature increase would be much more severe. As a result, the radiators were placed outside of the garage structure.

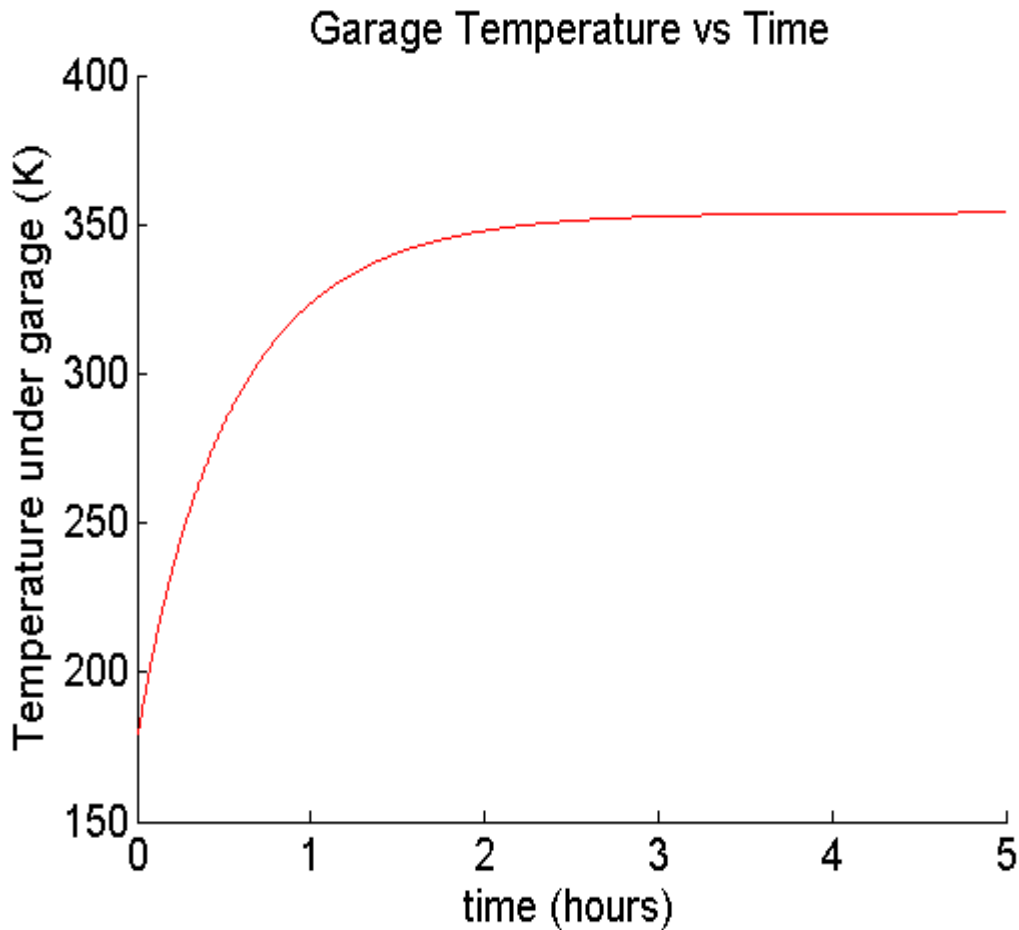


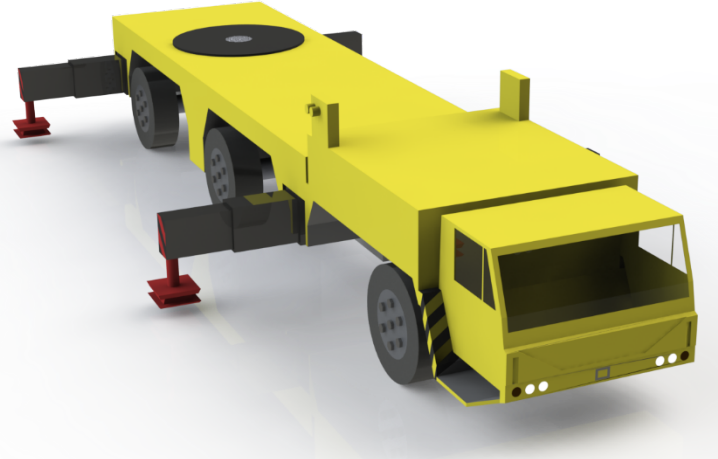
Figure 212. Garage Temperature vs. Time

10.4.4. The Atlas Martian Crane

The Atlas Martian Crane

The Atlas Martian Crane went through several different versions of chassis, boom arms, boom towers, and attachments before it arrived at its current design. All of the different designs are listed in the chart below.

Chassis

Chassis Series Development Number	Reason for Discontinuation and Comments
<p data-bbox="488 352 630 384">Version 1.0</p> 	<p data-bbox="959 520 1406 821">This was the first chassis design, it was modeled after the LTM1050 mobile crane with some modifications. This chassis was extremely bulky and overweight. It had a variety of unnecessary components that, though useful on Earth, would be near useless on Mars.</p>
<p data-bbox="488 1031 630 1062">Version 1.5</p> 	<p data-bbox="959 1119 1406 1535">This next iteration, we attempted to better modify the LTM1050 chassis to fit the needs of the martian surface. As seen in the picture, the chassis is stripped of all the accessories of what it once was, but still maintains the general shape of version 1.0. Just like its predecessor, the chassis was deemed too heavy and the suspension system would not work on Mars' rough terrain.</p>
<p data-bbox="488 1707 630 1738">Version 2.0</p>	<p data-bbox="979 1661 1390 1881">This version attempted to utilize a rocker bogie suspension system instead of the traditional split axle system so that it would be better equipped for the martian terrain. Though this type of suspension has</p>

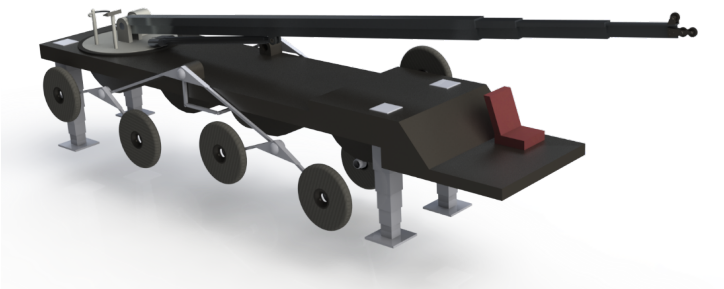
	<p>proved successful on smaller martian vehicles, such as Curiosity, it was found that it could not be scaled appropriately to match the weight and size of the crane.</p>
<p>Version 3.0</p> 	<p>This is the first design that uses the miner's triangular truss structure to create the chassis. It still uses the same general shape as the previous iterations, which was why it was scrapped. It had an unnecessary driving area, as well as an unneeded "hump" to protect the engine block.</p>
<p>Version 4.0</p> 	<p>This design uses the exact same chassis as the miner, however it was scrapped for being too narrow and short and did not provide the appropriate stability.</p>
<p>Version 5.0</p>	<p>This is the current crane design. It uses the same triangular truss components as the miner to make up its chassis. It is 2m longer and 2m wider than version 4.0.</p>



Table 88. The Atlas Martian Crane Evolution

Boom arm and Boom Tower

Boom Arm and Tower Series Development Number	Reason for discontinuation and comments
<p data-bbox="418 955 555 991">Version 1.0</p> 	<p data-bbox="808 955 1399 1264">The first design for the boom arm was used on chassis designs 1-4. It was made up of a telescoping T-beam, that at full extension, could reach 45m tall. It was discontinued since it had to reach so far, it had to be made very thick and heavy. The arm had such a large moment arm, that it also required an incredibly large counterweight just so the crane will not tip over.</p>
<p data-bbox="418 1663 555 1698">Version 2.0</p>	<p data-bbox="808 1621 1393 1768">This next iteration was a complete redesign, it incorporated two telescoping square trusses. This version was found to be too heavy and was discarded.</p>



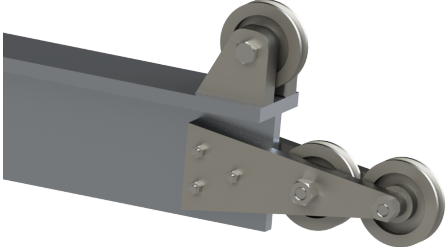
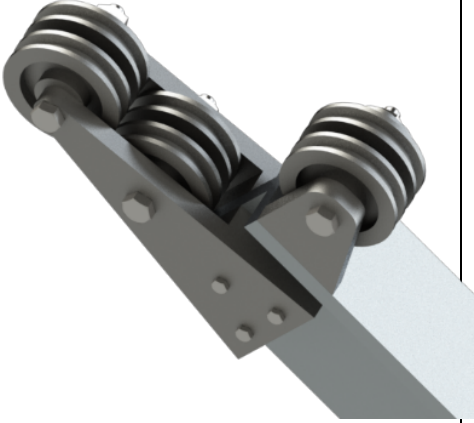
Version 3.0



Following the same general technique as the previous design, this current version uses two telescoping triangular trusses along with a variety of other components discussed in more detail in the Phase 5.

Table 89. Boom Arm and Tower Evolution

Attachments

Attachment Name and Series Development Number	Reason for discontinuation and comments
<p data-bbox="365 352 587 384">Pulley Version 1.0</p> 	<p data-bbox="792 352 1403 575">This is the first version of the pulley housing, it was designed to be used with boom arm version 1.0. It was decided that a two cable system would be needed in order to provide the crane with greater maneuverability and stability when lifting and moving the various payloads.</p>
<p data-bbox="365 793 587 825">Pulley Version 2.0</p> 	<p data-bbox="792 737 1386 846">This two cable system was designed for boom arm version 1.0, and had to be discarded when the new boom arm was designed.</p>
<p data-bbox="365 1409 587 1440">Pulley Version 3.0</p>	<p data-bbox="792 1388 1396 1497">This is the current two cable system pulley housing designed to be used with boom arms versions 2.0 and 3.0</p>

	
<p data-bbox="342 688 610 720">Drive Cab Version 1.0</p> 	<p data-bbox="789 688 1409 953">This attachment was designed Atlas chassis versions 4.0 and 5.0. It was designed to be mounted on the side of the crane upon human arrival to mars. Its goal was to provide a position to take manual control over the crane. This design had a very bulky roll cage, was heavy, and was could only be mounted at an awkward position on the crane.</p>

Table 90. Crane Attachments Evolution

10.4.5. Habitat Module Structure

For the first design of the Mars surface habitat halls and hubs, a slightly different approach was used. Originally, different materials were used for pressure vessel versus the ribs and longitudinal struts. For the pressure vessel Ti-6Al-2Sn was used and Al-7050-T6 was used for the ribs and longitudinal struts. Also, the ribs and longitudinal struts had a hollow cylinder cross-section because a circular cross-section is most resistant to buckling. This design was abandoned because it was made clear at the Preliminary Design Review that having a habitat consist of one single, cohesive structure would be preferable from a manufacturing standpoint.

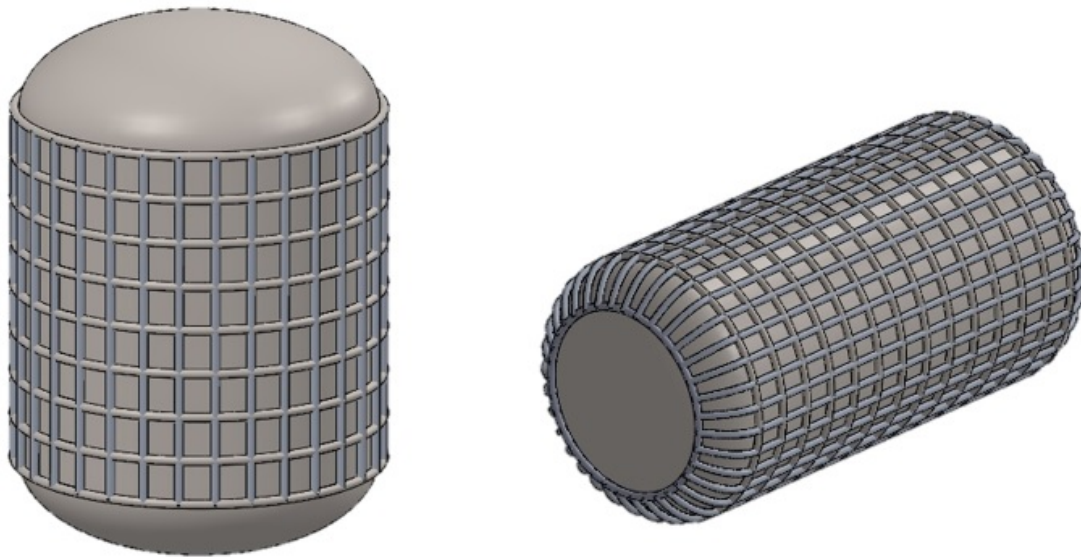


Figure 213. Preliminary Surface Habitat Design

10.4.6. Past Potential Power Sources

10.4.6.1. Solar Thermal

Solar thermal was under consideration as a power option for the Mars settlement, and an analysis was done to see if it was a viable option. Solar thermal is the process where heliostats reflect solar light onto heat exchanger that water is flowing through. The water picks up the heat and is converted into steam that then runs through a turbine where power is generated. Under the assumption that this thermodynamic cycle would be a Rankine cycle the amount of power generated from this cycle can be calculated using the amount of heat reflected by the heliostats and how that will correspond to the mass flow rate of the water.

$$\dot{Q}_{solar} = I_{summer} * A_{mirror} * n_{mirrors} * a$$

This equation represents the solar heat power reflected off the surface of the heliostat by relating the amount of solar flux onto heliostat, the surface area of said heliostat, the amount of heliostats reflecting the solar energy, and the reflectivity of the heliostat material. The assumption was made that the reflectivity is 90 percent.

Once the amount of solar power reflected onto the heat exchanger is calculated the mass flow rate of the water needed to pick up that amount of heat can be found. The mass flow is found by relating the solar power with the specific heat of the water at constant pressure and the change in temperature from the water storage temperature to the max operating temperature of the turbine, which in this case is about 400 degrees Celsius.^[241]

$$m_{H2O} = \frac{Q_{solar}}{Cp_{H2O} * (T_{turbine} - T_{storage})}$$

Now knowing the mass flow rate of the water the power generated by the turbine can be calculated using the equation

$$P_{turb} = m_{H2O}(\eta_{turb})(Cp_{vapor})(T_{turb}) \left(1 - \left(\frac{P1}{P2} \right)^{\frac{\gamma-1}{\gamma}} \right)$$

where the power is related to the mass flow rate of the water, the efficiency of the turbine “ η ”, the temperature of fluid flowing into the turbine “ T ”, the pressure ratio of before, the specific heat of water vapor “ Cp ” and the specific heat ratio of water vapor “ γ ”.

Once the power produced by the turbine is found, and once the power required for the pump is calculated the difference between the two will produce the total amount of power produced by the system.

The main reason that this power option was not chosen is that the system would be heavier than if we brought solar panels mainly because the turbine’s mass is the driving reason why the system is about three and a half metric tons greater than the mass of the solar panels producing 70 kW. The turbine itself, 4500 kg, weighs more than 1100 m² worth of solar panels. With the mission being very mass critical it did not seem feasible to use a system that would require more mass to produce the same amount of power. (See Appendix C “Solar_Thermal” for full calculations)

10.4.6.2. Wind Power

Wind turbines were considered as a potential power source at the beginning of this project. However, further research into the wind patterns on Mars showed that wind power would not be a successful power source on the Martian surface. Unfortunately, the atmosphere on Mars is extremely thin, resulting in a very low surface pressure. This low surface pressure causes the winds of Mars to be extremely weak, even at relatively high speeds. The wind velocity can reach up to 30 m/s, but the average wind velocity on Mars is about 10 m/s.²⁰¹ The figures below show the relationship between the lengths of the wind turbine blades and the power output of the wind turbine, based on a range of performance coefficients and at Martian atmospheric pressure. Figure 214 displays this relationship when the wind velocity remains at a constant 30 m/s.

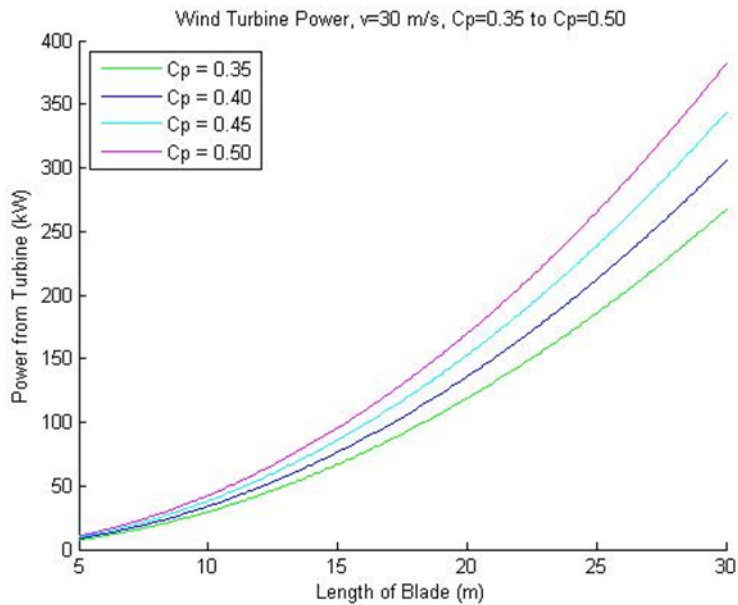


Figure 214. Wind Turbine Power Study 1

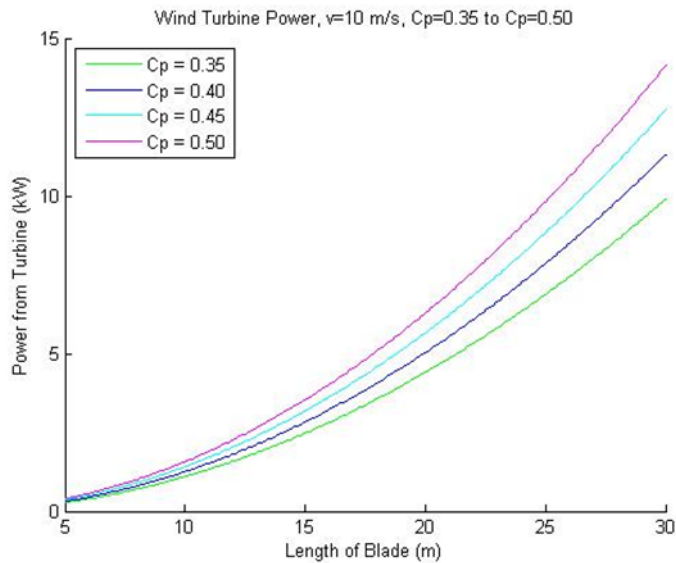


Figure 215. Wind Turbine Power Study 2

Figure 214 shows that a reasonably high amount of power could be gained if the wind turbine were interacting with wind at the highest possible velocities on Mars. If the wind constantly blew at 30 m/s and the coefficient of performance was relatively high, a wind turbine on Mars could potentially output about 300 kW (depending on the blade length). However, these wind speeds mostly occur during dust and wind storms, which have little pattern associated with them and are generally unpredictable.²⁰² Because they are unpredictable, there is no guarantee as to when the wind turbine will be interacting with wind at these high velocities. It is much more probable that the wind turbine would be interacting with an average wind speed of about 10 m/s. Figure 215 shows the same relationship as the previous graph, but this time with a

wind speed of 10 m/s. The power output would drop significantly with this decrease in wind speed. The blade lengths of the wind turbine would need to be nearly 30 m long just to produce 10-15 kW. The habitat would not be able to run on this low of a power output. The increasing blade length would also result in an increasing mass of the turbine. Because payload mass and volume is limited, it would not be ideal to transport a wind turbine with both a high mass and a large volume. Therefore, it was decided that the power that a wind turbine would produce on average would not be enough to make it a worthwhile investment.

10.4.6.3. Geothermal Power

Geothermal power was initially researched as a potential power source for the Martian settlement. A geothermal power plant produces energy through the manipulation of underground heat sources, such as reservoirs of steam or hot water.²⁰⁴ However, Mars has a significantly cooler interior than that of Earth due to its relatively smaller size. As a result, geothermal heat was not believed to exist within a reasonable distance from the surface of the planet, which would make access to the heat pockets difficult. There was no guarantee that this subsurface heat was even located at the estimated depths.²⁰⁵ Thus, it was decided that geothermal would be an impractical choice for a habitat power source.

10.4.6.4. Nuclear Power Trade Studies

There are various types of nuclear reactors, each with their own characteristics and systems. One of the main differences to emphasize would be the fuel types. The two fuel types that were focused on in this trade study were Uranium-based fuel and Thorium-based fuel. The advantages and disadvantages of each fuel type found after further research were summarized in the table below. The primary benefit to note for Uranium would be its high technology readiness level. Uranium-based fuel is well understood and used in commercial reactors around the world. Thorium-based fuel, on the other hand, is not well understood but is widely abundant on the surface of Mars. The ability to mine Thorium on Mars would increase the level of independence for the habitat.

	Uranium (enriched U-238)	Thorium (Th-232)
Advantages	<ul style="list-style-type: none"> • TRL 9 • Currently operational • Does not require a driver to commence chain reaction (fuel can be enriched) • Can be pre-enriched and safely transported 	<ul style="list-style-type: none"> • Operates at low pressure • Minimal nuclear waste • Minimal meltdown risk • High abundance: 6 ppm • Waste has lower levels of radioactivity • Higher fission probability (U-233 is 92%, U-235 is 85%)
Disadvantages	<ul style="list-style-type: none"> • Operates at very high pressures • Higher risk for accidents • Waste has higher level of 	<ul style="list-style-type: none"> • TRL 3 - 4 • Irradiation required • Requires a driver (U-233, U-235, Pu-239)

	radiotoxicity <ul style="list-style-type: none"> Low abundance: 2 ppm 	
--	--------------------------------------------------------------------------------------	--

Table 91. Nuclear Power Trade Studies

Multiple types of nuclear reactors were initially taken into consideration as potential power sources for the settlement. The following table summarizes the trade study that was done.^{[206][207]}

	LWR: Boiling Water Reactor	LWR: Pressurize d Water Reactor	Heavy Water Reactor	Graphite Moderated Reactor: Gas Cooled	Graphite Moderated Reactor: Water Cooled	Fast Breeder Reactor (Liquid Metal)	Molten Salt Reactor
Coolant	Water (H2O)	Water	Heavy Water (Deuterium-oxide, D2O)	Gas (CO2 or He)	Water	Molten, liquid sodium	Molten fluoride salts (Lithium Beryllium Fluoride, Lithium Fluoride)
Moderator	Water	Water	Heavy Water	Graphite	Graphite	Not required	-
Fuel	Uranium-Dioxide (UO2)	UO2	UO2 or metal	Uranium dicarbide (UC2) or uranium metal	Uranium dioxide (RBMK), metal (N-reactor)	Plutonium dioxide and uranium dioxide in various arrangements	Thorium (Th-232) to breed U-233
Enrichment	Low-enriched	Low	Natural Uranium (not enriched)	Slightly enriched, natural uranium	Slightly enriched	Various mixtures of Plutonium-235 and uranium-235	-

Table 92. Reactor Trade Study

After further research into nuclear reactors, it was discovered that one of the main issues would be minimizing the reactor mass. Most commercial reactors would be far too heavy to transport to Mars. Small Modular Reactors (SMRs) could be a potential solution to this. The SMRs have a lower technology readiness level, but are much smaller in mass and volume. The average power output of general commercial reactors would be far more than necessary. SMRs would solve this issue too since they produce significantly less power. Table 93 summarizes the SMRs that were researched.^[208,209]

	Reactor Type	Electric Capacity (MWe)	Thermal Capacity (MWt)	System Pressure (MPa)	Coolant	Moderator	Fuel	Fuel Cycle	Enrichment	Core Outlet Temp (C)
Unitherm	Light Water Reactor	2.5	20	16.5	Light Water	Light Water	UO2-ZrO2	25 years	19.75 %	330
AHWR300-LEU	Heavy Water Reactor	300	920	7.0	Light Water	Heavy Water	Th, 233U; Th, Pu	Close cycle	3-3.75% ; 2.5-4%	285
EC6	Heavy Water Reactor	740	2084	10.1	Heavy Water	Heavy Water	Natural Uranium	Close cycle	-	310
NuScale	Light Water Reactor	45	160	8.7	Light Water	Light Water	Uranium Oxide	24 months	4.95%	329

Table 93. Small Modular Reactor Trade Study

10.5. Phase 6 Iterations

10.5.1. Evolution of Mission Architecture Costing Strategy

The requirement to fund the Exploration Systems Development program imposed by RASC-AL motivated a cost-saving strategy involving efficient use of Space Launch System launch vehicles. The \$3,000M annual fee between 2015 and 2035 is equivalent to the program paying \$63B for 25 SLS vehicles, as no Orion capsules are used in the mission architecture. RASC-AL stipulated that the Exploration Systems team would be able to construct and launch an SLS every six months, with no potential to store the vehicles. Therefore, if the program had no hardware to launch every six month cycle, the SLS would be wasted, and the program would lose \$2,520M. Additionally, if all of the hardware was

not able to be sent via SLS, the program would be required to purchase additional launch vehicles, further adding to the cost.

In an attempt to mitigate these issues, the first strategy used in developing the mission architecture timeline was to make sure that each available SLS was used and all of the hardware was delivered to Mars by 2035. This resulted in a very rigid launch cycle for the Exploration, Resource Acquisition, and Habitat Delivery phases. Accounting for all the spacecraft development and production, Figure 216 shows a breakdown of the costs incurred using this strategy. Two major development thrusts are exhibited, the Exploration development occurring 2015-2024, and the Martian equipment development occurring 2027-2033. The Martian equipment development coincides with the Lunar Exploration spacecraft production and launch phases, leading to two overall extrema in the total cost. A small adjustment to the timeline caused the integrated balance to remain positive throughout the program. Therefore, spreading parameters could be tuned to ensure that these peaks fall under the curve. One notable feature of this plot is the very large margin after 2035. All spacecraft except for the Crew Transfer Vehicle were already developed and produced to ensure they could all launch on the provided SLS vehicles, so there was no cost associated with the out-years except for the crew missions.

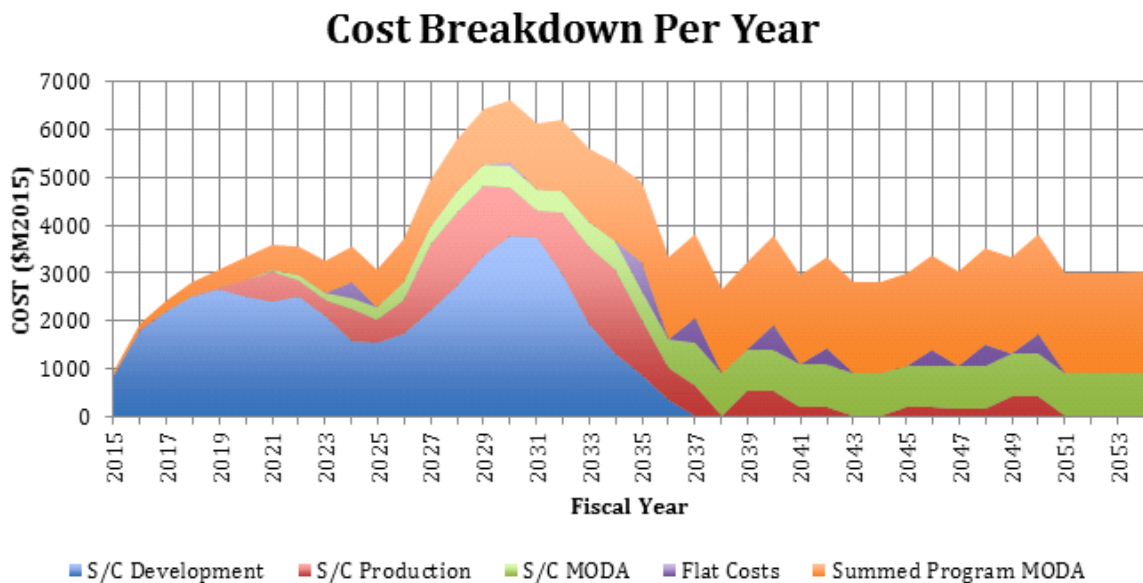


Figure 216. Previous Strategy Cost Division

10.5.2. Mars Buggy Revisions

10.5.2.1. Concept of Operations

The Mars Buggy was intended to be the unpressurized rover for the Mars settlement. The buggy will provide short-distance surface transport for the inhabitants of Mars. It will be used mostly for maintenance around the habitat, such as repairing solar panels. Since the Mars Buggy is unpressurized and only intended for short-distance travel, the inhabitants will not need to pack additional resources for trips like in the Magellan Rover.

10.5.2.2. Similarities to Apollo Lunar Roving Vehicle

The design of the Mars Buggy is simply a modification of the Apollo Lunar Roving Vehicle (2). The Mars Buggy will also have 2 seats, 4 metal wheels with double horizontal wishbone suspension, a communications antenna and room to stow small items.

10.5.2.3. Adjustments to Apollo LRV design

The original Apollo Lunar Roving Vehicle was intended for use on the surface of Moon, so the design will be updated for use on the surface of Mars. Mars has a higher surface gravity than the moon, so the wheels will need to be a different size to accommodate that. The suspension will also need to be adjusted accordingly for the different surface gravity. In addition to structural adjustments, the Mars Buggy will also have an updated communications array capable of communicating with the various systems set up on Mars. Most of the additional equipment from the Apollo Lunar Roving Vehicle will be removed from the buggy.

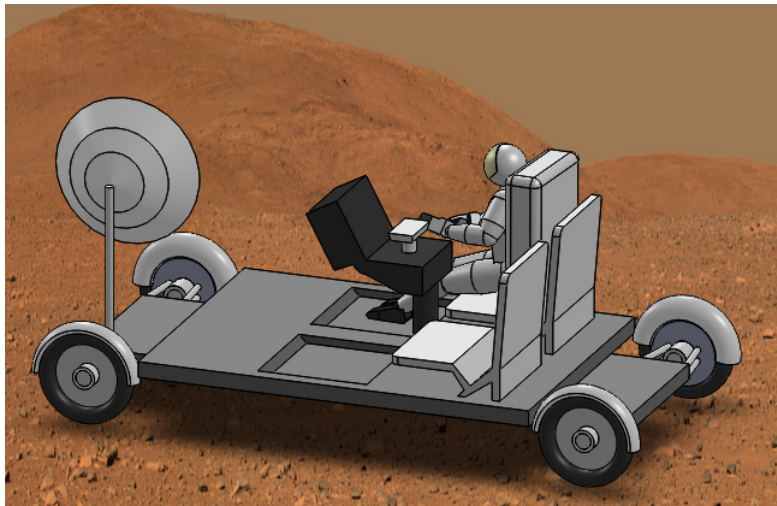


Figure 217. Buggy

11. Appendix C. MATLAB Code

11.1. Phase I: Exploration

11.1.1. DSx Aeroshell Ballistic Coefficients

Lauren Powers

1. Primary calculations for Mass vs. Diameter Assuming Constant Ballistic Coefficient

```
%Mars constants
p = 0.020; %kg/m^2
g = 3.8; %m/s

%From the original Deep Space 2 vehicle:
Vterm = 179; %m/s
Mds2 = 3.57; %kg
%According to NASA paper:
BC = 38; %kg/m^2 (for MARS MICROPROBES)

%% MASS vs. DIAM (with constant BC)

clear all

diameter=[1:3];
figure()
hold on
p1=plot(mass_V(diameter,20),diameter,'b') %Ballistics coeff = 20
p2=plot(mass_V(diameter,30),diameter,'g--') %Ballistics coeff = 30
p3=plot(mass_V(diameter,38),diameter,'k') %Ballistics coeff = 38
p4=plot(mass_V(diameter,50),diameter,'r') %Ballistics coeff = 50
p5=plot(mass_V(diameter,80),diameter,'m--') %Ballistics coeff = 80
p6=plot(mass_V(diameter,100),diameter,'y--') %Ballistics coeff = 100
p7=plot(mass_V(diameter,150),diameter,'g-') %Ballistics coeff = 150
%p8=plot(mass_V(diameter,260),diameter,'g') %Ballistics coeff = 260
hold off

set([p1 p2 p3 p4 p5 p6 p7],'LineWidth',2)
set(p1,'Color',[0,0,0])
set(p2,'Color',[0.4,0.4,0.4])
set(p3,'Color',[0.7,.7,0.7])
set(p4,'Color',[0.4,0.4,0.4])
set(p5,'Color',[0,0,0])
set(p6,'Color',[0.7,0.7,0.7])
set(p7,'Color',[0.2,0.2,0.2])
%set(p8,'Color',[0.4,0,1])
%set(gca,'XTickLabel',{labelList},'FontSize',8)
%set(gca,'YTickLabel',{labelList},'FontSize',8)

LEG=legend('BC=20kg/m^2','BC=30kg/m^2','BC=38kg/m^2','BC=50kg/m^2','BC=80kg/m^2','BC=100kg/m^2','BC=150kg/m^2')
Title('Spacecraft Diameter vs. Mass (Constant Ballistic Coefficient) ','FontSize',22)
```

```

set(gca,'FontSize',16)
xlabel('Mass (in kg)','FontSize',22)
ylabel('Diameter (in m)','FontSize',22)
axis([0 10,0,1]) %0 to 10 kg (about 22 lb) and 0 to 3 m diameter (about 10 feet)
set(gca,'XTick',0:1:10)
set(LEG,'FontSize',18)
grid on

```

2. Vehicle Mass Function (mass_v)

```
function [mass_S] = mass_V(d, B_coeff)
```

```

%calculates mass given the diameter and ballistic coefficient of a vehicle in the
%shape of a spherical cap along with the cross-sectional radius (larger
%radius) of the cap.

```

```
%MAKE SURE UNITS ARE METRIC!! i.e. N/m^2, Pascals, etc.
```

```
r = d./2;
```

```
h = (r./sind(45)) - (r./tand(45))
```

```
A = pi.*(r.^2 + h.^2);
```

```
Vterm = 180; %m/s
```

```
Cd = 0.4; %average for half sphere
```

```
mass_V=B_coeff.*A.*Cd;
```

```
mass_S=mass_V;
```

```
end
```

3. Primary calculations for Ballistic Coefficient vs. Diameter (with constant mass)

```
%% BC vs. DIAMETER (with constant mass)
```

```
%Constant variable: Mass
```

```
%GRAPH: BC vs. Diam.
```

```
clear all
```

```
Bcoeff=1:150;
```

```
figure()
```

```
hold on
```

```
p1=plot(diameter_vehicle(3.752,Bcoeff),Bcoeff,'--'); %3.752kg total (Deep Space 2 original mass)
```

```
p2=plot(diameter_vehicle(4.500, Bcoeff),Bcoeff); %4.5kg
```

```
p3=plot(diameter_vehicle(5.000, Bcoeff),Bcoeff); %5.0kg
```

```
p4=plot(diameter_vehicle(6.000,Bcoeff),Bcoeff); %6.0kg
```

```
p5=plot(diameter_vehicle(7.000, Bcoeff),Bcoeff); %7.0kg
```

```
p6=plot(diameter_vehicle(8.000, Bcoeff),Bcoeff); %8.0kg
```

```
p7=plot(diameter_vehicle(10.00, Bcoeff),Bcoeff); %10.0kg
```

```
%p8=plot(diameter_vehicle(12.00, Bcoeff),Bcoeff); %15.0kg
```

```
hold off
```

```
set([p1 p2 p3 p4 p5 p6 p7],'LineWidth',2)
```

```
set(p1,'Color',[1,0.2,0.4])
```

```
set(p2,'Color',[0.3,0.4,0.9])
```

```
set(p3,'Color',[0,.5,0])
```

```
set(p4,'Color',[0.9,0.5,0])
```

```
set(p5,'Color',[0,0,0])
```

```
set(p6,'Color',[0.3,0.8,0.5])
```

```
set(p7,'Color',[0.7,0,0.7])
%set(p8,'Color',[0.4,0,1])
```

```
LEG=legend('3.752kg vehicle (original)', '4.500kg vehicle', '5.000kg vehicle', '6.000kg vehicle', '7.000kg vehicle', '8.000kg vehicle', '10.00kg vehicle');
Title('Spacecraft Diameter vs. Ballistic Coefficient for Constant Vehicle Mass','FontSize',20)
xlabel('Diameter (m)','FontSize',20)
ylabel('\beta_c (Ballistic Coefficient, Pa)','FontSize',20)
axis([0,10,0,200])
set(LEG,'FontSize',17)
grid on
```

4. Vehicle Diameter Function (diameter_vehicle)

```
function [diam_v] = diameter_vehicle(mass, B_coeff)

%calculates diameter given the mass and ballistic coefficient of a vehicle in the
%shape of a spherical cap along with the cross-sectional radius (larger
%radius) of the cap.

%MAKE SURE UNITS ARE METRIC!! i.e. N/m^2, Pascals, etc.

Cd = 0.4; %approximated based on half sphere

A = mass./(B_coeff.*Cd);

rnew = solve((A./pi)==r.^3-r.^2+sqrt(2).*r,r);
diam = 2*rnew;

diam_v=diam;

end
```

11.1.2.Orbital Dynamics Calculations

Lemuel Carpenter

```
dV's for solar syetem bodies and dV's for yearly flight windows to Mars from C3 data (Lem)
%% Transfer Orbit
% http://space.stackexchange.com/questions/1380/how-to-calculate-delta-v-required-for-a-planet-to-planet-hohmann-transfer
% http://www.nasa.gov/content/how-will-nasas-asteroid-redirect-mission-help-humans-reach-mars/#.VMh-oGjF98F
mu_S=132712440018; % Sun
mu_E=398600.4418; % Earth
mu_m=4902.8; % Moon
mu_M=42828; % Mars
mu_c=63.1; % Ceres
mu_J=126686534; % Jupiter
mu_Sa=37931187; % Saturn
% Earth radius 6371km
% Earth LEO 1000km alt
```

```

% Moon a=382,823km
% Mars radius 3390km
% Mars LMO 250km alt
% Jupiter radius 69,911km
% Europa orbital radius 670,900km
% Saturn radius 58,232km
% Enceladus orbital radius 237,948km

mu_Mo=4902.8;    % Moon
%% Earth to Mars (C3)

% 2026-2045
C3_short=[11.11;9.048;9.00;8.412;10.19;17.07;18.65;14.86;9.032;9.061;];
C3_long=[9.14;8.928;8.237;7.781;17.52;14.84;12.17;9.818;8.969;8.587;];
r=300+6371;
Vesc=sqrt(2*mu_E/r);
Vc=sqrt(mu_E/r);
dv_short=zeros(10,1);
dv_long=zeros(10,1);
for i=1:10
dv_short(i)=sqrt((Vesc^2)+C3_short(i))-Vc;
dv_long(i)=sqrt((Vesc^2)+C3_long(i))-Vc;
end
dv_short
dv_long

%% LEO to NEO (Amor Astroids) (Hohmann)
% distance in AU
% convert to AU by multiplying by 149597871km
AU=149597871;
r1=300+6371;
r2=0.239*AU;
dv1=sqrt(mu_E/r1)*(sqrt(2*r2/(r1+r2))-1);
dv2=sqrt(mu_E/r2)*(1-sqrt(2*r1/(r1+r2)));
Total_Delta_V=abs(dv1)+abs(dv2)

%% Earth LEO to Phobos
mu1=mu_E;
mu2=mu_M;
r1=149513000; % radius of departure body orbit about the Sun, assumed to be circular
r2=227939100; % radius of arrival body orbit about the Sun, assumed to be circular
a1=6371+1000; % circular orbit radius of the spacecraft about the departure body
a2=9376; % circular orbit radius of the spacecraft about the arrival body
dv1=sqrt((sqrt(2*mu_S*r2/(r1*(r1+r2)))-sqrt(mu_S/r1))^2 + (2*mu1/a1))-sqrt(mu1/a1);
dv2=sqrt((sqrt(2*mu_S*r1/(r2*(r1+r2)))-sqrt(mu_S/r2))^2 + (2*mu2/a2))-sqrt(mu2/a2);
Total_Delta_V=abs(dv1)+abs(dv2)

%% Earth LEO to Deimos
mu1=mu_E;
mu2=mu_M;
r1=149513000;
r2=227939100;
a1=6371+1000;
a2=23463;
dv1=sqrt((sqrt(2*mu_S*r2/(r1*(r1+r2)))-sqrt(mu_S/r1))^2 + (2*mu1/a1))-sqrt(mu1/a1);

```

```

dv2=sqrt((sqrt(2*mu_S*r1/(r2*(r1+r2)))-sqrt(mu_S/r2))^2 + (2*mu2/a2))-sqrt(mu2/a2);
Total_Delta_V=abs(dv1)+abs(dv2)

```

```

%%% Earth LEO to Moon(alt) (Hohmann)

```

```

r1=6371+1000;% LEO of 1,000km alt
r2=382823;
dv1=sqrt(mu_E/r1)*(sqrt(2*r2/(r1+r2))-1);
dv2=sqrt(mu_E/r2)*(1-sqrt(2*r1/(r1+r2)));
Total_Delta_V=abs(dv1)+abs(dv2)

```

```

%%% Earth to Moon (Other)

```

```

mu1=mu_E;
mu2=mu_Mo;
r1=149513000;
r2=149513000+384400;
a1=6371+1000;
a2=1800; % radius of the moon is 1737.4 km
dv1=sqrt((sqrt(2*mu_S*r2/(r1*(r1+r2)))-sqrt(mu_S/r1))^2 + (2*mu1/a1))-sqrt(mu1/a1);
dv2=sqrt((sqrt(2*mu_S*r1/(r2*(r1+r2)))-sqrt(mu_S/r2))^2 + (2*mu2/a2))-sqrt(mu2/a2);
Total_Delta_V=abs(dv1)+abs(dv2)

```

```

%%% Moon to Mars

```

```

mu1=mu_E; % GM of the departure body
mu2=mu_M; % GM of the arrival body
r1=149513000; % radius of departure body orbit about the Sun, assumed to be circular
r2=227939100; % radius of arrival body orbit about the Sun, assumed to be circular
a1=382823; % circular orbit radius of the spacecraft about the departure body
a2=3390+300; % circular orbit radius of the spacecraft about the arrival body
dv1=sqrt((sqrt(2*mu_S*r2/(r1*(r1+r2)))-sqrt(mu_S/r1))^2 + (2*mu1/a1))-sqrt(mu1/a1);
dv2=sqrt((sqrt(2*mu_S*r1/(r2*(r1+r2)))-sqrt(mu_S/r2))^2 + (2*mu2/a2))-sqrt(mu2/a2);
Total_Delta_V=abs(dv1)+abs(dv2)

```

```

%%% Earth 1000 to Mars 300

```

```

mu1=mu_E;
mu2=mu_M;
r1=149513000; % radius of departure body orbit about the Sun, assumed to be circular
r2=227939100; % radius of arrival body orbit about the Sun, assumed to be circular
a1=6371+1000; % circular orbit radius of the spacecraft about the departure body
a2=3390+300; % circular orbit radius of the spacecraft about the arrival body
dv1=sqrt((sqrt(2*mu_S*r2/(r1*(r1+r2)))-sqrt(mu_S/r1))^2 + (2*mu1/a1))-sqrt(mu1/a1);
dv2=sqrt((sqrt(2*mu_S*r1/(r2*(r1+r2)))-sqrt(mu_S/r2))^2 + (2*mu2/a2))-sqrt(mu2/a2);
Total_Delta_V=abs(dv1)+abs(dv2)

```

```

%%% Mars to Phobos (Hohmann)

```

```

r1=3390+250; % 250km is out of mars atmo
r2=9376; % semimajor axis
dv1=sqrt(mu_M/r1)*(sqrt(2*r2/(r1+r2))-1);
dv2=sqrt(mu_M/r2)*(1-sqrt(2*r1/(r1+r2)));
Total_Delta_V=abs(dv1)+abs(dv2)

```

```

%%% Mars to Deimos (Hohmann)

```

```

r1=3390+250; % 250km is out of mars atmo
r2=23463; % semimajor axis
dv1=sqrt(mu_M/r1)*(sqrt(2*r2/(r1+r2))-1);
dv2=sqrt(mu_M/r2)*(1-sqrt(2*r1/(r1+r2)));

```

Total_Delta_V=abs(dv1)+abs(dv2)

%% Mars to Europa

mu1=mu_M;

mu2=mu_J;

r1=227939100;

r2=778547200;

a1=3390+250;

a2=670900;

dv1=sqrt((sqrt(2*mu_S*r2/(r1*(r1+r2)))-sqrt(mu_S/r1))^2 + (2*mu1/a1))-sqrt(mu1/a1);

dv2=sqrt((sqrt(2*mu_S*r1/(r2*(r1+r2)))-sqrt(mu_S/r2))^2 + (2*mu2/a2))-sqrt(mu2/a2);

Total_Delta_V=abs(dv1)+abs(dv2)

%% Mars to Enceladus

mu1=mu_M;

mu2=mu_Sa;

r1=227939100;

r2=1433449370;

a1=3390+250;

a2=237948; % Enceladus

dv1=sqrt((sqrt(2*mu_S*r2/(r1*(r1+r2)))-sqrt(mu_S/r1))^2 + (2*mu1/a1))-sqrt(mu1/a1);

dv2=sqrt((sqrt(2*mu_S*r1/(r2*(r1+r2)))-sqrt(mu_S/r2))^2 + (2*mu2/a2))-sqrt(mu2/a2);

Total_Delta_V=abs(dv1)+abs(dv2)

%% Mars to G-ring

mu1=mu_M;

mu2=mu_Sa;

r1=227939100;

r2=1433449370;

a1=3390+250;

a2=170000; % G-ring

dv1=sqrt((sqrt(2*mu_S*r2/(r1*(r1+r2)))-sqrt(mu_S/r1))^2 + (2*mu1/a1))-sqrt(mu1/a1);

dv2=sqrt((sqrt(2*mu_S*r1/(r2*(r1+r2)))-sqrt(mu_S/r2))^2 + (2*mu2/a2))-sqrt(mu2/a2);

Total_Delta_V=abs(dv1)+abs(dv2)

%% Mars to E-ring

mu1=mu_M;

mu2=mu_Sa;

r1=227939100;

r2=1433449370;

a1=3390+250;

a2=480000; % E-ring

dv1=sqrt((sqrt(2*mu_S*r2/(r1*(r1+r2)))-sqrt(mu_S/r1))^2 + (2*mu1/a1))-sqrt(mu1/a1);

dv2=sqrt((sqrt(2*mu_S*r1/(r2*(r1+r2)))-sqrt(mu_S/r2))^2 + (2*mu2/a2))-sqrt(mu2/a2);

Total_Delta_V=abs(dv1)+abs(dv2)

%% E-ring to G-ring

r1=480000;

r2=170000;

dv1=sqrt(mu_Sa/r1)*(sqrt(2*r2/(r1+r2))-1);

dv2=sqrt(mu_Sa/r2)*(1-sqrt(2*r1/(r1+r2)));

Total_Delta_V=abs(dv1)+abs(dv2)

%% E-ring to Enceladus

r1=480000;

```

r2=237948;
dv1=sqrt(mu_Sa/r1)*(sqrt(2*r2/(r1+r2))-1);
dv2=sqrt(mu_Sa/r2)*(1-sqrt(2*r1/(r1+r2)));
Total_Delta_V=abs(dv1)+abs(dv2)

```

```

%%% G-ring to Enceladus
r1=170000;
r2=237948;
dv1=sqrt(mu_Sa/r1)*(sqrt(2*r2/(r1+r2))-1);
dv2=sqrt(mu_Sa/r2)*(1-sqrt(2*r1/(r1+r2)));
Total_Delta_V=abs(dv1)+abs(dv2)

```

11.2. Phase II: Resource Acquisition and Infrastructure Setup

11.2.1. Magellan 2.0 Required Habitable Volume Curves

Jaelyn Rupert

```

%%%
clear all
close all
clc

%%%Magellan 2.0 Crew of 3
x=0;
for i=1:1:150
x=x+1;
NASA_Curve(x)=3*(4.8827*log(x)-3.9113);
Celentano(x)=3*(20*(1-exp(-x/20)));
Historical_data(x)=3*(62*(1-exp(-x/35)));
Small_Hab_Historical(x)=3*(20*(1-exp(-x/8)));
end
t=[1:1:150];

plot(t, NASA_Curve)
hold on
plot(t, Celentano)
hold on
plot(t, Historical_data)
hold on
plot(t, Small_Hab_Historical)
axis([0 130 0 200])
xlabel('Mission Duration (days)','fontsize',14)
ylabel('Habitable Volume (m^3)','fontsize',14)
title('Magellan Mk2.0 Habitable Volume (3-Person Crew)','fontsize',14)
legend('NASA 2011 HVW', 'Celentano Curve', 'NASA Historical Data', 'Small Hab Historical', 'Location','southeast')

%Habitable vol per crew of 3 on moon
days=120

NASA_Curve_3=(4.8827*log(days)-3.9113)*3

```

```

Celentano_3=(20*(1-exp(-days/20)))^3
Historical_data_3=(62*(1-exp(-days/35)))^3
Small_Hab_Historical_3=3*(20*(1-exp(-days/8)));

```

11.2.2. Magellan 2.0 Actual Habitable Volume

Chris Wells-Weitzner

%This code was written to determine the habitable volume for the crew in the Magellan 2.0

%Volume Magellan

%number of crew

```
crew_num = 3;
```

% 180days for 4 people

```
Days = 80:120;
```

```
Clothes = 1.0012/180/4*Days^3; %m^3
```

```
Food = 6.9/180/4*Days^3; %m^3
```

```
water = 178*3/42*Days;
```

```
rho_w = 999.97;
```

```
vol_H2O = water/rho_w
```

%Habitable volume in Mag

```
Front = 4/3*pi*(1.8-.16)^3; %m^3
```

```
Hull = 6.4*pi*(1.8-.16)^2; %m^3
```

```
End = 2.06; %m^3
```

```
Basement = 12.45; %m^3
```

```
Total_vol = Front + Hull + End + Basement
```

```
total_crew = Front + Hull + End - Basement-Clothes-Food-vol_H2O;
```

```
total_indiv = total_crew/crew_num
```

%From the NASA 2011 Habitable Volume Workshop, the required vol per crew

%for 120 days is

```
Days120_VpC = 19; %m^3
```

11.2.3. Solar Power on the Moon

Adam Buckingham (“Solar_Moon”)

%% Solar Power on the Moon

```
clear all
```

```
Is = 1360;
```

```

obl = 6.68;
lat = 85;
A_array = 1;
Solar_efficiency = 0.29;

Orb_P=238;
t = -6:1/3600:6;
for i = 1:length(t)
hour_angle(i) = 360*(t(i)/648);
dec = sind(obl)*sind(Orb_P);
zenith(i) = acosd(sind(lat)*sind(dec)+cosd(lat)*cosd(dec)*cosd(hour_angle(i)));

Sflat(i) = Is*cosd(zenith(i));
Sflat_dust(i) = (1-.26)*Sflat(i);

Pflat(i) = Sflat(i)*Solar_efficiency*A_array;
i = i+1;

end

Pflat_total = sum(Pflat);
display(Pflat_total/3600,'Flat Power in W-hr');

Ptotal = (Pflat_total/3600)/12

plot(t,zenith)

```

11.2.4. Lunar Mining

Dustin Zrelak

"Lunar Mining"

```

clear all
close all
clc

```

%FTV launch windows in units of days

```
ftv_window = 60;
```

% Constants

```
fuel_req = 300;    %Metric tons
```

```
window = 150;    %Days
```

```
fuelperday = fuel_req/window;    %Metric tons per day
```

```
n = 0.8;    %Assumed electrolysis efficiency
```

```
h20 = 0.055;    %55000 ppm water in soil
```

```

LOXden = 1.140; %Metric tons per cubic meter
LH2den = 0.071; %Metric tons per cubic meter

%Amount of regolith mining req per day
dirtperday = fuel_req/window/n/h20 %Metric tons

dirt_density = 0.75; %Metric tons per cubic meter

volumeperday = dirtperday/dirt_density %cubic meters per day

FTVLOXvol = (fuelperday*ftv_window/7)/LOXden; %Cubic meters
FTVLOXrad = (FTVLOXvol/(4*pi/3))^(1/3); %Meters

FTVLH2vol = (fuelperday*ftv_window/7*6)/LH2den; %Cubic meters
FTVLH2rad = (FTVLH2vol/(4*pi/3))^(1/3); %Meters

lunarLOXvol = FTVLOXvol*1.2 %Cubic meters
eachlunarLOXvol = lunarLOXvol/4 %Cubic meters
lunarLOXrad = ((eachlunarLOXvol)/(4*pi/3))^(1/3) %Meters

lunarLH2vol = FTVLH2vol*1.2 %Cubic meters
eachlunarLH2vol = lunarLH2vol/8 %Cubic meters
lunarLH2rad = ((eachlunarLH2vol)/(4*pi/3))^(1/3) %Meters

```

11.2.5. Lunar Regolith Heating

Dustin Zrelak

```

clear all
close all
clc

kW = 150000; % Power allotted (kW)
cp = 718; % Cp of soil
regolith = 45000/(24*60^2); %regolith mass processed per minute

dT=kW/(cp*regolith) % Resulting change in temperature

```

11.2.6. Dimensions for Fuel Transport Vehicle Tanks

Laura Martinez

```

% Dimensions for Fuel Transport Vehicle Tanks
%This script calculates the tank size for LOX and LH2 depending on
%propellant mass

clear
%run propellant.m
%close all

rho_lox = 1140; %density of LOX in kg/m^3
rho_lh2 = 71; %density of LH2 in kg/m^3

```

```

ratio = 5.85; %LOX/LH2 ratio

%-----From April's numbers
m_prop = 63*1000; %total propellant mass used in kg
m_struc = 15.4*1000; %structure mass in kg
m_pl = 40*1000; %payload mass in kg

%Masses of LH2 and LOX
m_lh2 = (1/ratio)*m_prop; % LH2 mass in kg
m_lox = (1 - 1/ratio)*m_prop; % LOX mass in kg

%Volumes and masses of tanks
v_lh2 = m_lh2/rho_lh2; %volume of LH2 in m^3
v_lox = m_lox/rho_lox; %volume of LOX in m^3
m_lh2_tank = 9.09*v_lh2; %mass of LH2 tank in kg
m_lox_tank = 12.16*v_lox; %mass of LOX tank in kg

%Assume spherical tanks
rad_lh2 = (v_lh2/(4*pi/3))^(1/3); %radius of LH2 tank in m
rad_lox = (v_lox/(4*pi/3))^(1/3); %radius of LOX tank in m
a_lh2 = 4*pi*rad_lh2^2; %area of LH2 tank in m^2
a_lox = 4*pi*rad_lox^2; %area of LOX tank in m^2
h_lh2 = 2*rad_lh2;
h_lox = 2*rad_lox;

%Assume cylindrical tanks
% {
rad_lh2 = 3/2; %radius of LH2 tank in m
rad_lox = 3/2; %radius of LOX tank in m
h_lh2 = v_lh2/(pi*rad_lh2^2); %height of LH2 tank in m
h_lox = v_lox/(pi*rad_lox^2); %height of LOX tank in m
if h_lh2>19
    h_tank = h_lh2/2; %height of fuel tanks in m
else
    h_tank = h_lh2; %height of fuel tanks in m
end
a_lh2 = 2*pi*rad_lh2 + 2*pi*rad_lh2^2; %surface area of LH2 tank in m^2
a_lox = 2*pi*rad_lox + 2*pi*rad_lox^2; %surface area of LOX tank in m^2
%}

%Insulation Masses
m_lh2_ins = 2.88*a_lh2; %mass of LH2 insulation in kg
m_lox_ins = 1.123*a_lox; %mass of LOX insulation in kg

%Payload Mass by Material
m_lh2_pl = (1/ratio)*m_pl; %in kg
m_lox_pl = (1 - 1/ratio)*m_pl; %in kg

%Total LH2 and LOX mass
m_lh2_tot = m_lh2 + m_lh2_pl; %in kg
m_lox_tot = m_lox + m_lox_pl; %in kg

%display(rad_lh2,'Radius of LH2 tank in m') %spherical tanks
%display(rad_lox,'Radius of LOX tank in m') %spherical tanks
display(h_lh2,'Height of LH2 tank in m') %spherical tanks

```

```

display(h_lox,'Height of LOX tank in m') %spherical tanks
%display(h_tank,'Height of tanks in m') %cylindrical tanks
display(m_struct/1000,'Estimated structure dry mass in MT')
display(m_lh2_pl/1000,'Payload mass of LH2 in MT')
display(m_lox_pl/1000,'Payload mass of LOX in MT')

```

11.2.7. Dimensions for Fuel Transport Vehicle

Laura Martinez

```

%% Dimensions for Fuel Transport Vehicle
% This one is the two spheres on a cylinder

%This script calculates the various masses of the lunar lander vehicle
%and indicates the distribution of mass too

clear
run sizing.m
clc

rho_al7078 = 2700; %density of aluminum 7078 in kg/m^3
rho_stl = 7850; %density of steel in kg/m^3
rho_al7075 = 2810; %density of aluminum 7075 in kg/m^3
rho_al6061 = 2700; %density of aluminum 6061 in kg/m^3
rho_FTV = rho_al6061; %density of chosen material in kg/m^3

%----From CAD sketch dimensions
r_cyl = 1.5; %Radius of lowest cylinder platform in m
h_cyl = 0.15; %Height of lowest cylinder platform in m

%Heights, thickness and area
h_tanks = h_lox + h_lh2; %height of both tanks in m
h_eng = 4.14; %height of RL10 in m
a_cyl = 4*pi*r_cyl^2; %area of cylinder in m^2

%Volumes
v_cyl = a_cyl*h_cyl; %volume of bottom cylinder in m^3
v_lh2_pl = m_lh2_pl/rho_lh2; %volume of LH2 payload in m^3
v_lox_pl = m_lox_pl/rho_lox; %volume of LOX payload in m^3

%Masses
m_cyl = v_cyl*rho_FTV; %mass of both lids in kg
m_eng = 277; %mass of RL10 engine in kg

%Tank calculations including payload propellant
v_lh2_true = v_lh2 + v_lh2_pl; %volume of full LH2 tank in m^3
v_lox_true = v_lox + v_lox_pl; %volume of full LOX tank in m^3
m_lh2_tank = 9.09*v_lh2_true; %mass of entire LH2 tank in kg
m_lox_tank = 12.16*v_lox_true; %mass of entire LOX tank in kg
r_lh2_true = (v_lh2/(4*pi/3))^(1/3); %radius of full LH2 tank in m
r_lox_true = (v_lox/(4*pi/3))^(1/3); %radius of full LOX tank in m

%Truss Masses

```

```

%m_tr_dock =
%m_tr_mid =
%m_tr_land =

%Totals for structure
h_tanks_true = 2*r_lh2_true + 2*r_lox_true; %height of tanks in m
h_lander = 6.68; %height of landing struts in m
h_struc = r_lh2_true + 2*r_lox_true + h_cyl + h_lander; %full structure height in m
m_FTV_dry = m_cyl + m_eng + m_lh2_tank + m_lox_tank;
%structure dry mass in kg
m_FTV_gross = m_FTV_dry + m_pl + m_prop;
%total vehicle mass in kg

display('FTV Mass Analysis')
display(r_lh2_true, 'LH2 tank radius in m')
display(r_lox_true, 'LOX tank radius in m')
display(m_lh2_tot/1000, 'Total LH2 mass in MT')
display(m_lox_tot/1000, 'Total LOX mass in MT')
display(h_tanks_true, 'Total tank height in m')
display(h_struc, 'Total structure height in m')
display(m_FTV_dry/1000, 'True structure dry mass in MT')
display(m_FTV_gross/1000, 'Loaded vehicle mass in MT')

```

11.2.8. Loads for Cylindrical Lunar Lander Vehicle

Laura Martinez

```

%% Loads for Cylindrical Lunar Lander Vehicle
% This one is the two spheres on a cylinder

%This script calculates the various loads of the lunar lander vehicle

clear
run mass_cyl.m
clc

%Structure weight on moon
grav_moon = 1.622; %gravity on moon in m/s^2
grav_earth = 9.81; %gravity on Earth in m/s^2
grav = grav_earth; %gravity used for crash calculations
weight_FTV_dry = m_FTV_dry*grav_moon; %dry structure weight on moon in N
weight_FTV_gross = m_FTV_gross*grav_moon; %fully loaded vehicle weight on moon in N

%Material Properties
str_al7075 = 503*10^6; %yield strength of aluminum 7075 in Pa
str_al6061 = 55.2*10^6; %yield strength of aluminum 6061 in Pa
str_FTV = str_al6061; %yield strength of chosen material
E_al7075 = 71.7*10^9; %young's modulus for al7075 in Pa
E_al6061 = 68.9*10^9; %young's modulus for al6061 in Pa
E_FTV = E_al6061; %young's modulus of chosen material

%LH2 and LOX tanks

```

```

pres_lh2 = 1*10^6; %pressure in LH2 tank in Pa from April
pres_lox = 4.7*10^6; %pressure in LOX tank in Pa from April
t_lh2_tank = 0.07; %LH2 tank thickness in m
t_lox_tank = 0.05; %LOX tank thickness in m

%Stress in tanks
str_hoop_lh2 = (pres_lh2*r_lh2_true)/(2*t_lh2_tank); %hoop stress for LH2 in Pa
str_hoop_lox = (pres_lox*r_lox_true)/(2*t_lox_tank); %hoop stress for LOX in Pa

%Forces
f_thrust = 110*10^3; %thrust of RL10-B in N
acc_land = 6*grav; %acceleration due to crash
f_crash = m_FTV_dry*acc_land; %all weight landing on 1 point (crash landing)
f_fland = f_crash/4; %flat landing on 4 points (distributed)
%f_dock = 6500; %dynamic docking force at top in N
f_dock = f_crash/4; %crash landing effect on dock truss in N

%Docking Truss
Ad = [1.7; 1.55; 1.4]; %points on truss in m, A at top of strut
Bd = [0; 0; 0]; %points on truss in m, B on bottom
r_rod_ot = 0.1/2; %radius of outer rod in m
t_rod = 0.02; %thickness of rod in m
r_rod_in = r_rod_ot - t_rod; %radius of inner rod in m
a_rod = pi*(r_rod_ot^2 - r_rod_in^2); %area of rod in m^2
%a_rod = pi*(r_rod_ot^2); %area of rod in m^2
L_rod = norm(Ad); %length of one landing strut rod
%I_rod = (pi/4)*(r_rod_ot^4 - r_rod_in^4); %moment of inertia for rod in m^4
I_rod = (pi/4)*(r_rod_ot^4); %moment of inertia for rod in m^4
K_buck = 0.5; %assumes a fixed-fixed connection
f_dock_DT = f_dock/4;
str_dock_DT = f_dock_DT/a_rod;
vol_DT = pi*Ad(3)*(r_rod_ot^2-r_rod_in^2); %volume of docking truss
m_DT = vol_DT*rho_FTV; %mass of docking truss in kg

%Middle Trusses
Am = [2.24; 2.4; 4.59]; %points on truss in m, A at top of strut
Bm = [0; 0; 0]; %points on truss in m, B on bottom
r_rod_ot = 0.1/2; %radius of outer rod in m
%t_rod = 0.05; %thickness of rod in m
%r_rod_in = r_rod_ot - t_rod; %radius of inner rod in m
%a_rod = pi*(r_rod_ot^2 - r_rod_in^2); %area of rod in m^2
a_rod = pi*(r_rod_ot^2); %area of rod in m^2
L_rod = norm(Am-Bm); %length of one landing strut rod
%I_rod = (pi/4)*(r_rod_ot^4 - r_rod_in^4); %moment of inertia for rod in m^4
I_rod = (pi/4)*(r_rod_ot^4); %moment of inertia for rod in m^4
K_buck = 0.5; %assumes a fixed-fixed connection
f_fland_MT = f_fland/2;
%force due to distributed landing over 2 legs
str_fland_MT = f_fland_MT/a_rod;
vol_MT = pi*Am(3)*(r_rod_ot^2); %volume of middle truss
m_MT = vol_MT*rho_FTV; %mass of middle truss in kg

%Landing Struts

```

```

Al = [3.47; 0; 0]; %points on strut in m, A at top of strut
Bl = [4.5; 4.5; 7.7]; %points on strut in m, B on bottom
r_rod_ot = 0.3/2; %radius of outer rod in m
t_rod = 0.02; %thickness of rod in m
r_rod_in = r_rod_ot - t_rod; %radius of inner rod in m
a_rod = pi*(r_rod_ot^2 - r_rod_in^2); %area of rod in m^2
L_rod = norm(Al-Bl); %length of one landing strut rod
I_rod = (pi/4)*(r_rod_ot^4 - r_rod_in^4); %moment of inertia for rod in m^4
K_buck = 0.699; %assumes a fixed-pinned connection
f_crash_LS = f_crash/3;
%force due to 5g crash + 1g inertia load distributed over 3 legs
str_crash_LS = f_crash_LS/a_rod;
vol_LS = pi*Bl(3)*(r_rod_ot^2 - r_rod_in^2); %volume of landing struts
m_LS = vol_LS*rho_FTV; %mass of landing struts in kg

%Margins of Safety
sf_pres = 2; %safety factor for pressure vessels
sf_land = 3; %safety factor for landings
sf_thrust = 1.2; %safety factor for thrust
sf_dock = 3; %safety factor for docking
mos_lh2 = str_FTV/(str_hoop_lh2*sf_pres) - 1; %MOS for LH2 tank
mos_lox = str_FTV/(str_hoop_lox*sf_pres) - 1; %MOS for LOX tank
mos_crash = str_FTV/(str_crash_LS*sf_land) - 1; %MOS for landing strut buckle
mos_fland = str_FTV/(str_fland_MT*sf_land) - 1; %MOS for middle truss buckle
%mos_thrust = str_FTV/(str_crash_MT*sf_thrust) - 1; %MOS for middle truss buckle
mos_dock = str_FTV/(str_dock_DT*sf_dock) - 1; %MOS for dock truss buckle

display('FTV Load Analysis')
display(weight_FTV_dry/(10^3),'Dry structure weight in kN')
display(weight_FTV_gross/(10^3),'Gross structure weight in kN')

display(str_hoop_lh2/(10^6),'LH2 hoop stress in MPa')
display(str_hoop_lox/(10^6),'LOX hoop stress in MPa')
display(mos_lh2,'Margin of Safety for LH2 tank')
display(mos_lox,'Margin of Safety for LOX tank')

display(f_crash/(10^3),'Crash Landing in kN')
display(f_fland/(10^3),'Distributed Landing in kN')
display(f_dock/(10^3),'Dynamic Docking in kN')
display(mos_crash,'Margin of Safety for Landing struts on Crash')
display(mos_fland,'Margin of Safety for Middle truss on Flat Landing')
display(mos_dock,'Margin of Safety for Docking truss on Docking')

display((m_MT+m_LS+m_DT)/1000,'Mass of all Trusses/Struts in MT')
%display(f_thrust/(10^3),'Thrust in kN')
%display(mos_thrust,'Margin of Safety for Middle truss on Thrust')

```

11.2.9. Dimensions for Moon Gas Station Tanks

Laura Martinez

```

%% Dimensions for Moon Gas Station Tanks
%This script calculates the tank size for LOX and LH2 depending on
%propellant mass

clear; clc

rho_lox = 1140; %density of LOX in kg/m^3
rho_lh2 = 71; %density of LH2 in kg/m^3
ratio = 5.85; %LOX/LH2 ratio

%-----From Sam's Mission Requirements
m_gas = 330*1000; %total propellant mass in kg

%Masses of LH2 and LOX
m_lh2 = (1/ratio)*m_gas; % LH2 mass in kg
m_lox = (1 - 1/ratio)*m_gas; % LOX mass in kg
t_tank = 0.35; %thickness of tanks in m

%Volumes and masses of tanks
v_lh2 = m_lh2/rho_lh2; %volume of LH2 in m^3
v_lox = m_lox/rho_lox; %volume of LOX in m^3
m_lh2_tank = 9.09*v_lh2; %mass of LH2 tank in kg
m_lox_tank = 12.16*v_lox; %mass of LOX tank in kg

%Assume half-spherical tanks as endcaps
rad_lh2 = 7/2; %radius of LH2 tank in m
rad_lox = 6.5/2; %radius of LOX tank in m
vs_lh2 = 2*(4*pi/3)*rad_lh2^3; %spherical volume of both LH2 tanks in m^3
vs_lox = (4*pi/3)*rad_lox^3; %spherical volume of LOX tank in m^3

%Use cylindrical tanks for the rest
vc_lh2 = v_lh2 - vs_lh2; %cylindrical volume for LH2 tanks in m^3
vc_lox = v_lox - vs_lox; %cylindrical volume for LOX tank in m^3
hc_lh2 = (vc_lh2/2)/(pi*rad_lh2^2); %height of LH2 tank in m
hc_lox = vc_lox/(pi*rad_lox^2); %height of LOX tank in m

%Full tanks with cap
h_lh2 = 2*rad_lh2 + hc_lh2; %full height of rounded LH2 tanks in m
h_lox = 2*rad_lox + hc_lox; %full height of rounded LOX tank in m

%Tank insulation
rad_lh2_out = rad_lh2 + t_tank; %outer radius of LH2 tanks in m
rad_lh2_in = rad_lh2; %inner radius of LH2 tanks in m
rad_lox_out = rad_lox + t_tank; %outer radius of LOX tank in m
rad_lox_in = rad_lox; %inner radius of LOX tank in m
v_lh2_tank = (4*pi/3)*(rad_lh2_out^3 - rad_lh2_in^3) + (pi*hc_lh2)*(rad_lh2_out^2 - rad_lh2_in^2);
v_lox_tank = (4*pi/3)*(rad_lox_out^3 - rad_lox_in^3) + (pi*hc_lox)*(rad_lox_out^2 - rad_lox_in^2);
%Volume of each tank in m^3
m_lh2_tank = 0.5*(9.09*v_lh2); %mass of LH2 tank in kg
m_lox_tank = 12.16*v_lox; %mass of LOX tank in kg

%Mass Totals
m_struc = m_lh2 + m_lox + 2*m_lh2_tank + m_lox_tank;
%full structure mass in kg
m_lox_tot = m_lox + m_lox_tank; %full LOX tank mass in kg

```

```
m_lh2_tot = m_lh2 + m_lh2_tank; %1 full LH2 tank mass in kg
```

```
display(m_gas/1000,'Total propellant mass on Moon Gas Station in MT')
display(2*rad_lh2+2*t_tank,'Diameter of LH2 tank in m')
display(h_lh2,'Full Height of each LH2 tank in m')
display(m_lh2_tank/1000,'Each LH2 tank mass in MT')
display(2*rad_lox+2*t_tank,'Diameter of LOX tank in m')
display(h_lox,'Full Height of LOX tank in m')
display(m_lox_tank/1000,'LOX tank mass in MT')
display((2*m_lh2_tank+m_lox_tank)/1000,'Mass of all tanks in MT')
display(m_struc/1000,'Total Structure Mass in MT')
```

11.2.10. Loads for Gas Stations

Laura Martinez

```
%% Loads for Gas Stations
% Author: Laura Martinez
%% Moon Gas Station
```

```
clear
run moon_gas_station.m
clc
```

```
%-----Lengths based on CTV requirements (Will + Jaclyn)
len_tc = 1; %length of truss in m
```

```
%-----Forces due to Stationkeeping (April)
a_STK = 2.07e-4; %acceleration due to stationkeeping in m/s^2
f_thrust = 590; %force created due to stationkeeping thrust in N
f_STK = f_thrust + m_lox_tot*a_STK; %largest force due to stationkeeping
```

```
%-----Forces due to Docking (IDS Paper)
f_dkT = 3900; %docking tension load in N
f_dkC = 6500; %docking dynamic compression load in N
f_dock_DT = 2.1915e+05; %same as FTV, in N
```

```
%Material Properties
str_al7075 = 503*10^6; %yield strength of aluminum 7075 in Pa
str_al6061 = 55.2*10^6; %yield strength of aluminum 6061 in Pa
str_FD = str_al6061; %yield strength of chosen material
E_al7075 = 71.7*10^9; %young's modulus for al7075 in Pa
E_al6061 = 68.9*10^9; %young's modulus for al6061 in Pa
E_FD = E_al6061; %young's modulus of chosen material
rho_al7075 = 2810; %density of aluminum 7075 in kg/m^3
rho_al6061 = 2700; %density of aluminum 6061 in kg/m^3
rho_FD = rho_al6061; %density of chosen material in kg/m^3
```

```
%Tank Connectors
mom_STK = len_tc*f_STK; %moment created due to station keeping in Nm
r_tc_ot = 0.15/2; %radius of outer rod in m
```

```

t_tc = 0.02; %thickness of rod in m
r_tc_in = r_tc_ot - t_tc; %radius of inner rod in m
a_rod = pi*(r_tc_ot^2 - r_tc_in^2); %area of rod in m^2
rad_tc = 0.4; %radius of tank connectors in m
I_tc = (pi/4)*(r_tc_ot^4 - r_tc_in^4); %moment of inertia in m^4
str_STK = mom_STK*rad_tc/I_tc;%bending stress due to station keeping in Pa

%LH2 and LOX tanks
pres_lh2 = 1*10^6; %pressure in LH2 tank in Pa from April
pres_lox = 4.7*10^6; %pressure in LOX tank in Pa from April
t_lh2_tank = 0.1; %LH2 tank thickness in m
t_lox_tank = 0.1; %LOX tank thickness in m

%Stress in tanks
str_hoop_lh2 = (pres_lh2*rad_lh2_out)/(2*t_lh2_tank); %hoop stress for LH2 in Pa
str_hoop_lox = (pres_lox*rad_lox_out)/(2*t_lox_tank); %hoop stress for LOX in Pa

%Docking Truss
Ad = [1.7; 1.55; 1.4]; %points on truss in m, A at top of strut
Bd = [0; 0; 0]; %points on truss in m, B on bottom
r_rod_ot = 0.1/2; %radius of outer rod in m
t_rod = 0.02; %thickness of rod in m
r_rod_in = r_rod_ot - t_rod; %radius of inner rod in m
a_rod = pi*(r_rod_ot^2 - r_rod_in^2); %area of rod in m^2
%a_rod = pi*(r_rod_ot^2); %area of rod in m^2
L_rod = norm(Ad); %length of one landing strut rod
%I_rod = (pi/4)*(r_rod_ot^4 - r_rod_in^4); %moment of inertia for rod in m^4
I_rod = (pi/4)*(r_rod_ot^4); %moment of inertia for rod in m^4
K_buck = 0.5; %assumes a fixed-fixed connection
str_dock_DT = f_dock_DT/a_rod;
vol_DT = pi*Ad(3)*(r_rod_ot^2-r_rod_in^2); %volume of docking truss
m_DT = vol_DT*rho_FD; %mass of docking truss in kg

%Margins of Safety
sf_pres = 2; %safety factor for pressure vessels
sf_dock = 3; %safety factor for landings
sf_STK = 2; %safety factor for station keeping
mos_lh2 = str_FD/(str_hoop_lh2*sf_pres) - 1; %MOS for LH2 tank
mos_lox = str_FD/(str_hoop_lox*sf_pres) - 1; %MOS for LOX tank
mos_dock = str_FD/(str_dock_DT*sf_dock) - 1; %MOS for docking truss buckle
mos_STK = str_FD/(str_STK*sf_STK) - 1; %MOS for upper truss buckle

display('Fuel Depot Load Analysis')
display(f_dkT,'Undocking Tension in N')
display(f_dkC,'Dynamic Docking Compression in N')
display(str_dock_DT/(10^6),'Dynamic Docking Stress in MPa')
display(mos_dock,'Margin of Safety for Dynamic Docking')

display(str_hoop_lh2/(10^6),'LH2 hoop stress in MPa')
display(str_hoop_lox/(10^6),'LOX hoop stress in MPa')
display(mos_lh2,'Margin of Safety for LH2 tank')
display(mos_lox,'Margin of Safety for LOX tank')

```

```

display(f_STK,'Stationkeeping in N')
display(str_STK/(10^6),'Stationkeeping Stress in MPa')
display(mos_STK,'Margin of Safety for Stationkeeping')

```

11.2.11. Dimensions for Mars Gas Station Tanks

Laura Martinez

```

%% Dimensions for Mars Gas Station Tanks
%% This script calculates the tank size for LOX and LH2 depending on
%% propellant mass

clear; clc

rho_lox = 1140; %density of LOX in kg/m^3
rho_lh2 = 71; %density of LH2 in kg/m^3
ratio = 5.85; %LOX/LH2 ratio

%-----From Sam's Mission Requirements
m_gas = (3*26)*1000; %total propellant mass in kg
m_gas = (3*40)*1000; %just in case propellant mass in kg
t_tank = 0.35; %thickness of tanks in m

%Masses of LH2 and LOX
m_lh2 = (1/ratio)*m_gas; % LH2 mass in kg
m_lox = (1 - 1/ratio)*m_gas; % LOX mass in kg

%Volumes and masses of tanks
v_lh2 = m_lh2/rho_lh2; %volume of LH2 in m^3
v_lox = m_lox/rho_lox; %volume of LOX in m^3
m_lh2_tank = 9.09*v_lh2; %mass of LH2 tank in kg
m_lox_tank = 12.16*v_lox; %mass of LOX tank in kg

%Assume half-spherical tanks as endcaps
rad_lh2 = 7/2; %radius of LH2 tank in m
rad_lox = 6.5/2; %radius of LOX tank in m
vs_lh2 = 2*(4*pi/3)*rad_lh2^3; %spherical volume of both LH2 tanks in m^3
vs_lox = (4*pi/3)*rad_lox^3; %spherical volume of LOX tank in m^3

%Use cylindrical tanks for the rest
vc_lh2 = v_lh2 - vs_lh2; %cylindrical volume for LH2 tanks in m^3
vc_lox = v_lox - vs_lox; %cylindrical volume for LOX tank in m^3
hc_lh2 = (vc_lh2/2)/(pi*rad_lh2^2); %height of LH2 tank in m
hc_lox = vc_lox/(pi*rad_lox^2); %height of LOX tank in m

%Full tanks with cap
h_lh2 = 2*rad_lh2 + hc_lh2; %full height of rounded LH2 tanks in m
h_lox = 2*rad_lox + hc_lox; %full height of rounded LOX tank in m

%Tank insulation
rad_lh2_out = rad_lh2 + t_tank; %outer radius of LH2 tanks in m
rad_lh2_in = rad_lh2; %inner radius of LH2 tanks in m

```

```

rad_lox_out = rad_lox + t_tank; %outer radius of LOX tank in m
rad_lox_in = rad_lox; %inner radius of LOX tank in m
v_lh2_tank = (4*pi/3)*(rad_lh2_out^3 - rad_lh2_in^3) + (pi*hc_lh2)*(rad_lh2_out^2 - rad_lh2_in^2);
v_lox_tank = (4*pi/3)*(rad_lox_out^3 - rad_lox_in^3) + (pi*hc_lox)*(rad_lox_out^2 - rad_lox_in^2);
all_tank = 2*m_lh2_tank+m_lox_tank; %mass of all tanks in kg
%Volume of each tank in m^3
m_lh2_tank = 0.5*(9.09*v_lh2); %mass of LH2 tank in kg
m_lox_tank = 12.16*v_lox; %mass of LOX tank in kg

display(m_gas/1000,'Total propellant mass on Mars Gas Station in MT')
display(2*rad_lh2+2*t_tank,'Diameter of LH2 tank in m')
display(h_lh2,'Full Height of each LH2 tank in m')
display(m_lh2_tank/1000,'Each LH2 tank mass in MT')
display(2*rad_lox+2*t_tank,'Diameter of LOX tank in m')
display(h_lox,'Full Height of LOX tank in m')
display(m_lox_tank/1000,'LOX tank mass in MT')
display(h_lh2*2+h_lox,'Height of all 3 tanks stacked in m')
display(all_tank/1000,'Mass of all tanks in MT')

```

11.2.12. Propellant Calculations with Multi-Stage Estimations

April Claus

```

%% PROPELLANT CALC with multi stage estimations ***
% FTV: surface to L1, then L1 to surface
% 63 t to get there and back with 0 left over

mS = 15; %t, includes empty tanks
mPL = 40; %t, prop for gas station
Isp = 460;
g0 = 9.81;
mprop_start1 = 0:0.1:100; % t, prop for FTV
moondV = 1.04*1.6337; % surface to LLO dV, with 4% margin
dVtot_max_md = 0.8892; % 4% margin already incorporated (LLO-L1)
dVtot_min_md = 0.8550; % 4% margin already incorporated (LLO-L1)

% accounting for dV from surface to LLO AND LLO to L1
dV_StoL1_min_md = moondV + dVtot_min_md; % using min L1 distance from moon
dV_StoL1_max_md = moondV + dVtot_max_md; % using max L1 distance from moon

for i = 1:length(mprop_start1)
    % MAX DISTANCE FROM MOON TO L1
    % prop it takes to get from surface to L1
    % PL in m_initial, PL in m_final (tanks dumped AFTER arrival at L1)
    mprop_left1(i) = ((exp(-dV_StoL1_max_md/(Isp*g0*0.001)))*(mprop_start1(i) + mS + mPL))-mS-mPL;

    % starting with prop leftover from first maneuver
    % getting from L1 to surface, powered descent
    % no PL in m_initial or m_final values
    mprop_left2(i) = ((exp(-dV_StoL1_max_md/(Isp*g0*0.001)))*(mprop_left1(i) + mS))-mS;

```

```

% MIN DISTANCE FROM MOON TO L1
% prop it takes to get from surface to L1
mprop_left3(i) = ((exp(-dV_StoL1_min_md/(Isp*g0*0.001)))*(mprop_start1(i) + mS + mPL))-mS-mPL;

% starting with prop leftover from first maneuver
% getting from L1 to surface, powered descent
mprop_left4(i) = ((exp(-dV_StoL1_min_md/(Isp*g0*0.001)))*(mprop_left3(i) + mS))-mS;

end
figure(7)
plot(mprop_start1,mprop_left1,'r')
hold on
plot(mprop_start1,mprop_left2,'k')
refline(0,0)
hold off

title('MAX R: Mass of Prop LEFT vs. Mass of PL on FTV, surface-L1-surface','FontSize',12)
xlabel('Mass of Starting Propellant (t)','FontSize',12)
ylabel('Mass of Propellant Left in Tank (t)','FontSize',12)
legend('surface - L1','L1 - surface','Location','NorthEast')

figure(8)
plot(mprop_start1,mprop_left3,'r')
hold on
plot(mprop_start1,mprop_left4,'k')
refline(0,0)
hold off

title('MIN R: Mass of Prop LEFT vs. Mass of PL on FTV, surface-L1-surface','FontSize',12)
xlabel('Mass of Starting Propellant (t)','FontSize',12)
ylabel('Mass of Propellant Left in Tank (t)','FontSize',12)
legend('surface - L1','L1 - surface','Location','NorthEast')

```

11.2.13. Payload Mass Calculations

April Claus

```

%% Payload Mass Calculations

mS = 4; %t, SLS Block IB Stage 2

mPL = 0:0.1:120; % t, max PL to LEO is 105 t
Isp = 460; % s, RL10 engines
g0 = 9.81; % m/s^2
mprop_start = 129; % t (assuming full refuel at L1)

dVLEOtoLLO = 4.08; % km/s
dVLEOtoL1_min_ed = 3.94;

```

```

dVescLLO = 2.78;
dVLLOtoLMO = 5.51;
dVL1toLMO = 3.23;
dVLEOtoLMO = 6.67;

for i = 1:length(mPL)

% LEO to LLO
mprop_left11(i) = ((exp(-dVLEOtoLLO/(Isp*g0*0.001)))*(mprop_start + mS + mPL(i)))-mS-mPL(i);
mprop_used11(i) = mprop_start - mprop_left11(i);

% LLO to Interplanetary: 2.78
% LLO to LMO: 5.51
% LLO to LMO after full refuel
mprop_left22(i) = ((exp(-dVLLOtoLMO/(Isp*g0*0.001)))*(mprop_start + mS + mPL(i)))-mS-mPL(i);
mprop_used22(i) = mprop_start - mprop_left22(i);

% LEO to L1, using max dV
mprop_left33(i) = ((exp(-dVLEOtoL1_min_ed/(Isp*g0*0.001)))*(mprop_start + mS + mPL(i)))-mS-mPL(i);
mprop_used33(i) = mprop_start - mprop_left33(i);

% L1 to LMO
mprop_left44(i) = ((exp(-dVL1toLMO/(Isp*g0*0.001)))*(mprop_start + mS + mPL(i)))-mS-mPL(i);
mprop_used44(i) = mprop_start - mprop_left44(i);

% no refuel
%dVLEOtoLMO = 6.67;
mprop_left55(i) = ((exp(-dVLEOtoLMO/(Isp*g0*0.001)))*(mprop_start + mS + mPL(i)))-mS-mPL(i);

end
figure(1)
plot(mPL,mprop_left11,'r')
hold on
plot(mPL,mprop_left22,'k')
refline(0,0) % refline(m,b)
hold off

title('Mass of Propellant Left vs. Mass of Payload, LEO-LLO-LMO','FontSize',14)
xlabel('Mass of Payload (t)','FontSize',14)
ylabel('Mass of Propellant Left in Tank (t)','FontSize',14)
legend('LEO-LLO','LLO-LMO','Location','NorthEast')

figure(2)
plot(mPL,mprop_left33,'r')
hold on
plot(mPL,mprop_left44,'k')

```

```
refline(0,0)
hold off
```

```
title('Mass of Propellant Left vs. Mass of Payload, LEO-L1-LMO','FontSize',14)
xlabel('Mass of Payload (t)','FontSize',14)
ylabel('Mass of Propellant Used (t)','FontSize',14)
legend('LEO-L1, Max dV','L1-LMO','Location','NorthEast')
```

```
figure(3)
plot(mPL,mprop_left55,'r')
hold on
refline(0,0)
hold off
```

```
title('Mass of Propellant Left vs. Mass of Payload, LEO-LMO','FontSize',14)
xlabel('Mass of Payload (t)','FontSize',14)
ylabel('Mass of Propellant Used (t)','FontSize',14)
legend('LEO-LMO, NO REFUEL','Location','NorthEast')
```

EML1 prop requirements

```
clear all;
```

```
dVmax = 0.15; % km/s, both x an y axis control, yearly cost
dVmin = 0.01;
Isp = 350;
mS = 10;
g0 = 9.81;
```

```
mprop_start1 = 0:0.01:20; %t
mPL = 330-mprop_start1; % full tanks
```

```
for n = 1:length(mprop_start1)
    mprop_left_min(n) = ((exp(-dVmin/(Isp*g0*0.001)))*(mprop_start1(n) + mS + mPL(n)))-mS - mPL(n);
    mprop_left_max(n) = ((exp(-dVmax/(Isp*g0*0.001)))*(mprop_start1(n) + mS + mPL(n)))-mS - mPL(n);
end
```

```
figure
plot(mprop_start1,mprop_left_min,'r')
hold on
plot(mprop_start1,mprop_left_max,'k')
refline(0,0)
hold off
title('Starting RCS Prop Mass vs Remaining Prop Mass','FontSize',14)
xlabel('Start RCS Prop Mass (t)','FontSize',14)
ylabel('Remaining RCS Prop Mass (t)','FontSize',14)
legend('Min Delta V','Max Delta V','Location','NorthWest')
```

11.2.14. EML1 RCS Design

April Claus

```

%% EML1 RCS Design
clear all;
clc;

gamma = 1.33; % steam, water
R1 = 8314.3; % J/molK
Mbar = 18; % H2O
T0 = 4000; %K, combustion temp of H2 and O2
%Pe = 14*10^3; % about 2 psi
%P0 = 2*10^6; % about 300 psi
g0 = 9.81; % m/s^2
R2 = 461.5; % J/kgK
hold off
P_ratio = (10^-6):0.000001:(10^-1); %Pe/P0
for i=1:length(P_ratio)
    ve(i) = sqrt((2*gamma/(gamma-1))*(R1*T0/Mbar)*(1-((P_ratio(i))^((gamma-1)/gamma)))); %m/s
    Isp(i) = ve(i)/g0;
    Te(i) = ((P_ratio(i))^((gamma-1)/gamma))*T0;
    Me(i) = ve(i)/sqrt(gamma*R2*Te(i));
end

figure(1)
plot(P_ratio,ve,'r')
title('Pe/P0 vs Exit Velocity')
xlabel('Pe/P0')
ylabel('Exit Velocity (m/s)')

figure(2)
plot(P_ratio,Isp,'k')
hold on
refline(0,300)
refline(0,350)
refline(0,400)
hold off
title('Pe/P0 vs Isp')
xlabel('Pe/P0')
ylabel('Isp (s)')
legend('Pe/P0 vs. Isp','Varying Isp Values','Location','NorthEast')

figure(3)
plot(P_ratio,Te,'r')
xlabel('Pe/P0')
ylabel('Exit Temperature (K)')
title('Pe/P0 vs Exit Temp')

figure(4)
plot(P_ratio,Me,'r')
xlabel('Pe/P0')
ylabel('Exit Mach Number')
title('Pe/P0 vs Exit Mach Number')

```

11.2.15. Mass Ratio Analysis for EML1 Depot

April Claus

```
%% Mass Ratio Analysis for EML1 Depot
clear all;
clc;

dVmax = 150; %m/s/year %max possible
g0 = 9.81; % m/s
m_depot = 340*10^3; % kg
% say that you run it constantly for the year
% instantaneous acceleration at any given time:
inst_accel = dVmax/((1*365*24*60*60)*(24/365)) % m/s^2, divide by number of seconds in year
F = m_depot*inst_accel % thrust, N

Isp = 250:0.1:450; %s
F2 = 25.5;
% ratio of propellant required with dVmax for range of Isp
for i=1:length(Isp)
    m_ratio(i) = exp(dVmax/(Isp(i)*g0));
    mdot(i) = (F2/(Isp(i)*g0))*1000; % g/s
end
% m_ratio = mprop-initial/ mfinal
% larger m_ratio means minitial is much bigger than mfinal
% more propellant is used
% want a small m_ratio
```

```
Figure(1)
plot(Isp,m_ratio,'r')
xlabel('Isp (s)','FontSize',16)
ylabel('Initial Mass/Final Mass ratio','FontSize',16)
title('Isp vs (Mi/Mf), EML1 Fuel Depot','FontSize',16)
```

```
Figure(2)
plot(Isp,mdot,'b')
xlabel('Isp (s)')
ylabel('Mass Flow Rate (g/s)','FontSize',16)
title('Isp vs. Mass Flow Rate','FontSize',16)
```

RCS nozzle sizing

```
clear all;
clc;

gamma = 1.33;

Mt = 1; % choked flow
Me = 1:0.01:6;
for k=1:length(Me)
    num(k) = 1 + (((gamma-1)/2)*(Me(k)^2));
    denom = 1 + (((gamma-1)/2)*(Mt^2));
    exp = (gamma+1)/(2*(gamma-1));
    A_ratio(k) = (Mt/Me(k))*((num(k)/denom)^exp);
end
figure
```

```

plot(Me,A_ratio)
xlabel('Me')
ylabel('Area ratio (Ae/At)')
title('Exit Mach Number vs Area Ratio')

```

11.2.16. EML1 Power Requirements

April Claus

```
%% EML1 Power Requirements
```

```

clear all;
rhoF = 71; % kg/m^3, LH2
rhoO = 1141; % kg/m^3, LOx

VtankF = 400; % m^3, rounded up, tank for LH2
mtankF_full = 30; % t, this would vary
% assuming max mass for this analysis

TtankF = 20; %K
TtankO = 90; %K

RF = 4124; %J/kgK
RO = 259.8; %J/kgK

Vtank0 = 240; % m^3

% 13 atm and 50 atm are the critical pressures for O2 and H2, vapor dome
p1F = 1*10^6; % Pa, 13 atm, slightly less to stay under vapor dome
p1O = 4.7*10^6; % Pa, 50 atm, slightly less to stay under vapor dome

n_pumpF = 0.8;
n_pumpO = 0.8;

% combustion chamber pressures (H2 and O2 go to same chamber)
p2 = 15*10^6; %Pa same as P0 above

% flow through pipes to combustion chamber
mdot = 0:0.00001:.01; %kg/s

% going from tank to combustion chamber
for m=1:length(mdot)
    PpumpF(m) = ((mdot(m)*(1/6.85))*(p2 - p1F)/(rhoF*n_pumpF));
    PpumpO(m) = ((mdot(m)*(5.85/6.85))*(p2 - p1O)/(rhoO*n_pumpO));
    Tot_power(m) = PpumpF(m)+PpumpO(m);
end
figure
plot(mdot*1000,PpumpF,'r')
hold on
plot(mdot*1000,PpumpO,'b')

```

```

plot(mdot*1000,Tot_power,'k')
title('Mdot vs. Pump Power','fontsize',16)
xlabel('Mdot (g/s)','fontsize',16)
ylabel('Power Required for Pump (W)','fontsize',16)
legend('Fuel Pump','Oxygen Pump','Total Pump Power','Location','NorthWest')

```

11.2.17. Propellant Required (CTV back to LEO with SLS Upper Stage)

April Claus

```

%% Propellant required: CTV back to LEO with SLS upper stage ***
% THIS IS WHERE I GOT THE 21.5 MT LIMIT FROM (but doesn't matter anymore)
% THIS IS WHERE I GOT 35 MT FROM LMO to L1 FOR THE CTV
clear all;
clc;

m_CTV = 29; %t, 29 max, includes structural and payload
mS_D = 4.2; % t
mprop_D = 1.85; %MT, RCS propellant, increased value from 1.290

Isp = 460; % SLS upper stage
g0 = 9.81;
mprop_start1 = 0:0.1:120; % MT

dV_LMOtoL1 = 3.2; % km/s, LMO to L1
dV_L1toLEO = 3.94; % km/s, max dV
dV_LEOtoLMO = 6.67; % km/s, dV1_abs + dV2_abs

mPL = m_CTV + mS_D + mprop_D; % set mPL, max it would ever be

for i = 1:length(mprop_start1)

    % LMO TO L1
    % prop it takes to get from LMO to L1
    % mCTV = 29 MT
    mprop_left1(i) = ((exp(-dV_LMOtoL1/(Isp*g0*0.001))))*(mprop_start1(i) + mS + mPL)-mS-mPL;

end

figure(1)
plot(mprop_start1,mprop_left1,'r')
% hold on
% plot(mprop_start1,mprop_left2,'g')
% plot(mprop_start1,mprop_left5,'k')
refline(0,0)
% hold off
title('Mass of Prop LEFT vs. Mass of Starting Prop, CTV','fontsize',14)
xlabel('Mass of Starting Propellant (t)','fontsize',14)
ylabel('Mass of Propellant Left in Tank (t)','fontsize',14)

```

```
% legend('LMO - L1','L1-LEO','LEO-L1','Location','NorthWest')
legend('LMO - L1','Location','NorthWest')
```

11.2.18. LMO Propellant Required

April Claus

```
%% LMO prop required
clear all;
clc;

dVmax = 0.15; % km/s, both x and y axis control, yearly cost
dVmin = 0.01;
Isp = 350;
mS = 6.3;
g0 = 9.81;

mprop_start1 = 0:0.01:6; %MT
mPL = 120-mprop_start1; % full tanks

for n = 1:length(mprop_start1)
    mprop_left_min(n) = ((exp(-dVmin/(Isp*g0*0.001))))*(mprop_start1(n) + mS + mPL(n))-mS - mPL(n);
    mprop_left_max(n) = ((exp(-dVmax/(Isp*g0*0.001))))*(mprop_start1(n) + mS + mPL(n))-mS - mPL(n);
end

figure
plot(mprop_start1,mprop_left_min,'r')
hold on
plot(mprop_start1,mprop_left_max,'k')
refline(0,0)
hold off
title('Starting RCS Propellant Mass vs Remaining Propellant Mass, LMO','FontSize',13')
xlabel('Start RCS Prop Mass (t)','FontSize',16)
ylabel('Remaining RCS Prop Mass (t)','FontSize',16)
legend('Min Delta V','Max Delta V','Location','NorthWest')
```

Extra LMO Depot Calculations

```
dVmax = 150; %m/s/year %max possible
g0 = 9.81; % m/s
m_depot = 126.3*10^3; % kg
% say that you run it constantly for the year
% instantaneous acceleration at any given time:
inst_accel = dVmax/((1*365*24*60*60)*(24/365)) % m/s^2, divide by number of seconds in year
% 6% duty cycle
F = m_depot*inst_accel % thrust, N

Isp = 350; %s
F2 = F/cosd(15); % accounting for thrust loss due to angled nozzle
```

```

mdot = (F2/(Isp*g0)) % kg/s

p1F = 1*10^6; % Pa, 13 atm, slightly less to stay under vapor dome
p1O = 4.7*10^6; % Pa, 50 atm, slightly less to stay under vapor dome

n_pumpF = 0.8;
n_pumpO = 0.8;
rhoF = 71; % kg/m^3, LH2
rhoO = 1141;
% combustion chamber pressures (H2 and O2 go to same chamber)
p2 = 15*10^6; %Pa same as P0 above

PpumpF = ((mdot*(1/6.85))*(p2 - p1F)/(rhoF*n_pumpF))
PpumpO = ((mdot*(5.85/6.85))*(p2 - p1O)/(rhoO*n_pumpO))
Tot_power = PpumpF+PpumpO

```

11.3. Phase III: Habitat Transport

11.3.1.Parachute Sizing for EDL

Lemuel Carpenter

%Parachute Study to Determine Sizing

```

clear all
close all

%% 20,000kg
figure
m=20000; % kg
g=3.711; % m/s^2
rho=0.01; % kg/m^3
Cd=1.2;
syms v

D=sqrt((8*m*g)/(pi*rho*Cd*(v^2)));
ezplot(D,[100,800])
setcurve('color','red','linewidth',1.5)
hold on
grid on

% Cd=0.55;
% D=sqrt((8*m*g)/(pi*rho*Cd*(v^2)));
% ezplot(D,[100,800])
% setcurve('color','blue','linewidth',1.5)
% hold on

% Three Chutes

m=20000; % kg

```

```

g=3.711; % m/s^2
rho=0.01; % kg/m^3
Cd=1.2;
syms v

D=sqrt((8*m*g)/(pi*rho*Cd*(v^2)));
Ar=pi*(D/2)^2;
Tre=(2*sqrt((Ar/3)/pi));

ezplot(Tre,[100,800])
setcurve('color','red','linestyle','--','linewidth',1.5)
hold on
grid on

set(gca,'fontsize', 30);
legend({'One Chute','Three Chutes'},'FontSize',30)
set(gca,'fontsize', 30);
% One Chute

Cd=0.7;
D=sqrt((8*m*g)/(pi*rho*Cd*(v^2)));
ezplot(D,[100,800])
setcurve('color','blue','linewidth',1.5)

title('20,000kg Entry Vehicle')
xlabel('Velocity (m/s)')
ylabel('Parachute Diameter (m)')
set(gca,'fontsize', 16);

% three chutes

% Cd=0.55;
% D=sqrt((8*m*g)/(pi*rho*Cd*(v^2)));
% Ar=pi*(D/2)^2;
% Tre=(2*sqrt((Ar/3)/pi));
% ezplot(Tre,[100,800])
% setcurve('color','blue','linestyle','--','linewidth',1.5)
% hold on

Cd=0.7;
D=sqrt((8*m*g)/(pi*rho*Cd*(v^2)));
Ar=pi*(D/2)^2;
Tre=(2*sqrt((Ar/3)/pi));
ezplot(Tre,[100,800])
setcurve('color','blue','linestyle','--','linewidth',1.5)

title('20,000kg Entry Vehicle')
xlabel('Terminal Velocity (m/s)')
ylabel('Parachute Diameter (m)')
set(gca,'fontsize', 30);
legend({'Cd=1.2','Cd=0.7'},'FontSize',15)

```

```

%% 10,000kg
figure
% single chute
m=10000; % kg
g=3.711; % m/s^2
rho=0.01; % kg/m^3
Cd=1.2;
syms v

D=sqrt((8*m*g)/(pi*rho*Cd*(v^2)));
ezplot(D,[100,800])
setcurve('color','red','linewidth',1.5)

hold on
grid on

% Cd=0.55;
% D=sqrt((8*m*g)/(pi*rho*Cd*(v^2)));
% ezplot(D,[100,800])
% setcurve('color','blue','linewidth',1.5)
%
% hold on

Cd=0.7;
D=sqrt((8*m*g)/(pi*rho*Cd*(v^2)));
ezplot(D,[100,800])
setcurve('color','blue','linewidth',1.5)

title('10,000kg Entry Vehicle')
xlabel('Velocity (m/s)')
ylabel('Parachute Diameter (m)')
set(gca,'fontsize', 16);

% three chutes
m=10000; % kg
g=3.711; % m/s^2
rho=0.01; % kg/m^3
Cd=1.2;
syms v

D=sqrt((8*m*g)/(pi*rho*Cd*(v^2)));
Ar=pi*(D/2)^2;
Tre=(2*sqrt((Ar/3)/pi));
ezplot(Tre,[100,800])
setcurve('color','red','linestyle','--','linewidth',1.5)

hold on
grid on

```

```

% Cd=0.55;
% D=sqrt((8*m*g)/(pi*rho*Cd*(v^2)));
% Ar=pi*(D/2)^2;
% Tre=(2*sqrt((Ar/3)/pi));
% ezplot(Tre,[100,800])
% setcurve('color','blue','linestyle','--','linewidth',1.5)
%
% hold on

Cd=0.7;
D=sqrt((8*m*g)/(pi*rho*Cd*(v^2)));
Ar=pi*(D/2)^2;
Tre=(2*sqrt((Ar/3)/pi));
ezplot(Tre,[100,800])
setcurve('color','blue','linestyle','--','linewidth',1.5)

title('10,000kg Entry Vehicle')
xlabel('Terminal Velocity (m/s)')
ylabel('Parachute Diameter (m)')
set(gca,'fontsize', 30);
% legend({'Cd=1.2','Cd=0.7'},'FontSize',15)

```

11.4. Phase IV: Crew Transport

11.4.1. Inflatables Optimization – Falcon Heavy

Jaclyn Rupert (Code #1)

```

%Falcon – Inflatables Optimization
clear all
close all
clc

%Set Values
LD=4.6; %Launch Diameter Falcon 4.6
%%%%%%%%%%
AD=1.255; %Airlock/ center cylinder diameter %%%%%%%%%%

n=0; nn=0;

for ii=2:1:6.6
nn=1+nn; %47
L=ii; %Length of module
%%%%%%%%%%
Length(nn)=(ii);

for i=1.2:.05:2
n=1+n;
RatioD=i; %Launch diameter to inflated diameter ratio 1.26, 1.91
Ratio(n)=i;

```

InflD=LD*RatioD; %Inflated diameter

St=.4; %Shell material thickness
%%%%%%%%%%
WWt=.1; %water wall thickness
%%%%%%%%%%
St_total=St+WWt; %Total shell thickness

L2=L-(2*St_total); %Interior Length (taking into account shell thickness)

HD=InflD-(2*St_total); %habitable diameter

if HD>2.5,
HD_array(n)=HD;
else
HD_array(n)=0;
end

MV(n)=3.14159*L*(InflD/2)^2; %total module volume
HV(n)=(3.14159*L2*(HD/2)^2); %Habitable volume

if HV(n)>110,
HV_array(n)=HV(n);
else
HV_array(n)=0;
end

HVC(n)=(3.14159*L2*(HD/2)^2)-(3.14159*L2*(AD/2)^2); %Habitable volume
%(w/ cylinder structure)

if HVC(n)>110,
HVC_array(n)=HVC(n);
else
HVC_array(n)=0;
end

SV(n)=MV(n)-HV(n); %Shell volume
SVC(n)=(MV(n)-HV(n))-(2*(3.14159*St_total*(AD/2)^2)); %Shell volume
%w/ cylinder vol taken out

%COMPARED TO HARD STRUCTURE:
HSV(n)=3.14159*(L-WWt)*((LD-(WWt*2))/2)^2; %habitable hard structure
%(metal) volume

Cyl_vol(n)=3.14159*L*(AD/2)^2; %(cyl vol- how tightly we can pack fairing)
PDC(n)=2*(sqrt((SVC(n)+Cyl_vol(n))/(3.14159*L))); %outer packed diam ...
%w/ cylinder structure

if PDC(n)<4.6,
PDC_array(n)=PDC(n);
else
PDC_array(n)=0;
end

PD(n)=2*(sqrt(SVC(n)/(3.14159*L))); %outer packed diameter w/ no cyl

```

if PD(n)<4.6,
PD_array(n)=PD(n);
else
  PD_array(n)=0;
end

end

end

%length array
xx=-16; yy=0; zz=1.9;
for j=1:1:47
xx=xx+17; yy=yy+17; zz=zz+.1;
length_array(xx:yy)=zz;
end

Array=[length_array; Ratio; HD_array; PD_array; PDC_array; ...
  HV_array; HVC_array];

disp('Falcon Fairing')
disp(' ')
Launch_Diameter=LD
Total_Shell_thickness=St_total
disp(' ')
disp('Column1-Length (2-6.6)')
disp('Column2-Ratio (1.2-2)')
disp('Column3-Habitable Diam (>2.5)')
disp('Column4-Packed Diam w/ no interior structure (<4.6)')
disp('Column5-Packed Diam (w/ Cyl in the middle (<4.6)')
disp('Column6-Habitable Vol (110-120)')
disp('Column7-Habitable Vol (w/ cyclinder in the middle (110-120)')
disp(' ')

for q=1:1:799

  if (Array(3,q) & Array(4,q) & Array(5,q) & ...
    Array(6,q) & Array(7,q) ~=0 ...
    & (Array(6,q) < 120)...
    & (Array(7,q) < 120)...
    & (Array(1,q) < 6.1))

    disp(Array(:,q))
  end
end
end

```

11.4.2. CTV Required Habitable Volume Curves

Jaclyn Rupert (Code #4)

```

clear all
close all

```

```

clc

%%CTV Crew of 4
x=0;
for i=1:1:400
x=x+1;
NASA_Curve(x)=4*(4.8827*log(x)-3.9113);
Celentano(x)=4*(20*(1-exp(-x/20)));
Historical_data(x)=4*(62*(1-exp(-x/35)));
Small_Hab_Historical(x)=4*(20*(1-exp(-x/8)));
end
t=[1:1:400];

plot(t, NASA_Curve)
hold on
plot(t, Celentano)
hold on
plot(t, Historical_data)
hold on
plot(t, Small_Hab_Historical)
axis([0 400 0 260])
xlabel('Mission Duration (days)','fontsize',14)
ylabel('Habitable Volume (m^3)','fontsize',14)
title('CTV Habitable Volume (4-Person Crew)','fontsize',14)
legend('NASA 2011 HVW', 'Celentano Curve', 'NASA Historical Data','Small Hab Historical','Location','southeast')

%%
%Habitable vol per crew of 4
days=360

NASA_Curve_4=(4.8827*log(days)-3.9113)*4
Celentano_4=(20*(1-exp(-days/20)))*4
Historical_data_4=62*(1-exp(-days/35))*4
Small_Hab_Historical_4=4*(20*(1-exp(-days/8)))

```

11.4.3. Atmospheric Composition Trade Study

William Bentz

```

% Title: "Atmospheric Composition Trade Study"
% This study was used to determine the composition of the atmospheres across % all of the vehicles by analyzing
the pre-breathe times.
clear
count=1;
for m=20:25;
pO2=m;
Percent_N2=[0:1:80];
Percent_O2=100-Percent_N2;
P_cabin=100.*pO2./Percent_O2;
p_N2=P_cabin.*(Percent_N2/100);
k=log(2)/240; %Assuming 240 minute tissue model
R=1.6; %"Generally safe" ENAE483 Presentation on Space Physiology
suitpress=29.6; %Iss suit pressure

```

```

Pdesired=R*suitpress;
[min_difference, array_position] = min(abs(p_N2-Pdesired));
Time_breathe(1:array_position)=0;
syms t;
for j=array_position+1:801;
Time_breathe(count,j)=real(solve(Pdesired==p_N2(j)*exp(-k*t)));
end;
count=count+1;
end;
plot(Percent_O2,Time_breathe(1,:))
hold all
plot(Percent_O2,Time_breathe(2,:),'--')
plot(Percent_O2,Time_breathe(3,:),'-')
plot(Percent_O2,Time_breathe(4,:),':')
plot(Percent_O2,Time_breathe(5,:),'c')
plot(Percent_O2,Time_breathe(6,:),'LineWidth',5)
xlabel('Percent O2')
ylabel('Prebreathe Time (min)')
legend('20 kPa O2','21 kPa O2', '22 kPa O2', '23 kPa O2', '24 kPa O2', '25 kPa O2')
title('Prebreathe Time Vs. Percent O2 for Various O2 pp')
hold off;

```

11.4.4. Mars Surface EVA Allocations as Determined by CTV Water Wall Thickness

William Bentz

```

% Title: "Mars Surface EVA Allocations as Determined by CTV Water Wall
% Thickness"
% This study was used to determine the necessary thickness of the CTV's
% waterwall to shield from GCR's.

```

```

male_limit=100; %Rem for 35 yr old
female_limit=60; %Rem for 35 yr old
water_thickness=[0:.01:10].*(10^-2);
water_mass=1000*2.5*pi*((3.5+water_thickness).^2-3.5.^2)
water_thicknesscm=water_thickness*100;
Decay_rate=17*exp(water_thickness*(-39.1202))+53; %Exponential fit of end points of the Cucinotta plot

```

```

for (count=1:length(water_thickness));
NoEVA_Exposure=Decay_rate(count)+.02*13*13; %Assuming 13 REM per year (10 in deep portions and 15 near
three craters)
syms x;
Male_Weeklyhours(count)=(male_limit-NoEVA_Exposure)*8760/(13*13*52);
Female_Weeklyhours(count)=(female_limit-NoEVA_Exposure)*8760/(13*13*52);
end
plot(water_thicknesscm, Male_Weeklyhours)
hold all
plot(water_thicknesscm, Female_Weeklyhours)

```

```

male_limit=150; %Rem for 45 yr old
female_limit=90; %Rem for 45 yr old
water_thickness=[0:.01:10].*(10^-2);

```

```
Decay_rate=17*exp(water_thickness*(-39.1202))+53; %Exponential fit of end points of the Cucinotta plot
```

```
for (count=1:length(water_thickness));  
NoEVA_Exposure=Decay_rate(count)+.02*13*13; %Assuming 13 REM per year (10 in deep portions and 15 near  
three craters)  
syms x;  
Male_Weeklyhours(count)=(male_limit-NoEVA_Exposure)*8760/(13*13*52);  
Female_Weeklyhours(count)=(female_limit-NoEVA_Exposure)*8760/(13*13*52);  
end  
plot(water_thicknesscm, Male_Weeklyhours)  
hold all  
plot(water_thicknesscm, Female_Weeklyhours)
```

```
male_limit=300; %Rem for 55 yr old  
female_limit=170; %Rem for 55 yr old
```

```
Decay_rate=17*exp(water_thickness*(-39.1202))+53; %Exponential fit of end points of the Cucinotta plot
```

```
for (count=1:length(water_thickness));  
NoEVA_Exposure=Decay_rate(count)+.02*13*13; %Assuming 13 REM per year (10 in deep portions and 15 near  
three craters)  
syms x;  
Male_Weeklyhours(count)=(male_limit-NoEVA_Exposure)*8760/(13*13*52);  
Female_Weeklyhours(count)=(female_limit-NoEVA_Exposure)*8760/(13*13*52);  
end  
plot(water_thicknesscm, Male_Weeklyhours)  
hold all  
plot(water_thicknesscm, Female_Weeklyhours)  
xlabel('Transfer vehicle water wall thickness (cm)')  
ylabel('Allowable EVA hours per week')  
legend('male-35 yr', 'female-35 yr', 'male-45 yr', 'female-45 yr', 'male-55 yr', 'female-55 yr')  
title('Nominal Crew EVA Hours/Week')  
hold off;
```

```
%construction crew  
male_limit=100; %Rem for 35 yr old  
water_thickness=[0:.01:10].*(10^-2);  
Decay_rate=17*exp(water_thickness*(-39.1202))+53; %Exponential fit of end points of the Cucinotta plot
```

```
for (count=1:length(water_thickness));  
NoEVA_Exposure=Decay_rate(count)+.02*13*11; %Assuming 13 REM per year (10 in deep portions and 15 near  
three craters)  
syms x;  
Male_Weeklyhours(count)=(male_limit-NoEVA_Exposure-(13*2))*8760/(11*13*52);  
end  
figure  
plot(water_thicknesscm, Male_Weeklyhours)  
hold all
```

```
male_limit=150; %Rem for 45 yr old  
water_thickness=[0:.01:10].*(10^-2);  
Decay_rate=17*exp(water_thickness*(-39.1202))+53; %Exponential fit of end points of the Cucinotta plot
```

```

for (count=1:length(water_thickness));
NoEVA_Exposure=Decay_rate(count)+.02*13*11; %Assuming 13 REM per year (10 in deep portions and 15 near
three craters)
syms x;
Male_Weeklyhours(count)=(male_limit-NoEVA_Exposure-(13*2))*8760/(11*13*52);
end
plot(water_thicknesscm, Male_Weeklyhours)

male_limit=300; %Rem for 55 yr old
water_thickness=[0:.01:10].*(10^-2);
Decay_rate=17*exp(water_thickness*(-39.1202))+53; %Exponential fit of end points of the Cucinotta plot

for (count=1:length(water_thickness));
NoEVA_Exposure=Decay_rate(count)+.02*13*11; %Assuming 13 REM per year (10 in deep portions and 15 near
three craters)
syms x;
Male_Weeklyhours(count)=(male_limit-NoEVA_Exposure-(13*2))*8760/(11*13*52);
end
plot(water_thicknesscm, Male_Weeklyhours)
xlabel('Transfer vehicle water wall thickness (cm)')
ylabel('Allowable EVA hours per week')
title('Construction Crew EVA Hours/Week After Garage Completion')
legend('male-35 yr', 'male-45 yr', 'male-55 yr')
hold off;

```

11.4.5. Reliability Analysis on UPA and WPA Components

William Bentz

```

% Title: "Reliability Analysis on Urine Processor and Water Processor
%Assembly Components"
%This short calculation predicts the reliability of the UPA and WPA units.

```

```

Quantity_Array=[2,3,2,2,14,2,2,3,2,8,2,4,4,6,2,2,3,3,2,3,2,3,3,3];
MTBF=[142525.2,27331.2,90140.4,181507.2,199640.4,384651.6,184222.8,25579.2,84008.4,296701.2,143488.8,29
6701.2,296701.2,717356.4,137181.6,87950.4,42398.4,56677.2,143664,359072.4,226884,53611.2,64561.2,44676];
Quantity_Array=Quantity_Array;
for j=1:24
R(j)=exp(-8640/MTBF(j));
R_mults(j)=(1-(1-R(j))^Quantity_Array(j));
end;
R_sys=prod(R_mults)

```

11.4.6. MLI Thermal Conductivity

Adam Buckingham (“MLI_thermal_conductivity”)

```

T_hot = 293*1.8; %conversion to Rankine from Kelvin
T_cold = 4*1.8;

```

$k_{therm} = (1.027 \cdot 10^{-7} \cdot ((T_{hot} - T_{cold})/2) + 3.333 \cdot 10^{-16} \cdot ((T_{hot}^{4.67} - T_{cold}^{4.67}) / (T_{hot} - T_{cold}))) \cdot 625 \cdot 1.73$ %from Akin's slides the 1.73 is a conversion from BTU/hrftR to W/mK

11.4.7.RCS Actual Propellant

Adam Buckingham ("RCS_actual")

%% Actual RCS Prop

Izz = 1388000; %[kg m^2] Mass moment of inertia in z-direction for Space Train
Iyy = 1365000; %[kg m^2] Mass moment of inertia in y-direction for Space Train

Max_phase = pi/2; % [rad] Max phase change for CTV (180 degrees)
t = [40:1:100]; % [sec] amount of time to make phase change

Ae = 0.002; %[m^2]

Ve_O2 = 644; %[m/s]
Ve_H2 = 2565; %[m/s]
Ve_Comb = 2820; %[m/s]
Rat_LH2 = (1/6.5);
Rat_LOX = 5.5/6.5;
syms m;

Pcham = 2.07; %[MPa]
Pcham_LOX = Pcham * Rat_LOX;
Pcham_LH2 = Pcham * Rat_LH2;

Pint_LH2 = 0.10135;
Pint_LOX = 1.5;

Pump_eff = 0.7;
den_LOX = 1141;
den_LH2 = 71;

Hvap_H2 = 461; %[kJ/kg]
Hvap_O2 = 214;

for i = 1:length(t)
TorqueZ(i) = 2 * Max_phase * Izz / (t(i)^2);
TorqueY(i) = 2 * Max_phase * Iyy / (t(i)^2);

%Since Torque in the Z-direction is larger then I will design towards that

TorqueDrag = 400 * 2 * 1.8; %Torque applied from the Dragon's RCS system

TorqueRCS(i) = TorqueZ(i) - TorqueDrag;
RCS_dist = 3.2725;
Thrust_RCS(i) = TorqueRCS(i) / (2 * RCS_dist);
Thrust_RCSwo(i) = TorqueZ(i) / (2 * RCS_dist);

```
%%%%%% Analyzing Power Requirements
```

```
mdot_O2(i) = double(solve(Thrust_RCS(i)==m*Ve_O2 + 13790*Ae,m));  
mdot_H2(i) = double(solve(Thrust_RCS(i)==m*Ve_H2 + 13790*Ae,m));  
mdot_Comb(i) = double(solve(Thrust_RCS(i)==m*Ve_Comb + 13790*Ae,m));
```

```
mdot_LH2(i) = mdot_Comb(i)*Rat_LH2;  
mdot_LOX(i) = mdot_Comb(i)*Rat_LOX;
```

```
Power_LOX(i) = mdot_LOX(i)*((Pcham_LOX-Pint_LOX)*10^6)/(den_LOX*Pump_eff);  
Power_LH2(i) = mdot_LH2(i)*((Pcham_LH2-Pint_LH2)*10^6)/(den_LH2*Pump_eff);
```

```
Power_Comb(i) = Power_LOX(i)+Power_LH2(i);
```

```
end  
figure(1)  
plot(t*2,Thrust_RCS,'r')  
xlabel('Maneuver Time (sec)')  
ylabel('Thrust Required (N)')  
title('Thrust needed vs Maneuver Time (with Dragon)')  
hold on  
refline(0,70)  
  
figure(2)  
plot(t*2,Thrust_RCSwo,'r')  
xlabel('Maneuver Time (sec)')  
ylabel('Thrust Required (N)')  
title('Thrust needed vs Maneuver Time (without Dragon)')  
hold on  
refline(0,70)
```

11.4.8. Thermal Analysis of Spacecraft to Mars

Scott Kindl (“SC_thermal”)

```
%% Thermal Analysis of Spacecraft to Mars  
% ALL CREDIT FOR CODE GOES TO SCOTT KINDL  
r = 1:.01:1.5;  
Is = 1394./r.^2;  
sigma = 5.67e-8;  
  
%% MLI characteristics  
a = 0.0037;  
e_eff = 0.02;  
%% Area illuminated of spacecraft (assuming cylindrical spacecraft)  
l = 5.6;  
d = 6.67;  
  
angle = 0:90;  
%A_illum = l*d*sind(angle) + 0.25*pi*d^2*cosd(angle);
```

```

A_illum = 1*d+pi*(d/2)^2;
Q_solar = zeros(length(r),length(angle));

for i = 1:length(r)
    Q_solar_alum(i,:) = Is(i)*A_illum*.65;
    Q_solar(i,:) = Q_solar_alum(i,:)*a;
end

%% Heat out from Spacecraft
A_sc = 0.5*4*pi*(d/2)^2+2*pi*(d/2)*1;
%Q_esc = A_sc*sigma*e_eff*293^4;
Q_esc = 200;
%% Internal power used in spacecraft
Q_int = 11000;

%% Radiated power
T_rad = 323;
e = 0.85;
A_rad = zeros(length(r),length(angle));
for i = 1:length(r)
    A_rad(i,:) = (Q_solar(i,:) + Q_int - Q_esc)/(e*sigma*T_rad^4);
end
plot(r,A_rad);
set(gca,'fontsize',15)
% scatter3(r(1),A_illum(1),A_rad(1,1),5)
% hold on
% for i = 1:length(r)
%     for j = 1:5:length(A_illum)
%         scatter3(r(i),A_illum(j),A_rad(i,j),10,'b')
%     end
% end
xlabel('Distance from Sun (AU)')
% ylabel('Illuminated Area (m^2)')
ylabel('Radiator Area (m^2)')
title('Radiator Area vs. Spacecraft Position')
% hold off

```

11.4.9. SpaceTrain (On SLS, Launch from LEO-L1 (refuel) - LMO)

April Claus

```

%%SpaceTrain: on SLS, launch from LEO-L1(refuel)-LMO
clear all;
clc;

g0 = 9.81;

%Crew Transport Vehicle
mCTV = 0:0.1:50; % max 29 t

%Dragon

```

```

mprop_D = 1.85;
mS_D = 4.2;
mD = mprop_D + mS_D;
% SLS Block 1B Upper Stage
mS_SLS = 4;
mprop_start_SLS = 129;
Isp_SLS = 460;
dVLEOtoL1_min_ed = 3.94;
dVL1toLMO = 3.23;
dVLEOtoLMO = 6.67;

for i = 1:length(mCTV)
mPL(i) = mCTV(i) + mD;
% WITH REFUEL
% LEO to L1 (max dV)
% SLS, CTV+D
    mprop_left1(i) = ((exp(-dVLEOtoL1_min_ed/(Isp_SLS*g0*0.001))))*(mprop_start_SLS + mS_SLS + mPL(i))-
mS_SLS - mPL(i);

    % L1 to LMO
    % SLS, CTV+D
    % same starting prop mass (full refuel at L1)
    mprop_left2(i) = ((exp(-dVL1toLMO/(Isp_SLS*g0*0.001))))*(mprop_start_SLS + mS_SLS + mPL(i))- mS_SLS
- mPL(i);

% NO REFUEL
% LEO to LMO
% SLS, CTV+D
    mprop_left3(i) = ((exp(-dVLEOtoLMO/(Isp_SLS*g0*0.001))))*(mprop_start_SLS + mS_SLS + mPL(i))-
mS_SLS - mPL(i);

end

figure(1)
plot(mCTV, mprop_left1,'r')
hold on
plot(mCTV, mprop_left2,'k')
plot(mCTV, mprop_left3,'g')
refline(0,0)
hold off
title('CTV Mass Limitations, Space Train','FontSize',14)
xlabel('CTV Mass (t)','FontSize',14)
ylabel('Propellant Mass Left in SLS Tanks (t)','FontSize',14)
legend('LEO-L1','L1-LMO','LEO-LMO, no refuel','Location','NorthEast')

%%%%%%

mS_D = 4.2; % t
mprop_D2 = 1.850; %t, RCS propellant
%(increased this amount from original 1.290)
mprop_D = 1.290; % original
mPL_D = 0:0.01:2; % t
dV_escL1 = 0.699; % km/s

```

```

Isp = 235; % s, SuperDraco
g0 = 9.81; % m/s^2
% starts with and ends with same payload
% only thing changing is propellant mass

for i = 1:length(mPL_D)
    %original prop mass
    mprop_left(i) = ((exp(-dV_escL1/(Isp*g0*0.001)))*(mprop_D + mS_D + mPL_D(i)))-mS_D-mPL_D(i);

    % slightly increased prop mass
    mprop_left2(i) = ((exp(-dV_escL1/(Isp*g0*0.001)))*(mprop_D2 + mS_D + mPL_D(i)))-mS_D-mPL_D(i);
end

figure
plot(mPL_D, mprop_left,'k')
hold on
plot(mPL_D, mprop_left2,'r')
refline(0,0)
xlabel('Payload Mass in Dragon (t)','FontSize',14)
ylabel('Propellant Left after Burn to Escape EML1 (t)','FontSize',14)
title('Dragon: Payload Mass vs. Propellant Left','FontSize',14)
legend('Original Prop Mass: 1.29 t','Increased Prop Mass: 1.85 t','Location','NorthEast')

```

11.5. Phase V: Mars Habitation

11.5.1. EDL/A with Refueling

Scott Kindl (“EDL/A with Refueling”)

```

%% EDL and Ascent with Refueling
clear all
clc
% First look at the fuel requirements for ascent with people and descent
% with people and cargo and find the limiting case.
Pamb = 636;
g = 9.8;
dVa = sqrt(2*42970/(300+3393))*1000;
dVd = sqrt(42970/(300+3393))*1000;

% Rocket properties
Isp = 465; % s

rho_LOX = 1140;
rho_LH2 = 71;
rho_CO2 = 36.48;

RCS_ratio = 0.1;
%% Ascent with people
% AD #2 (LOX and LH2)
mpl = 7.6*1000; % MT
% Inert mass will give estimate of inert plus tank mass

```

```

m_misc = (2+4+5)*1000; % MT -> 2 is given as a leg estimate

% Solving rocket equation
% First two lines give the final mass
% Third and fourth lines give initial mass
fun = @(x) Isp*g + dVa/log(((0.02*x+mpl+m_misc) +...
    (9.09*(1/7)*(1/rho_LH2)*x)+(12.16*(6/7)*(1/rho_LOX)*x))/...
    (mpl+x+m_misc +...
    (9.09*(1/7)*(1/rho_LH2)*x)+(12.16*(6/7)*(1/rho_LOX)*x)));
m_propAP = fsolve(fun,20000);

m_LOXAP = (6/7)*m_propAP;
V_LOXAP = m_LOXAP/rho_LOX;
m_LH2AP = (1/7)*m_propAP;
V_LH2AP = m_LH2AP/rho_LH2;

m_LOXtank = 12.16*(6/7)*(1/rho_LOX)*m_propAP;
m_LH2tank = 9.09*(1/7)*(1/rho_LH2)*m_propAP;

m_inL = m_misc + m_LH2tank + m_LOXtank;
mtot_AP = mpl+m_propAP+m_inL;

m_RCS_AP = RCS_ratio*mtot_AP;
V_RCS_AP = m_RCS_AP/rho_CO2;
m_RCStank = 12.16*V_RCS_AP;

%% Check miscellaneous masses using MERs
m_fair = 1.8*1000;
m_av = 10*mtot_AP^0.361;
m_wiring = 1.058*sqrt(mtot_AP)*15^0.25;
%Insulation:
r_LH2 = (3*V_LH2AP/4/pi)^(1/3);
A_LH2 = 4*pi*r_LH2^2;
m_LH2ins = 2.88*A_LH2;
r_LOX = (3*V_LOXAP/4/pi)^(1/3);
A_LOX = 4*pi*r_LOX^2;
m_LOXins = 2.88*A_LOX;

Po = 6e6; % Pa -> total pressure in tank
W = mtot_AP*3.711;
T = W*1.1/3; % Thrust required. 1.1 T/W if one engine goes out

M_eng = 4*(7.81e-4*T+3.37e-5*T*sqrt(277)+59);
M_ts = (4*2.55e-4*T);

m_misc_extra = (m_fair+m_av+m_wiring+m_LH2ins+m_LOXins+M_eng+M_ts);
% Amount available to capsule and struts
m_misc_leftover = (m_misc - m_misc_extra)/1000;

%% Descent with people
% AD #2 (LOX and LH2)

```

```

mpl = 7.6*1000; % MT
% Inert mass will give estimate of inert plus tank mass
m_misc = 6*1000; % MT

fun = @(x) Isp*g + dVd/log((0.02*x+mpl+m_misc + ...
    m_LH2tank+m_LOXtank+m_RCStank)/...
    (mpl+x+m_misc + m_LH2tank+m_LOXtank+m_RCStank+m_RCS_AP));
m_propDP = fsolve(fun,20000);

m_LOXDP = (6/7)*m_propDP;
V_LOXDP = m_LOXDP/rho_LOX;
m_LH2DP = (1/7)*m_propDP;
V_LH2DP = m_LH2DP/rho_LH2;

mtot_DP = mpl + m_propDP + m_RCS_AP + m_misc + m_LH2tank+m_LOXtank+m_RCStank;

%% Descent without people
% AD #2 (LOX and LH2)
mpl = 4*1000; % MT
% Inert mass will give estimate of inert plus tank mass
m_misc = 6*1000; % MT

fun = @(x) Isp*g + dVd/log((0.02*x+mpl+m_misc + ...
    (9.09*(1/7)*(1/rho_LH2)*x)+(12.16*(6/7)*(1/rho_LOX)*x))/...
    (mpl+x+m_misc + (9.09*(1/7)*(1/rho_LH2)*x)+...
    (12.16*(6/7)*(1/rho_LOX)*x + 0.1*(0.02*x+mpl+m_misc + ...
    (9.09*(1/7)*(1/rho_LH2)*x)+(12.16*(6/7)*(1/rho_LOX)*x)))));
m_propD = fsolve(fun,20000);

m_LOXD = (6/7)*m_propD;
V_LOXD = m_LOXD/rho_LOX;
m_LH2D = (1/7)*m_propD;
V_LH2D = m_LH2D/rho_LH2;

mtot_L = mpl+m_propD+m_inL;

%% Propulsion Calculations %%
g = 1.26;
Pamb = 636;
To = 3500;
R_uni = 8314.3;
M = 27;
R = R_uni/M;

W = 3.711*mtot_AP;
T = W*1.1/3;

c = Isp*9.8;
mdot = T/c;

Ae = pi*2.25^2/4;
Po = 8e6;

```

```

fun = @(x)[
% Thrust
    c - x(1) - (x(3)-Pamb)*Ae/mdot;
% Area Ratio
    x(2)/Ae - (((g+1)/2)^(1/(g-1)))*((x(3)/Po)^(1/g))*...
    sqrt(((g+1)/(g-1))*(1-((x(3)/Po)^((g-1)/g))));
% Exit Velocity
    x(1)^2 - ((2*g)/(g-1))*To*R*(1-((x(3)/Po)^((g-1)/g)));
x = fsolve(fun, [3000, 0.1, 10000]);
Ve = x(1)
At = x(2)
Pe = x(3)

```

11.5.2. EDL/A without Refueling

Scott Kindl (“EDL/A without Refueling”)

```

%% Calculating propellant masses for LOX/LH2 powered maneuvers
% Mass calculations for ascent and descent without refueling in orbit
clc
clear all
g = 9.8;
R = 8314.3;
dVa = sqrt(2*42970/(300+3393))*1000;
dVd = sqrt(42970/(300+3393))*1000;

rho_LOX = 1140;
M_LOX = 16;
R_LOX = R/M_LOX;

rho_LH2 = 71;
rho_CH4 = 422;

m_misc = (2+4+5)*1000;

Isp = 465;
%% Descent 1: (LOX and LH2)
% First human descent
mpl = 7.6*1000;

fun = @(mpr) Isp*g + dVd/log(...
...% Final Mass
(mpl+m_misc + 9.09*(1/7)*(1/71)*mpr+12.16*(6/7)*(1/1140)*mpr)/...
...% Initial Mass
(mpl+mpr+m_misc + 9.09*(1/7)*(1/71)*mpr+12.16*(6/7)*(1/1140)*mpr));
m_prop1L = fsolve(fun,5000);

%% AD #2 (LOX and LH2)
% Masses for an ascent immediately followed by descent
mpl = 7.6*1000;
fun = @(x) [Isp*g + dVa/log(... % Ascent
... % Final Mass

```

```

(x(1)*x(2)+mpl+m_misc + (9.09*(1/7)*(1/rho_LH2)*x(2))...
+(12.16*(6/7)*(1/rho_LOX)*x(2)))/...
...% Initial Mass
(mpl+x(2)+m_misc + (9.09*(1/7)*(1/rho_LH2)*x(2))...
+(12.16*(6/7)*(1/rho_LOX)*x(2)));
    Isp*g + dVd/log(... % Descent
    ... % Final Mass
(m_misc + (9.09*(1/7)*(1/rho_LH2)*x(2))+...
(12.16*(6/7)*(1/rho_LOX)*x(2)))/...
... % Initial Mass
(x(1)*x(2)+m_misc + (9.09*(1/7)*(1/rho_LH2)*x(2))...
+(12.16*(6/7)*(1/rho_LOX)*x(2)))]);
m_prop2L = fsolve(fun,[.75,70000]);

m_prop = 1.02*m_prop2L(2);
m_LOX = (6/7)*m_prop;
V_LOX = m_LOX/rho_LOX;
m_LH2 = (1/7)*m_prop;
V_LH2 = m_LH2/rho_LH2;

m_LOXtank = 12.16*(6/7)*(1/rho_LOX)*m_prop;
m_LH2tank = 9.09*(1/7)*(1/rho_LH2)*m_prop;
m_inL = m_misc + m_LH2tank + m_LOXtank;
mtot_L = mpl+m_prop+m_inL;

%% Check miscellaneous masses
m_fair = 1.8*1000;
m_av = 10*mtot_L^0.361;
m_wiring = 1.058*sqrt(mtot_L)*20^0.25;
%Insulation:
h_LH2 = V_LH2/pi/2.5^2-4/3;
A_LH2 = 4*pi*2.5^2+2*pi*2.5*h_LH2;
m_LH2ins = 2.88*A_LH2;
h_LOX = V_LOX/pi/2.5^2-4/3*1.25;
A_LOX = 27.13+2*pi*2.5*h_LOX;
m_LOXins = 2.88*A_LOX;

% Propulsion MERs:
Po = 6e6; % Pa
W = mtot_L*3.711;
T = W*1.1/3;

M_eng = 4*(7.81e-4*T+3.37e-5*T*sqrt(277)+59);
M_ts = (4*2.55e-4*T);

m_misc_extra = (m_fair+m_av+m_wiring+m_LH2ins+m_LOXins+M_eng+M_ts+M_gim);
%Amount available to capsule and struts
m_misc_leftover = (m_misc - m_misc_extra)/1000;

%% Descent 1: (LOX and LH2)
mpl = 7.6*1000;

```

```

fun = @(mpr) Isp*g + dVd/log((mpl+m_inL)/(mpl+mpr+m_inL));
m_prop1L = fsolve(fun,5000);

mtot_there = mpl+m_prop1L+m_inL;

```

11.5.3. RCS Thruster Design for EDL/A Vehicle

Scott Kindl (“RCS Thruster”)

```

%% RCS design
clc
clear all

g0 = 9.8;
Pamb = 636;

%% Storage
rhoL = 817.6;
rhoG = 163.4;
m = 5900;
vol = 15.4;

fun = @(V) [rhoL*V(1) + rhoG*V(2) - m;
            V(1) + V(2) - vol];
V = fsolve(fun,[5,10]);
qual = V(2)*rhoG/m;

% CO2 Properties
R_uni = 8314.3;
M = 44;
R = R_uni/M;
gamma = 1.289;

% Rocket Properties
% Total Conditions
To = 288.59; % K
Po = 5.14e6; % Pa

Isp = 67;
c = Isp*g0;

T = 311; % N

% Exit Area
Ae = pi/4*(6*0.0254)^2;
d_exit = sqrt(4*Ae/pi)*100;

% Mass flow rate required
mdot = T/c;

```

```

%% Solve for Exit Pressure and Exhaust Velocity
fun = @(x) [
    % Exit Velocity
    x(1) - sqrt(2*gamma/(gamma-1)*R_uni*To/M*...
    (1-(x(2)/Po)^((gamma-1)/gamma)));
    % Thrust
    x(1)+(x(2)-Pamb)*Ae/mdot-c];

x = fsolve(fun,[500 2000]);
Ve = x(1);
Pe = x(2);

% Area Ratio
AtAe = P2A( Pe/Po, gamma );

% Throat Area
At = AtAe*Ae
d_throat = sqrt(4*At/pi)*100

```

11.5.4. EDL/A Critical Loads and Margin of Safety

Chris Bohlman

MannedEDLCriticalLoads.m

```

h = 13; % radius (m)
R = 6; % radius (m)
t = .025; % thickness (m)
mWet = 59e3; % Wet Mass (kg)
mDry = 20e3; % Dry Mass (kg)
T = 320e3; % Thrust (kN)

E = 68.9e9; % Young's Mod. (Pa)
%sigY = 276e6; % Sigma yield (Pa)
sigU = 386e6; % Sigma Ultimate (Pa)
p = 200e3; % Tank Pressure
v = .33; % Poisson's Ratio

g = 9.81;

% Assuming Launch Loads
gx = 3*9.81; % Longitudinal Acceleratino(g)
gy = 3*9.81; % Lateral Acceleration, y component (g)
gz = 3*9.81; % Lateral Acceleration, z component (g)

% Safety Factors
SF = 1.4; % Using NASA standard factors of safety for structural fuel tanks.

%% Moment of Inertia
I = pi*(R^3)*t; % Moment of Inertia

```

```

%% Pressure Loads
sigHoop = (p*R)/t; % Hoop Stress
sigAx = (p*R)/(2*t); % Axial Stress

%% Buckling
sigCritBuck = (E*t)/(R*sqrt(3*(1-v^2))); % Critical Buckling Stress

%% Acceleration Loads
hCG = h/2; % Assuming Evenly Distributed
gTran = sqrt(gy^2 + gz^2);
M = gTran*(mWet*g);
sigLatAcc = ((M*R)/I);
sigLonAcc = (T/(pi*R^2))*gx;

%% Printing Results
fprintf('Critical Buckling Stress: %3.2f MPa \n',sigCritBuck*10^-6)
fprintf('Hoop Stress: %3.2f MPa \n',sigHoop*10^-6)
fprintf('Axial Stress: %3.2f MPa \n',sigAx*10^-6)
fprintf('Acceleration Lat Stress: %3.2f MPa \n',sigLatAcc*10^-6)
fprintf('Acceleration Lon Stress: %3.2f MPa \n',sigLonAcc*10^-6)

%% Printing MOS
sigDesignHoop = sigHoop*1.4;
sigDesignAx = sigAx*1.4;
sigDesignLatAcc = sigLatAcc*1.4;
sigDesignLonAcc = sigLonAcc*1.4;

sigDesignTot = sigDesignHoop + sigDesignAx + sigDesignLatAcc + sigDesignLonAcc;
fprintf('Total Design Stress: %3.2f MPa \n',sigDesignTot*10^-6)
MOSBuck = sigCritBuck/sigDesignTot - 1;
MOSUlt = sigU/sigDesignTot - 1;
fprintf('MOS Crit Buck: %f \n',MOSBuck)
fprintf('MOS Ultimate: %f \n',MOSUlt)

CargoEDLCriticalLoads.m

clear all; close all; clc;
h = 25; % radius (m)
R = 9; % radius (m)
t = .01; % thickness (m)
mWet = 59e3;
mDry = 20e3;
T = 634e3;

E = 68.9e9; % Young's Mod. (Pa)
%sigY = 276e6; % Sigma yield (Pa)
sigU = 316e6; % Sigma Ultimate (Pa)
p = 0; % Tank Pressure
v = .33; % Poisson's Ratio

g = 9.81; % Martian Gravity

% Assuming Launch Loads

```

```

gx = 6*9.81;
gy = 6*9.81;
gz = 6*9.81;

% Safety Factors
SF = 1.4;

%% Moment of Inertia
I = pi*(R^3)*t;

%% Pressure Loads
sigHoop = (p*R)/t;
sigAx = (p*R)/(2*t);

%% Buckling
sigCritBuck = (E*t)/(R*sqrt(3*(1-v^2)));

%% Acceleration Loads
hCG = h/2; % Assuming Evenly Distributed
gTran = sqrt(gy^2 + gz^2);
M = gTran*(mWet*g);
sigLatAcc = ((M*R)/I)
sigLonAcc = (T/(pi*R^2))*3*9.81;

%% Printing Results
fprintf('Critical Buckling Stress: %3.2f MPa \n',sigCritBuck*10^-6)
fprintf('Hoop Stress: %3.2f MPa \n',sigHoop*10^-6)
fprintf('Axial Stress: %3.2f MPa \n',sigAx*10^-6)
fprintf('Acceleration Lat Stress: %3.2f MPa \n',sigLatAcc*10^-6)
fprintf('Acceleration Lon Stress: %3.2f MPa \n',sigLonAcc*10^-6)

%% Printing MOS
sigDesignHoop = sigHoop*1.4;
sigDesignAx = sigAx*1.4;
sigDesignLatAcc = sigLatAcc*1.4;
sigDesignLonAcc = sigLonAcc*1.4;

sigDesignTot = sigDesignHoop + sigDesignAx + sigDesignLatAcc + sigDesignLonAcc;
fprintf('Total Design Stress: %3.2f MPa \n',sigDesignTot*10^-6)
MOSBuck = sigCritBuck/sigDesignTot - 1;
MOSUlt = sigU/sigDesignTot - 1;
fprintf('MOS Crit Buck: %f \n',MOSBuck)
fprintf('MOS Ultimate: %f \n',MOSUlt)

```

11.5.5.Freon Pump Radiator and Power Sizing

Adam Buckingham (“Material_For_engine”)

```

%% Radiator and Power required for Freon Pump
clear all
sig = 5.67*10^-8;
As = .2;

```

```

den_21 = 1405.5; %[kg/m^3]

%%%%%%%%%%%% Niobium and Magnesium
den_N = 8570; %[kg/m^3] Niobium
den_M = 1740; %[kg/m^3] Magnesium
Tm_M = 923;
Powrad_TN = sig*.39*.2*(2228^4-Tm_M^4);

Arad_TN = Powrad_TN/(sig*.77*(600^4-293^4));
mdot_TN = Powrad_TN/(1000*(.994*40));

Powpump_TN = mdot_TN*(.94-.9)*10^6/(den_21*.7);

mass_TN = den_N*.0025 + den_M*.055 + Arad_TN*2.2; %mass of total system

figure(1)
plot(mass_TN,Arad_TN,'*k')
hold on
figure(2)
plot(mass_TN,Powpump_TN,'*k')
hold on
%%%%%%%%%%%% Niobium and Titanium
den_N = 8570; %[kg/m^3] Niobium
den_t = 4430; %[kg/m^3] Titanium
Tm_M = 1900;
Powrad_Nt = sig*.39*.2*(2228^4-Tm_M^4);

Arad_Nt = Powrad_Nt/(sig*.77*(600^4-293^4));
mdot_Nt = Powrad_Nt/(1000*(.994*40));

Powpump_Nt = mdot_Nt*(.94-.9)*10^6/(den_21*.7);

mass_Nt = den_N*.0025 + den_t*.055 + Arad_Nt*2.2; %mass of total system

figure(1)
plot(mass_Nt,Arad_Nt,'*g')
title('Area of Radiator vs Mass')
xlabel('Mass (kg)')
ylabel('Area of Radiator (m^2)')
legend('Niob and Mag','Niob and Titan')
figure(2)
plot(mass_Nt,Powpump_Nt,'*g')
title('Power vs Mass')
xlabel('Mass (kg)')
ylabel('Coolant Pump Power (W)')
legend('Niob and Mag','Niob and Titan')

“Methane boiloff” (Adam Buckingham)
%% Methane boil off rate
clear all;
hold off;
Tamb = 321; %Ambient Temperature facing the sun
T = 111; %Temperature of the liquid

```

```

T_hot = Tamb*1.8; %conversion to Rankine
T_cold = T*1.8;

km =(1.027*10^-7*((T_hot-T_cold)/2) + 3.333*10^-16*((T_hot^4.67 - T_cold^4.67)/(T_hot-T_cold)))*.625*1.73;
%from Akin's slides the 1.73 is a conversion from BTU/hrftR to W/mK; %average thermal conductivity of
multilayer insolation W/mK
ks = 88; %thermal conductivity of the material holding propellant W/mK
% example ks is for steel
t = [3:.25:8]; %thickness of the multilayer insolation
Vol = 150; %m^3 for 200 metric tons
S = 4*pi*3.3^2; %surface area of inner shell of tank
alpha = .002/100; %ratio of the support junction area and total area: Ss/S
Beta = S/Vol; %Area density of tank : S/V
M_CH4 = 16*10^-3; %kg/mol

dT = Tamb - T;

rho = 422.36; %Density of liquid methane [kg/m^3]
A = -0.018; B= 1.1982; C= -9.8722*10^-3; D= 3.1670*10^-5;
%Coefficients found from tables

syms Ts;
Cpl = (A + B*Ts + C*Ts^2 + D*Ts^3)/(M_CH4*1000); %specific heat capacity for oxygen kJ/kgK
hl = int(Cpl,0,T); %enthalpy of the liquid going from 0K to Temperature of the liquid kJ/kg

Av = 10.312; Tc = 190.58; n = .265;
Hvap = (Av*(1-(T/Tc))^n)/M_CH4; %enthalpy of vaporization kJ/kg
hg = hl + Hvap;

for i = 1:length(t)
    for j= 1:length(alpha)
        boil_off(i,j) = double((dT*(km + ks*alpha(j))*Beta)/(rho*t(i)*0.0254*(hg-hl)*1000))*86400;
    end
end

for i = 1:length(t)
    plot(t,boil_off(:,i)*100)
    hold on
    title('Methane boil-off rate','fontsize',14)
    ylabel('% per day','fontsize',14)
    xlabel('Thickness (inches)','fontsize',14)
    end

“Brayton_Cycle” (Adam Buckingham)
%% Brayton Cycle Methane Combustion
clear all;

mass_CH4 = 800;

```

```

T3 = 2500; %
P2 = 4;
P1 = .1:.01:3;
gam = 1.4;
Cp = 1.003;

Tur_eff=.63;
Com_eff = .9;
g = 1;

Wnetf = 0;
Timef = 0;
Wnet_hourpre = 0;
for i =1:length(P1)
T1(i) = T3/((P2/P1(i))^(1/1.75));
T2(i)= T1(i)*(P2/P1(i))^(.4/1.4);
T4(i) = T3*(P1(i)/P2)^(.4/1.4);

Wt_m(i) = Cp*(T3 - T4(i))*Tur_eff;
Wc_m(i)= Cp*(T1(i) -T2(i))/Com_eff;
Qin_m(i) = Cp*(T3-T2(i));
Qout_m(i) = Cp*(T1(i)-T4(i));

Wnet_m(i) = Wt_m(i) - abs(Wc_m(i));

v1(i) = (259.8)*T1(i)/(P1(i)*10^6); %specific volume!
for q = .001:.001:1
mdot(g) = q/v1(i);
Power_Pump(g) = mdot(i)*((.3-.1)*10^6)/(1141*.7) + (mdot(i)/4)*((.3-.1)*10^6)/(422*.7) + (.503*((.94-.9)*10^6))/(1405.5*.7);
Wnet(g) = mdot(g)*Wnet_m(i)*35 - Power_Pump(g);
Time(g) = mass_CH4/(mdot(g)/5.8)*3600;
Wnet_hour(g) = Wnet(g)*Time(g);

if (g>=2)
if (Wnet(g) <= 40 && Wnet(g) >= 36)
if(Time(g) > Timef)
Wnet_hourpre = Wnet_hour(g);
Wnet_hourf = Wnet_hour(g);
Qout = Qout_m(i)*mdot(g);
Qin = Qin_m(i)*mdot(g);
mdotf = mdot(g);
Wnetf = Wnet(g);
v1f = v1(i);
Timef = Time(g);
qq = q;
Pressure = P1(i);
T1f = T1(i);
T2f = T2(i);
T4f = T4(i);
Qleft= 35*Qin-35*abs(Qout)-Wnetf;
end
end
end
g = g+1;

```

```
end
end
```

“Boil_off_Rate” (Adam Buckingham)

```
%% Oxygen boil off rate
clear all;
```

```
ks = 88; %thermal conductivity of the material holding propellant W/mK
% example ks is for aluminum
t = [5:.25:15]; %thickness of the multilayer insulation
Vol = 150; %m^3 for 200 metric tons
S = 4*pi*3.3^2; %surface area of inner shell of tank
alpha = .003/100; %ratio of the support junction area and total area: Ss/S
Beta = S/Vol; %Area density of tank : S/V
M_O2 = 32*10^-3; %kg/mol
```

```
Tamb = 321; %Ambient Temperature facing the sun
T = 90; %Temperature of the liquid
```

```
T_hot = Tamb*1.8; %conversion to Rankine
T_cold = T*1.8;
```

```
km = (1.027*10^-7*((T_hot-T_cold)/2) + 3.333*10^-16*((T_hot^4.67 - T_cold^4.67)/(T_hot-T_cold)))*.625*1.73;
%from Akin's slides the 1.73 is a conversion from BTU/hrftR to W/mK; %average thermal conductivity of
multilayer insulation W/mK
dT = Tamb - T;
```

```
rho = 1140; %Density of liquid oxygen [kg/m^3]
A = 46.432; B = 3.9506*10^-1; C = -7.0522*10^-3; D = 3.9897*10^-5;
%Coefficients found from tables
```

```
syms Ts;
Cpl = (A + B*Ts + C*Ts^2 + D*Ts^3)/(M_O2*1000); %specific heat capacity for oxygen kJ/kgK
hl = int(Cpl,0,T); %enthalpy of the liquid going from 0K to Temperature of the liquid kJ/kg
```

```
Av = 8.040; Tc = 154.58; n = .201;
Hvap = (Av*(1-(T/Tc))^n)/M_O2; %enthalpy of vaporization kJ/kg
hg = hl + Hvap;
```

```
for i = 1:length(t)
    for j = 1:length(alpha)
        boil_off(i,j) = double((dT*(km + ks*alpha(j))*Beta)/(rho*t(i)*0.0254*(hg-hl)*1000))*86400;
    end
end
figure(1)
for i = 1:length(t)
    plot(t,boil_off(:,i)*100)
hold on
```

```

title('Oxygen boil-off rate','fontsize',14)
ylabel('% per day','fontsize',14)
xlabel('Thickness (inches)','fontsize',14)
end

hold off;

%% Hydrogen Boil-off rate
clear all;

Tamb = 293; %Ambient Temperature facing the sun
T = 20; %Temperature of the liquid
dT = Tamb - T;

T_hot = Tamb*1.8; %conversion to Rankine
T_cold = T*1.8;

km = (1.027*10^-7*((T_hot-T_cold)/2) + 3.333*10^-16*((T_hot^4.67 - T_cold^4.67)/(T_hot-T_cold)))*.625*1.73;
%average thermal conductivity of multilayer insulation W/mK
ks = 88; %thermal conductivity of the material holding propellant W/mK
% example ks is for steel
t = [5:.25:25]; %thickness of the multilayer insulation
Vol = 400; %m^3 for 200 metric tons
S = 4*pi*4.57^2; %surface area of inner shell of tank
alpha = .003/100; %ratio of the support junction area and total area: Ss/S
Beta = S/Vol; %Area density of tank : S/V
M_H2 = 2*10^-3; %kg/mol

rho = 71; %Density of liquid oxygen [kg/m^3]
A = 50.607; B= -6.1136; C= 3.093*10^-1; D= -4.148*10^-3;
%Coefficients found from tables

syms Ts;
Cpl = (A + B*Ts + C*Ts^2 + D*Ts^3)/(M_H2*1000); %specific heat capacity for hydrogen kJ/kgK
hl = int(Cpl,0,T); %enthalpy of the liquid going from 0K to Temperature of the liquid kJ/kg

Av = .659; Tc = 33.18; n = .38;
Hvap = (Av*(1-(T/Tc))^n)/M_H2; %enthalpy of vaporization kJ/kg
hg = hl + Hvap;

for i = 1:length(t)
    for j= 1:length(alpha)
        boil_off(i,j) = double((dT*(km + ks*alpha(j))*Beta)/(rho*t(i)*0.0254*(hg-hl)*1000))*86400;
    end
end
figure(3)
for i = 1:length(t)
    plot(t,boil_off(:,i)*100)
end

```

```

hold on
title('Hydrogen boil-off rate','fontsize',14)
ylabel('% per day','fontsize',14)
xlabel('Thickness (inches)','fontsize',14)
end

```

11.5.6.Habitat Thermal

Scott Kindl

```

%% Heat Transfer
% Calculates heat flow out of the habitat and radiator fluid temperature
clc
clear all
T_env = 297;
% Specific Power Radiator
M = 6; % kg/m2
V = 0.06; % m3/m2
% Methanol
cp_m = 2300;
rho_m = 791;
% Water
cp_w = 4190;
rho_w = 1000;

sigma = 5.67e-8; %W/m2K4
e = 0.9;

h_env = 2.929; % W/m2-K
k_al = 88; %W/m-K

q_int = 232e3;

% Heat loss at lowest environmental temperature
q_reg = 7*0.8*2*0.085*pi*17.4*(295-177)/log(8.75/3.75)+...
        6*0.8*2*0.085*pi*12.1*(295-177)/log(8.75/3.75)+...
        7*0.2*2*0.085*pi*17.4*(295-177)/log(5.75/3.75)+...
        6*pi*3.75^2*0.085*(295-223)/2+...
        6*pi*3.75^2*0.085*(295-177)/5;

%% Radiator Analysis
% Greenhouse
q_g = 210e3/9;
mdot_gm = q_g/cp_m/20;
mdot_gw = mdot_ga*(cp_m/cp_w);
A_g = fsolve(@(A) q_g - A*(sigma*0.9*(323^4-T_env^4))-...
             h_env*A*(323-T_env),100);
M_g = A_g*M;
V_g = A_g*V;

P_g = mdot_gm*(28800)/(0.7*rho_m) + mdot_gw*(28800)/(0.7*rho_w);

% Human
q_h = 22e3/4;

```

```

mdot_hm = q_h/cp_m/20;
mdot_hw = mdot_hm*(cp_m/cp_w);
A_h = fsolve(@(A) q_h - A*(sigma*0.9*(323^4-T_env^4))-...
    h_env*A*(323-T_env),100);
M_h = A_h*M;
V_h = A_h*V;

P_h = mdot_hm*(28800)/(0.7*rho_m) + mdot_hw*(28800)/(0.7*rho_w);

%% Bypass Analysis
dT = 20;
T_set = 283;
F_load = 0.01:0.0005:1;

F_rad = zeros(length(F_load),1);
dT_rad = zeros(length(F_load),1);
T_out = zeros(length(F_load),1);

options.MaxFunEvals = 6000;
options.MaxIter = 400;

T_sink = 177;

C = (log((177-283)*(303+177)/((283+177)*(177-303)))+...
    2*atan(177/283)-2*atan(177/303))/22180932;
for i = 1:length(F_load)
    T_in(i) = T_set + dT*F_load(i);
    fun = @(x) [T_set - (1-x(1))*T_in(i)-x(1)*x(2);
        C/x(1) - (log((T_sink-x(2))*(T_in(i)+T_sink)/...
            ((x(2)+T_sink)*(T_sink-T_in(i)))))...
        +2*atan(T_sink/x(2))-2*atan(T_sink/T_in(i))]/22180932];
    if i == 1
        x = fsolve(fun,[0.01,176],options);
    else
        x = fsolve(fun,[F_rad(i-1),T_out(i-1)],options);
    end
    F_rad(i) = x(1);
    T_out(i) = x(2);
end

% Plot Results
figure(1);
plot(F_load,F_rad,'k');
xlabel('Load Fraction')
ylabel('Radiator Flow Fraction')
figure(2);
hold on
plot(F_load,T_out,'k');
xlabel('Load Fraction')
ylabel('Radiator Outlet Temp, K')
plot([0.01 1],[195 195],'g')
plot([0.01 1],[175 175],'r')
plot([0.01 1],[273 273],'b')
legend('T_s_i_n_k = 177 K','Freezing Point Ammonia, 195 K','Freezing Point Methanol 175 K','Freezing Point Water 273 K','Location','northwest')

```

hold off

11.5.7. Garage Temperature

Scott Kindl

```
%% Garage Temperature
% Calculates the temperature in the garage structure over time
clear all
```

```
t_start = 1/3600;
dt = 1;
```

```
%% day cycle
Tint = linspace(177,297,43200);
Tenv(1:43200) = Tint;
Tenv(43201:86400) = fliplr(Tint);
```

```
len = 86400;
time = 1:len;
```

```
%% Radiator Power Emmitted
Qdot = 14000; % W
```

```
%% soil properties
k = 0.085;
A = 4122; % Area of garage walls
dx = 5; % Regolith thickness
```

```
% ground
Ag = 39*60;
dxg = 2;
Tg = 223;
```

```
%% air properties
rho = 0.020;
V = 9*39*60 - 7*pi*13*(7.5/2)^2 - 6*pi*8*4^2; % Volume
m = rho*V;
gamma = 1.289;
cp = [175 0.709;
200 0.735;
225 0.763;
250 0.791;
275 0.819;
300 0.846;
325 0.871;
350 0.895;
375 0.918;
400 0.939;
450 0.978;
500 1.014;
```

```

550 1.046;
600 1.075;
650 1.102;
700 1.126;
750 1.148;
800 1.168;
850 1.187;
900 1.204;
950 1.220;
1000 1.234];

%% Temperature calculation
temp = zeros(len,1);

i0 = t_start*3600;
finish = i0-1;

T = Tenv(i0);

temp(1) = T;
count = 1;

% Calculate the temperature in the habitat at each time
for j = i0:length(Tenv)
    count = count + 1;
    for i = 1:length(cp)
        if T > cp(i,1)
            cp_i = (((cp(i+1,2)-cp(i,2))*(T-cp(i,1))/...
                (cp(i+1,1)-cp(i,1)))+cp(i,2))/gamma*1000;
            end
        end

        T = fzero(@(Ti) m*cp_i*(Ti-T)+k*A*(Ti-Tenv(j))/dx*dt+...
            k*Ag*(Ti-Tg)/10*dt-Qdot*dt,T);
        temp(count) = T;
    end

if i0 ~= 1
    for j = 1:finish
        count = count + 1;
        for i = 1:length(cp)
            if T > cp(i,1)
                cp_i = (((cp(i+1,2)-cp(i,2))*(T-cp(i,1))/...
                    (cp(i+1,1)-cp(i,1)))+cp(i,2))/gamma*1000;
                end
            end

            T = fzero(@(Ti) m*cp_i*(Ti-T)+k*A*(Ti-Tenv(j))/dx*dt+...
                k*Ag*(Ti-Tg)/10*dt-Qdot*dt,T);
            temp(count) = T;
        end
    end

% Plot results
plot(time/3600,temp(1:len),'r')
set(gca,'fontsize',15)

```

```

title('Garage Temperature vs Time')
xlabel('time (hours)')
ylabel('Temperature under garage (K)')

```

11.5.8. Martian Surface Pressurized Tank Sizing

Chris Wells-Weitzner

%This code was written to help determine the size of the tanks that stored the O2 and N2 on the Martian %surface. How big they would have to be in order to fully pressurize the rover and have excess gas to %account for the leakage from the pressurized tanks. I used an exponential decay model.

```

%Gas required to breathe for 120 days
psi_pa = 6894.75729; %Converts psi to pa
pO2 = 2000*psi_pa; %Units: pa ... 2000psi to pa
pN2 = 4500*psi_pa; %Units: pa ... 4500psi to pa
O2_day = .85; %Units: kg ... Oxygen required per day for each crew member
gas_loss_percent = 1.0014; %Loss of .14% gas per day due to leaks (multiplier)
T_mars = 297; %Units: K ... Hottest temperature on mars surface
R = 8.3144; %J/molK ... duh.

dayO2_120 = O2_day*120;%Units: kg ... Tells kg of O2 for 3 people for 42 days
kg_molO2 = .032; %kg/molO2

molO2_120days = dayO2_120/kg_molO2; %converts kgO2 to molO2
breathe_vO2 = molO2_120days*R*T_mars/pO2*3;

%% Oxygen needed to pressurize the Hull with O2

front_cap = 24.43; %m^3
hull = 54.97; %m^3
Cabin_vol = front_cap + hull;
T_room = 293; %K
pressure = 71.2*10^3; %Pa
percent = .295; %percent
Cabin_molO2 = pressure*Cabin_vol/T_room/R*percent;
mars_vO2 = R*Cabin_molO2*T_mars/pO2;
total = (mars_vO2+breathe_vO2);
total_mass = dayO2_120+Cabin_molO2*kg_molO2;
M_init = total_mass*exp(-log(.9986)*365*3);
mols = M_init/kg_molO2;

newvol = mols*R*T_mars/pO2

%% N2
Cabin_molN2 = pressure*Cabin_vol/T_room/R*(1-percent);
kg_molN2 = .028;
Cabin_kgN2 = Cabin_molN2*kg_molN2;
M_init_N2 = Cabin_kgN2*exp(-log(.9986)*365*3);

```

```

vol_N2 = M_init_N2/kg_molN2*R*T_mars/pN2

%% Watter
water = 178/2.5*3;
rho_w = 999.97;
vol_H2O = water/rho_w

----- Dusty -----
"Mars Mining"

clear all
close all
clc

% Constants
fuel_req = 30; %Metric tons
window = 360; %Days
fuelperday = 30/360; %Metric tons per day
n = 0.8; %Assumed electrolysis efficiency
h2o = 0.000250; %55000 ppm water in soil
LOXden = 1.140; %Metric tons per cubic meter
LH2den = 0.071; %Metric tons per cubic meter

%Amount of regolith mining req per day
dirtperday = fuel_req/window/n/h2o %Metric tons

dirt_density = 3.0; %Metric tons per cubic meter

volumeperday = dirtperday/dirt_density %cubic meters per day

marsLOXvol = (1.76)/LOXden %Cubic meters
marsLOXrad = (marsLOXvol/(4*pi/3))^(1/3) %Meters

marsLH2vol = (0.22)/LH2den %Cubic meters
marsLH2rad = (marsLH2vol/(4*pi/3))^(1/3) %Meters

```

11.5.9. Martian Surface Habitat Structural Optimization

Patrick Dunleavy (Codes # 1, 2)

MATLAB #1

```
clear;clc;close all
```

```
% This script was used to determine the optimal number of longitudinal
% struts to handle launch loads
```

```
% **To save space on ELMS I've posted this one script. A similar script was
% used for the Hub of the habitats. The only difference being R=4m and L=8m
```

```
% Yield strength [Pa] from SolidWorks
```

```
SigmaY = [370 500 345 345 377 1034.213594 744.63379 1070.000004 827.37088 930.7922346 792.89709 220 830
827 910 875 27.5742 75 90 105 125 30 34.5 27.5742 27.5742 96.5098 95 290 415 317.104 75.829 75 345 395 325
70 250 315 290 350 395 371.999997 41.3613 125 145 170 185 40 315 195 215 240 255 90 180 125 205 240 115
55.1485 62.05281564 227.5269907 275.0000009 50 90 90 145 215 240 435 470 490 505]*10^6;
```

```
% Density [kg/m^3]
```

```
den = [4510 4510 4510 4510 4500 4820 4480 4650 4428.78 4370 4730 4510 4820 4480 4370 4730 2700 2705 2705
2705 2705 2710 2700 2700 2800 2800 2800 2800 2800 2800 2780 2780 2780 2780 2840 2840 2840 2840
2840 2840 2760 2700 2730 2730 2730 2730 2730 2680 2680 2680 2680 2680 2680 2690 2690 2690 2690 2690
2700 2700 2700 2700 2700 2700 2700 2700 2700 2700 2830 2830 2830 2810];
```

```
% Elastic Modulus [Pa]
```

```
E = (10^10)*[10.5 10.5 10.5 10.5 10.5 10.40000019 11.03 12.30000018 10.480031 12.00000033 11.5 10.5 9.9
11.03 12 11.5 6.9 6.9 6.9 6.9 6.9 6.9 6.89 6.9 6.9 7.3 7.24 7.24 7.24 7.4 7.3 7.24 7.24 7.24 7.24 7.2 7.2 7.2 7.2
7.2 7.449999682 6.9 6.9 6.9 6.9 6.9 6.9 7.9 7 7 7 7 7 7 7 6.9 6.900000067 6.900000067 6.900000067 6.9 6.9
6.9 6.9 6.9 6.9 7.2 7.2 7.2 7.2];
```

```
M = 20*10^3; % [kg]
```

```
g = 9.81; % [m/s^2]
```

```
a = 5*g; % [m/s^2]
```

```
F = M*(a+g); % [N]
```

```
K = 0.5; % [unitless] fixed at both ends
```

```
L = 13; % [m]
```

```
FS = 1.4; % Factor of Safety
```

```
num = [4:32]; % Number of long. struts
```

```
% This loop finds all the positive thickness of cylindrical long. struts and
```

```
% calculates the r^4 term used in the area moment of inertia
```

```
Rin = 0:0.001:0.1;
```

```
Rout = 0:0.001:0.1;
```

```
for k=1:length(Rin)
```

```
    for e=1:length(Rout)
```

```
        if Rout(e)- Rin(k) > 0
```

```
            RR(k,e) = (Rout(e)^4)-(Rin(k)^4);
```

```
        else
```

```
            RR(k,e)=0;
```

```
        end
```

```
    end
```

```
end
```

```
disp('Done1')
```

```
% Determines the force each strut would take for each num scenerio
```

```
for i=1:length(num)
```

```
    ForcePerStruct(i) = F/num(i);
```

```
end
```

```
disp('Done2')
```

```
% Determines the I required for each num scenerio
```

```
for j=1:length(E)
```

```
    for i=1:length(num)
```

```
        m(j,i) = 10000000000000;
```

```
        I(j,i) = (FS*ForcePerStruct(i)*(K*L)^2)/(pi*E(j));
```

```
        r4(j,i) = (4/pi)*I(j,i);
```

```
        for k=1:length(Rin)
```

```
            for e=1:length(Rout)
```

```

% Finds an existing RR value close to the r4 (r^4)
% calculated above
if (RR(k,e) ~= 0) && (abs(RR(k,e) - r4(j,i)) < 0.000001)
    Area = pi*((Rout(e)^2)-(Rin(k)^2));
    Vol = L*Area*num(i);
    mass = Vol*den(j);
    if mass <= m(j,i)
        A(j,i) = Area;
        V(j,i) = Vol;
        m(j,i) = mass ;
        rin(j,i) = Rin(k);
        rout(j,i) = Rout(e);
        RR4(j,i) = RR(k,e);
    end
end
end
end
end
end
disp('Done3')

% This loop runs through to find the material, number of long. struts and
% dimensions of the long. struts to minimize mass
for j=1:length(E)
    mass = 10000000;
    for i=1:length(num)
        if m(j,i)<= mass
            mass = m(j,i);
            MassY(i) = m(j,i)*10^-3;
            t(i) = (rout(j,i)-rin(j,i))*10^3;
            Area = pi*(((rout(j,i))^2)-((rin(j,i))^2));
            fprintf('Index %d\n',j)
            disp(Name {j})
            fprintf('Mass = %f [tons]\nNum of Struts = %d\nI = %0.9f\nr4 = %0.9f\nRin = %0.9f\nRout = %0.9f\nt = %f
[mm]\nForce per strut = %f\n\n', MassY(i),num(i),I(j,i),r4(j,i),rin(j,i),rout(j,i),t(i), ForcePerStruct(i))
            Sigma = ForcePerStruct(1)/Area;
            end

        end
    end
end
disp('end')

```

MATLAB #2

```
clear;clc;close all
```

```
% Mars habitat analysis using a variety of aluminums to choose
% the material that will lead to the least mass
```

```
% **To save space I've posted this one script. A similar script was
% used for the Hub of the habitats. The only difference being R=4m and L=8m
```

```
% Names of Aluminum
```

```
Name = cell(57,1);
Name{1} = '1060 Alloy'; Name{2} = '1060-H12'; Name{3} = '1060-H14';
Name{4} = '1060-H16'; Name{5} = '1060-H18'; Name{6} = '1060-O';
Name{7} = '1100-O'; Name{8} = '1345 Alloy'; Name{9} = '1350 Alloy';
Name{10} = '2014 Alloy'; Name{11} = '2014-O'; Name{12} = '2014-T4';
Name{13} = '2014-T6'; Name{14} = '2018 Alloy'; Name{15} = '2024 Alloy';
Name{16} = '2024-O'; Name{17} = '2024-T3'; Name{18} = '2024-T361';
Name{19} = '2024-T4'; Name{20} = '2219-O'; Name{21} = '2219-T31';
Name{22} = '2219-T37'; Name{23} = '2219-T62'; Name{24} = '2219-T81';
Name{25} = '2219-T87'; Name{26} = '2618-T6(SS)'; Name{27} = '3003 Alloy';
Name{28} = '3003-H12'; Name{29} = '3003-H14'; Name{30} = '3003-H16';
Name{31} = '3003-H18'; Name{32} = '3003-O'; Name{33} = '4032-T6';
Name{34} = '5052-H32'; Name{35} = '5052-H34'; Name{36} = '5052-H36';
Name{37} = '5052-H38'; Name{38} = '5052-O'; Name{39} = '5454-H111';
Name{40} = '5454-H112'; Name{41} = '5454-H32'; Name{42} = '5454-H34';
Name{43} = '5454-O'; Name{44} = '6061-Alloy'; Name{45} = '6061-O(SS)';
Name{46} = '6061-T4(SS)'; Name{47} = '6061-T6(SS)'; Name{48} = '6063-O';
Name{49} = '6063-T1'; Name{50} = '6063-T4'; Name{51} = '6063-T5';
Name{52} = '6063-T6'; Name{53} = '6063-T83'; Name{54} = '7050-T73510';
Name{55} = '7050-T77451'; Name{56} = '7050-T7651'; Name{57} = '7050-T6';
```

```
% Yield strength [Pa] from SolidWorks for each material
```

```
SigmaY = (10^6)*[27.5742 75 90 105 125 30 34.5 27.5742 27.5742 96.5098 95 290 415 317.104 75.829 75 345
395 325 70 250 315 290 350 395 371.999997 41.3613 125 145 170 185 40 315 195 215 240 255 90 180 125 205
240 115 55.1485 62.05281564 227.5269907 275.0000009 50 90 90 145 215 240 435 470 490 505];
```

```
% Density [kg/m^3] from SolidWorks for each material
```

```
den = [2700 2705 2705 2705 2705 2705 2710 2700 2700 2800 2800 2800 2800 2800 2800 2780 2780 2780 2780
2840 2840 2840 2840 2840 2840 2760 2700 2730 2730 2730 2730 2730 2680 2680 2680 2680 2680 2680 2690
2690 2690 2690 2700 2700 2700 2700 2700 2700 2700 2700 2830 2830 2830 2810];
```

```
% Pressures
```

```
P_hab = 72*10^3; % [Pa] Pressure of habitat from CS
P_mars = 630; % [Pa] Average surface pressure on Mars from...
% ...An Introduction to the Solar System by...
% ...Rothery, McBride and Gilmour
P_eff = P_hab - P_mars; % [Pa]
```

```
% Dimensions of inner volume of habitat
```

```
R = 3.75; % [m] From CS
L = 13; % [m] From CS
```

```
% Determine the minimum thickness, t, of habitat walls for each material
% The following (*) equation was derived from the equation for hoop stress
% using the r in the equation to be the R defined above plus t/2. Also a
% factor of safety was used for stress. Solving that equation for t
% yields (*)
FS = 3;
```

```
% Array for required thickness of each material for FS=3
```

```
tmin = zeros(1,length(SigmaY));
```

```
% Array for resulting mass of each material. NOTE: This is the mass of a
% hollow, uncapped cylinder. Masses including endcaps are determined using
```



```

% Automatic linear interpolation of Beta coefficient
beta=interpolate(floor(aOverB*5)/5,betaTab(floor(aOverB*5)-4),...
    ceil(aOverB*5)/5,betaTab(ceil(aOverB*5)-4),aOverB);

% Calculation of maximum bending stress [Pa]
plateSigmaMax=beta*q*b^2/t^2;

% Calculation of Margin of Safety
MoS=520*10^6/(3*plateSigmaMax)-1;

--
function [si,so,A]=alash_2(a,b,t,L,FS)

% Physical constants
rhoReg=1500; % Regolith density [kg/m^3]
rhoAl=2590; % AL-2090-T83 density [kg/m^3]
E=76*10^9; % AL-2090-T83 Young's Modulus [Pa]
g=3.711; % Martian gravity [m/s^2]
K=2; % Buckling end condition

% Intermediate calculations
w=rhoReg*g*12; % Regolith pressure load for 12m thickness [Pa]
q=w+rhoAl*g*t; % Combined regolith and gravitational load [Pa]
F=a*b*q/4; % Per column compressive load [N]

% Solving for I [m^4]
I=FS*F*(K*L)^2/(pi^2*E);

% Varying geometric properties
si=[0:.001:1]; % Inner side length from 0 to .01 [m]
so=(si.^4+I*12).^25; % Calculating outer side length [m]
A=so.^2-si.^2; % Calculating area [m^2]

% Plot
Ffigure
ax=plotyy(so,si,so,A);
title('Column Cross Section Geometry')
ylabel(ax(1),'Inner Side Length [m]')
ylabel(ax(2),'Area [m^2]')
xlabel(ax(2),'Outer Side Length [m]')
-----

function [MoSBuckling, MoSCompression]=alash_3(a,b,t,L,si,so,FS)

% Physical constants
rhoReg=1500; % Regolith density [kg/m^3]
rhoAl=2590; % AL-2090-T83 density [kg/m^3]
E=76*10^9; % AL-2090-T83 Young's Modulus [Pa]
g=3.711; % Martian gravity [m/s^2]
K=2; % Buckling end condition

% Intermediate calculations
w=rhoReg*g*12; % Regolith pressure load for 12m thickness [Pa]
q=w+rhoAl*g*t; % Combined regolith and gravitational load [Pa]
F=a*b*q/4; % Per column compressive load [N]

```

```

A=so^2-si^2;    % Cross sectional area [m^2]
I=(so^4-si^4)/12; % Cross sectional moment of inertia [m^4]

% Buckling analysis
Fcrit=pi^2*E*I/(2*L)^2; % Critical buckling load [N]
MoSBuckling=Fcrit/(F*FS)-1; % Margin of Safety

% Compression analysis
sigmaAxial=F/A; % Axial compression stress [Pa]
MoSCompression=520*10^6/(3*sigmaAxial)-1; % Margin of Safety

```

11.5.11. Martian Surface Habitat Mass Estimation

Chris Wells-Weitzner

```

%This program is to estimate the Hall and Hub masses for the initial mars
%crew of 4

```

```

%Conservative Hall and Hub estimates from LSM as of 2/25/15
Hall = 10; %Metric Tons (MT)
Hub = 5; %MT

```

```

%%%%%%%%%% Hall 2 %%%%%%%%%%%
%From Will's CAD, the mass of interior bedroom equipment: walls, cubbies,
%clothing poles, table beds all made of plastic 2/25/15
rooms = 5.8; %MT

```

```

%Bathroom
%%including 2 toilets, and 4 sinks
toilet = 1*.028; %MT
sink = 1*.015; %MT
shower = 2*.05; %MT Placeholder
bath = toilet + sink + shower;

```

```

%Exercise
Treadmill = 2*.0898; %MT
Bike = .044; %MT Placeholder
Pullup = .024; %MT
Exerc = Treadmill + Bike + Pullup;

```

```

%Medical
Storage = .4; %Waiting on Jaclyn

```

```

%Laundry
%LGWM3431HS
Wash_dry = 2*.103; %MT

```

```

%Avionics

```

```

%Piping

```

```

%Hall total
Hall_1 = Hall + rooms + bath + Exerc + Med + Wash_dry

%%%%%%%%%%%%%%%%%%%%%%%%%%%%%%%%%%%%%%%%%%%%%%%%%%%%%%%%%%%%%%%%%%%%%%%% Hall 1 %%%%%%%%%
%From Will's CAD, the mass of interior bedroom equipment: walls, cubbies,
%clothing poles, table beds all made of plastic 2/25/15
rooms = 5.8; %MT

%Bathroom
%%including 2 toilets, and 4 sinks
toilet = 1*.028; %MT
sink = 1*.015; %MT
shower = 2*.05; %MT Placeholder
bath = toilet + sink + shower;

%This script is used to calculate the total length of pipe
% required to irrigate water to the plants on the habitats

%The current model is a cross design with an equal sign overlayed
% and end caps

floors = 2;
Shelf_num = 3;

%Each term is multiplied by 4 because there are 4 places for each path type
Longest_path = (8-.75)/2*4;
Connecting_path = 3.25*4;
Short_outter_path = 4*sin(35.7*pi/180)*4;

%multiplied by 2 for the 2 floors
total_hub = Longest_path+Connecting_path+Short_outter_path*floors;

Hall_Length = 12;
Hall_rows = 3;
Hall_total = Hall_Length*Hall_rows*floors*Shelf_num;

Total_length = Hall_total + total_hub;
%Assuming 1 in PVC
length = 3.048; %meters
weight = 1.47009; %kg

weight_per_length = weight/length;

total_mass = weight_per_length*Total_length

```

11.5.12. Crew Food Optimization

Henry Ludgate (Code # 1)

```

%% Food Optimization
% uses the linprog optimization function in order to find the minimum
% area required to allow the diet of a 75th percentile male to be
% completely met.

```

```

clear all
A=xlsread('Foodfda.xlsx');
%% requirements
tots(1:22,1)=A(1:22,9);
tots(1:22,2:31)=A(1:22,20:49);
calories=3200 %kcal
protein=65 %g
carbos=360; %g
fat=71; %g
fiber=38 %g
vita=900; %mcg
vitc=90 %mg
vitd=15; %mcg
vite=15; %mg
vitk=120; %mcg
thiamin=1.2; %mg
ribo=1.3; %mg
niacin=16; %mg
vitb6=1.3 %mg
folate=400; %mcg
vitb12=2.4 %mcg
panto=5; %mg
choline=550 %mg
calcium=1000 % mg
copper=.9 % mg
flouride=4000; %mcg
iron=8; %mg
magnesium=420; %mg
mangenes=2.3 %mg
phosphorous=700 %mg
potassium=4700 %mg
selenium=55 %mcg
sodium=1500; %mg
zinc=11 %mg

%% food data matrix
for i=1:22
    for k=1:28
        Aeq(k,i)=tots(i,k+2);
    end
    for j=1:28
        Aeq(j+k,i)=-tots(i,j+2);
    end
end
%% allowable ranges for each nutrient
xx=3000
beq=[calories+1000; protein+1000; fat+1000; carbos+1000; fiber+1000 ;calcium+xx ;iron+xx; magnesium+xx;
phosphorous+xx; potassium+xx+2000; sodium+xx; zinc+xx; copper+xx; mangenes+xx; selenium+xx; vitc+xx;
thiamin+xx; ribo+xx; niacin+xx; panto+xx; vitb6+xx; folate+xx; choline+xx; vitb12+xx; vita+xx; vite+xx; vitd+xx;
vitk+xx; -calories; -protein; -fat; -carbos; -fiber ; -calcium ; -iron; -magnesium; -phosphorous; -potassium; -sodium; -
zinc; -copper; -mangenes; -selenium; -vitc; -thiamin; -ribo; -niacin; -panto; -vitb6; -folate; -choline; -vitb12; -vita; -
vite; -vitd; -vitk];
%lb=zeros(22,1);
%% upper bound multiplier for each food
c=combnk(1:22,15);

```

```

for i=1:22
    ub(i,1)=20;
end
f=[tots(1,1) tots(2,1) tots(3,1) tots(4,1) tots(5,1) tots(6,1) tots(7,1) tots(8,1) tots(9,1) tots(10,1) tots(11,1) tots(12,1)
tots(13,1) tots(14,1) tots(15,1) tots(16,1) tots(17,1) tots(18,1) tots(19,1) tots(20,1) tots(21,1) tots(22,1)];

%% lower bound of each food multiplier/ optimizer
% placed into a for loop that cycles through different combinations of
% meals in order to add variety.

for ii=1:170544

    lb=zeros(22,1);
    for h=1:15
        u=c(ii,h);
        lb(u,1)=.4;
    end

    [x fval]=linprog(f,Aeq,beq,[],[],lb,ub);
    totalarea(ii,1)=fval*4;
    diet(:,ii)=x;
    totalarea(ii,2)=ii;
end
%%
best=sortrows(totalarea);

```

11.5.13. Solar Power Analysis for Martian Surface Habitat

Adam Buckingham

“Length_Mars_day”

```

%% Length of Mars Day
clear all;
day = [0:687];

Lat = -36.5;
for i = 1:length(day)

    a(i) = 90 - cos(pi*(day(i)/343.5))*25;
    m(i) = 1 + (tand(-Lat)/tand(a(i)));
    b(i) = acos(1-m(i))/pi; %length of Day

end

plot(day,b*24.7)
title('Hours of Sunlight vs Day in Year')
xlabel('Day of Mars year')
ylabel('Amount of sunlight (hour)')

```

“Solar_Tracking_Analysis”

```
%% Sun Tracker Analysis
mean_distance = 1.524; %AU
Is_mean = 1390*(1/mean_distance)^2; % Mean amount of Solar Irradiance on Mars
max_distance = 1.666; %AU
Is_min = 1394*(1/max_distance)^2; % Min amount
min_distance = 1.382; %AU
Is_max = 1394*(1/min_distance)^2; % Max amount
```

```
Is_spring = 1394*(1/1.56)^2; %Spring equinox
Is_summer = 1394*(1/1.65)^2; %Summer Solstice
Is_autumn = 1394*(1/1.45)^2; %Autumnal equinox
Is_winter = 1394*(1/1.38)^2; %Winter Solstice
```

```
%% Hellas Planitia
```

```
i = 1;
```

```
%Calculating zenith angle based on Latitude and declination on Mars
```

```
lat = -36.5; % Latitude of Hellas Planitia
obl = 25; % axis tilt of Mars
% Orb_P = 0:360; Orbital Position of Mars
%t = -6; %hours past noon, so t=0 is noon
%hour_angle = 360*(t/24.67);
%dec = sind(obl)*sind(Orb_P);
%zenith = acosd(sind(lat)*sind(dec)+cosd(lat)*cosd(dec)*cosd(hour_angle))
Solar_efficiency = 0.29;
% Is = Is_spring;
Is = Is_summer;
% Is = Is_autumn;
% Is = Is_winter;
% figure
```

```
A_array = 1;
```

```
Pflat_total = 0;
```

```
Pflat = 0;
```

```
for t = -4.8:1/3600:4.8
```

```
if(Is ==Is_spring)
```

```
    Orb_P = 0;
```

```
end
```

```
if(Is ==Is_summer)
```

```
    Orb_P = 90;
```

```
end
```

```
if(Is ==Is_autumn)
```

```
    Orb_P = 180;
```

```
end
```

```
if(Is ==Is_winter)
```

```
    Orb_P = 270;
```

```
end %Orbital Position of Mars 0 deg -> 360 deg
```

```

hour_angle(i) = 360*(t/24.67);
dec = sind(obl)*sind(Orb_P);
zenith(i) = acosd(sind(lat)*sind(dec)+cosd(lat)*cosd(dec)*cosd(hour_angle(i)));

error_tracking = -10:10; %Place Holder for how accurate the tracker would be

Sflat(i) = Is*cosd(zenith(i));
Sflat_dust(i) = (1-.26)*Sflat(i);
hold on;

worst_case = min(error_tracking);
Sw = Is*cosd(worst_case);
Sw_dust = Sw*(1-.26);
diff(i) = Sw - Sflat(i);

Pflat(i) = Sflat(i)*Solar_efficiency*A_array;
i = i+1;

end
t = [0:1/3600:9.6];
Pflat_total = sum(Pflat);
display(Pflat_total/3600,'Flat Power in W-hr');

plot(t,Pflat)
title('Power over the course of the summer day')
ylabel('Power (W)')
xlabel('Time (hours)')
Ptotal = (Pflat_total/3600)/9.6;

% figure
% plot(t,Sflat,'b',t,Sflat_dust,'r')
% hold on;
% plot(t,Sw,'k',t,Sw_dust,'g')
%
% legend('Flat','Flat with Dust','Tracking','Tracking with Dust')
% title('Solar Irradiance change over course of day at Hellas Planitia (Spring)')
% xlabel('Time (hr)')
% ylabel('Solar Irradiance (W/m^2)')
% hold off

% hold off;
% figure
% plot(t,diff)
% title('Difference between Tracking (worst case) vs Flat on ground')
% xlabel('Time (hr)')
% ylabel('Difference (W/m^2)')

%Just took efficiency of Si solar cells
% May change if use different solar cells
% m^2 chose an Area to compare how the Power output would differ from tracking vs flat on the ground

P_output_flat = Sflat*Solar_efficiency*A_array;

```

```

% P_output_track = Sw*Solar_efficiency*A_array;
%
% display(P_output_track*9.6,'Power output for Tracking');

% figure
% plot(t,P_output_flat);
% hold on;
% plot(t,P_output_track);
% title('Power output change over time at Hellas Planitia')
% xlabel('Time (hr)')
% ylabel('Power Output (W)')
% hold off;

% figure

% Ptrack = P_output_track;
% diff_Power = P_output_track - P_output_flat;

% plot(t,diff_Power)
% title('Difference between Tracking (worst case) vs Flat on ground')
% xlabel('Time (hr)')
% ylabel('Power output (W)')

```

11.6. Auxiliary Trade Studies

11.6.1.CTV Inflatables Optimization for Ariane 5

Jaclyn Rupert

```

%Ariane - Inflatables Optimization
clear all
close all
clc

%Set Values
LD=4.57; %Launch Diameter
%%%%%%%%%%
AD=1.255; %Airlock/ center cylinder diameter %%%%%%%%%%

n=0; nn=0;

for ii=2:1:10
nn=1+nn; %81
L=ii; %Length of module
%%%%%%%%%%
Length(nn)=(ii);

for i=1.2:.05:2
n=1+n;
RatioD=i; %Launch diameter to inflated diameter ratio
Ratio(n)=i;

```

```

InflD=LD*RatioD; %Inflated diameter

St=.4; %Shell material thickness
%%%%%%%%%%%%%%%%%%%%%%%%%%%%%%%%%%%%%%%%%%%%%%%%%%%%%%%%
WWt=.1; %water wall thickness
%%%%%%%%%%%%%%%%%%%%%%%%%%%%%%%%%%%%%%%%%%%%%%%%%%%%%%%%
St_total=St+WWt; %Total shell thickness

L2=L-(2*St_total); %Interior Length (taking into account shell thickness)

HD=InflD-(2*St_total); %habitable diameter

if HD>3,
HD_array(n)=HD;
else
HD_array(n)=0;
end

MV(n)=3.14159*L*(InflD/2)^2; %total module volume
HV(n)=(3.14159*L2*(HD/2)^2); %Habitable volume

if HV(n)>110,
HV_array(n)=HV(n);
else
HV_array(n)=0;
end

HVC(n)=(3.14159*L2*(HD/2)^2)-(3.14159*L2*(AD/2)^2); %Habitable volume ...
%(w/ cylinder structure)

if HVC(n)>110,
HVC_array(n)=HVC(n);
else
HVC_array(n)=0;
end

SV(n)=MV(n)-HV(n); %Shell volume
SVC(n)=(MV(n)-HV(n)-(2*(3.14159*St_total*(AD/2)^2))); %Shell volume ...
%w/ cylinder vol taken out

%COMPARED TO HARD STRUCTURE:
HSV(n)=3.14159*(L-WWt)*((LD-(WWt*2))/2)^2; %habitable hard structure...
%(metal) volume

Cyl_vol(n)=3.14159*L*(AD/2)^2; %(cyl vol- how tightly we can pack fairing)
PDC(n)=2*(sqrt((SVC(n)+Cyl_vol(n))/(3.14159*L))); %outer packed diam ...
%w/ cylinder structure

if PDC(n)<4.57,
PDC_array(n)=PDC(n);
else
PDC_array(n)=0;
end

PD(n)=2*(sqrt(SVC(n)/(3.14159*L))); %outer packed diameter w/ no cyl

```

```

if PD(n)<4.57,
PD_array(n)=PD(n);
else
    PD_array(n)=0;
end

end

end

%length array
xx=-16; yy=0; zz=1.9;
for j=1:1:81
xx=xx+17; yy=yy+17; zz=zz+.1;
length_array(xx:yy)=zz;
end

Array=[length_array; Ratio; HD_array; PD_array; PDC_array; ...
    HV_array; HVC_array];

disp('Ariane Fairing')
disp(' ')
Launch_Diameter=LD
Total_Shell_thickness=St_total
disp(' ')
disp('Column1-Length (2-10)')
disp('Column2-Ratio (1.2-2)')
disp('Column3-Habitable Diam (>5)')
disp('Column4-Packed Diam w/ no interior structure (<4.57)')
disp('Column5-Packed Diam (w/ Cyl in the middle (<4.57)')
disp('Column6-Habitable Vol (110-120)')
disp('Column7-Habitable Vol (w/ cylinder in the middle (110-120)')
disp(' ')

for q=1:1:1377

    if (Array(3,q) & Array(4,q) & Array(5,q) & ...
        Array(6,q) & Array(7,q) ~=0 ...
        & (Array(7,q) < 120)...
        & (Array(6,q) < 120)...
        & (Array(1,q) < 9))

        disp(Array(:,q))
    end
end
end

```

11.6.2. CTV Inflatables Optimization for SLS

Jaclyn Rupert

```

%SLS - Inflatables Optimization
clear all
close all
clc

```

```

%Set Values
AD=1.255; %Airlock/ center cylinder diameter %%%%%%%%%%

n=0; nn=0; nnn=0;
for iii=3.5:1:8 %launch diam
%%%%%%%%%
nnn=1+nnn;
LD=iii;
Launch_diam(nnn)=(iii); %(46) 1802

for ii=2.5:1:13 %length
%%%%%%%%%
nn=1+nn; %47
L=ii; %Length of module
Length(nn)=(ii); %4876 (17)

for i=1.2:0.05:2 %diam ratio
%%%%%%%%%
n=1+n;
RatioD=i; %Launch diameter to inflated diameter ratio
Ratio(n)=i; %82892

InflD=LD*RatioD; %Inflated diameter

St=.4; %Shell material thickness
%%%%%%%%%
WWt=.1; %water wall thickness
%%%%%%%%%
St_total=St+WWt; %Total shell thickness

L2=L-(2*St_total); %Interior Length (taking into account shell thickness)

HD=InflD-(2*St_total); %habitable diameter

if HD>2.5,
HD_array(n)=HD;
else
HD_array(n)=0;
end
MV(n)=3.14159*L*(InflD/2)^2; %total module volume

HV(n)=(3.14159*L2*(HD/2)^2); %Habitable volume
if HV(n)>110 & HV(n)<120,
HV_array(n)=HV(n);
else
HV_array(n)=0;
end

HVC(n)=(3.14159*L2*(HD/2)^2)-(3.14159*L2*(AD/2)^2); %Habitable volume...
%(w/ cylinder structure)
if HVC(n)>110 & HV(n)<120,
HVC_array(n)=HVC(n);
else
HVC_array(n)=0;
end

```

```

SV(n)=MV(n)-HV(n); %Shell volume
SVC(n)=(MV(n)-HV(n))-(2*(3.14159*St_total*(AD/2)^2)); %Shell volume...
%w/ cylinder vol taken out
HSV(n)=3.14159*(L-WWt)*((LD-(WWt*2))/2)^2; %habitable hard structure...
%(metal) volume

Cyl_vol(n)=3.14159*L*(AD/2)^2; %cyl vol (how tightly we can pack fairing)

PDC(n)=2*(sqrt((SVC(n)+Cyl_vol(n))/(3.14159*L))); %outer packed diam...
%w/ cylinder structure

if PDC(n)<8,
PDC_array(n)=PDC(n);
else
    PDC_array(n)=0;
end

PD(n)=2*(sqrt(SVC(n)/(3.14159*L))); %outer packed diameter (no cylinder)
if PD(n)<8,
PD_array(n)=PD(n);
else
    PD_array(n)=0;
end

end
end
end

%launch diam array
xx=-1801; yy=0; zz=3.4;
for j=1:1:46
xx=xx+1802; yy=yy+1802; zz=zz+.1;
launch_diam_array(xx:yy)=zz;
end

Length_array= repmat(Length,1,17);

Array=[launch_diam_array; Ratio; Length_array; HD_array; PD_array; ...
    PDC_array; HV_array; HVC_array];

disp('SLS Fairing')
disp(' ')
Launch_Diameter=LD
Total_Shell_thickness=St_total
disp(' ')

disp('Column1-Launch diam (3.5-8)')
disp('Column2-Ratio (1.2-2)')
disp('Column3-Length (2.5-13)')
disp('Column4-Habitable Diam (>2.5)')
disp('Column5-Packed Diam w/ no interior structure (<8)')
disp('Column6-Packed Diam (w/ Cyl in the middle (<8)')
disp('Column7-Habitable Vol (110-120)')
disp('Column8-Habitable Vol (w/ cylinder in the middle (110-120)')
disp(' ')

```

```

disp('Total Options (Removed rows with Packed D > Launch D)')
for q=1:1:21573

    if ((Array(4,q) & Array(5,q) & Array(6,q) & Array(7,q)...
        & Array(8,q) ~=0 ...
        & (Array(3,q) < 12) ...
        & (Array(1,q) > (Array(5,q) & Array(6,q))))

        disp(Array(:,q)')
    end
end

```

```

disp('vertical orientation (One level)')
for q=1:1:21573

    if (Array(4,q) & Array(5,q) & Array(6,q) & Array(7,q)...
        & Array(8,q) ~=0 ...
        & (Array(3,q) < 12) ...
        & (Array(3,q)>2.5 & Array(3,q)<3) ...
        & (Array(1,q) > (Array(5,q) & Array(6,q))))

        disp(Array(:,q)')
    end
end

```

```

disp('vertical orientation (Two level)')
for q=1:1:21573

    if (Array(4,q) & Array(5,q) & Array(6,q) & Array(7,q)...
        & Array(8,q) ~=0 ...
        & (Array(3,q) < 12) ...
        & (Array(3,q)>5 & Array(3,q)<5.5) ...
        & (Array(1,q) > (Array(5,q) & Array(6,q))))

        disp(Array(:,q)')
    end
end

```

```

disp('vertical orientation (Three level)')
for q=1:1:21573

    if (Array(4,q) & Array(5,q) & Array(6,q) & Array(7,q)...
        & Array(8,q) ~=0 ...
        & (Array(3,q) < 12) ...
        & (Array(3,q)>7.5 & Array(3,q)<8) ...
        & (Array(1,q) > (Array(5,q) & Array(6,q))))

        disp(Array(:,q)')
    end
end

```

```

disp('horizontal orientation (Two level)')
for q=1:1:21573

```

```

if (Array(4,q) & Array(5,q) & Array(6,q) & Array(7,q)...
    & Array(8,q) ~=0 ...
    & (Array(3,q) < 12) ...
    & (Array(4,q)>5 & Array(4,q)<5.5) ...
    & (Array(1,q) > (Array(5,q) & Array(6,q))))

disp(Array(:,q)')
end
end

disp('horizontal orientation (Three level)')
for q=1:1:21573

if (Array(4,q) & Array(5,q) & Array(6,q) & Array(7,q)...
    & Array(8,q) ~=0 ...
    & (Array(3,q) < 12) ...
    & (Array(4,q)>7.5 & Array(4,q)<8) ...
    & (Array(1,q) > (Array(5,q) & Array(6,q))))

    disp(Array(:,q)')
end
end

```

11.6.3. Zeolite Pressure Swing Absorber for Martian Surface Habitat

Chris Wells-Weitzner

%When we were originally going to use a Zeolite Pressure Swing Absorber to help remove the excess O2 I
 %wrote this code to help determine what size of PSA we needed and how long it would have to run for.

```

zeo = 2:1:5000; %cubic feet
zeo = zeo*28.31; %liters

%% pv = nrt

% t = 294; %70F to K
% r = 8.314; %L kPa K^-1 mol^-1
% v = zeo*.29; %.29 for percent O2
% p = 71.2*.29; %kPa
%
% n = p*v/r/t;
% mass_hour = n*32; %g
% totalO2 = 1200*24; %g*24crew
% hours_till_gone = totalO2./mass_hour/60;

zeo2 = 20*28.31; %liters

t = 294; %70F to K
r = 8.314; %L kPa K^-1 mol^-1
v = zeo2*.29; %.29 for percent O2
p = 71.2*.29; %kPa

n = p*v/r/t;
mass_hour = n*32; %g

```

```
totalO2 = 450*24; %g*24crew
hours_till_gone = totalO2./mass_hour/60
```

11.6.4.Solar Power at Alternate Landing Sites

Adam Buckingham

%% McLaughlin Crater

```
i = 1;

%Calculating zenith angle based on Latitude and declination on Mars
lat = 21.9; % Latitude of McLaughlin Crater
obl = 25; % axis tilt of Mars
Orb_P = 0;
A_array = 1;
% Is = Is_spring;
% Is = Is_summer;
% Is = Is_autumn;
% Is = Is_winter;
Is = 1360;
Solar_efficiency = 0.29;
% figure
for t = -6:1/3600:6
if(Is ==Is_spring)
    Orb_P = 0;
end
if(Is ==Is_summer)
    Orb_P = 90;
end
if(Is ==Is_autumn)
    Orb_P = 180;
end
if(Is ==Is_winter)
    Orb_P = 270;
end %Orbital Position of Mars 0 deg -> 360 deg
hour_angle(i) = 360*(t/24.67);
dec = sind(obl)*sind(Orb_P);
zenith(i) = acosd(sind(lat)*sind(dec)+cosd(lat)*cosd(dec)*cosd(hour_angle(i)));

    error_tracking = -10:10; %Place Holder for how accurate the tracker would be

    Sflat(i) = Is*cosd(zenith(i));
    hold on;

    worst_case = min(error_tracking);
    Sw = Is*cosd(worst_case);
    diff(i) = Sw - Sflat(i);

Pflat(i) = Sflat(i)*Solar_efficiency*A_array;

i = i+1;
```

```

end
t = -6:1/3600:6;
%
% Pflat_total = sum(Pflat);
% display(Pflat_total/3600,'Flat Power in kW-hr at McLaughlin Crater')
%
%
% % plot(t,Sflat)
% % plot(t,Sw)
% title('Solar Irradiance change over course of day at McLaughlin Crater')
% xlabel('Time (hr)')
% ylabel('Solar Irradiance (W/m^2)')
% hold off;
%
% % figure
% % plot(t,diff)
% title('Difference between Tracking (worst case) vs Flat on ground')
% xlabel('Time (hr)')
% ylabel('Difference (W/m^2)')

%Just took efficiency of Si solar cells
% May change if use different solar cells
% m^2 chose an Area to compare how the Power output would differ from tracking vs flat on the ground

P_output_flat = Sflat*Solar_efficiency*A_array;
P_output_track = Sw*Solar_efficiency*A_array

% display(P_output_track*12,'Power output for Tracking for McLaughlin Crater')

% figure
% plot(t,P_output_flat);
% hold on;
% plot(t,P_output_track);
% title('Power output change over time at McLaughlin Crater')
% xlabel('Time (hr)')
% ylabel('Power Output (W)')
% hold off;
%
%
% % figure
%
% Ptrack = P_output_track;
% diff_Power = P_output_track - P_output_flat;
%
% % plot(t,diff_Power)
% title('Difference between Tracking (worst case) vs Flat on ground')
% xlabel('Time (hr)')
% ylabel('Power output (W)')

%% Arisa Mons

i = 1;

%Calculating zenith angle based on Latitude and declination on Mars

```

```

lat = -8.35; % Latitude of Arisa Mons
obl = 25; % axis tilt of Mars

Is = Is_spring;
% Is = Is_summer;
% Is = Is_autumn;
% Is = Is_winter;

% figure
for t = -6:1/3600:6
if(Is ==Is_spring)
    Orb_P = 0;
end
if(Is ==Is_summer)
    Orb_P = 90;
end
if(Is ==Is_autumn)
    Orb_P = 180;
end
if(Is ==Is_winter)
    Orb_P = 270;
end
hour_angle(i) = 360*(t/24.67);
dec = sind(obl)*sind(Orb_P);
zenith(i) = acosd(sind(lat)*sind(dec)+cosd(lat)*cosd(dec)*cosd(hour_angle(i)));

    error_tracking = -10:10; %Place Holder for how accurate the tracker would be

    Sflat(i) = Is*cosd(zenith(i));
    hold on;

    worst_case = min(error_tracking);
    Sw = Is*cosd(worst_case);
    diff(i) = Sw - Sflat(i);

    Pflat(i) = Sflat(i)*Solar_efficiency*A_array;
    i = i+1;

end
t = -6:1/3600:6;

Pflat_total = sum(Pflat);
display(Pflat_total/3600,'Flat Power in kW-hr')

% plot(t,Sflat)
% plot(t,Sw)
title('Solar Irradiance change over course of day at Arisia Mons')
xlabel('Time (hr)')
ylabel('Solar Irradiance (W/m^2)')
hold off;

% figure
% plot(t,diff)
title('Difference between Tracking (worst case) vs Flat on ground')

```

```

xlabel('Time (hr)')
ylabel('Difference (W/m^2)')

%Just took efficiency of Si solar cells
% May change if use different solar cells
% m^2 chose an Area to compare how the Power output would differ from tracking vs flat on the ground

P_output_flat = Sflat*Solar_efficiency*A_array;
P_output_track = Sw*Solar_efficiency*A_array;

display(P_output_track*12,'Power output for Tracking')

% figure
% plot(t,P_output_flat);
% hold on;
% plot(t,P_output_track);
title('Power output change over time at Arsia Mons')
xlabel('Time (hr)')
ylabel('Power Output (W)')
hold off;

% figure

Ptrack = P_output_track;
diff_Power = P_output_track - P_output_flat;

% plot(t,diff_Power)
title('Difference between Tracking (worst case) vs Flat on ground')
xlabel('Time (hr)')
ylabel('Power output (W)')

```

11.6.5.Solar Thermal Power Analysis for Martian Surface Habitat

Adam Buckingham (“Solar_Thermal”)

```

%% Rankine Cycle with H2O

clear all;
Amount_of_Mirrors = 25:1:700;
Amirror = 2.3;
Cp_water = 4186; % Liquid water specific heat
Cp_watervapor = 2063.5; % Water Vapor specific heat @ 400 C
Den_water = 999.97; % kg/m^3
gam = 1.3; % Water Vapor

Po1 = .07; %MPA
P2 = 4; %MPA
Peff = 0.70;
Teff = 0.61;
g = 1;

Is_spring = 1394*(1/1.56)^2; %Spring equinox

```

```

Is_summer = 1394*(1/1.65)^2; %Summer Solstice
Is_autumn = 1394*(1/1.45)^2; %Autumnal equinox
Is_winter = 1394*(1/1.38)^2; %Winter Solstice
differencepre =0;
g=1;
for i = 1:length(Amount_of_Mirrors)
Qsolar(i) = (Is_summer)*Amirror*Amount_of_Mirrors(i)*.90;

Tst = 40;
mdot(g) = Qsolar(i)/(Cp_water*(400 - Tst));
Power_Pump(g) = (mdot(g)*(P2-Po1)*10^6)/(Peff*Den_water);
Power_Turbine(g) = mdot(g)*Teff*Cp_watervapor*(400+273)*(1-(Po1/P2)^((gam-1)/gam));
differenceP(g) = Power_Turbine(g) - Power_Pump(g);
if(Power_Turbine(g) < 80000)
    if (Power_Turbine(g) > Power_Pump(g))
        difference(g) = Power_Turbine(g) - Power_Pump(g);
        Turbine_Power(g) = Power_Turbine(g);
        Pump_Power(i) = Power_Pump(g);
        weight(g) = Amount_of_Mirrors(i)*11.3 + 4500;

        if(difference(g) < 70000)
            if(difference(g) > differencepre)
                differencepre = difference(g);
                AM = Amount_of_Mirrors(i);
                Tstf = Tst;
                weightf = Amount_of_Mirrors(i)*11.3 + 4500;
                mdotf = mdot(g);
            end
            end
            end
            end
            g=g+1;
end

% figure
% % plot(weight,Power_Turbine/(1*10^3));
% % hold on;
%
plot(mdot,differenceP/(1*10^3),'r');
%
% % legend('Turbine Produced','Pump needed','Total Power left over','Location','northwest');
ylabel('Power (kW)');
xlabel('Mass Flow rate (kg/s)')
title('Power produced vs Mass flow rate');
% axis([2*10^4 6.5*10^4 0

```

11.6.6. Feasibility of Wind Power Generation on the Martian Surface

April Claus

```

%% Cp = 0.1 to 0.5, v=30 m/s
% this code is specifically for 30 m/s, but the velocity can be altered below to any desired wind velocity (such
as 10 m/s)
Cp1 = 0.1;
Cp2 = 0.15;

```

```

Cp3 = 0.2;
Cp4 = 0.25;
Cp5 = 0.3;

Cp6 = 0.35;
Cp7 = 0.4;
Cp8 = 0.45;
Cp9 = 0.5;

%rho = 0.020; % kg/m3, this is where the Mars atmosphere is taken into account
rho = 1.2; % Earth density
r = 5:0.1:30; % test a range of sizes, maybe 10m - 40m
% A = swept area of turbine blades, variable
% wind speed, use min and max, usually between 25 - 35 at high altitude
v2 = 10; % m/s

for n=1:length(r)
    A(n) = pi*(r(n)^2);
    P(n) = (Cp1*0.5*rho*A(n)*(v2^3))/1000;
    figure(3)
    hold on
end
plot(r,P,'r')

hold on

for n=1:length(r)
    A(n) = pi*(r(n)^2);
    P(n) = (Cp2*0.5*rho*A(n)*(v2^3))/1000;
    figure(3)
    hold on
end
plot(r,P,'g')

for n=1:length(r)
    A(n) = pi*(r(n)^2);
    P(n) = (Cp3*0.5*rho*A(n)*(v2^3))/1000;
    figure(3)
    hold on
end
plot(r,P,'b')

for n=1:length(r)
    A(n) = pi*(r(n)^2);
    P(n) = (Cp4*0.5*rho*A(n)*(v2^3))/1000;
    figure(3)
    hold on
end
plot(r,P,'c')

for n=1:length(r)
    A(n) = pi*(r(n)^2);
    P(n) = (Cp5*0.5*rho*A(n)*(v2^3))/1000;
    figure(3)
    hold on
end

```

```

plot(r,P,'m')

xlabel('Length of Blade (m)')
ylabel('Power from Turbine (kW)')
title('Wind Turbine Power,v=30 m/s Cp=0.1 to Cp=0.3')
legend('Cp = 0.10','Cp = 0.15','Cp = 0.20','Cp = 0.25','Cp = 0.30','Location','NorthWest')

hold off

% higher Cp values
for n=1:length(r)
    A(n) = pi*(r(n)^2);
    P(n) = (Cp6*0.5*rho*A(n)*(v2^3))/1000;
    figure(4)
    hold on
end
plot(r,P,'g')
hold on

for n=1:length(r)
    A(n) = pi*(r(n)^2);
    P(n) = (Cp7*0.5*rho*A(n)*(v2^3))/1000;
    figure(4)
    hold on
end
plot(r,P,'b')

for n=1:length(r)
    A(n) = pi*(r(n)^2);
    P(n) = (Cp8*0.5*rho*A(n)*(v2^3))/1000;
    figure(4)
    hold on
end
plot(r,P,'c')

for n=1:length(r)
    A(n) = pi*(r(n)^2);
    P(n) = (Cp9*0.5*rho*A(n)*(v2^3))/1000;
    figure(4)
    hold on
end
plot(r,P,'m')

xlabel('Length of Blade (m)')
ylabel('Power from Turbine (kW)')
title('Wind Turbine Power, Earth, v=10 m/s, Cp=0.35 to Cp=0.50')
legend('Cp = 0.35','Cp = 0.40','Cp = 0.45','Cp = 0.50','Location','NorthWest')

hold off

```

11.6.7.Methane-powered EDL/A Crew Vehicle

Scott Kindl

```
%% Calculating propellant mass for methane powered maneuvers
% Propellant masses for ascent and descent with methane
clc
clear all
g = 9.8;
R = 8314.3;
dVa = sqrt(2*42970/(300+3393))*1000;
dVd = sqrt(42970/(300+3393))*1000;

rho_LOX = 1140;
M_LOX = 16;
R_LOX = R/M_LOX;

rho_CH4 = 422;

m_misc = (2+4+5)*1000;

Isp = 380;
%% Descent 1: (Methane)
% Fully powered descent to mars surface using a methane rocket. This is
% first descent of the rocket.
mpl = 7.6*1000;

fun = @(mpr) Isp*g + dVd/log((...
    ... % Final Mass
    mpl+m_misc+12.16/rho_CH4*(1/3.85)*mpr +...
    12.16/rho_LOX*(2.85/3.85)*mpr)/...
    ... % Initial Mass
    (mpl+mpr+m_misc+12.16/rho_CH4*(1/3.85)*mpr +...
    12.16/rho_LOX*(2.85/3.85)*mpr));
m_prop1M = fsolve(fun,5000);

%% AD #2 (Methane)
% Propellant necessary for ascent and descent in one fueling
mpl = 7.6*1000;
fun = @(x) [Isp*g + dVa/log(... % Ascent
    ... % Final Mass
    (x(1)*x(2)+mpl+m_misc+12.16/rho_CH4*(1/3.85)*x(2) + ...
    12.16/rho_LOX*(2.85/3.85)*x(2))/...
    ... % Initial Mass
    (mpl+x(2)+m_misc+12.16/rho_CH4*(1/3.85)*x(2) +...
    12.16/rho_LOX*(2.85/3.85)*x(2)));
    Isp*g + dVd/log(... % Descent
    ... % Final Mass
    (4000+m_misc+12.16/rho_CH4*(1/3.85)*x(2) +...
    12.16/rho_LOX*(2.85/3.85)*x(2))/...
    ...% Initial Mass
    (4000+x(1)*x(2)+m_misc+12.16/rho_CH4*(1/3.85)*x(2) +...
    12.16/rho_LOX*(2.85/3.85)*x(2))];
m_prop2M = fsolve(fun,[.75,40000]);

m_inM = m_misc + (12.16/422.36*(1/3.85)*m_prop2M(2)) + ...
```

```

(12.16/rho_LOX*(2.85/3.85)*m_prop2M(2));
mtot_M = mpl+m_prop2M(2)+m_inM;

%% Take two for cargo descent
% Descent 1: (Methane)
% Calculating new mass needed for initial descent because of size
% limitations for the ascent/descent
mpl = 7.6*1000;

fun = @(mpr) Isp*g + dVd/log((mpl+m_inM)/(mpl+mpr+m_inM));
m_prop1M = fsolve(fun,5000);

```

12. Appendix D. Works Cited & References

1. Norton, O. Richard (2002). *The Cambridge Encyclopedia of Meteorites*. Cambridge: Cambridge University Press. pp. 121–124. ISBN 0-521-62143-7.
2. "Phobos: Facts & Figures." *Solar System Exploration*. NASA.
3. Robin M. Camp. Boulder Office/Planetary Science Directorate(
4. Robin M. Camp. Boulder. *Planetary Science Directorate*.
<http://www.boulder.swri.edu/~robin/>
5. John P. Millis, Ph.D. *Mars Moon Mystery*. <http://space.about.com/od/mars/a/Mars-Moon-Mystery.htm>
6. StarDate. *Mars' Moons*. http://stardate.org/astro-guide/ssguide/mars_moons
7. <https://books.google.com/books?id=NBf2QyRBMXEC&pg=PA372&lpg=PA372&dq=zbo+cooling+power+input&source=bl&ots=BUfCndIW2v&sig=-hDCvloADlxa5sV-kcMWHpH3fQY&hl=en&sa=X&ei=5YosVdKEB462yQSCwYCYDw&ved=0CCcQ6AEwAQ#v=onepage&q=zbo%20cooling%20power%20input&f=false>
8. http://www.nasa.gov/centers/ames/research/technology-onepaggers/cryogenic-fluid-management_prt.htm
9. "CO₂CRC - Leaders in Research into Carbon Capture and Storage." *CO₂CRC - Leaders in Research into Carbon Capture and Storage*. The University of Melbourne, Carlton, VIC 3010, n.d.
10. Muscatello, Santiago-Maldonado, T. Gibson, R. Devor, J. Captain, Evaluation of Mars CO₂ Capture and Gas Separation Technologies. 2011.
11. Muscatello, Berggren, Zubrin, *Integrated Mars In Situ Propellant Production System*. 2013.
12. "Hydrogen (H₂)." Hydrogen (H₂). Matweb Material Property Data, n.d. Web.
13. "Methane (CH₄)." Methane (CH₄). Matweb Material Property Data, n.d. Web.
14. Kushnir, Peter. "Hydrogen As an Alternative Fuel." *Army Logistics University* (2000)
15. Muscatello, Santiago-Maldonado, *Mars In Situ Resource Utilization Technology Evaluation*. 2012
16. http://spacecraft.ssl.umd.edu/academics/483F14/483F14L19.power/483F14L19.power_x.pdf
17. <http://spacecraft.ssl.umd.edu/academics/483F14/483F14L09.costing/483F14L09.costing.pdf>
18. [http://spacecraft.ssl.umd.edu/academics/483F12/483F12Proj4/D10-Avionics,%20Sensors,%20Simulation%20Project%20\(2\).pdf](http://spacecraft.ssl.umd.edu/academics/483F12/483F12Proj4/D10-Avionics,%20Sensors,%20Simulation%20Project%20(2).pdf)
19. <http://nssdc.gsfc.nasa.gov/nmc/spacecraftDisplay.do?id=DEEPSP2>
20. <http://ieeexplore.ieee.org/stamp/stamp.jsp?tp=&arnumber=267903>
21. "Small Is Beautiful: US Military Explores Use of Microsatellites." Defense Industry Daily RSS News. N.p., n.d. Web. 05 May 2015.
22. "A Study on a Simple Communication Network by Microsats - 14th International Communication Satellite Systems Conference and Exhibit (AIAA)." A Study on a Simple Communication Network by Microsats - 14th International Communication Satellite Systems Conference and Exhibit (AIAA). N.p., n.d. Web. 05 May 2015.
23. Casani, John. Report on the Loss of the Mars Polar Lander and Deep Space 2 Missions. Pasadena, CA: Jet Propulsion Laboratory, California Institute of Technology, 2000. Web.
24. Consideration of Communications System for Future Mars Human Community Takashi Iida, Yoshinori Arimoto, and Yoshiaki Suzuki 26th International Communications Satellite Systems Conference (ICSSC).
25. Communication Architecture and Technologies for Missions to Moon, Mars, and Beyond Tapan Kulkarni, Avinash Dharne, and Daniele Mortari 1st Space Exploration Conference: Continuing the Voyage of Discovery. January

26. Communications During Critical Mission Operations: Preparing for InSight's Landing on Mars Sami W. Asmar, Kamal Oudrhiri, Susan Kurtik, and Stacy Weinstein-Weiss SpaceOps 2014 Conference. May
27. "Space Communications with Mars." Space Communications with Mars. N.p., n.d. Web. 05 May 2015.
28. "Busek Electro Spray Thrusters." Busek Electro Spray Thrusters. N.p., n.d. Web. 05 May 2015.
29. Small, fileserver1shareddocsadcopsadvertsapersadc-0807201305 - R0, Spacecraft Antenna Selection Tutorial.doc, Revision R0, and Date: 7/20/08 Status = Active Disposal = T/e. Fileserver1shareddocsADCopsAdvertsPapersADC-0807201305 - R0 Small Spacecraft Antenna Selection Tutorial.doc (n.d.): n. pag. Web.
30. http://www.lpi.usra.edu/opag/meetings/july2014/posters/3-HPSC_Poster_OPAG.pdf← this should probably be removed...
31. MSFC SKYLAB CREW SYSTEMS MISSION EVALUATION. Tech. no. TM X-64825. Huntsville, AL: Skylab Program Office, 1974. Print.
32. Shellhammer, Kaley, and Samantha Jeswald, eds. "FORMULA SAE ANTHROPOMETRIC REFERENCE DATA 5TH PERCENTILE FEMALE & 95TH PERCENTILE MALE." SAE Collegiate Design Series News 4.7 (2007): n. pag. Web. 22 Feb. 2015. <<http://www.sae.org/students/cdsnewsletter1207.pdf>>.
33. Thomas J. Stapleton, United Technologies Corporation; James L. Broyan, NASA Johnson Space Center; Shelly Baccus, NASA Johnson Space Center; William Conroy, United Technologies Corporation
34. Perchonok, Michele, Ph.D., Grace Douglas, Ph.D., and Maya Cooper, M.S. Risk of Performance Decrement and Crew Illness Due to an Inadequate Food System. Evidence Report. Houston, Texas: NASA, 2012. Print.
35. Catauro, Patricia M., and Michele H. Perchonok. "Assessment of the Long-Term Stability of Retort Pouch Foods to Support Extended Duration Spaceflight." Journal of Food Science 77.1 (2012): S29-39. Web.
36. Perchonok, Michele and Charles Bourland. "NASA food systems: Past, present, and future." Nutrition, Volume 18, Issue 10, October 2002, Pages 913-920.
37. Hanford, Anthony J., Ph.D., ed. Advanced Life Support Baseline Values and Assumptions Document. Tech. N.p.: NASA, 2004. Print. NASA/CR—2004–208941
38. Dismukes, Kim. "Food for Space Flight." HumanSpaceFlight. NASA, 07 Apr. 2002. Web. 07 May 2015. <<http://spaceflight.nasa.gov/shuttle/reference/factsheets/food.html>>.
39. Lange, Kevin E., Alan T. Perka, Bruce E. Duffield, and Frank F. Jeng. Bounding the Spacecraft Atmosphere Design Space for Future Exploration Missions. Tech. no. NASA/CR-2005-213689. Houston, Texas: Jacobs Sverdrup ESC Group, 2005. Print.
40. Cucinotta, Francis A. "Space Radiation Cancer Risk Projections and Uncertainties-2010." NASA/TP-2011-216155 (n.d.): n. pag. Web.
41. Parsons, Jennifer L., and Lawrence W. Townsend. "Interplanetary Crew Dose Rates for the August 1972 Solar Particle Event." Radiation Research 153.6 (2000): 729-33. Web.
42. Kerr, Richard A. "Radiation Will Make Astronauts' Trip to Mars Even Riskier." SCIENCE 31 May 2013: 1031. Web.
43. Cosmic Ray Environment. Digital image. NASA JPL. 1 Mar. 2002. Web.
44. Holt, John W., and Ali Safeinili. "Radar Sounding Evidence for Buried Glaciers in the Southern Mid-Latitudes of Mars." SCIENCE 21 Nov. 2008: 1235-238. Web.
45. Morthekai P, Jain M, Dartnell L et al (2007) Modeling of the dose rate variations with depth in the Martian regolith using GEANT4. Nucl Instrum Methods Phys Res Sect A 580:667–670
46. Francis A. Cucinotta, Myung-Hee Y. Kim, and Lei Ren, Managing Lunar and Mars Mission Radiation Risks Part I: Cancer Risks, Uncertainties, and Shielding Effectiveness NASA/TP-2005-213164, July, 2005

47. Mitchell, Julie. "Ion Exchange Technology Development in Support of the Urine Processor Assembly." - Nasa Tech Briefs. N.p., 1 Sept. 2013. Web. 09 May 2015.
<<http://www.techbriefs.com/component/content/article/5-ntb/tech-briefs/materials/17191>>.
48. "NASA Facts: International Space Station Environmental Control and Life Support System." Huntsville, AL: George C. Marshall Space Flight Center, 2008. Print.
49. Iacomini, Christine S. "Water Requirements and Exhaust Products of Solid Oxide Electrolysis Systems with Embedded Sabatier Reactors for 100% Oxygen Regeneration." AIAA 41st International Conference on Environmental Systems (2011): n. pag. Web. 9 May 2015.
50. Cockell, Charles S., and Anthony L. Andrady. "The Martian and Extraterrestrial UV Radiation Environment—1. Biological and Closed-loop Ecosystem Considerations." *Acta Astronautica* 44.1 (1999): 53-62. Web.
51. "UND Human Spaceflight Laboratory." UND Human Spaceflight Laboratory. N.p., n.d. Web. 11 May 2015.
52. NASA. NASA, 12 July 2014. Web. 11 May 2015.
53. Golombek, M. P. "Overview of the Mars Pathfinder Mission and Assessment of Landing Site Predictions." *Science* 278.5344 (1997): 1743-748. Web.
54. Squyres, S. W. "The Opportunity Rover's Athena Science Investigation at Meridiani Planum, Mars." *Science* 306.5702 (2004): 1698-703. Web.
55. Clark, Benton. "SURVIVAL AND PROSPERITY USING REGOLITH RESOURCES ON MARS." *Journal of the British Interplanetary Society* 42 (1989): 161-66. Print.
56. Mackenzie, Bruce (1988) Building Mars Habitats Using Local Materials, Case for Mars III conference proceedings, AAS 87-216, vol 74.
57. Boston, Penelope J., Mikhail V. Ivanov, and Christopher P. McKay. "On the Possibility of Chemosynthetic Ecosystems in Subsurface Habitats on Mars." *Icarus* 95.2 (1992): 300-08. Web.
58. Bodiford, Melanie, Michael Fiske, Walter McGregor, and Regina Pope. "In Situ Resource-Based Lunar and Martian Habitat Structures Development at NASA/MSFC." AIAA (2005): n. pag. Web.
59. Badgery-Parker, Jeremy. "Light in the Greenhouse." (1999): 2. NSW Agriculture. Web. Murphy, Tom. "Maximum Efficiency of White Light." (2011): 2. University of California, San Diego. Web.
60. "Mars Dust." NASA Science. NASA, 9 July 2003. Web. 11 May 2015.
61. "Mars Fact Sheet." NASA, 25 Apr. 2014. Web. 11 May 2015.
62. "LED Light Bulbs: Comparison Charts." Eartheasy. N.p., n.d. Web. 11 May 2015.
63. "LED Bulb Efficiency Expected to Continue Improving as Cost Declines." U.S. Energy Information Administration - EIA - Independent Statistics and Analysis. U.S. Energy Information Administration, 19 Mar. 2014. Web. 11 May 2015.
64. "Light Absorption for Photosynthesis." Hyper Physics. N.p., n.d. Web. 11 May 2015.
65. "3M Ceramic Textiles & Composites - Nextel(tm) Woven Fabric 440." *3M Ceramic Textiles & Composites - Nextel(tm) Woven Fabric 440*. 3M, 2007. Web. 11 May 2015.
66. Lichodziejewski, Leo, Christopher Kelley, Ben Tutt, David Jurewicz, Glen Brown, and Brian Gilles. *Design and Testing of the Inflatable Aeroshell for the IRVE-3 Flight Experiment*. Honolulu: AIAA, Apr. 2012. PDF.
67. "Liquid Oxygen & Liquid Methane." *Rocket and Space Technology*. Braeunig.us, n.d. Web. 11 May 2015.
68. "Lox/LCH4." *Encyclopedia Astronautica*. Encyclopedia Astronautica, n.d. Web. 11 May 2015.
69. "Lox/LH2." *Encyclopedia Astronautica*. Encyclopedia Astronautica, n.d. Web. 11 May 2015.
70. Nowlin, Samuel, and Luke Thimons. *SURVIVING THE HEAT: THE APPLICATION OF PHENOLIC IMPREGNATED CARBON ABLATORS*. Pittsburgh: University of Pittsburgh Swanson School of Engineering, 1 Mar. 2013. PDF.
71. *Returning from Space: Re-entry*. N.p.: Federal Aviation Administration, n.d. PDF.
72. "RL10 Engine." Aerojet Rocketdyne. Aerojet Rocketdyne, n.d. Web. 11 May 2015.

73. "Thermophysical Properties of Fluid Systems." *NIST Chemistry WebBook*. NIST, n.d. Web. 11 May 2015.
74. Venkatapathy, Ethiraj, Christine E. Szalai, Bernard Laub, Helen H. Hwang, Joseph L. Conley, and James Arnold. *Thermal Protection System Technologies for Enabling Future Sample Return Missions*. Houston: Lunar and Planetary Institute, 2011. PDF
75. Cobos, Douglas, Gaylon Campbell, and Colin Campbell. *Soil Physical Measurements by the Thermal and Electrical Conductivity Probe aboard NASA's Mars Phoenix Scout Mission*. Brisbane: World Congress of Soil Science, Aug. 2010. PDF.
76. Gori, F., and S. Corasanti. *Theoretical Prediction of the Thermal Conductivity and Temperature Variation inside Mars Soil Analogues*. Rome: Elsevier, Aug. 2003. PDF.
77. Leovy, C. *Note on Thermal Properties of Mars*. Santa Monica: The RAND Corporation, 28 Apr. 1965. PDF.
78. Ungar, Eugene K. *Spacecraft Radiator Freeze Protection Using a Regenerative Heat Exchanger with Bypass Setpoint Temperature Control*. San Francisco: 38th International Conference on Environmental Systems, June-July 2008. PDF.
79. Zuber, Maria T. "Constraints on the Volatile Distribution within Shackleton Crater at the Lunar South Pole." *Nature*. N.p., 20 June 2012. Web. 11 May 2015.
<http://www.nature.com/nature/journal/v486/n7403/full/nature11216.html#FWT.ec_id%3DNATURE-20120621>.
80. "The Altair Lunar Lander." NASA Facts. NASA, 7 Sept. 2008. Web. 11 May 2015.
<http://www.nasa.gov/pdf/289914main_fs_altair_lunar_lander.pdf>.
81. "Lunar Module: Quick Reference Data." (n.d.): n. pag. Apollo News Reference. Grumman. Web. 11 May 2015. <https://www.hq.nasa.gov/alsj/LM04_Lunar_Module_ppLV1-17.pdf>.
82. Klaus, Kurt. SLS and Lunar Missions. USRA. LEAG, 15 Oct. 2013. Web. 11 May 2015.
<<http://www.hou.usra.edu/meetings/leag2013/presentations/klaus.pdf>>.
83. Donahue, Ben. Global Exploration Workshop: Moon Mission Concept with Re-usable Lunar Lander. Boeing, 15 Nov. 2011. Web. 11 May 2015. <http://www.nasa.gov/pdf/604643main_2-Panel%202_Donahue_Final.pdf>.
84. Chai, Siew Wah, Mayuresh V. Kothare, and Shivaji Sircar. "Rapid Pressure Swing Adsorption for Reduction of Bed Size Factor of a Medical Oxygen Concentrator." *Industrial & Engineering Chemistry Research* 50.14 (2011): 8703-710. Web.
85. Malik, Muhammad Arif, Abdul Ghaffar, and Salman Akbar Malik. "Water Purification by Electrical Discharges." *Plasma Sources Science and Technology* 10.1 (2001): 82-91. Web.
86. Al-Shamma'a, A. I., I. Pandithas, and J. Lucas. "Low-pressure Microwave Plasma Ultraviolet Lamp for Water Purification and Ozone Applications." *Journal of Physics D: Applied Physics* 34.18 (2001): 2775-781. Web.
87. Hanley, J., V. F. Chevrier, and M. Mellon. "DISTRIBUTION, DETECTION, AND IMPLICATIONS OF CHLORINE SALTS ON MARS." *44th Lunar and Planetary Science Conference (2013)* (n.d.): n. pag. Lunar and Planetary Institute, 2013. Web.
88. Boduch, Michael. "Standards of Human Comfort." *Meadows Seminar*. The University of Texas at Austin, Fall 2009. Web.
89. Edwards, L., and Paul A. Torcellini. *A Literature Review of the Effects of Natural Light on Building Occupants*. Golden, CO: National Renewable Energy Laboratory, 2002. July 2002. Web.
90. Doyle, Richard, Raphael Some, Wesley Powell, Gabriel Mounce, Montgomery Goforth, Stephen Horan, and Michael Lowry. "High Performance Spaceflight Computing (HPSC)." *High Performance Spaceflight Computing (HPSC)* (2014): n. pag. Lunar and Planetary Institute. 23 July 2014. Web.
91. Mudgett, Paul D. "Multi-Gas Monitor (Multi-Gas Monitor) - 05.06.15." NASA. NASA, n.d. Web. <http://www.nasa.gov/mission_pages/station/research/experiments/1187.html#publications>.

92. High-definition image of JPL's ENose air contamination sensor. Digital image. *NASA | Jet Propulsion Lab*. NASA, n.d. Web. <<http://enose.jpl.nasa.gov/images/DSCN0287b.PNG>>.
93. Phillips, Tony. "Curiosity, the Stunt Double - NASA Science." *Curiosity, the Stunt Double - NASA Science*. Science@NASA, 24 Feb. 2012. Web. <http://science.nasa.gov/science-news/science-at-nasa/2012/24feb_stuntdouble/>.
94. Semones, Edward. *Passive Environmental Neutron Dosimeter*. Oak Ridge, TN: United States. Dept. of Energy. Technical Information Center, 1974. *NASA*. NASA. Web. <https://www.nasa.gov/centers/johnson/pdf/514208main_ES-01_Passive_Dosimetry_Area_%26_Crew_Monitoring_E.Semones.pdf>.
95. "Aircraft Pitch: Digital Controller Design." *Control Tutorials for MATLAB and Simulink* -. University of Michigan, n.d. Web. <<http://ctms.engin.umich.edu/CTMS/index.php?example=AircraftPitch&ion=ControlDigital>>.
96. Aalok, A, A.K Tripathi, and P Soni. "Vermicomposting: A Better Option for Organic Solid Waste Management." *JOURNAL OF HUMAN ECOLOGY -DELHI-* 24.1 (2008): 59–64. Print.
97. Hanford, A. J. "Advanced Life Support Baseline Values and Assumptions Document." NASA Lyndon B. Johnson Space Center. (2004). Print.
98. "Bioenergy Research Group." N.p., n.d. Web. 12 May 2015.
99. Chynoweth DP et al. "Anaerobic Digestion of Space Mission Wastes." *Water science and technology : a journal of the International Association on Water Pollution Research* 53.8 (2006): 177–85. Print.
100. Jourdan, J. "GROW YOUR OWN SPIRULINA." (2001). Print.
101. "Guarantee Your Tilapia Farming Success with Advice from the Experts." *lakewaytilapia*. N.p., n.d. Web. 12 May 2015.
102. "Interactive DRI for Healthcare Professionals." N.p., n.d. Web. 12 May 2015.
103. Key, Suzie, Julian K-C Ma, and Pascal MW Drake. "Genetically Modified Plants and Human Health." *Journal of the Royal Society of Medicine* 101.6 (2008): 290–298. *PubMed Central*. Web. 12 May 2015.
104. "NDL/FNIC Food Composition Database Home Page." N.p., n.d. Web. 12 May 2015.
105. Wamelink, G. W. Wieger et al. "Can Plants Grow on Mars and the Moon: A Growth Experiment on Mars and Moon Soil Simulants." *PLoS ONE* 9.8 (2014): e103138. *PLoS Journals*. Web. 12 May 2015.
106. Wang, Chi-Fei et al. "Bulleyaconitine A Isolated from Aconitum Plant Displays Long-Acting Local Anesthetic Properties in Vitro and in Vivo." *Anesthesiology* 107.1 (2007): 82–90. *PubMed Central*. Web. 12 May 2015.
107. "What Are the Physical and Mental Benefits of Gardening?" *MSU Extension*. N.p., n.d. Web. 12 May 2015.
108. Baguer, Guy G. "Proceedings of the 19th International Cryogenic Engineering Conference." *Google Books*. ICEC, 2002. Web. 07 May 2015.
109. Plachta, David. "Results of an Advanced Development Zero Boil-Off Cryogenic Propellant Storage Test." *40th AIAA/ASME/SAE/ASEE Joint Propulsion Conference and Exhibit* (2004): n. pag. Web.
110. "Cryorefridgerator Purchase Data/Specification Sheet." *Cryomech* (1998): 203-05. Web.
111. Kittel, Peter. "Propellant Preservation for Mars Mission." *Space Technology* (2004): 101-08. Web.
112. United States. Department of the Air Force. Operations. Ed. Brig Gen Giovanni K. Tuck. US Air Force, 17 Oct. 2014. Web. 23 May 2015. <http://static.e-publishing.af.mil/production/1/af_a3_5/publication/afpam11-419/afpam11-419.pdf>.
113. Mars Next. "2020 Landing Site for Mars Rover Mission." Jet Propulsion Laboratory, 2014.
114. Bell, J. F., and J. N. Maki. "MASTCAM-Z: A GEOLOGIC, STEREOSCOPIC, AND MULTISPECTRAL INVESTIGATION ON THE NASA MARS-2020 ROVER." *Solar System Exploration Division* (2014)

115. NASA JPL. "Los Alamos Laser Selected for 2020 Mission". Jet Propulsion Laboratory, 2014, <http://mars.nasa.gov/mars2020/news/whatsnew/index.cfm?FuseAction=ShowNews&NewsID=1684>
116. NASA JPL. "SHERLOC to Micro-Map Mars Minerals and Carbon Rings". Jet Propulsion Laboratory 2014, <http://mars.nasa.gov/mars2020/news/whatsnew/index.cfm?FuseAction=ShowNews&NewsID=1684>
117. NASA JPL. "Mission Instruments", 2014, <http://mars.nasa.gov/mars2020/mission/instruments/>
118. NASA JPL. "Going To the Red Planet", 2014, <http://mars.nasa.gov/mars2020/news/whatsnew/index.cfm?FuseAction=ShowNews&NewsID=1683>
119. Harman, Svein-Erik, Amundsen E.F. et al. "The Ground Penetrating Radar RIMFAX on the Mars 2020 Mission". *Solar System Exploration Division* (2014).
120. Mueller, P.J., J.C. Betty, and R.M. Zubrin. "High-pressure Cryogenic Hydrogen Storage System for a Mars Sample Return Mission." *Elsevier Science Limited* 36 (1996).
121. Vinokhodova, A.G., Gushin, V.I. (2012). Study of values and interpersonal perception in cosmonauts on board of International Space Station. Paper # IAC-12-A1.1.8. International Astronautical Federation. Proceedings, 63rd International Astronautical Congress, Naples, Italy, October 1–5, 2012.
122. Kanas, Nicholas; Manzey, D. (2008). *Space Psychology and Psychiatry* (2nd ed.). El Segundo, California, and Dordrecht, The Netherlands: Microcosm Press and Springer.
123. Vickers, Zata M., Ph.D., University of Minnesota, Traci L. Mann, Ph.D., Department of Psychology, Minneapolis, MN, and Joseph P. Redden, MBA, Ph.D., Marketing Department, Minneapolis, MN. "Factors Contributing to Food Acceptability and Consumption, Mood and Stress on Long-Term Space Mission (Astro Palate)." *NASA*. NASA, 12 Mar. 2015. Web. 12 May 2015.
124. Meyer, William V., Ph.D., Glenn Reserach Center, Cleveland, OH. "Binary Colloidal Alloy Test Low Gravity Phase Kinetics - 1- Product Shelf Life (BCAT-KP1-Shelf Life)." *NASA*. NASA, ZIN Technologies Incorporated, National Laboratory (NL), 17 Apr. 2015. Web. 12 May 2015.
125. Park, University Of Maryland College, Department Of Aerospace Engineering Undergraduate Program, Jhason Abuan, Jorge Aviles, Ryan Dickson, Oscar Hsu, Michael Kessler, Mehdi Khoali, Daniel Maloney, Karen, and Mitchell, Nicholas Patregnani, Peter Pawlowski, Lisa Policastri, Jonathan Quigg, Robert Reed, Molly Simmons,. *Project Magellan: First Human Circumnavigation of the Moon* (n.d.): n. pag. Web.
126. Turnbull, Margaret C. "The Search for Habitable Worlds. 1. The Viability of a Starshade Mission." *Publications of the Astronomical Society of the Pacific* 124.915 (2012): 418-47. Web.
127. Simon, Matthew A. Factors Impacting Habitable Volume Requirements: Results from the 2011 Habitable Volume Workshop. Rep. no. NASA/TM-2011-217352. NASA, Dec. 2011. Web. 12 May 2015. <<http://ston.jsc.nasa.gov/collections/trs/techrep/TM-2011-217352.pdf>>.
128. Akin, David L. "Spacecraft Habitability." Dave Akin's Web Site. Web. 12 May 2015. <http://spacecraft.ssl.umd.edu/academics/483F14/483F14L14.habitability/483F14L14.habitability_x.pdf>.
129. Ijsselstein, Sylvie, European Space Agency. "Electronic - Learning (E-Learning)." *NASA, International Space Station*. NASA, 17 Sept. 2014. Web. 12 May 2015.
130. Miller, Cole, Ph.D. "Astroseismology." 9 Apr. 2015. E-mail.
131. Jones, Mark R. "Deployment and Applications of L1 Gateway Space Station." *Colorado Center for Astrodynamics Research*. Colorado Center for Astrodynamics Research, n.d. Web.
132. Bonskill, Marianne R., Ph.D., and Mark Lupisella, Ph.D. "Earth-Moon L1/L2 Infrastructure - What Role Does It Play?" *Human Exploration Community Workshop on the Global Exploration Roadmap* (2011): 1-10. *NASA*. NASA. Web.

133. RGB3 Cohen, B. A., and R. G. Sellar. "Lunar Flashlight: Finding Lunar Volatiles Using CubeSats." *Annual Meeting of Lunar Exploration Analysis Group* (n.d.): 1-2. Web.
134. RJB2 Staehle, Robert, Barbra Cohen, and Courtney Duncan. "Lunar Flashlight: Finding Lunar Volatiles Using CubeSats." *Third International Workshop on LunarCubes* (n.d.): n. pag. Web.
135. RJB1 Landis, Geoffrey. "Origin of Martian Moons from Binary Asteroid Dissociation." *American Association for Advancement of Science Annual Meeting* (2002): 3-4. Web.
136. NASA. "Deep Space 2." *National Aeronautics and Space Administration*. NASA, 26 Aug. 2014. Web.
137. NASA. "Deep Space 2." *Deep Space 2*. NASA, 15 Sept. 200. Web. 12 May 2015.
138. ESA. "Traces of the Martian past in the Terby Crater." *European Space Agency*. ESA, 25 Jan. 2008. Web. 12 May 2015.
139. Dunbar, Brian. "Martian Crater May Once Have Held Groundwater-Fed Lake." *NASA*. NASA, 20 Jan. 2013. Web. 12 May 2015.
140. IAU, USGS Astrogeology Science Center, and NASA. "Planetary Names: Crater, Craters: McLaughlin on Mars." *Gazetteer of Planetary Nomenclature*. International Astronomical Union (IAU) Working Group for Planetary System Nomenclature (WGPSN), n.d. Web.
141. JPL, and NASA. "Estimated Radiation Dosage on Mars." *JPL*. Jet Propulsion Laboratory, 1 Mar. 2002. Web. 11 May 2015.
142. IAU, USGS Astrogeology Science Center, and NASA. "Planetary Names: Planitia, Planitiae: Hellas Planitia on Mars." *Gazetteer of Planetary Nomenclature*. International Astronomical Union (IAU) Working Group for Planetary System Nomenclature (WGPSN), n.d. Web. 12 May 2015.
143. Bergin, Chris. "Modifications Planned for Atlas V SLC-41 Pad and SLS Mobile Launcher." *Modifications Planned for Atlas V SLC-41 Pad and SLS Mobile Launcher*. NASA Spaceflight, 8 Nov. 2012. Web. 11 May 2015.
144. National Aeronautics and Space Administration. JPL. *Mars Polar Lander/Deep Space 2. Jet Propulsion Laboratory*. NASA, n.d. Web. 12 May 2015.
145. Dunbar, Brian. "Martian Crater May Once Have Held Groundwater-Fed Lake." *NASA*. NASA, 20 Jan. 2013. Web. 12 May 2015.
146. Vittorio De Balsio, Fabio. "INVESTIGATING THE HYDROLOGY OF THE ALLEGED HELLAS PLANITIA LAKE IN SOUTHERN MARS." *45th Lunar and Planetary Science Conference (2014)* (n.d.): n. pag. Universities Space Research Association. Web. 2014.
147. Planetary Science Institute. "Explorer's Guide to Impact Craters." *Planetary Science Institute*. PSI, 2015. Web.
148. Dunbar, Brian, and NASA. "Three Craters." *NASA*. NASA, 22 Dec. 2008. Web. 12 May 2015.
149. "Weather on Mars: The Hellas Plantia Region." *Weather on Mars: The Hellas Plantia Region*. N.p., Jan. 2005. Web. 12 May 2015.
150. Akin, David L. "Applications of Ultra-Low Ballistic Coefficient Entry Vehicles to Existing and Future Space Missions." *SpaceOps 2010 Conference* (2010): 1-12. AIAA. Web.
151. "Hellas Planitia." 41°52'12.91" S and 72°38'19.60" E elev -20839 ft. **Google Earth**. February 22, 2015.
152. "East Hellas Planitia." 39°36'20.26 S and 82°16'17.87" E elev -20049 ft. **Google Earth**. February 27, 2015.
153. "Northern Hellas Planitia." 28°23'08.95" S and 72°32'57.26" E elev -12120 ft. **Google Earth**. February 27, 2015.
154. "Hadriacus Mons at Hellas Planitia." 33°47'09.13" S and 96°01'58.10" E elev -9904 ft. **Google Earth**. February 27, 2015.
155. "McLaughlin Crater." 21°50'14.75" N and 22°23'43.25" W elev -16598ft. **Google Earth**. February 27, 2015.
156. Lee, Pascal. "PADME: A Proposed NASA Discovery Mission to Investigate the Two Moons of MArS." (n.d.): n. pag. 17 Mar. 2015. Web. 12 Apr. 2015.

157. "Lunar Atmosphere and Dust Environment Explorer (LADEE) Launch Press Kit." (n.d.): n. pag. NASA.Gov. Aug. 2013. Web. 13 Apr. 2015.
158. Glarner, Herbert. "Length of Day and Twilight." Herbert Gandraxa. Herbert Glarner, 15 Jan. 2006. Web. 5 Apr. 2015.
159. Beish, Jeff. "DAYS AND SEASONS ON MARS." *General Information - Observing Mars*. Association of Lunar & Planetary Observers, 4 Mar. 2015. Web. 7 Apr. 2015.
160. "Hour Angle." *Encyclopedia Britannica Online*. Encyclopedia Britannica, n.d. Web. 09 May 2015.
161. "Battery Statistics." *Battery University*. Cadex, 2011. Web. 10 May 2015.
162. Benoit. "Solar Irradiance on Mars." *Solar Irradiance on Mars*. Colorado Center for Astrodynamics Research, 2001. Web. 10 May 2015.
163. "HSF -- TransHab." NASA. NASA, 27 June 2003. Web. 10 May 2015.
164. Fuente, Horacio, and Jasen Raboin. *TRANSHAB: NASA's LARGE-SCALE INFLATABLE SPACECRAFT*. Tech. NASA, 3 Apr. 2000. Web. 10 Apr. 2015.
165. Gilmore, D.G, ed., *Spacecraft Thermal Control Handbook AIAA*, 2002
166. Blau, Patrick. "Dragon Spacecraft Information." *Spaceflight101*. Spaceflight101, n.d. Web. 11 May 2015.
167. Chen, Q. S., J. Wegrzyn, and V. Prasad. "Analysis of Temperature and Pressure Changes in Liquified Natural Gas Cryogenic Tanks." *Cryogenics* 44 (2002): 701-09. 16 Mar. 2004. Web. 14 Apr. 2015.
168. Fleming, Lan. "Thrusters, Light Flashes, and Ice Particles." *VGL*. N.p., n.d. Web. 5 May 2015.
169. Coker, A. Kayode., and Ernest E. Ludwig. "Appendix C: PHYSICAL PROPERTIES OF LIQUIDS AND GASES." *Ludwig's Applied Process Design for Chemical and Petrochemical Plants: Distillation, Packed Towers, Petroleum Fractionation, Gas Processing and Dehydration*. 4th ed. Oxford: Gulf Professional, 2010. 827-62. Print.
170. Howard, Maahs, Wallace, Vaughn "Carbon-Carbon Composite Radiator Development for the EO-1 Spacecraft." (n.d.): n. pag. NASA. Web. 10 May 2015.
171. Tombouliau, Briana N., "Lightweight, High-Temperature Radiator for In-Space Nuclear-Electric Power and Propulsion" (2014). Doctoral Dissertations 2014-current. Paper 247.
172. Jordan, Dirk C., and Sarah R. Kurtz. "Photovoltaic Degradation Rates." *An Analytical Review: Preprint* (n.d.): n. pag. *National Renewable Energy Laboratory*. Alliance for Sustainable Energy, June 2012. Web. 28 Feb. 2015.
173. Dean, Wendy S. "Revised Data Sheet Solopanel SP3L." (n.d.): n. pag. *SoloPower.com*. SoloPower Systems. Web. Feb. 2015.
174. "260W Solar Panel Solopower SP3L-260 CIGS." *FreeCleanSolar.com*. FreeCleanSolar, Inc, n.d. Web. Feb. 2015. <<http://www.freecleansolar.com/260W-solar-panel-Solopower-SP3L-260-CIGS-p/sp3l-260.htm>>.
175. SunPower. N.p.: SunPower, n.d. *SunPower*. SunPower Corporation. Web. 8 Feb. 2015. <<http://us.sunpower.com/sites/sunpower/files/media-library/spec-sheets/sp-e-series-residential-solar-panels-supplementary-technical-spec.pdf>>.
176. "SunPower 327 Solar Panels." *FreeCleanSolar.com*. FreeCleanSolar, Inc, n.d. Web. 10 Feb. 2015. <<http://www.freecleansolar.com/SunPower-327-Solar-Panels-s/4580.htm>>.
177. "Photovoltaics." *Spectrolab*. Spectrolab, Inc., n.d. Web. 26 Feb. 2015. <<http://www.spectrolab.com/faqs-space.htm>>.
178. "Space Solar Panels." (n.d.): n. pag. *Spectrolab*. Spectrolab, Inc. Web. Feb. 2015.
179. "Advanced Triple-Junction Solar Cell For Space Applications." *ZTJ Photovoltaic Cell* (n.d.): n. pag. *Emcore*. Emcore, Sept. 2012. Web. Feb. 2015.
180. "PowerFLEX™ BIPV." (n.d.): n. pag. 2013. Web. 20 Feb. 2015.
181. Cotal, Hector, Chris Fetzer, Joseph Boisvert, Geoffrey Kinsey, Richard King, Peter Hebert, Hojun Yoon, and Nasser Karam. "III-V Multijunction Solar Cells for Concentrating

- Photovoltaics." *Energy & Environmental Science* 2.2 (2009): 174-92. Royal Society of Chemistry, 10 Dec. 2009. Web. 02 Mar. 2015.
182. Caplinger, Mike. "Seasons on Mars." *Malin Space Science Systems*. N.p., Sept. 1994. Web. 17 Mar. 2015.
- 183.
184. "Cost Estimating Web Site." *NASA - Johnson Space Center*. 21 Jan. 2005. 30 Oct. 2006 [http://www1.jsc.nasa.gov/bu2/beta.html] *Internet Archive*. [https://web.archive.org/web/20061103063550/http://www1.jsc.nasa.gov/bu2/index.htm] Web. 12 May 2015.
185. "Spacecraft/Vehicle Level Cost Model." *NASA - Johnson Space Center*. 21 Jan. 2005. 30 Oct. 2006 [http://www1.jsc.nasa.gov/bu2/beta.html] *Internet Archive*. [https://web.archive.org/web/20061030224001/http://www1.jsc.nasa.gov/bu2/SVLCM.html] Web. 12 May 2015.
186. "Advanced Missions Cost Model." *NASA - Johnson Space Center*. 21 Jan. 2005. 29 Sept. 2006 [http://www1.jsc.nasa.gov/bu2/AMCM.html] *Internet Archive*. [https://web.archive.org/web/20060929030639/http://www1.jsc.nasa.gov/bu2/AMCM.html] Web. 12 May 2015.
187. "Cost Spreading Calculator." *NASA - Johnson Space Center*. 21 Jan. 2005. 30 Oct. 2006 [http://www1.jsc.nasa.gov/bu2/beta.html] *Internet Archive*. [https://web.archive.org/web/20061030223738/http://www1.jsc.nasa.gov/bu2/beta.html] Web. 12 May 2015.
188. "Mission Operations Cost Model." *NASA - Johnson Space Center*. 21 Jan. 2005. 29 Sept. 2006 [http://www1.jsc.nasa.gov/bu2/beta.html] *Internet Archive*. [https://web.archive.org/web/20060929030605/http://www1.jsc.nasa.gov/bu2/index.html] Web. 12 May 2015.
189. "Capabilities & Services." *SpaceX*. Space Exploration Technologies Corp. Web. 12 May 2015.
190. *FY 2016 President's Budget Request Summary*. National Aeronautics and Space Administration. PDF.
191. Reeves, JD. "NASA Cost Estimating." RASC-AL Costing Webinar. Web. 26 Mar. 2015. Lecture.
192. *NASA New Start Inflation Indices*. Computer software. *CAD Publications*. Vers. FY14. NASA Cost Analysis Division, 14 Feb. 2014. Web. 12 May 2015.
193. United States. NASA/ DOE. Fission Surface Power Team. *Fission Surface Power System: Initial Concept Definition*. By Lee Mason, Dave Poston, Donald Palac, and Scott Harlow. N.p.: NASA, 2010. Print.
194. "FSP System Inquiry." Message to Donald Palac. 30 Apr. 2015. E-mail.
195. Harlow, Scott, Lee Mason, Donald Palac, and Michael Houts. "Robust Optimization for Power Systems Capacity Expansion under Uncertainty." *The Journal of the Operational Research Society* 45.9 (1994): 1040-049. NASA. Web
196. Holbert, K. E. "Neutron Reactions." *EEE-460 Handout* (n.d.): n. pag. Arizona State University. Web
197. National Aeronautics and Space Administration. *NASA Technical Standard*. 6 Aug. 2014. Technical Standards Manual.
198. "Xenon Poisoning." *Hyper Physics*. Georgia State University, n.d. Web. <http%3A%2F%2Fhyperphysics.phy-astr.gsu.edu%2Fhbase%2Fnucene%2Fxenon.html>.
199. "Fast Neutron Reactors." World Nuclear Association, May 2015. Web. <http://www.world-nuclear.org/info/Current-and-Future-Generation/Fast-Neutron-Reactors/>.
200. "Uranium: Uranium Dioxide." *Uranium»uranium Dioxide [WebElements Periodic Table]*. WebElements, n.d. Web. <http://www.webelements.com/compounds/uranium/uranium_dioxide.html>.

201. Boumis, Robert. "The Average Wind Speed on Mars." *Science*. Opposing Views, n.d. Web. 13 May 2015. <<http://science.opposingviews.com/average-wind-speed-mars-3805.html>>.
202. Grant, John, Dr. "Interview with Dr. John Grant." Personal interview. 11 Feb. 2015.
203. Folta, David, and Frank Vaughn. "A Survey Of Earth-Moon Libration Orbits: Stationkeeping Strategies And Intra-Orbit Transfers." NASA, n.d. Web. 4 Apr. 2015. <<http://ntrs.nasa.gov/archive/nasa/casi.ntrs.nasa.gov/20040171140.pdf>>.
204. "Geothermal Electricity Production." *Geothermal Energy*. Renewable Energy World, n.d. Web. <<http://www.renewableenergyworld.com/rea/tech/geothermal-energy/geoelectricity/>>.
205. Hargrave, Michael L. "Geophysical Detection of Features and Community Plan at New Philadelphia, Lllinois." *Historical Archaeology* 44.1, New Philadelphia: Racism, Community, and the Illinois Frontier (2010): 43-57. La Trobe University. Web.
206. "Molten Salt Reactors." World Nuclear Association, n.d. Web. 26 Feb. 2015. <<http://www.world-nuclear.org/info/Current-and-Future-Generation/Molten-Salt-Reactors/>>.
207. "Types of Nuclear Reactors." ». Institute for Energy and Environmental Research, 2012. Web. 24 Feb. 2015. <<http://ieer.org/resource/classroom/types-of-nuclear-reactors/>>.
208. Kuznetsov, Vladimir, and Alexey Lokhov. "Current Status, Technical Feasiblity and Economics of Small Nuclear Reactors." (n.d.): n. pag. Nuclear Energy Agency: Organization of Economic Cooperation and Development, 2011. Web. <<http://www.oecd-nea.org/ndd/reports/2011/current-status-small-reactors.pdf>>.
209. "Status of Small and Medium Sized Reactor Designs." (n.d.): n. pag. *IAEA.org*. International Atomic Energy Agency, Sept. 2012. Web. <<https://www.iaea.org/NuclearPower/Downloadable/SMR/files/smr-status-sep-2012.pdf>>.
210. "Aluminium 2090-T86." Aluminium 2090-T86 Matweb Material Property Data, n.d. Web.
211. "Just Like Home." Educator Features. Ed. Shelley Canright. NASA, 10 Apr. 2009. Web. 13 May 2015. <http://www.nasa.gov/audience/foreducators/k-4/features/F_Just_Like_Home.html>.
212. "14 CFR 1214.604 - Personal Preference Kit (PPK)." 14 CFR 1214.604. Cornell University Law School, n.d. Web. 13 May 2015. <<https://www.law.cornell.edu/cfr/text/14/1214.604>>.
213. "World's First 'Head-Up Display for Soldier' in Field Testing." Newsroom. BAE Systems, 19 Feb. 2014. Web. 15 May 2015. <http://www.baesystems.com/article/BAES_165373/worlds-first-head-up-display-for-soldier-in-field-testing?_adf.ctrl-state=1575jxsgn6_4&_afLoop=1786787039277000&_afWindowMode=0&_afWindowId=null#!%40%40%3F_afWindowId%3Dnull%26_afLoop%3D1786787039277000%26_afWindowMode%3D0%26_adf.ctrl-state%3Dna0jv63tr_4>.
214. Maxey, Kyle. "Q-Warrior Is the Soldier's Google Glass." *Engineering.com*, 27 Feb. 2014. Web. 15 May 2015. <<http://www.engineering.com/DesignerEdge/DesignerEdgeArticles/ArticleID/7228/Q-Warrior-is-the-Soldiers-Google-Glass.aspx>>.
215. "The NASA Z-2 Suit." Z-2. NASA, 30 Apr. 2014. Web. 15 May 2015. <<https://jscfeatures.jsc.nasa.gov/z2/>>.
216. Barta, Daniel J., Ph.D. Next Generation Life Support Project: Development of Advanced Technologies for Human Exploration Missions. Tech. AIAA, n.d. Web. 15 May 2015. <<http://ntrs.nasa.gov/archive/nasa/casi.ntrs.nasa.gov/20120011664.pdf>>.
217. Hammond, Teena. "Ultimate Wearable Tech: NASA Using 3D Printing to Design Mars Spacesuit." *Tech Republic*. CBS Interactive, 18 Sept. 2014. Web. 15 May 2015. <<http://www.techrepublic.com/article/ultimate-wearable-tech-nasa-using-3d-printing-to-design-mars-spacesuit/>>.
218. Ayrey, William. ILC Space Suits & Related Products. Rep. no. 0000-712731. ILC Dover, 28 Nov. 2007. Web. 15 May 2015. <<http://history.nasa.gov/alsj/ILC-SpaceSuits-RevA.pdf>>.
219. SpaceNews Staff. "NASA Picks ILC Dover To Build Next-gen Spacesuit." *SpaceNews*, 26 Apr. 2013. Web. 15 May 2015. <http://spacenews.com/35077nasa-picks-ilc-dover-to-build-next-gen-spacesuit/#.UX3X5MrdP_o>.

220. Akin, David. "Mass Estimating Relations." ENAE483. Martin Hall, College Park. 2 Oct. 2014. Lecture.
221. Colaprete, Anthony, Peter Shultz, and Jennifer Heldmann. "Detection of Water in the LCROSS Ejecta Plume." *Science* 330.6003 (2010): 463-68. Web. 02 Feb. 2015.
222. Bussey, D.Bj., J.A. McGovern, P.D. Spudis, C.D. Neish, H. Noda, Y. Ishihara, and S.A. Sorensen. "Illumination Conditions of the South Pole of the Moon Derived Using Kaguya Topography." *Icarus* 208.2 (2010): 558-64. *ScienceDirect*. Aug. 2010. Web.
223. Meyer, C. "Lunar Regolith." *Lunar Sample Catalog* (2003): 46-48. *Curation | Lunar*. NASA, 2003. Web.
224. "Specific Heat of Some Common Substances." *Specific Heat of Some Common Substances*. N.p., n.d. Web. <http://www.engineeringtoolbox.com/specific-heat-capacity-d_391.html>.
225. Dopp, Robert B. "High Rate and High Efficiency Hydrogen Generation via Water Electrolysis Catalyzed by Nano Powders." Thesis. DoppStein Enterprises Inc., 2013. *Grid-Shift.com*. GridShift, Inc., 8 Jan. 2013. Web. <http://www.grid-shift.com/white_papers/docs/3D%20Water%20Electrolysis%20Whitepaper%20Jan%2012a.pdf>.
226. Bigelow Aerospace Colonizing Space One Module at a Time." Google Books. N.p., n.d. Web. 05 May 2015.
227. "HSF -- TransHab." HSF -- TransHab. NASA, n.d. Web. 16 May 2015. <<http://www.spaceflight.nasa.gov/history/station/transhab/index.html>>.
228. Roberts M. Inflatable Habitation For Lunar Base (n.d.): n. pag. Web. Apr.-May 2015.
229. Technical Report on Space Debris: Text of the Report Adopted by the Scientific and Technical Subcommittee of the United Nations Committee on the Peaceful Uses of Outer Space. New York: United Nations, 1999. United Nation Technical Report on Space Debris. Web. <http://www.unoosa.org/pdf/reports/ac105/AC105_720E.pdf>.
230. 3. "Developing a Habitat for Long Duration, Deep Space Missions." Michelle A. Rucker NASA Johnson Space Center, USA, Spacecraft and Mission Operations, Subsystem Equipment, Logistics and Resupply, and Contingency Operations. NASA. Web. Apr.-May 2015.
231. Valentin Stavrev, and Raffi Tomasian. High Transparency Inflatable Modules for Space Habitats (n.d.): n. pag. High Transparency Inflatable Modules for Space Habitats. Web.
232. "Carp Aquaponics - Aqua Allotments UK Aquaponic Systems and Supplies." N.p., n.d. Web. 15 May 2015.
233. "CATFISH FARMING -- SMALL-SCALE & HOME-USE." N.p., n.d. Web. 15 May 2015.
234. Chaudhuri, H., and S. B. Singh. "Induced Breeding of Carps." (1984): 82 pp. Print.
235. corporateName=Department of Agriculture, Fisheries and Forestry; jurisdiction=Queensland; address=GPO Box 46. "Growing and Harvesting Jade Perch." Collection; Text. N.p., 20 Feb. 2012. Web. 15 May 2015.
236. "FAO: Rainbow Trout Home." N.p., n.d. Web. 15 May 2015.
237. "Murray Cod - Aquaculture Prospects | NSW Department of Primary Industries." N.p., n.d. Web. 15 May 2015.
238. Tidwell, James H. et al. "Effect of Stocking Density on Growth and Water Quality for Largemouth Bass *Micropterus Salmoides* Growout in Ponds." *Journal of the World Aquaculture Society* 29.1 (1998): 79-83. Wiley Online Library. Web. 15 May 2015.
239. Watson, Craig, Jeffrey Hill, and Deborah Poudar. "Species Profile: Koi and Goldfish." Southern Regional Aquaculture Center September 2004 6. Print.
240. "FAO Fisheries & Aquaculture - Cultured Aquatic Species Information Programme - *Oreochromis Niloticus* (Linnaeus, 1758)." Accessed May 15, 2015. http://www.fao.org/fishery/culturedspecies/Oreochromis_niloticus/en.
241. "Predesigned Steam Turbine SST-040." (n.d.): n. pag. *Www.siemens.com*. Siemens AG Energy Sector, 2011. Web. 24 Feb. 2015.
242. Steinfeldt, Bradley A. "Guidance, Navigation, and Control Technology System Trades for Mars Pinpoint Landing." *Space Systems Design Lab* (2008)

243. Dutta, Soumyo, Robert D. Braun, and Christopher D. Karlgaard. "Uncertainty Quantification for Mars Entry, Descent, and Landing Reconstruction Using Adaptive Filtering." *Journal of Spacecraft and Rockets* (2014): 1-11.
244. ARL. "Terrain Relative Navigation." *Terrain Relative Navigation* (2008).
245. Korzun, Ashley M. "Supersonic Aerodynamic Characteristics of Blunt Body Trim Tab Configurations." NASA Langley (2014)
246. Johnson, Andrew, and Yang Cheng. "Real-Time Terrain Relative Navigation Test Results from a Relevant Environment for Mars Landing." AIAA (2015)
247. Brugararoles, Paul B. "Entry Attitude Controller for the Mars Science Laboratory." IEEE Xplore.
248. Ploen, Scott, and Behcet Acikmese. "A Comparison of Powered Descent Guidance Laws for Mars Pinpoint Landing." AIAA/AAS (2006)
249. Acikmese, Behcet, and Scott Ploen. "A Powered Descent Guidance Algorithm for Mars Pinpoint Landing." (2005)
250. Akin, David L. "Aerospace Physiology." Dave Akin's Web Site. Web. 18 May 2015. http://spacecraft.ssl.umd.edu/academics/483F14/483F14L11.physiology/483F14L11.physiology_x.pdf
251. Akin, David L. "Physiology and Radiation." Dave Akin's Web Site. Web. 18 May 2015. http://spacecraft.ssl.umd.edu/academics/483F14/483F14L12.radiation/483F14L12.radiation_x.pdf
252. Akin, David L. "Space Life Support Systems." Dave Akin's Web Site. Web. 18 May 2015. http://spacecraft.ssl.umd.edu/academics/483F14/483F14L15.life_support/483F14L15.life_support_x.pdf
253. "Corporate Site – RASC-AL Themes." Web. 18 May 2015. <http://nia-cms.nianet.org/RASCAL/Program-Info/RASC-AL-THEMES.aspx>
254. Aluminum 2090 Alloy." AZoMaterials. AZoNetwork, 11 June 2013. Web.
255. Young, Warren C., and Richard G. Budynas. *Roark's Formulas for Stress and Strain*. New York: McGraw-Hill, 2002. Print.
256. Noffke Nora. *Astrobiology*. February 2015, 15(2): 169-192. doi:10.1089/ast.2014.1218.
257. Engler, Simon. "Testing Robotic Companions on a Simulated Mission to Mars." *IEEE SPECTRUM*. 26 Sept. 2013. Web. 3 May 2015.
258. Williams, Dave R. "Isolation and integrated testing- An introduction to the Lunar-Mars Life Support Test Project." *Isolation: NASA Experiments in Closed-Environment Living- Advanced Human Life Support Enclosed System Final Report* 104 (2002): 1-5.
259. Hawkey, A. "The Physical Price of a Ticket Into Space." *Journal of the British Interplanetary Society* 56.May-June (2003): 152-59. Print.
260. Gradie et al. pp. 316-335 in *Asteroids II*. edited by Richard P. Binzel, Tom Gehrels, and Mildred Shapley Matthews, Eds. University of Arizona Press, Tucson, 1989, ISBN 0-8165-1123-3
261. <http://www.astronomysource.com/tag/c-type-asteroids/>
262. **Near-Earth Object Human Space Flight Accessible Targets Study (NHATS);** <http://neo.jpl.nasa.gov/cgi-bin/nhats>
263. Dr. Akin's Mass Estimation Lecture
264. Adams, John C. "Atmospheric Re-Entry." *Atmospheric Re-Entry*. Arnold Engineering Department Center, n.d. Web. 12 May 2015.
265. Reuben R. Rohrschneider and Robert D. Braun. "Survey of Ballute Technology for Aerocapture." *Journal of Spacecraft and Rockets*, Vol. 44, No. 1 (2007), pp. 10-23.
266. <http://www.nss.org/settlement/moon/LUNOX.html>